

VOL. **593** NOS. **1 + 2** FEBRUARY 28, **1992**

COMPLETE IN ONE ISSUE

**15th International Symposium  
on Column Liquid Chromatography  
Basel, June 3-7, 1991  
Part II****Period.**

JOURNAL OF

# CHROMATOGRAPHY

INCLUDING ELECTROPHORESIS AND OTHER SEPARATION METHODS

## SYMPOSIUM VOLUMES

### EDITORS

E. Heftmann (Orinda, CA)  
Z. Deyl (Prague)

### EDITORIAL BOARD

E. Bayer (Tübingen)  
S. R. Binder (Hercules, CA)  
S. C. Churms (Rondebosch)  
J. C. Fetzer (Richmond, CA)  
E. Gelpí (Barcelona)  
K. M. Gooding (Lafayette, IN)  
S. Hara (Tokyo)  
P. Helboe (Brønshøj)  
W. Lindner (Graz)  
T. M. Phillips (Washington, DC)  
S. Terabe (Hyogo)  
H. F. Walton (Boulder, CO)  
M. Wilchek (Rehovot)

ELSEVIER

# JOURNAL OF CHROMATOGRAPHY

INCLUDING ELECTROPHORESIS AND OTHER SEPARATION METHODS

**Scope.** The *Journal of Chromatography* publishes papers on all aspects of chromatography, electrophoresis and related methods. Contributions consist mainly of research papers dealing with chromatographic theory, instrumental development and their applications. The section *Biomedical Applications*, which is under separate editorship, deals with the following aspects: developments in and applications of chromatographic and electrophoretic techniques related to clinical diagnosis or alterations during medical treatment; screening and profiling of body fluids or tissues with special reference to metabolic disorders; results from basic medical research with direct consequences in clinical practice; drug level monitoring and pharmacokinetic studies; clinical toxicology; analytical studies in occupational medicine.

**Submission of Papers.** Manuscripts (in English; *four* copies are required) should be submitted to: Editorial Office of *Journal of Chromatography*, P.O. Box 681, 1000 AR Amsterdam, Netherlands, Telefax (+31-20) 5862 304, or to: The Editor of *Journal of Chromatography, Biomedical Applications*, P.O. Box 681, 1000 AR Amsterdam, Netherlands. Review articles are invited or proposed by letter to the Editors. An outline of the proposed review should first be forwarded to the Editors for preliminary discussion prior to preparation. Submission of an article is understood to imply that the article is original and unpublished and is not being considered for publication elsewhere. For copyright regulations, see below.

**Publication.** The *Journal of Chromatography* (incl. *Biomedical Applications*) has 39 volumes in 1992. The subscription prices for 1992 are:

*J. Chromatogr.* (incl. *Cum. Indexes, Vols. 551-600*) + *Biomed. Appl.* (Vols. 573-611):  
Dfl. 7722.00 plus Dfl. 1209.00 (p.p.h.) (total ca. US\$ 4880.25)

*J. Chromatogr.* (incl. *Cum. Indexes, Vols. 551-600*) only (Vols. 585-611):  
Dfl. 6210.00 plus Dfl. 837.00 (p.p.h.) (total ca. US\$ 3850.75)

*Biomed. Appl.* only (Vols. 573-584):

Dfl. 2760.00 plus Dfl. 372.00 (p.p.h.) (total ca. US\$ 1711.50).

**Subscription Orders.** The Dutch guilder price is definitive. The US\$ price is subject to exchange-rate fluctuations and is given as a guide. Subscriptions are accepted on a prepaid basis only, unless different terms have been previously agreed upon. Subscriptions orders can be entered only by calendar year (Jan.-Dec.) and should be sent to Elsevier Science Publishers, Journal Department, P.O. Box 211, 1000 AE Amsterdam, Netherlands, Tel. (+31-20) 5803 642, Telefax (+31-20) 5803 598, or to your usual subscription agent. Postage and handling charges include surface delivery except to the following countries where air delivery via SAL (Surface Air Lift) mail is ensured: Argentina, Australia, Brazil, Canada, China, Hong Kong, India, Israel, Japan\*, Malaysia, Mexico, New Zealand, Pakistan, Singapore, South Africa, South Korea, Taiwan, Thailand, USA. \*For Japan air delivery (SAL) requires 25% additional charge of the normal postage and handling charge. For all other countries airmail rates are available upon request. Claims for missing issues must be made within three months of our publication (mailing) date, otherwise such claims cannot be honoured free of charge. Back volumes of the *Journal of Chromatography* (Vols. 1-572) are available at Dfl. 217.00 (plus postage). Customers in the USA and Canada wishing information on this and other Elsevier journals, please contact Journal Information Center, Elsevier Science Publishing Co. Inc., 655 Avenue of the Americas, New York, NY 10010, USA, Tel. (+1-212) 633 3750, Telefax (+1-212) 633 3990.

**Abstracts/Contents Lists** published in Analytical Abstracts, Biochemical Abstracts, Biological Abstracts, Chemical Abstracts, Chemical Titles, Chromatography Abstracts, Clinical Chemistry Lookout, Current Contents/Life Sciences, Current Contents/Physical, Chemical & Earth Sciences, Deep-Sea Research/Part B: Oceanographic Literature Review, Excerpta Medica, Index Medicus, Mass Spectrometry Bulletin, PASCAL-CNRS, Pharmaceutical Abstracts, Referativnyi Zhurnal, Research Alert, Science Citation Index and Trends in Biotechnology.

**See inside back cover** for Publication Schedule, Information for Authors and information on Advertisements.

© ELSEVIER SCIENCE PUBLISHERS B.V. — 1992

0021-9673/92/\$05.00

All rights reserved. No part of this publication may be reproduced, stored in a retrieval system or transmitted in any form or by any means, electronic, mechanical, photocopying, recording or otherwise, without the prior written permission of the publisher, Elsevier Science Publishers B.V., Copyright and Permissions Department, P.O. Box 521, 1000 AM Amsterdam, Netherlands.

Upon acceptance of an article by the journal, the author(s) will be asked to transfer copyright of the article to the publisher. The transfer will ensure the widest possible dissemination of information.

Submission of an article for publication entails the authors' irrevocable and exclusive authorization of the publisher to collect any sums or considerations for copying or reproduction payable by third parties (as mentioned in article 17 paragraph 2 of the Dutch Copyright Act of 1912 and the Royal Decree of June 20, 1974 (S. 351) pursuant to article 16 b of the Dutch Copyright Act of 1912) and/or to act in or out of Court in connection therewith.

**Special regulations for readers in the USA.** This journal has been registered with the Copyright Clearance Center, Inc. Consent is given for copying of articles for personal or internal use, or for the personal use of specific clients. This consent is given on the condition that the copier pays through the Center the per-copy fee stated in the code on the first page of each article for copying beyond that permitted by Sections 107 or 108 of the US Copyright Law. The appropriate fee should be forwarded with a copy of the first page of the article to the Copyright Clearance Center, Inc., 27 Congress Street, Salem, MA 01970, USA. If no code appears in an article, the author has not given broad consent to copy and permission to copy must be obtained directly from the author. All articles published prior to 1980 may be copied for a per-copy fee of US\$ 2.25, also payable through the Center. This consent does not extend to other kinds of copying, such as for general distribution, resale, advertising and promotion purposes, or for creating new collective works. Special written permission must be obtained from the publisher for such copying.

No responsibility is assumed by the Publisher for any injury and/or damage to persons or property as a matter of products liability, negligence or otherwise, or from any use or operation of any methods, products, instructions or ideas contained in the materials herein. Because of rapid advances in the medical sciences, the Publisher recommends that independent verification of diagnoses and drug dosages should be made.

Although all advertising material is expected to conform to ethical (medical) standards, inclusion in this publication does not constitute a guarantee or endorsement of the quality or value of such product or of the claims made of it by its manufacturer.

This issue is printed on acid-free paper.

Printed in the Netherlands

JOURNAL OF CHROMATOGRAPHY

VOL. 593 (1992)





# JOURNAL of CHROMATOGRAPHY

INCLUDING ELECTROPHORESIS AND OTHER SEPARATION METHODS

## SYMPOSIUM VOLUMES

### EDITORS

E. HEFTMANN (Orinda, CA), Z. DEYL (Prague)

### EDITORIAL BOARD

E. Bayer (Tübingen), S. R. Binder (Hercules, CA), S. C. Churms (Rondebosch), J. C. Fetzer (Richmond, CA), E. Gelpí (Barcelona), K. M. Gooding (Lafayette, IN), S. Hara (Tokyo), P. Helboe (Brønshøj), W. Lindner (Graz), T. M. Phillips (Washington, DC), S. Terabe (Hyogo), H. F. Walton (Boulder, CO), M. Wilchek (Rehovot)



ELSEVIER

AMSTERDAM — LONDON — NEW YORK — TOKYO

---

*J. Chromatogr.*, Vol. 593 (1992)

© 1992 ELSEVIER SCIENCE PUBLISHERS B.V. All rights reserved.

0021-9673/92/\$05.00

All rights reserved. No part of this publication may be reproduced, stored in a retrieval system or transmitted in any form or by any means, electronic, mechanical, photocopying, recording or otherwise, without the prior written permission of the publisher, Elsevier Science Publishers B.V., Copyright and Permissions Department, P.O. Box 521, 1000 AM Amsterdam, Netherlands.

Upon acceptance of an article by the journal, the author(s) will be asked to transfer copyright of the article to the publisher. The transfer will ensure the widest possible dissemination of information.

Submission of an article for publication entails the authors' irrevocable and exclusive authorization of the publisher to collect any sums or considerations for copying or reproduction payable by third parties (as mentioned in article 17 paragraph 2 of the Dutch Copyright Act of 1912 and the Royal Decree of June 20, 1974 (S. 351) pursuant to article 16 b of the Dutch Copyright Act of 1912) and/or to act in or out of Court in connection therewith.

**Special regulations for readers in the USA.** This journal has been registered with the Copyright Clearance Center, Inc. Consent is given for copying of articles for personal or internal use, or for the personal use of specific clients. This consent is given on the condition that the copier pays through the Center the per-copy fee stated in the code on the first page of each article for copying beyond that permitted by Sections 107 or 108 of the US Copyright Law. The appropriate fee should be forwarded with a copy of the first page of the article to the Copyright Clearance Center, Inc., 27 Congress Street, Salem, MA 01970, USA. If no code appears in an article, the author has not given broad consent to copy and permission to copy must be obtained directly from the author. All articles published prior to 1980 may be copied for a per-copy fee of US\$ 2.25, also payable through the Center. This consent does not extend to other kinds of copying, such as for general distribution, resale, advertising and promotion purposes, or for creating new collective works. Special written permission must be obtained from the publisher for such copying.

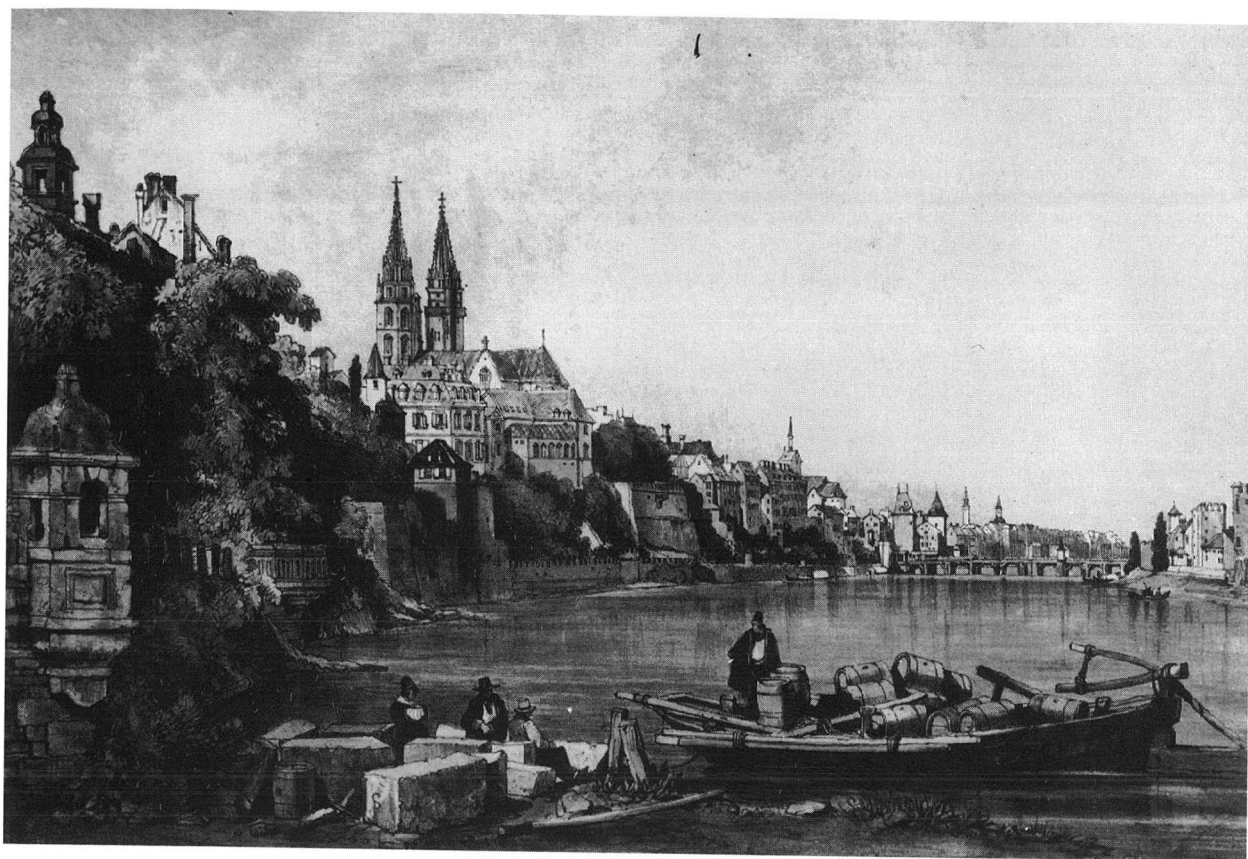
No responsibility is assumed by the Publisher for any injury and/or damage to persons or property as a matter of products liability, negligence or otherwise, or from any use or operation of any methods, products, instructions or ideas contained in the materials herein. Because of rapid advances in the medical sciences, the Publisher recommends that independent verification of diagnoses and drug dosages should be made.

Although all advertising material is expected to conform to ethical (medical) standards, inclusion in this publication does not constitute a guarantee or endorsement of the quality or value of such product or of the claims made of it by its manufacturer.

This issue is printed on acid-free paper.

Printed in the Netherlands

SYMPOSIUM VOLUME



**15TH INTERNATIONAL SYMPOSIUM  
ON  
COLUMN LIQUID CHROMATOGRAPHY**

**PART II**

*Basel (Switzerland), June 3–7, 1991*

*Guest Editor*

**F. ERNI**  
(Basel)

The proceedings of the *15th International Symposium on Column Liquid Chromatography, Basel, June 3–7, 1991*, are published in two consecutive volumes of the *Journal of Chromatography*: Vols.

592 and 593 (1992). The Foreword to the proceedings only appears in Vol. 592. A combined Author Index to both Vols. 592 and 593 only appears in Vol. 593.



## CONTENTS

## 15TH INTERNATIONAL SYMPOSIUM ON COLUMN LIQUID CHROMATOGRAPHY, BASEL, JUNE 3-7, 1991, PART II

COLUMN LIQUID CHROMATOGRAPHY (*Continued*)*Applications: pharmacological*

Assessment of the biotransformation of the cardiotonic agent piroximone by high-performance liquid chromatography and gas chromatography-mass spectrometry by M. Berg-Candolfi, J. T. Borlakoglu, B. Dulery, F. Jehl and K. D. Haegele (Strasbourg, France)	1
Determination of amphetamines by high-performance liquid chromatography with ultraviolet detection. On-line pre-column derivatization with 9-fluorenylmethyl chloroformate and preconcentration by G. Maeder, M. Pelletier and W. Haerdi (Geneva, Switzerland)	9
High-performance liquid chromatographic determination of penicillin G, penicillin V and cloxacillin in beef and pork tissues by W. A. Moats (Beltsville, MD, USA)	15
Automated high-performance liquid chromatographic method for the determination of rifampicin in plasma by K. J. Swart and M. Paggis (Bloemfontein, South Africa)	21
High-performance liquid chromatographic analysis of FCE 24304 (6-methylenandrosta-1,4-diene-3,17-dione) and FCE 24928 (4-aminoandrosta-1,4,6-triene-3,17-dione), two new aromatase inhibitors by S. Del Nero, M. Di Somma and A. Vigevani (Milan, Italy)	25
High-performance liquid chromatographic determination of monohydroxy compounds by a combination of pre-column derivatization and post-column reaction detection by V. K. Boppana, R. C. Simpson, K. Anderson, C. Miller-Stein, T. J. A. Blake, B. Y.-H. Hwang and G. R. Rhodes (King of Prussia, PA, USA)	29
Direct high-performance liquid chromatographic resolution of a novel benzothiazine $\text{Ca}^{2+}$ antagonist and related compounds by A. Ota, S. Ito and Y. Kawashima (Osaka, Japan)	37
Simple reversed-phase high-performance liquid chromatographic method for 13- <i>cis</i> -retinoic acid in serum by R. R. Gadde and F. W. Burton (Buffalo, NY, USA)	41
Stability studies with a high-performance liquid chromatographic method for the determination of a new anthracycline analogue, 3'-deamino-3'-[2-( <i>S</i> )-methoxy-4-morpholino]doxorubicin (FCE 23762), in the final drug formulation by M. L. Rossini and M. Farina (Milan, Italy)	47
Use of direct injection precolumn techniques for the high-performance liquid chromatographic determination of the retinoids acitretin and 13- <i>cis</i> -acitretin in plasma by R. Wyss and F. Bucheli (Basle, Switzerland)	55
Determination of the catechol-O-methyltransferase inhibitor Ro 40-7592 in human plasma by high-performance liquid chromatography with coulometric detection by U. Timm and R. Erdin (Basle, Switzerland)	63
High-performance liquid chromatography method for the determination of aminoglycosides based on automated pre-column derivatization with <i>o</i> -phthalaldehyde by M. C. Caturla and E. Cusido (Barcelona, Spain) and D. Westerlund (Uppsala, Sweden)	69
Determination of Zy 17617B in plasma by solid-phase extraction and liquid chromatography with automated pre-column exchange by C. Chollet and M. Salanon (Nyon, Switzerland)	73
Determination of ( <i>S</i> )-(-)-cathinone and its metabolites ( <i>R,S</i> )-(-)-norephedrine and ( <i>R,R</i> )-(-)-norpseudoephedrine in urine by high-performance liquid chromatography with photodiode-array detection by K. Mathys and R. Brenneisen (Berne, Switzerland)	79
Determination of psychotropic phenylalkylamine derivatives in biological matrices by high-performance liquid chromatography with photodiode-array detection by H.-J. Helmlin and R. Brenneisen (Berne, Switzerland)	87

High-performance liquid chromatographic determination of $\alpha$ -tocopheryl nicotinate in cosmetic preparations by A. Baruffini, E. De Lorenzi, C. Gandini, M. Kitsos and G. Massolini (Pavia, Italy) . . . . .	95
<i>Applications: proteins and their constituents</i>	
Rapid determination of amino acids by high-performance liquid chromatography: release of amino acids by perfused rat liver ( <i>Short Communication</i> ) by F. Zezza, J. Kerner, M. R. Pascale, R. Giannini and E. A. Martelli (Rome, Italy) . . . . .	99
High-performance liquid chromatography of amino acids, peptides and proteins. CXV. Thermodynamic behaviour of peptides in reversed-phase chromatography by A. W. Purcell, M. I. Aguilar and M. T. W. Hearn (Clayton, Australia) . . . . .	103
Direct determination of kallikrein by high-performance liquid chromatography by G. Raspi, A. Lo Moro and M. Spinetti (Pisa, Italy) . . . . .	119
Isolation and characterization of $\alpha$ -glucosidase from <i>Aspergillus niger</i> by K. Břizová, B. Králová, K. Demnerová and I. Vinš (Prague, Czechoslovakia) . . . . .	125
<i>Applications: other biological applications</i>	
Reversed-phase high-performance liquid chromatography–thermospray mass spectrometry of radiation-induced decomposition products of thymine and thymidine by M. Berger and J. Cadet (Grenoble, France) and R. Berube, R. Langlois and J. E. van Lier (Québec, Canada) . . . . .	133
Improved determination of individual molecular species of phosphatidylcholine in biological samples by high-performance liquid chromatography with internal standards by A. Cantafora and R. Masella (Rome, Italy) . . . . .	139
Determination of benzene metabolites in urine of mice by solid-phase extraction and high-performance liquid chromatography by H. Schad, F. Schäfer, L. Weber and H. J. Seidel (Ulm, Germany) . . . . .	147
Determination of 5-hydroxymethylfurfural by ion-exclusion chromatography with UV detection ( <i>Short Communication</i> ) by H.-J. Kim and M. Richardson (Natick, MA, USA) . . . . .	153
Determination of inositol polyphosphates from human T-lymphocyte cell lines by anion-exchange high-performance liquid chromatography and post-column derivatization by A. H. Guse and F. Emmrich (Erlangen, Germany) . . . . .	157
Separation of flavonol-2-O-glycosides from <i>Calendula officinalis</i> and <i>Sambucus nigra</i> by high-performance liquid and micellar electrokinetic capillary chromatography by P. Pietta, A. Bruno and P. Mauri (Milan, Italy) and A. Rava (Pavia, Italy) . . . . .	165
High-performance liquid chromatographic method with fluorescence detection for the determination of total homocyst(e)ine in plasma by I. Fermo, C. Arcelloni, E. De Vecchi, S. Vigano' and R. Paroni (Milan, Italy) . . . . .	171
High-performance liquid chromatographic analysis of the pigments of blood-red prickly pear ( <i>Opuntia ficus indica</i> ) by E. Forni, A. Polesello, D. Montefiori and A. Maestrelli (Milan, Italy) . . . . .	177
Determination of catecholamines in urine by liquid chromatography and electrochemical detection after on-line sample purification on immobilized boronic acid by B.-M. Eriksson and M. Wikström (Mölnådal, Sweden) . . . . .	185
Determination of cinnamic acid and paeoniflorin in traditional chinese medicinal preparations by high-performance liquid chromatography by K.-C. Wen, C.-Y. Huang and F.-S. Liu (Taipei, Taiwan) . . . . .	191
Analysis and isolation of indole alkaloids of fungi by high-performance liquid chromatography by M. Wurst, R. Kysilka and T. Koza (Prague, Czechoslovakia) . . . . .	201
Use of high-performance liquid chromatographic peak deconvolution and peak labelling to identify antiparasitic components in plant extracts by N. Perez-Souto (Havana, Cuba) and R. J. Lynch, G. Measures and J. T. Hann (Cambridge, UK) . . . . .	209
Improved high-performance liquid chromatographic method for the determination of coenzyme Q <sub>10</sub> in plasma by G. Grossi, A. M. Bargossi, P. L. Fiorella and S. Piazzi (Bologna, Italy), M. Battino (Ancona, Italy) and G. P. Bianchi (Bologna, Italy) . . . . .	217

*Applications: miscellaneous*

- Reversed-phase high-performance liquid chromatography of anionic and ethoxylated non-ionic surfactants and pesticides in liquid pesticide formulations  
by T. Bán (Budapest, Hungary) and E. Papp and J. Inczédy (Veszprém, Hungary) . . . . . 227
- Analysis of block copolymers by high-performance liquid chromatography under critical conditions  
by T. M. Zimina, J. J. Kever and E. Yu. Melenevskaya (St. Petersburg, USSR) and A. F. Fell (Bradford, UK) . . . . . 233
- Comparison of several methods for the determination of trace amounts of polar aliphatic monocarboxylic acids by high-performance liquid chromatography  
by A. J. J. M. Coenen, M. J. G. Kerkhoff, R. M. Heringa and S. van der Wal (Geleen, Netherlands) . . . . . 243

## ELECTROPHORESIS AND ELECTROKINETIC CHROMATOGRAPHY

- Planar chips technology for miniaturization and integration of separation techniques into monitoring systems. Capillary electrophoresis on a chip  
by A. Manz, D. J. Harrison, E. M. J. Verpoorte, J. C. Fettingier, A. Paulus, H. Lüdi and H. M. Widmer (Basle, Switzerland) . . . . . 253
- Separation of leucinoatins by capillary zone electrophoresis  
by M. G. Quaglia, S. Fanali and A. Nardi (Rome, Italy) and C. Rossi and M. Ricci (Perugia, Italy) . . . . . 259
- Separation of naphthalene-2,3-dicarboxaldehyde-labeled amino acids by high-performance capillary electrophoresis with laser-induced fluorescence detection  
by T. Ueda, R. Mitchell, F. Kitamura, T. Metcalf and T. Kuwana (Lawrence, KS, USA) and A. Nakamoto (Kyoto, Japan) . . . . . 265
- Determination of substituted purines by body fluids by micellar electrokinetic capillary chromatography with direct sample injection  
by W. Thormann, A. Minger, S. Molteni, J. Caslavská and P. Gebauer (Bern, Switzerland) . . . . . 275
- Factors affecting the separation of inorganic metal cations by capillary electrophoresis  
by A. Weston and P. R. Brown (Kingston, RI, USA) and P. Jandik, W. R. Jones and A. L. Heckenberg (Milford, MA, USA) . . . . . 289
- Prediction of migration behavior of oligonucleotides in capillary gel electrophoresis  
by A. Guttman, R. J. Nelson and N. Cooke (Palo Alto, CA, USA) . . . . . 297
- Capillary electrophoresis with electrochemical detection employing an on-column Nafion joint  
by T. J. O'Shea, R. D. Greenhagen, S. M. Lunte and C. E. Lunte (Lawrence, KS, USA), M. R. Smyth (Dublin, Ireland), D. M. Radzik (Kansas City, MO, USA) and N. Watanabe (Tokyo, Japan) . . . . . 305
- Electrokinetic reversed-phase chromatography with packed capillaries  
by H. Yamamoto, J. Baumann and F. Erni (Basle, Switzerland) . . . . . 313

## OTHER SEPARATION METHODS

- Analytical study of heavy crude oil fractions by coupling of the transalkylation reaction with supercritical fluid chromatography  
by P.-L. Desbène and A. Abderrezag (Evreux, France) and B. Desmazières (Paris, France) . . . . . 321
- Retention behaviour of closely related coumarins in thin-layer chromatographic preassays for high-performance liquid chromatography according to the "PRISMA" model  
by P. Härmälä, H. Vuorela, E.-L. Rahko and R. Hiltunen (Helsinki, Finland) . . . . . 329
- Asymmetric-channel flow field-flow fractionation with exponential force-field programming  
by J. J. Kirkland, C. H. Dilks, Jr., S. W. Rementer and W. W. Yau (Wilmington, DE, USA) . . . . . 339
- Simple solution of velocity profiles of laminar flows in channels of various cross-sections used in field-flow fractionation  
by J. Pazourek and J. Chmelik (Brno, Czechoslovakia) . . . . . 357
- Separation of pristnamycins by high-speed counter-current chromatography. I. Selection of solvent system and preliminary preparative studies  
by S. Drogue, M.-C. Rolet, D. Thiébaud and R. Rosset (Paris, France) . . . . . 363
- Author Index Vols. 592 and 593* . . . . . 373

\*\*\*\*\*  
\* In articles with more than one author, the name of the author to whom correspondence should be addressed is indicated \*  
\* in the article heading by a 6-pointed asterisk (\*). \*  
\*\*\*\*\*





# Assessment of the biotransformation of the cardiotonic agent piroximone by high-performance liquid chromatography and gas chromatography–mass spectrometry

Martine Berg-Candolfi, Jürgen T. Borlakoglu and Bertrand Dulery

*Departments of Clinical Biochemistry and Drug Metabolism, Marion Merrell Dow, 16 Rue d'Ankara, B.P. 447 R/9, 67009 Strasbourg Cédex (France)*

François Jehl

*Institute of Bacteriology, Faculty of Medicine, University Louis Pasteur, Strasbourg (France)*

Klaus D. Haegele\*

*Departments of Clinical Biochemistry and Drug Metabolism, Marion Merrell Dow, 16 Rue d'Ankara, B.P. 447 R/9, 67009 Strasbourg Cédex (France)*

---

## ABSTRACT

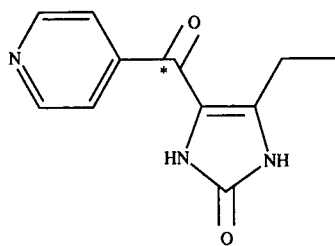
<sup>14</sup>C-labelled piroximone was administered to rats at a dose of 10 mg/kg body weight. Of the total radioactivity administered,  $74.9 \pm 7.9\%$  ( $n=4$ ) and  $87.8 \pm 1.7\%$  ( $n=3$ ) were recovered in the 8-h urine collection after oral and intravenous administration, respectively. Two major metabolites,  $M_1$  and  $M_2$ , were detected in methanol extracts and accounted for  $7.1 \pm 1.2\%$  ( $n=4$ ) ( $M_1$ ) and  $4.3 \pm 0.4\%$  ( $n=4$ ) ( $M_2$ ) in response to oral administration and  $5.7 \pm 0.8\%$  ( $n=3$ ) ( $M_1$ ) and  $6.7 \pm 2.0\%$  ( $n=3$ ) ( $M_2$ ) in response to intravenous administration. In addition, three minor metabolites were detected;  $M_3$  and  $M_4$  in the 8-h urine collection and  $M_5$  in the 12-h urine collection. Separation of piroximone and metabolites was achieved by high-performance liquid chromatography on a  $C_{18}$  column by gradient elution with 0.05 M ammonium acetate (pH 7) using 0–60% methanol over 20 min at a flow-rate of 1 ml/min, followed by isocratic elution with 60% methanol for 10 min.  $M_1$  and  $M_2$  were isolated by fraction collection following the addition of 1 mM tetrabutylammonium acetate in the mobile phase. Between each injection a column re-equilibration time of 45 min was necessary to achieve optimum collection of  $M_1$  and  $M_2$  fractions. Gas chromatography–mass spectrometry of  $M_1$  provided evidence for a molecular structure consistent with isonicotinic acid methyl ester. Corroborative evidence for this identification was obtained by comparison with a synthetic standard. Isonicotinic acid is assumed to be the actual metabolite while esterification with methanol had occurred as a result of the work-up procedure. *In vitro* studies carried out with rat liver microsomes resulted in a mean total metabolite formation rate of 94.3 pmol/mg microsomal protein/min.

---

## INTRODUCTION

Piroximone [4-ethyl-1,3-dihydro-5(4-pyridinyl-carbonyl)-2H-imidazol-2-one; MDL 19205] (Fig. 1), is a cardiotonic agent with positive inotropic properties [1–3]. It is a specific inhibitor of a high-affinity cAMP phosphodiesterase type III [4] and is

being developed for the treatment of congestive heart failure [5]. The pharmacokinetics of piroximone in healthy volunteers and patients with congestive heart failure have been reported previously [6]; however, its metabolism and the unequivocal identification of metabolites remained to be evaluated.

\*  $^{14}\text{C}$ Fig. 1. Structure of piroximone and  $^{14}\text{C}$ -label position.

The present report presents results on the separation and tentative identification of *in vivo* and *in vitro* biotransformation products of piroximone.

## EXPERIMENTAL

### Reagents and chemicals

Unlabelled piroximone was provided as ampoules containing 1.5 mg/ml in physiological saline (total volume 20 ml) and was packed by the Marion Merrell Dow Research Institute (Winnersh, UK).  $^{14}\text{C}$ -labelled piroximone with a specific activity of 17.4 Ci/mol was synthesized by Dr. Eugene R. Wagner (Marion Merrell Dow Research Institute, Indianapolis, IN, USA). The position of the radio-labelled carbon atom is shown in Fig. 1. Hydroxy-piroximone (MDL 20770) was obtained from Marion Merrell Dow Research Institute (Cincinnati, OH, USA), isonicotinic acid and ammonium acetate were purchased from Sigma (St. Louis, MO, USA), methanol (spectroscopic grade) from Merck (Darmstadt, Germany) and tetrabutylammonium acetate from Aldrich (Milwaukee, WI, USA).

### *In vivo* metabolic study

Adult male Sprague-Dawley rats with an average body weight of 200 g were obtained from Charles River (Cl  on, France). They were fasted and acclimatized to metabolic cages 16 h before dosing and subsequent collection of urine and faeces.

Each rat received a single dose of 10 mg/kg body weight of piroximone (*i.e.*, 46  $\mu\text{mol/kg}$ ) containing 100  $\mu\text{Ci}$  of  $^{14}\text{C}$ -labelled piroximone in a 0.9% NaCl isotonic saline solution. The dose solution was administered alternatively by gastric intubation or intravenously into a tail vein. The volume infused did not exceed 1.3 ml. Food and water were given *ad*

*libitum*. Urine and faeces were collected over 48 h at time intervals of 0–8, 8–12, 12–24 and 24–48 h. All samples were stored at  $-20^\circ\text{C}$  prior to analysis.

### *In vitro* metabolic study

**Induction *in vivo* of drug metabolizing enzymes.** Adult female Sprague-Dawley rats ( $n = 3$ ) with an average body weight of 200 g were treated at 10 a.m. with a single intraperitoneal injection of 600  $\mu\text{mol/kg}$  body weight of Aroclor 1254 dissolved in corn oil and were killed 5 days later. Aroclor 1254 is a mixture of polychlorinated biphenyls (PCBs). The latter induce distinctively isoforms of cytochrome P-450 dependent monooxygenases, as detailed previously [7].

**Preparation of hepatic microsomes.** Control and treated rats were killed and the livers were weighed and washed free of superficial blood, cooled to  $4^\circ\text{C}$  and used within 1 h. All of the operations described below were performed at  $4^\circ\text{C}$ .

The liver was finely chopped with scissors and homogenized for 2 min in an MSE homogeniser with 0.15 M KCl (3 ml/g wet weight of liver). The homogenate was then centrifuged at 11 000  $g_{av}$  for 30 min using an  $8 \times 50$  or an  $8 \times 14$  ml titanium angle-head rotor in an MSE 3 PrepSpin 50 or a Sorvall OTD 50B ultracentrifuge. The supernatant was centrifuged at 104 000  $g_{av}$  for 60 min and the microsomal pellet resuspended in 0.15 M KCl using a Potter-Elvehjem glass-Teflon homogenizer. The microsomal suspension was then washed by recentrifugation at 104 000  $g_{av}$  for a further 30–60 min and the pellet was resuspended in 0.25 M sucrose–20 mM Tris buffer–5 mM EDTA (pH 7.4) at a final concentration of *ca.* 20 mg protein/ml [9].

***In vitro* metabolic assay.** Hepatic microsomes that were isolated from control and treated rats were incubated with 0.55  $\mu\text{mol}$  of piroximone containing 2.2  $\mu\text{Ci}$  of  $^{14}\text{C}$ -labelled piroximone by adjusting the microsomal protein concentration to *ca.* 10 mg (equivalent to 0.5 g of liver) per flask. The incubations were carried out in a shaking water-bath at  $37^\circ\text{C}$  for 20 or 40 min with a buffer system containing 1.8 mmol of Tris buffer (pH 7.4), 0.6 mmol of  $\text{MgCl}_2$ , 2.2 mmol of nicotinamide and 0.2 ml of an NADPH-generating system consisting of 21.2  $\mu\text{mol}$  of glucose-6-phosphate, 4.6  $\mu\text{mol}$  of  $\text{NADP}^+$  and 1.6 I.U. of glucose-6-phosphate dehydrogenase (E.C. 1.1.1.49). The enzymatic reactions were stop-

ped by protein precipitation with 40% trichloroacetic acid (Merck) [8].

#### *Sample treatment*

Radioactivity was measured by liquid scintillation using an LS 5000 CE counter (Beckman, San Ramon, CA, USA) and Aquasol-2 (Dupont de Nemours, France). Urine samples and liver supernatant samples were added to the scintillator directly. Radioactivity in faecal samples was measured after treatment with Lumasolve (Lumac, Landgraaf, Netherlands) according to the manufacturer's recommendations.

Piroximone and metabolites were extracted from urine samples with the addition of methanol, followed by centrifugation at 10 500 *g* for about 10 min (Zentrifuge 3200, Eppendorf, Hamburg, Germany); the supernatant contained >99% of radioactivity. A similar recovery was obtained with other biological samples.

#### *High-performance liquid chromatography (HPLC)*

The chromatograph consisted of a WISP Model 710 B automatic sample injector (Waters, Milford, MA USA), two pumps (Waters Model 6000), a gradient programmer (Waters Model 660), a Waters Model 450 variable-wavelength UV detector and a Flo-one HP-HS radioactivity detector (Radiomatic, Tampa, FL, USA). Quickszint Flow 302 (Zinsser Analytic, Maidenhead, UK) was used as the scintillator at a flow-rate of 4 ml/min using a liquid cell with a volume of 1.6 ml. Samples were separated on an IP-Ultrasphere C<sub>18</sub> (5- $\mu$ m particles size) column (25 cm  $\times$  4.6 mm I.D.) (Beckman, San Ramon, CA, USA) that was connected with a Waters  $\mu$ Bondapack C<sub>18</sub> guard column.

UV detection of piroximone and metabolites was carried out at 230 nm [9]. The separation of piroximone and metabolites was achieved using a combination of gradient and isocratic elution as follows: the two major metabolites (M<sub>1</sub> and M<sub>2</sub>) were eluted by concave gradient elution (curve type 9) using 0.05 *M* ammonium acetate (pH 7) and 0–60% methanol over a period of 20 min at a flow-rate of 1 ml/min followed by an isocratic elution of the two minor metabolites (M<sub>3</sub> and M<sub>4</sub>) and of piroximone with 60% methanol for a period of 10 min.

The HPLC conditions were optimized by an addition of 1 mM tetrabutylammonium acetate (TBA)

to the mobile phase to increase the retention times of M<sub>1</sub> and M<sub>2</sub>. They were isolated automatically with a FOXY fraction collector (Roucaire, Lincoln, NE, USA). TBA was removed from the fractions by cation-exchange chromatography using a Dowex 50W-X8 resin (Bio-Rad Labs, Richmond, CA, USA). The resin was conditioned prior to use as described previously [10]. A 0.5-ml volume of resin suspended in water was used to elute M<sub>1</sub> and M<sub>2</sub> using 4.5 and 5.5 ml of 0.2 *M* NaCl, respectively. The purified M<sub>1</sub> and M<sub>2</sub> fractions were lyophilized and concentrated in methanol. Sodium chloride was removed by sedimentation at 10 500 *g* for 10 min.

#### *Gas chromatography–mass spectrometry (GC–MS)*

Mass spectrometric analysis was carried out with QMD 1000 GC–MS system (Erba Sciences, Massy, France). The chromatographic column was a 5% phenylmethylsilicone fused-silica capillary column (12.5 m  $\times$  0.32 mm I.D.) with a film thickness of 0.52  $\mu$ m (Hewlett Packard, les Ulis, France).

The column temperature was kept at 70°C for 1 min and then programmed to 280°C at 35°C/min. The pressure of the injector head was set at 70 kPa. Injection was carried out in the splitless mode and the injector port was kept at 250°C. The interface of chromatograph and mass spectrometer was maintained at 250°C and the ion source temperature was set at 180°C.

Mass spectra were obtained in the positive-ion chemical ionization (PCI) mode with an electron energy of 70 eV and a filament current of 300  $\mu$ A. Ammonia was used as the reagent gas. The instrument was scanned over the mass range 90–600 a.m.u.

## RESULTS AND DISCUSSION

Of the total radioactivity administered, within 48 h after dosing,  $82.4 \pm 8.3\%$  ( $n = 4$ ) and  $92.2 \pm 2.5\%$  ( $n = 3$ ) were recovered in urine samples in response to oral and intravenous treatment, respectively. Approximately 2% of the total radioactivity was recovered in faeces. These results indicate the importance of renal excretion as compared with biliary excretion into the gut and subsequent elimination by faeces.

Of the total radioactivity administered orally,

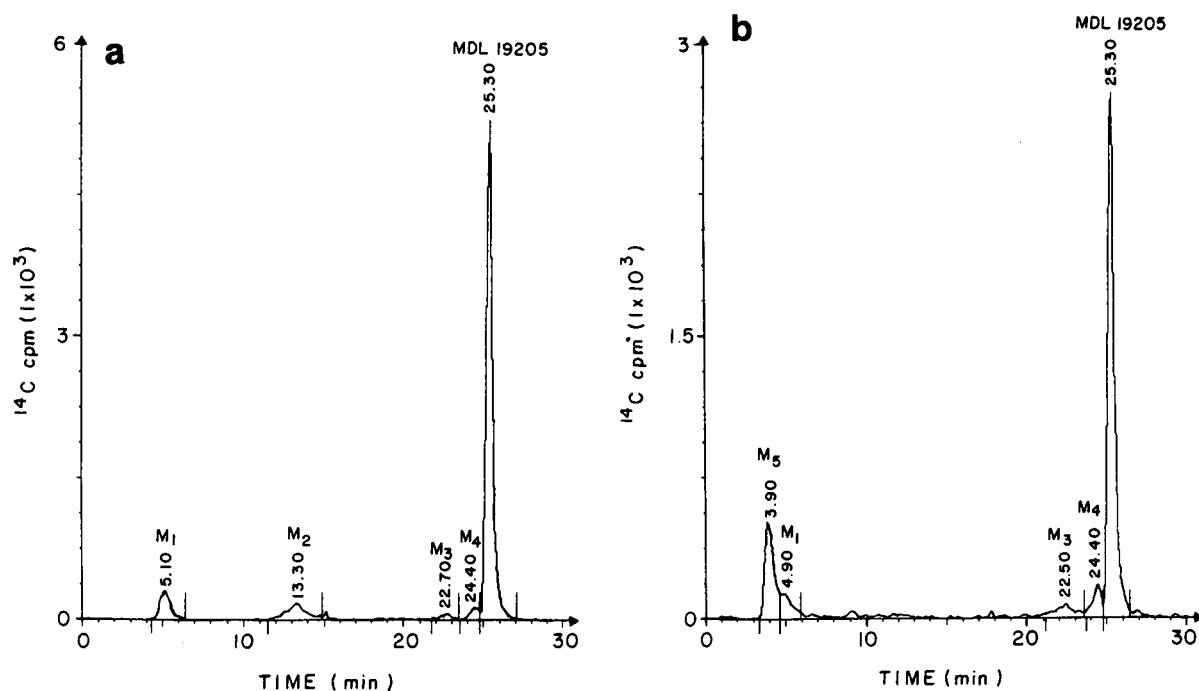


Fig. 2. HPLC of  $^{14}\text{C}$ -labelled piroximone and metabolites in a urinary extract: (a) 8 h post-treatment; (b) 12 h post-treatment.

$74.9 \pm 7.9\%$  ( $n = 4$ ) was recovered in the first 8 h of urine collection, which corresponds to a urinary excretion rate of  $34.5 \pm 3.6 \mu\text{mol/kg}$  body weight per 8 h. Two major (M<sub>1</sub> and M<sub>2</sub>) and two minor (M<sub>3</sub> and M<sub>4</sub>) metabolites were detected (Fig. 2a). M<sub>1</sub> and M<sub>2</sub> accounted for  $7.1 \pm 1.2\%$  ( $n = 4$ ) and

$4.3 \pm 0.4\%$  ( $n = 4$ ) (Fig. 3), thus implying urinary excretion rates of  $3.3 \pm 0.6$  and  $2.0 \pm 0.2 \mu\text{mol/kg}$  body weight per 8 h for M<sub>1</sub> and M<sub>2</sub>, respectively.

In contrast, of the total radioactivity administered intravenously,  $87.8 \pm 1.7\%$  ( $n = 3$ ) was recovered in the first 8 h of urine collection. This corre-

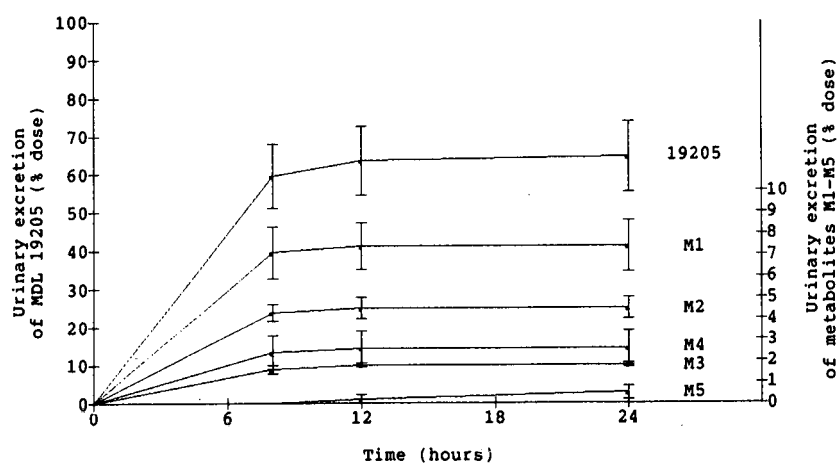


Fig. 3. Cumulative urinary excretion of MDL 19205 and metabolites after oral administration of  $^{14}\text{C}$ -labelled piroximone.



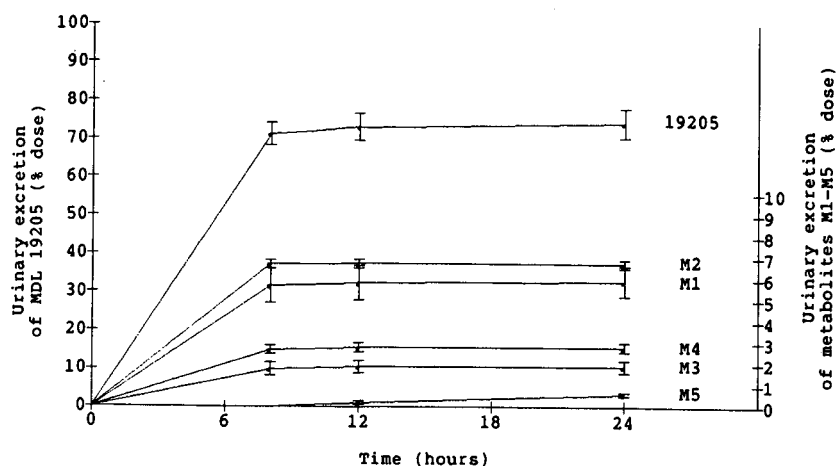


Fig. 4. Cumulative urinary excretion of MDL 19205 and metabolites after intravenous administration of  $^{14}\text{C}$ -labelled piroximone.

spends to a urinary excretion rate of  $40.4 \pm 0.8 \mu\text{mol/kg}$  body weight per 8 h. Two major ( $\text{M}_1$  and  $\text{M}_2$ ) and two minor ( $\text{M}_3$  and  $\text{M}_4$ ) metabolites were detected (Fig. 2a).  $\text{M}_1$  and  $\text{M}_2$  accounted for  $5.7 \pm 0.8\%$  ( $n = 3$ ) and  $6.7 \pm 2.0\%$  ( $n = 3$ ) (Fig. 4), thus implying urinary excretion rates of  $2.6 \pm 0.4$  and  $3.1 \pm 0.9 \mu\text{mol/kg}$  body weight per 8 h for  $\text{M}_1$  and  $\text{M}_2$ , respectively.

The urine analysis shows that piroximone and its metabolites were essentially excreted within the first 8 h following treatment. The ratio of metabolites  $\text{M}_1$  and  $\text{M}_2$  was 1.7 for oral administration and 0.9 for intravenous administration. This suggests increased formation of  $\text{M}_2$  following intravenous administration. The reasons for these differences due to alternate administration routes are unknown. A minor metabolite ( $\text{M}_5$ ) was detected in the 12-h urine collection (Fig. 2b). The cumulative urinary excretion of piroximone and its metabolites after oral administration is shown in Fig. 3 and after intravenous administration in Fig. 4.

When TBA was added to the mobile phase the retention times of  $\text{M}_1$  and  $\text{M}_2$  increased. TBA is a lipophilic positive counter ion which increases the retention time of the negative ions on a reversed-phase column [11,12]. With 1 mM TBA there is a relationship between the re-equilibration time of the column and the retention times of  $\text{M}_1$  and  $\text{M}_2$ . It was found that a column re-equilibration time of 45 min between sample injections resulted in optimum purity of the  $\text{M}_1$  and  $\text{M}_2$  fractions for sub-

sequent mass spectrometric analysis.

CI-MS of  $\text{M}_1$  yielded a molecular ion at  $m/z$  138, corresponding to the  $\text{MH}^+$  of isonicotinic acid methyl ester (Fig. 5a and b). In addition, the observed GC retention time of  $\text{M}_1$  and of a standard sample of isonicotinic acid methyl ester were identical (Fig. 6a and b), suggesting that the *in vivo* biotransformation of piroximone led to the formation

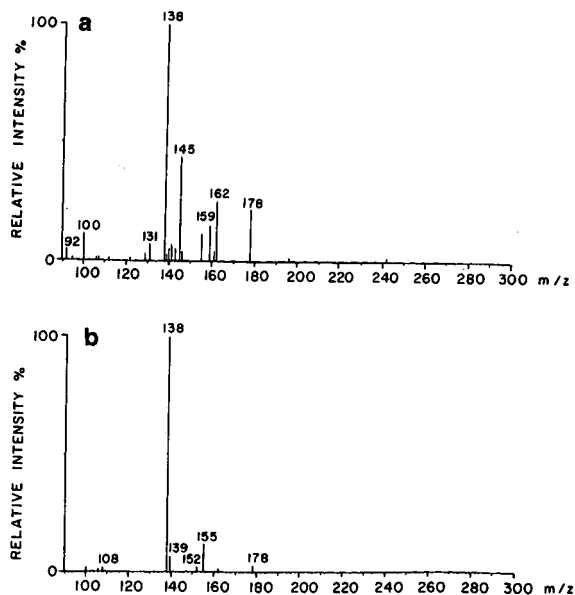


Fig. 5. PICI mass spectra of (a)  $\text{M}_1$  and (b) isonicotinic acid methyl ester.

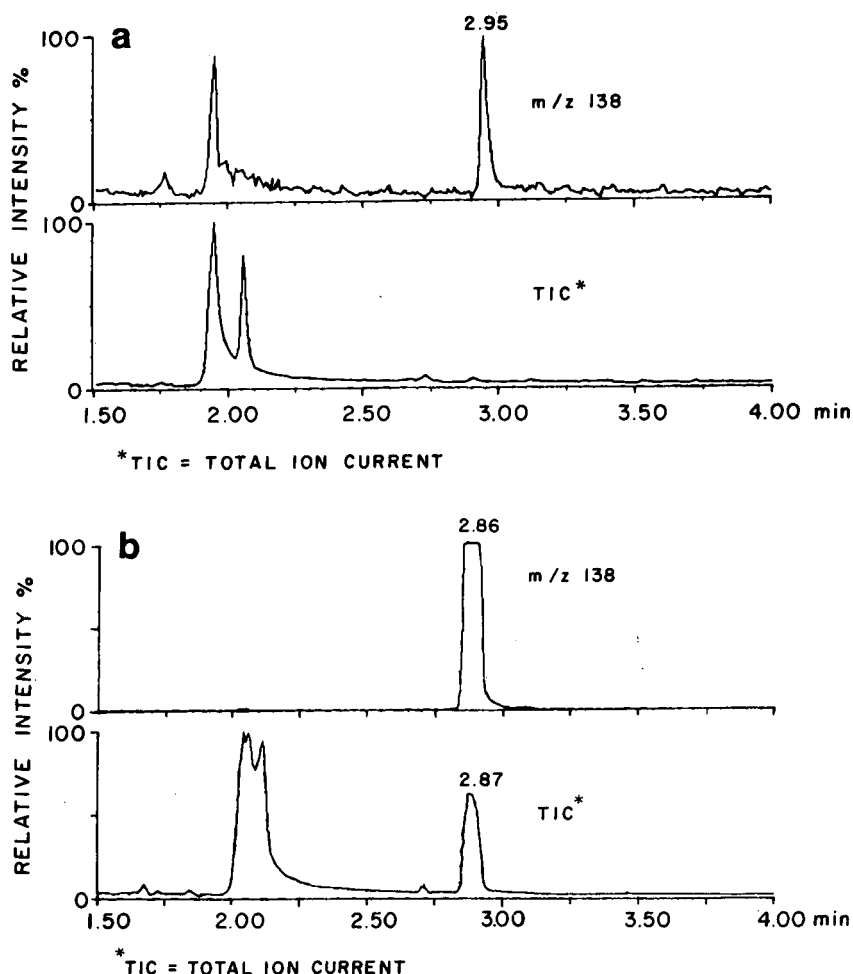


Fig. 6. Ion chromatograms (PICl) of (a)  $M_1$  and (b) isonicotinic acid methyl ester.

of isonicotinic acid. Moreover, isonicotinic acid is the only degradation product of piroximone under basic conditions [0.1 M NaOH (pH 13) at 60°C] and

was found to be the major degradation product in 1% hydrogen peroxide solution [10]. Isonicotinic acid methyl ester could, however, be the result of non-enzymatic methylation, probably owing to the work-up procedure with methanol.

*In vitro* metabolic studies of piroximone with rat hepatic microsomes resulted in a total metabolite formation of 94.3 pmol/mg microsomal protein/min (Table I). This represents an approximate mean rate of metabolism of 13.7  $\mu$ mol in the liver per 8 h, which compares favourably with the above-calculated urinary excretion rate. It is noteworthy that only  $M_1$  and  $M_4$  could be detected in *in vitro* incubations using hepatic microsomal membranes. Induction of hepatic cytochrome P-450-dependent

TABLE I  
METABOLISM WITH RAT LIVER MICROSOMES

	Microsomal protein (mg/g liver) <sup>a</sup>	Metabolite (pmol/ml microsomal protein/min) <sup>a</sup>	
		$M_1$	$M_4$
Control	22.9 $\pm$ 1.8	72.6 $\pm$ 13.7	21.7 $\pm$ 5.0
PCB	23.1 $\pm$ 1.1	74.4 $\pm$ 13.4	14.9 $\pm$ 1.1

<sup>a</sup> Mean  $\pm$  S.D. ( $n = 4$ ).

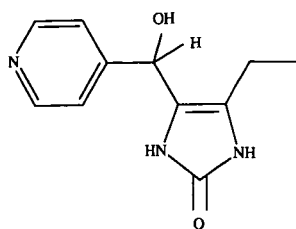


Fig. 7. Structure of hydroxypiroximone.

monooxygenases by treatment with Aroclor 1254 [9] did not increase the rate of  $M_1$  and  $M_4$  formation (89.3 pmol/mg microsomal protein/min) (Table I), and consequently induced isoforms of hepatic cytochrome P-450-dependent monooxygenases by PCB are not involved in the formation of  $M_1$  and  $M_4$ .

#### CONCLUSION

Piroximone is metabolized *in vivo* and *in vitro*. The *in vivo* biotransformation of piroximone resulted in the formation of two major metabolites ( $M_1$  and  $M_2$ ) representing approximately 15% of the administered dose.  $M_1$  was identified as isonicotinic acid.

Preliminary studies in dogs (data not shown) provided evidence for a large interspecies variation in the metabolism of piroximone. Unlike rats,  $M_4$  was found to be the major metabolite in dogs. This me-

tabolite co-chromatograms (UV detection) with the synthetic standard hydroxypiroximone (Fig. 7), thus providing evidence for interspecies variation in the metabolism of piroximone.

#### ACKNOWLEDGEMENT

We thank Muriel Rohfritsch for excellent secretarial assistance.

#### REFERENCES

- 1 R. A. Schnettler, R. C. Dage and J. M. Grisar, *J. Med. Chem.*, 25 (1982) 1477-1481.
- 2 R. C. Dage, L. E. Roebel, C. P. Hsieh and J. K. Woodward, *J. Cardiovasc. Pharmacol.*, 6 (1984) 35-42.
- 3 L. E. Roebel, R. C. Dage, C. P. Hsieh and J. K. Woodward, *J. Cardiovasc. Pharmacol.*, 6 (1984) 43-49.
- 4 T. Kariya, L. J. Wille and R. C. Dage, *J. Cardiovasc. Pharmacol.*, 6 (1984) 50-55.
- 5 K. Chatterjee, *Crit. Care Med.*, 18 (1990) S34-S38.
- 6 K. D. Haegeler, G. G. Belz, T. T. Meinicke and P. J. Schechter, *Eur. J. Clin. Pharmacol.*, 31 (1986) 239-242.
- 7 J. T. Borlakoglu, J. D. Edwards-Webb, R. R. Dils, J. P. G. Wilkins and L. W. Robertson, *FEBS Lett.*, 247 (1989) 327-329.
- 8 J. T. Borlakoglu, M. G. B. Drew, J. P. G. Wilkins and R. R. Dils, *Biochim. Biophys. Acta*, 1036 (1990) 167-175.
- 9 T. M. Chen, J. E. Coutant, A. D. Sill and R. R. Fike, *J. Chromatogr.*, 396 (1987) 382-388.
- 10 Y. Kakimoto and M. D. Armstrong, *J. Biol. Chem.*, 237 (1962) 208-214.
- 11 R. Gloor, and E. L. Johnson, *J. Chromatogr. Sci.*, 15 (1977) 413-423.
- 12 B. A. Bidlingmeyer, *J. Chromatogr. Sci.*, 18 (1980) 525-539.





# Determination of amphetamines by high-performance liquid chromatography with ultraviolet detection

## On-line pre-column derivatization with 9-fluorenylmethyl chloroformate and preconcentration

Gabrielle Maeder\*

*Department of Inorganic, Analytical and Applied Chemistry, University of Geneva, 30 Quai Ernest-Ansermet, CH-1211 Geneva 4 (Switzerland)*

Michel Pelletier

*Institute of Forensic Medicine, University of Geneva, CMU, 9 Avenue de Champel, CH-1211 Geneva 4 (Switzerland)*

Werner Haerdi

*Department of Inorganic, Analytical and Applied Chemistry, University of Geneva, 30 Quai Ernest-Ansermet, CH-1211 Geneva 4 (Switzerland)*

---

### ABSTRACT

An on-line pre-column derivatization method for the determination of low concentrations of amphetamines using ultraviolet detection has been developed. In this work 9-fluorenylmethyl chloroformate (FMOC-Cl) has been used as the derivatizing agent. The optimum conditions for derivatization such as pH, reaction time and FMOC-Cl/amphetamine concentration ratio have been investigated. Attempts have been made to extend the sensitivity of the method by preconcentration of the derivatives on a micro-column packed with  $C_{18}$  bonded silica. Derivatization and preconcentration of the samples were carried out at low pressure on a flow injection analysis system. Quantitative determination of amphetamines as low as  $2 \cdot 10^{-8}$  mol/l can be made using this on-line method with preconcentration. The sensitivity of this technique is about 50 times greater than the equivalent off-line method.

---

### INTRODUCTION

Quantitative analysis of drugs such as amphetamine, methamphetamine, ephedrine, norephedrine and other amphetamine-related compounds which are used as stimulants has become important in clinical and forensic sciences.

Amphetamine and methamphetamine are the only drugs of this family which have been included in Swiss drug abuse legislation. However, stimulants such as ephedrine and norephedrine are banned by

the International Olympic Committee because they are considered as dopants. Ephedrine and norephedrine in nose sprays are used as the starting products for amphetamine and methamphetamine synthesis [1].

Many analytical methods have been developed for their determination, including gas chromatography (GC) [2], thin-layer chromatography (TLC) [3] and high-performance liquid chromatography (HPLC) [4–6]. Biological samples often contain low concentrations of these drugs. Although GC and

TLC are sensitive enough for their determination, they require time-consuming sample preparation. HPLC has the advantage that it is simple and aqueous samples, especially urine, may be analysed with a minimum of sample preparation.

The determination of amphetamines and amphetamine-related compounds by HPLC with UV detection has not gained much popularity due to the low absorbances of these compounds (molar absorptivity about  $200 \text{ l cm}^{-1} \text{ mol}^{-1}$  at 257 nm in water).

Improvements in the detection limits is possible by using pre-column or post-column derivatization. In fact, a number of derivatizing agents such as *o*-phthalaldehyde (OPA), 4-chloro-7-nitrobenzo-2-oxa-1,3-diazole (NBD-Cl) and sodium  $\beta$ -naphthoquinone-4-sulphonate (NQS) have been used to overcome the detection problem. These pre-column derivatization reagents have been used for the qualitative and quantitative analysis of amphetamines in urine and plasma samples [7].

The derivatizing agent 9-fluorenylmethyl chloroformate (FMOC-Cl) was first introduced for the derivatization of amino acids by Einarsson *et al.* [8]. It is suitable for the pre-column derivatization of primary and secondary amino acids [8,9] and amines [10,11]. The products formed with FMOC-Cl are stable, as opposed to those with OPA, which forms unstable derivatives and does not react with secondary amino acids.

As FMOC-Cl is a good derivatization agent for amines, it would be expected to be a good derivatizing agent for amphetamines, which also have amine groups. This was shown by Veuthey and Haerdi [12] and Gao *et al.* [13]. FMOC-Cl was therefore chosen as a derivatizing agent for amphetamines in this study.

The aim of this work was to develop an analytical method with on-line pre-column derivatization with FMOC-Cl for the determination of low concentrations of amphetamines using UV detection. The optimum conditions for derivatization such as pH, choice of solvent, reaction time and derivatization agent/amphetamine concentration ratio have been investigated. Attempts have been made to extend the sensitivity of the method by preconcentration of the derivatives on a micro-column packed with  $\text{C}_{18}$  bonded silica. Derivatization and preconcentration of the samples were carried out at low pressure by a flow injection analysis (FIA) system.

## EXPERIMENTAL

### Apparatus

The chromatographic system consisted of a Varian 5000 high-performance liquid chromatograph. An HP 1050 series variable-wavelength detector coupled to an HP 3390A integrator was used. A Gilson Minipuls-3 peristaltic pump and a Knauer 64 pump were used in the FIA system for the on-line derivatization and preconcentration steps. PTFE tubings (0.8 mm I.D.) were used in all instances. The reaction coil consisted of a glass tube ( $10 \text{ m} \times 2 \text{ mm I.D.}$ ). The FIA system was coupled to the HPLC system via a six-way Rheodyne 7000 valve coupled to a trace enrichment cartridge (pre-column), which is a cylindrical stainless-steel tube ( $13 \text{ mm} \times 2 \text{ mm I.D.}$ ) (Fig. 1) packed with 40–63- $\mu\text{m}$  Nucleosil  $\text{C}_{18}$  silica (MN, Düren, Germany). The analytical column ( $200 \text{ mm} \times 4 \text{ mm I.D.}$ ) was packed with 5- $\mu\text{m}$  Nucleosil  $\text{C}_{18}$  (MN).

### Chemicals

Acetonitrile (HPLC grade) was obtained from Romil (Loughborough, UK). Distilled water was used for the preparation of the aqueous mobile phase. The mobile phase was filtered through a 0.45- $\mu\text{m}$  Schleicher and Schuell membrane. FMOC-Cl, sodium carbonate (reagent grade) and sodium hydrogencarbonate (reagent grade) were obtained from Merck (Darmstadt, Germany), (–)-Ephedrine and D-(+)-norephedrine from Fluka Chemie (Buchs, Switzerland), DL-amphetamine sulphate from Siegfried (Zofingen, Switzerland) and DL-methamphetamine hydrochloride from the Federal Office of Public Health (Switzerland) were used. Stock solutions (0.01 mol/l) of each of the amphetamines in 0.1 mol/l hydrochloric acid were stored at

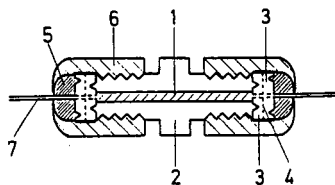


Fig. 1. Enrichment cartridge. 1 = Internal volume ( $13 \text{ mm} \times 2 \text{ mm I.D.}$ ) packed with 40–63  $\mu\text{m}$  Nucleosil  $\text{C}_{18}$  silica; 2 = pre-column; (3) PTFE O-ring; 4 = sintered stainless steel (porosity 20  $\mu\text{m}$ ); 5 = adaptor for sealed capillary; 6 = nut "Serto"; 7 = stainless-steel capillary.

5°C. A stock solution (0.01 mol/l) of FMOC-Cl in acetonitrile was prepared. Sodium hydrogencarbonate-sodium carbonate (0.1 mol/l) buffer solution (pH 9.0) was prepared for the off-line derivatization. For the on-line derivatization the concentration of the buffer was 0.2 mol/l.

### Procedure

**Off-line derivatization.** To 35 ml of 0.1 mol/l carbonate buffer (pH 9.0) placed in a 50-ml volumetric flask, 5 ml of an aqueous solution containing the four amphetamines ( $1 \cdot 10^{-6}$ – $1 \cdot 10^{-4}$  mol/l) and 10 ml of  $5 \cdot 10^{-4}$  mol/l FMOC-Cl in acetonitrile were added and diluted to the mark with carbonate buffer. After a 10-min reaction time, 200  $\mu$ l of the mixture were injected into the HPLC system for separation.

**On-line derivatization and preconcentration.** A schematic diagram of the system used is shown in Fig. 2. The sample solution was pumped by a peristaltic pump to tee 1 (6) where it was mixed with the carbonate buffer. Switch valve 4 was used for pumping  $5 \cdot 10^{-5}$  mol/l FMOC-Cl in acetonitrile to tee 2 (7). FMOC-Cl and the sample solutions were pumped simultaneously. Once the desired volume of sample solution had been pumped, the six-port valve 3 was switched to pump water for the clean-up of the tubes. Valve 4 was switched 1 min after switching valve 3 to allow the FMOC-Cl solution to circulate back into the reservoir. Before linking the pre-column to the analytical column for the separation of the derivatized products, using valve 5,

the glass coil and the pre-column were flushed with the pumping solution, the volume used being slightly greater than the capacity of the coil (31.4 ml).

It is important to note that preliminary tests using a PTFE or nylon reaction coil showed that these coils were unsuitable as a result of adsorption problems and only glass reaction coils gave satisfactory results.

### RESULTS AND DISCUSSION

Amphetamines react with FMOC-Cl under alkaline conditions to form amino derivatives. In addition, FMOC-Cl undergoes hydrolysis to produce FMOC-OH. These reactions are shown in Fig. 3. The derivatization and hydrolysis reactions are influenced by factors such as pH, FMOC-Cl/amphetamine ratio and derivatization time. The effect of these parameters was studied by the batch method using HPLC.

The spectral characteristics of the derivatives is important in optimizing the sensitivity of the detector. Therefore, the UV spectra of the derivatized amphetamines and the hydrolysed FMOC-Cl (FMOC-OH) were run. The spectra of derivatized amphetamines and FMOC-OH show absorption maxima at 208 and 265 nm (Fig. 4). Although the absorbance at 208 nm is much higher than at 265 nm, 265 nm was chosen for these measurements as at 208 nm the absorbances due to the eluent (acetonitrile-water) and interfering substances in the test solution were fairly high.

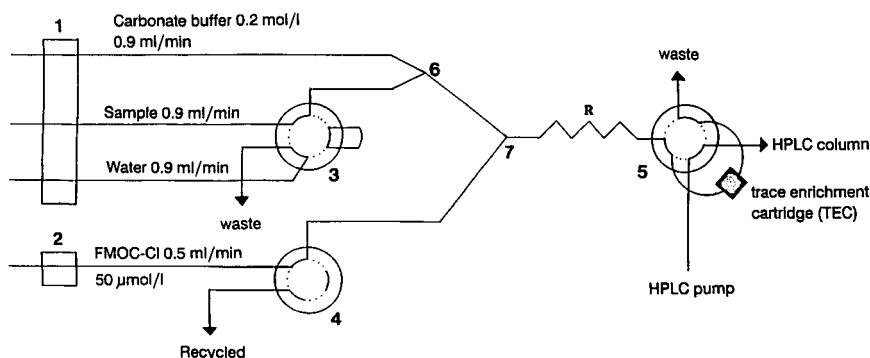


Fig. 2. Schematic diagram of the system used for on-line preconcentration and derivatization. 1, 2 = Pumps; 3, 4, 5 = switch valves; 6 = tee 1; 7 = tee 2; R = glass coil (capacity 31.4 ml).

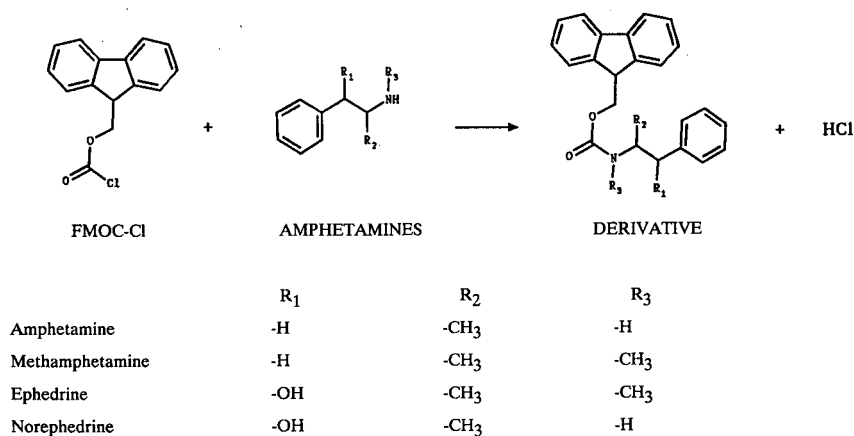
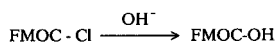
PRIMARY REACTION:SECONDARY REACTION:

Fig. 3. Reaction between FMOC-Cl and amphetamines under alkaline conditions.

*Effect of pH*

The optimum pH for derivatization was between 9 and 10. For pH > 10, the hydrolysis of FMOC-Cl

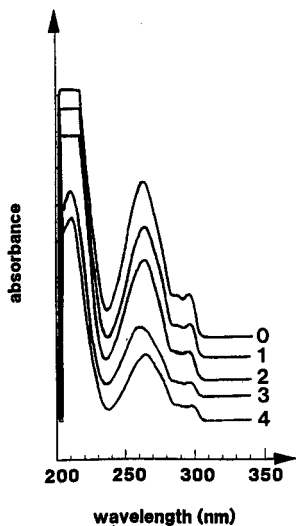


Fig. 4. Spectra of the derivatized amphetamines and FMOC-OH. 0 = FMOC-OH; 1 = methamphetamine; 2 = ephedrine; 3 = norephedrine; 4 = amphetamine.

is considerably higher than at lower pH values. In addition, the silica degrades at this pH. For pH < 9 the derivatization time for amphetamines was too long. Thus pH 9 was chosen for derivatization and a carbonate buffer was used to maintain this constant pH.

*Stability of the derivatives*

The derivatives remained stable for 1 week if they were stored at 5°C.

*Effect of FMOC-Cl/amphetamine ratio*

As the hydrolysis of FMOC-Cl depends on its concentration, measurements were made keeping its initial concentration constant and varying the amphetamine concentration. The derivatization of amphetamine was independent of the FMOC-Cl/amphetamine ratio when this ratio was between 10 and 1000.

*Optimum reaction time*

A preliminary study of the reaction time indicated that for reaction times greater than or equal to 10 min, peak areas were independent of time for all

the amphetamines tested. Thus, for the on-line derivatization reaction, the capacity of the reaction coil was chosen such that the reaction time is greater than 10 min for the flow-rates used in this work.

#### Separation of amphetamines

Amphetamines were separated by HPLC using the optimum conditions of flow-rate, 1.5 ml/min, and eluent acetonitrile–water (58:42, v/v). A typical chromatogram obtained for the separation of amphetamines from a solution containing four different amphetamines is shown in Fig. 5 (off-line method). The peak at 42.13 min is probably the carbonic acid ester of FMOC, a product resulting from the condensation reaction between FMOC-Cl and FMOC-OH. UV spectra do not discriminate between this compound and FMOC-Cl.

Analogous chromatograms were obtained for on-line derivatized and preconcentrated samples.

#### Breakthrough volume

To determine the loading capacity of the pre-column, a solution containing the four different amphetamines ( $1 \cdot 10^{-5}$  mol/l each) was derivatized by the off-line method and passed through the column. Aliquots of the mixture were collected every 5 min at the outlet of the column and injected into the HPLC system for separation. The volume of solu-

tion passed through the column may be computed from the flow-rate and the time of passage. The breakthrough volume was 45 ml using this procedure.

#### Calibration graph

*Off-line method.* Linear calibration graphs were obtained over the range  $1 \cdot 10^{-6}$ – $1 \cdot 10^{-4}$  mol/l for each of the amphetamines corresponding to  $2 \cdot 10^{-11}$ – $2 \cdot 10^{-9}$  mol injected, the correlation coefficient being greater than 0.999.

The reproducibility of the injections was tested by making five replicate measurements. The results showed that the reproducibility at low concentrations was 10% and that for high concentrations it never exceeded 2%.

*On-line method.* Linear graphs were obtained in the range  $2 \cdot 10^{-8}$ – $1 \cdot 10^{-7}$  mol/l for each of the amphetamines. Correlation coefficients ( $r$ ) for methamphetamine and norephedrine were 0.979 and 0.958, respectively, whereas for the other two substances they were greater than 0.997. Despite the fact that the  $r$  values for methamphetamine and norephedrine are not very good, they are acceptable for quantification considering the low levels of these substances. A comparison of these results with those obtained by the off-line method shows that the sensitivity of the method is increased by a factor

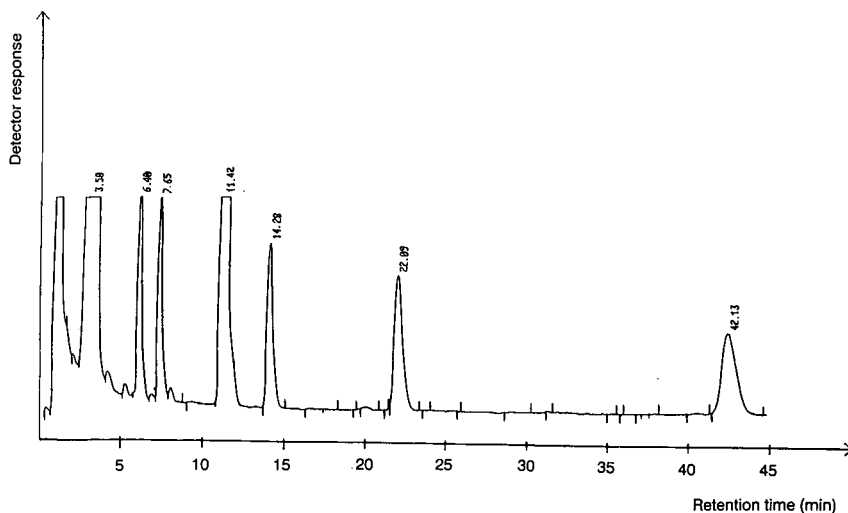


Fig. 5. Typical chromatogram obtained for a mixture of four derivatized amphetamines (off-line method). The injected amounts ( $2 \cdot 10^{-10}$  mol) were the same for all the amphetamines. Retention times (min): FMOC-OH, 3.50; norephedrine, 6.40; ephedrine, 7.65; FMOC-Cl, 11.42; amphetamine, 14.28; methamphetamine, 22.09; (FMOC)<sub>2</sub> carbonic acid ester, 42.13.

of about 50. The reproducibility for methamphetamine and norephedrine was 13.5 and 16.1%, respectively, whereas for ephedrine and amphetamine it was 4.8 and 5.0%, respectively. Better reproducibilities, particularly for methamphetamine and norephedrine, may be achieved by making slight alterations to the experimental procedure.

#### CONCLUSION

The results of this study have shown that amphetamines may be determined quantitatively using FMOC-Cl as a prederivatizing agent. Good separation of the amphetamines was observed. In contrast to the batch method, the on-line prederivatization-preconcentration method enhanced the sensitivity of the analytical determination. The application of the method to biological samples is currently under investigation.

#### REFERENCES

- 1 F. T. Noggle, J. DeRuiter and C. R. Clark, *J. Chromatogr. Sci.*, 28 (1990) 529.
- 2 *Application Bulletin No. 810C*, Supelco SA, Gland 1988.
- 3 H. Spahn, H. Weber, E. Mutschler and W. Möhrke, *J. Chromatogr.*, 310 (1984) 167.
- 4 M. L. Chan, C. Whetsell and J. D. McChesney, *J. Chromatogr. Sci.*, 12 (1974) 512.
- 5 I. Jane, *J. Chromatogr.*, 111 (1975) 227.
- 6 P. J. Twitchett and A. C. Moffat, *J. Chromatogr.*, 111 (1975) 149.
- 7 B. M. Farrell and T. M. Jefferies, *J. Chromatogr.*, 272 (1983) 111.
- 8 S. Einarsson, B. Josefsson and S. Lagerkvist, *J. Chromatogr.*, 282 (1983) 609.
- 9 S. Einarsson, *J. Chromatogr.*, 348 (1985) 213.
- 10 J. A. Shah and D. J. Weber, *J. Chromatogr.*, 309 (1984) 95.
- 11 Z. Harduf, T. Nir and B. J. Juven, *J. Chromatogr.*, 437 (1988) 379.
- 12 J. L. Veuthey and W. Haerdi, *J. Chromatogr.*, 515 (1990) 385.
- 13 C. X. Gao, T. Y. Chou and I. S. Krull, *Anal. Chem.*, 61 (1989) 1538.

# High-performance liquid chromatographic determination of penicillin G, penicillin V and cloxacillin in beef and pork tissues

William A. Moats

US Department of Agriculture, Agricultural Research Service, Product Quality and Development Institute, Meat Science Research Laboratory, Building 201, BARC-East, 10300 Baltimore Avenue, Beltsville, MD 20705-2350 (USA)

---

## ABSTRACT

The objective was to develop confirmatory high-performance liquid chromatographic methods for penicillin residues in animal tissues with detection limits of  $\leq 10$  ng/g. A previously described procedure was modified by using a larger sample size and isocratic analysis. Tissues (15 g) were blended with 45 ml of water and 20 ml of homogenate were mixed with 40 ml acetonitrile and filtered. The filtrate (30 ml) was mixed with 10 ml of 0.2 M  $H_3PO_4$  and extracted with methylene chloride. The combined methylene chloride layers were mixed with acetonitrile and hexane, washed with two 4-ml portions of water and then extracted with four 1-ml portions of 0.01 M phosphate buffer (pH 7). The combined buffer extracts were concentrated to 1 ml under reduced pressure. Analysis was isocratic during 0.01 M phosphate buffer (pH 7)–acetonitrile with proportions 85:15 (penicillin G), 82:18 (penicillin V) or 78:22 (cloxacillin). A polystyrene–divinylbenzene copolymer column,  $150 \times 4.6$  mm I.D. (Polymer Labs. PLRP-S), was used with a flow-rate of 1 ml/min and detection at 210 nm. The presence of penicillins was confirmed by treating a duplicate sample with penicillinase. Recoveries were  $> 90\%$  in most instances. Detection limits were 5 ng/g in muscle and higher in liver and kidney. The procedure is a simple and sensitive method for confirming the presence of penicillins in animal tissues.

---

## INTRODUCTION

Penicillins, especially penicillin G, are widely used in food animal production, both therapeutically and as growth promotants in feeds. Although penicillins are relatively non-toxic, residual amounts in foods have caused allergic reactions in sensitive individuals [1].

Although penicillins can be detected in tissues by microbiological assays, they cannot be distinguished from one another. Some progress has been made in the development of specific chromatographic methods for the determination of penicillin G and other  $\beta$ -lactam antibiotics [2–7] in tissues. However, the development of chromatographic methods of adequate sensitivity has been difficult and it is only recently that methods capable of detecting  $< 10$  ng/g of penicillin residues in tissues have been reported. Meetschen and Petz [7] de-

scribed a sensitive gas chromatographic method capable of determining  $\beta$ -lactam antibiotics with neutral side-chains at levels of  $\leq 3$  ng/g in a variety of substrates. Their procedure requires lengthy clean-up and derivatization. Boison *et al.* [2] recently described a high-performance liquid chromatographic (HPLC) method for penicillin G sensitive to 5 ng/g in tissues using tungstic acid precipitation, solid-phase extraction and derivatization.

The method described in this paper is a modification of that described previously [3], using a simple partitioning clean-up. By use of larger samples, a different type of HPLC column and isocratic elution at neutral pH, the sensitivity was increased about tenfold. The procedure is simpler than other reported procedures in that no derivatization is required. The use of the procedure with three penicillins with neutral side-chains is described.

## EXPERIMENTAL

*Chemicals and materials*

Acetonitrile, hexane and methylene chloride were of Omnisolv grade (EM Science, Gibbstown, NJ, USA) or equivalent. The penicillins were obtained from Sigma (St. Louis, MO, USA), and used as received. Stock solution of 1 mg/ml were prepared in distilled water and diluted as appropriate. Stock solutions of penicillin G were prepared fresh weekly and others were prepared biweekly and stored refrigerated. Other chemicals were of analytical-reagent grade from various sources.

To prepare 0.2 M  $\text{H}_3\text{PO}_4$ , 13.6 ml of concentrated phosphoric acid was diluted to 1 l. To prepare 0.01 M buffer of pH 7, 1.36 g of  $\text{KH}_2\text{PO}_4$  and 2.84 g of  $\text{Na}_2\text{HPO}_4$  were dissolved in 3 l of water. The  $\beta$ -lactamase preparation used was Bacto penase concentrate obtained from Difco Labs. (Detroit, MI, USA).

Final filtration was done with 13-mm Acrodisc LCPVDF filter cartridges, 0.45- $\mu\text{m}$  pore size, obtained from Gelman Sciences (Ann Arbor, MI, USA).

*Sample preparation procedure*

Tissue (15 g) was blended with 45 ml (60 ml for liver and kidney) of water in 300- or 500-ml blender jars for 2 min at half full-power (or less to reduce foaming) as controlled by a variable-resistance transformer. A 20-ml aliquot of the homogenate was measured into a 125-ml conical flask and mixed with 40 ml of acetonitrile. After 5 min, the supernatant was decanted through a plug of glass-wool in the stem of a funnel and 30 ml (= 2.5 g of muscle or 2.0 of liver and kidney) of filtrate were collected. The filtrate was transferred to a separating funnel and 10 ml of 0.2 M  $\text{H}_3\text{PO}_4$  and 20 ml of methylene chloride were added with vigorous shaking. The methylene chloride layer was drawn off into a flask and the water layer in the separating funnel was extracted with 10 ml methylene chloride (and 10 ml of acetonitrile for liver and kidney) and combined with the first extract. The water layer was discarded and the separating funnel was rinsed with water. The combined methylene chloride layers were returned to the separating funnel and 15 ml of acetonitrile and 40 ml of hexane were added. The mixture was washed twice with 4-ml portions of water,

which were discarded. In the partitioning steps, the layers ordinarily separated quickly without formation of emulsions. If significant emulsion was present, a few milliliters of acetonitrile were added and the mixture was shaken again. The organic layer was then extracted with four successive 1-ml portions of 0.01 M buffer pH 7 and the extracts were combined in a calibrated 15-ml centrifuge tube.

A few drops (0.1–0.2 ml) of *tert*.-butanol were added to each tube to suppress foaming and they were placed in a Buchler (Fort Lee, NJ, USA) Rotary Evapomix. Vacuum was applied cautiously without heating. After the contents had become cold, the water-bath was warmed to a final temperature of 50°C with the tubes rotating under vacuum. The contents were concentrated to  $\leq 1$  ml, adjusted to a final volume of 1 ml and filtered into auto-sampler vials through a Gelman Acrodisc LCPVDF filter. Evaporation can also be done under a stream of air or nitrogen, but this was slower and required more heating of the sample solution.

*HPLC analysis*

For HPLC analysis a Varian (Sugarland, TX, USA) Model 5000 pump and a Varian Model 9090 autosampler were used with either a Beckman (Fullerton, CA, USA) System Gold diode-array detector or a Hewlett-Packard (Rockville, MD, USA) Model 1050 UV-visible detector with a Varian Model 650 data system. A Polymer Labs. (Amherst, MA, USA) PLRP-S polystyrene-divinylbenzene copolymer HPLC column 150 mm  $\times$  4.6 I.D., 5  $\mu\text{m}$  particle size, 100 Å pore diameter) was used with a matching guard cartridge. The mobile phase was 0.01 M phosphate buffer (pH 7) (A)–acetonitrile (B). Analysis was isocratic with the proportions (A:B) adjusted to give a retention time of 9–11 min for each compound; these were 85:15 for penicillin G, 82:18 for penicillin V and 78:22 for cloxacillin. The injection volume was 200  $\mu\text{l}$  with a flow-rate of 1 ml/min and detection at 210 nm. After 12 min, a flushing program was started to A–B (65:35) at 15–20 min and then to the starting conditions at 21 min. After 30 min, the next sample was injected. After use, the column was flushed for 5 min with water and then for 10 min with water–acetonitrile (40:60) for storage. Quantification was based on comparison with a 1  $\mu\text{g/ml}$  standard injected in the same sample series. Peak area was more accurate



than peak height, but either was linear with concentration up to at least 2  $\mu\text{g}$  injected. The blank (if any) found after penicillinase treatment was subtracted for more accurate quantification, especially at low levels.

#### *Spiked samples*

The indicated amount of the penicillin was added in 150  $\mu\text{l}$  of solution to the tissue in a blender jar and equilibrated for 30 min before blending with water. An equivalent amount of 0.01 *M* buffer (pH 7) was added at the same time to serve as a standard. In some instances, a larger amount of tissue was homogenized and the 20-ml aliquots were spiked.

#### *Penicillinase treatment*

The time required to reduce or eliminate the penicillin peak was determined by adding 0.2 ml of penicillinase concentrate to 20 ml of spiked water and incubating at room temperature for 15 min for penicillin G, 1 h for penicillin V and 3 h for cloxacillin. A 20-ml aliquot of sample homogenate was mixed with 0.2 ml of penicillinase concentrate and incubated for the indicated time before adding acetonitrile.

### RESULTS AND DISCUSSION

The approaches developed in our laboratory for determining low levels of penicillin G [8,9] and other penicillins with neutral side-chains in milk were not satisfactory with tissue. When the acetonitrile filtrates were evaporated directly, a precipitate, almost certainly phospholipid, formed when the acetonitrile was driven off and recovery of the penicillins in the water layer was poor, indicating that penicillins were bound to the precipitate. When methylene chloride and hexane were added to the acetonitrile filtrate to separate the water layer, the recoveries of penicillins in the water layer were also poor. Penicillins were evidently complexed with something in the filtrate, probably phospholipids. The positively charged phospholipid molecules could act as ion pairs with the anionic penicillins. The penicillins were present in the acetonitrile filtrate and could be recovered by the partitioning technique described previously [3,4] and in this paper.

The partitioning clean-up described previously [3,4] proved adequate for isocratic analysis in pH 7 buffer. Some minor modifications in the earlier procedure together with improved detection systems increased the sensitivity about ten-fold with detection limits lowered from 0.05 to 0.005 ppm. A larger sample size was used. This required more acid to overcome the buffering action of the sample extract so that the penicillins could be converted to the acid form for extraction into methylene chloride. Addition of 10 ml of 0.2 *M* buffer (pH 2.2) was not satisfactory, pH 2 buffer gave a partial recovery and 0.2 *M* phosphoric acid gave essentially quantitative recoveries. Wiese and Martin [10] observed that penicillin G deteriorated rapidly in aqueous solutions below pH 3. However, it is probably more stable when organic solvents are present. No noticeable degradation occurred in 0.01 *M* phosphoric acid-acetonitrile during a run time of up to 20 min for HPLC analysis [3,4]. In the present instance, the effective pH of the methylene chloride extract was not known. However, there was no evidence of significant deterioration of penicillin G during the extraction procedure. The methylene chloride extracts were partitioned back into pH 7 buffer without undue delay, usually within 1 h.

The solvent composition used during partitioning usually gave rapid and clean separations of the layers. If stable emulsions were present, 5-ml portions of acetonitrile were added with shaking until the layers separated quickly.

Some samples, especially from liver and kidney, were turbid after final concentration and required filtration. Nylon 66 filters retained the penicillins quantitatively from water and, indeed, show promise for solid-phase extraction of these compounds. The PVDF filters specified were satisfactory. Some very fine turbidity sometimes passed through the filter but did not affect the chromatographic system. Isocratic analysis in pH 7 buffer improved the separation of penicillins from interferences over that achieved previously by gradient elution in 0.01 *M*  $\text{H}_3\text{PO}_4$ . Isocratic analysis had the disadvantage that retentions of the penicillins were so different that a different mobile phase was required for each penicillin. It also had the disadvantage that the column was not flushed between samples and late-eluting peaks were sometimes a problem, particularly with liver and kidney. A column flush was used af-

ter each sample to eliminate this problem.

Extraction/deproteinization with acetonitrile was rapid and effective. However, others [3,6] have successfully used tungstic acid. The partitioning clean-up used is simple, effective and reproducible. Reproducibility has sometimes been a problem when solid-phase extraction techniques were used [3,4,8]. Derivatization using imidazole or triazole and mercury (II) chloride has been used to form a derivative with a UV absorption maximum of 325 nm, where fewer interferences absorb than at the lower end of the UV range where penicillins have significant UV absorption. Wiese and Martin [10] observed that the molar absorptivity of penicillin G at 193 nm at acid pH was greater ( $38\,000/\text{l mol} \cdot \text{cm}$ ) than that of the derivative at 325 nm ( $20\,000/\text{l mol} \cdot \text{cm}$ ). Derivatization is therefore neither necessary nor advantageous if an adequate chromatographic separation of the parent compound can be achieved. At pH 7, use of absorbance at 210 nm was more satisfactory as the baseline noise was less than at shorter wavelengths.

Although the sensitivity of both UV-visible and diode-array detectors has improved considerably in recent years, the former are still better with respect

to sensitivity. The present procedure was used successfully to measure incurred residues of penicillin G at levels  $<0.01$  ppm in muscle and spiked levels of 0.01–0.02 ppm in muscle using a UV-visible detector connected to a data system. Detection at these low levels in liver and kidney and less certain because more interferences were present. However, residues were readily determined at 0.1 ppm in these tissues. Quantification was based on one or more external standards run at the same time as the samples and was generally based on peak area.

Treatment of the sample with penicillinase is a simple and effective method of confirming that a suspect chromatographic peak is indeed a penicillin [8,11]. Wiese and Martin [11] used a "digital subtraction" technique for samples with and without penicillinase treatment to determine low levels of penicillin G in milk. Penicillin G was rapidly inactivated by penicillinase. However, many other penicillins such as cloxacillin are resistant to penicillinase and require several hours for complete inactivation.

The application of this method to meat samples revealed unsuspected low levels of penicillin G residues. The compound was so ubiquitous that it was

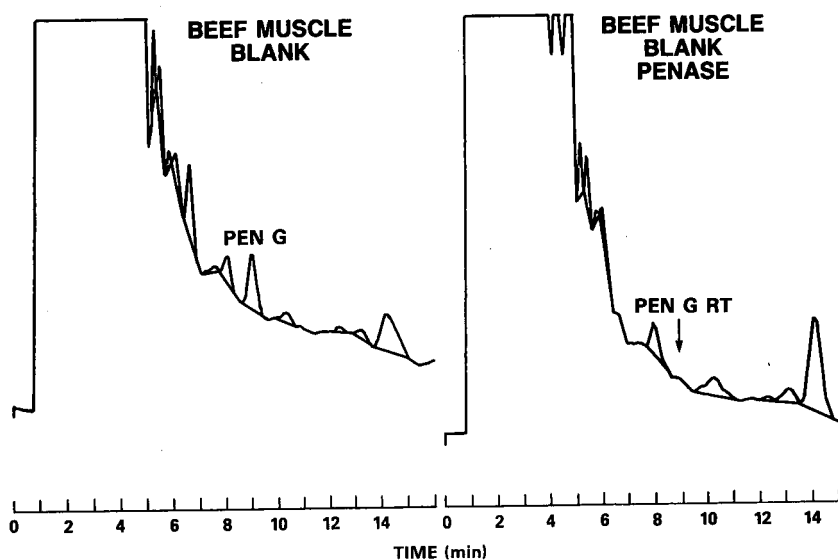


Fig. 1. Beef muscle, isocratic analysis: 0.01 M phosphate buffer pH 7.0–acetonitrile (85:15); flow-rate, 1 ml/min; Polymer Labs. PLRP-S column ( $150 \times 4.6$  mm I.D.); UV detection at 210 nm, 0.5 g equivalent injected, 0.0078 a.u.f.s., Hewlett-Packard Model 1050. UV-visible detector, Varian Model 650 data system. (Left) before and (Right) after treatment with penicillinase. The presence of penicillin G equivalent to 0.022 ppm of penicillin G sodium salt was confirmed. PEN G = Penicillin G; RT = retention time.

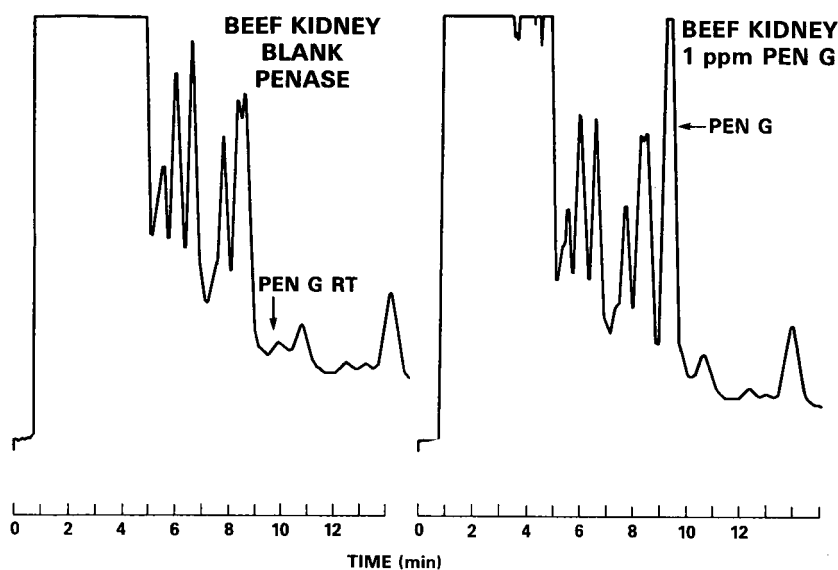


Fig. 2. Beef kidney: Conditions as in Fig. 1; 0.4 g equivalent injected; blank treated with penicillinase and spiked with 1 ppm of sodium penicillin G.

difficult to obtain suitable blank tissue for recovery experiments. The levels found from subsamples of the same tissue were variable. It was therefore necessary to prepare a uniform sample homogenate and spike subsamples of the homogenate to determine recoveries of penicillin G. The background levels were generally below the US tolerance limit of 0.05 ppm [12]. No background levels of penicillin V or cloxacillin were observed.

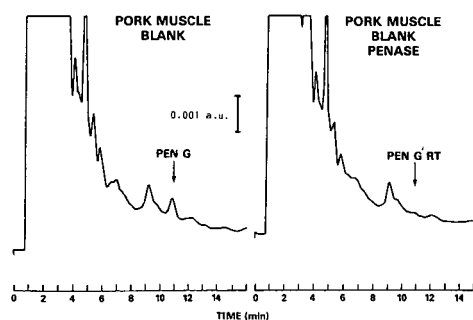


Fig. 3. Pork muscle; conditions as in Fig. 1, except mobile phase, 0.01 M phosphate buffer (pH 7)-acetonitrile (86:14). (Left) before and (right) after treatment with penicillinase. The presence of the equivalent of 0.019 ppm of sodium penicillin G was confirmed.

Fig. 1 shows a beef chuck sample with incurred penicillin G residue confirmed by penicillinase treatment. The residue is equivalent to 0.022 ppm of sodium penicillin G. Fig. 2 shows beef kidney blank and spiked with 1.0 ppm of penicillin G. There was no detectable penicillin G in the blank. Fig. 3 shows pork with an incurred penicillin G residue equivalent to 0.019 ppm of sodium penicillin G, confirmed by penicillinase treatment. With penicillinase treatment, penicillins can be differentiated from interferences with similar retention times.

Recoveries from spiked samples are shown in Table I. Recoveries from beef muscle were >90% for all three compounds. Recoveries of penicillin G were >90% except from beef kidney. Recovery of cloxacillin was lower from pork muscle and kidney. Cloxacillin was not recovered from beef liver.

This is a simple, specific and sensitive HPLC confirmatory test for penicillin G, penicillin V and cloxacillin. It should be applicable to any penicillin with a neutral side-chain. The use of penicillinase for confirmation enhances the sensitivity and makes the method suitable for regulatory confirmation of penicillin residues.

TABLE I  
RECOVERY OF PENICILLINS ADDED TO TISSUES

Compound	Tissue	Amount added (μg/g) and recovery <sup>a</sup> (%)	Mean recovery ± S.D. (%)
Penicillin G	Beef muscle	1.5(98) <sup>b</sup> , 1(86,100,92), 0.15(99) <sup>b</sup> , 0.015(96) <sup>b</sup>	95 ± 5
	Beef kidney	1(71)	
	Pork muscle	1(101,95) <sup>b</sup> , 0.1(92) <sup>b</sup>	
	Pork liver	1(102,89), 0.1(98)	
	Pork kidney	1(96)	
Penicillin V	Beef muscle	10(98), 1(97,105,98)	99 ± 3
	Beef kidney	1(67,76), 0.1(118)	99 ± 4
	Pork muscle	10(104) <sup>b</sup> , 1(100), 0.1(97 <sup>b</sup> ,93)	
Cloxacillin	Beef muscle	10(91), 2(89), 1(89,97,91), 0.2(92), 0.02(91)	91 ± 2
	Beef kidney	1(85), 0.1(86)	84 ± 12
	Beef liver	No recovery	
	Pork muscle	1.5(76) <sup>b</sup> , 1(85) <sup>b</sup> , 0.15(74) <sup>b</sup> , 0.1(77) <sup>b</sup> , 0.015(107) <sup>b</sup>	
	Pork kidney	10(69)	

<sup>a</sup> In parentheses.  
<sup>b</sup> Spiked homogenate.

REFERENCES

1 W. G. Huber, in A. G. Rico (Editor), *Drug Residues in Animals*, Academic Press, Orlando, FL, 1986, pp. 33–50.

2 J. O. Boison, C. D. C. Salisbury, W. Chan and J. D. MacNeil, *J. Assoc. Off. Anal. Chem.*, 74 (1991) 497.

3 W. A. Moats, *J. Chromatogr.*, 317 (1984) 311.

4 W. A. Moats, E. W. Harris and N. C. Steele, *J. Agric Food Chem.*, 34 (1986) 425.

5 H. Yoshimura, O Itoh and S. Yonezawa, *Jpn. J. Vet. Sci.*, 43 (1981) 833.

6 H. Terada, M. Asanoma and Y. Sakabe, *J. Chromatogr.*, 318 (1985) 299.

7 U. Meetschen and M. Petz, *J. Assoc. Off. Anal. Chem.*, 73 (1990) 373.

8 W. A. Moats, *J. Chromatogr.*, 507 (1990) 177.

9 W. A. Moats and R. Malisch, *J. Assoc. Off. Anal. Chem.*, in press.

10 B. Wiese and K. Martin, *J. Pharm. Biomed. Anal.*, 7 (1989) 67.

11 B. Wiese and K. Martin, *J. Pharm. Biomed. Anal.*, 7 (1989) 107.

12 *United States Code of Federal Regulations*, 21.566.510.

# Automated high-performance liquid chromatographic method for the determination of rifampicin in plasma

K. J. Swart\* and M. Paggis

*Department of Pharmacology, G6, Faculty of Medicine, UOFS, P.O. Box 339, Bloemfontein 9300 (South Africa)*

## ABSTRACT

Due to the unstable nature of rifampicin, a rapid automated high-performance liquid chromatographic method had to be developed for the analysis of a large number of plasma samples generated during a bioavailability trial. Extraction and injection of the samples were automatically done by a sample preparation system using  $C_2$ , 100 mg Bond Elut extraction columns. The extracts were chromatographed on a 4- $\mu$ m reversed-phase  $C_{18}$  column with a citrate buffer and acetonitrile as mobile phase. The analytes were detected at 342 nm. Calibration curves were linear to at least 20  $\mu$ g/ml and the limit of quantification was 0.16  $\mu$ g/ml.

## INTRODUCTION

Rifampicin, 3-(4-methylpiperazin-1-yl)iminomethyl) rifamycin SV, a semisynthetic antibiotic drug, is widely used alone or in combination with other drugs such as isoniazid and pyrazinamide in the treatment of tuberculosis.

Rifampicin spontaneously oxidizes to a quinone derivative in atmospheric oxygen above pH 8. In aqueous solutions with lower pH values, rifampicin hydrolyses to 3-formylrifamycin SV and amino 4-methylpiperazine [1,2]. Rifampicin is extensively metabolized in the liver, especially during its first passage through the hepatportal system, mainly to its active metabolite 25-desacetyl rifampicin [3] and 3-formyl-25-desacetyl rifampicin [4].

A number of microbiological [5,6], thin-layer chromatographic (TLC) [7] and high-performance liquid chromatographic (HPLC) [1,8–12] methods have been published for the determination of rifampicin and its metabolites in plasma and urine. These methods did not meet our requirements, since we needed a fully automated method to determine large numbers of samples generated during a bioavailability trial. Owing to the unstable nature of rifampicin we wanted to minimize the time between sample generation, extraction and chromatography of the samples.

This article describes a fully automated procedure for the quantitation of rifampicin in plasma using sulindac as internal standard.

## EXPERIMENTAL

### *Materials*

Rifampicin was obtained from Lennon (Port Elizabeth, South Africa) and sulindac from Adcock-Ingram (Johannesburg, South Africa). Ascorbic acid (BDH, Poole, UK) was used to protect rifampicin from oxidative degradation. All the other reagents were of guaranteed analytical grade, and were used as received. Water was purified by passing through a Millipore Milli-Q filtration system (18 m $\Omega$  cm resistivity) (Waters Assoc., Milford, MA, USA).

### *Analytical systems*

A modular HPLC system was used which consisted of a pump (Shimadzu LC-6A, Shimadzu, Kyoto, Japan), a Waters Radial pak, Nova Pak  $C_{18}$ , 4  $\mu$ m particle size, 100  $\times$  8 mm cartridge, held in an RCM 8  $\times$  10 compression unit (Waters) protected by a Waters Guard Pak with a  $\mu$ Bondapak  $C_{18}$  RCSS precolumn insert. A Shimadzu SPD-6A UV detector was used to measure the absorbance of the eluate. The chromatograms were recorded on a

Spectra-Physics SP4290 integrator (Spectra-Physics, San Jose, CA, USA) and the data sent via a LABNET network to a Spectra-Physics ChromStation for automated data manipulation.

Sample processing and injections were done by an ASPEC system (automated sample preparation with extraction columns) from Gilson (Villiers Le Bel, France) utilizing Bond Elut (100 mg, C<sub>2</sub>) extraction columns (Analytichem International).

#### Chromatography

The mobile phase consisted of acetonitrile–0.05 M sodium citrate buffer adjusted to pH 4.3 with 0.05 M hydrochloric acid (42:58) and pumped at a flow-rate of 2.3 ml/min at ambient temperature. The analytes were detected by a UV detector at 342 nm. Retention times for rifampicin and the internal standard sulindac were 4.65 and 3.07 min, respectively. A peak was found at 2.52 min, which was probably the 25-desacetyl-rifampicin metabolite.

#### Sample preparation

**Plasma standards.** An accurately weighed amount of rifampicin was dissolved in methanol and an aliquot immediately spiked into drug-free plasma to obtain a stock solution containing approximately 22 µg of rifampicin per millilitre of plasma. Subsequent dilutions with plasma were made to obtain adequate standards covering the expected range. All plasma samples contained 200 µg of ascorbic acid per millilitre as an antioxidant. Plasma standards were prepared freshly each week, divided into aliquots and stored in polypropylene tubes at –80°C.

The internal standard sulindac was prepared freshly each week in methanol to obtain an approximate concentration of 19 µg/ml.

**Samples from trial subjects.** Blood (10 ml) was sampled at predetermined intervals in heparinized Venoject tubes from twenty healthy male volunteers after receiving 450 mg of rifampicin in a double-blind, randomized, crossover design in a comparative bioavailability study. The samples were immediately centrifuged for 5 min at 4°C, and 2-ml plasma aliquots, to which 400 µg of ascorbic acid were added, were immediately frozen in solid carbon dioxide. The samples were stored at –80°C until analysed. All the samples were analysed within 4 days after sampling.

**Procedure.** Plasma samples (0.5 ml) were transferred to 5-ml glass tubes and mixed with 0.5 ml of 0.1 M hydrochloric acid to which 50 µl of the internal standard solution were added. The samples were briefly vortexed to obtain thorough mixing and placed in the ASPEC system.

The apparatus was programmed to condition each Bond Elut extraction column with 1 ml of methanol, followed by 1 ml of 0.1 M hydrochloric acid just before use. The plasma mixture was loaded onto the column and the column washed afterwards with 1 ml of 0.1 M hydrochloric acid to get rid of excess protein and plasma components. The analytes were eluted with 400 µl of methanol-acetonitrile (3:2) into a clean tube, mixed by repeatedly aspirating/dispensing the fraction, and a 20-µl aliquot automatically injected onto the HPLC column.

#### RESULTS AND DISCUSSION

Fig. 1 shows representative chromatograms obtained from plasma determinations and demonstrates the lack of interfering endogenous compounds in the blank plasmas.

Quantifications was achieved using the peak-height ratio of rifampicin to the internal standard. All calibration curves were shown to be linear over a wide concentration range with the curves almost passing through the origin. Calibration curves were linear to at least 20 µg/ml and had good correlation coefficients with eight different standard concentrations. The mean recovery for rifampicin was 98% and for sulindac 73%.

The precision and accuracy of the method are indicated in Table I and are expressed as the relative standard deviation (%) and bias (%) for replicates of eight different concentrations covering the expected range. These results were obtained during the analysis of the trial samples. Although good results were obtained at 0.08 µg/ml with a signal-to-noise ratio of 9 during the validation of the method, the limit of quantification was set after the trial to 0.16 µg/ml (fifteen times base value) owing to the larger than expected coefficient of variation experienced in the day-to-day analysis of the low concentrations.

The extraction and chromatography procedures are fully automated and take only 9.5 min from in-

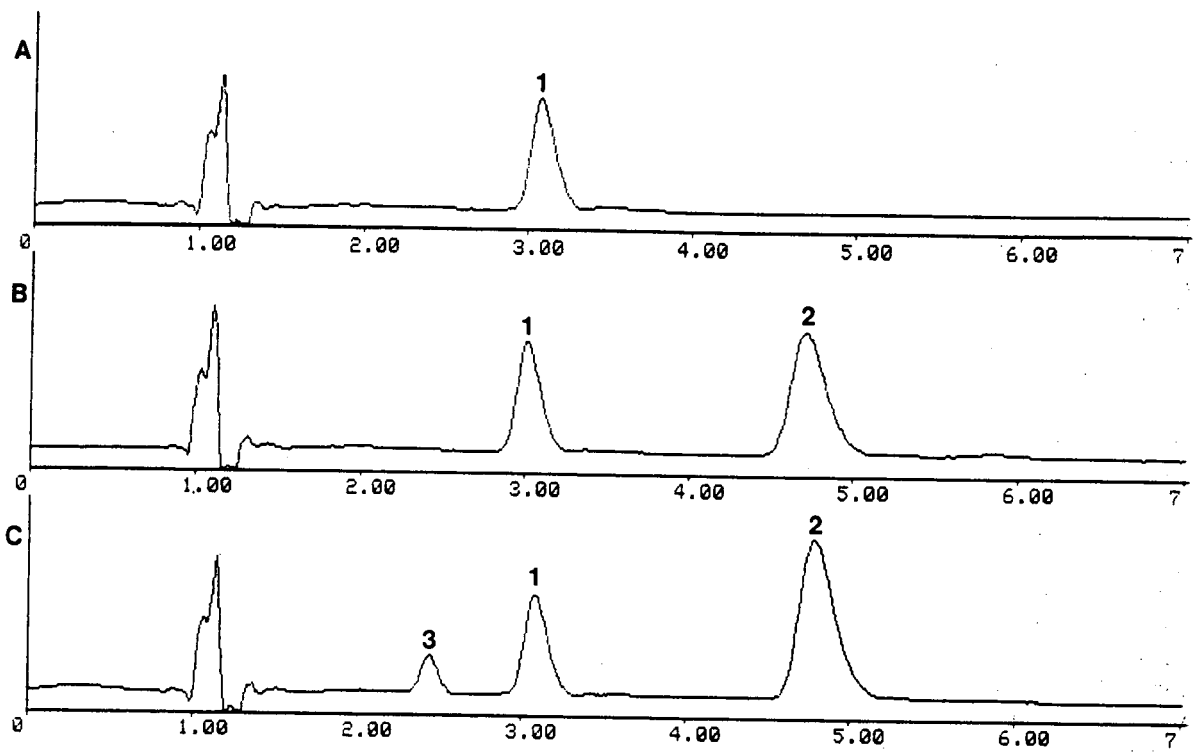


Fig. 1. Chromatograms: (A) blank plasma containing internal standard; (B) plasma standard of 5.2  $\mu\text{g/ml}$ ; (C) trial plasma sample equal to 7.2  $\mu\text{g/ml}$ . Peaks: 1 = sulindac (internal standard); 2 = rifampicin; 3 = rifampicin metabolite. For HPLC conditions, see text.

jection of a sample to extraction and injection of a second sample. Minimum sample handling is required, and determinations can be done 24 h a day, as was done during the determination of the plasma

samples during the trial. Fig. 2 represents a concentration-time profile of the mean plasma rifampicin values of twenty healthy volunteers after receiving an oral dose of 450 mg of rifampicin.

TABLE I

RELATIVE STANDARD DEVIATIONS (R.S.D.) AND BIAS OF QUALITY CONTROLS OBTAINED DURING THE TRIAL TO INDICATE THE PRECISION AND ACCURACY OF THE METHOD

<i>n</i>	Rifampicin concentration ( $\mu\text{g/ml}$ )	Accuracy (bias, %)	Precision (R.S.D., %)
6	22.19	3.1	3.6
7	12.06	3.6	4.0
6	5.80	2.4	2.5
7	2.93	-3.2	4.7
5	1.40	-5.4	3.3
7	0.69	-5.0	3.8
6	0.32	-8.9	5.9
6	0.17	-2.5	5.0

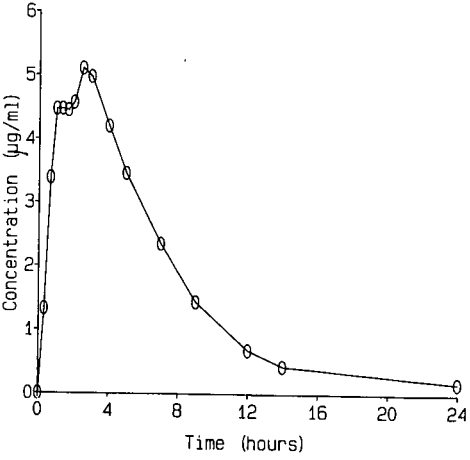


Fig. 2. Concentration-time profile of the mean rifampicin plasma values of twenty volunteers after each receiving a 450-mg rifampicin dose.

Since this method was used only during a study of comparative bioavailability, other substances were not tested for interference with rifampicin. However, no interference from plasma substances was found during chromatography.

Since we were perturbed about the stability of rifampicin when stored in plasma for some time, we checked the stability of rifampicin when plasma samples were stored at  $-80^{\circ}\text{C}$  for 1 month. To these samples were added 200  $\mu\text{g}$  of ascorbic acid per millilitre of plasma, and weekly determinations were carried out. No decrease in the rifampicin content was observed over this time. Degradation of rifampicin in organic solvents such as methanol occurs quite rapidly, so that these solutions should be kept for the shortest time possible.

The data from the integrators were sent to a ChromStation via a LABNET communication system. Calibration curves were automatically constructed from the eight standards processed with each batch using software developed in our laboratory. These standards and seven quality controls were scattered between the 64 samples of each batch to exclude possible variations due to degradation of rifampicin. No degradation peaks could be found in the standards or quality controls over this period. Calculations of the quality controls and trial samples were done from a linear calibration curve. Wherever deviations from linearity occurred, which is not unusual at low concentrations, a calibration curve including only the four lowest standards was

constructed using the appropriate regression equation (usually a second order or power curve).

## CONCLUSION

The procedure provided us with a method that was sensitive enough to determine concentrations of rifampicin in low plasma volumes for 24 h after a single 450-mg oral dose. Determinations could be done 24 h a day since the extraction, injection, chromatography and data manipulation steps were completely automated.

## REFERENCES

- 1 A. Weber, K. E. Opheim and A. L. Smith, K. Wong, *Reviews of Infectious Diseases*, 5, Suppl. 3 (1983) S433.
- 2 G. Binda, Domenichini, E. Gottardi, B. Orlandi, E. Ortelli, B. Pacini and G. Fowst, *Arzneim-Forsch.*, 21 (1971), 1907.
- 3 G. Acocella, *Reviews of Infectious Diseases*, 5 Suppl. 3 (1983) S428.
- 4 K. Sono and H. Hakusui, *Jpn. J. Antibiot.*, 23 (1970) 416.
- 5 H. J. Simon and E. J. Yin, *Appl. Microbiol.*, 19 (1970) 573.
- 6 S. Furesz, K. Scotti, R. Pollanza and E. Mapelli, *Arzneim.-Forsch.*, 17 (1967) 534.
- 7 O. T. Kolos and L. L. Eidus, *J. Chromatogr.*, 68 (1972) 294.
- 8 L. B. Lecaillon, N. Febure, J. P. Metayer and C. Souppart, *J. Chromatogr.*, 145 (1978) 319.
- 9 M. Ishii and H. Ogata, *J. Chromatogr.*, 426 (1988), 412.
- 10 A. B. M. Jamaluddin, G. S. Larwar, M. A. Rahim, and M. K. Rahmon, *J. Chromatogr.*, 625 (1990) 496.
- 11 K. Chang, *Methods Find. Exp. Clin. Pharmacol.*, 8 (1986) 721.
- 12 S. Oldfield, J. D. Berg, H. J. Stiles and B. M. Buckley, *J. Chromatogr.*, 377 (1986) 423.



CHROMSYMP. 2422

# High-performance liquid chromatographic analysis of FCE 24304 (6-methylenandrosta-1,4-diene-3,17-dione) and FCE 24928 (4-aminoandrosta-1,4,6-triene-3,17-dione), two new aromatase inhibitors

Stefano Del Nero\*, Mario Di Somma and Aristide Vigevani

Department of Analytical Chemistry, R & D Farmitalia Carlo Erba Srl, Erbamont Group, Via Dei Gracchi 35, 20146 Milan (Italy)

## ABSTRACT

The cytochrome P-450-dependent aromatase enzyme plays an important role in hormone-dependent diseases. Many products that inhibit this type of enzyme were obtained: FCE 24304 (I) and FCE 24928 (II) proved to possess remarkable activity and are presently under development. Compounds I and II and their synthetic intermediates are analyzed by means of a high-performance liquid chromatographic method, affording rapid and efficient separation, good resolution and identification of all the examined compounds. The linearity, specificity, sensitivity, precision and accuracy for the method are also provided.

## INTRODUCTION

Aromatase, a cytochrome P-450-dependent enzyme, catalyzes the conversion of androgens to estrogens [1]. This enzyme affects the rate-limiting step in estrogen production and therefore it is supposed to play a key role in the pathogenesis of estrogen-dependent diseases.

The conversion of androgens to estrogens by aromatase has been demonstrated [1–4], the mechanism of aromatization reported [5], and the enzyme purified from human placental microsomes [5–9].

A series of steroid compounds were synthesized and tested for their aromatase inhibitory activity. Among them FCE 24304 (I, 6-methylenandrosta-1,4-diene-3,17-dione) and FCE 24928 (II, 4-aminoandrosta-1,4,6-triene-3,17-dione) (Fig. 1) exhibited good activity and remarkable stability [10,11].

In this paper a high-performance liquid chromatographic (HPLC) method for quantitation of FCE 24304 (I) and FCE 24928 (II) and separation of related synthetic intermediates is reported, and the experimental parameters for separation of artifi-

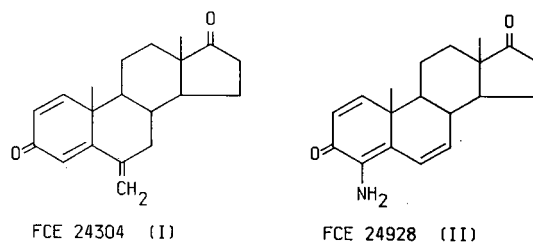


Fig. 1. Chemical structures of FCE 24304 (I) and FCE 24928 (II).

cial mixtures of I, II, and related substances are described (Figs. 2 and 3).

## EXPERIMENTAL

HPLC-grade acetonitrile and other chemicals of analytical grade were obtained from Carlo Erba (Milan, Italy). Buffer solutions were filtered before use through a Millipore 0.45- $\mu$ m filter.

The HPLC system consisted of a Hewlett-Packard (HP) 1090 LUSI chromatograph equipped with

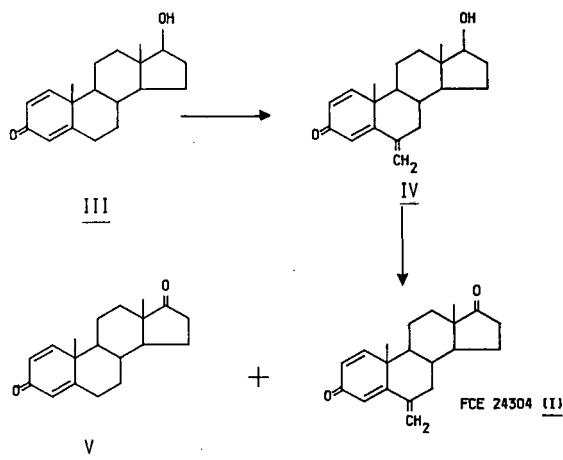


Fig. 2. Synthesis of FCE 24304 (I).

an HP 79847B temperature-controlled autosampler, and HP 1040A variable-wavelength detector (with a DPU multichannel integrator and an HP 85 B computer), an HP 2225 think-jet printer and an HP 7470A plotter.

Phosphate buffer (eluent A) was prepared by dissolving dibasic ammonium phosphate (6.60 g, 0.05 mol) in deionized water (1000 ml) filtered with a Milli-Q3 system (Waters), and adjusting to pH 6.0 with concentrated phosphoric acid; eluent B consisted of a mixture of eluent A and acetonitrile (30:70, v/v).

Isocratic elution with 45% B for 3 min followed by a linear gradient to 96% B in 20 min was used.

A Partisphere 5C<sub>18</sub> cartridge (Whatman, 110 ×

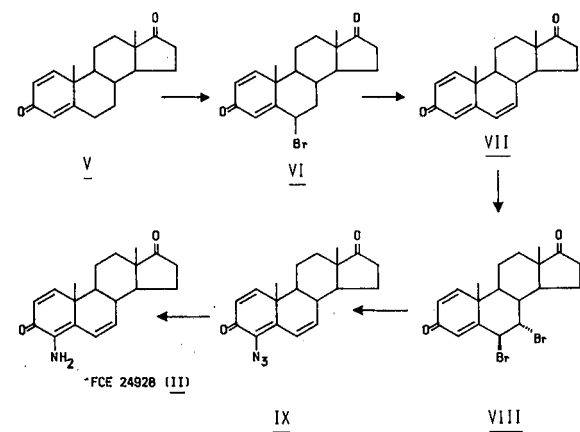


Fig. 3. Synthesis of FCE 24928 (II).

4.7 mm I.D., 5  $\mu$ m particle size), at 40°C with flow-rate of 1 ml/min was used.

UV detection was at 245 and 220 nm. The samples were dissolved in eluent A–acetonitrile (90:10, v/v) immediately before use.

## RESULTS AND DISCUSSION

The described gradient elution, with increasing acetonitrile content, is necessary for selective elution of the synthetic intermediates.

The reproducibility of the chromatographic system is high: the resolution of the compounds of interest does not change whereas, as expected, the relative retention times decrease with increasing column lifetime. The retention times of the compounds change by no more than approximately 1% during an 8-h run; however, it is possible to use the column for several months of continuous use.

Two chromatograms of an artificial mixture of compounds I and III–V and compounds II and V–IX are shown in Fig. 4; all the products were dissolved in eluent A (ammonium phosphate 0.05 M, pH 6.0) containing a small amount of acetonitrile (about 10%).

Note that the by-product (V) in the synthesis of FCE 24304 (I) is also the starting material for the synthesis of FCE 24928 (II) (see Figs. 2 and 3).

The elution patterns, with increasing retention times, are in the order: III, V, IV, I and II, VII, V, VI, VIII, IX. Other impurities are also well separated. The chromatographic method provides good resolution of all peaks and allows separation, identification and quantitative determination of these compounds, if present.

Satisfactory results for FCE 24304 (I) and FCE 24928 (II), in terms of both linearity and of sensitivity [quantitation limits are better than 0.5  $\mu$ g/ml (I) and 0.75  $\mu$ g/ml (II)] were obtained; linear relationships between peak areas and amounts of products injected are observed in the ranges 10–90  $\mu$ g/ml (I) and 60–490  $\mu$ g/ml (II).

### Regression equations

Area = slope  $\times$  concentration + intercept.

(I) Area counts = 109.4  $\times$  (concentration in  $\mu$ g/ml) + 15.6

(II) Area counts = 33.1  $\times$  (concentration in  $\mu$ g/ml) + 227.7

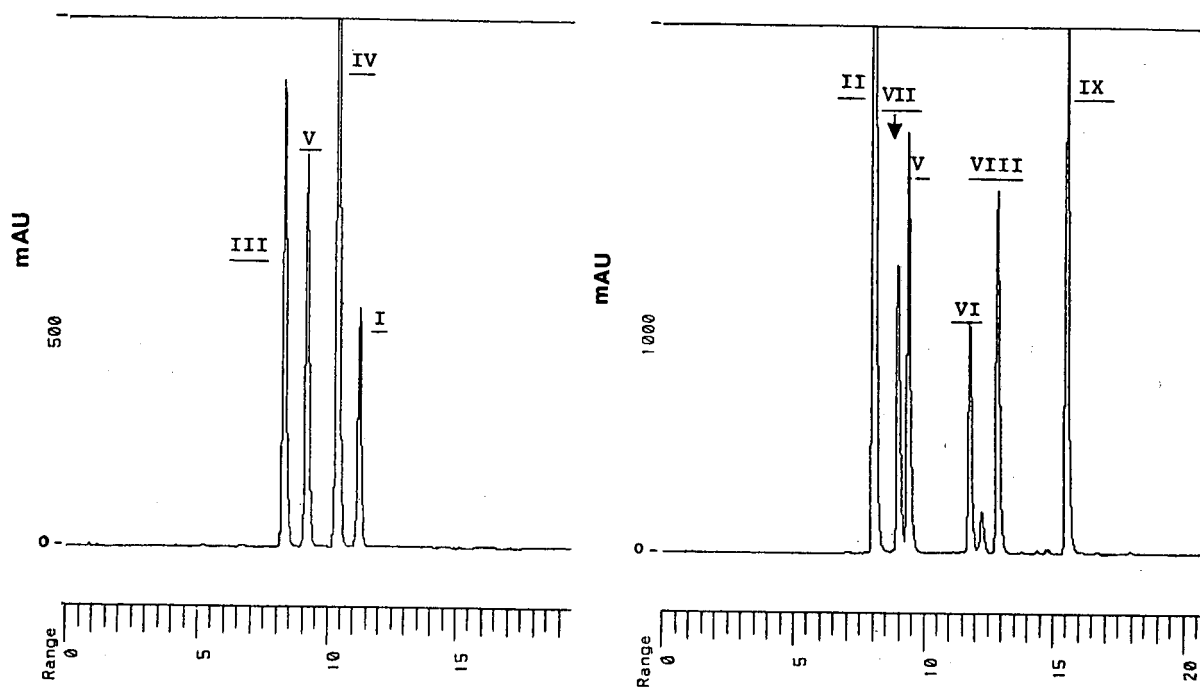


Fig. 4. Chromatograms of artificial mixtures of products I and III-V and products II and V-IX; conditions as reported in the text.

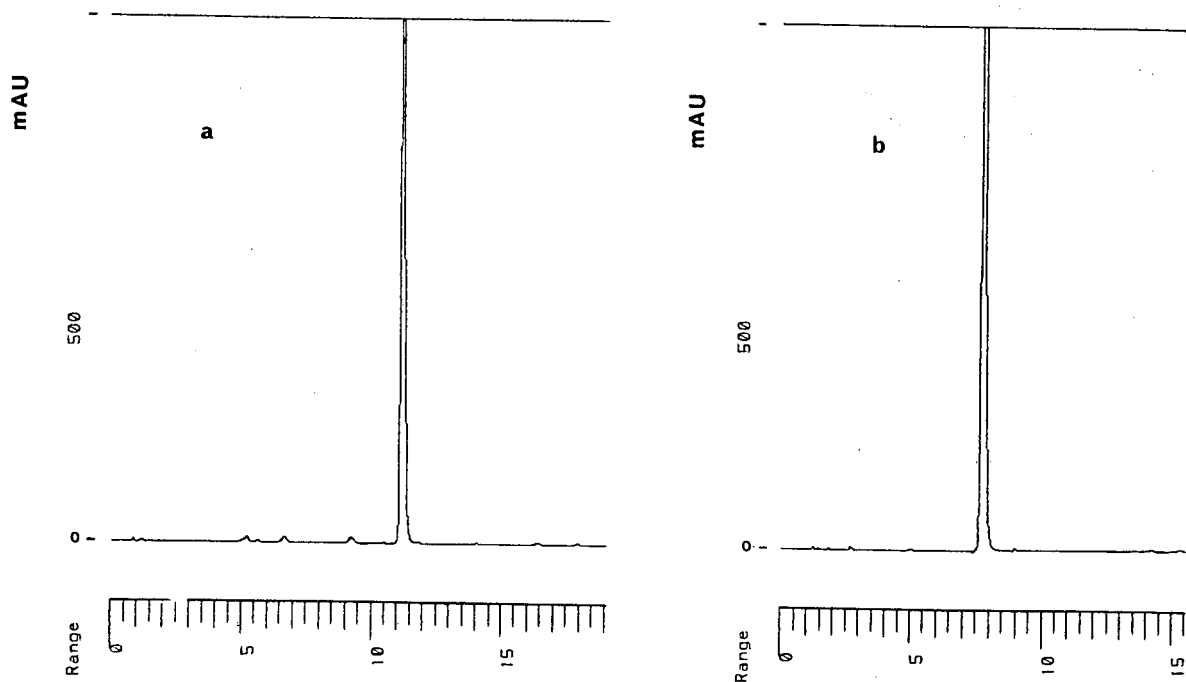


Fig. 5. Chromatograms of representative lots of I (a) and II (b).

From calibration plots, the relative correlation coefficients are: FCE 24304 (I),  $r = 0.99968$ ; FCE 24928 (II),  $r = 0.99753$ .

The chromatographic method provides also satisfactory specificity, precision and accuracy for I and II analyses.

#### Specificity

No interferences of sample solvent [0.05 M ammonium phosphate, pH 6.0–acetonitrile (90:10, v/v)] and synthetic impurities (see Figs. 2 and 3) could be observed at the detection wavelength (245 nm), as shown in Fig. 5.

From the chromatograms, only product (V) is recognized as an impurity in FCE 24304 (I), but it was not determined quantitatively. However, the separation of very low amounts of unknown impurities is also observed.

#### Precision

The following results were obtained from seven replicate injections of the same solutions. FCE 24304 (I): concentration = 105.6  $\mu\text{g/ml}$ ; S.D. =  $\pm 0.389$ ; precision =  $\pm 0.95\%$ . FCE 24928 (II): concentration = 220.2  $\mu\text{g/ml}$ ; S.D. =  $\pm 0.248$ ; precision =  $\pm 0.60\%$ .

#### Accuracy

From three replicate injections of every solution at five different concentrations the accuracy was for FCE 24304 (I), S.D. =  $\pm 0.761$ ; for FCE 24928 (II), S.D. =  $\pm 0.540$ .

#### Stability

The stabilities of I and II in the injection solution were also studied with the present chromatographic system. The solutions (at concentrations of about 100 and 200  $\mu\text{g/ml}$ , respectively) were stored at room temperature (about 25°C) and the area counts of the relative peaks with respect to the initial time

were measured as function of the time.

Under these conditions FCE 24304 (I) proved to be stable, whereas FCE 24928 (II) slowly decomposed with formation of one degradation product (with a shorter retention time than that of FCE 24928), at present unidentified.

#### CONCLUSIONS

The use of the described HPLC method allows a selective and quantitatively accurate analysis of steroid aromatase inhibitor compounds and the determination of possible impurities in the active drug substance. The chromatographic method is sufficiently specific, accurate, precise and sensitive for the purpose of analytical characterization.

#### ACKNOWLEDGEMENTS

We wish to thank Mr. G. Vasconi for participation in the set-up of the FCE 24304 analytical method, and Mr. M. Stefani for technical assistance.

#### REFERENCES

- 1 H. Taniguchi, H. R. Feldmann, M. Kaufmann and W. Pyerin, *Anal. Biochem.*, 181 (1989) 167.
- 2 R. D. H. Heard, P. H. Jellink and V. J. O'Donnel, *Endocrinology*, 57 (1955) 200.
- 3 K. J. Ryan, *J. Biol. Chem.*, 234 (1959) 268.
- 4 E. A. Thompson and P. K. Suteri, *J. Biol. Chem.*, 249 (1974) 5373.
- 5 J. T. Kellis and L. E. Vickery, *J. Biol. Chem.*, 262 (1987) 4413.
- 6 L. Tan and N. Muto, *J. Biochem.*, 156 (1986) 243.
- 7 N. Harada, *J. Biochem.*, 103 (1988) 106.
- 8 S. Nakajin, M. Shinoda, and P. F. Hall, *Biochem. Biophys. Res. Commun.*, 134 (1986) 704.
- 9 D. D. Hagermann, *J. Biol. Chem.*, 262 (1987) 2398.
- 10 A. Longo and P. Lombardi, *Br. Pat.* GB-B-2 177 700 (1985).
- 11 F. Faustini, R. D'Alessio, V. Villa, E. Di Salle, and P. Lombardi, *Br. Pat.*, GB-B-2 171 100 (1985).

# High-performance liquid chromatographic determination of monohydroxy compounds by a combination of pre-column derivatization and post-column reaction detection

Venkata K. Boppana\*, Richard C. Simpson, Kathleen Anderson, Cynthia Miller-Stein, Timothy J. A. Blake, Bruce Y.-H. Hwang and Gerald R. Rhodes

*Department of Drug Metabolism and Pharmacokinetics, SmithKline Beecham Pharmaceuticals, P.O. Box 1539, Mail Code L-712, King of Prussia, PA 19406 (USA)*

---

## ABSTRACT

A novel high-performance liquid chromatographic method was developed for the determination of monohydroxy compounds using the combined approach of pre-column derivatization and post-column reaction with fluorescence detection. Monohydroxy-containing drugs were modified by pre-column derivatization with propyl isocyanate (in pyridine, 50°C, 1 h) to form the corresponding *n*-propyl carbamate esters. Excess of reagent, reagent impurities and solvent were then removed by evaporation. Following chromatographic separation on a reversed-phase octadecylsilica column, the *n*-propyl carbamate ester derivative was subjected to post-column reaction and detection using alkaline hydrolysis to generate free propylamine, which was subsequently derivatized in-line using *o*-phthalaldehyde and 3-mercaptopropionic acid to form a fluorescent isoindole. The fluorescence emission of the isoindole product was measured at 455 nm following excitation at 340 nm. As propyl isocyanate is highly volatile and physico-chemically different to many drug molecules, problems associated with reagent impurities and reaction by-products were substantially minimized. The method was highly sensitive, allowing detection of sub-nanogram amounts of monohydroxy-containing drugs, hydroxy steroids and hydroxamic acids. The utility of this derivatization scheme was demonstrated by the highly sensitive measurement in human plasma of oxiracetam (4-hydroxy-2-oxo-1-pyrrolidineacetamide), an investigational drug intended for use in dementia and other memory disorders.

---

## INTRODUCTION

The chemical modification of hydroxyl groups to improve the detectability of certain analyte molecules for high-performance liquid chromatographic (HPLC) applications typically involves pre-column derivatization with relatively large non-volatile chromophoric [1] or fluorescent reagents [2–7]. However, the use of such an approach to develop highly sensitive methodology for the determination of hydroxy-containing drugs at trace levels in biological fluids is complicated by several difficulties. The large excess of reagent concentration necessary to ensure complete and reproducible reaction with the analyte and the physico-chemical similarity between many chromophoric and fluorescent reagents and drug molecules necessitate extensive sample clean-up following reaction to remove excess of re-

agent and reagent impurities, in addition to derivatized interferences resulting from endogenous compounds. In most instances, clean-up approaches following derivatization are only partly successful, and interferences from reagent impurities limit the ultimate sensitivity that can be achieved.

In our approach, hydroxy-containing drugs were modified by pre-column derivatization with propyl isocyanate to form the corresponding *n*-propyl carbamate esters. Excess of reagent, reagent impurities and solvent were then removed by evaporation. Following chromatographic separation on a reversed-phase column, the *n*-propyl carbamate ester derivatives were subjected to post-column alkaline hydrolysis to generate free propylamine, which was subsequently derivatized in-line using *o*-phthalaldehyde and 3-mercaptopropionic acid to form a fluorescent isoindole. As propyl isocyanate is highly

volatile and physico-chemically different to many drug molecules, problems associated with reagent impurities and reaction by-products were substantially minimized. The utility of this derivatization scheme was demonstrated by the sensitive measurement in human plasma of an investigational drug, oxiracetam (4-hydroxy-2-oxo-1-pyrrolidineacetamide), intended for use in dementia and other memory disorders.

## EXPERIMENTAL

### Materials

Oxiracetam (SK&F 107823, I, Fig. 1) and the internal standard (ISF 2839, I.S.) were obtained from ISF Laboratories (Milan, Italy). HPLC-grade water (Milli-Q water purification system; Millipore, Bedford, MA, USA) was used in the preparation of standard solutions, buffers and mobile phase. Analytical-reagent grade glacial acetic acid and sodium hydroxide were purchased from Mallinckrodt (Paris, KY, USA), HPLC-grade methanol and acetonitrile from J. T. Baker (Phillipsburg, NJ, USA), silylation-grade pyridine and *o*-phthalaldehyde (OPA) from Pierce (Rockford, IL, USA), propyl isocyanate (99%), phenyl isocyanate and benzohydroxamic acid from Aldrich (Milwaukee, WI, USA) and 3-mercaptopropionic acid and all steroid compounds from Sigma (St. Louis, MO, USA). All other chemicals were analytical-reagent grade. Phenylboronic acid (PBA) solid-phase extraction columns (100 mg/ml) were purchased from Analytichem International (Harbor City, CA, USA).

### *o*-Phthalaldehyde reagent solution

Sodium hydroxide (2 g) was first dissolved in 1 l of degassed HPLC-grade water and then 2 ml of freshly prepared methanolic solution of *o*-phthalaldehyde (2 mg/ml) and 80  $\mu$ l of 3-mercaptopropionic acid were added. The solution was filtered through

a 0.45- $\mu$ m nylon 66 filter. The reagent was stable for 48 h at room temperature.

### Standard solutions

The stock (1 mg/ml) and working standard solutions (100, 10, 1 and 0.1  $\mu$ g/ml) of oxiracetam and the internal standard were prepared in water. The solutions were stable for 1 month. The stock and standard solutions of steroids and hydroxamic acids were prepared in pyridine.

### Pre-column derivatization of monohydroxy compounds

To the tubes containing oxiracetam or monohydroxy-containing analytes, anhydrous pyridine (200  $\mu$ l) and propyl isocyanate (50  $\mu$ l) were added and the solution was vortex mixed. The tube was sealed with Parafilm and placed in a water-bath maintained at 50°C for 1 h. The solvents were evaporated at 50°C under nitrogen and the residue was dissolved in the mobile phase.

### Mass spectrometric (MS) analysis of *n*-propyl carbamate derivatives

LC-MS was performed using an HP 1090A HPLC system (Hewlett-Packard, Waldbronn, Germany) interfaced to a Finnigan MAT (San Jose, CA, USA) TSQ 70 triple quadrupole mass spectrometer via a Finnigan MAT thermospray ionization (TSP) interface. Chromatographic separations were carried out on a Hypersil ODS column (10 cm  $\times$  4.6 mm I.D.) (Hewlett-Packard) using a mobile phase of ammonium formate (0.1 M, pH 3.8)-acetonitrile at a flow-rate of 1 ml/min. Subsequent to injection (3.5 min), the concentration of acetonitrile was increased linearly from 0 to 35% over a period of 25 min, held at that level for 2 min and then cycled back to the initial conditions. Mobile phase components were filtered through a 0.2- $\mu$ m nylon 66 filter and degassed before use. The TSP vaporizer temperature was 108°C and the jet temperature was 260°C.

LC-MS with continuous-flow fast atom bombardment (CF-FAB) ionization was performed using the same HPLC system as above interfaced to the Finnigan MAT TSQ 70 via a Finnigan MAT BIO Probe ion source. Ionization was accomplished using xenon as the bombarding gas and a VCR Group (San Francisco, CA, USA) saddle-field gun



Fig. 1. Structures of oxiracetam (I) and the internal standard (I.S.).

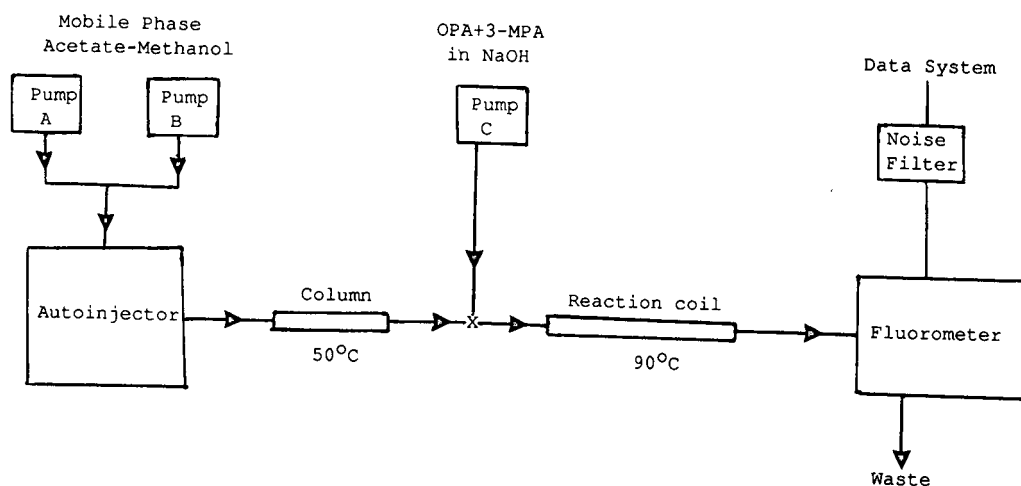


Fig. 2. Schematic diagram of the chromatographic system.

operated at 6 kV and 2 mA. Isocratic chromatographic separations were carried out on Zorbax Rx octyl column (15 cm  $\times$  2.1 mm I.D.) (Mac Mod Analytical, Chadds Ford, PA, USA) using a mobile phase consisting of 60% water and 40% organic modifier [acetonitrile-methanol (50:7, v/v)]. The mobile phase contained 5% glycerol and 0.1% trifluoroacetic acid. The flow-rate of the mobile phase was 250  $\mu$ l/min. A flow splitter was placed before the UV flow cell, which reduced the flow of mobile phase into the mass spectrometer to 2  $\mu$ l/min. The probe tip temperature was held at 26°C to prevent freezing. For all analyses, the mass spectrometer was operated in alternating positive-negative ion full-scan modes.

#### High-performance liquid chromatography

The HPLC system (Fig. 2) consisted of a Hitachi 665A-12 high-pressure gradient semi-micro solvent delivery system (EM Science), a post-column reactor module (PCRS Model 520; ABI Analytical, Ramsey, NJ, USA) and a Hitachi F-1000 fluorescence detector (EM Science). Chromatographic separations were carried out on a 25 cm  $\times$  2.0 mm I.D., octadecylsilica (5  $\mu$ m) column (Ultrasphere) (Beckman Instruments, Palo Alto, CA, USA), maintained at 50°C, at a flow-rate of 300  $\mu$ l/min. The initial mobile phase composition was 0.05 M acetate buffer (pH 6.0)-methanol (90:10, v/v). Following injection, the methanol concentration was held at 10% for 5 min, then raised to 20% over a

period of 4 min, held for 1 min, then increased to 50% in 1 min, held at 50% for 5 min and cycled back to the initial conditions in 1 min. The system was equilibrated at the initial mobile phase composition for 14 min before injecting the next sample. Mobile phase components were filtered through a 0.2- $\mu$ m nylon 66 filter and degassed before use. Samples were injected using an HPLC autosampler (WISP, Model 710B; Waters Assoc., Milford, MA, USA). The post-column reactor module contains two independently heated zones which are used, in this instance, as a column heating chamber and a reaction coil heating block. One additional pump (Model 114, Beckman Instruments) was utilized to deliver the OPA reagent solution at a flow-rate of 200  $\mu$ l/min to the post-column reactor where they were mixed with the column effluent utilizing a low-dead-volume mixer. Following formation of the fluorescent reaction product, detection was accomplished utilizing excitation at 340 nm while monitoring the fluorescence emission at 455 nm. The chromatographic data were collected with a computerized automated laboratory system (Access\*Chrom; PE-Nelson, Cupertino, CA, USA).

#### RESULTS AND DISCUSSION

Initial attempts to derivatize monohydroxy-containing drugs with various commercially available fluorogenic reagents, such as 9-anthrolylnitrile [3], 7-methoxycoumarin-3-(and 4-)-carbonyl azides [4]

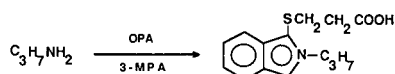
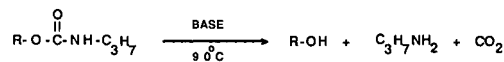
PRE-COLUMNPOST-COLUMN

Fig. 3. Schematic representation of reactions showing the pre-column conversion of hydroxy compounds to *n*-propyl carbamate compounds and post-column conversion of the latter into fluorescent isindole structures.

and 7-[(chlorocarbonyl)methoxyl]-4-methylcoumarin [6], were problematic owing to the difficulties associated with the stability of these reagents. Various environmental factors, such as moisture, temperature and light, affect the stability during storage and lead to very short shelf lives for these reagents. These problems often require either custom synthesis or repurification of reagents. Moreover, the large excess of reagent concentration employed to ensure the complete and reproducible reaction with the analyte and the physico-chemical similarity between the derivatized products and the reagent typically necessitate extensive sample purification following reaction to remove excess of reagent and numerous reagent impurities, in addition to derivatized interferences due to endogenous compounds. In our approach, hydroxy-containing drugs were first modified by pre-column derivatization with propyl isocyanate to form the corresponding *n*-propyl carbamate esters. Following removal of the excess reagent and solvent by evaporation, the carbamate esters were separated by reversed-phase HPLC and then subjected to simultaneous post-column base hydrolysis and derivatization of the liberated propylamine with OPA–thiol (Fig. 3).

Several aliphatic and aromatic isocyanates were examined for pre-column derivatization of monohydroxy compounds to form carbamate esters.

Based on the use of oxiracetam as a model compound, propyl isocyanate was chosen owing to its superior physico-chemical properties, such as ease of handling, safety, reactivity and ease of removal from the reaction medium. Propyl isocyanate is a liquid which is less volatile than its lower homologues, and can be handled safely. In comparison with phenyl isocyanate, however, the volatility and ease of hydrolysis of carbamate esters favored propyl isocyanate for pre-column derivatization of monohydroxy compounds.

The formation of the *n*-propyl carbamate ester of oxiracetam was confirmed by both post-column reaction detection via fluorescence response and mass spectral evidence. The *n*-propyl carbamate ester of oxiracetam was subjected to LC–TSP–MS analysis, and the positive ion mass spectrum is shown in Fig. 4A. The protonated molecular ion ( $[M+H]^+$ ,  $m/z = 244$ ) was observed as the base peak of the spectrum. The corresponding ammonium, sodium and potassium adduct ions were observed at  $m/z$  261, 266 and 282, respectively. Loss of propyl isocyanate ( $C_3H_7N=C=O$ ) from the  $[M+H]^+$  ion yielded the ion at  $m/z$  159. The ion at  $m/z$  141 indicated loss of the elements of *n*-propyl carbamate. The negative ion mass spectrum is shown in fig. 4B. It shows a base peak ion at  $m/z$  288, which corresponds to the formate molecular anion adduct ( $[M+HCOO]^-$ ) of the *n*-propyl carbamate derivative of oxiracetam. Loss of *n*-propyl ketene from the ion at  $m/z$  288 yielded the ion at  $m/z$  203.

The pre-column formation of *n*-propyl carbamate esters of hydroxy compounds was optimized by using oxiracetam as a model compound. As oxiracetam was highly hydrophilic in nature, pyridine was chosen to conduct the reaction. The reaction was carried out at different temperatures for various times and the HPLC with post-column hydrolysis and fluorescence detection was used to obtain peak heights. Derivatized oxiracetam was separated by gradient elution HPLC using the mobile phase conditions described under Experimental. By varying the pre-column reaction temperature between 30 and 80°C, it was observed that the reaction rate was optimum when the temperature of the reaction was maintained between 50 and 60°C. The effect of pre-column reaction time was also examined by allowing the reaction to proceed from 30 to 240 min at 50°C. The results from this experiment indicated



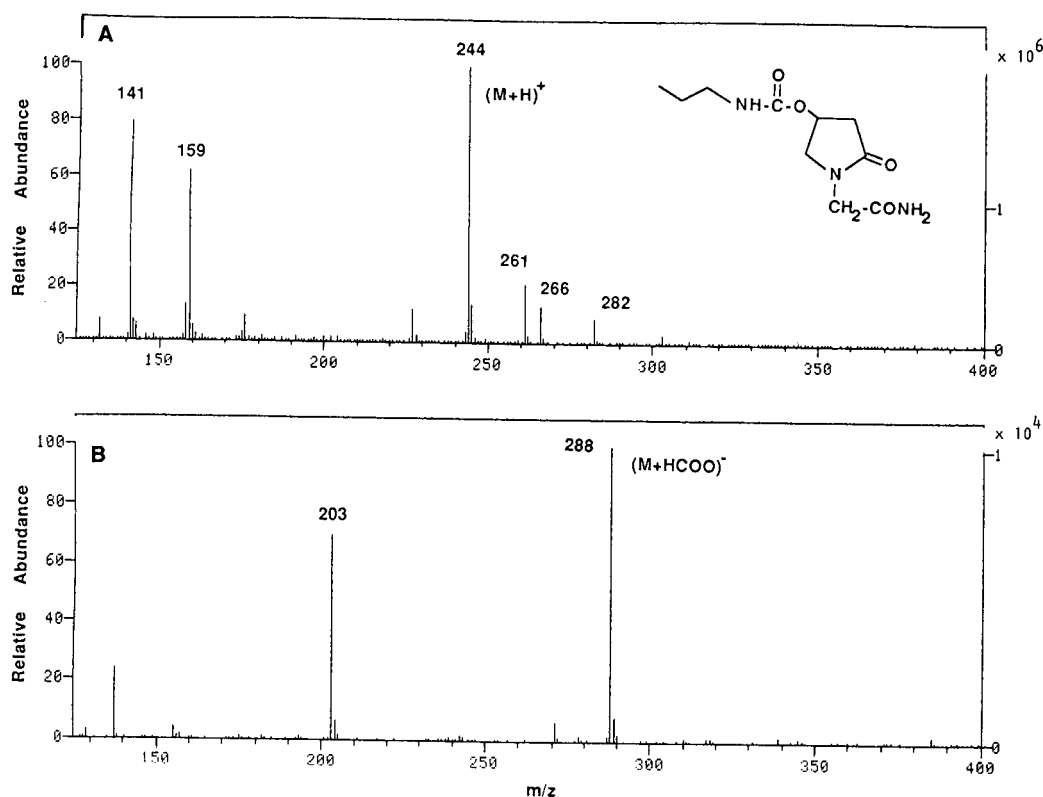


Fig. 4. LC-TSP-MS of oxiracetam *n*-propyl carbamate: (A) positive ion mass spectrum; (B) negative ion mass spectrum.

that a reaction time of 60 min was necessary to obtain optimum yields of the carbamate derivative. Using  $^3\text{H}$ -labelled oxiracetam, and following the disappearance of oxiracetam and the formation of the carbamate ester in the reaction mixture by isocratic HPLC with radiometric detection (Beckman), it was determined that the conversion of oxiracetam to the *n*-propyl carbamate derivative was quantitative.

Post-column fluorescence detection of carbamates typically involves a two-stage (two-pump) reaction system [8]. The carbamate esters were first hydrolyzed to release a primary amine, which was subsequently derivatized on-line with *o*-phthalaldehyde and a thiol to form highly a fluorescent substituted isoindole. Of the several approaches available for post-column hydrolysis of carbamate esters, we selected base hydrolysis owing to its ease and simplicity. Moreover, it has been shown that *o*-phthalaldehyde and 3-mercaptopropionic acid

can both be added to the hydrolytic reagent solution [9], eliminating the need for a second post-column pump. This allows for the simultaneous hydrolysis and fluorescence detection of carbamates without compromising the sensitivity and offers the same advantages as offered by solid-phase reactors [10,11] and photolytic hydrolysis methods [12].

In order to optimize the reaction conditions for the 2.0 mm I.D. reversed-phase columns used here, certain post-column reaction parameters were examined using the *n*-propyl carbamate ester of oxiracetam as a model substrate. In these experiments, the post-column flow-rate and concentration of OPA and thiol reagent solution were maintained as described under Experimental. The post-column reaction conditions for the concentration of sodium hydroxide, temperature and reaction time were then optimized by injecting 10 ng of derivatized oxiracetam on to the column and monitoring the intensity of the fluorescence signal obtained.

The effect of base concentration was examined by varying the sodium hydroxide concentration from 0.01 to 0.3 *M*. The results indicated that a base concentration of 0.05 *M* provided the optimum fluorescence signal for derivatized oxiracetam. The effect of temperature on the post-column reaction was then examined by varying the reaction coil temperature from 40 to 110°C. A reaction temperature of 90°C was found to be optimum for the post-column derivatization. The effect of reaction coil volume (0.5–2.0 ml) on the post-column reaction was also examined. The 1.0-ml reaction coil provided the optimum chromatographic peak height without a significant change in peak broadening. These conditions were utilized in subsequent work.

In order to establish the applicability of this approach for the routine determination of monohydroxy compounds, the linearity and precision of the combined pre- and post-column reaction detection system were examined. The linearity was evaluated by analysis of a series of standard solutions of oxiracetam, and a linear response over the range 2–2000 ng injected on-column was obtained. The curves were highly reproducible and correlation coefficients were typically >0.999. The precision of the method was determined by repetitive pre-column derivatization of a standard solution of oxiracetam followed by post-column reaction detection and measurement of the resulting chromatographic peak heights. The method displayed excellent precision, yielding relative standard deviations (R.S.D) of <3% (*n*=6). The limit of detection (signal-to-noise ratio = 3) for oxiracetam was 0.5 ng.

The application of the method to the determination of monohydroxy-containing compounds was exemplified by the HPLC assay developed to determine the concentration of oxiracetam in human plasma. The assay involved precipitation of plasma protein with acetonitrile followed by application of the supernatant to a phenylboronic acid column and collection and evaporation of the breakthrough liquid containing the analyte. Other endogenous polyhydroxy compound interferences remained on the column. The residue obtained was then subjected to the pre-column derivatization and post-column reaction detection scheme described above. Typical chromatograms from extracts of a drug-free plasma sample and a plasma sample spiked with 1 µg/ml of oxiracetam are shown in Fig. 5. The

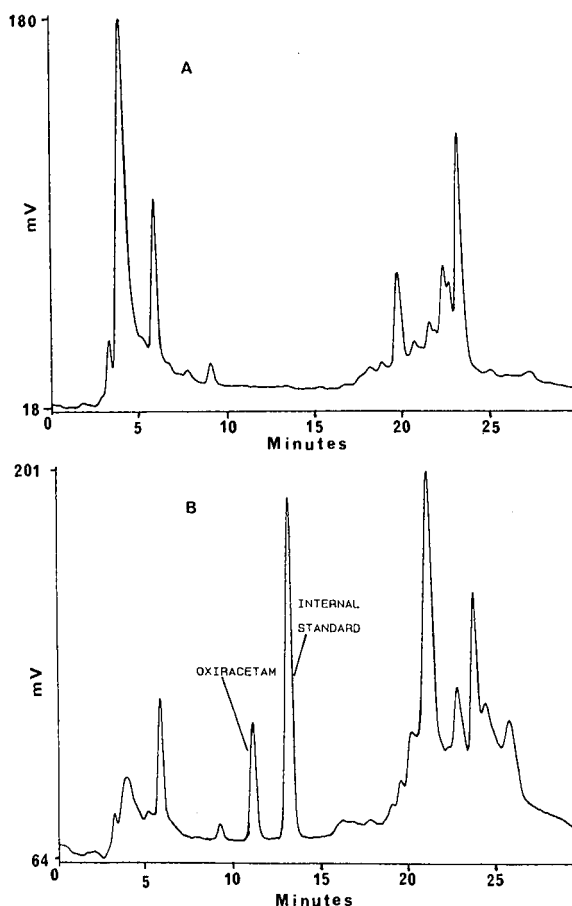


Fig. 5. Chromatograms of extracts of (A) drug-free plasma and (B) plasma sample spiked with 1 µg/ml of oxiracetam.

retention times for oxiracetam and the internal standard were 10.1 and 12 min, respectively. The chromatograms displayed no endogenous interfering peaks in the region of oxiracetam or the internal standard. Under the conditions utilized in this assay, the lowest concentration of oxiracetam that could be determined in 0.2 ml of plasma was 40 ng/ml, which corresponds to an injected amount of *ca.* 2 ng. The correlation coefficients for plasma calibration graphs were typically >0.99.

The method reported here may have general utility. This approach has also been applied to the HPLC detection of other classes of monohydroxy compounds such as steroids and hydroxamic acids. Of the various hydroxy steroids subjected to this carbamate derivatization procedure, aromatic ste-

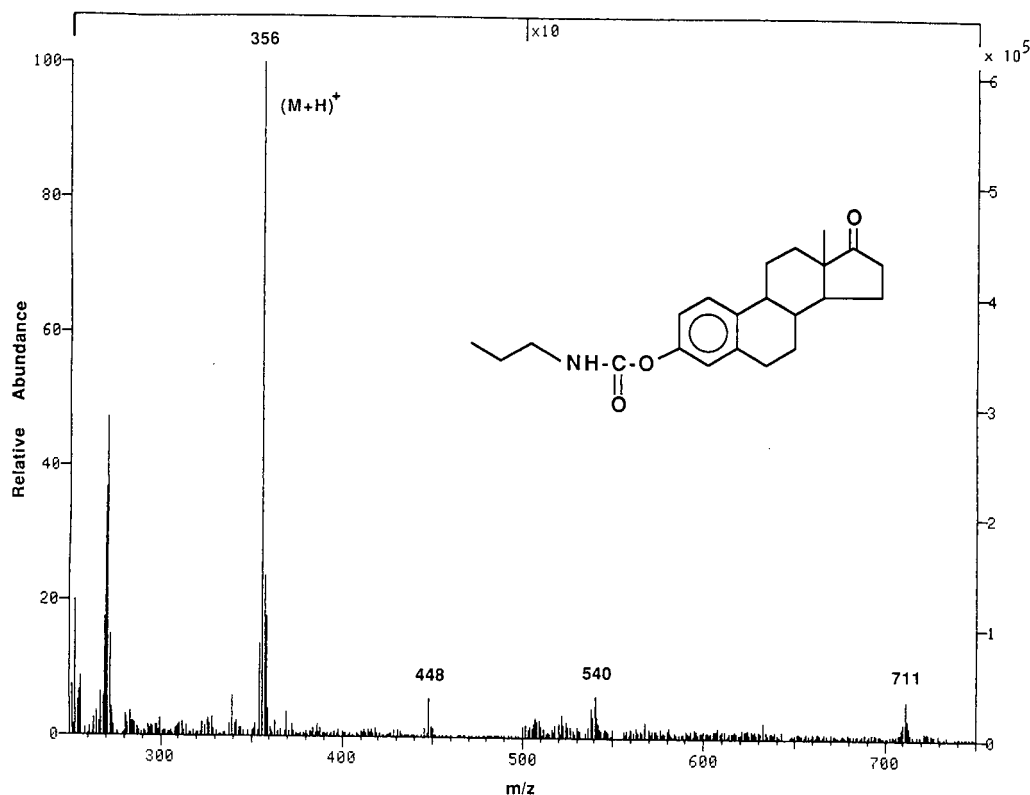


Fig. 6. LC-CF-FAB-MS of estrone *n*-propyl carbamate (positive ion mass spectrum).

roids, such as estrone, and steroids with a primary hydroxy group, such as cortisone, readily yielded the corresponding *n*-propyl carbamates, which were subsequently measured by HPLC with post-column reaction detection. The formation of estrone *n*-propyl carbamate was also confirmed by the positive ion CF-FAB mass spectrum (Fig. 6). The protonated molecular ion ( $[M+H]^+$ ,  $m/z = 356$ ) was observed as the base peak in the mass spectrum. The corresponding glycerol adduct ions were observed at  $m/z$  448 and 540. A protonated dimer of the molecular ion ( $[2M+H]^+$ ) was also observed at  $m/z$  711. The ion at  $m/z$  253 indicated loss of  $C_3H_7=N=C=O$ . Steroids such as progesterone, cholic acid and testosterone did not form the corresponding *n*-propyl carbamates under these conditions, presumably owing to steric hindrance effects [13]. Benzohydroxamic acid also readily yielded the *n*-propyl carbamate derivative, which was detectable by post-column reaction and fluorescence detection. The results of these studies suggest that certain

hydroxy compounds with complex structures may require additional optimization of the reaction conditions used to form the corresponding *n*-propyl carbamate derivatives. To achieve this, one may have to use different solvents, adjust the basicity of the reaction medium or employ various catalysts. As with many pre-column derivatization approaches, the potential reactivity of other functional groups with *n*-propyl isocyanate may lead to the formation of other by-products, thus complicating the analysis. In this instance, reaction of primary and secondary amine groups with *n*-propyl isocyanate has been observed, leading to the formation of substituted urea products.

The combined pre- and post-column reaction detection system described here provided a highly sensitive method for the fluorescence detection of certain monohydroxy compounds such as oxiracetam. The sensitivity of the method allowed its successful application to the determination of oxiracetam in human plasma samples. In addition, the method

may have some general utility as highly sensitive detection was also achieved with certain steroid compounds and hydroxamic acids.

## REFERENCES

- 1 F. Fitzpatrick and S. Siggia, *Anal. Chem.*, 45 (1973) 2310.
- 2 J. Goto, S. Komatsu, N. Goto and T. Nambara, *Chem. Pharm. Bull.*, 29 (1981) 899.
- 3 J. Goto, N. Goto, F. Shamsa, M. Saito, S. Komatsu, K. Suzaki and T. Nambara, *Anal. Chim. Acta*, 147 (1983) 397.
- 4 A. Takadate, M. Iwai, H. Fujino, K. Tahara and S. Goya, *Yakugaku Zasshi*, 103 (1983) 962.
- 5 A. Takadate, M. Irikura, T. Suehiro, H. Fujino and S. Goya, *Chem. Pharm. Bull.*, 33 (1985) 1164.
- 6 K. Karlsson, D. Wiesler, M. Alasandro and M. Novotny, *Anal. Chem.*, 57 (1985) 229.
- 7 Y. Tsuruta and K. Kohashi, *Anal. Chim. Acta*, 192 (1987) 309.
- 8 H. A. Moye, S. J. Scherer and P. A. St. John, *Anal. Lett.*, 10 (1977) 1049.
- 9 B. D. McGarvey, *J. Chromatogr.*, 481 (1989) 445.
- 10 L. Nondek, U. A. Th. Brinkman and R. W. Frei, *Anal. Chem.*, 54 (1983) 141.
- 11 L. Nondek, R. W. Frei and U. A. Th. Brinkman, *J. Chromatogr.*, 282 (1983) 141.
- 12 C. J. Miles and H. A. Moye, *Anal. Chem.*, 60 (1988) 220.
- 13 J. Goto, M. Saito, T. Chikai, N. Goto and T. Nambara, *J. Chromatogr.*, 276 (1983) 289.

# Direct high-performance liquid chromatographic resolution of a novel benzothiazine $\text{Ca}^{2+}$ antagonist and related compounds

Atsutoshi Ota\*, Susumu Ito and Yoichi Kawashima

Central Research Laboratories, Santen Pharmaceutical Co., Ltd., 9-19 Shimoshinjo 3-chome, Higashiyodogawa-ku, Osaka 533 (Japan)

## ABSTRACT

Enantiomers of 3,4-dihydro-2-(5-methoxy-2-[3-(N-methyl-N-{2-[(3,4-methylenedioxy)phenoxy]ethyl}amino)propoxy]phenyl)-4-methyl-3-oxo-2H-1,4-benzothiazine hydrogen fumarate (I), a novel and potent  $\text{Ca}^{2+}$  antagonist, and its synthetic precursors, phenol (II) and bromide (III), were directly resolved by high-performance liquid chromatography on a chiral column, with a stationary phase of cellulose carbamate-coated silica gel. Further, the resolution of some 2-(substituted-phenyl)benzothiazines (IVa–IVl) was investigated to study the effects of 2-phenyl ring substituents on chiral recognition. As an index of the characteristics of substituents, substituent constants for quantitative structure–activity relationship studies were used. The correlations between the resolution efficiency ( $R_s$ ) and the substituent constants for these benzothiazines were investigated by regression analysis. As a result, for 2-(4-substituted-phenyl)-benzothiazines,  $R_s$  showed good correlation with  $E_s$ , Taft's steric parameter [correlation coefficient ( $r$ ) = 0.99]. It was also shown that  $R_s$  correlated with  $R$ , an electronic constant for the resonance effect, for 2-(2-hydroxy-5-substituted-phenyl)benzothiazines ( $r$  = 0.92). These findings suggest that the 2-phenyl ring plays an important role in chiral recognition in the resolution of these benzothiazines.

## INTRODUCTION

In the course of our recent studies on sulphur-containing heterocyclic compounds [1–4], we found a novel 2-aryl-3-oxo-2H-1,4-benzothiazine derivative I (Fig. 1) with a potent  $\text{Ca}^{2+}$  antagonistic activity [5].  $\text{Ca}^{2+}$  antagonists are useful in the treatment of hypertension, angina pectoris and certain cardiac arrhythmias [6–8]. Compound I has an asymmetric carbon on the C-2 position of the benzothiazine ring. In an *in vitro* study, the  $\text{Ca}^{2+}$  antagonistic activity of the (*R*)-enantiomer was about seven times more than that of the (*S*)-enantiomer. The (*R*)-enantiomer (SD-3211) is now undergoing clinical trials.

During the progress of this research, an analytical method for the determination of optical purity was required for I and its synthetic precursors II and III (Fig. 1). In the present study, the direct resolution of enantiomers of these compounds with high-performance liquid chromatography (HPLC)

on a commercially available chiral column (Chiralcel OG) was investigated. The stationary phase of this chiral column is cellulose carbamate-coated silica gel [9]. Further, we became interested in the chiral recognition mechanism for these benzothiazine

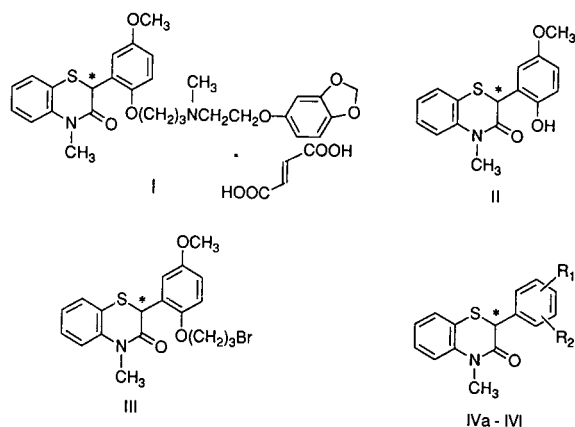


Fig. 1. Structures of benzothiazine derivatives I, II, III and IV.

derivatives. Since we had already developed a convenient method of synthesizing 2-(substituted-phenyl)benzothiazines [3], it was intended to study the effects of 2-phenyl ring substituents on chiral recognition by using these benzothiazines. In the present study, the correlations between the resolution efficiency and physicochemical properties of the substituents on the 2-phenyl ring for benzothiazines IVa–IVl (Fig. 1) were studied by applying the quantitative structure–activity relationship (QSAR) procedure.

## EXPERIMENTAL

### Materials

The benzothiazine derivatives I–III [5] and IVa–IVl [3], except IVj, were prepared as reported previously. Compound IVj was synthesized from a mandelic acid derivative, which was prepared from *m*-anisaldehyde and 2-methylaminobenzenethiol in accordance with the preparation of IVl.

### Liquid chromatography

Chiralcel OG (250 mm × 4.6 mm I.D.) was purchased from Daicel Chemical Industries. The chromatographic system was from Shimadzu (Kyoto, Japan) and consisted of a solvent-delivery pump (Model LC-6A) equipped with a UV detector (Model SPD-6A). The column was maintained at 30°C by a column oven (Model CTO-2A). The flow-rate was adjusted to 1.5 ml/min, and the detector was set to 238 nm. Chromatograms were recorded on a recorder (Model C-R2AX Chromatopac). Ethanol (1 ml) solutions of the samples (10 μmol) were diluted with mobile phase to give a 1 mM solution. Aliquots of 20 μl of the solutions were injected. The dead time ( $t_0$ ) of the column was estimated to be 2.2 min with 1,3,5-tri-*tert*-butylbenzene as a non-retained compound [10]. Capacity factors ( $k'_1$ ,  $k'_2$ ) were estimated as  $(t_1 - t_0)/t_0$  and  $(t_2 - t_0)/t_0$ , respectively. The separation factor ( $\alpha$ ) was calculated as  $k'_2/k'_1$ . Resolution ( $R_s$ ) was conveniently calculated as  $2(t_2 - t_1)/(W_1 + W_2)$ , where  $t_1$  and  $t_2$  are elution

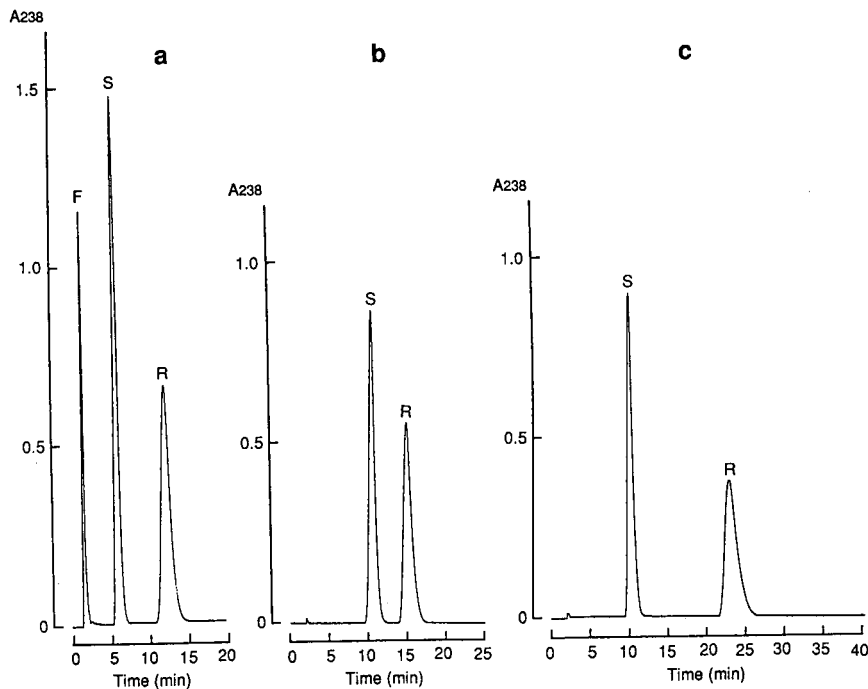


Fig. 2. Chromatograms of benzothiazine derivatives I (a), II (b) and III (c). In each chromatogram, R and S are (*R*)- and (*S*)-enantiomers, respectively. In the chromatogram of I (a), F is fumaric acid.

times and  $W_1$  and  $W_2$  are band widths. Subscripts 1 and 2 represent the first- and the second-eluting enantiomers, respectively.

## RESULTS AND DISCUSSION

### *Resolution of enantiomers of I and its synthetic precursors, II and III*

In the investigation of resolution, *n*-hexane and alcohol (methanol and/or ethanol and/or 2-propanol) mixtures were examined as eluents. Of these, a *n*-hexane-ethanol (85:15) mixture gave the best results for II and III. Under this condition, enantiomers of II and III were completely resolved.  $k'_1$  and  $k'_2$  were estimated as 3.63 and 5.69, respectively for II, and as 3.63 and 9.29, respectively for III;  $\alpha$  was found to be 1.57 and 2.56, respectively.  $R_s$  values were 2.63 and 6.28, respectively. In the case of I, addition of a small amount of diethylamine to the eluent was required. Without diethylamine, I could not be eluted. Enantiomers of I were completely resolved by using a *n*-hexane-ethanol-diethylamine (50:450:1) mixture as the eluent, with  $k'_1 = 1.64$ ,  $k'_2 = 4.39$ ,  $\alpha = 2.67$  and  $R_s = 4.31$ . Chromatograms of I-III are shown in Fig. 2. In all cases, the (*S*)-enantiomer was the first-eluting isomer.

### *Resolution of enantiomers of 2-(substituted-phenyl)-benzothiazines IVa-IVl*

The resolution of the enantiomers of 2-(substituted-phenyl)benzothiazines IVa-IVl was investigated under the same condition as that for II and III. The results are summarized in Table I. For most of the compounds, the enantiomers were partially or completely resolved.

In order to study the effects of 2-phenyl ring substituents on chiral recognition, the QSAR procedure was applied. Of the QSAR procedures, the Hansch-Fujita approach has been most widely used [11]. It assumes that the potency of a certain biological activity is expressible in terms of a function of the substituent constants [12], which represent the various physicochemical characteristics. Thus, correlations between the resolution efficiency, which was used instead of biological activity, and several substituent constants were investigated for these 2-(substituted-phenyl)benzothiazines by regression analysis. As a result, the following correlations were found. First, as shown in Fig. 3a,  $R_s$  showed good correlation with  $E_s$ , Taft's steric parameter, for 2-(4-substituted-phenyl)benzothiazines IVa-IVe [correlation coefficient ( $r$ ) = 0.99]. The compounds whose *para*-substituent on the 2-phenyl ring had an  $E_s$  value close to 0 gave better resolution. It seems

TABLE I  
RESOLUTION OF ENANTIOMERS (COMPOUNDS II AND IVa-IVl)

Compound	$R_1$	$R_2$	$k'_1$	$k'_2$	$\alpha$	$R_s$
IVa	H	H	1.51	1.94	1.28	1.33
IVb	4-OH	H	3.66	4.34	1.18	0.99
IVc	4-OCH <sub>3</sub>	H	2.33	2.69	1.16	0.86
IVd	4-Cl	H	1.26	1.45	1.15	0.60
IVe	4-CH <sub>3</sub>	H	1.31	1.43	1.10	0.30
IVf	2-OH	H	1.90	2.25	1.18	0.83
II	2-OH	5-OCH <sub>3</sub>	3.63	5.69	1.57	2.63
IVg	2-OH	5-Cl	1.48	1.69	1.14	0.50
IVh	2-OH	5-CH <sub>3</sub>	1.56	1.81	1.16	0.62
IVi	2-OH	5-NO <sub>2</sub>	2.85	2.95	1.04	~0
IVj	H	3-OCH <sub>3</sub> (5-OCH <sub>3</sub> )	2.24	3.03	1.35	1.86
IVk	2-OCH <sub>3</sub>	5-OCH <sub>3</sub>	3.20	5.93	1.85	3.76
IVl	2-OBz <sup>a</sup>	5-OCH <sub>3</sub>	3.39	5.46	1.61	2.76

<sup>a</sup> Bz = benzyl group.

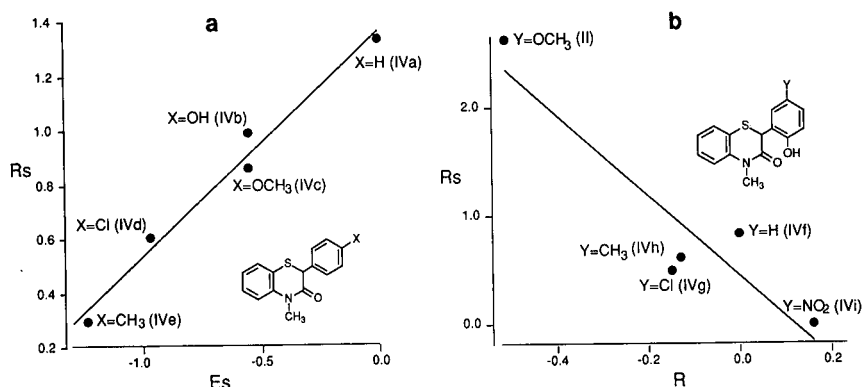


Fig. 3. Plots of resolution factor ( $R_s$ ) against substituent constant. (a) Correlation between  $R_s$  and Taft's steric parameter ( $E_s$ ) for 4-(substituted-phenyl)benzothiazines (IVa–IVe). (b) Correlation between  $R_s$  and Swain–Lupton's constant for resonance effect ( $R$ ) for 2-(2-hydroxy-5-substituted-phenyl)benzothiazines (II and IVf–IVi).

that a smaller *para*-substituent is better for resolution. Second, as shown in Fig. 3b,  $R_s$  showed a correlation with  $R$ , an electronic constant for the resonance effect, for 2-(2-hydroxy-5-substituted-phenyl)benzothiazines II and IVf–IVi ( $r = 0.92$ ). The compounds in which the substituent on the 5-position of 2-phenyl ring had a smaller  $R$  were resolved more efficiently. This suggested that substituents donating their electrons to the 2-phenyl ring by the resonance effect are favourable for good resolution. The fact that IVj gave better resolution than IVa might be also explained by this correlation. These findings suggest that the electron-rich 2-phenyl ring is desirable for resolution. This could be supported by the fact that 2-(2-substituted-5-methoxyphenyl)benzothiazines with a hydroxy or alkoxy group as a substituent, *i.e.* II, IVk and IVl, showed significant resolution.

Okamoto *et al.* [9] showed the importance of hydrogen bonding between the carbamate group of the stationary phase and the solute for chiral recognition. Since the benzothiazine derivatives examined in this study have an amido carbonyl group, such hydrogen bonding is likely to occur. This interaction might play an important role in chiral recognition. In addition, Okamoto *et al.* [9] also pointed out the participation of  $\pi$ – $\pi$  interaction of phenyl groups on the stationary phase with aromatic groups of the solute. The data shown in Fig. 3b, in which the electronic character is correlated with resolution efficiency, show the possibility that the 2-phenyl ring of these benzothiazines could be involved in  $\pi$ – $\pi$  interaction.

The present data suggest that the 2-phenyl ring of these benzothiazines is an important recognition site for resolution.

#### ACKNOWLEDGEMENT

The authors thank Dr. Shiro Mita for valuable suggestions.

#### REFERENCES

- 1 M. Oya, T. Baba, E. Kato, Y. Kawashima and T. Watanabe, *Chem. Pharm. Bull.*, 30 (1982) 440.
- 2 K. Yamamoto, M. Fujita, K. Tabashi, Y. Kawashima, E. Kato, M. Oya, T. Iso and J. Iwao, *J. Med. Chem.*, 31 (1988) 919.
- 3 M. Fujita, A. Ota, S. Ito, K. Yamamoto and Y. Kawashima, *Synthesis*, (1988) 599.
- 4 M. Fujita, A. Ota, S. Ito, K. Yamamoto, Y. Kawashima, T. Iso and J. Iwao, *Chem. Pharm. Bull.*, 38 (1990) 936.
- 5 M. Fujita, S. Ito, A. Ota, N. Kato, K. Yamamoto, Y. Kawashima, H. Yamauchi and J. Iwao, *J. Med. Chem.*, 33 (1990) 1898.
- 6 A. Fleckenstein, *Circ. Res.*, 52 (Suppl. I) (1983) 3.
- 7 R. A. Janis and D. J. Triggle, *J. Med. Chem.*, 26 (1983) 775.
- 8 H. Purcell, D. G. Waller and K. Fox, *Br. J. Clin. Pract.*, 43 (1989) 369.
- 9 Y. Okamoto, M. Kawashima and K. Hatada, *J. Chromatogr.*, 363 (1986) 173.
- 10 H. Koller, K.-H. Rimbock and A. Mannschreck, *J. Chromatogr.*, 282 (1983) 89.
- 11 C. Hansch and T. Fujita, *J. Am. Chem. Soc.*, 86 (1964) 1616.
- 12 C. Hansch and A. J. Leo, *Substituent Constants for Correlation Analysis in Chemistry and Biology*, Wiley, New York, 1979.



CHROMSYMP. 2479

# Simple reversed-phase high-performance liquid chromatographic method for 13-*cis*-retinoic acid in serum

R. Rao Gadde\* and Frederick W. Burton

Bristol-Myers Squibb Company, Pharmaceutical Research Institute, 100 Forest Avenue, Buffalo, NY 14213 (USA)

## ABSTRACT

An isocratic reversed-phase high-performance liquid chromatographic method for the analysis of 13-*cis*-retinoic acid in serum is developed. Sample preparation includes deproteination with acetonitrile–perchloric acid–acetic acid followed by centrifugation. 9-Methylanthracene is used as the internal standard. Chromatographic separation is achieved on a C<sub>18</sub> column (Zorbax) using an acetonitrile–aqueous 0.5% acetic acid (85:15, v/v) eluent containing 0.05% (w/v) sodium hexanesulfonate. The limit of detection is 12 ng/ml in serum, using 0.5 ml samples. Quantitative recoveries and excellent intra-day and inter-day precision are reported.

## INTRODUCTION

13-*cis*-Retinoic acid (CRA) (Fig. 1) is a very effective drug in the treatment of severe, recalcitrant cystic acne [1]. It is also under study for the treatment of several keratinizing disorders (psoriasis, ichthyosis, etc.) and epithelial cancers. The pharmacology, clinical pharmacokinetics and therapeutic efficacy of CRA have been reviewed [1–3]. It has been extensively studied in animals and humans to evaluate the safety and efficacy of this drug. Different chromatographic methods used to monitor the retinoids, including CRA, in biological fluids and tissues have been discussed in a recent review [4].

CRA, like most retinoids, is very sensitive to light and oxidation [4–8]. Multiple degradation products, isomers as well as oxidation products, were reported [9,10]. Extreme precautions to protect CRA from white light to minimize exposure to oxygen by inert gas purge, and to maintain storage of samples at low temperatures (–17°C to –70°C) are recommended in handling CRA and its solutions [4–8,11]. The assay method for biological fluids analysis should therefore be simple with few sample handling manipulations, yet specific to resolve CRA from its metabolite, degradation products and matrix components. However, most of the pub-

lished methods are cumbersome and complex for routine use.

Lengthy sample preparation schemes including extractions with an organic solvent, evaporation of solvent and reconstitution prior to high-performance liquid chromatographic (HPLC) analysis were used in several published procedures [11–14]. Lyo-

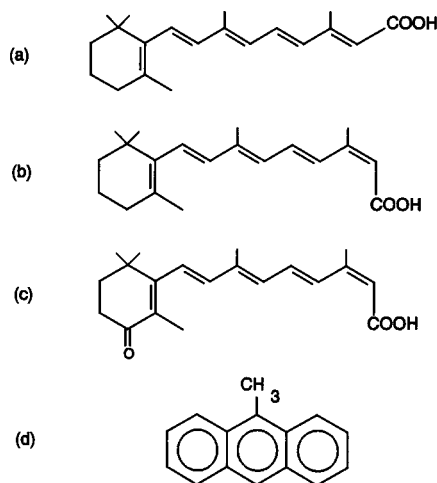


Fig. 1. Structural configurations. a = All-*trans*-retinoic acid, b = 13-*cis*-retinoic acid, c = 4-oxo-13-*cis*-retinoic acid and d = 9-methylanthracene.

philization of the sample before extraction is required in other methods [15,16]. Solvent gradient programming is required in some methods [7,13,14,17,18]. Both column switching and gradient elution were used in one fully automated method [19,20]. The present report describes an isocratic reversed-phase HPLC method for CRA in human serum which is precise, accurate and sensitive and requires only minimal sample preparation.

## EXPERIMENTAL

### *Apparatus*

A Waters Assoc. (Milford, MA, USA) Model 204 liquid chromatograph was used. It was equipped with Model 6000A low-volume displacement pump, a Model U6K universal injector, Model 710A intelligent sample processor (WISP), Model 440 absorbance detector (365 nm) and Zorbax 5  $\mu$ m ODS column (25 cm  $\times$  4.6 mm I.D., DuPont, Wilmington, DE, USA). The chromatograms were recorded using an OmniScribe B5117-1 recorder (Houston Instruments, Austin, TX, USA). A Hewlett-Packard Model 3352D Laboratory Data System was used for peak height determination and data analysis.

The HPLC mobile phase used was acetonitrile–aqueous 0.5% acetic acid (85:15, v/v) containing 0.05% (w/v) sodium hexanesulfonate. The flow-rate was 2 ml/min. The injection volume for samples and standards was 50  $\mu$ l. The detection wavelength was 365 nm.

### *Reagents and chemicals*

CRA was obtained from BASF Wyandotte (Wyandotte, MI, USA). 4-Oxo-13-*cis*-retinoic acid (OCRA) was provided by Midwest Research Institute (Kansas City, MO, USA). All-*trans*-retinoic acid (TRA) and sodium hexanesulfonate were acquired from Eastman Kodak (Rochester, NY, USA). ACS grade methanol and glacial acetic acid, HPLC grade acetonitrile and also certified reagent perchloric acid solution (0.1 M in acetic acid) were purchased from Fisher Scientific (Rochester, NY, USA). Dimethyldichlorosilane was obtained from Pierce (Rockford, IL, USA), 9-methylanthracene from Aldrich (Milwaukee, WI, USA) and human serum from Interstate Blood Bank (Philadelphia, PA, USA). Reagent grade water from a Milli-Q wa-

ter purification system (Millipore, Bedford, MA, USA) was used in making the HPLC mobile phase.

### *General procedures*

All solvents, serum and mobile phase were deaerated before use by sonication under vacuum. The headspace over the solutions was flushed with argon. All CRA solutions were also protected from UV light by using low actinic glassware and performing the solution transfers in yellow light only. The 4-ml vials (Sun Brokers, Wilmington, NC, USA) used for sample preparation and also as vials for automatic injector (WISP) are silanized before use, with dimethyldichlorosilane.

### *Preparation of standards*

A CRA stock standard solution (0.5 mg/ml) was prepared in methanol and standardized periodically using a combination of spectrophotometric and liquid chromatographic methods described earlier [5]. When not in use, it was stored in a refrigerator (5°C). Dilute CRA solution (25  $\mu$ g/ml) in methanol for use in preparing calibration standards were prepared fresh by diluting the stock solution. The stock solution of internal standard 9-methylanthracene (50  $\mu$ g/ml nominal concentration) was also prepared in methanol and diluted further as needed.

Six different spiking standard solutions were prepared from the above dilute CRA solution and the methyl anthracene solution, to contain 25–1000 ng/ml of CRA and 6  $\mu$ g/ml of 9-methylanthracene. Serum CRA standards were prepared by pipeting 0.5 ml of pooled serum, 100  $\mu$ l of the spiking standard solution, 1.5 ml of acetonitrile and 100  $\mu$ l of 0.1 M perchloric acid solution. The head space in vials was flushed with argon, and the vials were capped with self-seal septa and mixed over a vortex mixer. The vials were then centrifuged at 10°C until the solution was clear (approximately 5 min, 300 g) and transferred to an automatic injector for HPLC analysis.

The spiked serum standards prepared as above represent CRA concentrations in the range of 50–2000 ng CRA/ml in serum. These standards were used in the routine analysis of serum and plasma samples. Standards out of this concentration range were prepared and used as needed in evaluating the method.

### Preparation of samples

A 0.5-ml aliquot of plasma or serum sample in a 4-ml vial was spiked with 100  $\mu$ l of dilute internal standard solution (6  $\mu$ g/ml) and then treated with 1.5 ml of acetonitrile and 100  $\mu$ l of 0.1 *M* perchloric acid solution. The headspace over the mixture was then flushed with argon, and the vial was capped, vortexed, centrifuged and loaded into an HPLC automatic injector for analysis.

## RESULTS AND DISCUSSION

### Chromatography

For the analysis of CRA and its metabolite in biological fluids and tissues, reversed-phase HPLC methods using octadecylsilane columns have been the methods of choice. Different sample preparation procedures, eluent systems and also octadecylsilane columns from different manufacturers have been used to advantage. Most of these methods reviewed recently [4] have either used lengthy sample preparation schemes (lyophilization, solid phase or liquid-liquid extractions), gradient elution systems or both. Our efforts were focussed on simplifying the sample preparation process and developing a

sensitive and specific method for CRA and its metabolites.

Our early trials with the  $\mu$ Bondapak C<sub>18</sub> (Waters) column showed that although symmetrical peaks were obtained for CRA and TRA using the most commonly employed acetonitrile-aqueous ammonium acetate eluents, their resolution was not satisfactory. While the acetonitrile-aqueous acetic acid systems allowed good separation of CRA and TRA, both peaks showed tailing. Noticeable improvement in resolution and tailing was obtained using an acetonitrile-aqueous 0.5% acetic acid (60:40, v/v) eluent when modified with 0.05% (w/v) sodium hexanesulfonate. However, this system could not resolve TRA from retinol, which is endogenous in serum. Good baseline separation of TRA, retinol, CRA and the metabolite 4-oxo-13-*cis*-retinoic acid (OCRA) was obtained using Zorbax C<sub>18</sub> column (DuPont) and acetonitrile-aqueous 0.5% acetic acid (85:15, v/v) eluent containing 0.05% (w/v) sodium hexanesulfonate (Fig. 2). The major metabolite in human plasma after oral administration of CRA is OCRA [2,4]; TRA and its 4-oxo metabolite are present only at very low concentrations. Hence the above HPLC system performs well for the assay of CRA plasma and serum if the sample preparation adequately removes the matrix components.

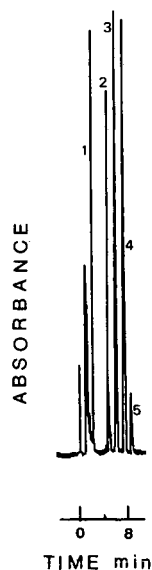


Fig. 2. Chromatogram of spiked serum sample showing separation of OCRA (1), 9-methylanthracene (2), CRA (3), TRA (4) and endogenous retinol (5). Detection wavelength 365 nm. See text for sample preparation procedure and HPLC conditions.

### Sample and standard preparation

The deproteination of plasma and serum by simple treatment with solvents (acetonitrile, methanol) with or without buffer modifiers have been used in the analysis of CRA and metabolites [7,12,21]. In our experience, the use of acetonitrile alone, while appearing satisfactory for deproteination, led to high variability in CRA assays of plasma. Improved precision in assay results as well as quick and very effective deproteination was achieved by a mixture of acetonitrile-perchloric acid-acetic acid. The addition of this mixture to both standards and samples appears to have stabilizing influence on CRA which improved both precision and linearity of response.

Full details of samples and standards preparation are given in the experimental section. Typical chromatograms of CRA spiked serum samples are shown in Fig. 3. A peak due to endogenous retinol was observed in all samples. CRA and internal

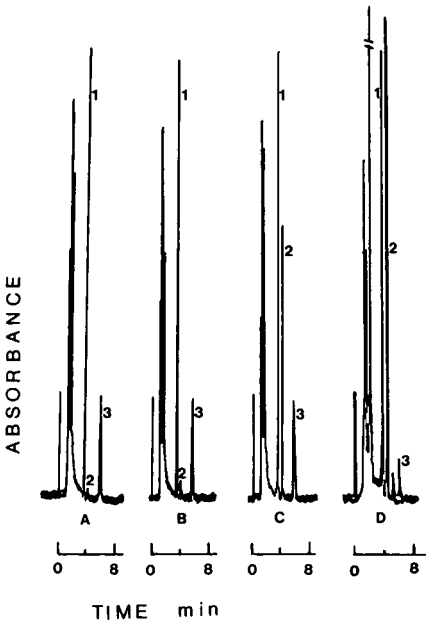


Fig. 3. Chromatograms of serum CRA standards (A, B, C) and clinical samples (D). CRA standards: A = 9.7 ng/ml; B = 19.4 ng/ml and C = 388 ng/ml. Clinical sample: plasma sample from volunteer treated with a single oral dose of 40 mg CRA. Detector wavelength 365 nm. See text for other HPLC conditions and the procedures for sample and standards preparation.

standard (9-methylanthracene) peaks in these chromatogram are well resolved from each other and from TRA, OCRA and retinol. CRA peak at the

lowest CRA concentration, 9.7 ng/ml is easily noticeable.

A typical chromatogram of plasma from volunteer dosed orally with CRA is shown in Fig. 3D. The CRA and internal standard peaks are clearly separated from the metabolite and matrix component peaks. The CRA peak purity was further checked by monitoring the peak heights at two wavelengths, 365 nm and 313 nm. For six plasma samples from a volunteer (1.5 to 6 hr after dosing orally with 40 mg of CRA), the average peak height ratio was 2.46 [relative standard deviation (R.S.D.) 1.6%] compared to 2.43 (R.S.D. 1.6%) observed for three serum CRA standards.

*Linearity and limit of detection*

The calibration curve from spiked serum standards was linear over the range 9.7 to 2912 ng CRA/ml. Linear regression analysis of data on ten standards in this range, each analyzed in duplicate, gave a correlation coefficient 0.999, slope 0.0158 ng/ml and *y*-intercept 0.0069. Similar study with standards in a slightly narrower concentration range 50 to 2000 ng CRA/ml (6 standards, each analyzed in duplicate) led to a correlation coefficient greater than 0.999, on 7 different days performed over a period of 12 weeks.

Serum samples from ten separate individuals were spiked separately with CRS standard in methanol or with methanol only and analyzed without the use of internal standard in the HPLC method.

TABLE I  
STABILITY OF CRA AT LOW CONCENTRATION IN SERUM AT -90°C  
CRA concentration (theory) 157 ng/ml.

Storage time (weeks)	Assay (ng/ml)					Mean	R.S.D. (%)	Initial (%)
	Individual results							
0	163	162	160	158	161	160.8	1.2	(100)
4	181	158	173	165	165	168.4	5.2	104.7
7	157	164	158	161	153	158.6	2.6	98.6
14	159	159	164	156	161	159.8	1.8	99.4
28	162	160	159	163	163	161.4	1.1	100.4
43	169	167	163	165	164	165.6	1.5	103.0
56	161	160	158	164	162	161.0	1.4	100.1
84	155	160	157	156	152	156.0	1.9	97.0
Inter-day R.S.D. (%)	6.1	1.8	3.2	2.4	3.1			

TABLE II

STABILITY OF CRA AT HIGH CONCENTRATION IN SERUM AT  $-90^{\circ}\text{C}$ 

CRA concentration (theory) 1253 ng/ml.

Storage time (weeks)	Storage					Mean	R.S.D. (%)	Initial (%)
	Individual results							
0	1298	1244	1272	1253	1257	1265	0.2	(100)
4	1281	1243	1211	1304	1258	1259	2.8	99.5
7	1271	1238	1248	1226	1241	1245	1.3	98.4
14	1236	1263	1225	1252	1219	1240	1.5	98.0
28	1298	1271	1282	1352	1267	1294	2.7	102.3
43	1286	1320	1320	1311	1275	1302	1.6	102.9
56	1262	1268	1258	1256	1275	1264	0.4	99.9
84	1251	1241	1207	1208	1214	1224	1.7	96.8
Inter-day R.S.D. (%)	1.7	2.2	3.1	3.8	1.9			

The methanol spiked samples showed no detectable CRA peak while the samples spiked at a level 12.1 ng CRA/ml in serum gave an average peak height response of 29 with a standard deviation of 11.6 ( $n = 10$ ). These data suggest that CRA at 12 ng/ml level can be easily detected.

#### Recovery and precision

Two sets of CRA standards, one with and another without pooled serum, were prepared. Each set contained twelve standards, two at each concentration of 52.2, 104.4, 208.9, 417.7, 1044 and 2089 ng CRA/ml. All standards were treated the same prior to HPLC analysis, except that the standards without serum were not centrifuged since they require no clarification. Essentially identical linear response was observed with both sets. The CRA recovery of serum standards calculated using the linear regression equation of non-serum standards gave an average value of 100.5% ( $n = 12$ , R.S.D. 1.9%) which demonstrates excellent recovery of CRA by this sample preparation method.

Two CRA spiked samples in pooled serum were prepared to contain 157 and 1253 ng CRA/ml and ten replicate analyses were performed on each sample using serum CRA standards. The results for the 157 ng/ml sample showed intra-day assay precision of 2.1% R.S.D. ( $n = 10$ , recovery 101.6%), and 1.8% R.S.D. ( $n = 10$ , recovery 100.2%) was found for the 1253 ng/ml sample. Additional discussion

on intra-day precision and also inter-day precision data is presented in the next section.

#### Stability of CRA in serum

Serum CRA solutions (0.5 ml) at concentrations of 157 ng/ml and 1253 ng/ml were aliquotted into 4-ml vials, the head space in the vial was flushed with argon, and the vials were tightly capped and stored at  $-90^{\circ}\text{C}$  until analysis. Five vials at selected storage times were analyzed independently. The data are summarized in Tables I and II and show that CRA is stable in serum for extended periods. Also, the data reveal that % R.S.D. ( $n = 5$ ) is in the range 0.2 to 5.2 for the intra-day analysis. The mean % R.S.D. for the 8 days is 2.1% at 157 ng/ml concentration and 1.5% at 1253 ng/ml concentration.

The excellent stability of CRA in serum at  $-90^{\circ}\text{C}$ , as shown in Tables I and II allows us to use the same data for assessing the inter-day precision of the method. Calculating the % R.S.D. for assay results in each column (one result from each of 8 days) gave values of 6.1, 1.8, 3.2, 2.4 and 3.1 with a mean % R.S.D. of 3.3 for the 157 ng/ml samples. Similarly, the % R.S.D. values for the 1253 ng/ml samples are 1.7, 2.2, 3.1, 3.8 and 1.9, with a mean % R.S.D. of 2.5.

#### Stability of processed samples

The stability of deproteinated samples (in contact with the protein mass at the bottom of the vial) at

room temperature was studied by analyzing five processed plasma samples from a single subject, initially and 20 h later using freshly prepared serum CRA standards. These samples which had CRA concentrations in the range 694 to 2083 ng/ml were found to degrade in 20 h to 97.4% of initial ( $n = 5$ , R.S.D. 1.3%).

#### *Advantages of the current method*

Simplicity in both the sample preparation and isocratic reversed-phase HPLC analysis are the major benefits of the method. The deproteinization of plasma or serum samples is achieved efficiently by simple, addition of acetonitrile and perchloric acid (in acetic acid). The sample is handled in one 4-ml vial for the entire analysis, which made it very easy to minimize losses due to adsorption to surfaces and also protect CRA and metabolites from degradation by light and air. The excellent accuracy and precision achieved by this method is better than most published methods. The only methods which show comparable performance [14,18,19] are more complex, requiring sample preparation using solid phase or solvent extraction and chromatography employing gradient elution.

#### CONCLUSION

The isocratic reversed-phase HPLC method described for the determination of CRA in serum is sensitive, precise and accurate. The simple sample preparation procedure coupled with the relatively fast isocratic HPLC analysis (10 min) makes it highly suited for monitoring serum CRA levels in clinical studies.

#### ACKNOWLEDGEMENTS

The authors thank Drs. J. DiNunzio and J. Allison and also C. Miller and S. Gadde for their assistance in the preparation of the manuscript.

#### REFERENCES

- 1 A. Ward, R. N. Brogden, R. C. Heel, T. M. Speight and G. S. Avery, *Drugs*, 28 (1984) 6.
- 2 R. W. Lucek and W. A. Coburn, *Clin. Pharmacokin.*, 10 (1985) 38.
- 3 J. A. Rumsfeld, D. P. West, C. S. T. Tse, M. L. Eaton and L. A. Robinson, *Drug Intell. Clin. Pharm.*, 17 (1983) 329.
- 4 R. Wyss, *J. Chromatogr.*, 531 (1990) 481.
- 5 R. R. Gadde and F. W. Burton, *J. Chromatogr. Sci.*, 28 (1990) 543; also see correction in 29 (1991) 8A.
- 6 P. Jakobsen, F. G. Larsen and C. G. Larsen, *J. Chromatogr.*, 415 (1987) 413.
- 7 C. J. L. Bugge, L. C. Rodriguez and F. M. Vane, *J. Pharm. Biomed. Anal.*, 3 (1985) 269.
- 8 G. E. Goodman, J. E. Einspahr, D. S. Alberts, T. P. Davis, S. A. Leigh, R. S. G. Chen and F. L. Meyskens, *Cancer Res.*, 42 (1982) 2087.
- 9 J. P. Boehlert, *Drug. Dev. Ind. Pharm.*, 10 (1984) 1343.
- 10 R. W. Curley Jr. and J. W. Fowble, *Photochem. Photobiol.*, 47 (1988) 831.
- 11 C. V. Puglisi and J. A. F. DeSilva, *J. Chromatogr.*, 152 (1978) 421.
- 12 J. G. Besner, R. Leclaire and P. R. Band, *J. Chromatogr.*, 183 (1980) 346.
- 13 F. M. Vane and C. J. L. Bugge, *Drug Metab. Dispos.*, 9 (1981) 515.
- 14 F. M. Vane, J. K. Stoltzenberg and C. J. L. Bugge, *J. Chromatogr.*, 227 (1982) 471.
- 15 C. A. Frolik, T. W. Tavela, G. L. Peck and M. B. Sporn, *Anal. Biochem.*, 86 (1978) 743.
- 16 P. R. Sundaresan and A. Kornhauser, *Ann. N. Y. Acad. Sci.*, 359 (1981) 422.
- 17 P. R. Sundaresan and P. V. Bhat, *J. Lipid Res.*, 23 (1982) 448.
- 18 C. Eckhoff and H. Nau, *J. Lipid Res.*, 31 (1990) 1445.
- 19 R. Wyss and F. Bucheli, *J. Chromatogr.*, 424 (1988) 303.
- 20 J. Creech Kraft, Ch. Echhoff, W. Kuhn, B. Lofberg and H. Nau, *J. Liq. Chromatogr.*, 11 (1988) 2051.
- 21 R. Shelley, J. C. Price, H. W. Jun, D. E. Cadwallader and A. C. Capomacchia, *J. Pharm. Sci.*, 71 (1982) 262.

# Stability studies with a high-performance liquid chromatographic method for the determination of a new anthracycline analogue, 3'-deamino-3'-[2-(*S*)-methoxy-4-morpholino]doxorubicin (FCE 23762), in the final drug formulation

Maria Luisa Rossini and Marina Farina\*

Galenical Research and Development, Farmitalia Carlo Erba, Via Carlo Imbonati 24, 20159 Milan (Italy)

## ABSTRACT

A high-performance liquid chromatographic method was studied to optimize the separation of FCE 23762, a new antitumour agent, from both synthetic impurities and degradation products having very similar molecular structures. The main problems faced in the analytical method development using the most common reversed-phase columns available arose from the presence of analytical peaks with poor symmetry, a long analysis time and the separation between FCE 23762 and its *R*-isomer, which was often unsuitable for the correct determination of the drug substance. The use of a new stationary phase, Zorbax R<sub>x</sub>-C8, together with a suitable mobile phase resulted in a good separation between the diastereomers, with satisfactory peak symmetry and run time. The method permitted the study of the stability of the drug substance in formulations for clinical trials.

## INTRODUCTION

3'-Deamino-3'-[2-(*S*)-methoxy-4-morpholino]-doxorubicin (Fig. 1), laboratory code FCE 23762, is a new antitumour agent belonging to the anthracycline group, showing marked growth-inhibiting properties similar to those of its parent drug, doxorubicin [1], whose clinical use in acute leukaemias, malignant lymphomas and solid tumour is well known [2–7].

In order to obtain good separation and selectivity among anthracyclines, different analytical methods [8–26] have been developed in the last decade, both for stability and pharmacokinetic studies, applying a wide variety of reversed-phase columns. The application of the official analytical method for doxorubicin [27], which involves the use of a reversed-phase trimethylsilane column (Zorbax TMS), was unsatisfactory, mainly owing to the low level of peak symmetry achieved. The use of a new stationary phase with deactivated silanol groups [28,29],

Zorbax R<sub>x</sub>-C8, designed for the analysis of basic and polar compounds, and optimization of the analytical conditions (mobile phase pH, buffer concentration and temperature) allowed us to develop an appropriate method for the determination of the active drug and for its separation from related substances, especially its *R*-isomer, to be used in stability studies on final dosage forms.

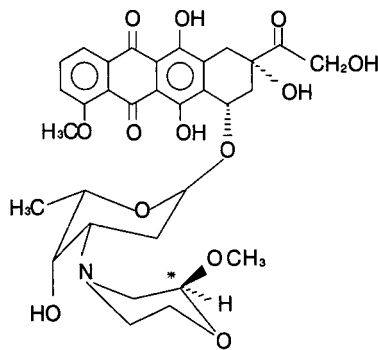


Fig. 1. Structural formula of FCE 23762.

## EXPERIMENTAL AND RESULTS

*Apparatus and chromatographic conditions*

The experiments were carried out on a Milton Roy (Rochester, NY, USA) CM 4000 liquid chromatograph equipped with a Zorbax R<sub>x</sub>-C8 analytical column (25/cm × 4.6 mm I.D.; average particle size 5 μm) manufactured by Rockland Technologies (Newport, DE, USA), a Gilson (Worthington, OH, USA) Model 231 autosampler, a Shimadzu (Tokyo, Japan) SPD-6A spectrophotometric detector and a Spectra-Physics (San Jose, CA, USA) Model SP 4270 integrating recorder.

The analytical wavelength chosen was 254 ± 1 nm. The mobile phase was water-acetonitrile (70:30, v/v), containing 2 ml/l of 85% H<sub>3</sub>PO<sub>4</sub>, adjusted to pH 6.0 with 2 M NaOH. A LABNET/IBM system (Spectra-Physics) was used for collecting and processing data.

Sample solutions were stored at ambient temperature and used within 24 h of preparation.

*Chemicals*

FCE 23762, its *R*-isomer, the synthetic intermediate doxorubicin and the most probable degradation product likely to be present, adriamycinone,

were kindly supplied by Carlo Erba R&D Chemical Department. The chemicals used were of analytical-reagent grade and the solvents for the high-performance liquid chromatographic (HPLC) analyses were of HPLC grade.

*Mobile phase study*

*Water to acetonitrile ratio.* During the trials on mobile phase optimization, a solution in water-acetonitrile (50:50, v/v) of FCE 23762 (about 50 μg/ml), the *R* diastereomer (about 15 μg/ml) and adriamycinone (about 10 μg/ml) was injected into the chromatographic system and analysed using mobile phases with different proportions of the two solvents.

After several experiments with mobile phase compositions varying from 50:50 to 90:10 (v/v), the optimum composition was found to be water-acetonitrile (70:30, v/v), which gave the best results for the determination of related substances with low-polarity characteristics.

*Influence of pH.* Water-acetonitrile (70:30, v/v) mixtures were prepared and adjusted to different pH values in the range 2.5–7.5 by means of 85% H<sub>3</sub>PO<sub>4</sub> and 2 M NaOH. The ionic strength was kept constant at 0.08 by adding NaCl in appropriate

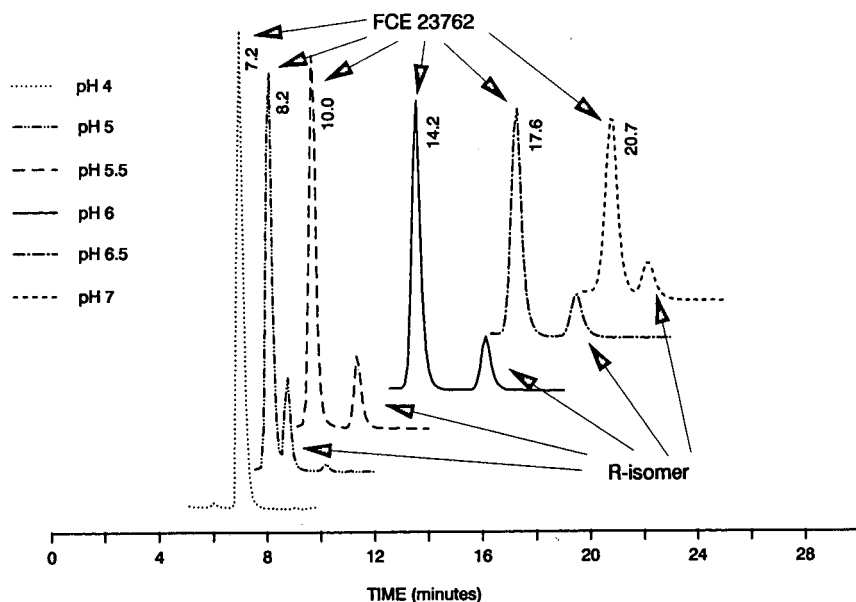


Fig. 2. Chromatograms showing the separation of FCE 23762 from its *R*-diastereomer when the pH of the mobile phase is varied ( $I = 0.08$ ).



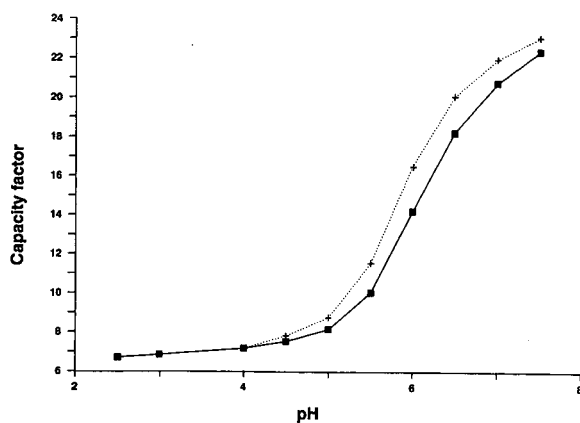


Fig. 3. Capacity factors ( $k'$ ) of (■) FCE 23762 and (+) its *R*-isomer versus pH.

amounts to guarantee that the variations observed in the chromatographic traces were dependent only on the pH effect.

The chromatograms obtained (Fig. 2) show that the retention times of both diastereomers increase as the pH increases, and the optimum symmetry of the peaks is achieved at low pH values.

Plots of the capacity factor ( $k'$ ) versus pH are given in Fig. 3 for FCE 23762 and its *R*-isomer and indicate that only the pH range *ca.* 4.5–7.5 can be considered suitable for the separation of the two isomers. Complete separation of the diastereomers is obtained solely in the pH range 5.5–6.5 as shown by the resolution values [30] reported in Table I, which also indicates that pH 6.0 is the optimum for resolution of the peaks.

As the  $k'$  values of the two ionizable solutes in phases buffered at different pH values depend on their  $pK_a$  values [31–33] and the major variations of this parameter are observed at pH values close to the  $pK_a$  value, it is likely that the separation between the

two diastereomers under our analytical conditions is strongly influenced by their different  $pK_a$  values (6.25 and 6.02 for FCE 23762 and its *R*-isomer, respectively, determined by potentiometric titration).

**Influence of buffer concentration.** To the water–acetonitrile (70:30, v/v) mobile phase were added phosphate buffer (pH 6.0) at different concentrations (from 0.0008 to 0.4 *M*), and the resulting mixtures were tested for the separation of FCE 23762 and its *R*-isomer. On increasing the buffer concentration the symmetry of the peaks improves and the retention times of both the isomers decrease; on lowering the buffer concentration the elution time of the two isomers is reversed.

Optimum separation of the isomers and peak symmetry were obtained when 2 ml/l of 85%  $H_3PO_4$  were added to the mobile phase, the pH then being adjusted to 6.0 with 2 *M* NaOH (buffer concentration = 0.04 *M*). Under these conditions, the separation of related substances from the main peaks was also better, allowing a more precise determination.

**Influence of temperature.** The influence of temperature on the separation of FCE 23762 from its *R*-isomer was studied using the optimized mobile phase on a Zorbax  $R_x$ -C8 column maintained at 2, 12, 22, 32, 42 and 52°C by means of a thermostat.

At higher temperatures (32, 42 and 52°C) the symmetry of the peaks decreases and the retention times increase, and at the lowest (2°C) and highest (52°C) temperatures tested the separation of the *S*- and *R*-isomers is significantly reduced, hence the optimum column temperature is 22°C. Therefore, for practical reasons, the stability studies on FCE 23762 formulations can be conducted at room temperature.

#### Validation of the HPLC method

The method was validated for the assay of freeze-dried vials dosed at 50 and 500  $\mu$ g, and showed the following performances.

**Precision.** Repeated determinations on six different samples showed a relative standard deviation (R.S.D.) of 0.73% for the 50- $\mu$ g dosage and R.S.D. = 0.56% for the 500- $\mu$ g dosage.

**Accuracy.** Samples prepared extemporaneously with FCE 23762 in amounts close to the limits of acceptance (85–115% of the label claim) showed an accuracy of  $99.55 \pm 0.75\%$  for the 50- $\mu$ g dosage and

TABLE I

RESOLUTION BETWEEN THE PEAKS OF FCE 23762 AND ITS *R*-ISOMER VERSUS pH

pH	Resolution	pH	Resolution
4.0	0	6.0	4.2
5.0	1.2	6.5	3.2
5.5	2.3	7.0	1.6

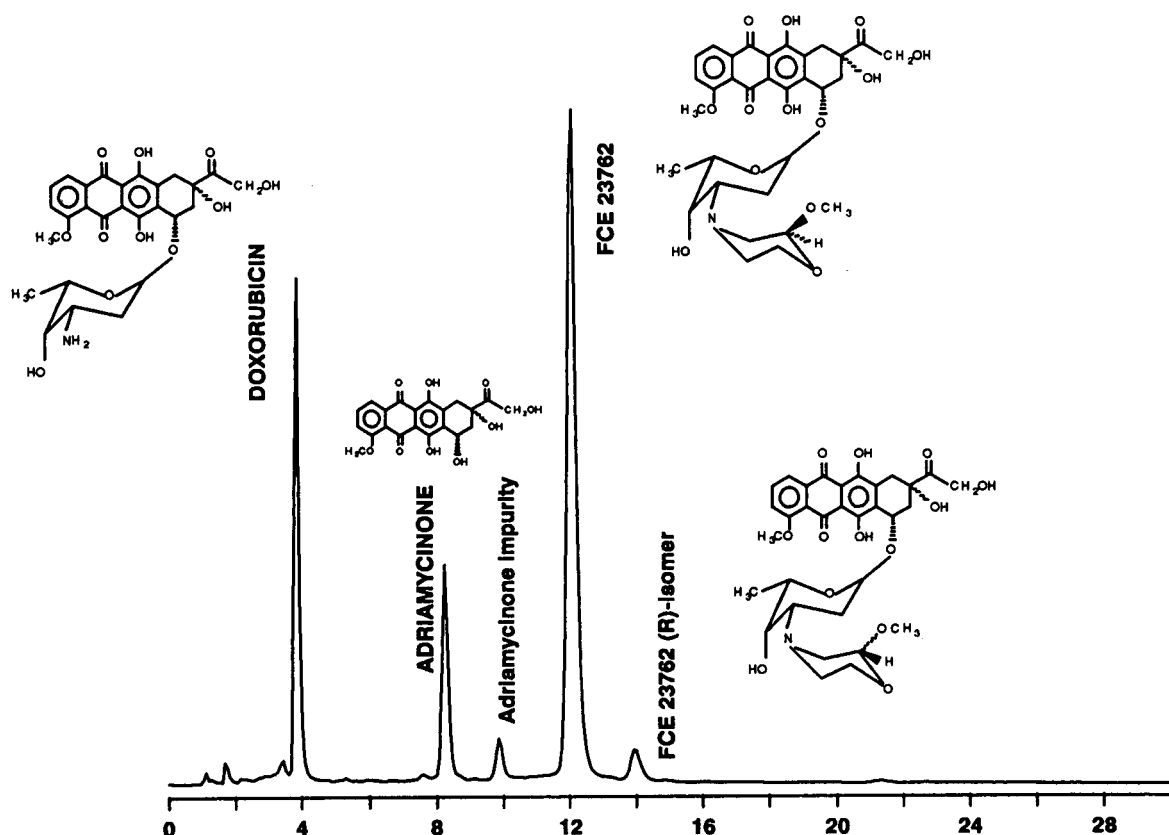


Fig. 4. Chromatogram of a mixture of FCE 23762, its *R*-diastereomer, doxorubicin and adriamycinone analysed under the optimized experimental conditions.

$99.67 \pm 0.88\%$  for the 500- $\mu\text{g}$  dosage (both as means of twelve determinations).

**Linearity.** Calibration standard solutions prepared spanning a concentration range of 10–160  $\mu\text{g}/\text{ml}$  showed a correlation coefficient  $r = 0.999687$ .

**Specificity.** The method is capable of assaying FCE 23762 in the final dosage forms without interference arising from the presence of structurally related compounds. This was confirmed by chromatographing a mixture of FCE 23762 (ca. 50  $\mu\text{g}/\text{ml}$ ), its *R*-isomer (ca. 5  $\mu\text{g}/\text{ml}$ ), doxorubicin (ca. 30  $\mu\text{g}/\text{ml}$ ) and adriamycinone (ca. 15  $\mu\text{g}/\text{ml}$ ) dissolved in water–acetonitrile (70:30, v/v) under the optimized analytical conditions (Fig. 4).

**Stability-indicating power.** The method allows the determination of FCE 23762 in samples forcibly degraded under acidic and basic conditions, under

intense white light and in the presence of a strong oxidizing agent, without interference arising from the side-products formed (Fig. 5 and Table II).

#### Stability trials

The HPLC method was applied to the assay of FCE 23762 in its final dosage forms, freeze-dried vials dosed at 50 and 500  $\mu\text{g}$ , with the aim of determining the provisional shelf-life of the drug product for clinical studies. The freeze-dried vials, supplied by Carlo Erba Galenical Development Department, were reconstituted with water–acetonitrile (70:30, v/v) at concentrations of 50 and 100  $\mu\text{g}/\text{ml}$ , respectively, and then injected into the chromatographic system. Tables III and IV show the stability results obtained for FCE 23762, its *R*-isomer and total related substances.

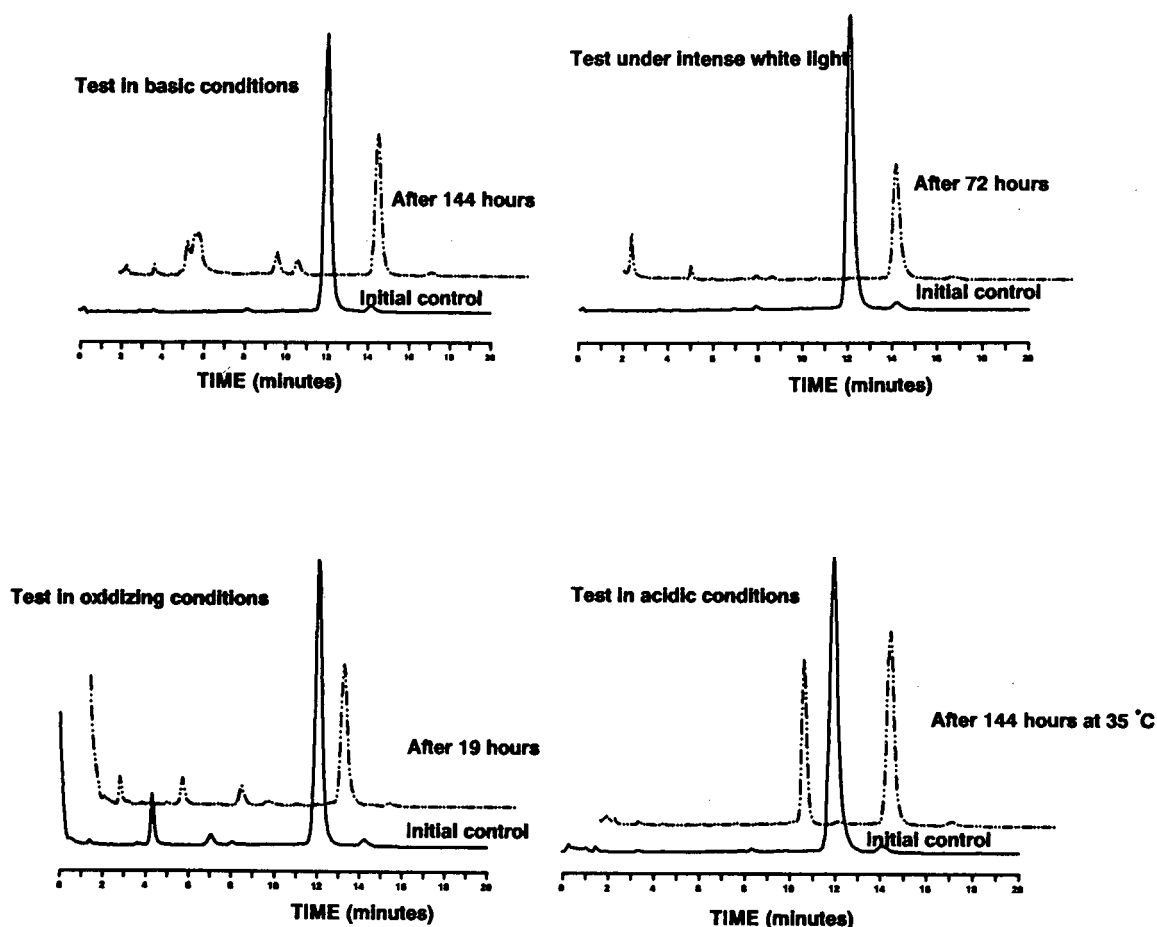


Fig. 5. Stability-indicating power of the HPLC method: chromatograms showing the forced degradation of FCE 23762 under acidic and basic conditions, in the presence of a strong oxidizing agent and under intense white light.

TABLE II

STABILITY-INDICATING NATURE OF THE HPLC ASSAY METHOD FOR FCE 23762

Results relative to initial control = 100%.

Conditions	Time (h)	Residual concentration (%)
Acidic	144	53.8
Basic	144	48.2
Intense white light	72	39.9
Oxidizing	19	52.1

## CONCLUSIONS

The results demonstrate the excellent power of the Zorbax R<sub>x</sub>-C8 column in reducing peak tailing and giving constant performance and high efficiency for long periods. The developed and validated HPLC method proved capable of identifying and separating FCE 23762 from related substances and in particular from its *R*-diastereomer, and can be applied to the assay of the active principle in its final dosage forms to establish the shelf-life of the drug product.

TABLE III  
STABILITY DATA FOR FCE 23762  
50-μg freeze-dried vials, batch No. TF/23659. R.S. = Related substances.

Tempera- ture (°C)	Parameter	Initial control	1 month	2 months	3 months
55	Assay (%)	100.0	102.2		
	Total R.S. (%)	3.33	3.74		
	R-isomer (%)	1.89	2.35		
45	Assay (%)	100.0	100.9	100.7	96.8
	Total R.S. (%)	3.33	3.80	3.68	3.47
	R-isomer (%)	1.89	2.44	2.52	2.09
35	Assay (%)	100.0	102.3	102.2	100.1
	Total R.S. (%)	3.33	3.54	3.28	3.10
	R-isomer (%)	1.89	2.36	2.19	1.99
30	Assay (%)	100.0	102.9	102.1	98.2
	Total R.S. (%)	3.33	3.69	3.69	3.15
	R-isomer (%)	1.89	2.40	2.29	2.07
25	Assay (%)	100.0	102.3	101.1	101.4
	Total R.S. (%)	3.33	3.25	3.60	3.41
	R-isomer (%)	1.89	2.27	2.33	2.11

TABLE IV  
STABILITY DATA FOR FCE 23762  
500-μg freeze-dried vials, batch No. TF/23660.

Tempera- ture (°C)	Parameter	Initial control	1 month	2 months	3 months
55	Assay (%)	100.0	101.6		
	Total R.S. (%)	3.47	3.92		
	R-isomer (%)	2.20	2.48		
45	Assay (%)	100.0	102.3	99.9	98.7
	Total R.S. (%)	3.47	3.83	3.50	3.58
	R-isomer (%)	2.20	2.44	2.26	2.09
35	Assay (%)	100.0	101.0	100.5	98.2
	Total R.S. (%)	3.47	3.77	3.66	3.51
	R-isomer (%)	2.20	2.47	2.22	2.14
30	Assay (%)	100.0	100.5	99.9	99.1
	Total R.S. (%)	3.47	3.75	3.77	3.45
	R-isomer (%)	2.20	2.47	2.18	2.17
25	Assay (%)	100.0	101.7	101.0	98.8
	Total R.S. (%)	3.47	3.73	3.63	3.37
	R-isomer (%)	2.20	2.47	2.28	2.19

## REFERENCES

- 1 F. Arcamone, *Doxorubicin Anticancer Antibiotics*, Academic Press, New York, 1981.
- 2 M. Ghione, J. Fetzter and H. Maier (Editors), *Ergebnisse der Adriamycin-Therapie*, Springer, New York, 1975.
- 3 W. B. Pratt and R. W. Ruddon, *The Anticancer Drugs*, Oxford University Press, Oxford, New York, 1979, pp. 155–170.
- 4 R. T. Dorr and W. L. Frits, *Cancer Chemotherapy Handbook*, Elsevier, Amsterdam, 1980, pp. 373–378 and 388–401.
- 5 C. E. Myers, in B. Chabner (Editor), *Pharmacological Principles of Cancer Treatment*, W. B. Saunders, Philadelphia, PA, 1982, pp. 416–434.
- 6 J. R. Brown, *Prog. Med. Chem.*, 15 (1978) 125–64.
- 7 J. R. Brown and S. H. Imam, *Prog. Med. Chem.*, 21 (1984) 170–236.
- 8 A. Vigevani and M. J. Williamson, in K. Florey (Editor), *Analytical Profiles of Drug Substances*, Vol. 9, Academic Press, New York, 1980, pp. 245–274.
- 9 J. A. Benvenuto, R. W. Anderson, K. Kerkof, R. G. Smith and T. L. Loo, *Am. J. Hosp. Pharm.*, 38 (1981) 1914–1918.
- 10 E. Tomlinson and L. Malspeis, *J. Pharm. Sci.*, 71 (1982) 1121–1125.
- 11 A. M. B. Bots, W. J. van Oort, J. Noordhoek, A. van Dijk, S. W. Klein and Q. G. C. M. van Hoesel, *J. Chromatogr.*, 272 (1983) 421–427.
- 12 E. Moro, V. Bellotti, M. G. Jannuzzo, S. Stegnaich and G. Valzelli, *J. Chromatogr.*, 274 (1983) 281–287.
- 13 S. Eksborg and H. Ehrsson, *J. Pharm. Biomed. Anal.*, 2 (1984) 297–303.
- 14 J. H. Beijnen, G. Wiese and W. J. M. Underberg, *Pharm. Weekbl., Sci. Ed.*, 7 (1985) 109–116.
- 15 M. J. H. Janssen, D. J. A. Crommelin, G. Storm and A. Hulshoff, *Int. J. Pharm.*, 23 (1985) 1–11.
- 16 A. N. Kotake, N. J. Vogelzang, R. A. Larson and N. Choporis, *J. Chromatogr.*, 337 (1985) 194–200.
- 17 A. G. Bosanquet, *Cancer Chemother. Pharmacol.*, 17 (1986) 1–10.
- 18 P. A. Maessen, K. B. Mross, H. M. Pinedo and W. J. F. van der Vijgh, *J. Chromatogr.*, 417 (1987) 339–346.
- 19 P. A. Maessen, H. M. Pinedo, K. B. Mross and W. J. F. van der Vijgh, *J. Chromatogr.*, 424 (1988) 103–110.
- 20 L. M. Rose, K. F. Tillery, S. M. El Dareer and D. L. Hill, *J. Chromatogr.*, 425 (1988) 419–423.
- 21 P. K. Gupta, F. C. Lam and C. T. Hung, *Drug Dev. Ind. Pharm.*, 14 (1988) 1657–1671.
- 22 C. M. Camaggi, R. Comparsi, E. Stocchi, F. Testoni and F. Pannuti, *Cancer Chemother. Pharmacol.*, 21 (1988) 216–220.
- 23 J. Wood, *Pharm. J.*, 241 (1988) HS12.
- 24 R. Mariani, M. Farina and W. Sfreddo, *J. Pharm. Biomed. Anal.*, 7 (1989) 1877–1882.
- 25 O. Bekers, J. H. Beijnen, M. Otagiri, A. Bult and W. J. M. Underberg, *J. Pharm. Biomed. Anal.*, 8 (1990) 671–674.
- 26 R. Ficarra, P. Ficarra, M. L. Calabro, G. Altavilla, T. Giacobello and V. Adamo, *Boll. Chim. Farm.*, 130 (1991) 17–21.
- 27 *US Pharmacopeia, XXII Revision*, US Pharmacopeial Convention, Rockville, MD, 1990, p. 478.
- 28 D. Chan Leach, M. A. Stadalius, J. S. Berus and L. R. Snyder, *LC · GC Int.*, 1 (1988) 22–30.
- 29 J. Kohler and J. J. Kirkland, *J. Chromatogr.*, 385 (1987) 125–150.
- 30 *US Pharmacopeia, XXII Revision*, US Pharmacopeial Convention, Rockville, MD, 1990, p. 1567.
- 31 C. Horváth and W. Melander, *J. Chromatogr. Sci.*, 15 (1977) 393.
- 32 C. Horváth, W. Melander and I. Molnar, *Anal. Chem.*, 49 (1977) 142–154.
- 33 C. Herrenknecht, D. Ivanovic, E. Guernetnivand and M. Guernet, *J. Pharm. Biomed. Anal.*, 8 (1990) 1071–1074.



# Use of direct injection precolumn techniques for the high-performance liquid chromatographic determination of the retinoids acitretin and 13-*cis*-acitretin in plasma

R. Wyss\* and F. Bucheli

Pharma Division, Preclinical Research, F. Hoffmann-La Roche Ltd, PRPK, 68/121A, CH-4002 Basle (Switzerland)

## ABSTRACT

A previously developed highly sensitive high-performance liquid chromatographic method for the determination of retinoids, using direct injection of large plasma volumes, on-line solid-phase extraction and ultraviolet detection, was improved and fully validated for the determination of acitretin and 13-*cis*-acitretin in plasma samples. The addition of acetonitrile to improve the recovery was performed on-line by a T-piece, avoiding any *cis-trans* isomerization which could occur when acetonitrile was added prior to storage in the autosampler. About 30 injections could be made onto one precolumn despite the large injection volume (1 ml of plasma containing the internal standard). Full automation was attained by the use of automated precolumn replacement. In addition, forward- and back-flush purging of the precolumn enhanced the longevity of the analytical column. This consisted of three coupled C<sub>18</sub> columns of 125 mm length each. The quantification limit was 0.3 ng/ml, using ultraviolet detection at 360 nm, and the mean inter-assay precision was 3.8% for the two compounds.

## INTRODUCTION

Acitretin (Neotigason®, **1**, Fig. 1) is a synthetic retinoid which is used in the treatment of psoriasis [1]. Its ethyl ester, etretinate (Tigason®), which has been used for many years for the same indication, is now regarded as a pro-drug of acitretin [2]. Compared with etretinate, acitretin has a profound pharmacokinetic advantage because of its more rapid elimination from the body [3]. As acitretin is teratogenic [4], a more thorough investigation of its elimination characteristics is of great interest. For this purpose, highly sensitive methods are needed

for the determination of acitretin and its main metabolite, 13-*cis*-acitretin (**2**) [3], after oral or topical administration.

High-performance liquid chromatography (HPLC) is the method most often used for the determination of retinoids [5]. Gas chromatography is not suitable as a result of isomerization of the tetraene side-chain. On-line solid-phase extraction with automated column switching is especially useful for the pretreatment of biological fluids in HPLC to minimize photoisomerization and oxidation of the retinoids. In this way, liquid-liquid extraction under light protection and evaporation of the extraction solvents are avoided. On the other hand, on-line solid-phase extraction requires special injection conditions to overcome high and strong protein binding of the retinoids [6]. Plasma samples (two volumes) containing isotretinoin, tretinoin (13-*cis*- and all-*trans*-retinoic acid) and their 4-oxo metabolites were diluted either with three volumes of sodium hydroxide-acetonitrile (8:2) [7,8] or with *ca.* eight volumes of ammonium acetate-acetonitrile

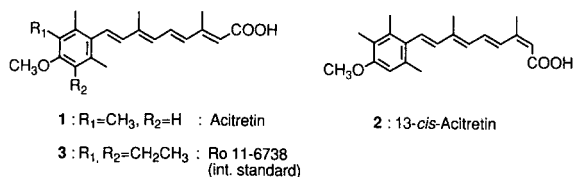


Fig. 1. Structures of the studied compounds.

(5:1), followed by semi-automated on-line solid-phase extraction using the Varian AASP system [9]. As an alternative, protein precipitation was performed prior to injection, either with ethanol for the simultaneous determination of etretinate and its two acid metabolites **1** and **2** [8,10], or with propan-2-ol for the above-mentioned retinoic acids [11].

However, the most sensitive methods using HPLC with on-line solid-phase extraction require the injection of large plasma volumes with only minimal dilution. This has been achieved by adding 0.2 ml of acetonitrile to 1 ml of plasma, and the injection of 1 ml of sample by the autosampler. In addition, automated precolumn replacement, when a precolumn became clogged, was inserted into the column switching system for overnight injections [12]. This technique works well with arotinoids, and was successfully applied to sumatriptan (Ro 14-9706), an arotinoid methyl sulphone [13]. However, during the routine analysis of acitretin samples, isomerization (mainly from **2** to **1**) was observed in some of the patient samples. This problem was not encountered during method validation with blood bank plasma from volunteers. A detailed investigation revealed that 10–20% of the blood bank plasmas did, in fact, show this effect, and, probably, an even higher proportion of the plasma samples from patients. However, the degree of isomerization varied from sample to sample from the same patient and was often completely absent. The isomerization only became relevant after the plasma samples had been stored for more than 10 h in the autosampler before injection.

Shih *et al.* [14] investigated the isomerization of 13-*cis*- and all-*trans*-retinoic acid by thiol-containing compounds in a non-enzymatic chemical reaction. Catalytic activity was found for glutathione, mercaptoethanol, L-cysteine methyl ester, apoferritin (a thiol-containing protein) and native, and even (to a lesser extent) boiled, microsomes. The ability of the ubiquitous glutathione to catalyse the *cis*-*trans* isomerization of retinoids was also confirmed by Jewell and McNamara [15] for **1** and **2**. To test the hypothesis that glutathione or a thiol-containing enzyme could be responsible for the observed isomerization in the plasma samples in the acitretin method [12], several inhibitors of this interconversion, proposed previously [14,15], were investigated

for plasma stabilization. Sodium *p*-hydroxymercuribenzoate [15], L-cysteine and iodoacetate [14], as well as the addition of sodium hydroxide [7], inhibited the isomerization. Surprisingly, this was also true for glutathione, which was reported to be a catalyst [14,15]. However, all these substances only partially prevented the isomerization of **2** to **1** when they were added to the plasma sample (containing *ca.* 17% acetonitrile). All substances produced accelerated clogging of the precolumn, which excluded overnight injections. Finally, it was found that the isomerization only occurred in the presence of acetonitrile, and that undiluted plasma samples were completely stable for more than 20 h in the autosampler. Therefore, in this work, a modified HPLC method for **1** and **2** was developed, using a direct injection technique with acetonitrile addition by a T-piece, to avoid long contact of the retinoids with this solvent. This resulted in good recoveries without isomerization.

## EXPERIMENTAL

The preparation of plasma standards, handling of samples and the addition of the internal standard were performed under diffuse light conditions. The materials and solvents, preparation of calibration standards and other general conditions were as described by Wyss and Bucheli [10,12].

### *Chromatographic system and conditions*

A schematic representation of the modular HPLC column-switching system is given in Fig. 2. A 420 LC pump (P1A; Kontron, Zurich, Switzerland) delivered mobile phase M1A (or alternatively M3) at a flow-rate of 1.4 ml/min. Plasma samples (1.0 ml) were injected by a WISP 712 automatic sample injector with cooling module (I1; Waters, Milford, MA, USA; 10°C) onto one of the precolumns (PC). To inject sample volumes larger than 200 µl, the autosampler was used with a 1-ml syringe, the 2-ml auxiliary sample loop and a syringe motor rate of 1.85 µl/s. In addition, a 2 m × 0.18 mm I.D. capillary was used as a restrictor. The injected sample plug was diluted on-line with a mobile phase containing acetonitrile (M1B) by the HPLC pump P1B (Spectroflow 400 solvent delivery system, Kratos, Westwood, NJ, USA; flow-rate 0.7 ml/min) and a T-piece (T; Valco Instruments, Hous-



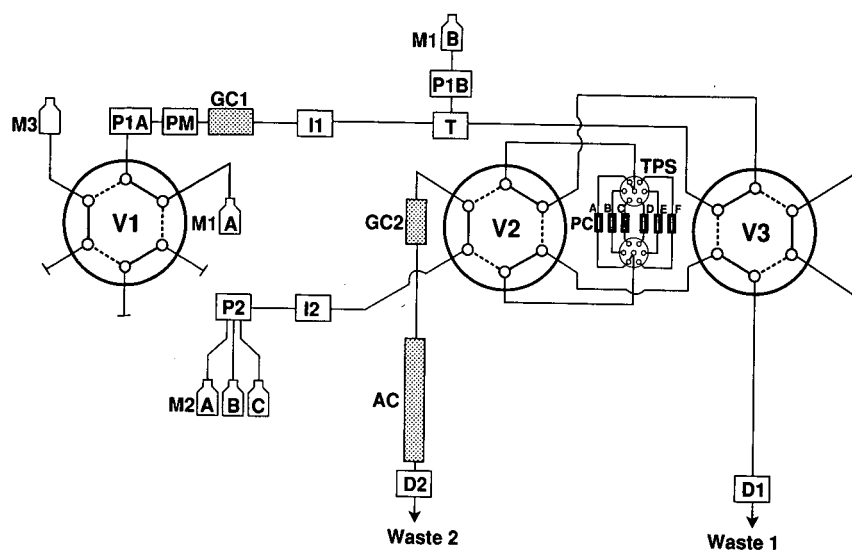


Fig. 2. Schematic representation of the HPLC column-switching system. Position of the valves: V1 = T5, V2 = T4 and V3 = T8. After valve switching the positions are defined as V1 = T6, V2 = T3 and V3 = T7 (see text for further details).

ton, TX, USA; 1/16 in., bore 0.25 mm). The UV detector D1 (Spectroflow 773, Kratos), operating at 230 nm, together with a W + W recorder 600 (Kontron) were used to monitor the removal of plasma components from the precolumn during the purge step; they were not needed for routine analysis. The gradient pump P2 (Model 480, Gynkoteck, Germering b. München, Germany) delivered mobile phase M2 (flow-rate 1 ml/min), which was degassed on-line (Shodex DEGAS KT-35M degassing device, Showa Denko, Tokyo, Japan). A manual injector (I2; Model 7125 with a 200- $\mu$ l loop, Rheodyne, Cotati, CA, USA) was used for direct injection onto the analytical column (*e.g.* for recovery experiments). Detection of the eluted compounds was carried out at 360 nm with a UV detector (D2; Spectroflow 783, Kratos; rise time 1 s, range 0.01 a.u.f.s.), and integration was performed by a computing integrator (Model SP 4200, Spectra-Physics, San Jose, CA, USA; sensitivity 8 mV, chart speed 0.5 cm/min).

The low-pressure three-way rotary valve (V1; Model 5032P, Rheodyne) and the two high-pressure switching valves (V2 and V3; Model 7000P, Rheodyne), all pneumatically operated and connected to three solenoid valves (Model 7163, Rheodyne), were controlled by the external time events

(T3–T8) of the integrator. To achieve compatibility, an interface, produced in the electronic workshop at F. Hoffmann-La Roche, was placed between the integrator output and the solenoid valve input. The positions of the valves in Fig. 2 are V1 = T5 (alternative flow T6), V2 = T4 (T3) and V3 = T8 (T7). During injection and purging of the PC, the pressure was measured by a pressure monitor (PM; Bischoff-Analysentechnik, Leonberg, Germany). When a pressure of 80 bar was reached, indicating PC clogging during the following injections, a signal was sent to a second interface which, after obtaining an end-of-run signal from the gradient pump, effected replacement of the PC by the tandem precolumn selector (TPS; Model 7066, Rheodyne).

#### Columns and mobile phases

The guard column GC1 and the PC (all 14 mm  $\times$  4.6 mm I.D.; Bischoff) were packed with Bondapak C<sub>18</sub> Corasil, 37–50  $\mu$ m (Waters). The analytical column (AC; three coupled columns, 125 mm  $\times$  4 mm I.D. each) and the guard column GC2 (30 mm  $\times$  4 mm I.D., all from E. Merck, Darmstadt, Germany) were packed with Spherisorb ODS 1, 5  $\mu$ m (Phase Separations, Queensferry, UK), using a slurry technique.

Mobile phase M1A consisted of 1% ammonium acetate–acetonitrile (100:2, v/v), M1B of 1% ammonium acetate–acetonitrile (6:4, v/v) and M3 of acetonitrile–water (8:2, v/v). The gradient mobile phase 2 (M2) contained three components: (A) 0.1% ammonium acetate–acetonitrile–acetic acid (40:60:3, v/v/v); (B) 0.8% ammonium acetate–acetonitrile–acetic acid (5:95:1, v/v/v); (C) water–acetonitrile–acetic acid (20:980:1, v/v/v).

### Procedure

A 5- $\mu$ l aliquot of internal standard solution [5  $\mu$ g/ml **3** in acetonitrile–ethanol (95:5, v/v)] was added to 1.2 ml of plasma. After vortex-mixing and centrifugation (6 min at 3400 g), 1 ml was injected. The total sequence of automated analysis required 31 min, and included the following steps.

(1) Step A (0–8 min, V1 = T5, V2 = T4, V3 = T8). Injection and pre-concentration of the sample on PC. Proteins and polar compounds were washed out to waste 1 with M1. AC was equilibrated with M2 (100% A).

(2) Step B (8–10 min, V1 = T5, V2 = T4, V3 = T7). PC was purged in the back-flush mode by M1.

(3) Step C (10–14 min, V1 = T6, V2 = T3, V3 = T7; 14–16 min, V1 = T6, V2 = T4, V3 = T7; 16–17 min, V1 = T6, V2 = T4, V3 = T8). Transfer of the retained components from PC to AC in the back-flush mode by a gradient of 100% A to 100% B (10–26 min). In the meantime, the capillaries between V1 and D1 were purged with M3.

(4) Step D (17–31 min, V1 = T5, V2 = T4, V3 = T8). Gradient of 100% B to 100% C (26–27 min), 100% C (27–30 min), 100% C to 100% A (30–31 min). Meanwhile, PC was re-equilibrated with M1.

## RESULTS AND DISCUSSION

### Analytical system and chromatography

The addition of acetonitrile or another water-miscible organic solvent was found to be necessary for a good recovery in the on-line solid-phase extraction of retinoids [6,7,9]. For very lipophilic compounds (e.g. etretinate), protein precipitation with an organic solvent may be indispensable [6]. However, for **1** and **2**, protein precipitation was not necessary, and the addition of acetonitrile alone (0.2 ml to 1 ml of plasma) was sufficient to obtain a good recovery. The omission of additional dilution

with water or buffer resulted in a higher sensitivity [12]. As acetonitrile addition prior to storage in the autosampler induced isomerization, on-line dilution with an acetonitrile-containing mobile phase (M1B) via a T-piece was used. Table I shows the absence of a time-dependent *cis*–*trans* isomerization of **2** using this technique, compared with the acetonitrile addition used previously.

The addition of an internal standard is recommended for the control of the autosampler injection volume and possible decrease in the peak height on the analytical column after many injections onto the same precolumn. Ro 11-6738 (**3**) showed better results in this respect compared with the previously used isotretinoin (13-*cis*-retinoic acid) [10]. The wash-out time of 8 min (step A of the procedure) needed careful investigation to keep the total run time as short as possible, and to exclude any transfer of plasma proteins to the analytical column, which would reduce the efficiency and the longevity of the analytical column.

The number of injections possible (1 ml of plasma per injection) onto one precolumn was about 30, resulting in a pressure increase to about 80 bar. This was the limit set at the pressure monitor to give a signal for precolumn replacement. During sample injection onto a new precolumn, the pressure was constant (about 30 bar) over many injections. It then increased relatively sharply to >100 bar. The

TABLE I

COMPARISON OF TIME DEPENDENT *cis*–*trans* ISOMERIZATION

A plasma sample spiked with 100 ng/ml 13-*cis*-acitretin (**2**) was stored in the autosampler at 10°C. Acitretin (**1**) was formed by isomerization in the same sample. Conditions: (A) 1 ml of plasma injected, analytical conditions as described in the text. (B) 1 ml of plasma was diluted with 0.2 ml of acetonitrile prior to storage in the autosampler, and 1 ml of the mixture was injected as under (A).

Condition	Storage time (h)	Peak heights	
		1	2
A	2.9	2567	73 169
	26.0	3045	74 667
B	3.6	4323	50 059
	26.7	17 147	38 285

injection of 30 ml of plasma onto one precolumn is about twice the volume which is normally possible. This is, however, still considerably less than the 64.5 ml which could be injected after acetonitrile addition to the plasma sample prior to injection [12]. The immediate addition of acetonitrile appears to be better for the dissolution of plasma components. This could also be observed from stored samples without acetonitrile, which often contained lipid layers or suspended particles. In addition, large numbers of injections could only be obtained by using sieves instead of frits [16].

The peak heights of 1 and 2 were relatively stable during the injection of plasma standards onto the same precolumn. The decrease of less than 10% (until the pressure had reached 80 bar) was compensated sufficiently by the internal standard. After automatic precolumn replacement, the initial peak heights were again obtained. This indicates that the plasma injections resulted in an alteration of the precolumn, probably by coating with lipids. The gradient mobile phase (M2) and the purge mobile phase (M3) eluted part of these lipids. A higher acetonitrile content (100%) in M3 would probably enhance the number of injections onto one precolumn. However, a change from the ammonium acetate containing M1 to 100% acetonitrile in M3 was not possible due to solubility problems, and would have required an intermediate purge step which was not used in this method. In the previous method without a T-piece [12], purging of the capillaries was performed with M2, and not with M3. In that configuration, the precolumn was cleaned for 4 min with M2 containing 99% acetonitrile. This may have resulted in the elution of a higher amount of lipids and, therefore, could be another explanation of the higher number of injections possible onto one precolumn under these conditions. The use of the low-pressure valve V1 resulted in a *ca.* 8 min shorter run time.

The benefits of back-flush purging of the precolumn was also investigated under the experimental conditions described. Whereas the number of injections onto two precolumns tested without back-flush purging (step B of the procedure) was high (>40), an increase in the pressure on the analytical column of 5–10 bar was observed. This confirms the advantage of this additional purge step [6,12] which prevents a pressure increase on the analytical column.

### Selectivity

The injection of large plasma volumes makes high demands on the selectivity of the chromatographic system. These requirements were adequately fulfilled by the use of three coupled 125-mm columns and gradient elution, allowing improved separation, compared with the method of Wyss and Bucheli [12], of the internal standard from endogenous interferences. The pressure was about 200 bar using acetonitrile as an organic modifier in the mobile phase (M2). Typical chromatograms of spiked plasma samples are presented in Fig. 3. Fig. 4 shows a plasma sample from a patient before and 24 h after receiving the drug.

### Recovery

Recoveries without the addition of acetonitrile (on- or off-line) were low, independent of the amount of acetonitrile in M1A. Therefore, the addition of acetonitrile by M1B was used. Mixing of the

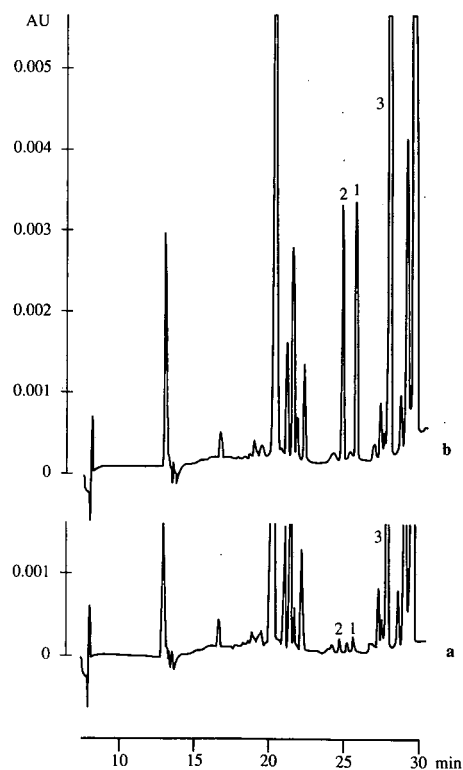


Fig. 3. Chromatograms of human plasma samples. Spiked with (a) 0.3 ng/ml and (b) 5 ng/ml acitretin (1) and 13-*cis*-acitretin (2); 3 is the internal standard.

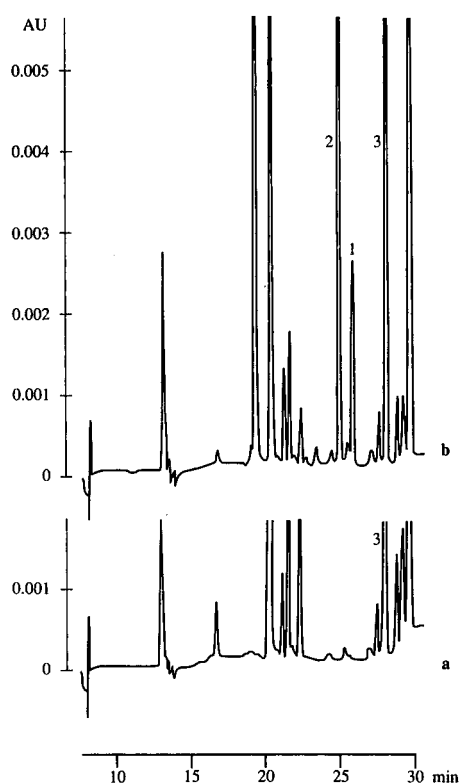


Fig. 4. Chromatograms of patient plasma samples. (a) Pre-dose sample; (b) sample taken 24 h after an oral daily dose of 50 mg acitretin over three weeks. Measured concentrations: acitretin (1) 5.77 ng/ml, 13-*cis*-acitretin (2) 56.6 ng/ml; 3 is the internal standard.

injected plasma sample, delivered by P1A, and M1B in the 50-cm-long steel capillary (0.5 mm I.D.) between the T-piece and V3 was efficient. Only a minimal improvement was obtained when a coiled, 2-m-long capillary of the same diameter was used. How-

TABLE II

INFLUENCE OF THE ACETONITRILE PORTION OF MOBILE PHASE M1B (ADDED BY THE T-PIECE) ON THE RECOVERIES OF 1, 2 AND 3

Plasma samples spiked with 100 ng/ml acitretin (1) and 13-*cis*-acitretin (2) and 20.8 ng/ml internal standard (3) ( $n = 3$ ).

Acetonitrile (%)	Recovery (%)		
	1	2	3
2	58.4	38.3	28.3
10	69.3	74.1	40.6
20	82.6	91.3	64.0
30	84.7	94.8	78.1
40	88.4	99.0	83.3
50	80.7	92.5	88.8
60	68.8	83.3	87.3

ever, the amount of acetonitrile added by the T-piece was crucial for good recoveries of the individual compounds. Table II shows the influence of the acetonitrile content in M1B on the recoveries of 1–3. More lipophilic compounds (*e.g.* the internal standard 3) needed a higher proportion of acetonitrile in M1B to achieve maximum recovery. The actual conditions of the method were 40% acetonitrile. The 100% values for recovery experiments were established by replicate injections of 100  $\mu$ l of 1–3 in M2A directly onto the analytical column (using I2). The recoveries under the conditions used are shown in Table III.

#### Linearity

The method was linear in at least the range 0.3–1000 ng/ml. Standard curves (0.3–500 ng/ml) were

TABLE III

RECOVERIES OF 1, 2 AND 3 ( $n = 5$ –8)

Concentration (ng/ml)	1		2		3	
	Recovery (%)	R.S.D. (%)	Recovery (%)	R.S.D. (%)	Recovery (%)	R.S.D. (%)
0.3	86.3	10.3	91.4	2.2	84.2	1.1
1	88.5	2.1	104	2.4	85.7	1.3
100	88.4	1.9	100	1.5	86.5	2.4
500	87.9	0.8	95.9	1.5	86.0	0.7

calculated by weighted least-squares regression, using  $1/y^2$  as the weighting factor.

#### Limit of quantification

The limit of quantification of **1** and **2** was 0.3 ng/ml. This high sensitivity was obtained by the injection of 1-ml plasma volumes. In contrast to off-line extraction methods, this technique prevents any loss of analyte by the re-injection of aliquots of dissolved extracts. Full automation of the method was realized using precolumn replacement by a tandem precolumn selector. A chromatogram of a spiked plasma sample at the quantification limit of 0.3 ng/ml is shown in Fig. 3a. The inter-assay ( $n = 6$ ) relative standard deviations (R.S.D.) at this concentration were 7.9 and 5.9% for **1** and **2**, respectively (see Table IV). The detection limit, defined by a signal-to-noise ratio of 3:1, was *ca.* 0.1 ng/ml. Even though simple UV detection was used, this is the highest sensitivity attained for these compounds, even considering liquid chromatography-mass spectrometry [17].

#### Precision and accuracy

The inter-assay precision and accuracy of the

TABLE IV  
INTER-ASSAY PRECISION AND ACCURACY ( $n = 6$ )

Concentration (ng/ml)		R.S.D. (%)	Difference between found and added (%)
Added	Found		
<i>Compound 1</i>			
0.3	0.30	7.9	-1.7
0.5	0.51	6.9	+1.3
1	1.01	4.2	+1.0
5	5.06	3.1	+1.1
20	20.3	2.0	+1.6
100	101	3.7	+0.6
200	197	1.2	-1.7
500	499	1.3	-0.1
<i>Compound 2</i>			
0.3	0.29	5.9	-2.7
0.5	0.50	8.4	-0.6
1	1.00	5.1	+0.3
5	5.13	2.4	+2.5
20	20.6	1.2	+2.9
100	101	4.2	+1.4
200	198	1.8	-1.1
500	505	1.4	+1.0

method were evaluated by analysing one series of calibration standards over six days against an independent calibration set. The results are given in Table IV. The overall precision was 3.8% for the two compounds.

#### Stability

The stability of retinoids in general and of **1** and **2** in particular have been discussed [5,10]. Plasma samples stored in the autosampler at 10°C were stable for at least 24 h. Therefore, after having prevented any *cis-trans* isomerization, fully automated routine analyses could be performed for 20–22 h per day.

#### CONCLUSIONS

A previously developed highly sensitive HPLC method for retinoids, using the direct injection of large plasma volumes, on-line solid-phase extraction and UV detection, was improved and fully validated for the determination of acitretin (**1**) and 13-*cis*-acitretin (**2**) in plasma samples. The addition of acetonitrile, which is necessary for good recovery in the on-line solid-phase extraction of retinoids, was performed on-line by a T-piece. In this way, long contact of the retinoids with acetonitrile in the autosampler could be avoided; this was shown to be responsible for the unexpected *cis-trans* isomerization in some of the plasma samples. About 30 injections could be made onto one precolumn, despite the large injection volume (1 ml of plasma). Full automation was attained with automated precolumn replacement. In addition, forward- and back-flush purging of the precolumn enhanced the number of injections possible onto the analytical column. The potential *cis-trans* isomerization, using the conditions described previously [12], also exists for other first- and second-generation retinoids (with a tetraene side-chain), but apparently not for third-generation retinoids [13]. Other ways to prevent the isomerization other than that proposed here would either only allow the analysis of short sample series, or, alternatively, result in less sensitive methods lacking full automation. Two examples of the latter are protein precipitation with ethanol [10] and solid-phase extraction using the Varian AASP system [9].

As a possible alternative to the on-line addition

of acetonitrile to an aqueous plasma sample, large injection volumes containing organic solvent could be diluted on-line with water (instead of acetonitrile) to prevent elution from the precolumn. This technique was used successfully in *in vitro* studies with incubated liver homogenates, where up to 20 ml of ethanol-containing solutions of acitretin and etretinate were injected [18]. The same procedure can also be applied to routine injections of relatively large volumes (> 1 ml) obtained after deproteinization of plasma samples with ethanol. Until now this has not been possible due to the breakthrough of polar compounds. Which of the two precolumn techniques, fully automated direct injection of large plasma volumes, or the more robust injection of deproteinized supernatants (the latter being more flexible with respect to recoveries), is superior will depend on the analyte, the matrix and the preference of the analyst.

HPLC methods with on-line solid-phase extraction and automated column switching are very useful for the determination of retinoids in biological samples because of their high automation potential, high precision and sensitivity. In this respect, this HPLC precolumn technique is superior to liquid chromatography-mass spectrometry, which has been introduced recently for the determination of retinoids in plasma samples [17, 19]. Whereas this latter technique is more specific, simplicity, economics, absence of manual extraction and derivatization, and even higher sensitivity are the advantages of HPLC with on-line solid-phase extraction and UV detection, making it the more direct of these two less travelled roads.

## ACKNOWLEDGEMENTS

The authors thank Dr. M. Klaus for supplying the internal standard, Mr. B. Maurer for the drawings and Drs. D. Dell and J. Burckhardt for correction of the manuscript.

## REFERENCES

- 1 J.-M. Geiger and B. Czarnetzki, *Dermatologica*, 176 (1988) 182.
- 2 W. Bollag, in J. H. Saurat (Editor), *Retinoids: New Trends in Research and Therapy*, Karger, Basle, 1985, p. 274.
- 3 C. J. Brindley, *Dermatologica*, 178 (1989) 79.
- 4 B. Löfberg, I. Chahoud, G. Bochert and H. Nau, *Teratology*, 41 (1990) 707.
- 5 R. Wyss, *J. Chromatogr.*, 531 (1990) 481.
- 6 R. Wyss and F. Bucheli, *J. Chromatogr.*, 456 (1988) 33.
- 7 R. Wyss and F. Bucheli, *J. Chromatogr.*, 424 (1988) 303.
- 8 R. Wyss, *Methods Enzymol.*, 189 (1990) 146.
- 9 C. Eckhoff and H. Nau, *J. Lipid Res.*, 31 (1990) 1445.
- 10 R. Wyss and F. Bucheli, *J. Chromatogr.*, 431 (1988) 297.
- 11 J. Creech Kraft, C. Eckhoff, W. Kuhn, B. Löfberg and H. Nau, *J. Liq. Chromatogr.*, 11 (1988) 2051.
- 12 R. Wyss and F. Bucheli, *J. Pharm. Biomed. Anal.*, 8 (1990) 1033.
- 13 R. Wyss and F. Bucheli, *J. Chromatogr.*, submitted for publication.
- 14 T. W. Shih, Y. F. Shealy, D. L. Strother and D. L. Hill, *Drug Metab. Dispos.*, 14 (1986) 698.
- 15 R. C. Jewell and P. J. McNamara, *J. Pharm. Sci.*, 79 (1990) 444.
- 16 K. Zech and R. Huber, *J. Chromatogr.*, 353 (1986) 351.
- 17 B. E. Fayer, C. A. Huselton, W. A. Garland and D. J. Liberato, *J. Chromatogr.*, 568 (1991) 135.
- 18 R. C. Chou, R. Wyss, C. A. Huselton and U.-W. Wiegand, *Life Sci.*, in press.
- 19 W. A. Garland, C. A. Huselton, F. Kolinsky and D. J. Liberato, *Trends Anal. Chem.*, 10 (1991) 177.

# Determination of the catechol-O-methyltransferase inhibitor Ro 40-7592 in human plasma by high-performance liquid chromatography with coulometric detection

U. Timm\* and R. Erdin

Pharma Division, Preclinical Research, F. Hoffmann-La Roche Ltd, CH-4002 Basle (Switzerland)

## ABSTRACT

A sensitive and specific high-performance liquid chromatographic method has been developed to measure the catechol-O-methyltransferase (COMT) inhibitor 3,4-dihydroxy-4'-methyl-5-nitrobenzophenone (Ro 40-7592) in human plasma. The compound and the internal standard were extracted from plasma at pH 2 with *n*-butyl chloride–ethyl acetate (95:5, v/v). The extract was chromatographed on a reversed-phase column (Hypersil ODS, 5  $\mu$ m) using a mixture of phosphate buffer (0.05 M, pH 2), methanol and tetrahydrofuran (45:55:5, v/v/v) as the mobile phase. Long-retained components were removed from the system by means of a simple column-switching system. Quantification of the catechol-O-methyltransferase inhibitor was performed by means of coulometric detection (0.15 V). The limit of quantification was about 1 ng/ml, using a 1-ml specimen of plasma. The recovery from human plasma was > 88%. The mean inter-assay precision was 5.3% in the range 2.5–1000 ng/ml. Linearity of the standard curve was obtained in the concentration range 2.5–500 ng/ml. The catechol-O-methyltransferase inhibitor was stable in human plasma when stored for six months at  $-20^{\circ}\text{C}$  and for 24 h at room temperature. The practicability of the new method was demonstrated by the analysis of more than 400 plasma samples from a tolerance study performed in human volunteers.

## INTRODUCTION

Parkinson's disease is one of the most common chronic progressive neurological diseases, and is characterized by the gradual degeneration of a group of neurons located in the brain stem in the substantia nigra. Although Madopar and Sinemet [combinations of 3,4-dihydroxyphenyl-L-alanine (L-DOPA) with the peripheral decarboxylase inhibitor benserazide or carbidopa, respectively] are still the

best treatments available for this condition, many patients experience significant side-effects and require frequent dosing, more than three times a day. These problems are related to markedly fluctuating L-DOPA levels as a result of peripheral degradation of L-DOPA to 3-O-methyldopa by the enzyme catechol-O-methyltransferase (COMT) [1].

In order to optimize L-DOPA therapy of Parkinson's disease, attempts have been made to discover compounds which would inhibit COMT. 3,4-Dihydroxy-4'-methyl-5-nitrobenzophenone (Ro 40-7592, I; see Fig. 1) is a novel nitrocatechol derivative which has been shown both *in vitro* and *in vivo* to be a potent, selective, competitive and reversible COMT inhibitor [2,3]. Adding I to L-DOPA-containing medications could optimize L-DOPA therapy of Parkinsonism.

A new reversed-phase high-performance liquid chromatography (HPLC) assay with coulometric

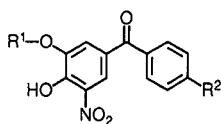


Fig. 1. Structures for the compounds referred to in the text: I,  $\text{R}^1 = \text{H}$ ,  $\text{R}^2 = \text{CH}_3$ , parent compound; II,  $\text{R}^1 = \text{CH}_3$ ,  $\text{R}^2 = \text{CH}_3$ , potential metabolite; III,  $\text{R}^1 = \text{H}$ ,  $\text{R}^2 = \text{Cl}$ , internal standard.

detection is described here for the determination of I in human plasma using the chlorinated analogue III as internal standard. Because of the high sensitivity of the assay (1 ng/ml, using 1-ml specimens) it was possible to follow plasma levels of I for a period of six elimination half-lives after a single 5-mg oral dose to human volunteers.

## EXPERIMENTAL

### Materials, reagents and solvents

Ethyl acetate (for pesticide residue analysis), methanol (gradient grade) and hydrochloric acid (titrisol, p.a.) were obtained from Merck (Darmstadt, Germany). *n*-Butyl chloride (HPLC grade) and tetrahydrofuran (unstabilized, HPLC grade) were purchased from Fisons (Loughborough, UK). Phosphate buffer (0.05 M, pH 2) was prepared by dissolving sodium dihydrogenphosphate monohydrate (p.a.; Merck) in water (HPLC grade; Baker, Deventer, Netherlands), titrating the solution with phosphoric acid (85%, suprapur; Merck) to pH 2 and filtering the buffer through a 0.22- $\mu$ m membrane filter (Millipore, Bedford, MA, USA). Plasma standards were prepared using pre-tested fresh-frozen plasma, which was obtained from a blood bank (Blutspendezentrum SRK, Basle, Switzerland).

### Preparation of standards

A stock solution was obtained by dissolving 10 mg of compound I in 10 ml of methanol. Aliquots of the stock solution were diluted in methanol, providing the working solutions. The plasma standards were obtained by spiking human blank plasma (25 ml) with 250  $\mu$ l of the corresponding working solution, providing concentrations between 1 and 500 ng/ml. The plasma standards were divided into aliquots of 2.5 ml and stored deep frozen ( $-20^{\circ}\text{C}$ ) until required for analysis.

### Sample preparation procedure

The samples were thawed at room temperature and homogenized by vortex-mixing. An aliquot of plasma (1 ml) was mixed with 50  $\mu$ l of internal standard solution containing 250 ng of III in hydrochloric acid (5 M). The sample was extracted with 5 ml of *n*-butyl chloride-ethyl acetate (95:5, v/v) by shaking for 15 min at 15 rpm on a rotating shaker

(Heidolph, Kelheim, Germany). After centrifugation for 5 min, 4 ml of the separated organic phase were transferred to a tapered tube and evaporated to dryness at  $45^{\circ}\text{C}$  by means of a gentle stream of pure (99.999%) nitrogen. For HPLC analysis, the extraction residue was dissolved in 200  $\mu$ l of mobile phase by vortex-mixing for 15 s.

### Instrumentation

A schematic representation of the column-switching system is given in Fig. 2. It consisted of a double-piston pump (P1; Model L6200; Merck), an automatic sample injector (A; Model Wisp 712; Waters, Milford, MA, USA), an analytical column (C1; 125  $\times$  4 mm; Merck), slurry-packed with Hypersil ODS 5  $\mu$ m (Shandon) in our laboratory, a stainless-steel precolumn (C2; 30  $\times$  4 mm; Merck), slurry-packed with 5- $\mu$ m Hypersil ODS (Shandon,

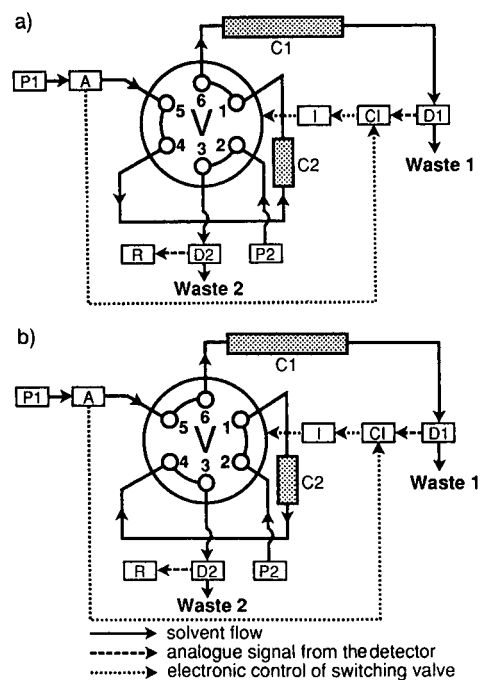


Fig. 2. Schematic representation of the column-switching system assembled for the analysis of I in plasma (see text for details). (a) Valve position 0-4 min and 16-18 min after injection. (b) Valve position 4-16 min after injection. P1 = double-piston pump; A = autosampler; C1 = analytical column; C2 = precolumn; D1 = electrochemical detector; P2 = single-piston pump; D2 = LC-UV detector; R = recorder; V = automatic switching valve; CI = computing integrator; I = interface.



Astmoor, UK), a column oven operating at 30°C (Model 7930; Jones, Hengoed, UK), a coulometric detector (D1; Model 5100, potential 0.15 V; ESA, Bedford, MA, USA), an analytical cell (Model 5011; ESA), a single-piston pump (P2; Model L6000; Merck), an air-actuated switching valve (V; Model 7000 assembled with a Model 7001 pneumatic actuator and a Model 7163 solenoid valve; Rheodyne, Cotati, CA, USA) and a laboratory-made interface (I) for actuating the switching valve by means of a computing integrator (CI; Model SP 4200; Spectra Physics, San Jose, CA, USA) [4]. Although not necessary, a LC-UV detector (D2; Model Spectroflow 773, 254 nm; Kratos, Ramsey, NJ, USA) and a recorder (R; Model W+W 600; Kontron, Zurich, Switzerland) were desirable for proper control of the column-switching process.

Data acquisition was performed by means of the computing integrator (CI), working with a special BASIC program originally developed for the integrator SP 4100 [5]. The acquired data were sent via Ethernet to the host computer for further data reduction and reporting by the KINLIMS system, recently developed in our company [6].

#### Chromatography and system operation

A mixture of phosphate buffer (0.05 M, pH 2), methanol and tetrahydrofuran (45:55:5, v/v/v) was used as the mobile phase for both pumps. The mobile phase was degassed before use with a stream of helium for 1 min. The flow-rates of the two pumps, P1 and P2, were adjusted to 1 ml/min.

The extraction residue was dissolved in 200  $\mu$ l of the mobile phase. After mixing for 30 s on a vortex mixer, an aliquot (100  $\mu$ l) of the clear solution was injected by the autoinjector A onto the precolumn (C2) (Fig. 2a). Immediately after the elution of compounds I and III from the precolumn (about 4 min), the HPLC valve (V) was switched to the second position by means of the computing integrator (CI) (Fig. 2b). The two compounds of interest were then chromatographed in the usual manner on the analytical column (C1), while longer-retained plasma constituents were removed from the HPLC system by back-flushing the precolumn (C2). When the chromatography of I and III was completed (about 16 min) the valve (V) switched back to the initial position (Fig. 2a). After an equilibrium time of about 1–2 min the system was ready for the next injection.

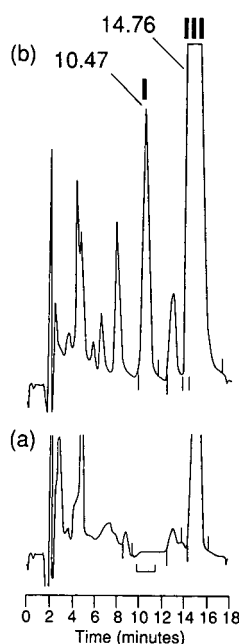


Fig. 3. Chromatograms of human plasma samples: (a) before application; (b) collected 6 h after a single oral dose of 5 mg I; measured concentration, 8.1 ng/ml. Detector, D1; potential, 0.15 V; gain,  $5 \times 10$ ; response time, 10 s.

The retention times of I and III were about 10.5 and 14.8 min, respectively (Fig. 3b). A complete cycle lasted about 18 min.

#### Calibration and calculations

At least six different plasma standards covering the expected concentration range were processed as described above, together with the biological samples. The standard curve was established by weighted linear least-squares regression (weighting factor =  $1/y^2$ ) of the measured peak-height ratios I/III ( $y$ ) versus the concentrations of I ( $x$ ) added to the plasma. This regression equation was then used to calculate concentrations of I in unknown plasma samples from the measured peak-height ratios I/III.

## RESULTS AND DISCUSSION

#### Sample preparation procedure

Because of the acidic nature of the nitrocatechol group ( $pK_a = 4.3$ ), maximum recovery of I was obtained around pH 2; this was achieved by mixing the plasma samples with 50  $\mu$ l of hydrochloric acid (5 M; also containing the internal standard) before

extraction. Several non-polar solvents (e.g. hexane, *n*-butyl chloride, chloroform) were tested as extractants; however, owing to the polar character of I, a more polar solvent was required to isolate the compound from plasma. A mixture of *n*-butyl chloride and ethyl acetate (95:5, v/v) provided the best compromise between high recovery of I and an acceptable degree of coextraction of interfering plasma components.

#### *Analytical system and chromatography*

From various suitable 5- $\mu$ m stationary phases (e.g. Spherisorb ODS-1, Spherisorb ODS-2), Hypersil ODS 5  $\mu$ m was selected as packing material for the analytical separation. However, long-term experience with this material showed that broad and tailing peaks for I and III were obtained for certain batches of Hypersil. This problem was overcome by purging new columns for 48 h with methanol-water, containing *n*-hexylmethyl amine (10 mM) as modifier. After removing the excess of amine with methanol-water, the columns were ready for use.

Good separation between I and III was achieved with the mobile phase system described in the Experimental section. Phosphate buffer (0.05 M, pH 2) was used as aqueous constituent, in order to suppress ionization of the nitrocatechol group in I and III during chromatography, and to provide a certain conductivity in the mobile phase, which was necessary for the electrochemical detection.

For some samples, late-eluting plasma constituents were observed which interfered in subsequent chromatograms. In order to keep the analysis time for these samples acceptable, the chromatographic system was extended by a simple column-switching unit, allowing a back-flush of the precolumn.

The relatively polar extraction conditions led to

considerable coextraction of plasma constituents, which could not be separated completely from I and III during chromatography. The problem was overcome by replacing the UV detector by a highly specific coulometric detector. The COMT inhibitor is a suitable candidate for electrochemical detection, because of the nitrocatechol group, which easily undergoes electrochemical oxidation. However, the voltage of the detector had to be kept at low values (around 0.15 V), in order to suppress the electrochemical response of plasma interferences. Unfortunately, the potential 3-O-methylated metabolite II could not be detected under these conditions, because the nitrophenol group needed a higher potential (ca. 0.6 V) for electrochemical oxidation than the nitrocatechol system. Further work on a simultaneous assay for I and II is planned.

#### *Recovery*

Human blank plasma was spiked with compounds I and III at concentrations of 10, 50 and 250 ng/ml. The plasma was divided into 1-ml aliquots, extracted as described but without adding the internal standard. The extraction residues were reconstituted in mobile phase and chromatographed as described.

A second series of control samples, providing the 100% values, was prepared by extracting 1-ml aliquots of human blank plasma and then adding equimolar amounts of I and III in mobile phase to the dry residues.

The analytical recoveries for compounds I and III were calculated by comparing the peak heights of the extracted samples to the peak heights obtained from the control samples to which I and III had been added after extraction. The overall recoveries were calculated by correcting the analytical recoveries with the aliquot factors.

TABLE I  
RECOVERY OF THE COMT INHIBITOR FROM HUMAN PLASMA

Concentration added (ng/ml)	Concentration found (ng/ml)	Number of replicates (n)	Relative standard deviation (%)	Recovery (%)
10.0	9.11	5	8.71	91.1
50.0	44.0	5	2.93	88.0
250	244	5	4.60	97.6

TABLE II

## RECOVERY OF THE INTERNAL STANDARD FROM HUMAN PLASMA

Concentration added (ng/ml)	Concentration found (ng/ml)	Number of replicates (n)	Relative standard deviation (%)	Recovery (%)
10.0	8.58	5	8.91	85.8
50.0	42.2	5	2.14	84.3
250	233	5	4.49	93.1

The data in Tables I and II indicate a satisfactory overall recovery of >88% and >84% for compound I and the internal standard III, respectively.

*Selectivity*

The electrochemical method was very specific with respect to endogenous components coextracted from plasma. In more than 100 clinical blank plasma samples (pre-dose, placebo) from 18 different volunteers analysed so far, in only one case was an interfering compound observed coeluting with the COMT inhibitor. Fig. 3a shows a representative chromatogram of a human plasma sample collected before administration.

*Precision, accuracy and linearity*

The inter-assay precision was measured at different concentration levels around therapeutic concentrations in human plasma. For each level (10, 50

and 250 ng/ml) a spiked plasma sample was prepared and analysed on different days (using a separate calibration line on each day). The data in Table III demonstrate an acceptable precision and accuracy over the concentration range investigated.

The correlation between the peak-height ratio I/III *versus* the concentration of I was linear in the range 2.5–500 ng/ml of plasma. Some clinical samples contained more than 500 ng of COMT inhibitor per ml. In this case the samples were diluted before work-up and the calculated concentration was corrected by means of a scale factor.

According to Table III, the standard deviations and, therefore, also the variances were not constant over this wide concentration range. For this reason, the calibration curve had to be calculated by means of a weighted linear least-squares regression procedure, using  $1/y^2$  as weighting factor [7]. The standard software of the computing integrator provided

TABLE III

## INTER-ASSAY PRECISION

Concentration added (ng/ml)	Concentration found (mean $\pm$ S.D.) (ng/ml)	Number of replicates (n)	Relative standard deviation (%)	Inaccuracy <sup>a</sup> (%)
2.50	2.76 $\pm$ 0.4195	5	15.2	10.4
5.00	4.96 $\pm$ 0.3258	5	6.57	– 0.8
10.0	9.98 $\pm$ 0.4082	5	4.09	– 0.1
25.0	24.4 $\pm$ 1.210	5	4.96	– 2.5
50.0	50.9 $\pm$ 1.639	5	3.22	1.9
100	101 $\pm$ 2.151	5	2.13	0.6
250	247 $\pm$ 3.359	5	1.36	– 1.2
500	489 $\pm$ 25.53	5	5.22	– 2.4
10.3	10.3 $\pm$ 0.2482	34	2.41	0.4
51.1	51.0 $\pm$ 1.117	32	2.19	– 0.1
231	237 $\pm$ 10.50	35	4.43	2.4

<sup>a</sup> (Concentration found – concentration added) / concentration added  $\times$  100.

TABLE IV  
STABILITY OF PARENT COMPOUND IN HUMAN PLASMA

Storage conditions	Concentration added (ng/ml)	Concentration found (ng/ml)	Change of concentration after storage (%)	90% Confidence interval (%)	Number of replicates (n)
Six months at -20°C	10.0	10.2	2.1	-8.5 to +13.8	5
	50.0	51.1	2.3	-1.7 to +6.4	5
	250	260	3.9	-3.9 to +12.3	5
24 h at +25°C	10.0	10.0	0.0	-5.0 to +5.3	5
	50.0	50.2	0.3	-2.7 to +3.5	5
	250	253	1.1	-0.9 to +3.2	5

only conventional linear regression and had, therefore, to be modified by means of additional programs [5].

#### Limit of quantification

By careful adjustment of the conditions of the coulometric detector, less than 1 ng/ml COMT inhibitor could be detected with a signal-to-noise ratio of 3:1. However, the limit of quantification, defined here as the minimum concentration that can be measured routinely with acceptable precision (<20%) and accuracy (>80%), was 1–2.5 ng/ml (see Table III).

#### Stability

Control plasma was prepared at concentrations of 10, 50 and 250 ng/ml. One portion of these samples was stored at room temperature for 24 h and then analysed. The other portion was frozen, stored at -20°C for six months and then analysed. With each set of stored samples, an equal number of freshly prepared samples was analysed to provide the 100% values. The statistical interpretation of the data followed the procedure recently developed [8]. The data presented in Table IV indicate that compound I was stable in human plasma under the storage conditions investigated.

#### Application to biological samples

The method has been applied successfully to the analysis of more than 400 plasma samples from a dose proportionality study performed in man. Fig. 3b shows a representative chromatogram from this study. All samples of the study could be analysed by means of the same precolumn and analytical column. Additionally, the electrochemical cell needed

no special treatment or readjustment of potential, demonstrating the robustness of the new method. The method was sensitive enough to measure precisely the low concentrations of I in plasma for up to 10 h (corresponding to a period of approximately six elimination half-lives) after a single oral dose of 5 mg to human volunteers.

#### ACKNOWLEDGEMENTS

The authors thank Dr. A. Saner, Dr. J. Borgulya and Mr. G. Zürcher for their helpful advice, Dr. D. Dell and Dr. J. Burckhardt for correcting the manuscript, Mr. H. Suter for drawing the figures and Mrs. S. Klein for preparing the manuscript.

#### REFERENCES

- 1 M. Da Prada, in W. Birkmayer, U. K. Rinne, J. Worm-Petersen, E. Dupont and W. Schwarz (Editors), *Parkinson's Disease, Actual Problems and Management*, Editiones Roche, Basle, 1984, 25.
- 2 K. Bernauer, J. Borgulya, H. Bruderer, M. Da Prada and G. Zürcher, *Swiss Pat. Appl.*, CH 980/86, (1986).
- 3 G. Zürcher, H. H. Keller, R. Kettler, J. Borgulya, E. P. Bonetti, R. Eigenmann and M. Da Prada, in M. B. Streifler, A. D. Korczyn, E. Melamed and M. B. H. Youdim (Editors), *Advances in Neurology, Vol. 53 Parkinson's Disease: Anatomy, Pathology, and Therapy*, Raven Press, New York, 1990, p. 497.
- 4 U. Timm and A. Saner, *J. Chromatogr.*, 378 (1986) 25.
- 5 U. Timm, D. Dell and D. A. Ord, *Instrum. Comput.*, 3 (1985) 29.
- 6 U. Timm and B. Hirth, *Scientific Computing and Automation (Europe) 1990*, Elsevier, Amsterdam, 1990, pp. 329–340.
- 7 E. L. Johnson, D. L. Reynolds, D. S. Wright and L. A. Pachla, *J. Chromatogr. Sci.*, 26 (1988) 372.
- 8 U. Timm, M. Wall and D. Dell, *J. Pharm. Sci.*, 74 (1985) 972.

# High-performance liquid chromatography method for the determination of aminoglycosides based on automated pre-column derivatization with *o*-phthalaldehyde

M. C. Caturla\* and E. Cusido

*Analytical Chemistry Department, Centro de Investigación y Desarrollo Aplicado, S.A.L., C.I. Santiga, Argenters 6, 08130-STA. Pèrpetua de Mogoda, Barcelona (Spain)*

D. Westerlund

*Department of Analytical Pharmaceutical Chemistry, Uppsala University, P.O. Box 574, S-751 23 Uppsala (Sweden)*

---

## ABSTRACT

Aminoglycosides, such as amikacin, kanamycin, tobramycin and gentamycin, are often determined, after derivatization, by high-performance liquid chromatography with UV detection. The aim of this work was to develop a sensitive and precise automated method to determine amikacin in pharmaceutical formulations from a stability study. A liquid chromatograph fitted with an autosampler, a diode-array detector set at 340 nm and a  $C_{18}$  column was used. The method uses an automated pre-column derivatizing with *o*-phthalaldehyde for compounds containing derivatizable primary amino groups. The derivatization is fast at ambient temperatures, improving the precision and sensitivity (0.5  $\mu\text{g/ml}$ ), and there is a wide linearity range.

---

## INTRODUCTION

The use of high-performance liquid chromatography (HPLC) as an analytical method for therapeutic drug monitoring of aminoglycosides [1–7] and their determination in pharmaceutical formulations [8–12] has been reported previously. As aminoglycosides do not have a suitable UV absorption or fluorescence emission for on-line detection after separation by HPLC, either pre- or post-column derivatization is necessary for their determination.

Various liquid chromatography procedures have been reported for the determination of amikacin in pharmaceuticals [7, 11] using pre-column derivatization with 1-fluoro-2,4-dinitrobenzene [7] or 2,4,6-trinitrobenzenesulphonic acid [11]. These reagents have slow reaction rates and require heating for the derivatization to occur. *o*-Phthalaldehyde (OPA) is one of the most commonly used reagents for the derivatization of aminoglycosides, mainly due to the fact that the reaction is relatively fast, even at

ambient temperatures. However, OPA-derivatized aminoglycosides are unstable [3] and differing delay times after the derivatization affect the precision of the method. This method aims to avoid some of the drawbacks by using an automated derivatization injection procedure. This automated method is fast, simple and shows good precision and sensitivity compared with manual methods. It has been used for the determination of amikacin in pharmaceutical solutions from a stability study.

## EXPERIMENTAL

### *Chemicals and reagents*

Amikacin sulphate, kanamycin acid sulphate, sodium heptane sulphonate and OPA were all obtained from Sigma (St. Louis, MO, USA). Mercaptoethanol was of synthesis grade (Merck, Schuchardt, Hohenbrunn, Germany). Methanol (HPLC grade) was supplied by Scharlau (Barcelona, Spain). Glacial acetic acid and potassium hydroxide

were of analytical reagent grade (Merck, Darmstadt, Germany).

#### Chromatographic system

**Apparatus.** The HPLC analyses were performed using a modular liquid chromatographic system consisting of a 6000A pump from Waters, (Milford, MA, USA) and a Model 1000S diode-array detector from Applied Biosystems (Foster City, CA, USA), together with a Promis II autosampler from Spark-Holland (Emmen, Netherlands) or a Rheodyne 7125 manual injector. Data collection and reduction were performed using a computing integrator program (Nelson Analytical 2600 version 5; Perkin-Elmer Nelson System).

**Column and mobile phase.** Separations were performed using a C<sub>18</sub> reversed-phase column (Hypersil ODS 3  $\mu$ m; 15  $\times$  0.40 cm, Tracer). The mobile phase consisted of a mixture of acetic acid–heptane-sulphonate–methanol (4.5:22.5:73, v/v/v). The chromatographic separation was performed isocratically at ambient temperature at a flow-rate of 0.4–0.5 ml/min and UV detection at 340 nm was used.

#### Derivatizing reagent

Potassium borate buffer was prepared from boric acid (24.7 g) and potassium hydroxide (21.3 g) dissolved in 900 ml of water. A pH range of 10.38–10.42 was acceptable and adjustment was not usually necessary. The solution was diluted to 1.0 l. The reagent was prepared by dissolving OPA (100 mg) in 1 ml of methanol, followed by the addition of 200  $\mu$ l of mercaptoethanol and then diluting to 20 ml with potassium borate buffer. The solution was prepared weekly and stored in an air-tight amber bottle at 4°C.

#### Derivatization procedures

Manual pre-column derivatization (MAN) was performed by adding 100  $\mu$ l of the OPA solution to 100  $\mu$ l of the amikacin standard solution. At exactly 2 min after this addition (measured by a chronometer), 25  $\mu$ l were injected into the chromatograph.

Automatic pre-column derivatization (AUT) was performed by programming the autosampler (provided with a special cassette) to take 100  $\mu$ l each of the OPA and amikacin solutions, waiting for 2 min and then injecting 25  $\mu$ l of the mixture into the chromatograph.

## RESULTS

The representative chromatogram of amikacin and kanamycin (internal standard) is given in Fig. 1.

#### Derivatization products

The amikacin solution generated two peaks [retention times ( $t_R$ ) 6.20 and 6.80 min] giving qualitatively identical spectra by diode-array detection (Fig. 2).

When different reaction times (1, 2, 3 and 5 min) were investigated with OPA, the first peak decreased with the reaction time and the second increased. The increase was less than 1.5% between 2 and 5 min of reaction time. The results indicate that the first peak ( $t_R$  = 6.2 min) is a product of incomplete derivatization; only the second amikacin peak ( $t_R$  = 6.8 min) was used for the determination.

#### Method validation

Linearity was determined in the concentration range 2–100  $\mu$ g/ml (AUT), resulting in a coefficient

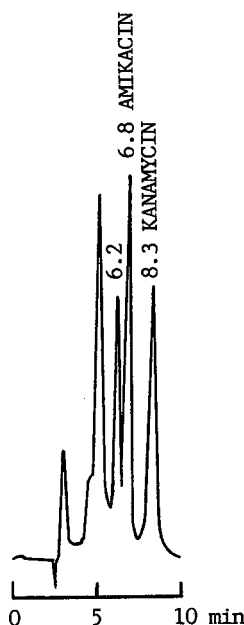


Fig. 1. Typical chromatogram for a sample of 50  $\mu$ g/ml amikacin and kanamycin (internal standard) solution. The peak with  $t_R$  = 6.2 min is the incompletely derivatized amikacin. Flow-rate = 0.5 ml/min.

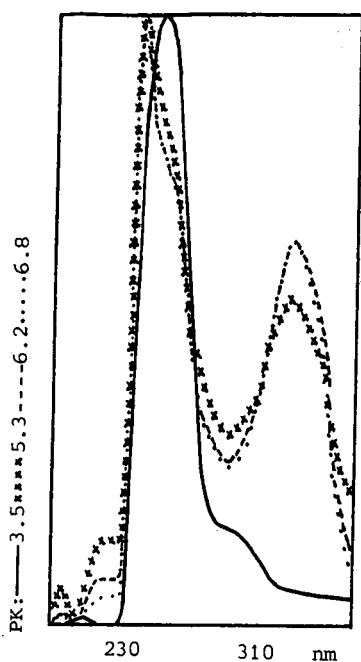


Fig. 2. "On-the-fly" spectra of the two peaks using diode-array detection. --- = First amikacin peak; ... = second amikacin peak (used for determination); — = excess of OPA reagent.

of regression of  $r=0.998$ , and the range 5–100  $\mu\text{g/ml}$  (MAN), giving  $r=0.994$ .

Fluorimetric detection severely restricted the linear range to 2–32 and 1–16  $\mu\text{g/ml}$  [2,5] compared with this UV detection method.

TABLE I

INTRA- AND INTER-DAY PRECISION: COMPARISON OF AUTOMATED (AUT) AND MANUAL (MAN) DERIVATIZATION

Concentration ( $\mu\text{g/ml}$ )	<i>n</i>	Coefficient of variation (%)	
		MAN method	AUT method
<i>Intra-day precision:</i>			
5	5	11.5	2.1
25	5	6.8	0.3
45	5	2.4	2.0
55	5	9.6	3.9
100	5	8.7	4.2
<i>Inter-day precision:</i>			
45	5	22.0	7.4
50	5	18.6	5.3
55	5	17.8	6.2

The limit of quantitation, defined as the lowest concentration that can be determined with a coefficient of variation (C.V.) less than 15%, was about 5 and 0.5  $\mu\text{g/ml}$  for the MAN and AUT methods, respectively.

Intra-day precision, calculated by the C.V., was determined for the MAN and AUT methods at five different concentrations. The values ( $n=5$ ) were 2.4–11.5% for the MAN and 0.3–4.2% for the AUT methods. The day-to-day C.V. ranged from 17.8 to 22.0% for the MAN and 5.3 to 7.4% for the AUT methods (Table I).

## DISCUSSION

Liquid chromatography with post-column derivatization using OPA is well suited to the determination of aminoglycosides in pharmaceutical formulations [6]. However, the post-column reaction method shows some disadvantages [5]: baseline noise is enhanced due to pumping the derivatization reagent through the detector; the flow cell may be soiled by the reaction products; the consumption of reagent is high; and the reaction time can only be increased by the increased column volume, resulting in additional peak broadening and loss of sensitivity.

The critical point for the pre-column derivatization with OPA has been the need to carefully control the reaction time to provide reproducible results. In the method presented here, the reaction is automatically controlled, improving the precision and sensitivity. The derivatization is fast at ambient temperatures and the linearity range wide.

The procedure has been successfully applied to the determination of the aminoglycosides amikacin, gentamycin, tobramycin and kanamycin.

## CONCLUSIONS

This automated method, as a result of its precision, limit of quantitation, capacity and simplicity, offers a suitable procedure for the determination of compounds containing derivatizable primary amino groups.

## ACKNOWLEDGEMENTS

We acknowledge the technical assistance of Carolina Sevillano.

## REFERENCES

- 1 J. D'Souza and R. I. Ogilvie, *J. Chromatogr.*, 232 (1982) 212.
- 2 J. P. Anhalt and S. D. Brown, *Clin. Chem.*, 24 (1978) 1940.
- 3 S. E. Bäch, I. Nilsson-Ehle and P. Nilsson-Ehle, *Clin. Chem.*, 25 (1979) 1222.
- 4 G. Lachatre, G. Nicot, C. Gonnet, J. Tronchet, L. Merle, J. P. Valette and N. Nonaille, *Analisis*, 11 (1983) 168.
- 5 L. Essers, *J. Chromatogr.*, 305 (1984) 345.
- 6 H. Fabre, M. Sekkat, M. D. Blanchin and B. Mandrou, *J. Pharm. Biomed. Anal.*, 7 (1989) 1711.
- 7 D. M. Barends, J. S. Blauw, M. H. Smiths and A. Hulshoff, *J. Chromatogr.*, 276 (1983) 385.
- 8 P. M. Kabra, P. K. Bhatnager and M. A. Nelson, *J. Chromatogr.*, 307 (1984) 224.
- 9 D. M. Barends, J. C. A. M. Brouwers and A. Hulshoff, *J. Pharm. Biomed. Anal.*, 5 (1987) 613.
- 10 N. K. Athanikar, R. W. Jurgens, R. J. Sturgeon and L. A. Zober, *J. Parenter. Sci. Technol.*, 37 (1983) 125.
- 11 P. Gambardella, R. Punziano, M. Gionti, C. Guadalupi and G. Mancini, *J. Chromatogr.*, 348 (1985) 229.
- 12 M. Freeman, P. A. Hawkins, J. S. Loran and J. A. Stead, *J. Liq. Chromatogr.*, 2 (1979) 1305.



CHROMSYMP. 2432

# Determination of Zy 17617B in plasma by solid-phase extraction and liquid chromatography with automated pre-column exchange

D. Chollet\* and M. Salanon

Zyma S.A., Department of Toxicology and Pharmacokinetics, Nyon (Switzerland)

## ABSTRACT

An automated chromatographic system, combining solid-phase extraction and automated pre-column exchange, is described for the routine determination of Zy 17617B at the pmol/ml level in human plasma. The sample extraction and elution onto the analytical column were performed automatically and concomitantly using a conventional liquid chromatographic apparatus equipped with a Merck OSP-2 on-line sample preparator. Validation data demonstrate the reliability of the method.

## INTRODUCTION

Zy 17617B, 1,3-dihydro-1-[(4-methyl-4H,6H-pyrrolo[1,2a][4,1]benzoxazepin-4-yl)methyl]-4-piperidiny]-2H-benzimidazol-2-one maleate (Fig. 1), is a pharmaceutical product with antidiarrheal properties [1]. A sensitive assay is required for the determination of pharmacokinetic data after oral intake of this drug.

Solid-phase extraction of drugs from plasma, via disposable extraction pre-columns or by column switching, is being increasingly used in combination with liquid chromatography (LC) as an alternative to time-consuming liquid-liquid extraction. Semi-automated or fully automated systems have been introduced for off-line analysis [2–4]; however, very

few of them allow complete on-line analysis with automated pre-column exchange [5].

In this study, a system is described for the routine quantification of Zy 17617B in human plasma. Both sample extraction, carried out using a new pre-column, and elution onto the analytical column were performed automatically and concomitantly using a conventional LC apparatus equipped with an OSP-2 on-line sample preparator from Merck.

## EXPERIMENTAL

### Materials

Anhydrous sodium dihydrogenphosphate of Suprapur grade was from Merck (Darmstadt, Germany). Orthophosphoric acid (85%, w/v), sodium hydroxide and tetrahydrofuran (THF) were of analytical grade and were also from Merck. THF was freshly distilled. Methanol and acetonitrile (high-performance liquid chromatography grade) were purchased from Mächler (Basle, Switzerland). Water was bidistilled.

Zy 17617B was from Ciba-Geigy (Summit, NJ, USA). A typical reference stock solution was prepared by dissolving 1.14 mg of Zy 17617B in 5 ml of acetonitrile and diluting to 100 ml with water. Di-

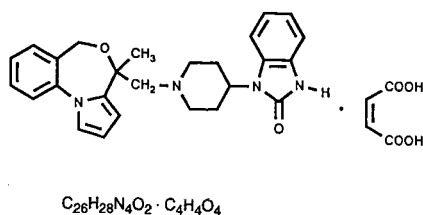


Fig. 1. Molecular structure of Zy 17617B; mol.wt. 544.61.

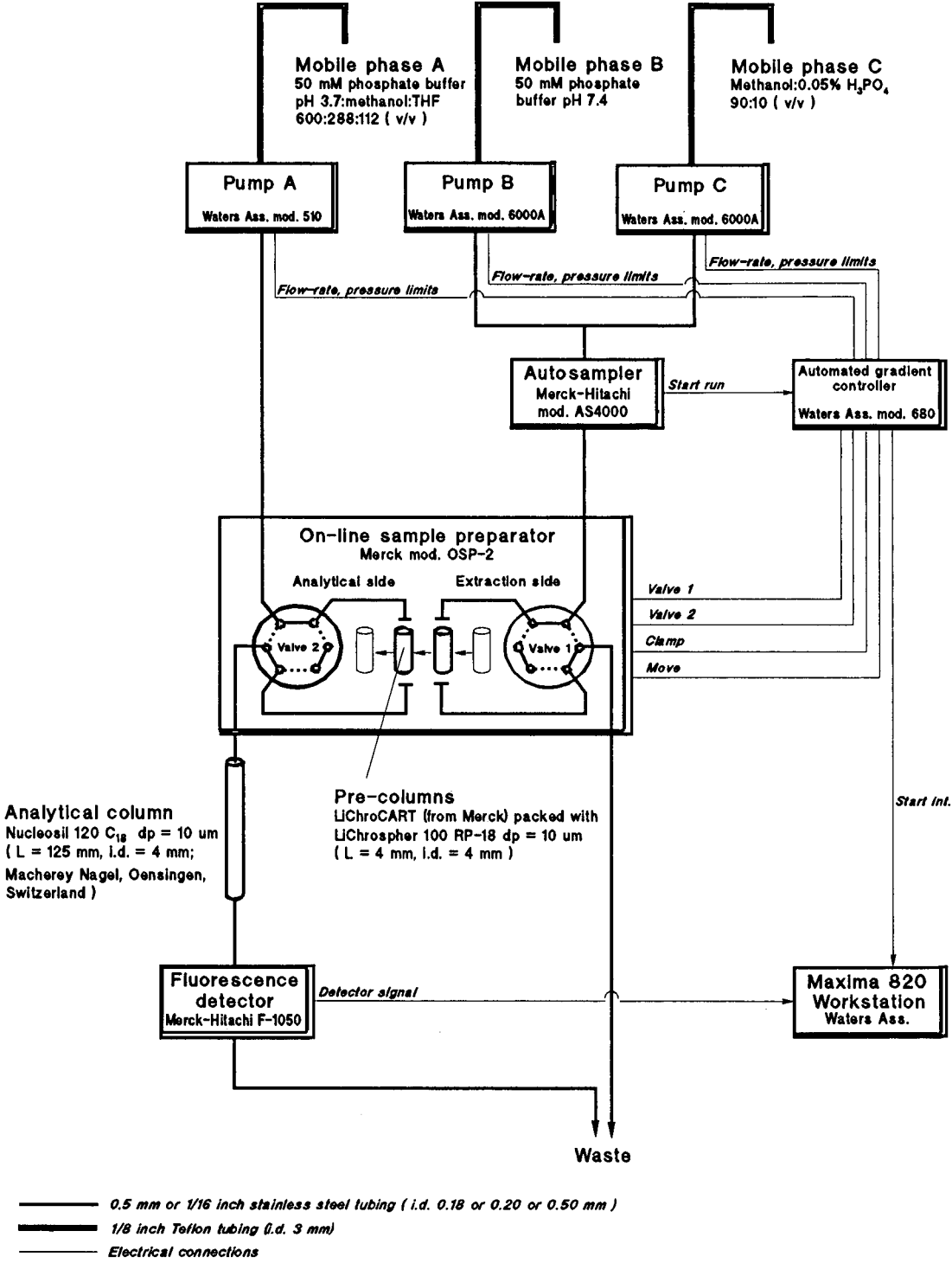


Fig. 2. Scheme of the chromatographic system.

luted solutions were obtained by successive dilutions with water. The reference solutions were stored at 4°C.

### Apparatus

The chromatographic system is described in Fig. 2. The autosampler was equipped with a 400- $\mu$ l

fixed loop and a temperature-controlled rack set to 10°C. The mobile phases are also described in Fig. 2.

### Method

Sample extraction was performed on LiChro-CART pre-columns (4 mm  $\times$  4.0 mm I.D.; from

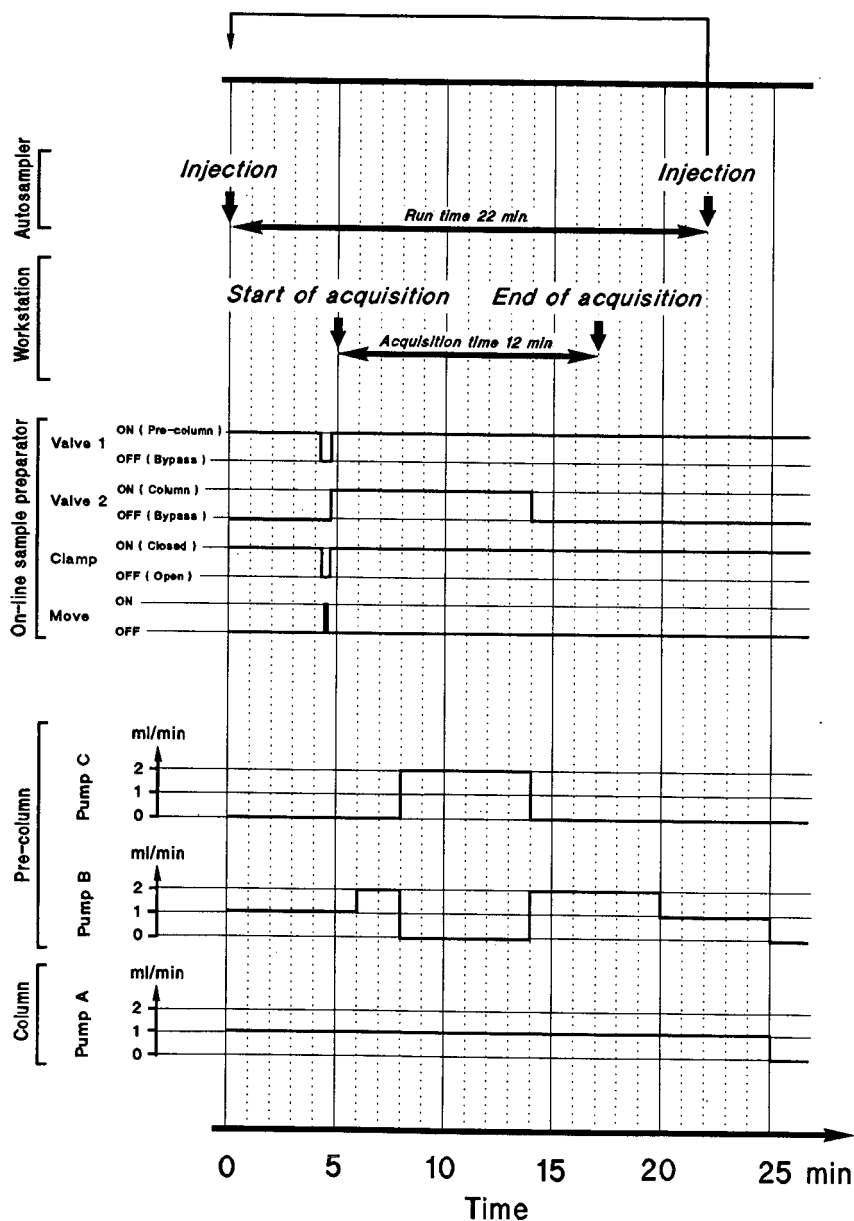


Fig. 3. Experimental conditions.

Merck), which were packed with LiChrospher 100 RP-18 (particle diameter,  $d_p = 10 \mu\text{m}$ ). These were conditioned following the instructions in Figs. 2 and 3. Concomitantly, the analytical column (Nucleosil 120  $\text{C}_{18}$ ,  $d_p = 5 \mu\text{m}$ ,  $125 \text{ mm} \times 4.0 \text{ mm I.D.}$ ) was eluted isocratically using mobile phase A (Fig. 2). The flow-rates were set as shown in Fig. 3. Detection was performed by spectrofluorimetry at an excitation wavelength of 285 nm and an emission wavelength of 315 nm.

#### Sample preparation

An aliquot of 1.0 ml of thawed plasma was diluted with 1.0 ml of mobile phase B (Fig. 2) in a glass tube, vortexed for 1 min and filtered on a single-use  $0.22\text{-}\mu\text{m}$  filter unit (Model Millex-GS, Millipore). The resulting solution was then placed in the auto-sampler rack for analysis (injection of  $400 \mu\text{l}$ ).

#### Standard preparation

Standard plasma samples were prepared by diluting drug-free plasma with reference solutions followed by further dilution with mobile phase B.

#### Calibration and quantification

Calibration was performed by linear regression analysis of the detector response over the concen-

tration range 10–84 pmol/ml. The concentration of Zy 17617B in each sample was quantified using the calibration curves.

## RESULTS AND DISCUSSION

Zy 17617B was extracted from the plasma by solid-phase extraction by means of an OSP-2 on line sample preparator. This device allowed the on-line extraction of a sample whilst another was being eluted onto the analytical column in a continuous automatic fashion (Fig. 2). A new or reconditioned pre-column was used for each analysis. Typical chromatograms are given in Fig. 4.

#### Solid-phase extraction

Solid-phase extraction of Zy 17617B was performed on short  $\text{C}_{18}$  reversed-phase pre-columns ( $4 \text{ mm} \times 4 \text{ mm I.D.}$ ,  $d_p = 10 \mu\text{m}$ ) using phosphate buffer pH 7.4 (50 mM) as the mobile phase.

The total recovery of the analysis was found to be  $81.5 \pm 1.4\%$  ( $n = 3$ ) for a plasma standard of 41.9 pmol/ml. Zy 17617B was strongly adsorbed onto plastic or glassware. In a set of experiments, the volume fraction of plasma in a standard sample was increased from 0.00 to 1.00. As shown in Fig. 5, the increase in the level of plasma proteins reduced this

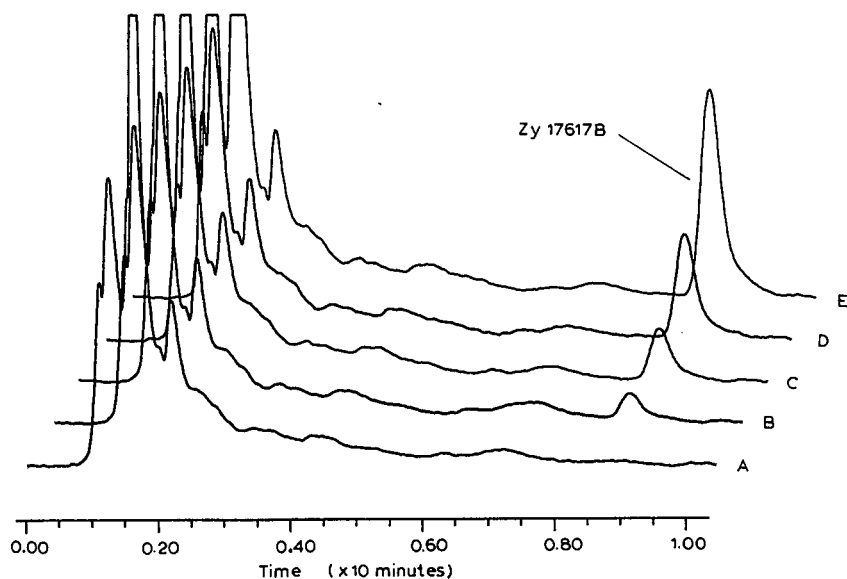


Fig. 4. Typical chromatograms of plasma standards: (A) 0.0 pmol/ml; (B) 10.5 pmol/ml; (C) 21.0 pmol/ml; (D) 41.9 pmol/ml; and (E) 83.7 pmol/ml. For experimental conditions see Fig. 3.

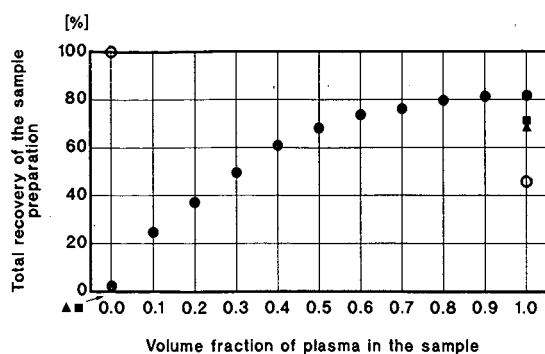


Fig. 5. Recovery of the sample preparation. Sample 1.00 ml + 41.9 pmol of Zy 17617B in 200  $\mu$ l of water + 0.80 ml of mobile phase B (pH 7.4, closed symbols) or 0.80 ml of diluted acetic acid (pH 3.0, open symbols). ● = glass tubes; ▲ = polyethylene tubes; ■ = polystyrene tubes.

adsorption at physiological pH. This is probably the result of protein binding. This effect was less pronounced in acidic medium.

The recovery of the extraction step was found to be approximately 99%. Liquid-liquid extraction in basic medium with diisopropyl ether, ethyl acetate and *n*-hexane gave values of 87, 47 and 7% respectively.

The capacity of the pre-columns was found to be more than 400 pmol of Zy 17617B. The pre-col-

umns may be used up to eighteen times. Pre-column to pre-column variations as well as peak broadening were found to be negligible.

### Chromatography

Zy 17617B was desorbed from the pre-column and eluted onto a C<sub>18</sub> reversed-phase analytical column by isocratic elution with a mobile phase containing phosphate buffer pH 3.7 (50 mM-methanol-tetrahydrofuran (600:288:112, v/v). The flow-rate was set to 1.0 ml/min. The data acquisition was started when the pre-column was switched to the analytical column. The retention time of Zy 17617B was about 9 min. Spectrofluorimetric detection was selected for its enhanced selectivity and sensitivity compared with UV detection.

### Method validation

The precision and the accuracy were determined over the range 10.5–83.7 pmol/ml. The results are given in Table I. The intra-assay and inter-assay precisions ranged from 1.5 to 4.8% and from 3.0 to 8.3% ( $n = 6$ ), respectively. The intra-assay and inter-assay accuracies ranged from –5.7 to +0.3% and from –5.5 to +4.9% ( $n = 6$ ), respectively.

The calibration graphs relating the Zy 17617B peak height to its concentration in prepared standards were linear in the range 10.5–83.7 pmol/ml in

TABLE I

### PRECISION AND ACCURACY OF Zy 17617B ASSAY

Analyses carried out using the experimental conditions of Fig. 3.

Nominal concentration (pmol/ml)	Concentration found (mean $\pm$ S.D., $n = 6$ ) (pmol/ml)	Relative standard deviation (%)	Confidence interval of the mean value ( $P = 95\%$ ) (pmol/ml)	Accuracy <sup>a</sup> (%)
<i>Intra-assay variability</i>				
10.47	10.01 $\pm$ 0.48	4.8	10.01 $\pm$ 0.50	–4.4
20.93	19.74 $\pm$ 0.35	1.8	19.74 $\pm$ 0.37	–5.7
41.86	41.99 $\pm$ 0.62	1.5	41.99 $\pm$ 0.66	0.3
83.73	84.01 $\pm$ 1.82	2.2	84.01 $\pm$ 1.91	0.3
<i>Inter-assay variability</i>				
10.47	10.98 $\pm$ 0.39	3.5	10.98 $\pm$ 0.40	4.9
20.93	20.60 $\pm$ 0.62	3.0	20.60 $\pm$ 0.66	–1.6
41.86	39.55 $\pm$ 1.47	3.7	39.55 $\pm$ 1.54	–5.5
83.73	85.11 $\pm$ 7.03	8.3	85.11 $\pm$ 7.38	1.6

<sup>a</sup> Defined as the percentage deviation between the mean concentration found and the theoretical concentration.

plasma. The regression characteristics were typical: slope = 0.000949, intercept = 0.06, with a correlation coefficient ( $r$ ) of 0.999.

The limit of quantification for the assay was of the order of 4 pmol/ml.

Zy 17617B was found to be stable under the experimental conditions for up to 12 h.

#### CONCLUSION

The developed method is suitable for the determination of Zy 17617B in plasma at the pmol/ml level. It allows automated extraction and analysis of plasma samples to be carried out. Full validation data demonstrate its reliability.

#### REFERENCES

- 1 K. H. Antonin, B. Ensslin-Haasis, R. Schulz and P. R. Bieck, *Eur. J. Gastroenterol. Hepatol.*, 2(Suppl. 1) (1990) 54.
- 2 M. W. F. Nielen, R. W. Frei and U. A. Th. Brinkman, in R. W. Frei and K. Zech (Editors), *Selective Sample Handling and Detection in HPLC, Part A (Journal of Chromatography Library, Vol. 39A)*, Elsevier, Amsterdam, 1988, Ch. 1, pp. 1–80.
- 3 R. Huber and K. Zech, in R. W. Frei and K. Zech (Editors), *Selective Sample Handling and Detection in HPLC, Part A (Journal of Chromatography Library, Vol. 39A)*, Elsevier, Amsterdam, 1988, Ch. 2, pp. 81–143.
- 4 M. C. Rouan, J. Campestrini, J. B. Lecaillon, J. P. Dubois, M. Lamontagne and B. Pichon, *J. Chromatogr.*, 456 (1988) 45.
- 5 M. W. F. Nielen, A. J. Valk, R. W. Frei, U. A. Th. Brinkman, Ph. Mussche, R. de Nijs, B. Ooms and W. Smink, *J. Chromatogr.*, 393 (1987) 69.

# Determination of (*S*)-(–)-cathinone and its metabolites (*R,S*)-(–)-norephedrine and (*R,R*)-(–)-norpseudoephedrine in urine by high-performance liquid chromatography with photodiode-array detection

Karoline Mathys and Rudolf Brenneisen\*

Institute of Pharmacy, University of Berne, Baltzerstr. 5, CH-3012 Berne (Switzerland)

## ABSTRACT

A high-performance liquid chromatographic (HPLC) procedure with photodiode-array detection (DAD) is described for the determination of (*S*)-(–)-cathinone (*S*-CA) and its metabolites (*R,S*)-(–)-norephedrine (*R*-NE) and (*R,R*)-(–)-norpseudoephedrine (*R*-NPE) in urine. Extraction and clean-up of 1-ml urine samples were performed on a cyano-bonded solid-phase column using (±)-amphetamine as internal standard. The concentrated extracts were separated on a 3- $\mu$ m ODS-1 column with acetonitrile–water–phosphoric acid–hexylamine as the mobile phase. Peak detection was done at 192 nm. The detection limits for *S*-CA and *R*-NE/*R*-NPE in urine were 50 and 25 ng/ml, respectively. The differentiation of the enantiomers of cathinone and norephedrine was achieved by derivatization with (*S*)-(–)-1-phenylethyl isocyanate to the corresponding diastereomers followed by HPLC–DAD on a 5- $\mu$ m normal-phase column. The *R* and *S* enantiomers of norpseudoephedrine were determined by gas chromatography–mass spectrometry after on-column derivatization with (*S*)-(–)-*N*-trifluoroacetylpropyl chloride. Following a single oral dose of 0.5 mg/kg of *S*-CA, the concentrations found in urine ranged from 0.2 to 3.8  $\mu$ g/ml of *S*-CA, from 7.2 to 46.0  $\mu$ g/ml of *R*-NE and from 0.5 to 2.5  $\mu$ g/ml of *R*-NPE.

## INTRODUCTION

Khat, the leaves or short tops of the evergreen shrub *Catha edulis* Forsk., is very popular in East Africa and the Arabian peninsula, where it is habitually chewed for its stimulating effects. As only fresh leaves are active, the habit of chewing khat has been confined to the areas where the plant grows. Mainly owing to the possibility of air transportation, fresh khat has recently been introduced in certain developed countries, *e.g.*, USA, UK, Italy and Switzerland.

Phytochemical studies [1–4] and animal experiments [5,6] have shown that the phenylalkylamine (*S*)-(–)-cathinone (see Fig. 7: *S*-CA) is the main psychoactive alkaloid of khat. Since 1985, *S*-CA has been scheduled as an internationally controlled substance. An experiment to study the effects and

pharmacokinetic characteristics of *S*-CA in humans has recently been completed [7]. Therefore, a method for the pharmacokinetic profiling of *S*-CA and its main metabolite (*R,S*)-(–)-norephedrine (*R*-NE) in human plasma has been developed [8]. An earlier study on the metabolism of *S*-CA using 24-h urine samples showed *R*-NE and its corresponding diastereomer (*R,R*)-(–)-norpseudoephedrine (*R*-NPE) in a ratio of 8:1 to be the main metabolites of *S*-CA [9]. In that study it was not clear whether the occurrence of *R*-NPE was due to the use of optically impure *S*-CA or the partial racemization of *S*-CA to (*R*)-(+)-cathinone (*R*-CA) during absorption and partition.

The purpose of this work was to develop a method for the rapid and sensitive clean-up of small urine samples and an improved high-performance liquid chromatographic (HPLC) method with pho-

todiode-array detection (DAD) for the pharmacokinetic profiling of *S*-CA and its metabolites in human urine.

## EXPERIMENTAL

### Instrumentation

Urine analyses were performed on a Hewlett-Packard (Waldbronn, Germany) HPLC system consisting of a Model 1090M liquid chromatograph, a Model 1090L autosampler, a Model 1040M photodiode-array detector, a Model 79994A Chemstation (software version 1.05), a Model 7470A *x-y* plotter and a Model 2225A Thinkjet printer.

For the determination of the *S* and *R* enantiomers of cathinone and norephedrine the same system was used, whereas the determination of the enantiomers of norpseudoephedrine was performed on a Hewlett-Packard gas chromatographic-mass spectrometric (GC-MS) system consisting of a Model 5990 gas chromatograph, a Model 5970 mass-selective detector, a Chemstation (Pascal Rev. 3.1), a Model 2225A Thinkjet printer and a Model 7470A *x-y* plotter.

### Chromatographic conditions

For the analysis of urine samples a 150 mm  $\times$  4.6 mm I.D. column directly coupled to a 20 mm  $\times$  4 mm I.D. precolumn and packed with Spherisorb 3- $\mu$ m ODS-1 (Stagroma, Wallisellen, Switzerland) was used. The mobile phase was acetonitrile-water (8.5:91.5, v/v) containing 8.5 g/l of orthophosphoric acid (85%) and 200  $\mu$ l/l of hexylamine. The flow-rate was 1 ml/min. The mobile phase was filtered under vacuum with a 0.45- $\mu$ m nylon membrane filter (RC 55, Schleicher & Schüll) and degassed by sonication before use and with a constant flow of helium during use. Methanol was used for column washing. All measurements were carried out at room temperature. Peak detection was done at 192 nm, and peak identity and homogeneity were ascertained by on-line scanning of UV spectra from 190 to 300 nm.

The separation of the *S* and *R* enantiomers of cathinone and norephedrine as their diastereomers was done on a 250 mm  $\times$  4.6 mm I.D. column packed with LiChrosorb Si 60, 5  $\mu$ m (Merck, Basel, Switzerland). The mobile phase was isooctane-iso-

propanol-acetic acid (>99.5%) (90:9:1, v/v/v). The flow-rate was 1 ml/min. Peak detection of the enantiomers after derivatization was done simultaneously at 254 and 236 nm.

The separation of the enantiomers of norephedrine and norpseudoephedrine was done after on column derivatization on a J & W DB-5 bonded-phase capillary column (J & W Scientific, Rancho Cordova, CA, USA), 20 m  $\times$  0.18 mm I.D. with a 0.40- $\mu$ m coating, that was inserted directly into the ion source. The injector and transfer line temperatures were 275 and 280°C, respectively. The oven temperature was programmed from 220°C (held for 3 min) at 10°C/min to 280°C (held for 7 min). The scan range was *m/z* 33–250, and the scan rate was set at 1.97 scans/s. Helium was used as the carrier gas at a flow-rate of 0.7 ml/min (velocity 49 cm/s). Injection was done manually through a silanized split liner (split ratio 1:15) packed with 3% OV-1 on 80–100-mesh Supelcoport (Supelco, Gland, Switzerland) held in place with silanized glass-wool.

### Chemicals and reagents

Optically pure (>98%) hydrochlorides of (*S*)-(-)-cathinone (*S*-CA) and (*R*)-(+)-cathinone (*R*-CA) were kindly donated by Dr. J. P. Wolf (Institute of Organic Chemistry, University of Berne). (*R,S*)-(-)-Norephedrine hydrochloride (*R-NE*), (*S,R*)-(+)-norephedrine (*S-NE*) and (*S*)-(-)-1-phenylethyl isocyanate (PEIC, >98%) were provided by Fluka (Buchs, Switzerland). (*S,S*)-(+)-Norpseudoephedrine hydrochloride (*S-NPE*) and ( $\pm$ )-amphetamine sulphate were obtained from Siegfried (Zofingen, Switzerland) and (*R,R*)-(-)-norpseudoephedrine hydrochloride (*R-NPE*) and (*S*)-(-)-*N*-trifluoroacetylpropyl chloride (TPC; 0.1 *M* in dichloromethane) from Sigma-Aldrich (St. Louis, MO, USA). All other chemicals and reagents were of HPLC or analytical-reagent grade from Merck and Fluka.

### Solid-phase extraction of urine samples

Extraction and clean-up of urine samples were carried out using an Adsorbex SPU sample preparation unit (Merck, Darmstadt, Germany). Frozen urine (stored at -20°C) was warmed to room temperature in an ultrasonic bath. After centrifugation (2000 *g*, for 5 min) a 1-ml aliquot was transferred into a 2.5-ml vial and 2  $\mu$ g/ml of internal standard



solution [I.S.; 200  $\mu\text{g/ml}$  ( $\pm$ )-amphetamine sulphate in water] were added. After vortex mixing for 1 min the sample was applied to a Baker-10 SPE cyano (CN) 3-ml column (Stehelin, Basel, Switzerland) and the vial washed with 1 ml of water. The sorbent was preconditioned using  $2 \times 3$  ml of methanol followed by  $2 \times 3$  ml of water, and was not allowed to dry out at the end of the conditioning step. Urine interferences were removed by washing the cartridge with  $3 \times 3$  ml of water followed by drying the column for about 1 min under vacuum. For the elution  $2 \times 500$   $\mu\text{l}$  of phosphate buffer (pH 3) [1.466 g of sodium dihydrogenphosphate dihydrate and 0.197 g of orthophosphoric acid (85%) in 100 ml of water] and  $2 \times 500$   $\mu\text{l}$  of eluent consisting of methanol-phosphate buffer (pH 3) (50:50, v/v) were used. The eluents were allowed to percolate through the column first without vacuum and for complete elution with slow aspiration under vacuum. The combined eluates were concentrated to about 100  $\mu\text{l}$  under a stream of nitrogen (which took about 1 h, but parallel working was possible), filtered if necessary through the tip of a Pasteur pipette filled with cotton-wool, and 10- $\mu\text{l}$  aliquots were used for duplicate HPLC analyses. When frozen and stored at  $-20^\circ\text{C}$ , urine samples and extracts were stable for at least 3 months.

*Derivatization of urine extracts and standards for the determination of enantiomers as diastereomers*

The urine extracts from one volunteer (about 300  $\mu\text{l}$ ) were combined, evaporated to dryness and the residue dissolved in 150  $\mu\text{l}$  of tetrahydrofuran. After filtration through the tip of a Pasteur pipette filled with cotton-wool, 10  $\mu\text{l}$  of PEIC and 5  $\mu\text{l}$  of triethylamine were added. Immediately after vortex mixing the sample in an ultrasonic bath for 5 min, 10- $\mu\text{l}$  aliquots were used for HPLC analysis. The PEIC derivatives were stable for only about 1 h. The minimum amounts of isomers of cathinone and norphedrine/norpseudoephedrine for the derivatization to take place were 10 and 100  $\mu\text{g}$ , respectively.

For the determination of the *R* and *S* enantiomers of norpseudoephedrine, the extract of one urine sample was evaporated to dryness and the residue dissolved in 50  $\mu\text{l}$  of methanol. Methanolic standard solutions of *R*-NE, *S*-NE, *R*-NPE and *S*-NPE were prepared to give a final concentration of about 20 ng/ $\mu\text{l}$ . On-column derivatization was ef-

fectured by taking up 4  $\mu\text{l}$  of each solution, 0.5  $\mu\text{l}$  of air and 1  $\mu\text{l}$  of TPC in a 10- $\mu\text{l}$  syringe and rapidly injecting the mixture into the GC-MS system.

*Quantitation*

Urine samples were analyzed by the internal standard method, measuring the peak areas of *S*-CA, *R*-NE, *R*-NPE and the I.S. at 192 nm. Calibration graphs (linear regression analysis) were obtained by analyzing four times pooled blank urine spiked with 0.25, 0.75, 2.00, 6.00, 10.00 and 15.00  $\mu\text{g/ml}$  of *S*-CA, *R*-NE and *R*-NPE and 2.00  $\mu\text{g/ml}$  of the I.S. (aqueous solution, calculated as base). The extractions were done as described above.

*Precision*

The inter-day precision was determined by analyzing three replicates of three blank urine samples spiked with 0.75, 2.00 and 10.00  $\mu\text{g/ml}$  of *S*-CA, *R*-NE and *R*-NPE and 2.00  $\mu\text{g/ml}$  of the I.S. Duplicate analyses were repeated on three different days during a 2-week period. The extractions were performed as described above.

*Recovery*

Six pooled blank urine samples were spiked with 0.25, 0.75, 2.00, 6.00, 10.00 and 15.00  $\mu\text{g/ml}$  of *S*-CA, *R*-NE and *R*-NPE and analyzed using the procedure described above. After the solid-phase extraction the eluates were concentrated to a definite volume. The efficiency of extraction was determined by comparing the peak areas of *S*-CA, *R*-NE and *R*-NPE with those of similar aqueous standard solutions.

## RESULTS AND DISCUSSION

The sample clean-up of low urine volumes containing *S*-CA and its main metabolites *R*-NE and *R*-NPE can be done rapidly and effectively by the use of short cyano-bonded solid-phase extraction columns. The standardized extraction procedure avoids any basic conditions which could cause racemization or oxidative dimerization of the unstable ketoamine *S*-CA [3]. As demonstrated with the chromatogram of a pooled blank urine extract (Fig. 1), most of the interfering endogenous matrix can be eliminated. The recovery of *S*-CA and its metabolites at the 6  $\mu\text{g/ml}$  level was determined to be 87.4

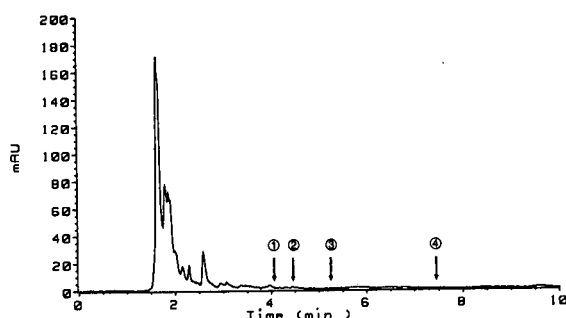


Fig. 1. Chromatogram of an extract of pooled blank urine recorded at 192 nm. Arrows indicate the peak position of *R*-NE (1), *R*-NPE (2), *S*-CA (3) and the I.S. (4). For chromatographic conditions, see Experimental.

$\pm 2.0\%$  (relative standard deviation, R.S.D. =  $2.3\%$ ,  $n = 6$ ) for *S*-CA,  $90.2 \pm 1.5\%$  (R.S.D. =  $1.7\%$ ) for *R*-NE and  $97.9 \pm 3.3\%$  (R.S.D. =  $3.4\%$ ) for *R*-NPE. All data from the recovery study are summarized in Table I. The recovery of amphetamine (I.S.) at the  $2 \mu\text{g/ml}$  level was  $99.2 \pm 2.4\%$  (R.S.D. =  $2.4\%$ ,  $n = 6$ ). Therefore, the method described could also be used for the determination of amphetamine and its derivatives in human urine.

The chromatographic system used was originally developed for screening urine for cocaine and its metabolites [10]. Hexylamine serves as a modifier and masking agent for residual silanol groups [11]. By making small changes in the concentration of hexylamine and in the ratio of the acetonitrile–water mixture, the potentially interfering matrix, which was not eliminated by the sample clean-up, could be separated chromatographically from the compounds of interest (Figs. 2 and 3).

For peak detection DAD was used. Peak homogeneity was ascertained by a peak purity check (part of the workstation software, up-slope, apex and down-slope peak spectra match). Owing to the very low UV cut-off of the mobile phase, it was possible to use 192 nm as the detection wavelength and to obtain a very high sensitivity. Fig. 4 shows the on-line UV spectra and the chromatogram of a standard mixture containing *S*-CA, *R*-NE, *R*-NPE and the I.S. At 192 nm and a signal-to-noise ratio of 5 the detection limit for *S*-CA was 5 ng (corresponding to 50 ng/ml), whereas 2.5 ng (25 ng/ml) was the minimum detectable amount of *R*-NE and *R*-NPE ( $\log \epsilon_{192} = 10.5$ ).

Human urine samples were collected from six

TABLE I  
RECOVERY OF *S*-CA, *R*-NE AND *R*-NPE FROM HUMAN URINE

Spiked urine ( $\mu\text{g/ml}$ )	Compound	Mean amount determined ( $\mu\text{g/ml}$ ) ( $n = 6$ )	Recovery $\pm$ S.D. (%)	R.S.D. (%)
0.25	<i>S</i> -CA	0.20	$78.7 \pm 3.5$	4.0
	<i>R</i> -NE	0.22	$89.5 \pm 4.9$	5.5
	<i>R</i> -NPE	0.25	$100.2 \pm 7.9$	7.9
0.75	<i>S</i> -CA	0.54	$72.5 \pm 2.0$	2.8
	<i>R</i> -NE	0.62	$82.5 \pm 0.6$	0.7
	<i>R</i> -NPE	0.70	$93.6 \pm 1.5$	1.6
2.00	<i>S</i> -CA	1.45	$72.3 \pm 4.4$	6.1
	<i>R</i> -NE	1.70	$85.1 \pm 1.6$	1.9
	<i>R</i> -NPE	1.96	$97.9 \pm 2.2$	2.3
6.00	<i>S</i> -CA	5.24	$87.4 \pm 2.0$	2.3
	<i>R</i> -NE	5.41	$90.2 \pm 1.5$	1.7
	<i>R</i> -NPE	5.87	$97.9 \pm 3.3$	3.4
10.00	<i>S</i> -CA	9.49	$94.9 \pm 5.8$	6.1
	<i>R</i> -NE	8.83	$88.3 \pm 3.5$	4.0
	<i>R</i> -NPE	9.80	$98.0 \pm 10.8$	11.0
15.00	<i>S</i> -CA	13.94	$93.0 \pm 5.0$	5.4
	<i>R</i> -NE	12.40	$82.6 \pm 3.5$	4.2
	<i>R</i> -NPE	14.73	$98.2 \pm 5.2$	5.3

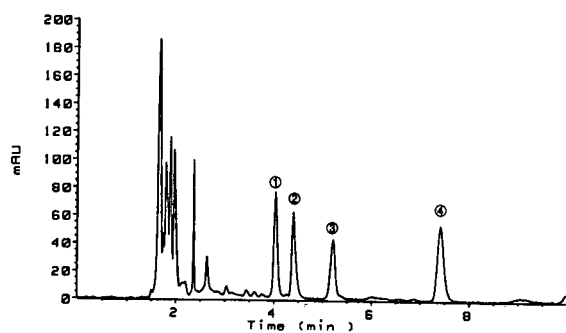


Fig. 2. Chromatogram of an extract of pooled blank urine spiked with 2 µg/ml each of *R*-NE (1), *R*-NPE (2), *S*-CA (3) and the I.S. (4).

male volunteers 2, 4, 6 and 8 h after the oral administration of 0.5 mg/kg of *S*-CA. Before admission to the experiment the subjects underwent medical and psychiatric examination and had agreed of refrain from any psychotropic drugs and medication for the 3 weeks preceding the experiment. The urine levels ranged from 0.2 to 3.8 µg/ml of *S*-CA, from 7.2 to 46.0 µg/ml of *R*-NE and from 0.5 to 2.5 µg/ml of *R*-NPE. Urine samples containing >20 µg/ml of *R*-NE were reanalyzed after dilution with water (1:1) before the extraction. The *R*-NE/*R*-NPE ratio ranged from about 10 to 23. The excretion patterns are summarized in Table II.

The linearity between the peak-area ratios of *S*-CA, *R*-NE and *R*-NPE vs. the I.S. and the urinary concentrations of *S*-CA, *R*-NE and *R*-NPE was checked in the range 0.25–15.00 µg/ml. The correlation coefficient (*r*) for *S*-CA, *R*-NE and *R*-NPE was 0.9982, 0.9996 and 0.9994, respectively (Fig. 5). The

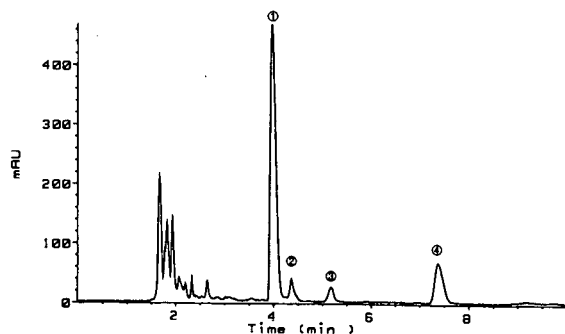


Fig. 3. Chromatogram of an extract of a human urine sample obtained 4 h after oral administration of 0.5 mg/kg of *S*-CA. Peaks as in Fig. 2.

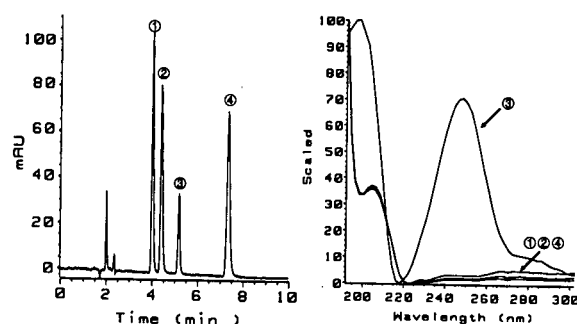


Fig. 4. Chromatogram and on-line DAD UV spectra of *R*-NE, *R*-NPE, *S*-CA and the I.S. Peaks as in Fig. 2.

TABLE II

EXCRETION OF *S*-CA AND ITS METABOLITES *R*-NE AND *R*-NPE IN HUMAN URINE AFTER ORAL ADMINISTRATION OF 0.5 mg/kg OF *S*-CA

Subject	Time after administration (h)	Compounds excreted in urine (µg/ml)			<i>R</i> -NE/ <i>R</i> -NPE ratio
		<i>S</i> -CA <sup>a</sup>	<i>R</i> -NE	<i>R</i> -NPE	
1	2	n.d.	9.09	0.50	18.1
	4	1.79	40.68	2.34	17.1
	6	n.d.	16.44	1.03	16.0
	8	n.d.	14.53	1.14	12.8
2	2	0.20	17.08	1.05	16.3
	4	1.72	26.84	1.76	15.2
	6	0.78	18.80	1.54	12.2
	8	0.70	14.29	1.36	10.5
3	2	1.73	46.04	2.49	18.5
	4	3.81	30.48	2.01	15.2
	6	1.06	15.11	1.24	12.1
	8	0.16	12.59	1.16	10.9
4	2	0.27	28.04	1.22	23.0
	4	0.90	37.31	2.02	18.5
	6	0.70	32.48	1.92	16.9
	8	n.d.	27.40	2.40	11.4
5	2	0.24	8.26	0.54	15.4
	4	0.30	10.16	0.77	13.3
	6	0.31	7.67	0.64	12.1
	8	0.30	11.71	1.05	11.2
6	2	2.92	16.62	1.22	13.6
	4	1.99	7.20	0.64	11.2
	6	0.28	19.64	1.55	12.7
	8	n.d.	15.48	1.54	10.1

<sup>a</sup> n.d. = Not detectable (below detection limit).

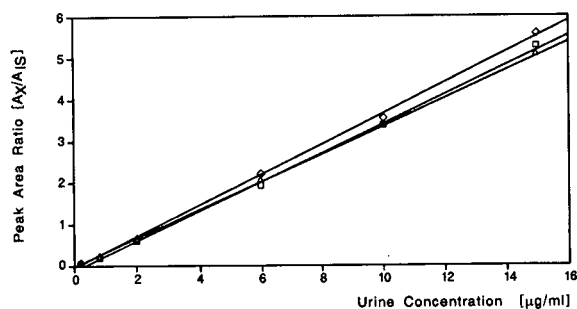


Fig. 5. Calibration graphs for (□) *R*-NE, (Δ) *R*-NPE and (◇) *S*-CA extracted from urine.

inter-day precision measured at low (0.75 μg/ml), medium (2.00 μg/ml) and high (15.00 μg/ml) concentration levels is summarized in Table III.

The determination of the enantiomers in urine by derivatization with PEIC was only practicable for cathinone and norephedrine and not for the very low concentrated norpseudoephedrine, as at least 100 μg of the amino alcohols was necessary for the reaction to take place. By comparing the results of the derivatization with the chromatogram for a standard solution containing derivatized *S*-CA, *R*-CA, *R*-NE and *S*-NE (Fig. 6), the enantiomers in urine samples were found to be *S*-CA and *R*-NE. The determination of the *R*- and *S*-NPE enantiomers was performed by GC-MS after on-column derivatization with chiral TPC to the corresponding diastereomers. To ensure that there was

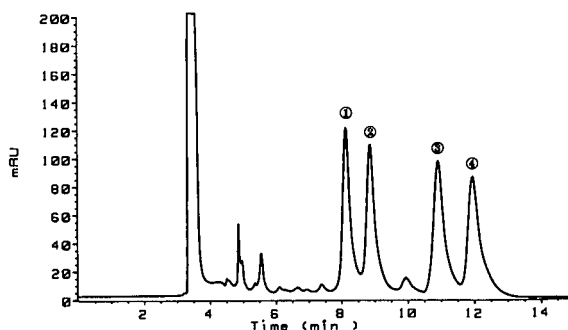


Fig. 6. Chromatogram of the PEIC derivatives of *S*-CA (1), *R*-CA (2), *R*-NE (3) and *S*-NE (4). For chromatographic conditions, see Experimental.

no interference with the simultaneously derivatized *R*-NE, the results were compared with those for a derivatized standard solution containing *R*-NE (*R*-NE-TPC:  $m/z$  238, 237, 194, 166, 139;  $t_R$  = 7.14 min), *S*-NE (*S*-NE-TPC:  $t_R$  = 6.87 min), *R*-NPE (*R*-NPE-TPC:  $m/z$  238, 237, 194, 166, 139;  $t_R$  = 6.96 min) and *S*-NPE (*S*-NPE-TPC:  $t_R$  = 7.21 min). The enantiomers found in the urine samples were *R*-NPE and *R*-NE. Therefore, it could be confirmed that, as shown in Fig. 7, orally administered *S*-CA is metabolized by a stereospecific 1*R* keto reduction to the corresponding amino alcohols [9].

As in this study the *S*-CA administered was optically pure (>98%) the simultaneous occurrence of

TABLE III

INTER-DAY PRECISION OF THE ASSAY FOR *S*-CA, *R*-NE AND *R*-NPE EXTRACTED FROM HUMAN URINE

Spiked urine (μg/ml)	Compound	Mean concentration determined ± S.D. (μg/ml) ( <i>n</i> = 6)	R.S.D. (%)
0.75	<i>S</i> -CA	0.77 ± 0.02	2.98
	<i>R</i> -NE	0.76 ± 0.04	4.63
	<i>R</i> -NPE	0.77 ± 0.02	2.87
2.00	<i>S</i> -CA	1.99 ± 0.06	2.97
	<i>R</i> -NE	1.92 ± 0.14	7.25
	<i>R</i> -NPE	1.97 ± 0.03	1.68
10.00	<i>S</i> -CA	10.20 ± 0.13	1.28
	<i>R</i> -NE	9.73 ± 0.18	1.82
	<i>R</i> -NPE	9.69 ± 0.13	1.31

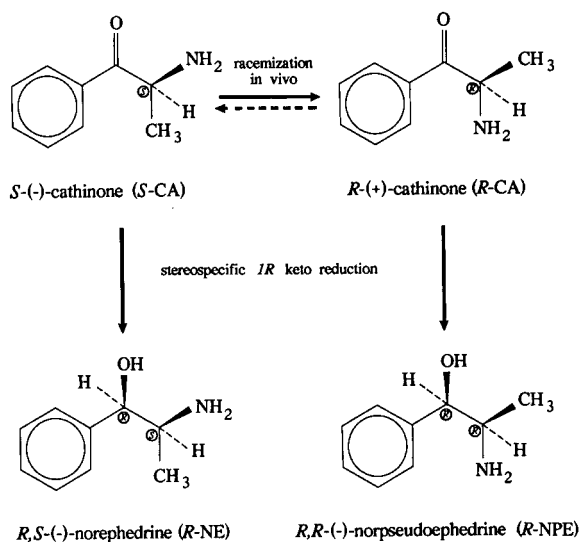


Fig. 7. Biotransformation of *S*-CA.

the corresponding diastereomeric amino alcohol *R*-NPE is probably the result of partial racemization of *S*-CA to *R*-CA during absorption and partition. The significant decrease in the *R*-NE/*R*-NPE ratio (see Table II) after oral administration also confirms this hypothesis. As only a small part (<10%) of the administered *S*-CA is racemized, the presence of *R*-CA in urine samples could not be proved. Compared with the concentration of *R*-NE, the concentration of *R*-NPE found in human urine is very low (<10%). This could explain why *R*-NPE (detection limit 12.5 ng/ml) could not be found in human plasma samples, where the maximum concentration of *R*-NE after oral administration was about 100 ng/ml [8].

#### ACKNOWLEDGEMENTS

Part of this work was supported by the E. Steingger Foundation for Medicinal Plant Research and the Foundation for Narcotics Research of the Swiss Federal Office of Public Health.

#### REFERENCES

- 1 X. Schorno, *Dissertation*, University of Berne, Berne, 1979.
- 2 K. Szendrei, *Bull. Narcot.*, 32 (1980) 5.
- 3 R. Brenneisen and S. Geissshüsler, *Pharm. Acta Helv.*, 60 (1985) 290.
- 4 S. Geissshüsler and R. Brenneisen, *J. Ethnopharmacol.*, 15 (1987) 269.
- 5 P. Kalix, *Gen. Pharmacol.*, 15 (1984) 179.
- 6 P. Kalix and O. Braenden, *Pharmacol. Rev.*, 37 (1985) 149.
- 7 P. Kalix, H. U. Fisch, U. Koelbing, S. Geissshüsler and R. Brenneisen, *Br. J. Clin. Pharmacol.*, 30 (1990) 825.
- 8 R. Brenneisen, K. Mathys, S. Geissshüsler, H. U. Fisch, U. Koelbing and P. Kalix, *J. Liq. Chromatogr.*, 14 (1991) 271.
- 9 R. Brenneisen, S. Geissshüsler and X. Schorno, *J. Pharm. Pharmacol.*, 38 (1986) 298.
- 10 D. Bourquin and R. Brenneisen, in *Proceedings of the 41th AAFS Meeting, Las Vegas, 1989*, American Academy of Forensic Sciences, Colorado Springs, CO, 1989, p. 143.
- 11 R. Gill, S. P. Alexander and A. C. Moffat, *J. Chromatogr.*, 246 (1982) 39.



# Determination of psychotropic phenylalkylamine derivatives in biological matrices by high-performance liquid chromatography with photodiode-array detection

Hans-Jörg Helmlin and Rudolf Brenneisen\*

Institute of Pharmacy, University of Berne, Baltzerstrasse 5, CH-3012 Berne (Switzerland)

## ABSTRACT

Several procedures using high-performance liquid chromatography with photodiode-array detection have been developed to create phytochemical and toxicological profiles of phenylalkylamine derivatives in biological samples (e.g. plant materials and urine). Mescaline-containing cactus samples were extracted with basic methanol, using methoxamine as internal standard; the extraction and clean-up of urine samples were performed on cation-exchange solid-phase extraction columns. The extracts were separated on a 3- $\mu$ m ODS column with acetonitrile–water–phosphoric acid–hexylamine as the mobile phase. Peak detection was performed at 198 or 205 nm; peak identity and homogeneity were ascertained by on-line scanning of the UV spectra from 190 to 300 nm. The detection limit of phenylalkylamine derivatives in urine and cactus material was 0.026–0.056  $\mu$ g/ml and 0.04  $\mu$ g/mg, respectively. Following a single oral dose of 1.7 mg/kg methylenedioxymethylamphetamine (MDMA) the concentrations found in urine ranged from 1.48 to 5.05  $\mu$ g/ml MDMA and 0.07–0.90  $\mu$ g/ml methylenedioxyamphetamine (a metabolite of MDMA). The mescaline content of the cactus *Trichocereus pachanoi* varied between 1.09 and 23.75  $\mu$ g/mg.

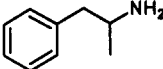
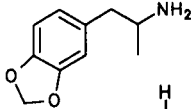
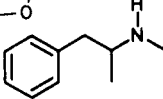
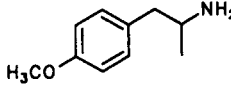
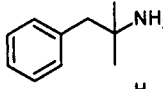
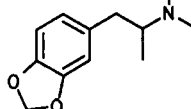
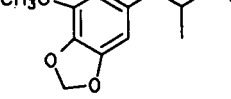
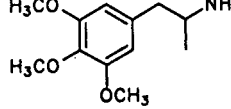
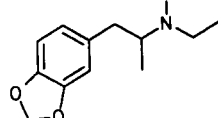
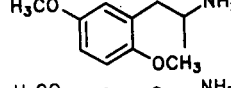
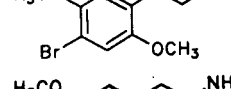
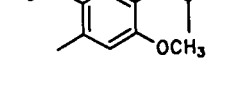
## INTRODUCTION

Many natural and synthetic phenylalkylamine derivatives such as mescaline, amphetamine, methamphetamine and 4-bromo-2,5-dimethoxyphenethylamine (see Table I) are known for their stimulant and/or hallucinogenic properties. Some very active ring-substituted amphetamines such as 3,4-methylenedioxyamphetamine (MDA), 3,4-methylenedioxyethylamphetamine (MDMA) and 3,4-methylenedioxyethylamphetamine (MDE) have now appeared as “designer drugs” on the illicit market, produced by clandestine laboratories [1]. Owing to their high potential of abuse, most of these popular recreational substances are now internationally controlled. Despite this, MDMA (“Ecstasy”, “XTC”, “Adam”) is used more frequently as a controversial adjunct in psychotherapy [2,3]. *Trichocereus pachanoi* Britt. et Rose (“San Pedro”) grows in subtropical and temperate areas of

South America, especially in the Andean regions and belongs, together with *Lophophora williamsii* (Lem. ex Salm-Dyck) Coult. [4], to the mescaline-containing cactus species which are commercially available without legal restrictions in Switzerland and other European countries.

Considering the potential of abuse of phenylalkylamine derivatives and mescaline-containing cactus species, it was the aim of this work to develop a selective, specific and sensitive analytical procedure using high-performance liquid chromatography with photodiode-array detection (HPLC–DAD). This method should allow not only the identification of such compounds, but also the acquisition of phytochemical and pharmacokinetic profiles in complex biological samples to estimate their toxicological or therapeutic potency. The efficiency of HPLC–DAD in drug analysis, analytical toxicology, forensic chemistry and phytochemistry of psychotropic drugs has been shown previously [5–18].

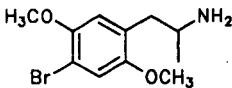
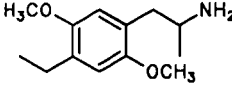
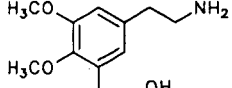
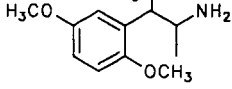
TABLE I  
STRUCTURES OF PHENYLALKYLAMINE DERIVATIVES

Structure	Peak no.	Compound
	1	Amphetamine
	2	3,4-Methylenedioxyamphetamine (MDA)
	3	Methamphetamine
	4	4-Methoxyamphetamine
	5	Phentermine
	6	3,4-Methylenedioxymethamphetamine (MDMA)
	7	5-Methoxy-3,4-methylenedioxyamphetamine (MMDA)
	8	3,4,5-Trimethoxyamphetamine
	9	3,4-Methylenedioxyethylamphetamine (MDE)
	10	2,5-Dimethoxyamphetamine
	11	4-Bromo-2,5-dimethoxyphenylethylamine (DOBP, 2-CB)
	12	2,5-Dimethoxy-4-methylamphetamine (DOM, STP)

(Continued on p. 89)



TABLE I (continued)

Structure	Peak No.	Compound
	13	4-Bromo-2,5-dimethoxyamphetamine (DOB)
	14	2,5-Dimethoxy-4-ethylamphetamine (DOET)
	15	Mescaline
	16	Methoxamine

## EXPERIMENTAL

*Instrumentation*

The HPLC-DAD system consisted of a Hewlett-Packard 1090M liquid chromatograph (Hewlett-Packard, Waldbronn, Germany), an HP 1090L autosampler, an HP 1040M photodiode-array detector, an HP 79994A Chemstation (software version 1.05), an HP 7470A *x/y* plotter and an HP 2225A Thinkjet printer.

*Chromatographic conditions*

The separation of fourteen phenylalkylamine derivatives was performed at 40°C on a 125 × 4.0 mm I.D. column packed with 3- $\mu$ m Spherisorb ODS-1 (Phase Separations), filled by Stagroma (Wallisellen, Switzerland). The solvent gradient was developed by using the CARTAGO (computer assisted retention time prediction and gradient optimization) software; details of this procedure are published elsewhere [19,20]. Solvent A was water containing 5.0 ml (8.5 g) orthophosphoric acid (85%) and 0.28 ml (0.22 g) hexylamine per 1000 ml; solvent B was acetonitrile containing 100 ml water, 5.0 ml (8.5 g) orthophosphoric acid (85%) and 0.28 ml (0.22 g) hexylamine per 1000 ml. The gradient profile was as follows: 0–10.6 min, 5.5% B in A (isocratic); 10.6–21.6 min, 5.5–39% B in A (linear gradient). The flow-rate was 0.8 ml/min. The eluent was filtered

through a membrane filter (regenerated cellulose, 0.45  $\mu$ m, Schleicher and Schuell) and degassed by sonication and during use with a constant flow of helium. Methanol was used for washing the column.

The separation of urine samples containing MDMA and MDMA metabolites was performed isocratically at 40°C on a 125 × 4.0 I.D. column packed with 3- $\mu$ m Spherisorb ODS-1. The mobile phase was acetonitrile–water (72:928, v/v; 57:943, w/w), containing 5.0 ml (8.5 g) orthophosphoric acid (85%) and 0.28 ml (0.22 g) hexylamine per 1000 ml. The flow-rate was 0.8 ml/min.

The separation of the cactus samples was performed isocratically at 25°C on a 150 × 4.6 mm I.D. column with a 20 × 4.0 mm I.D. precolumn, packed with 3- $\mu$ m Spherisorb ODS-1. The mobile phase was acetonitrile–water (108:892, v/v), containing 5.0 ml (8.5 g) orthophosphoric acid (85%) and 0.28 ml (0.22 g) hexylamine per 1000 ml. The flow-rate was 1 ml/min.

*Chemicals and reagents*

Amphetamine sulphate was obtained from Siegfried (Zofingen, Switzerland) and methylamphetamine hydrochloride from Dr. Grogg Chemie (Berne, Switzerland). Mescaline hydrochloride was supplied by Laboratoires Plan (Geneva, Switzerland), methoxamine hydrochloride and MDA were

provided by Sigma (St. Louis, MO, USA). MDMA, MDE, 5-methoxy-3,4-methylenedioxyamphetamine (MMDA), 4-methoxyamphetamine, 2,5-dimethoxyamphetamine, 2,5-dimethoxy-4-methylamphetamine (DOM,STP), 2,5-dimethoxy-4-ethylamphetamine (DOET), 3,4,5-trimethoxyamphetamine, 4-bromo-2,5-dimethoxyamphetamine (DOB) and phentermine were donated by the Division of Narcotic Drugs, United Nations (Vienna, Austria). 4-Bromo-2,5-dimethoxyphenethylamine (DOBP,2-CB) was a gift of the Swiss Association for Psycholytic Therapy. All other chemicals and reagents were of HPLC or analytical-reagent grade and were purchased from Merck (Darmstadt, Germany) or Fluka (Buchs, Switzerland).

#### *Urine and cactus samples*

The urine samples were obtained from patients treated with MDMA by psychiatrists of the Swiss Association for Psycholytic Therapy. Urine samples were collected approximately 6 h after the administration of 1.7 mg/kg MDMA. The specimens of *Trichocereus pachanoi* Britt. et Rose and *Lophophora diffusa* (Croizat) Bravo (Cactaceae) were bought at flower shops and shopping centres in Switzerland, or obtained from private collections.

#### *Sample preparation*

The extraction and clean-up of urine samples (real, spiked, blank) were carried out on Adsorbex SCX (100 mg) cation-exchange extraction columns (Merck), using an Adsorbex SPU sample preparation unit. Frozen urine samples (stored at  $-20^{\circ}\text{C}$ ) were warmed to room temperature in an ultrasonic bath and centrifuged, if necessary (2000 g for 5 min). An aliquot of 1.0 ml was added to 0.5 ml of 0.05 M  $\text{KH}_2\text{PO}_4$  and then sonicated for 1 min in a stoppered 2.5-ml vial. The Adsorbex columns were preconditioned with 2 ml of methanol, 1 ml of water and 1 ml of 0.017 M  $\text{KH}_2\text{PO}_4$ . The sample was then applied to the preconditioned extraction column, which was not allowed to dry out at the end of the preconditioning step. The vial was rinsed with 0.05 ml of 0.05 M  $\text{KH}_2\text{PO}_4$ . After drying the extraction column for about 1 min, urine interferences were removed by washing the cartridge with  $3 \times 0.5$  ml of 0.017 M  $\text{KH}_2\text{PO}_4$  and 1 ml of methanol; followed by drying the column for about 1 min under vacuum. The elution step was carried out with 4

$\times 0.5$  ml of methanol-hydrochloric acid (7.3%; 97.5:2.5) at a flow-rate of about 0.5 ml/min. Aliquots of 10  $\mu\text{l}$  of the defined volume of the eluates were injected into the HPLC-DAD system for the determination of MDMA and MDA. For low MDMA and MDA levels a concentration step may be necessary. An aliquot of 1.5 ml of the eluates was added to 68  $\mu\text{l}$  of 1 M  $\text{K}_2\text{HPO}_4$ , concentrated to about 100  $\mu\text{l}$  under a stream of nitrogen and reconstituted to 150.0  $\mu\text{l}$  with methanol-water (50:50). The resulting solution, with a pH of about 4–5, was then sonicated for 2 min and filtered through the tip of a Pasteur pipette filled with cotton wool. Aliquots of 10  $\mu\text{l}$  were used for determination by HPLC-DAD.

The cactus samples were cut in half, lyophilized and stored in a desiccator under vacuum and protected from light until used for analysis. A representative sample of the cactus specimen was pulverized with a grinder. An accurately weighed amount of the powdered sample (about 10 mg) was then washed four times with 1 ml of diethyl ether by sonication (5 min) and filtration through a 0.2- $\mu\text{m}$  regenerated cellulose filter (Spartan 13/30, Schleicher & Schuell). The defatted sample was extracted four times with 0.5 ml of methanol-ammonia (33%; 99:1), containing 150.0  $\mu\text{g}/\text{ml}$  methoxamine hydrochloride as internal standard (I.S.), by sonication (5 min) and filtration through a 0.2- $\mu\text{m}$  regenerated cellulose filter. Aliquots of 5  $\mu\text{l}$  were injected into the HPLC-DAD system.

#### *Quantitation*

Quantitation of the urine samples was performed at 198 nm by measuring the peak areas of MDMA and MDA and using the external standard method. The calibration graphs for MDMA and MDA (linear regression analysis) were obtained by analyzing twice pooled blank urine spiked with MDMA and MDA in the concentration ranges 0.5–17 and 0.08–1.6  $\mu\text{g}/\text{ml}$ , respectively. The extraction was performed as described earlier. Quantitation of the cactus samples was performed by measuring the peak areas of mescaline and the I.S. at 205 nm. The calibration graph was obtained by measuring three times standard solutions in the concentration range 20–75  $\mu\text{g}/\text{ml}$  mescaline with an addition of 128  $\mu\text{g}/\text{ml}$  I.S. (aqueous solution, calculated as base).

### Precision

The inter-day precision of MDMA in urine was determined by analyzing two pooled urine samples spiked with 1.8 and 8.8  $\mu\text{g/ml}$  MDMA. The inter-day precision of MDA in urine was determined by analyzing two pooled urine samples spiked with 0.4 and 0.8  $\mu\text{g/ml}$  MDA. The intra-day precision of mescaline in the cactus material was determined by analyzing a dried and pulverized mescaline-free cactus specimen (*Lophophora diffusa*) spiked with a methanolic solution of 1 mg/ml mescaline (corresponding to 10  $\mu\text{g/mg}$  dried material). The solvent was evaporated before analysis. All analyses were repeated three times on two different days during a one-week period using the described procedures.

### Recovery study

The recoveries of MDMA and MDA from urine specimens were measured with the spiked samples used for the determination of the precision. The recovery of mescaline from cactus material was determined with a dried and pulverized mescaline-free cactus sample (*Lophophora diffusa*) spiked with a solution of 1 mg/ml mescaline (corresponding to 10  $\mu\text{g/mg}$  dried material). The efficiency of the extraction and clean-up procedures was calculated by comparing the peak areas of MDMA, MDA and mescaline with those of similar aqueous standard solutions. All analyses were performed three times following the described procedures, but without adding I.S. for the cactus material.

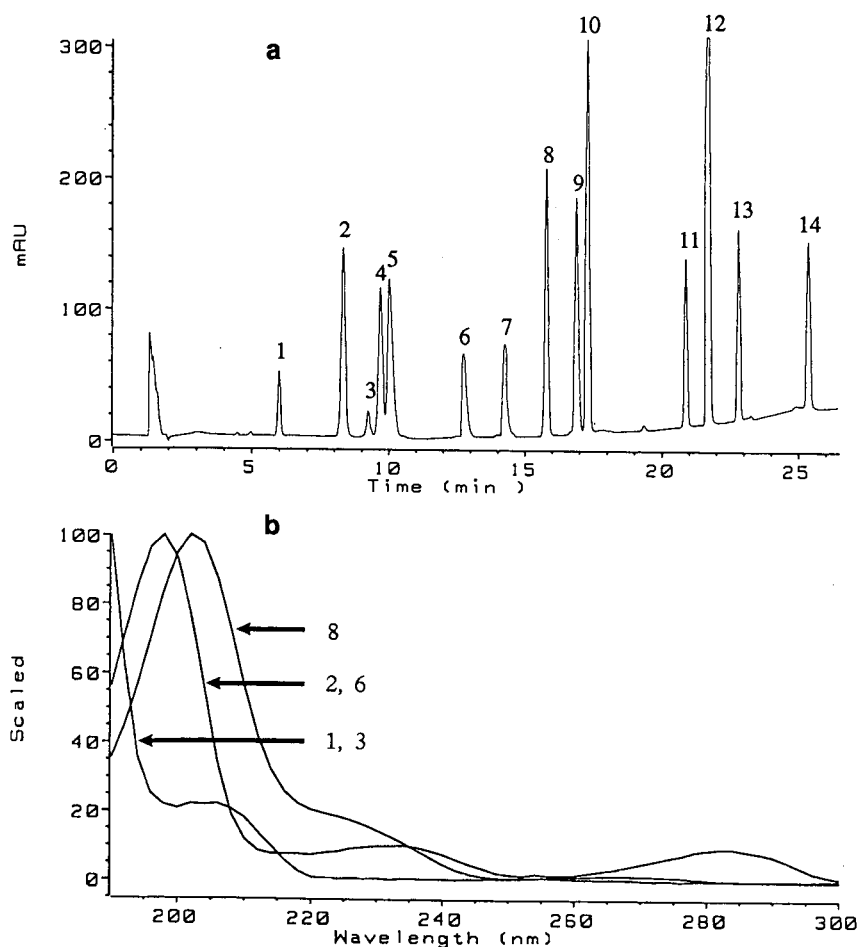


Fig. 1. (a) Chromatogram recorded at 198 nm and (b) on-line UV spectra of a standard mixture of phenylalkylamine derivatives. For peaks, see Table I. Chromatographic conditions as described under Experimental.

## RESULTS AND DISCUSSION

*HPLC-DAD*

Among the reversed-phase materials tested ( $C_8$ ,  $C_{18}$ ), with particle sizes of 3, 4 and 5  $\mu\text{m}$  and from different manufacturers, only the 3- $\mu\text{m}$  spherical  $C_{18}$  phase with a minimum plate number of 120 000/m showed the efficiency necessary to obtain the HPLC profiles of a complex mixture of fourteen structurally related phenylalkylamine derivatives (Fig. 1a) and to produce peak shapes which were generally sharp and symmetrical. It is well known that basic compounds may show a pronounced tailing effect on certain reversed-phase columns due to interactions with the residual polar silanol groups of the stationary phase [21,22]. The addition of an amine modifier to the mobile phase as a masking agent for the silanol groups improves the peak shape and changes the capacity factor ( $k'$ ) of basic substances [23,24]. It has to be noted that the selectivity of the chromatographic system can be widely influenced by changing not only the ratio of acetonitrile–water but also the concentration of hexylamine. With the addition of orthophosphoric acid to the mobile phase, an acidic eluent with a pH of approximately 2 is obtained, so that the components of interest, such as MDMA, MDA, mescaline and other basic phenylalkylamine derivatives, are protonated and eluted as associates with phosphate ions. The gradient was designed by the application of the CARTAGO software, a computer-based method development tool which can be extremely useful in the selection and optimization of chromatographic conditions for complex mixtures. The details of CARTAGO are reported elsewhere [19,20].

The selectivity of HPLC is significantly improved by coupling with a photodiode-array detector, allowing peak identification through the retention time and UV spectrum as well as peak purity checks through up-slope, apex and down-slope spectra matching. Fig. 1b, with the UV spectra (190–300 nm) of amphetamine sulphate, methylamphetamine hydrochloride, MDMA, MDA and 3,4,5-trimethoxyamphetamine (see Table I) shows that only phenylalkylamine derivatives with a distinct ring-substitution pattern can be differentiated. The low UV cut-off of the water–acetonitrile modifier phase gives the possibility of measuring in a range (190

210 nm) where the phenylalkylamine derivatives exhibit the highest absorption. At the optimum detection wavelengths of 198 and 205 nm the sensitivity is approximately ten times greater for MDMA and MDA ( $\log \epsilon_{198}$  4.557 and 4.569) and more than 60 times greater for mescaline ( $\log \epsilon_{205}$  4.675) compared with the absorption maxima and detection wavelengths reported previously (233–234 nm for MDMA and MDA [25,26] and 268 nm for mescaline [27]). The detection limit for MDA at 198 nm and a signal-to-noise ratio of 5:1 was about 0.03  $\mu\text{g/ml}$  in urine (Table II). The excellent sensitivity, the wide linearity range and the good overall reproducibility allow the detection and reliable determination of phenylalkylamine derivatives in biological matrices, even at very low concentrations.

*Determination of MDMA and MDA in urine*

The use of solid-phase extraction as an alternative to liquid–liquid extraction for the isolation of xenobiotics from body fluids is recommended because of excellent recoveries and ease of operation [5,18]. The sample clean-up of small volumes of urine containing MDMA and its main metabolite MDA can be performed rapidly and effectively by the use of short cation-exchange solid-phase extraction columns. Fig. 2 shows that MDMA and MDA are well resolved and separated from the endoge-

TABLE II  
VALIDATION DATA FOR MDMA AND MDA

Parameter	MDMA	MDA
Linearity range ( $\mu\text{g/ml}$ )	0.5–17	0.08–1.6
Correlation coefficient	0.999	0.999
Mean recovery (%; $n = 3$ ):		
0.4 $\mu\text{g/ml}$ sample	—	97.7
0.8 $\mu\text{g/ml}$ sample	—	100.7
1.8 $\mu\text{g/ml}$ sample	98.5	—
8.8 $\mu\text{g/ml}$ sample	99.2	—
Mean precision ( $\mu\text{g/ml}$ ; C.V., %; $n = 6$ )		
0.4 $\mu\text{g/ml}$ sample	—	0.39; 11.6
0.8 $\mu\text{g/ml}$ sample	—	0.78; 6.1
1.8 $\mu\text{g/ml}$ sample	1.77; 0.9	—
8.8 $\mu\text{g/ml}$ sample	8.69; 0.8	—
Detection limit <sup>a</sup>		
Absolute (ng)	2.8	1.3
Relative ( $\mu\text{g/ml}$ )	0.056	0.026

<sup>a</sup> Signal-to-noise ratio = 5:1.

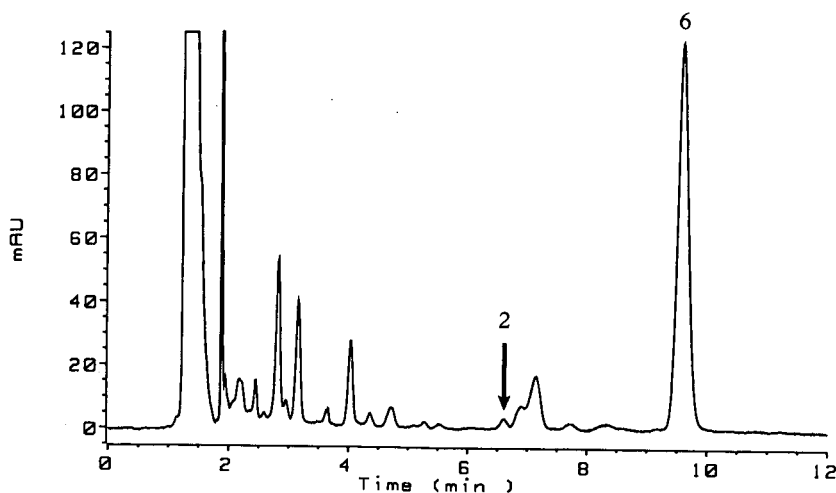


Fig. 2. Chromatogram of a human urine sample obtained after oral administration of 1.7 mg/kg MDMA. For peaks, see Table I.

nous matrix. The results of the recovery study for MDMA and MDA, listed in Table II with further validation data, show the efficiency of the extraction procedure. The volatility of MDMA and MDA may cause sample loss during the concentration step. This can be avoided by the addition of hydrochloric acid to the eluent and  $K_2HPO_4$  to the extract before evaporation. After oral administration, MDMA is mainly excreted unchanged in urine. The concentrations found in the urine of four patients who received an oral dose of 1.7 mg/kg ranged from 1.48 to 5.05  $\mu\text{g}/\text{ml}$ . The main metabolite

identified was MDA, formed by N-demethylation and excreted in concentrations of 0.07 to 0.90  $\mu\text{g}/\text{ml}$ . The pharmacokinetic data will be published in detail elsewhere.

#### *Determination of mescaline in cactus plants*

Solvent extraction was chosen for the extraction of cactus material. Mescaline is almost quantitatively extracted from the finely powdered and defatted cactus matrix by sonication with alkalized methanol (solvent/sample, 200:1, v/w). The selected I.S. (methoxamine) is a synthetic ring-substituted

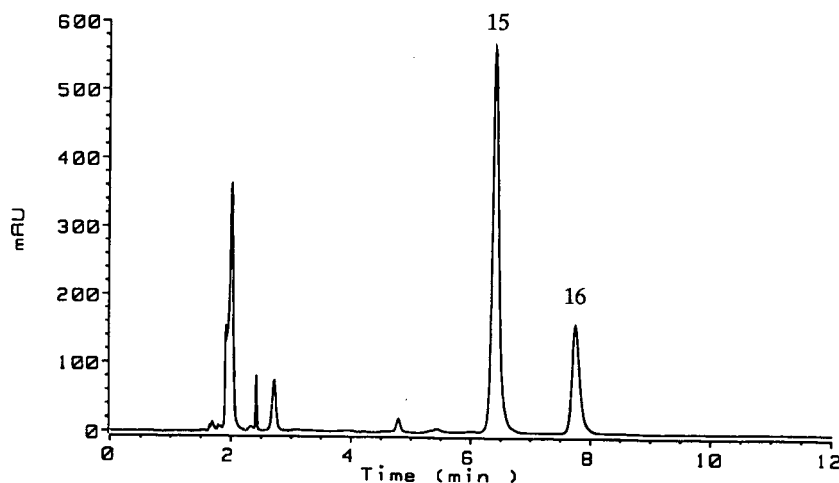


Fig. 3. Chromatogram of a *Trichocereus pachanoi* cactus specimen. For peaks, see Table I.

TABLE III  
VALIDATION DATA FOR Mescaline

Parameter	Mescaline
Linearity range ( $\mu\text{g/ml}$ )	20–75
Correlation coefficient	0.999
Mean recovery (%; $n = 3$ )	99.1
Mean precision ( $\mu\text{g/mg}$ ; C.V., %; $n = 6$ )	9.9; 3.3
Detection limit <sup>a</sup>	
Absolute (ng)	1
Relative ( $\mu\text{g/mg}$ )	0.04

<sup>a</sup> Signal-to-noise ratio = 5.1.

phenylalkylamine derivative with chemical properties very similar to those of mescaline but not interfering chromatographically (Fig. 3). The efficiency of extraction was tested by spiking mescaline-free cactus material with mescaline hydrochloride. The recovery of mescaline (Table III) was >99%, showing that the loss of mescaline during the defatting process, which is necessary to remove interfering lipids and waxes, is not significant. The mescaline content of six *Trichocereus pachanoi* specimens ranged from 1.09 to 23.75  $\mu\text{g/mg}$  dried cactus material, showing the extreme variability of the psychotropic potency.

#### ACKNOWLEDGEMENTS

This work was supported by grants from the E. Steinegger Foundation for Medicinal Plant Research and the Swiss Federal Office of Public Health (Foundation of Narcotics Research). We thank Dr. J. W. Roth, Chairman of the Swiss Association for Psycholytic Therapy, for providing the urine samples. We also thank the Division of Narcotic Drugs of the United Nations for the donation of phenylalkylamine derivatives and Mr. J. Lüthy, Institute of Botany, University of Berne, for the identification and supply of *Trichocereus pachanoi* specimens.

#### REFERENCES

- 1 R. M. Baum, *Chem. Eng. News*, 63 (1985) 7.
- 2 D. E. Nichols, in K. K. Redda, C. A. Walker and G. Barnett (Editors), *Cocaine, Marijuana, Designer Drugs: Chemistry, Pharmacology, and Behavior*, CRC Press, Boca Raton, FL, 1989, p. 175.
- 3 S. J. Peroutka (Editor), *Ecstasy: The Clinical, Pharmacological and Neurotoxicological Effects of the Drug MDMA*, Kluwer, Dordrecht, 1990.
- 4 H.-J. Helmlin and R. Brenneisen, in preparation.
- 5 B. K. Logan, D. T. Stafford, I. R. Tebbett and C. M. Moore, *J. Anal. Toxicol.*, 14 (1990) 154.
- 6 K. Zech and R. Huber, *J. Chromatogr.*, 282 (1983) 161.
- 7 A. Fell, B. J. Clark and H. P. Scott, *J. Chromatogr.*, 316 (1984) 423.
- 8 R. O. Fullinlaw, R. W. Bury and R. F. W. Moulds, *J. Chromatogr.*, 415 (1987) 347.
- 9 E. I. Minder, R. Schaubhut, C. E. Minder and D. J. Vonderschmitt, *J. Chromatogr.*, 419 (1987) 135.
- 10 D. W. Hill and K. J. Langner, *J. Liq. Chromatogr.*, 10 (1987) 377.
- 11 I. S. Lurie, J. M. Moore, D. A. Cooper and T. C. Kram, *J. Chromatogr.*, 405 (1987) 273.
- 12 R. Brenneisen and S. Geissshüsler, *Pharm. Acta Helv.*, 60 (1985) 290.
- 13 R. Brenneisen and S. Borner, *Pharm. Acta Helv.*, 60 (1985) 302.
- 14 D. Bourquin and R. Brenneisen, *Anal. Chim. Acta*, 198 (1987) 183.
- 15 S. Borner and R. Brenneisen, *J. Chromatogr.*, 408 (1987) 402.
- 16 H. H. Helmlin, D. Bourquin, M. de Bernardini and R. Brenneisen, *Pharm. Acta Helv.*, 64 (1989) 178.
- 17 D. Bourquin and R. Brenneisen *Proceedings of the 41th AAFS Meeting, Las Vegas, NV*, American Academy of Forensic Sciences, Colorado Springs, CO, 1989, p. 143.
- 18 R. Brenneisen, K. Mathys, S. Geissshüsler, H. U. Fisch, U. Koelbing and P. Kalix, *J. Liq. Chromatogr.*, 14 (1991) 271.
- 19 H.-J. Helmlin, L. Szajek, D. Bourquin and J. T. Clerc, *Proceedings of the 15th International Symposium on Column Liquid Chromatography (HPLC '91)*, Basel, 1991, Poster 118/1, Abstract book p. 76.
- 20 H.-J. Helmlin, D. Bourquin and J. T. Clerc, in preparation.
- 21 D. Chan Leach, M. A. Stadalius, J.S. Berus and L. R. Snyder, *LC · GC Int.*, 1 (1988) 22.
- 22 H. Engelhardt and M. Jungheim, *Chromatographia*, 29 (1990) 59.
- 23 R. Gill, S. P. Alexander and A. C. Moffat, *J. Chromatogr.*, 247 (1982) 39.
- 24 I. S. Lurie and S. M. Carr, *J. Liq. Chromatogr.*, 6 (1983) 1617.
- 25 *Analytical Profiles of Substituted 3,4-Methylenedioxyamphetamine: Designer Drugs Related to MDA*, CND Analytical, Auburn, AL, 1988.
- 26 C. R. Clark, A. K. Valaer and W. R. Ravis, *J. Liq. Chromatogr.*, 13 (1990) 1375.
- 27 A. C. Moffat (Editor), *Clarke's Isolation and Identification of Drugs in Pharmaceuticals, Body Fluids, and Post-Mortem Material*, Pharmaceutical Press, London, 1986.

# High-performance liquid chromatographic determination of $\alpha$ -tocopheryl nicotinate in cosmetic preparations

A. Baruffini, E. De Lorenzi, C. Gandini, M. Kitsos and G. Massolini\*

*Department of Pharmaceutical Chemistry, Via Taramelli 12, 27100 Pavia (Italy)*

## ABSTRACT

$\alpha$ -Tocopheryl nicotinate ( $\alpha$ -TN) accelerates blood circulation and stimulates hair follicle cells, hence it is an active ingredient in a broad range of cosmetic products. A reversed-phase high-performance liquid chromatographic method was developed to determine  $\alpha$ -TN in cosmetic preparations with  $\alpha$ -tocopheryl acetate as internal standard. The method was found to be rapid, precise and specific.

## INTRODUCTION

Various derivatives of tocopherol are employed in drugs as peripheral vasodilators [1]. In particular, nicotinic acid esters (methyl and benzyl) are mainly used in cosmetic preparations as circulation accelerators.  $\alpha$ -Tocopheryl nicotinate ( $\alpha$ -TN) combines the effects of its constituents, vitamin E and nicotinic acid [2], without displaying the adverse side-effects shown by other nicotinate derivatives, *i.e.*, erythema and heat sensation.  $\alpha$ -TN accelerates blood circulation and stimulates hair follicle cells, hence it is an active ingredient in a broad range of cosmetic products [3–12] such as skin conditioners (lotions and creams) and hair growth-promoters (lotions and shampoos).

Some reversed-phase high-performance liquid chromatographic (HPLC) methods for the separation of tocopherol derivatives have been reported [13–16]. Only one study considered the determination of  $\alpha$ -TN in plasma [16] but it was not found suitable for monitoring this compound in cosmetics.

This paper describes a rapid and specific method for the determination of  $\alpha$ -TN in cosmetic preparations.

## EXPERIMENTAL

### Materials

$\alpha$ -Tocopheryl nicotinate ( $\alpha$ -TN) and the internal

standard,  $\alpha$ -tocopheryl acetate ( $\alpha$ -TA), were purchased from Sigma (St. Louis, MO, USA) and Carlo Erba (Milan, Italy), respectively. Span 60 was obtained from Fluka (Buchs, Switzerland), Tween 61 from Auschem (Milan, Italy), stearic acid, stearyl alcohol, Tween 80, propylparaben, propylene glycol and methylparaben from Aldrich-Chemie (Steinheim, Germany), squalane, ethoxylated hydrogenated lanolin, alkylimidoabetaine, cocamide DEA and coconut oil from Esperis (Milan, Italy), sodium lauryl sulphate from Janssen (Beerse, Belgium) and mineral oil, triethanolamine and ethanol from Carlo Erba. All solvents used were of HPLC grade.

### Equipment

Determinations were performed on an HP 1090M liquid chromatograph (Hewlett-Packard, Palo Alto, CA, USA) equipped with a sample valve (Rheodyne Model 7410) with a 10- $\mu$ l loop, connected to an HP 1090M UV-VIS diode-array detector controlled by an HP 9000 Model 310 workstation.

### Analytical conditions

The column was ODS Hypersil C<sub>18</sub> (100  $\times$  4.6 mm I.D.) (5- $\mu$ m spherical particles) from Hewlett-Packard (Cernusco sul Naviglio, Milan, Italy).

Isocratic elution was carried out with the mobile phase methanol–water–2-propanol (97:2:1, v/v/v) at a flow-rate of 1 ml/min. The analytes were monitored at 210 nm (bandwidth 4 nm).

### Standard solutions

A 1 mg/ml standard solution of  $\alpha$ -TN in 2-propanol was prepared and diluted to obtain concentrations ranging from 10 to 100  $\mu$ g/ml. A 1 mg/ml stock standard solution of  $\alpha$ -TA internal standard was prepared in 2-propanol. The solutions were kept in brown bottles, refrigerated at 4°C.

### Cosmetic preparations

Four laboratory-made products were prepared containing the common concentrations of  $\alpha$ -TN and excipients and formulations as reported [12].

A skin cream was prepared consisting of 3 g of Span 60, 3 g of Tween 61, 8 g of coconut oil, 0.5 g of  $\alpha$ -TN, 6 g of stearic acid, 5 g of stearyl alcohol, 7 g of squalane, 0.1 g of propylparaben, 8 g of ethoxylated hydrogenated lanolin, 5 g of propylene glycol, 0.2 g of methylparaben and deionized water to 100 g.

A skin milk was prepared consisting of 10 g of mineral oil, 1 g of stearyl alcohol, 3 g of stearic acid, 0.5 g of  $\alpha$ -TN, 1.8 g of triethanolamine, 0.2 g of methylparaben and deionized water to 100 g.

A hair lotion was prepared consisting of 0.3 g of  $\alpha$ -TN, 40 g of ethanol, 2 g of Tween 80, 5 g of propylene glycol and deionized water to 100 g.

A shampoo was prepared consisting of 0.5 g of  $\alpha$ -TN, 4 g of sodium lauryl sulphate, 25 g of alkylimidobetaine (30%), 2 g of cocamide DEA, 0.2 g of methylparaben and deionized water to 100 g.

### Sample preparation

A 0.5-g and a 1.0-g sample of cosmetic product [for formulations containing 0.5% and 0.3% (w/w) of  $\alpha$ -TN, respectively] were accurately weighed into a 100-ml volumetric flask, 2.5 ml of internal stan-

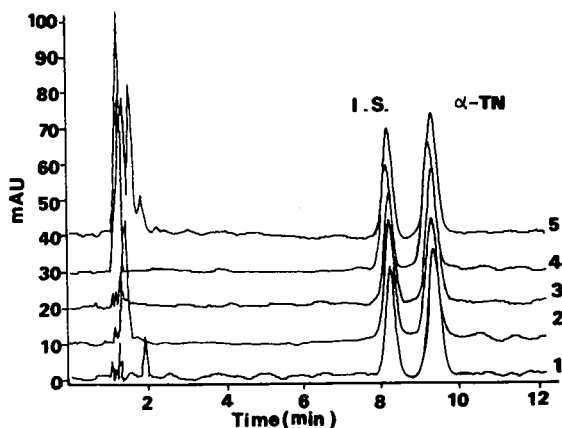


Fig. 1. Chromatograms of  $\alpha$ -TN in different products: 1 = standard solution; 2 = skin milk; 3 = lotion; 4 = skin cream; 5 = shampoo. I.S. = Internal standard ( $\alpha$ -TA).

dard stock solution and about 30 ml of 2-propanol were added and the mixture was stirred until complete solution was effected. The solutions were diluted to a final volume of 100 ml with 2-propanol and filtered over a FHL 0.5- $\mu$ m filter (Millipore) prior to injection.

### RESULTS AND CONCLUSIONS

The chromatographic conditions described above were selected to obtain a good resolution of  $\alpha$ -TN and peaks from excipients and to optimize the peak shape.

Typical chromatograms of  $\alpha$ -TN standard and  $\alpha$ -TN extracted from cosmetic samples are shown in Fig. 1. No interferences at the location of either the  $\alpha$ -TN or  $\alpha$ -TA peaks occurred.

TABLE I  
DETERMINATION OF  $\alpha$ -TN IN COSMETIC PREPARATIONS

Product	Amount added (%, w/w)	Average found <sup>a</sup> (%, w/w)	Mean recovery $\pm$ S.D. (%)	R.S.D. <sup>b</sup> (%)
Skin cream	0.50	0.5091	101.62 $\pm$ 0.9555	0.94
Skin milk	0.50	0.5074	101.48 $\pm$ 0.7000	0.69
Lotion	0.30	0.3069	102.29 $\pm$ 1.3858	1.35
Shampoo	0.50	0.5078	101.56 $\pm$ 0.6581	0.64

<sup>a</sup> Mean values for five samples.

<sup>b</sup> Relative standard deviation.



A calibration graph was constructed by plotting the peak-height ratio ( $\alpha$ -TN to internal standard) versus the concentration of  $\alpha$ -TN. The response was linear in the range investigated (10–100  $\mu\text{g/ml}$ ,  $n = 6$ ,  $r = 0.999$ ,  $y = 0.932x + 0.0503$ ). The equation describing the graph was selected to correspond to the common concentrations in cosmetic products.

For each laboratory-made preparation five samples were analysed in triplicate and the results are summarized in Table I.

The method was found to be rapid, precise and specific for application to the determination of  $\alpha$ -TN in cosmetic preparations.

#### REFERENCES

- 1 M. Kamimura, *Am. J. Clin. Nutr.*, 27 (1974) 1110.
- 2 F. G. M. Vogel, K. Sperling and P. T. Pugliese, *Cosmet. Toiletries, Ed. Ital.*, 102 (1987) 51.
- 3 K. Hasunuma (Kanebo Ltd.), *Jpn. Kokai Tokkyo Koho*, JP 63 139 104 (1988); *C.A.*, 110 (1989) 198932m.
- 4 T. Miyamoto and K. Maeno (Kanebo Ltd.), *Jpn. Kokai Tokkyo Koho*, JP 62 103 006 (1987); *C.A.*, 107 (1987) 183325e.
- 5 T. Miyamoto and T. Toshiyuki (Kanebo Ltd.), *Jpn. Kokai Tokkyo Koho*, JP 62 132 809 (1987); *C.A.*, 107 (1987) 161378x.
- 6 T. Miyamoto and K. Maeno (Kanebo Ltd.), *Jpn. Kokai Tokkyo Koho*, JP 62 103 005 (1987); *C.A.*, 107 (1987) 183324d.
- 7 T. Shinomiya and T. Abe (Kanebo Ltd.), *Jpn. Kokai Tokkyo Koho*, JP 62 72 605 (1987); *C.A.*, 107 (1987) 83705k.
- 8 H. Minamino and K. Mori (Kanebo Ltd.), *Jpn. Kokai Tokkyo Koho*, JP 62 192 312 (1987); *C.A.*, 108 (1988) 11014g.
- 9 K. Hasunuma (Kanebo Ltd.), *Jpn. Kokai Tokkyo Koho*, JP 62 175 417 (1987); *C.A.*, 108 (1988) 62465n.
- 10 K. Hasunuma (Kanebo Ltd.), *Jpn. Kokai Tokkyo Koho*, JP 62 255 409 (1987); *C.A.*, 108 (1988) 209987v.
- 11 Shiseido Co. Ltd., *Jpn. Kokai Tokkyo Koho*, JP 69 116 617 (1985); *C.A.*, 104 (1986) 10383g.
- 12 M. Orishige, H. Horikawa, M. Suzuki and T. Ishida (Pola Chemical Industry Co. Ltd.), *Jpn. Pat.*, 72 47 663 (1972); *C.A.*, 80 (1974) 40933q.
- 13 N. D. Mostow, R. O'Neill, D. Noon and B. R. Bacon, *J. Chromatogr.*, 344 (1985) 137.
- 14 D. D. Stump, E. F. Roth, J. Gilbert and H. S. Gilbert, *J. Chromatogr.*, 306 (1984) 371.
- 15 K. E. Savolainen, K. M. Pynnonen, S. P. Lapinjoki and M. T. Vidgren, *J. Pharm. Sci.*, 77 (1988) 802.
- 16 T. Ijitsu, M. Ueno and S. Hara, *J. Chromatogr.*, 427 (1988) 29.



## Short Communication

# Rapid determination of amino acids by high-performance liquid chromatography: release of amino acids by perfused rat liver

F. Zezza\*, J. Kerner, M. R. Pascale, R. Giannini and E. Arrigoni Martelli

Department of Biochemistry, Research and Development, Sigma-tau SpA, Rome (Italy)

### ABSTRACT

Perfused rat liver can be considered as one of the most suitable *ex vivo* models for studies of liver metabolism. To assess the possible effect of L-carnitine and some of its acyl esters on proteolysis in the rat liver, the amino acid derivatization and high-performance liquid chromatographic separation of Tapuhi *et al.* [*Anal. Biochem.*, 115 (1981) 123] was modified.

### INTRODUCTION

The method for amino acid derivatization and separation by high-performance liquid chromatography (HPLC) of Tapuhi *et al.* [1] has been modified and applied to determine amino acids released by perfused rat liver *in situ*. The amount of L-valine in the perfusate was taken as an indicator of liver proteolysis because its metabolism in the liver is very slow and quantitatively insignificant.

The aim of this work was to evaluate the possible inhibitory effect of different acyl-L-carnitine derivatives on liver proteolysis in normal rats.

### EXPERIMENTAL

Male Wistar rats (130–150 g body weight) were used and were maintained on standard laboratory chow and water *ad libitum*. The animals were anaesthetized with ketamine (Inoketam), 3 µl/g body weight, and heparinized (200 µl of a 5000 U/ml solution).

The perfusion was performed according to the method of Mortimore *et al.* [2]. In the first step (non-recirculating), Krebs Ringer hydrogencarbonate buffer containing 4% bovine serum albumin (fraction V, Sigma) was used for 40 min. This was followed (recirculating step) by a second Krebs Ringer buffer (50 ml) without glucose, but containing 18 µM cycloheximide, to stop hepatic protein synthesis.

The acyl-L-carnitine derivatives to be tested were added to the recirculating buffer at 0.22 or 0.88 mM concentrations. Control livers were perfused as described, but without the carnitine derivatives.

The buffer pH was adjusted to 7.40–7.45 by gassing for 1 h before the perfusion with a mixture of oxygen and carbon dioxide (95:5) and the solutions were filtered through a 0.45-µm Millipore filter. After 15 min of recirculating perfusion, samples were taken and 750 µM L-norvaline was added as an internal standard. A 1-ml volume of perfusate was deproteinized with 75 µl of ice-cold perchloric acid (60% solution). The supernatant was then neutral-

ized with 200 mM potassium carbonate. A 0.5 M solution of potassium carbonate–potassium hydrogencarbonate (30:70, v/v) was added and the pH adjusted to 9.40–9.50 with 5 M potassium hydroxide. Dansyl chloride was prepared (1.25 mg/ml final concentration) in acetonitrile and 100  $\mu$ l of this solution were added to 200  $\mu$ l of each sample. Derivatization was carried out at room temperature for 1 h in the dark. The reaction was stopped by adding methylamine (6  $\mu$ l of a 0.2% solution in water) to neutralize any excess dansyl chloride.

Acetic acid was then added to the samples (3% final concentration) to avoid the possible formation of bubbles following sample injection and mixing with the mobile phase.

A Varian high-performance liquid chromatograph was used for the analysis. This consisted of a STAR 9095 autosampler, a STAR 9010 solvent delivery system, a Merck-Hitachi F-1050 fluorescence spectrophotometer, a Biosil C<sub>18</sub> reversed-phase ODS-5S, 250  $\times$  4 mm column (Biorad) with a Biosil ODS-5S guard column with a microguard refill cartridge (30  $\times$  4.6 mm). The whole system was controlled by a Compaq personal computer.

Dansylated amino acids were separated using mobile phases of: (a) water–methanol (85:15, v/v), containing 1% (v/v) of glacial acetic acid and 0.030% (v/v) of triethylamine; and (b) methanol–acetonitrile (70:30, v/v) containing 3% (v/v) of glacial acetic acid and 0.030% (v/v) triethylamine.

For elution the following gradient was used: 0–52 min, linear increase from 30 to 50% solvent B; 52–73 min, linear increase from 50 to 75% solvent B. Solvent B (75%) was maintained for 5 min, followed by a linear decrease of solvent B to 30% in 7 min (return to initial conditions). The flow-rate was held at 1.0 ml/min throughout the analysis. The separation was performed at room temperature and the effluent monitored and recorded at 340 and 520 nm (excitation and emission wavelengths).

## RESULTS

Using this method it was possible to evaluate the release of amino acids (proteolysis) in rat liver. L-Valine, considered to be the best indicator of liver proteolysis, was calculated as the total amount released in the total recirculating buffer plus liver wa-

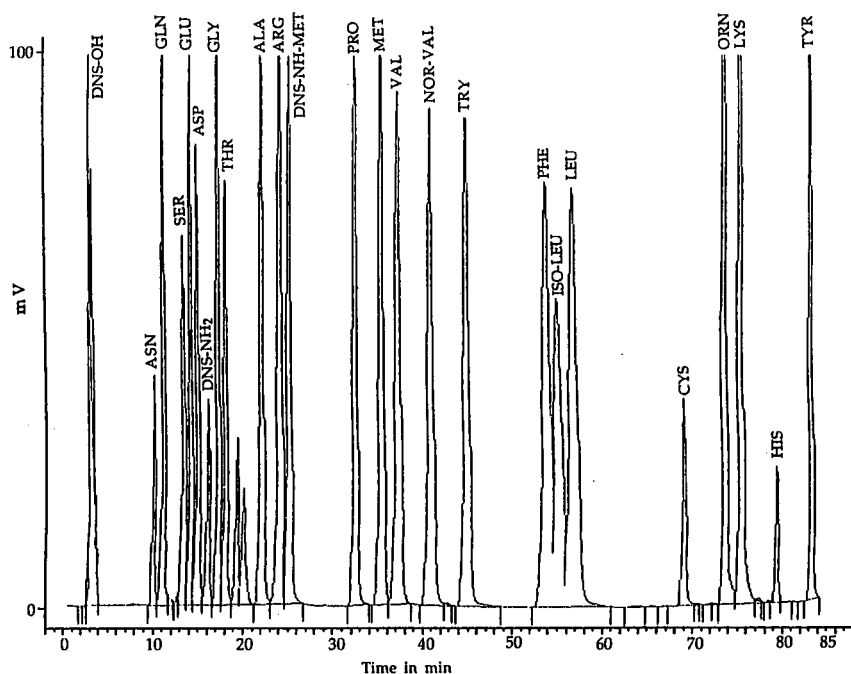


Fig. 1: Representative chromatogram for the standard analysis of amino acids with norvaline as the internal standard. The injection volume was 20  $\mu$ l and the amino acid concentration 37.5  $\mu$ M. Dansylated amino acids were separated as described under Experimental.

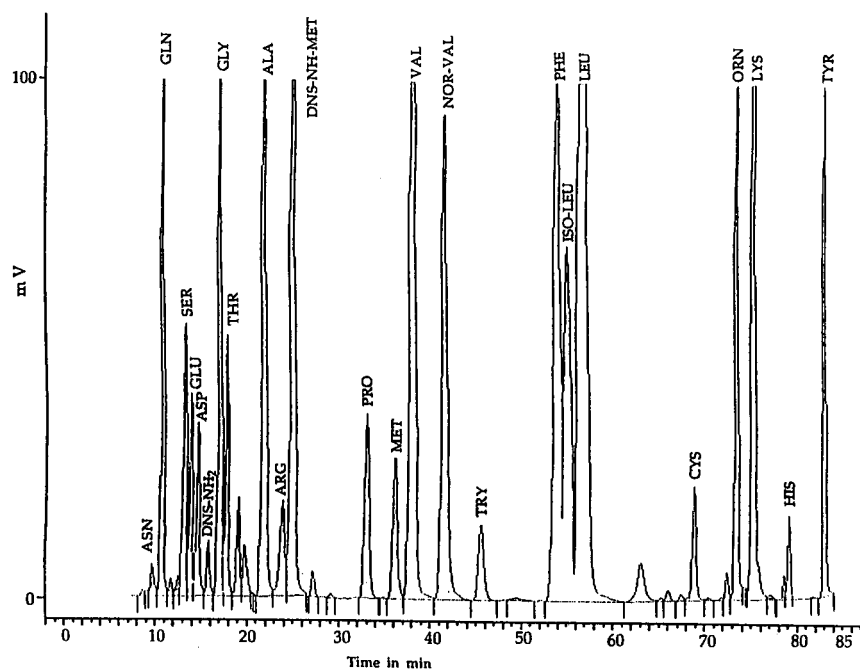


Fig. 2. Representative HPLC analysis of liver perfusate. Experimental conditions as in Fig. 1.

ter [3]. Representative chromatograms are shown in Figs. 1 and 2.

The rate of L-valine release into the perfusate buffer was expressed as nmol/ml of perfusate per g liver wet weight.

For each group of rats (control and those treated with L-carnitine, L-leucyl-L-carnitine or isovaleryl-L-carnitine- $\gamma$ -hydroxybutyrate) at least four livers were perfused. Each compound was tested at two different concentrations (0.22 and 0.88 mM).

In these experiments L-carnitine, L-leucyl-L-carnitine and isovaleryl-L-carnitine- $\gamma$ -hydroxybutyrate inhibited the release of L-valine acids from rat liver, lowering the proteolysis by over 20% at the higher concentration. The results obtained with L-leucyl-L-carnitine are similar to those found with L-leucine by other workers [4].

## DISCUSSION

The aim of this study was to evaluate the possible effect of L-carnitine and some of its acyl derivatives on rat liver proteolysis. It has been shown that leucine is a strong inhibitor of rat liver proteolysis, suppressing proteolysis by about 50% at a concentration four times its normal plasma level [5]. It has also been shown that isovaleryl-L-carnitine, and to

a lesser extent L-carnitine, inhibits proteolysis in perfused rat liver induced by amino acid deprivation [4].

In these experiments L-carnitine and two of its acyl esters (L-leucyl-L-carnitine and isovaleryl-L-carnitine- $\gamma$ -hydroxybutyrate) were studied and it was found that both esters have a pronounced inhibitory effect on liver proteolysis. The inhibitory action of isovaleryl-L-carnitine seems to be very specific, as neither isovalerate alone nor isovalerate plus L-carnitine have a comparable effect [4].

It is intended to use this method to test other carnitine derivatives to find a compound (or compounds) which are superior in their antiproteolytic effects to those compounds studied here.

## REFERENCES

- 1 Y. Tapuhi, D. E. Schmidt, W. Lindner and B. L. Karger, *Anal. Biochem.*, 115 (1981) 123.
- 2 G. E. Mortimore, A. R. Pösö, M. Kadowaki and J. J. Wert, *J. Biol. Chem.*, 262 (1987) 16322.
- 3 G. E. Mortimore, K. H. Woodside and J. E. Henry, *J. Biol. Chem.*, 247 (1972) 2776.
- 4 G. Miotto, R. Venerando and N. Siliprandi, *Biochem. Biophys. Res. Commun.*, 158 (1989) 797.
- 5 A. R. Pösö, J. J. Wert and G. E. Mortimore, *J. Biol. Chem.*, 257 (1982) 12 114.



# High-performance liquid chromatography of amino acids, peptides and proteins

## CXV<sup>☆</sup>. Thermodynamic behaviour of peptides in reversed-phase chromatography

A. W. Purcell, M. I. Aguilar and M. T. W. Hearn\*

*Department of Biochemistry and Centre for Bioprocess Technology, Monash University, Wellington Road, Clayton 3168, Victoria (Australia)*

---

### ABSTRACT

The thermodynamic behaviour of three peptides, bombesin,  $\beta$ -endorphin and glucagon, was studied under reversed-phase high-performance liquid chromatographic conditions. Experimental data related to the interactive surface contact area ( $S$  values) and solute affinity ( $\log k_0$ ) were derived over a range of temperatures between 5 and 85°C. These experimental conditions allowed changes in the secondary structure of the solute to be monitored. The influence of the nature of the stationary phase ligand on the relative conformational stability of the three peptides was analysed by acquiring data with *n*-octadecyl silica ( $C_{18}$ ) and *n*-butyl silica ( $C_4$ ) sorbents. Values for the relative changes in entropy and enthalpy associated with the interactive process were also determined. The results provide further insight into the factors involved with the stabilization of secondary structure and the mechanism of the interaction of peptides with hydrophobic surfaces.

---

### INTRODUCTION

The development of interactive modes of chromatography to investigate the physico-chemical nature of peptide and protein surface interactions has advanced considerably over the past decade. These powerful techniques have gained wide recognition as rapid and extremely useful procedures for elucidating, in structural and molecular terms, biopolymer behaviour at liquid–solid interfaces under a wide range of experimental conditions [2–4]. The hydrophobic modes of chromatography, namely reversed-phase high-performance liquid chromatography (RP-HPLC) and hydrophobic interaction chromatography (HIC), have especially been used in strategies employed for studies of the mechanistic basis of chromatographic separations. The useful-

ness of modern LC techniques stems from the ability of the stationary phase ligands to probe the solute surface. Different ligands may be employed to explore different physical and chemical properties of the interfacial region of the solute recognized by the stationary phase. The fact that this approach, aptly coined chromatotopography [5,6], also enables kinetic properties of the solute to be followed thus allows insight into the dynamic nature of the protein–ligand interaction. This attribute of modern LC methods with appropriate on-line detection systems clearly represents an advantage over many of the conventional techniques such as X-ray crystallography and other static methods of spectroscopic measurement hitherto used to evaluate biopolymer–ligand interactions.

It was postulated 15 years ago [7] that the hydrophobic surface in RP-HPLC may be a useful probe for investigating amphipathic helices and

---

\* For part CXIV, see ref. 1.

other helices of biopolymers induced or stabilized in hydrophobic environments and the behaviour of peptides and proteins at a hydrophobic interface, such as a lipid bilayer. This paper examines the potential of this technique and the validity of the above considerations by examining the thermodynamic behaviour of three biologically significant peptides, bombesin,  $\beta$ -endorphin and glucagon. The secondary and tertiary structures of these peptides in solution have been characterized [8–13], and each contains significant amounts of  $\alpha$ -helical structure under certain conditions. The relative stability of the secondary structure components within these peptides was studied by varying the temperature and the stationary phase composition upon which they were allowed to interact in the RP-HPLC mode.

## EXPERIMENTAL

### *Apparatus*

All chromatographic measurements were performed on a Perkin-Elmer (PE) Series 4 chromatograph (Perkin-Elmer, Norwalk, CT, USA) utilizing a PE ISS-100 autosampler, PE LC-95 UV-visible spectrophotometer and a PE 7500 professional computer with CHROM 3 software. All peak profiles were routinely monitored at 215 nm and stored on the Winchester disk of the PE 7500 and processed simultaneously by a PE LCI-100 computing integrator. Further peak analysis was performed using software packages included in the CHROM 3 framework. Temperature was controlled by either immersing the column in a thermostated column water-jacket coupled to a recirculating cooler (FTS Systems, New York, USA) or by an ICI TC 1900 column oven (ICI Instruments, Dingley, Victoria, Australia).

Chromatography was performed on Bakerbond wide-pore butylsilica and octadecylsilica columns (J. T. Baker, Phillipsburg, NJ, USA) with dimensions of 250  $\times$  4.6 mm I.D. and containing sorbents of 5  $\mu$ m nominal particle size and 30 nm average pore size.

All pH measurements were made with an Orion (Cambridge, MA, USA) Model SA520 pH meter.

### *Chemicals and reagents*

Acetonitrile (HPLC grade) was obtained from Mallinckrodt (Paris, KY, USA) and trifluoroacetic

acid (TFA) from Pierce (Rockford, IL, USA). Water was distilled and deionized in a Milli-Q system (Millipore, Bedford, MA, USA). N-Acetyl-L-tryptophanamide, N-acetyl-L-phenylalanine ethyl ester, penta-L-phenylalanine, bombesin and glucagon were all obtained from Sigma (St. Louis, MO, USA) and were of >95% purity by RP-HPLC and amino acid composition analysis.  $\beta$ -Endorphin (of purity >95%) was obtained from Organon (Oss, Netherlands) and Sigma; both batches gave identical HPLC profiles.

### *Chromatographic procedures*

Bulk solvents were filtered and degassed by sparging with nitrogen. Linear gradient elution was performed using 0.1% TFA in water (buffer A) and 0.09% TFA in acetonitrile–water (65:35) (buffer B) over gradient times of 30, 45, 60 and 90 min with a flow-rate of 1 ml/min at temperatures of 5, 15, 25, 37, 45, 55, 65, 75 and 85°C. Peptide solutions were prepared by dissolving the solute at a concentration of 0.5 mg/ml in 0.1% TFA and the injection size varied between 1 to 5  $\mu$ g. All data points are derived from at least duplicate measurements with retention times between replicates varying typically by less than 1%.

The column dead volume was taken as the retention time of the non-interactive solute, sodium nitrate. Various chromatographic parameters were calculated using the Pek-n-ese program [14] written in Pascal for an IBM PC, and statistical analysis involved ANOVA linear regression analysis. In all figures presented, the standard deviations of replicate experiments were as shown, or smaller than the data points.

## RESULTS AND DISCUSSION

### *Theoretical background*

The retention of a solute in interactive modes of chromatography is dictated by the equilibria established for the distribution of the solute in the mobile and stationary phases as described by

$$K = \frac{[P]_s}{[P]_m} \quad (1)$$

where  $[P]_s$  and  $[P]_m$  are the concentrations of solute in the stationary and mobile phases respectively. The dependence of the capacity factor,  $k'$ , on the



chromatographic equilibrium constant,  $K$ , can be equated to

$$k' = \phi K \quad (2)$$

where  $\phi$  is the phase ratio, that is, the ratio of volumes of stationary to mobile phases in the chromatographic bed.

For linear gradient elution systems, a mathematical model known as the linear solvent strength (LSS) model has been shown to provide useful information associated with the physico-chemical properties of the solute [3,14,15].

Under regular reversed-phase gradient elution conditions, a linear relationship typically exists between the medium capacity factor,  $\log \bar{k}$ , and the median organic mole fraction,  $\bar{\psi}$ , according to the empirical equation.

$$\log \bar{k} = \log k_0 - S\bar{\psi} \quad (3)$$

The values of  $S$  and  $\log k_0$  can then be determined by multivariate linear regression analysis of  $\log \bar{k}$  vs.  $\bar{\psi}$  plots according to eqn. 3.

The significance of the slope,  $S$ , of  $\log \bar{k}$  vs.  $\bar{\psi}$  plots in RP-HPLC resides in its relationship to the magnitude of the surface contact area and the number of interactive sites established at the interface between the solute and the stationary phase ligands. The  $S$  value as evaluated through eqn. 3 can be related to the hydrophobic contact area as derived from the solvophobic theory [7,16] as follows:

$$\log k' = \log k_0 - \gamma \cdot \frac{N\Delta A_h + 4.836N^{\frac{1}{3}}(\kappa^e - 1)V^{\frac{2}{3}}}{2.303RT} \quad (4)$$

where  $\Delta A_h$  is the relative hydrophobic contact area,  $\gamma$  is the mobile phase surface tension, which is directly related to the organic mole fraction,  $\bar{\psi}$ ,  $N$  is Avogadro's number,  $V$  is the mean molar volume of the solvent,  $R$  is the gas constant and  $T$  is the absolute temperature. The parameter  $\kappa$  is defined as the ratio of the energy required for the formation of a cavity with the surface area equal to solute surface area and the energy required to extend the planar surface of the liquid by the same area. The value of  $\log k_0$  is related to the change in free energy associated with the adsorption of the solute in the absence of organic modifier, and can thus be related to the affinity of the solute for the stationary phase at  $\bar{\psi} = 0$  (i.e., initial conditions).

The determination of these parameters at different temperatures allows a detailed analysis of the thermodynamic behaviour of the solute during the interaction with the stationary phase. The thermodynamic equilibrium constants can be equated to the overall standard unitary free-energy changes ( $\Delta G_{\text{assoc}}^0$ ) associated with the transfer of the solute from the mobile phase to the stationary phase, such that

$$\log K = -\frac{\Delta G_{\text{assoc}}^0}{RT} \quad (5)$$

Solute retention under equilibrium binding conditions can therefore be described as

$$\log \bar{k} = \frac{-\Delta H_{\text{assoc}}^0}{RT} + \frac{\Delta S_{\text{assoc}}^0}{R} + \log \phi \quad (6)$$

where  $\Delta H_{\text{assoc}}^0$  and  $\Delta S_{\text{assoc}}^0$  are the changes in enthalpy and entropy, respectively, for the association

TABLE I  
PHYSICAL DATA FOR THE SOLUTES STUDIED

Solute	Sequence <sup>a</sup>	Molecular weight
N-Acetyltryptophanamide	N-Ac-W-NH <sub>2</sub>	230
N-Acetylphenylalanine ethyl ester	N-Ac-F-OEt	210
Penta-L-phenylalanine	H <sub>2</sub> N-FFFFF-OH	760
Bombesin	H <sub>2</sub> N-XQRLGNQWAVGHLM-OH	1640
$\beta$ -Endorphin	H <sub>2</sub> N-YGGFMTSEKSQTPLVFKNAIKNAYKKGE-OH	3470
Glucagon	H <sub>2</sub> N-HSQGTFTSDYSKYLDSSRAQDFVQWLMNT-OH	3520

<sup>a</sup> Ac = Acetyl.

process. The  $\Delta H_{\text{assoc}}^0$  and  $\Delta S_{\text{assoc}}^0$  values can then be derived from the slope and intercept values determined by regression analysis of Van 't Hoff plots (*i.e.*  $\log \bar{k}$  vs.  $1/T$ ). Linear relationships in such plots are generally obtained for small organic molecules with no significant secondary or tertiary structure. However, the interactive surface of a peptide or protein solute in RP-HPLC will consist of sequentially and non-sequentially linked amino acids brought together spatially as a result of the secondary or tertiary constraints of the solute structure. For solutes with well developed secondary structure, chromatographed over a wide range of temperatures, significant deviation from linearity has been observed in Van 't Hoff plots [3]. This behaviour is a result of temperature-induced conformational changes which affect the molecular composition of the interactive surface of the solute and will therefore be reflected in both the retention behaviour of the solute and the thermodynamic parameters derived from Van 't Hoff plots.

#### Dependence of $S$ and $\log k_0$ on temperature

The retention behaviour of a range of peptide solutes with known  $\alpha$ -helical structure [8–13] was studied to provide further information on the factors which influence the chromatographic behaviour of peptides and proteins. The gradient elution behaviour of two amino acid derivatives, N-acetyltryptophanamide and N-acetylphenylalanine ethyl ester and four peptides, penta-L-phenylalanine and the peptide hormones bombesin,  $\beta$ -endorphin and glucagon, was measured under a range of experimental conditions. The molecular weights and sequences of these solutes are summarized in Table I.

As solution conformation is substantially influenced by environmental temperature, and can be generally perturbed within the temperature range available in chromatographic studies, the influence of temperature on the RP-HPLC behaviour of these peptides was studied. Gradient elution data were accumulated at gradient times between 30 and 90 min at a flow-rate of 1 ml/min and at temperatures ranging between 5 and 85°C. In order to study the influence of different hydrocarbonaceous ligands, samples were chromatographed on  $C_4$  and  $C_{18}$  silicas. Plots of  $\log \bar{k}$  vs.  $\psi$  were used to derive  $S$  and  $\log k_0$  values for each solute and the temperature dependencies of these values are represented graphically in Figs. 1–5.

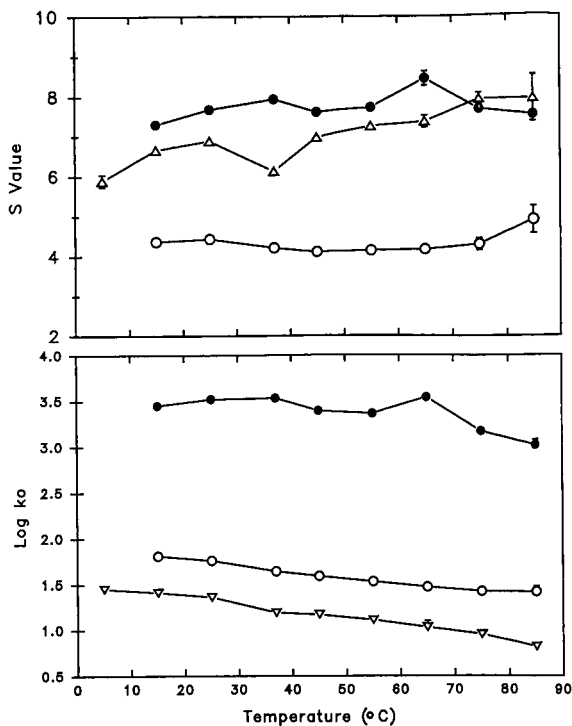


Fig. 1. Top, dependence of  $S$  values on temperature for the control solutes (●) penta-L-phenylalanine, (○) N-acetylphenylalanine ethyl ester and (△) N-acetyltryptophanamide chromatographed on the  $C_{18}$  stationary phase. Bottom, dependence of  $\log k_0$  on temperature for the same solutes chromatographed on the  $C_{18}$  stationary phase.

N-Acetyltryptophanamide, N-acetylphenylalanine ethyl ester and penta-L-phenylalanine were chromatographed as control solutes. These solutes are small molecules with no secondary structure. Changes in retention behaviour over the temperature range studied will therefore not be related to conformational changes in the interactive structure. N-Acetyltryptophanamide was only retained on the  $C_{18}$  stationary phase. These three solutes on the  $C_{18}$  stationary phase had essentially constant  $S$  values over the range of temperatures examined and the corresponding affinity ( $\log k_0$ ) demonstrated a constant or small uniform decrease in value with increases in temperature (Fig. 1). Similar trends in the temperature dependencies of the  $S$  and  $\log k_0$  values were also observed for these solutes when chromatographed on the  $C_4$  phase, as depicted in Fig. 2. However, the magnitude of the affinity of the

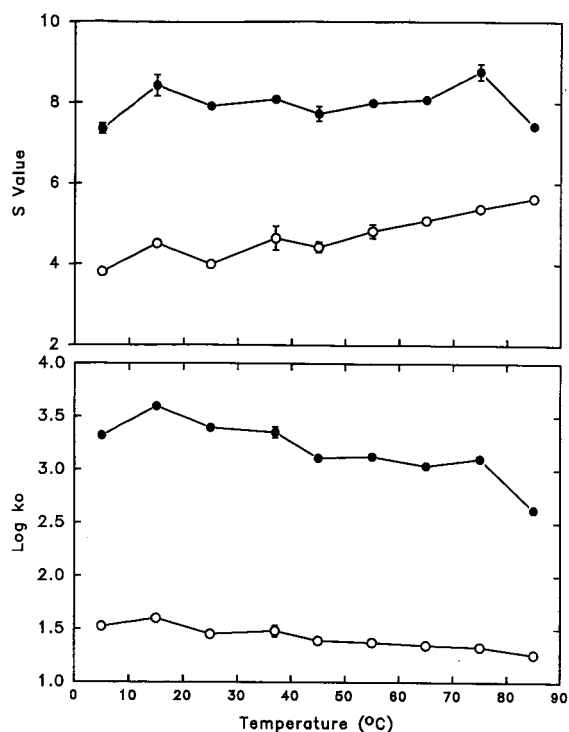


Fig. 2. Top, dependence of *S* values on temperature for the control solutes (●) penta-L-phenylalanine and (○) N-acetylphenylalanine ethyl ester chromatographed on the *C*<sub>4</sub> stationary phase. N-Acetyltryptophanamide was not retained at high temperatures on this phase. Bottom, dependence of log *k*<sub>0</sub> on temperature for the same solutes chromatographed on the *C*<sub>4</sub> stationary phase.

control solutes chromatographed on the *C*<sub>18</sub> stationary phase was generally higher than that on the *C*<sub>4</sub> stationary phase. Thus, for these solutes chromatographed over a wide range of temperatures, the two stationary phases behaved as would be empirically predicted on the basis of the relative hydrophobicity of the ligands when conformationally rigid solutes are chromatographed. It would also appear that similar interactive regions are involved in the interaction between the control solutes and the two stationary phase types, which is reflected in the similar magnitude for the derived chromatographic *S*-values for both the *C*<sub>18</sub> and *C*<sub>4</sub> phases.

As these control solutes are small organic molecules, the results in Figs. 1 and 2 represent the degree of change in *S* and log *k*<sub>0</sub> which would be expected for solutes which undergo no structural perturbation with increased temperature. Penta-L-phenyl-

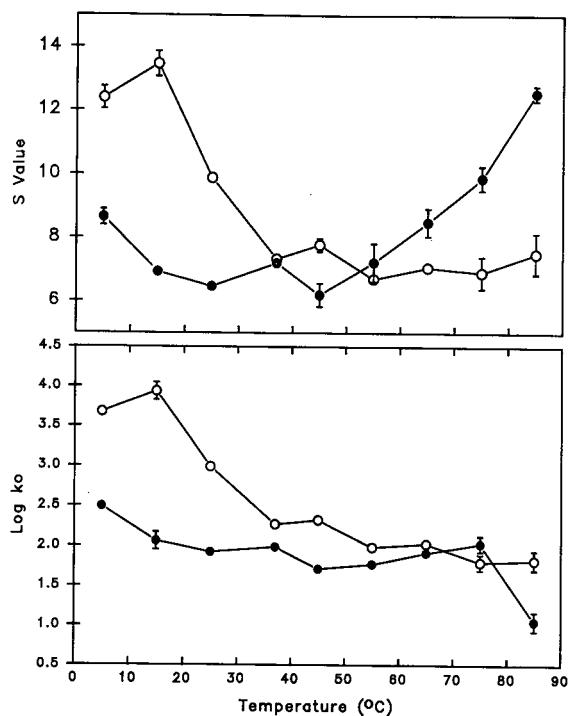


Fig. 3. Top, dependence of *S* values on temperature for bombesin chromatographed on the (○) *C*<sub>18</sub> and (●) *C*<sub>4</sub> stationary phases. Bottom, dependence of log *k*<sub>0</sub> on temperature for bombesin on these two stationary phases.

alanine displays some minor fluctuations with temperature, as would be expected for a molecule of greater conformational flexibility. However, similar *S* values were obtained with both *C*<sub>4</sub> and *C*<sub>18</sub> ligands. Moreover, these solutes represent useful probes for the changes in *n*-alkyl ligand structure which may occur at different temperatures.

Fig. 3 illustrates the relationship between *S* values and temperature for bombesin on the two different stationary phases studied. A transition at *ca.* 25°C corresponding to two different interactive structures with high and low contact areas was observed on the *C*<sub>18</sub> phase. The affinity vs. temperature plot (Fig. 3) also indicates a similar transition with significantly elevated log *k*<sub>0</sub> values in the 5–25°C range for bombesin on the *C*<sub>18</sub> phase. Thus, at higher temperature, bombesin is interacting through a much smaller proportion of its molecular surface area and with a diminished affinity.

In contrast to the *C*<sub>18</sub> phase, bombesin shows

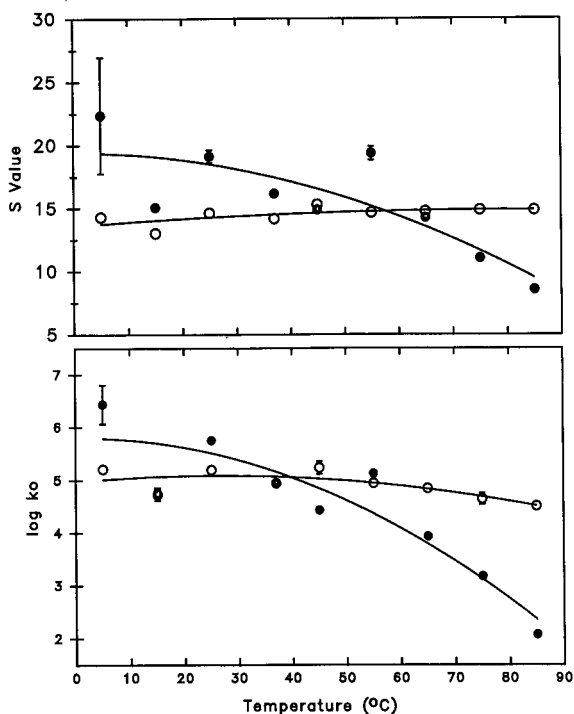


Fig. 4. Top, dependence of *S* values on temperature for  $\beta$ -endorphin chromatographed on the (○)  $C_{18}$  and (●)  $C_4$  stationary phases. Bottom, dependence of  $\log k_0$  on temperature for  $\beta$ -endorphin on these two stationary phases.

marked increases in *S* value on the  $C_4$  phase at temperatures above 50°C, which coincided with a decrease in affinity for this region of temperature. This result implies that whilst a larger surface area is exposed by bombesin to the  $C_4$  ligands at these higher temperatures, the affinity of the peptide for the sorbent at high temperatures is lower than when the solute exists with a more compact interactive structure at the lower temperature range. These observations suggest that at higher temperatures bombesin presents a more diffuse surface distribution of hydrophobic amino acids to the probing  $C_4$  stationary phase ligands.

The relative changes in affinity and chromatographic contact area with temperature for bombesin are much greater compared with the control solutes. In particular, on the  $C_{18}$  phase, the *S* value for bombesin changes from 12.5 to 7.0 at *ca.* 25°C, whereas the *S* value for penta-L-phenylalanine remained constant. The results for these two solutes chromatographed on the  $C_4$  phase indicate an

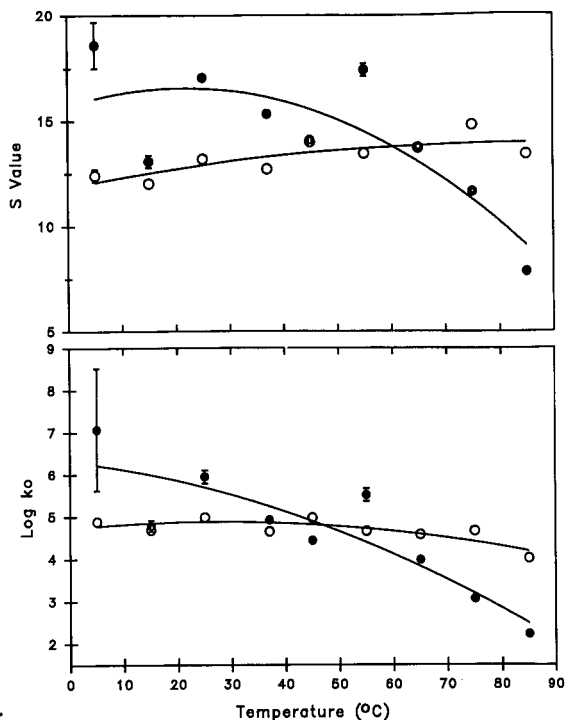


Fig. 5. Top, dependence of *S* value on temperature for glucagon chromatographed on the (○)  $C_{18}$  and (●)  $C_4$  stationary phases. Bottom, dependence of  $\log k_0$  on temperature for glucagon on these two stationary phases.

opposite trend, where at temperatures below 50°C similar *S* values are observed both for penta-L-phenylalanine and bombesin, but at the higher temperatures significantly higher *S* values and hence contact areas are observed for bombesin. Penta-L-phenylalanine also had a relatively constant *S*-value over the temperature range investigated on the  $C_4$  phase.

The affinity values also reflect these differences in chromatographic behaviour between penta-L-phenylalanine and bombesin. On the  $C_{18}$  phase, bombesin has a lower affinity compared with the control solute at high temperatures, whereas similar values for both solutes are observed at the low temperatures. Penta-L-phenylalanine demonstrated a small but uniform decrease in affinity with increasing temperature, whereas transitions were apparent for bombesin. Comparison of  $\log k_0$  values determined for both solutes on the  $C_4$  phase indicate that bombesin has overall lower affinity values than the control solute over the temperature range stud-

ied, but both solutes demonstrated a uniform decrease in affinity with temperature. These significant changes in chromatographic behaviour of bombesin are consistent with changes in the interactive structure of bombesin relative to penta-L-phenylalanine and the other control solutes. Hence it appears that bombesin adopts, in the presence of *n*-alkyl ligands, some degree of secondary structure, which may be helical as bombesin is known to possess an  $\alpha$ -helical structure in hydrophobic conditions [8,9].

The differences in the behaviour of bombesin on the  $C_4$  and  $C_{18}$  stationary phases also indicates that the two structurally disparate ligands are either probing different areas of the solute surface or that bombesin adopts a different structure in the presence of the two ligands. The difference in dynamic behaviour of the two stationary phases is well documented [17,18], with the  $C_4$  ligands tending to be more sterically rigid than the  $C_{18}$  ligands, which have the potential to self-associate owing to their higher degree of flexibility. The  $C_4$  stationary phase has been described as a "picket-fence" with  $C_4$  ligands projecting away from the silica surface [19] into the mobile phase whereas the  $C_{18}$  stationary phase comprises a "lawn" of alkyl chains forming a hydrophobic surface that coats the silica particles. Other workers have shown that transitions occur in the structure of longer chain alkyl ligands. These phase transitions have been shown to cause non-linear relationships between solute retention and temperature. Gilpin and Squires [20] studied phase transitions for  $C_8$ -,  $C_9$ - and  $C_{10}$ -alkylsilicas and determined phase transition temperatures of *ca.* 40, 50 and 60°C, respectively. The temperature increment of 10°C in the phase transition with each additional methylene group added suggests that the theoretical transition for the  $C_{18}$  stationary phase would be well outside the experimental temperature range utilized in this study, and that changes in the ligand structure do not account for the observed changes in retention behaviour of bombesin.

Jinno *et al.* [21] recently conducted a study on a series of polymeric  $C_{18}$  stationary phases and observed a non-linear retention dependence on temperature for planar polycyclic aromatic hydrocarbon solutes for some of the stationary phases investigated. This retention behaviour was attributed to changes in the ligand structure between 40 and 50°C. Although this transition range is not in accordance

with the work of Gilpin and Squires, different solvent systems were employed. Jinno *et al.* [21] used an organic solvent system of methanol–dichloromethane (80:20, v/v), whereas Gilpin and Squires used a totally aqueous system.

Although it is possible that a phase transition may occur in the experimental temperature region used in this study, several observations suggest that this phenomenon does not significantly influence the retention behaviour of the solutes employed in this study. First, a linear dependence of the derived retention parameters on temperature was obtained for the control solutes, which strongly suggests that should changes occur in the structure of the stationary phase ligand, they are not responsible for the observed peptide transitions. Additionally, of the peptides studied only bombesin shows a significant transition in *S* value on the  $C_{18}$  stationary phase. Hence, if a significant change occurred in the structure of the ligand, it should be manifested in the retention properties of all solutes. These observations strongly suggest that the observed non-linear temperature dependence of the derived retention parameters is due to solute-specific structural changes and not phase transitions of the immobilized ligands.

The dependence of *S* and  $\log k_0$  on temperature for the two larger peptides,  $\beta$ -endorphin and glucagon, on the  $C_{18}$  phase are shown in Figs. 4 and 5, respectively. The behaviour observed on the  $C_{18}$  phase for both  $\beta$ -endorphin and glucagon indicates a gradual increase in chromatographic *S* value with increasing temperature. The magnitude of this change was smaller than that observed for bombesin (Fig. 3) with the same phase. The plots of  $\log k_0$  vs. temperature indicate a small, uniform decrease in affinity between  $\beta$ -endorphin or glucagon and the  $C_{18}$  phase over the temperature range examined.

For both  $\beta$ -endorphin and glucagon on the  $C_4$  stationary phase, a sharp decrease in *S* values between 50 and 85°C was observed (Figs. 4 and 5 for  $\beta$ -endorphin and glucagon, respectively), as opposed to bombesin, which underwent a rapid increase in *S* value over this temperature range. This decrease in chromatographic contact area for both of these solutes also corresponded to a large decrease in affinity (Figs. 4 and 5), which is consistent with a decrease in the number of amino acid residues participating in the interaction at these higher

TABLE II

GIBB'S FREE ENERGY CHANGES FOR THE SOLUTES STUDIED ON BOTH PHASES

Temperature (°C)	Change in Gibb's free energy ( $\Delta G_{\text{assoc}}^0$ ) (kJ mol <sup>-1</sup> )					
	Bombesin		$\beta$ -Endorphin		Glucagon	
	C <sub>18</sub>	C <sub>4</sub>	C <sub>18</sub>	C <sub>4</sub>	C <sub>18</sub>	C <sub>4</sub>
5	-9.4	-6.6	-12.9	-17.2	-12.2	-15.7
15	-10.3	-5.8	-12.2	-12.3	-12.1	-12.3
25	-8.3	-5.7	-13.8	-15.6	-13.3	-15.1
37	-6.8	-6.1	-13.7	-13.6	-12.9	-13.7
45	-7.1	-5.5	-14.8	-12.7	-14.1	-12.7
55	-6.4	-5.8	-14.5	-16.0	-13.7	-15.0
65	-6.7	-6.4	-14.6	-12.2	-13.9	-12.1
75	-6.3	-6.9	-14.5	-9.9	-14.5	-10.2
85	-6.5	-4.2	-14.5	-7.7	-13.1	-7.3

TABLE III

CHANGES IN ENTHALPY AND ENTROPY FOR THE SOLUTES STUDIED

Solute	$\bar{\psi}$	C <sub>18</sub> -silica <sup>a</sup>		C <sub>4</sub> -silica <sup>a</sup>	
		$\Delta H_{\text{assoc}}^0$ (kJ mol <sup>-1</sup> )	$\Delta S_{\text{assoc}}^0$ (J mol <sup>-1</sup> K <sup>-1</sup> )	$\Delta H_{\text{assoc}}^0$ (kJ mol <sup>-1</sup> )	$\Delta S_{\text{assoc}}^0$ (J mol <sup>-1</sup> K <sup>-1</sup> )
N-Acetylphenylalanine ethyl ester	0.1	-5.4	-5.9	-4.6	-5.3
	0.3	-6.0	-14.7	-8.4	-25.3
N-Acetyltryptophanamide <sup>b</sup>	0.1	-8.2	-20.7		
	0.3	-12.2	-45.0		
Penta-L-phenylalanine	0.1	-5.8	-7.7	-8.6	-5.0
	0.3	-5.1	7.3	-7.9	-17.0
Bombesin	0.1	9.8 <sup>5-15</sup>	58.6		
		-36.3 <sup>15-37</sup>	-102.1	-5.6	-4.5
		-11.0 <sup>45-85</sup>	-19.1		
	0.3	1.0 <sup>5-55</sup>	6.2	-1.8 <sup>4-45</sup>	-5.2
		-16.8 <sup>65-85</sup>	-47.5	-29.9 <sup>45-85</sup>	-94.4
$\beta$ -Endorphin	0.1	-0.8 <sup>5-45</sup>	30.7	-15.6 <sup>25-55</sup>	-18.3
		-15.8 <sup>45-85</sup>	-16.0	-69.4 <sup>55-85</sup>	-180.0
	0.3	-5.0 <sup>5-45</sup>	-7.3	-5.9 <sup>5-45</sup>	-15.2
			-14.4 <sup>45-85</sup>	-36.6	-27.2 <sup>45-85</sup>
				-17.8 <sup>55-85</sup>	-4.8
Glucagon	0.1	-1.9 <sup>5-45</sup>	26.1	-39.9 <sup>25-45</sup>	-97.6
		-17.0 <sup>45-85</sup>	-23.7	-65.6 <sup>55-85</sup>	-169.0
	0.3	-7.2 <sup>5-45</sup>	-13.0	-1.7 <sup>15-25</sup>	2.1
			-18.2 <sup>45-85</sup>	-47.4	-15.9 <sup>25-75</sup>
				4.3 <sup>75-85</sup>	12.6

<sup>a</sup> Superscripts denote the temperature region (°C) of the Van 't Hoff plot used to derive the corresponding parameters.<sup>b</sup> N-Acetyltryptophanamide was not fully retained over the temperature studied on the C<sub>4</sub> stationary phase.

temperatures. As the compositional properties of the interactive region will determine both the affinity and the magnitude of the contact area for a particular solute, the results of this study suggest that the changes in retention behaviour with increasing temperature for these three peptidic solutes are due primarily to the conformational changes. These conformational changes over the temperature range investigated will in turn dictate the accessible interactive surface that will be presented to the probing stationary phase ligands.

#### Dependence of thermodynamic parameters on temperature

Consideration of the thermodynamic parameters underlying the biomolecular structural characteristics [22] of peptide and protein-surface interactions provides further insight into the chromatographic process. Changes in  $\Delta G_{\text{assoc}}^0$  were calculated at the individual temperatures from  $\log k_0$  values according to eqn. 5. As adsorption is a favourable process, the derived  $\Delta G_{\text{assoc}}^0$  values which are given in Table II are all negative. Van't Hoff plots ( $\log \bar{k}$  vs.  $1/T$ ) were also examined in order to derive the changes in enthalpy ( $\Delta H_{\text{assoc}}^0$ ) and entropy ( $\Delta S_{\text{assoc}}^0$ ) for the association process by regression analysis of the dependence of  $\log \bar{k}$  on  $1/T$  (as described by eqn. 6). In order to assess the influence of the organic

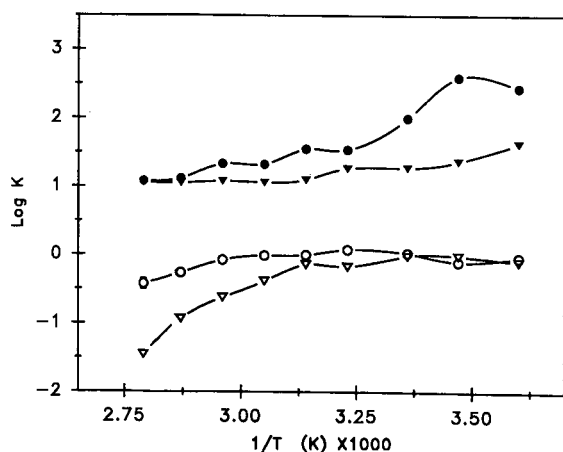


Fig. 6. Van't Hoff plot for bombesin chromatographed on the ( $\nabla, \blacktriangledown$ )  $C_4$  and ( $\circ, \bullet$ )  $C_{18}$  stationary phases at the different  $\log \bar{k}$  values ( $\bar{\psi} = 0.1$  and  $0.3$ , closed and open symbols, respectively).

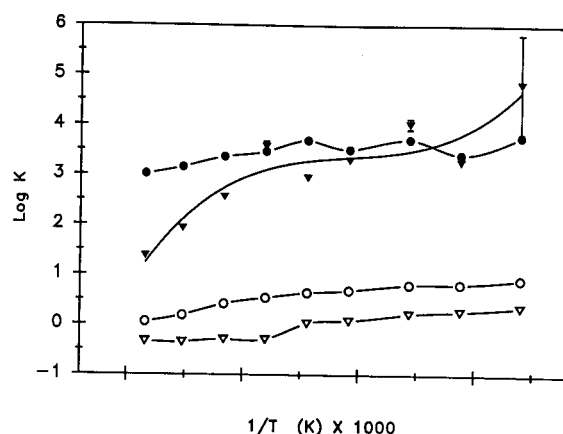


Fig. 7. Van't Hoff plot for  $\beta$ -endorphin chromatographed on the ( $\nabla, \blacktriangledown$ )  $C_4$  and ( $\circ, \bullet$ )  $C_{18}$  stationary phases at the two  $\log \bar{k}$  values ( $\bar{\psi} = 0.1$  and  $0.3$ , closed and open symbols, respectively).

modifier concentration on the structure of the solute and on the interactive process,  $\log \bar{k}$  values extrapolated from two different regions of the retention plots ( $\log \bar{k}$  vs.  $\bar{\psi}$ ) were examined.  $\log \bar{k}$  values extrapolated to  $\bar{\psi} = 0.1$  and  $0.3$  were determined and the corresponding  $\Delta S_{\text{assoc}}^0$  and  $\Delta H_{\text{assoc}}^0$  values are given in Table III.

Van't Hoff plots for bombesin,  $\beta$ -endorphin and glucagon are shown in Figs. 6–8. Non-linear relationships were found to exist for the three large

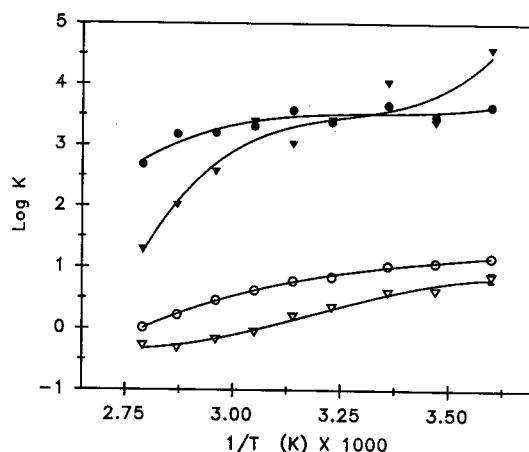


Fig. 8. Van't Hoff plot for glucagon chromatographed on the ( $\nabla, \blacktriangledown$ )  $C_4$  and ( $\circ, \bullet$ )  $C_{18}$  stationary phases at the two  $\log \bar{k}$  values ( $\bar{\psi} = 0.1$  and  $0.3$ , closed and open symbols, respectively).

peptidic solutes. This result is in contrast to the Van 't Hoff plots for the control solutes, which generally gave linear relationships for both stationary phases examined (data not shown). The non-linear behaviour of the larger polypeptides correlates with changes observed for these solutes in retention parameters discussed in the previous section, and also provides further support for the existence of conformational changes that occur during chromatographic migration.

Two important generalizations about the entropy of the interactive process can be made [3], namely that positive values for the change in entropy for the association process ( $\Delta S_{\text{assoc}}^0$ ) indicate an increase in the total disorder of the system during adsorption, whereas it is inherent in the corollary that negative values of  $\Delta S_{\text{assoc}}^0$  indicate an increased ordering of the system during adsorption. For the control solutes N-acetylphenylalanine ethylester and N-acetyltryptophanamide, negative values for  $\Delta S_{\text{assoc}}^0$  were obtained for both stationary phases and at both extrapolated values of  $\log \bar{k}$ . This result can be interpreted as an overall ordering of the system on interaction with the stationary phase, reflecting a solute that is less flexible when bound to the stationary phase than when it is in the mobile phase. In addition, values of  $\Delta S_{\text{assoc}}^0$  for  $\log \bar{k}$  at  $\bar{\psi} = 0.1$  are less negative than those at  $\bar{\psi} = 0.3$ . This result indicates that the solutes are more flexible in mobile phases containing organic solvents than in more aqueous solutions, which in turn suggests that they interact more readily with the organic solvent molecules than with the water molecules. This conclusion forms the basis of the solvophobic mechanism underlying retention in RP-HPLC and is also consistent with the observation that at  $\bar{\psi} = 0.3$ , lower  $\log \bar{k}$  values are obtained. As a result of this behaviour, the solute will be less constrained and the total system will be more disordered, thus accounting for the more negative  $\Delta S_{\text{assoc}}^0$  values at  $\log \bar{k}$  with  $\bar{\psi} = 0.3$ .

The same trends are evident for penta-L-phenylalanine, where negative  $\Delta S_{\text{assoc}}^0$  values were observed for all conditions except on the  $C_{18}$  phase at  $\log \bar{k}$  ( $\bar{\psi} = 0.3$ ). A small positive  $\Delta S_{\text{assoc}}^0$  value was observed under the latter conditions, indicating a possible disordering on binding to this stationary phase at the high organic solvent concentration. This result reflects a more rigid solution structure in

comparison with the bound molecule, suggesting that some form of conformational change on association with the stationary phase may occur.

**Bombesin on  $C_{18}$  phase.** Fig. 6 displays the Van 't Hoff plots for bombesin chromatographed on both stationary phases at the two extrapolated values of  $\log \bar{k}$ . Changes in enthalpy and entropy for the interactive process are given in Table III. Negative  $\Delta H_{\text{assoc}}^0$  values were generally observed for all solutes and indicate that heat is liberated on adsorption of the solute on the stationary phase. These decreases in enthalpy are presumably related to the changes in solvation of the solute and the corresponding changes in solvation energies for the melted structure.

Two opposing processes may contribute to a change in disorder or entropy on denaturation of the solute. First, the perturbation of secondary structure requires increased solvation of the newly exposed atoms which originally formed the "internal" core. These atoms, previously involved in intramolecular interactions, would not have been solvated prior to the thermal disruption of the solute. This solvation would in turn cause a corresponding decrease in entropy of the desorbed state, owing to the decreased number of free solvent molecules. However, this process will be compensated for by an increased disordering of the unbound system due to the increase in the conformational repertoire of the more flexible peptide. Thus, on interaction with the stationary phase, increased ordering would be apparent owing to the more static nature of the bound peptide and the conformational restraints conferred by the interactive process. This interactive process would then be expected to yield overall negative  $\Delta S_{\text{assoc}}^0$  values and is represented schematically in Fig. 9.

Analysis of the Van 't Hoff plot for bombesin at  $\bar{\psi} = 0.1$  chromatographed on the  $C_{18}$  phase reveals a curvilinear dependence corresponding to three apparently linear temperature ranges, 5–15, 15–37 and 45–85°C, with a transition around 25°C. This transition correlates with the observed decrease in contact area noted earlier. At low temperatures,  $\Delta S_{\text{assoc}}^0$  was found to equal 58.6 J mol<sup>-1</sup> K<sup>-1</sup>, which then decreased significantly to -102.1 J mol<sup>-1</sup> K<sup>-1</sup> over the transition range. At high temperatures a value of -19.1 J mol<sup>-1</sup> K<sup>-1</sup> for  $\Delta S_{\text{assoc}}^0$  was obtained. These  $\Delta S_{\text{assoc}}^0$  changes reflect an initially



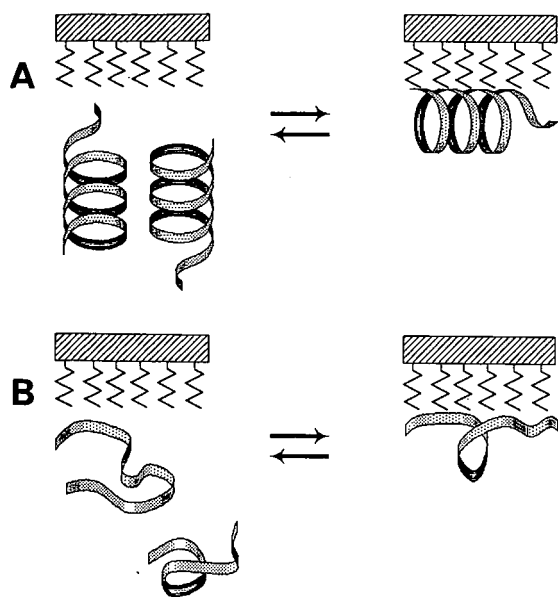


Fig. 9. Schematic view of the thermodynamic considerations involved in the interactive process of a polypeptide, with and without a well developed secondary structure, interacting with a hydrocarbonaceous ligand. In (A), the solute molecule has a rigid solution structure, which on interaction with the stationary phase undergoes conformational changes that cause disordering of the solute molecular population, resulting in a small positive value for the change in entropy ( $\Delta S^0_{\text{assoc}}$ ). Alternatively, the rigid solution structure may become slightly more constrained, thus yielding a small negative value of  $\Delta S^0_{\text{assoc}}$ . In (B), polypeptide of random solution structure binds to the stationary phase. This induces a more constrained conformation on the solute molecular population, which in turn causes an increase in ordering of the system, leading to a large negative value of  $\Delta S^0_{\text{assoc}}$ .

rigid solution structure that becomes more disordered on interaction with the stationary phase at low temperatures (5–15°C). The difference between the entropy of the bound and unbound states is much larger at the transition temperature (15–37°C) than at the lower (<15°C) and higher temperatures (>37°C). These results are consistent with the peptide existing as a much more flexible molecule in the transition range, and remaining flexible at the higher temperatures. It is interesting that the 45–85°C region yielded a smaller negative  $\Delta S^0_{\text{assoc}}$  than the transitional region, indicating that the molecule is still more flexible in solution than when bound, but at these temperatures either the conformational repertoire is restricted to a smaller population or the

elevated temperatures cause a more rapidly “time-averaged” structure to be observed. Here the difference in the entropy of the bound structure and solution structure would not be large owing to the rapid conformational interconversions occurring to both the sorbed and desorbed states of the molecule at these temperatures.

The Van 't Hoff plot for bombesin derived from  $\log \bar{k}$  values at  $\bar{\psi} = 0.3$  on the  $C_{18}$  phase demonstrates a biphasic relationship, with two distinct regions within the curve. These regions correspond to segments at 5–55 and 65–85°C, with an apparent transition around 60°C. The  $\Delta S^0_{\text{assoc}}$  values derived from these two regions were 6.2 and  $-47.5 \text{ J mol}^{-1} \text{ K}^{-1}$  respectively. At the higher temperatures a more negative change in entropy is observed. These results also indicate that the molecule is more flexible in solution at temperatures above 60°C than when bound to the stationary phase ligands. However, below this temperature the molecule is not significantly more flexible in solution than when bound, suggesting that bombesin may possess a more rigid solution structure at the lower temperatures. These data also suggest that the increased organic modifier concentration may be stabilizing the bombesin secondary structure, as is evident from the increased transition temperature observed at the higher organic modifier concentration. This finding correlates well with other physico-chemical studies on bombesin using NMR and circular dichroism spectroscopy [8,9,23], where it has been found that bombesin exists in a helical conformation in the presence of organic solvents such as trifluoroethanol or lipid micelles.

**Bombesin on  $C_4$  phase.** The Van 't Hoff plot for bombesin at extrapolated values of  $\log \bar{k}$  at  $\bar{\psi} = 0.1$  on the  $C_4$  phase was essentially linear, whereas on the  $C_{18}$  phase a transition at *ca.* 25°C was observed. The  $\Delta S^0_{\text{assoc}}$  value derived for these conditions was  $-4.5 \text{ J mol}^{-1} \text{ K}^{-1}$ , indicating little change in the flexibility between the bound and unbound bombesin molecule. For  $\log \bar{k}$  ( $\bar{\psi} = 0.3$ ) a biphasic relationship exists for the Van 't Hoff plot, with two distinct regions corresponding to segments at 5–45°C and 45–85°C. The  $\Delta S^0_{\text{assoc}}$  values derived from these two regions were  $-5.2$  and  $-94.4 \text{ J mol}^{-1} \text{ K}^{-1}$ , respectively. These values reflect a transition from a rigid or conformationally constrained solute molecule to a more flexible structure. The transition

at *ca.* 45°C is lower than the observed transition at 60°C for the C<sub>18</sub> stationary phase.

These results indicate that the C<sub>18</sub> ligands are more capable of stabilizing a "low-temperature" peptide conformational structure, which is either not present with the C<sub>4</sub> ligands or the transition for the same structure on the C<sub>4</sub> phase is shifted towards lower temperatures. If the experimental results with the C<sub>4</sub> and C<sub>18</sub> ligands are compared, the latter possibility appears to be more likely, that is, the conformational transition is moved to a lower temperature on the C<sub>4</sub> phase, as is observed for the transition temperatures at  $\log \bar{k}$  ( $\bar{\psi} = 0.3$ ). This finding suggests that the C<sub>18</sub> phase can enhance the stability of the solute secondary structure. Similar results have been observed with the binding of enzymes to agarose gels substituted with *n*-alkyl chains and weakly hydrophobic silica sorbents [24, 25].

***β-Endorphin on C<sub>18</sub> phase.*** Fig. 7 represents Van 't Hoff plots for *β*-endorphin chromatographed on both C<sub>18</sub> and C<sub>4</sub> phases. The Van 't Hoff relationship for  $\log \bar{k}$  values determined at  $\bar{\psi} = 0.1$  for the solute chromatographed on the C<sub>18</sub> stationary phase is non-linear with a transition occurring around 50°C. Two distinct regions of the curve, namely 5–45 and 45–85°C, are apparent. The lower temperature region yields a positive  $\Delta S_{\text{assoc}}^0$  value of 30.7 J mol<sup>-1</sup> K<sup>-1</sup>. This result indicates that the molecules become more disordered on binding to the stationary phase, reflecting a static solution structure at these temperatures, which becomes less ordered on adsorption. At the elevated temperatures, a negative  $\Delta S_{\text{assoc}}^0$  value of -16.0 J mol<sup>-1</sup> K<sup>-1</sup> was derived for *β*-endorphin from the Van 't Hoff plot. This result reflects a more flexible high-temperature solution structure for *β*-endorphin compared with the lower temperature structure, and this high-temperature structure becomes more constrained on binding to the stationary phase, resulting in an overall increase in the order of the system. Perturbation of the solution structure of the molecule would thus occur at the higher temperatures, a conclusion consistent with the gradual increase in *S* values observed with increasing temperature for this solute when chromatographed on the C<sub>18</sub> phase.

The Van 't Hoff plots for *β*-endorphin chromatographed on the C<sub>18</sub> stationary phase at  $\log \bar{k}$  values determined at  $\bar{\psi} = 0.3$  gave a non-linear relation-

ship with an apparent transition at 50°C, similar to that observed for the low organic mole fraction condition on this phase. In this instance two distinct regions of the Van 't Hoff curve were again apparent, at 5–45 and 45–85°C. The  $\Delta S_{\text{assoc}}^0$  value derived from the lower temperature region was small and negative (-7.3 J mol<sup>-1</sup> K<sup>-1</sup>), which is in contrast to the positive  $\Delta S_{\text{assoc}}^0$  value observed at the lower organic modifier concentration for this temperature range. Hence the increased concentration of organic modifier seems to make the molecule more flexible in solution at these temperatures. At higher temperatures, the derived  $\Delta S_{\text{assoc}}^0$  value was large and negative (-36.6 J mol<sup>-1</sup> K<sup>-1</sup>), and is also more negative than the observed value at the lower organic modifier concentration. Thus, again it would appear that solute is more flexible in the higher organic modifier concentration. It would also appear that the system is more disordered at higher organic mole fractions, indicating that the secondary structure of the *β*-endorphin solute is less well defined at the higher organic solvent concentration. This behaviour is in contrast to that observed for bombesin, which appeared to be stabilized by the increased organic modifier concentration, and may represent solvation of residues normally involved in intramolecular interactions. This possible structural change could then explain the observed increase in disorder illustrated by the  $\Delta S_{\text{assoc}}^0$  values obtained for *β*-endorphin.

***β-Endorphin on C<sub>4</sub> phase.*** Van 't Hoff plots for *β*-endorphin chromatographed on the C<sub>4</sub> phase are also displayed in Fig. 7. For the Van 't Hoff plot of  $\log \bar{k}$  values determined at  $\bar{\psi} = 0.1$ , the curve has two distinct regions, at 5–55 and 55–85°C, with an apparent transition around 55°C, a value similar to the observed transition at  $\bar{\psi} = 0.1$  on the C<sub>18</sub> phase.  $\Delta S_{\text{assoc}}^0$  values were derived from both regions of the Van 't Hoff plot and at the lower temperature range a  $\Delta S_{\text{assoc}}^0$  value of -18.3 J mol<sup>-1</sup> K<sup>-1</sup> was obtained. This behaviour reflects a total increase in ordering of the system on adsorption to the stationary phase, and thus indicates a flexible solution structure.  $\log \bar{k}$  at the higher temperature range yielded a  $\Delta S_{\text{assoc}}^0$  value of -180.0 J mol<sup>-1</sup> K<sup>-1</sup>, which indicates a large increase in ordering of the system on adsorption and reflects a very flexible solution structure at these elevated temperatures. A much larger relative increase in ordering occurs under these C<sub>4</sub> condi-

tions compared with the  $C_{18}$  phase, and can be attributed to the more rigid structure of the  $C_4$  ligand [17–19].

The Van 't Hoff plots for  $\beta$ -endorphin chromatographed on the  $C_4$  phase, with  $\log \bar{k}$  values at  $\bar{\psi} = 0.3$ , showed three distinct regions, 5–45, 45–55 and 55–85°C, with an apparent transition at 50°C. This behaviour is similar to the lower organic mole fraction transition temperature on this phase, and also similar to both transition temperatures observed on the  $C_{18}$  phase. Hence it would appear that the ligand hydrophobicity does not affect the observed transitions for  $\beta$ -endorphin, unlike the observed stabilization of bombesin on the  $C_{18}$  phase noted earlier. The  $\Delta S_{\text{assoc}}^0$  value derived from the lowest temperature region (5–45°C) was  $-15.2 \text{ J mol}^{-1} \text{ K}^{-1}$ . This value reflects an overall increase in order of the system on adsorption, and thus reflects a more flexible molecule in solution than when associated with the stationary phase. At the transition region (45–55°C) a  $\Delta S_{\text{assoc}}^0$  value of  $-82.4 \text{ J mol}^{-1} \text{ K}^{-1}$  was obtained, indicating an increased flexibility in solution at these temperatures relative to the lower temperatures. In contrast, at the higher temperatures a  $\Delta S_{\text{assoc}}^0$  value of  $-4.8 \text{ J mol}^{-1} \text{ K}^{-1}$  was derived. This value suggests that the molecule is least flexible in solution at these high temperatures or, more likely, that a rapidly interconverting time-averaged structure is being observed. Such a structure would undergo rapid conformational interconversions both in solution and when bound, hence the relative change in the ordering of the system would be relatively small for the association process.

Unlike the results on the  $C_{18}$  phase for this solute, the magnitude of  $\Delta S_{\text{assoc}}^0$  on the  $C_4$  phase at  $\bar{\psi} = 0.1$  is larger and more negative than the corresponding value at  $\bar{\psi} = 0.3$ . This behaviour indicates that there is a larger increase in ordering on adsorption in the presence of a lower organic mole fraction for this solute.

**Glucagon on  $C_{18}$  phase.** Fig. 8 displays Van 't Hoff plots for glucagon chromatographed on both  $C_{18}$  and  $C_4$  phases at the two extrapolated values of  $\bar{\psi}$ . The Van 't Hoff relationship for  $\log \bar{k}$  values at  $\bar{\psi} = 0.1$  is non-linear for glucagon chromatographed on the  $C_{18}$  phase. The Van 't Hoff curve is biphasic, possessing two distinct regions, at 5–45 and 45–85°C, with an apparent transition around 50°C. The  $\Delta S_{\text{assoc}}^0$  values derived from these two regions were

26.1 and  $-23.7 \text{ J mol}^{-1} \text{ K}^{-1}$ , respectively. Again, the decrease in ordering of the system on adsorption at the lower temperatures can be noted, indicating a stable solution structure which becomes more flexible on interaction with the stationary phase. At the elevated temperatures an overall increase in ordering of the system is apparent, reflecting a more flexible solution structure relative to the low-temperature structure. Thermal disruption of solution structure and hence a gradual increase in the  $S$  value and hence chromatographic contact area observed on this phase would account for this behaviour.

The Van 't Hoff relationship for  $\log \bar{k}$  values determined at  $\bar{\psi} = 0.3$  was also biphasic, with two distinct regions spanning 5–45 and 45–85°C, and an apparent transition at around 50°C. This value is similar to the transition temperature observed for the lower organic modifier concentration. The  $\Delta S_{\text{assoc}}^0$  values derived for the lower and higher temperature regions were  $-13.0$  and  $-47.4 \text{ J mol}^{-1} \text{ K}^{-1}$ , respectively. Again, this result indicates a flexible molecule in solution at both temperature ranges, with an overall increase in ordering on association with the stationary phase in both instances. The relatively larger increase in ordering at the higher temperatures suggests a more flexible molecule than at the lower temperatures, again indicating possible disruption of the solution structure at the higher temperatures. Further, the influence of increased organic mole fraction appears to be the increased flexibility in solution of the solute molecule, as was observed for  $\beta$ -endorphin on the  $C_{18}$  phase.

**Glucagon on  $C_4$  phase.** The Van 't Hoff plot for glucagon chromatographed on the  $C_4$  phase at  $\log \bar{k}$  values determined at  $\bar{\psi} = 0.1$  displays a biphasic relationship. The curve consists of two regions spanning 5–45 and 45–85°C, with a transition around 50°C, which is similar to the transitions observed for glucagon on the  $C_{18}$  phase. Ligand hydrophobicity therefore does not seem to affect the observed transition temperature, as was also observed for  $\beta$ -endorphin. The  $\Delta S_{\text{assoc}}^0$  values derived from these two regions were  $-97.6$  and  $-169.0 \text{ J mol}^{-1} \text{ K}^{-1}$ , respectively. These results indicate a considerably flexible structure at low temperatures that increases in flexibility with increasing temperature. In both instances the association process involves significantly large increases in the ordering

of the system, with a larger degree of ordering at the higher temperatures, which reflects changes in the solution structure of glucagon. As was evident with the other peptidic solutes, the magnitude of the increase in ordering of the system on adsorption was much larger on the  $C_4$  phase than the  $C_{18}$  phase.

The Van 't Hoff plot for glucagon determined for  $\log \bar{k}$  values at  $\bar{\psi} = 0.3$  gives a curve that can be divided into three regions, 5–25, 25–75 and 75–85°C. The  $\Delta S_{\text{assoc}}^0$  values derived from these temperature regions were 2.1, –45.4 and 12.6 J mol<sup>–1</sup> K<sup>–1</sup>, respectively. These values suggest an initially rigid molecule undergoing a transition around 50°C which corresponds to an increase in ordering on association with the stationary phase and indicates that at these temperatures the molecule is flexible in solution. At the higher temperatures a time-averaged structure is observed with rapid conformational interconversion both in solution and when bound to the stationary phase explaining the positive  $\Delta S_{\text{assoc}}^0$  value obtained.

The difference in magnitude of the  $\Delta S_{\text{assoc}}^0$  for the two organic modifier concentrations on the butyl stationary phase demonstrate a general trend of the  $\Delta S_{\text{assoc}}^0$  values being more negative at  $\bar{\psi} = 0.1$ . The behaviour of glucagon is thus similar to the corresponding case with  $\beta$ -endorphin. It can be concluded from these observations that glucagon is characterized by a higher degree of flexibility in solution at the lower organic modifier concentration on the  $C_4$  phase.

## CONCLUSIONS

Overall, the thermodynamic data for bombesin,  $\beta$ -endorphin and glucagon illustrate transitions in the 50–60°C region, suggesting that the interactive structure is dramatically disrupted over this temperature range. This value is also the temperature range over which helices tend to be disrupted, reiterating the hypothesis that the amphipathic helical portions of these molecules are either directly involved in the interaction between the stationary phase ligands or are able to stabilize the peptide surface exposed to the stationary phase ligands. When these helical conformations are perturbed, the corresponding change in the hierarchical structure and the interactive surface presented to the stationary phase will result in the observed changes in retention behaviour.

The differences in retention and thermodynamic parameters derived for each solute and the differing temperature dependencies of these parameters clearly demonstrate that the peptide sequence plays a crucial role in the interactive properties of peptide solutes. In this study, bombesin exhibited retention behaviour which was generally distinct to that observed with  $\beta$ -endorphin and glucagon. Although  $\beta$ -endorphin and glucagon are larger molecules than bombesin, it is not the molecular size *per se* that controls the chromatographic behaviour, but rather the ability of larger molecules to stabilize their secondary structure without external influences.

For both  $\beta$ -endorphin and glucagon the  $\Delta S_{\text{assoc}}^0$  values are all more negative at the higher temperatures, that is, the peptides are more flexible in solution at higher than at lower temperatures. The large negative value of  $\Delta S_{\text{assoc}}^0$  would suggest that on binding to the hydrocarbonaceous ligands the number of available conformations of the polypeptide dramatically decreases. The  $\Delta S_{\text{assoc}}^0$  values for these peptides for the postulated melted structure (*i.e.*, the high temperature structures) were generally more negative for the  $C_4$  phase than the corresponding values derived from the  $C_{18}$  stationary phase. This observation means there is a larger relative increase in the structural ordering of the solutes on their adsorption to the  $C_4$  phase than to the  $C_{18}$  phase, that is, the peptide is restricted to fewer conformations when bound to the ligand than for the corresponding interaction with the  $C_{18}$  ligand. This is consistent with the proposal that the  $C_4$  ligand is rigid as opposed to the more flexible  $C_{18}$  ligands.

The change in enthalpy follows the same trends as seen for the changes in entropy. These changes are presumably a consequence of related changes in solvation energies as the entropically driven changes in the solute structure occur.

The factors which stabilize  $\alpha$ -helical or any other secondary structure of a polypeptide include sequence-specific intramolecular charged interactions, hydrogen bonding and also the amphipathic arrangement of polar and non-polar residues along the peptide sequence. The ability to monitor changes in these stabilizing influences by employing hydrophobic stationary phases and varied temperature gives an insight into the underlying principles of peptide folding and peptide–surface interactions. In this investigation the influence of temperature on the

chromatographic behaviour of several peptide solutes was examined. The temperature range covered the region where secondary structure is normally perturbed. The three peptidic hormone solutes studied have a major portion of their structure stabilized by  $\alpha$ -helices at ambient temperature [8–13]. This study has shown that conformational transitions, such as the melting of the solution structure of the peptide, may be observed by utilizing chromatographic techniques. It is clear that the two different ligands studied have different abilities to monitor conformational changes of the solute. This discriminatory ability may be due either to differences in stabilizing forces associated with the ligand–solute interaction or to the solvated structure of the ligand themselves. Structurally disparate ligand surfaces would be expected to interact with different mechanisms [17], which would then be manifested as different dependencies of  $S$  and  $\log k_0$  on temperature. Similar conclusions have been reached from evaluating peptide–ligand interactions by principle component analysis [18]. Generally, it appears that the  $C_{18}$  stationary phase tended to stabilize interactive structures relative to the  $C_4$  stationary phase. In addition, increasing the organic modifier concentration resulted in destabilization of the interactive secondary structures of  $\beta$ -endorphin and glucagon, but stabilization of the bombesin secondary structure. The molecular basis of this interaction requires further analysis of the solution conformation and dynamics of these peptides, and is the subject of ongoing investigations.

#### ACKNOWLEDGEMENTS

These investigations were supported by grants from the Australian Research Council, the National Health and Medical Research Council of Australia and the Monash University Research Grants Committee.

#### REFERENCES

- 1 A. Johnson, Q. M. Mao and M. T. W. Hearn, *J. Chromatogr.*, 557 (1991) 335.
- 2 A. W. Purcell, M. I. Aguilar and M. T. W. Hearn, *J. Chromatogr.*, 476 (1989) 113.
- 3 A. W. Purcell, M. I. Aguilar and M. T. W. Hearn, *J. Chromatogr.*, 476 (1989) 125.
- 4 M. T. W. Hearn and M. I. Aguilar, *J. Chromatogr.*, 352 (1986) 35.
- 5 M. T. W. Hearn and M. I. Aguilar, *J. Chromatogr.*, 397 (1987) 47.
- 6 M. T. W. Hearn and M. I. Aguilar, in A. Neuberger and L. L. M. van Deenen (Editors), *Modern Physical Methods in Biochemistry, Part B*, Elsevier, Amsterdam, 1988, p. 107.
- 7 Cs. Horvath, W. Melander and I. Molnar, *J. Chromatogr.*, 125 (1976) 129.
- 8 P. Cavorta, G. Farrugia, L. Masotti, G. Sartor and A. G. Szabo, *Biochem. Biophys. Res. Commun.*, 141 (1986) 99.
- 9 J. A. Carver, *Eur. J. Biochem.*, 168 (1989) 193.
- 10 A. P. Korn and F. P. Ottensmeyer, *J. Theor. Biol.*, 105 (1983) 403.
- 11 V. J. Hruby, *Mol. Cell. Biochem.*, 44 (1982) 49.
- 12 W. L. Mattice and R. M. Robinson, *Biopolymers*, 20 (1981) 1421.
- 13 W. L. Mattice and R. M. Robinson, *Biochem. Biophys. Res. Commun.*, 101 (1981) 1311.
- 14 M. I. Aguilar, A. N. Hodder and M. T. W. Hearn, *J. Chromatogr.*, 327 (1985) 115.
- 15 M. A. Stadalius, H. S. Gold and L. R. Snyder, *J. Chromatogr.*, 296 (1984) 31.
- 16 W. R. Melander, D. Corradini and Cs. Horvath, *J. Chromatogr.*, 317 (1984) 67.
- 17 K. D. Lork, K. K. Unger, H. Brückner and M. T. W. Hearn, *J. Chromatogr.*, 476 (1989) 135.
- 18 M. C. J. Wilce, M. I. Aguilar and M. T. W. Hearn, *J. Chromatogr.*, 548 (1991) 105.
- 19 E. Bayer, A. Paulus, B. Peters, G. Laupp, J. Reniers and K. Alberts, *J. Chromatogr.*, 364 (1986) 25.
- 20 R. K. Gilpin and J. A. Squires, *J. Chromatogr. Sci.*, 19 (1981) 195.
- 21 K. Jinno, T. Nagoshi, N. Tanaka, M. Okamoto, J. C. Fetzer and W. R. Biggs, *J. Chromatogr.*, 436 (1988) 1.
- 22 P. L. Privalov, E. I. Tiktopulo, S. Yu. Venyaminov, Yu. V. Griko, G. I. Makhataдзе and N. N. Khechinashvili, *J. Mol. Biol.*, 205 (1989) 737.
- 23 J. A. Carver and J. G. Collins, *Eur. J. Biochem.*, 187 (1990) 645.
- 24 P. Oroszlan, R. Blanco, X.-M. Lu, D. Yaramush and B. L. Karger, *J. Chromatogr.*, 500 (1990) 481.
- 25 H. Jennissen, in I. M. Chaiken, M. Wilchek and I. Parikh (Editors), *Affinity Chromatography and Biological Recognition*, Academic Press, New York, 1983, p. 281.



# Direct determination of kallikrein by high-performance liquid chromatography

Giorgio Raspi\*, Antonino Lo Moro and Maria Spinetti

*Dipartimento di Chimica e Chimica Industriale, Università di Pisa, Via Risorgimento 35, I-56126 Pisa (Italy)*

## ABSTRACT

A direct and specific identification of porcine pancreatic kallikrein by high-performance hydrophobic chromatography is proposed; the minimum amount which can be injected is 2.5 U. An application to the quantitative determination of the enzyme by high-performance size-exclusion chromatography is reported; the method is precise with a mean coefficient of variation of 2.8% and the minimum amount which can be injected is 0.02 U of kallikrein. The results obtained with determinations in real biological samples (porcine pancreatic powder and human urine) are reported. The method is based on direct and specific chromatographic signals and does not destroy the biological activity of this enzyme.

## INTRODUCTION

Kallikrein is a serine protease occurring in various tissues and body fluids of humans and other mammals. Various methods [1–17] have been reported for the determination of kallikrein activity. Measurement by a synthetic peptide substrate assay using esters [6–12], e.g. N<sup>α</sup>-benzoyl-L-arginine ethyl ester (BAEE) [6], is commonly used; however, these substrates are not specific for kallikrein, but show a generic esterase activity.

This paper proposes a direct and specific identification of porcine pancreatic kallikrein by high-performance hydrophobic interaction chromatography (HPHIC) and an application to the quantitative determination of this enzyme by high-performance size-exclusion chromatography (HPSEC) in various batches of commercial products. The determination of the enzyme is accomplished without the use of a substrate and possible errors owing to the presence of compounds with esterase activity are avoided.

This is a preliminary contribution to the study of the behaviour of mammalian kallikreins in high-performance liquid chromatography (HPLC) owing to the limited number of reports [13–16] describing the use of HPLC for this analysis.

## EXPERIMENTAL

### *Reagents and materials*

All chemicals were of analytical-reagent grade or the highest purity available and were stored, when necessary, as recommended by the manufacturer. HPLC-grade ammonium sulphate was from Bio-Rad Labs. (Richmond, CA, USA); porcine pancreatic kallikrein was from several lots from Sigma (St. Louis, MO, USA), Calbiochem-Behring Diagnostics (Scoppito L'Aquila, Italy) and Unibios (Trecate Novara, Italy); aprotinin was from Sigma. Water was distilled once and then deionized using a Milli-Q water purification system (Millipore, Bedford, MA, USA). Aprotinin was bound to cyanogen bromide (CNBr)-activated Sepharose 4B according to the method given by the manufacturer (Pharmacia, Uppsala, Sweden); prolonged washing cycles of alternately high and low pH were necessary to obtain an acceptable HPLC background.

Econo columns, 10 × 1.0 cm I.D. (Bio-Rad), were used for the affinity chromatography.

### *Columns*

HPHIC was performed on a 75 × 7.5 mm I.D. column of Bio-Gel TSK Phenyl-5-PW (Bio-Rad). HPSEC was performed on a 300 × 7.5 mm I.D.

Ultropac column of TSK G3000 SW (LKB-Pharmacia).

#### Apparatus

An LKB-Pharmacia DfB HPLC System One, equipped with a Rheodyne 7125 injector, a 100- $\mu$ l injection loop and a LC 2249 gradient pump was connected to a variable-wavelength 2141 monitor. The UV detector was operated at 220 nm. The output from the detector was displayed on the 2221 integrator (LKB-Pharmacia).

#### Chromatographic separations

HPHIC was carried out at a flow-rate of 1.0 ml/min with a 30-min linear salt gradient obtained controlling buffer A (1.8 *M* ammonium sulphate in 0.1 *M* phosphate, pH 7.0) and buffer B (0.1 *M* phosphate, pH 7.0) using a solvent programmer at 20–25°C.

HPSEC was performed using a mobile phase of 0.15 *M* phosphate buffer in 0.1 *M* sodium chloride at a flow-rate of 1.0 ml/min. Bovine serum albumin (MW 67 000), ovalbumin (45 000),  $\alpha$ -chymotrypsinogen (25 000) and cytochrome C (12 400) were used as standards for the calculation of molecular weight. A linear calibration graph of retention time *versus* log molecular weight is shown in Fig. 1.

#### Inhibition assays

Inhibition assays were performed using BAEE as a substrate according to the method of Trautschold and Werle [6]. A Perkin-Elmer Lambda 17 spectrophotometer was used for absorbance measurements.

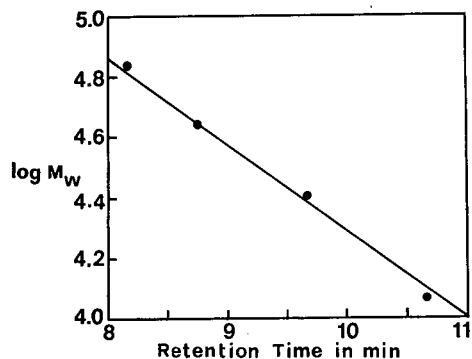


Fig. 1. Calibration graph obtained using protein molecular weight standards.

#### Procedure

Aqueous solutions of porcine pancreatic kallikrein, buffered with 0.1 *M* phosphate (pH 8.0) containing *ca.* 100 U of enzyme, were prepared and 100  $\mu$ l, containing about 10 U were directly assayed by the HPHIC technique.

Samples prepared as above were transferred onto the aprotinin–Sephacrose 4B column (bed volume *ca.* 2 ml) previously equilibrated with 0.1 *M* sodium hydrogencarbonate in 0.5 *M* sodium chloride (pH 8.3). The eluate was passed through the same column twice. The column was then washed with at least ten bed volumes of the same buffer solution to remove unbound substances prior to elution. The kallikrein bound to immobilized aprotinin was fully recovered by elution with 0.1 *M* sodium acetate–acetic acid (pH 4.5) in 1.0 *M* sodium chloride. At this pH value, the enzymatic activity does not decrease. The resulting solution, *ca.* 80 ml, was concentrated by ultrafiltration through an Amicon YM-10 membrane to 5.0 ml, and a 100- $\mu$ l aliquot was assayed by the HPHIC technique.

Amounts of kallikrein in the 1–10 U range were processed through the aprotinin column as described above and were recovered in 5.0 ml. A 100- $\mu$ l volume of the resulting solution was assayed by HPSEC.

#### Calibration graph

Aliquots of porcine pancreatic kallikrein resulting from the second procedure were standardized by the BAEE method and analysed by HPSEC as calibration samples. The calibration graph of peak area *versus* units of kallikrein injected (0.02–20) was obtained from a least-squares linear regression.

#### RESULTS AND DISCUSSION

Preliminary investigations carried out with reversed-phase (RP) HPLC columns were unsuccessful, despite the different hydrophobicities of the phases used. With the HPHIC column good results were obtained in terms of resolution, the reproducibility of peak areas and recovery. Fig. 2 shows the chromatogram resulting from the direct injection of an aliquot of a commercial sample. Extraneous substances, inactive *versus* aprotinin, can be removed by processing, as described under Experimental.

Fig. 3 shows the elution profile obtained; it is typ-



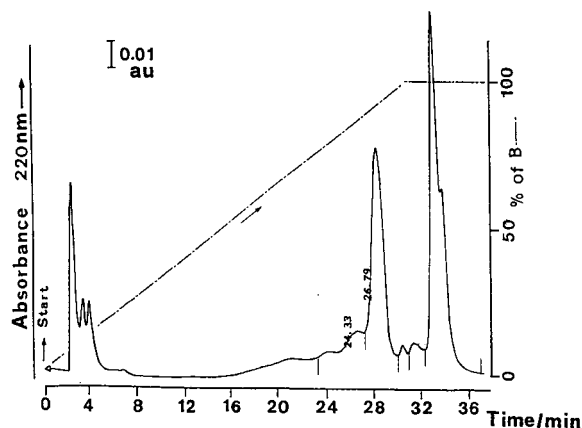


Fig. 2. Chromatogram of commercial pure porcine pancreatic kallikrein (2.5 U in 0.1 ml) obtained on Bio-Gel TSK Phenyl 5PW column (75 × 7.5 mm) at a flow-rate of 1.0 ml/min with a 30-min linear gradient of ammonium sulphate concentration from 1.8 to 0 M in 0.1 M phosphate buffer (pH 7.0). Percentage of B indicates the percentage of buffer B.

ical for all batches of porcine pancreatic kallikrein (Sigma and Calbiochem) examined and is characterized by the appearance of peaks a–d. According to other workers [3], multiple forms are observed for this enzyme, explained in terms of an intra-chain split occurring in the various purification steps. The volume fraction corresponding to the elution profile of the various peaks of kallikrein (Fig. 3) was examined for enzymatic activity. As a reference, an

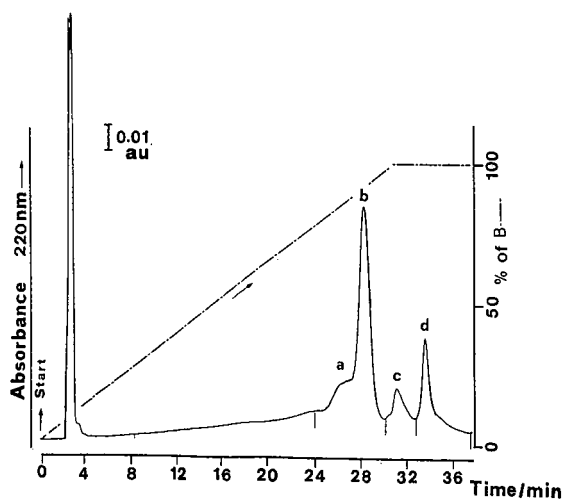


Fig. 3. Chromatogram of processed pure porcine pancreatic kallikrein (2.5 U in 0.1 ml). Conditions as in Fig. 2.

amount of kallikrein equal to that injected was diluted to the same volume fraction with the same chromatographic eluent mixture; the esterase activity shown by the chromatographic effluent and by the reference solution was almost identical, indicating a quantitative recovery from the HPLC column. The minimum injectable amount which could be determined by the HPHIC technique was 2.5 U.

Among the active substances which can be expected in samples containing kallikrein is trypsin, although this enzyme can be selectively inhibited by the addition of soybean trypsin inhibitor [3]. Eluate fractions corresponding to the single peaks a–d (Fig. 3) were collected and separately injected for measurement by HPSEC. All the forms gave the peak shown in Fig. 4. The molecular weight of this compound was calculated to be *ca.* 30 000, compatible with that of porcine pancreatic kallikrein [3]. These results show that the multiple peaks observed in the elution profile obtained with HPHIC (Fig. 3) are due to forms of kallikrein with similar structures.

The response obtained with HPSEC has been used for the quantitative determination of kallikrein in the diluted samples, owing to its higher sensitivity than HPHIC. The results are reported in Table I. The minimum amount in the original samples which can be detected is 1.0 U. The minimum amount which can be injected is 0.02 U.

These results are promising enough to justify de-

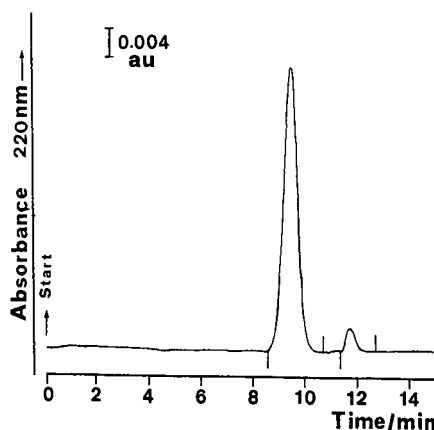


Fig. 4. Chromatogram of processed pure porcine pancreatic kallikrein obtained on TSK G3000 SW column (300 × 7.5 mm) using a mobile phase of 0.15 M phosphate buffer (pH 7.0) in 0.1 M sodium chloride at a flow-rate of 1.0 ml/min.

TABLE I

## EVALUATION OF THE ACCURACY, PRECISION AND RECOVERY OF THE METHOD

Mean coefficient of variation is 2.8%.

Sample No.	Amount of kallikrein processed <sup>a</sup> (U)	Amount of kallikrein found <sup>b</sup> (U)	C.V. (%)	Recovery <sup>c</sup> (%)
1	1.00	0.96 ± 0.043	4.5	96
2	2.00	1.94 ± 0.04	2.6	97
3	5.00	4.90 ± 0.11	2.2	98
4	8.00	7.60 ± 0.19	2.5	95
5	10.0	9.90 ± 0.22	2.2	99

<sup>a</sup> Standardized by BAEE method.<sup>b</sup> Mean ± S.D. (*n* = 5).<sup>c</sup> Calculated from the activity measured in the samples collected after chromatographic elution.

termining the chromatographic behaviour of kallikrein in real biological samples such as crude kallikrein from porcine pancreatic powder (Unibios) and human urine.

*Crude kallikrein*

Porcine pancreatic powder was suspended in buffer solution B and filtered through a Minisart NML Sartorius 0.2- $\mu$ m filter. Figs. 5 and 6 show the chromatograms obtained before and after purification with aprotinin according to the first and second procedures. In Fig. 5 the elution profile of kallikrein

is hidden by several peaks of extraneous substances present in the raw material. Only peak d is predominant in Fig. 6 and the elution profile is similar to that showed in Fig. 3; the predominance of only peak d can be explained by the small number of purification steps undergone by the raw material.

*Human urine*

The pH of a measured volume of urine (1500 ml) from a normal subject was adjusted to pH 8.0 by the addition of 2 *M* sodium hydroxide. After centrifugation (4390 *g*) for 10 min, the supernatant was transferred by a peristaltic pump (P1, Pharmacia, flow-rate 5.0 ml/min) to the aprotinin-Sepharose

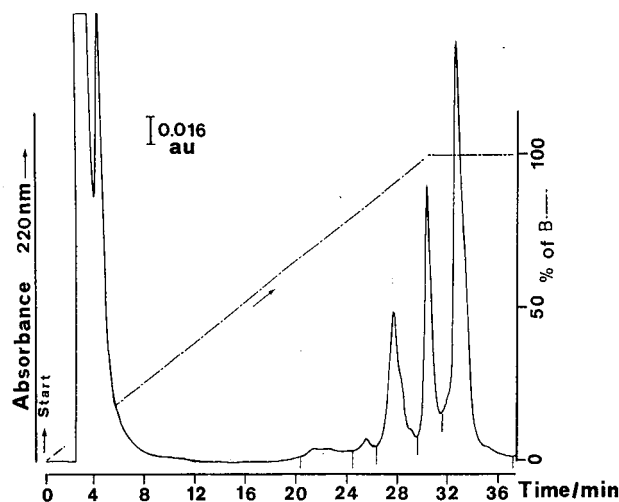


Fig. 5. Chromatogram obtained from porcine pancreatic powder dissolved in buffer B, filtered through a Minisart NML Sartorius 0.2- $\mu$ m filter and directly injected onto the column. Conditions as in Fig. 2.

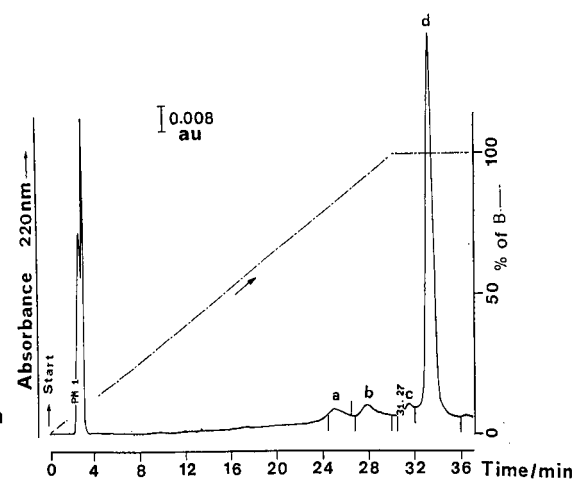


Fig. 6. Chromatogram of processed kallikrein from the crude material of Fig. 5. Conditions as in Fig. 2.

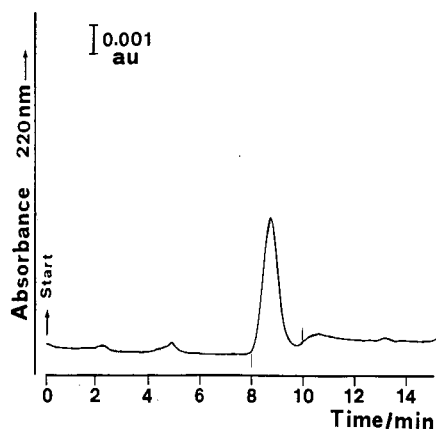


Fig. 7. Chromatogram of processed human urinary kallikrein. Conditions as in Fig. 4.

4B column. The affinity column was washed with about 200 ml of equilibrating buffer (0.1 M sodium hydrogencarbonate in 0.5 M sodium chloride, pH 8.3) before the elution of urinary kallikrein. The enzyme was eluted with 0.1 M acetate buffer, pH 4.5, and collected in 5.0 ml of buffers. The very low amount of urinary kallikrein recovered does not allow a signal to be obtained with the HPHIC column.

Fig. 7 shows the elution profile obtained by injecting 100  $\mu$ l of sample onto the HPSEC column. The molecular weight was calculated to be ca. 45 000, according to the reported value [16,17].

Work is now in progress to establish a precise, specific and convenient assay for urinary kallikrein.

## CONCLUSIONS

From the data presented here, it can be seen that HPHIC and HPSEC are suitable methods for the identification and determination of kallikrein. The procedures provide adequate alternatives to the sometimes complicated separation techniques and the unspecific determination currently used. The methods show an adequate accuracy, which is indicated by the almost complete recovery of kallik-

rein over the concentration range studied, and does not destroy the biological activity of this substance. The method could be used as a control in the production of kallikrein; the method is advantageous because it is based on direct and specific chromatographic signals.

## ACKNOWLEDGEMENTS

This work was supported by Ministero dell'Università e della Ricerca Scientifica e Tecnologica (MURST) and Consiglio Nazionale delle Ricerche (CNR), Italy.

## REFERENCES

- 1 R. Geiger and H. Fritz, *Methods Enzymol.*, 80 (1981) 466.
- 2 R. Geiger, R. Hell and H. Fritz, *Hoppe-Seyler's Z. Physiol. Chem.*, 363 (1982) 527.
- 3 F. Fiedler, E. Fink, H. Tschesche and H. Fritz, *Methods Enzymol.*, 80 (1981) 493.
- 4 A. Chung, J. W. Ryan, G. Pena and N. B. Oza, *Adv. Exp. Med. Biol.*, 120A (1979) 115.
- 5 H. Kato, N. Adachi, S. Iwanaga, K. Abe, K. Tanaka, T. Kimura and S. Sakakibara, *J. Biochem.*, 87 (1980) 1127.
- 6 I. Traustchold and E. Werle, *Z. Physiol. Chem.*, 325 (1961) 48.
- 7 A. M. Siegelman, A. S. Carlson and T. Robertson, *Arch. Biochem. Biophys.*, 97 (1962) 159.
- 8 V. H. Beaven, J. V. Pierce and J. Pisano, *Clin. Chim. Acta*, 32 (1971) 67.
- 9 R. Geiger, U. Stuckstedte and H. Fritz, *Z. Physiol. Chem.*, 361 (1980) 1003.
- 10 E. Amundsen, J. Putter, P. Friberger, M. Knos, M. Larsbraaten and G. Claeson, *Adv. Exp. Med. Biol.*, 120A (1979) 83.
- 11 Y. Hitomi, M. Niinobe and S. Fujii, *Clin. Chim. Acta*, 100 (1980) 275.
- 12 R. Geiger, *Methods Enzym. Anal.*, 5(1984) 129.
- 13 W. Gau, G. L. Haberland, H. I. Ploschke and K. Schmidt, *Adv. Exp. Med. Biol.*, 156A (1983) 483.
- 14 Y. Funae, H. Ariyama, S. Imaoka, M. Takaoka and S. Morimoto, *J. Chromatogr.*, 264 (1983) 249.
- 15 J. P. Girolami, J. L. Bascands and C. Pecher, *J. Immunoassay*, 8 (1987) 115.
- 16 V. Hial, C. R. Diniz and M. Mares-Guia, *Biochemistry*, 13 (1974) 4311.
- 17 J. W. Ryan, *Methods Enzymol.*, 163 (1988) 160.



# Isolation and characterization of $\alpha$ -glucosidase from *Aspergillus niger*

Kateřina Břízová, Blanka Králová\* and Kateřina Demnerová

Department of Biochemistry, Institute of Chemical Technology, Technická 1905, 166 28 Prague (Czechoslovakia)

Ivan Vinš

Tessek Ltd., Křižovnická 3, 110 00 Prague (Czechoslovakia)

---

## ABSTRACT

$\alpha$ -Glucosidase is an enzyme widely used in biochemical analytical methods. *Aspergillus niger* was selected as a potential source for its production. Conditions for glucosidase production were optimized and the enzyme was isolated from the culture supernatant by dialysis and anion-exchange chromatography. The activity of the enzyme was determined by maltose hydrolysis to glucose, which was determined using a glucose-specific electrode or by high-performance liquid chromatography. The isolated enzyme was further characterized by sodium dodecyl sulphate–polyacrylamide gel electrophoresis, substrate specificity and fast protein liquid chromatography. The Michaelis constant, optimal temperature and stability of the enzyme preparation were determined.

---

## INTRODUCTION

$\alpha$ -Glucosidase ( $\alpha$ -D-glucoside glucohydrolase, E.C. 3.2.1.20) [1] is a hydrolytic enzyme which is used mainly in clinical biochemistry for determination of  $\alpha$ -amylase activity [2–4] in blood and serum. This determination is important for the diagnosis of diseases of the gall bladder and pancreas. Fleet *et al.* [5] have suggested that there is a relation between  $\alpha$ -glucosidase and human immunodeficiency virus (HIV) activity.

It is found in many microorganisms, however, often together with glucoamylase ( $\alpha$ -1,4-glucan glucohydrolase, E.C. 3.2.1.3). As long as both those enzymes hydrolyse maltose, they are not always properly differentiated. Glucoamylase hydrolyses  $\alpha$ -1,4-polysaccharide (glucan) bonds with the release of glucose. It is also possible to break  $\alpha$ -1,6 bonds.  $\alpha$ -Glucosidase hydrolyses  $\alpha$ -1,4 or  $\alpha$ -1,6 bonds in short oligosaccharides. Enzymes isolated from different sources sometimes possess different specificity towards maltose and isomaltose, and to

*p*-nitrophenyl- $\alpha$ -D-glucopyranoside, sometimes distinguished as maltase and  $\alpha$ -glucosidase.

Both extracellular and intracellular  $\alpha$ -glucosidase producers and the substrate specificity and other characteristics of isolated enzymes are reviewed by Kelly *et al.* [6]. The production of  $\alpha$ -glucosidase by selected microorganisms can be enhanced by selection of a suitable medium, usually containing a substrate [7,8] of the enzyme reaction as an inducer.

The isolation and purification of enzyme from fermentation broth is performed after the separation of cells by centrifugation or filtration. For extracellular enzyme the dialysis of supernatant is recommended [9–11]. Precipitation by ammonium sulphate [10,11] or isopropanol [12] has been described as the next step. Ethanol was not recommended by Martin-Rendon *et al.* [13] because it inhibited the activity of  $\alpha$ -glucosidase from *Saccharomyces* and *Candida*. However, precipitation does not separate the amylase activity, and this is a main goal of the purification. The enzyme can be further purified by chromatographic techniques. Gel permeation chro-

matography [10,14] on Sephadex G-150 has been applied to the separation of  $\alpha$ -glucosidase and maltase activity in *Bacillus licheniformis*. Ion-exchange chromatography has been applied to the separation of  $\alpha$ -glucosidase and amylase activity on DEAE-Bio-Gel A [12].

Measurement of  $\alpha$ -glucosidase activity is usually based on determination of the glucose released by the enzyme. Glucoamylase can be distinguished by its ability to hydrolyse starch [15].

The different authors cited above used different nomenclature for the enzymes which catalyse the hydrolysis of  $\alpha$ -glucosidic bonds. Thus the aim of our paper was not only to find a quick and simple method of separating glucosidases with different specificity, but also the proper characterization of these enzymes, produced by *Aspergillus niger*.

## EXPERIMENTAL

### Materials

Tested microorganisms were obtained from the collection of the Department of Biochemistry and Microbiology, Institute of Chemical Technology, Prague.

### Chemicals

Yeast autolysate, peptone and casein hydrolysate were from Imuna Šarišské Michalany, Czechoslovakia. *p*-Nitrophenyl- $\alpha$ -D-glucopyranoside, Coomassie Blue R-250, acrylamide, N,N-methylene bis-acrylamide and sodium persulphate were from Serva, Heidelberg, Germany. Tris(hydroxymethyl)amino-methane (Tris) was from Fluka, Buchs, Switzerland, N,N,N',N'-tetramethylethylenediamine (TEMED) and sodium dodecyl sulphate (SDS) were from Sigma, St. Louis, MO, USA, and starch (Zulkovski) was from Merck, Darmstadt, Germany. Other chemicals used were of reagent grade from Lachema, Brno, Czechoslovakia. Urasol (3.7 mM uranyl acetate in 0.15 M sodium chloride) was from the Oxochrom glucose diagnostic kit (Lachema).

### Instruments

Cultivation was performed in an RT-50 rotary shaker (Developing Workshops, Czechoslovak Academy of Sciences, Prague, Czechoslovakia). The cooled centrifuge was a Model K-24 from Janetzky, Germany. A 195 D UV spectrometer (Spectromom,

Budapest, Hungary) was used to measure protein content. Ultrafiltration membranes were from Milipore, Milford, MA, USA, Dialysis membranes were from Serva, Heidelberg, Germany. The fast protein liquid chromatography (FPLC) system with a Mono-Q HR 5/5 column was from Pharmacia LKB, Bromma, Sweden. The high-performance liquid chromatography (HPLC) system used for activity measurement consisted of a 64 HPLC pump (Knauer, Bad Homburg, Germany), a 7125 injection valve (Rheodyne, Palo Alto, CA, USA), and an RIDK 102 refractometric detector (Laboratory Instruments, Prague, Czechoslovakia). A 250  $\times$  4 mm I.D. (Tessek Separon SGX RPS 5  $\mu$ m) with coupled 3  $\times$  30 mm compact glass cartridge guard columns (Tessek Separon HEMA-BIO 1000 SB 10  $\mu$ m in hydrogen form) and HEMA-BIO 1000 Q 10  $\mu$ m in hydroxide form, as well as HEMA-cart DEAE cartridges were from Tessek, Prague, Czechoslovakia. The oxygen-selective electrode and MMP 003 low current measurement instrument were from Chemoprojekt, Satalice, Czechoslovakia. Vertical electrophoresis unit EV1 was from Developing Workshops. The Multitemp 2219 cooling unit was from LKB, Bromma, Sweden and the OK-104 conductometer and pH meter were from Radelkis, Budapest, Hungary.

### Cultivation media

(a) Complete medium contained 5 g of yeast autolysate, 3 g of peptone, 3 g of casein hydrolysate, 10 g of glucose and distilled water to 1000 ml.

(b) Czapek-Dox medium contained 2 g of NaNO<sub>3</sub>, 0.5 g of KH<sub>2</sub>PO<sub>4</sub>, 0.5 g of K<sub>2</sub>HPO<sub>4</sub>, 0.5 g of MgSO<sub>4</sub> · 7H<sub>2</sub>O, 0.01 g of FeSO<sub>4</sub> · 7H<sub>2</sub>O, 10 g of glucose and distilled water to 1000 ml.

(c) Modified Czapek-Dox medium contained the same as above except 10 g of glucose were substituted by 1 g of glucose and 9 g of maltose.

(d) Modified Czapek-Dox medium contained the same as above except 10 g of glucose were substituted by 1 g of glucose and 9 g of soluble starch.

### Cultivation of microorganisms

A 150-ml aliquot of culture medium was inoculated with 7 ml of inoculum (medium A inoculated with cells from agar plate for 24 h at 28°C). The cultivation proceeded for 48 h at 28°C on a rotary shaker. The cells were then separated by centrifugation at 1500 g for 20 min at 4°C.

For the *Aspergillus niger*, which produced a pellet-form biomass, another inoculation method was used. The spores were washed from the agar plate with sterile distilled water, and the suspension was filtered and used for medium inoculation. Cultivation proceeded for 72 h at 28°C on a rotary shaker. The biomass was then separated by filtration through a Büchner funnel.

#### Dialysis

Dialysis was performed against 0.01 M phosphate buffer (pH 6.5) at 4°C for 16 h with several changes of buffer. The process was controlled by conductivity measurement.

#### Ultrafiltration

The medium after cultivation and dialysis was ultrafiltered at 4°C through Pellicone membrane with an exclusion limit of  $10^4$  at 0.5 MPa. After concentration to one-quarter of the original volume the ultrafiltrate was diluted twice and again concentrated to one-quarter of the volume.

#### Precipitation

The medium remaining after cell separation was precipitated with solid ammonium sulphate for 20 h at 4°C. The precipitate was separated by centrifugation and resolved in 0.1 M phosphate buffer pH 5.8.

#### Anion-exchange chromatography on HEMA-cart DEAE

A 5-ml aliquot of dialysed medium was applied on an equilibrated cartridge (5 ml of distilled water and 5 ml of 0.01 M phosphate buffer pH 6.5) from a hypodermic syringe and eluted with 3-ml portions of increasing sodium chloride concentration in phosphate buffer.

#### Anion-exchange chromatography on Mono-Q HR 5/5 column

A 2-ml aliquot of dialysed medium was applied on a column equilibrated with 0.01 M phosphate buffer pH 6.5 and eluted with a sodium chloride gradient at 1 ml/min. Fractions of 1 ml were collected.

#### Protein content measurement

The protein content was determined [16] from the adsorbance at 260 and 280 nm using the formula  $1.45 \times A_{280} - 0.74 \times A_{260}$  (in mg/ml). The cell

mass was determined gravimetrically after washing with distilled water and drying to constant weight.

SDS-polyacrylamide gel electrophoresis was performed according to Laemmli [17].

#### Activity measurement

Enzyme activity was measured by determination of glucose released from maltose. A 1-ml aliquot of 2% maltose in 0.1 M phosphate buffer pH 5.8 was incubated with 1 ml of sample for 30 min at 40°C. The reaction was terminated with 0.5 ml of the deproteinization reagent Urasol. After 10 min, the precipitate was separated by centrifugation and the glucose in the supernatant was determined. Two blank controls containing no maltose and no enzyme were measured simultaneously. Substrate specificity was measured for *p*-nitrophenyl- $\alpha$ -D-glucopyranoside and soluble starch using the same procedure.

#### Glucose determination [18]

The oxygen-selective electrode was covered with a nylon mesh containing immobilized glucose oxidase and catalase. The determination was performed at 30°C in a mixture of 1.4 ml of phosphate buffer and 0.1 ml of sample. Oxygen depletion was measured and evaluated from maxima height. The system was calibrated before each measurement with standard glucose solutions. Alternatively, HPLC determination on a 250  $\times$  4 mm I.D. steel column (Tessek Separon SGX RPS 5  $\mu$ m octadecyl-modified silica column) was performed with distilled water as the

TABLE I

EXTRACELLULAR ACTIVITY OF  $\alpha$ -GLUCOSIDASE IN THE MEDIUM AFTER CULTIVATION

Microorganism	Activity (nkat/ml)
<i>Endomyces magnusii</i>	0
<i>Hansenula anomala</i>	51.0
<i>Saccharomyces cerevisiae</i>	71.0
<i>Saccharomyces cerevisiae</i> type Malaga	99.6
<i>Saccharomyces cerevisiae</i> type Palestina	99.6
<i>Schizosaccharomyces pombe</i>	63.9
<i>Aspergillus niger</i>	105.0
<i>Penicillium citrinum</i>	112.4
<i>Penicillium brevicompactum</i>	51.3

eluent at a flow-rate of 0.5 ml/min with refractometric detection. When coupled with HEMA-BIO 1000 SB and HEMA-BIO 1000 Q guard columns the system enabled direct injection of buffered samples without disturbance normally caused by the salts. The system was calibrated with glucose and maltose.

RESULTS AND DISCUSSION

Cultivation conditions

From nine tested producers (Table I) *Aspergillus niger* was selected as a promising source owing to its high production rate.

Surprisingly, inoculation with a suspension of spores led to higher activity production than the classical inoculation with a culture inoculum. Many smaller uniform pellets were formed, rather than only a few non-uniform pellets. The activity produced is compared in Table II.

In agreement with the literature, the highest activity production was achieved with maltose as a carbon source (Table III). The maximum activity was produced after 4 days of cultivation later the activity decreased (Fig. 1).

Isolation

As the first step in enzyme isolation after filtration dialysis, ultrafiltration and ammonium sulphate precipitation were tested. The results are given in Table IV. Ultrafiltration caused a high loss of activity, while, probably because of a low protein concentration, precipitation was unsuccessful, no filterable precipitate being formed even under 100% saturation. The filtrate was thus dialysed and further purified by ion-exchange chromatography on anion exchangers. The results from HEMA-cart DEAE

TABLE II  
PRODUCTION OF  $\alpha$ -GLUCOSIDASE BY *A. NIGER* AFTER DIFFERENT INOCULATION METHODS

Method	Activity (nkat/ml)	Dry mass (g/ml)	Specific activity (nkat per g of dry mass)
Standard	9.0	0.1	90
Suspension of spores	26.7	0.09	297

TABLE III  
DEPENDENCE OF EXTRACELLULAR  $\alpha$ -GLUCOSIDASE PRODUCTION ON THE CARBON SOURCE

Carbon source	Activity (nkat/ml)
Glucose	7.0
Glucose + starch	11.2
Glucose + maltose	26.7

separation are given in Fig. 2, while the FPLC separation on Mono-Q column is shown in Fig. 3. The results are summarized in Tables V and VI.

In addition to better recovery in the first case, *i.e.*, with DEAE HEMA cartridges, the method is very quick, simple and does not require special equipment. Good separation of glucosidases with different substrate specificity was achieved in two isolation steps, dialysis and ion-exchange chromatography, which is a significant simplification in comparison with the procedures stated in literature. The degree of purification achieved in the chromatographic step, especially for maltase fraction, was very good (10.5).

Characterization

Two active fractions were isolated, the first exhibiting maltase activity, the second glucoamylase activity. Substrate specificity is compared in

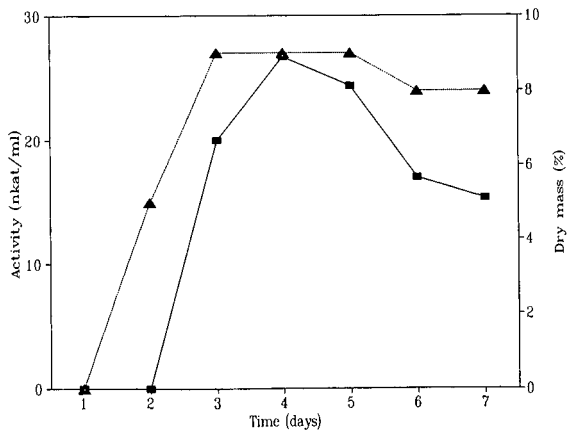


Fig. 1. Time dependence of the  $\alpha$ -glucosidase production in *Aspergillus niger*. ■—■ = Activity; ▲···▲ = dry mass.



TABLE IV  
EFFECTIVENESS OF FIRST ISOLATION STEPS

Method	Activity (nkat/ml)	
	Before	After
Dialysis	24.0	21.5
Ultrafiltration	24.2	13.0
Precipitation	24.0	No precipitate formed

Table VII. The characteristic parameters for both isolated enzyme fractions are summarized in Table VIII. The dependence of activity on temperature is given in Fig. 4, while the pH dependence of the crude enzyme preparation is shown in Fig. 5. According to SDS-PAGE, two and three protein impurities are present in the enzyme fractions,

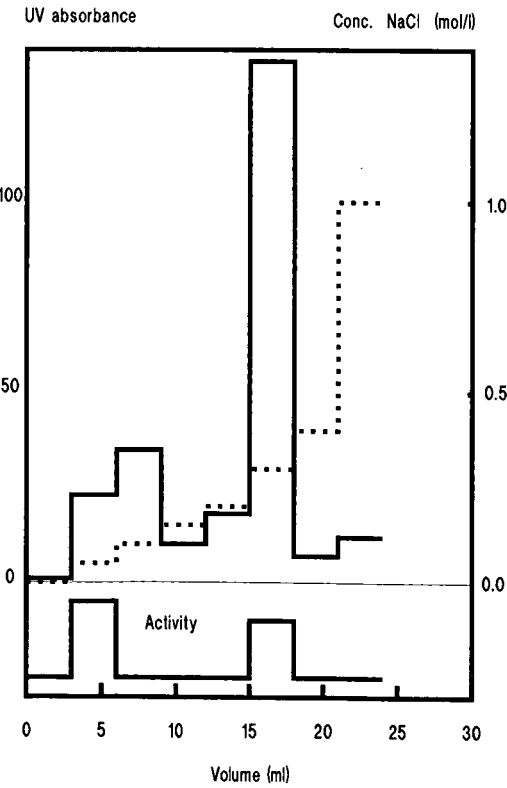


Fig. 2. Anion-exchange chromatography on HEMA-cart DEAE. 1 =  $\alpha$ -Glucosidase; 2 = glucoamylase. For conditions see Experimental section.

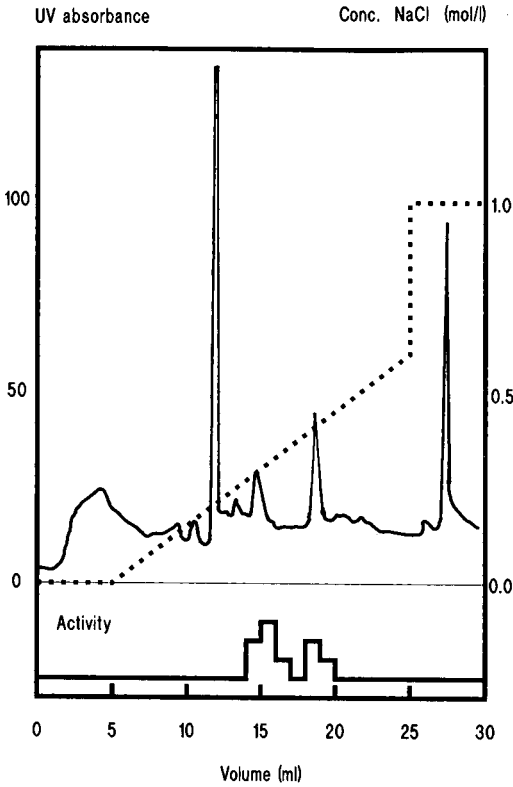


Fig. 3. Anion-exchange chromatography on Mono-Q HR 5/5 column. For conditions see Experimental section.

respectively, none of which possessed  $\alpha$ -amylase activity. To obtain a homogeneous preparation, further purification steps would thus be necessary.

*Activity determination by HPLC*

As a routine method for activity measurement the glucose-selective enzymic electrode was used throughout the work. For comparison, the HPLC

TABLE V  
ANION-EXCHANGE CHROMATOGRAPHY ON HEMA-CART DEAE

Sample	Total activity (nkat)	Total protein (mg)	Specific activity (nkat/mg)	Purification factor	Recovery (%)
Applied	71.56	1.25	57.32		
Fraction 1	42.00	0.07	600	10.47	
Fraction 2	24.00	0.41	58.54	1.02	92.1

TABLE VI  
ANION-EXCHANGE CHROMATOGRAPHY ON MONO-Q  
HR 5/5

Sample	Total activity (nkat)	Total protein (mg)	Specific activity (nkat/mg)	Purification factor	Recovery (%)
Applied	28.00	0.52	53.85		
Fraction 1	13.34	0.05	266.80	4.95	69.07
Fraction 2	6.00	0.11	54.54	1.01	

TABLE VII  
SUBSTRATE SPECIFICITY OF ISOLATED FRACTIONS  
Glucoside = *p*-nitrophenyl- $\alpha$ -D-glucopyranoside.

Substrate	Activity (nkat/ml)	
	Fraction 1	Fraction 2
Maltose	12.5	7.3
Starch	0	25.0
Glucoside	0	0

TABLE VIII  
CHARACTERISTIC PARAMETERS OF ISOLATED ENZYME FRACTIONS

Parameter	Fraction 1	Fraction 2
Substrate specificity	Maltase	Glucoamylase
Weight-average mol. wt. (SDS-PAGE)	131 000	89 000
Optimal temperature	40°C	60°C
Michaelis constant (Substrate)	$7.87 \cdot 10^{-3}$ mol/l	$3.13 \cdot 10^{-2}$ g/ml
Limiting velocity ( $V_{lim}$ )	Maltose 12.93 nkat/ml	Starch 82.7 nkat/ml
Remaining activity		
15 days at 4°C	79%	54%
15 days at -20°C	59%	79%
No. of protein impurities	2	3

determination was tested. The HPLC method enables determination of both substrate (maltose) and product (glucose), and has the potential to determine higher oligossaccharides also. A comparison of the results is given in Table IX. The agreement of

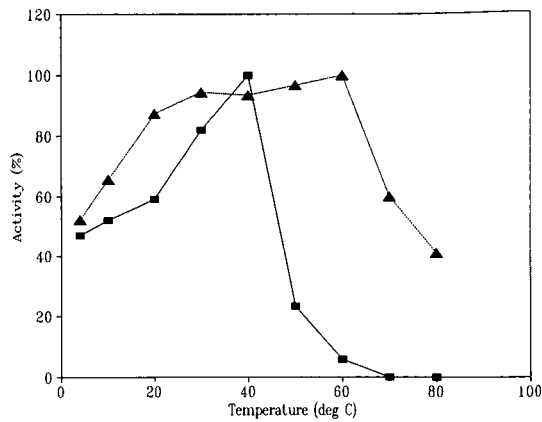


Fig. 4. Temperature dependence of activity of enzyme fractions. Highest activity taken as 100%.  $\blacktriangle \cdots \blacktriangle$  = Glucoamylase;  $\blacksquare \cdots \blacksquare$  = maltase.

both methods is satisfactory; the differences can be probably explained by a wider substrate specificity of the enzyme electrode. The chromatograms are given in Fig. 6. As long as the method takes only a little longer time to perform (analysis time 6 min) and the filtrate after protein precipitation is injected without any pretreatment, it can be an useful alternative method. The advantages will be better specificity and use of lower sample volumes.

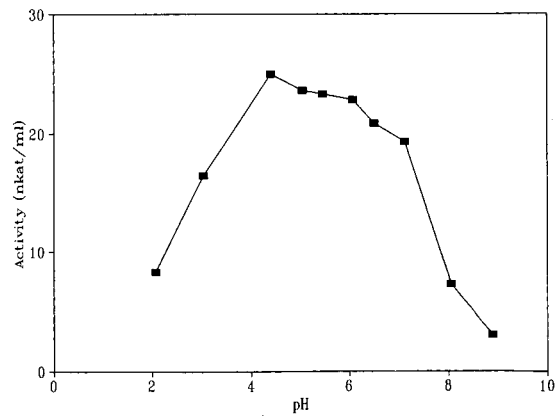


Fig. 5. pH dependence of crude enzyme activity (before separation of fractions).

TABLE IX

COMPARISON OF GLUCOSE DETERMINATION BY ENZYMIC ELECTRODE AND BY HPLC

Sample	Electrode	HPLC
<i>Enzyme sample</i>		
Glucose	6.9 mmol/l	6.14 mmol/l
Maltose		5.88 mmol/l
<i>Blank without enzyme</i>		
Glucose	2.2 mmol/l	0.0 mmol/l
Maltose		10.17 mmol/l
<i>Blank without substrate</i>		
Glucose	0.5 mmol/l	0.45 mmol/l
Maltose		0.22 mmol/l
Activity	14 nkat/ml	19 nkat/ml

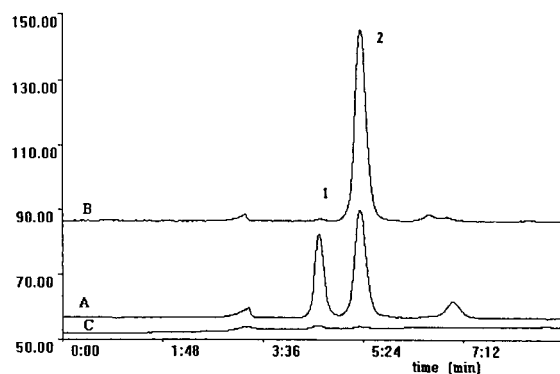


Fig. 6. HPLC determination of glucose and maltose for activity measurement. 1 = Glucose; 2 = maltose. (A) Measured sample; (B) blank (no sample); (C) blank (no maltose).

## CONCLUSIONS

Two enzyme fractions isolated from *Aspergillus niger* exhibited maltase and glucoamylase activities

as determined by anion-exchange chromatography. Basic characterization of both fractions was performed.

## REFERENCES

- 1 T. E. Barman, *Enzyme Handbook, Vol. II*, Springer, Berlin, Heidelberg, New York, 1969, pp. 564 and 576.
- 2 M. J. Batchelor, S. C. Williams and M. J. Green, *J. Electroanal. Chem.*, 246 (1988) 307.
- 3 S. Satomura, Y. Sakata, K. Omichi and T. Ikenaka, *Clin. Chim. Acta*, 174 (1988) 315.
- 4 E. Rausher, U. Neumann, E. Schaich and S. Bulow, *Clin. Chem. (Winston-Salom, N.C.)*, 31 (1985) 14.
- 5 G. W. J. Fleet, A. Karpas, R. A. Dwek, L. E. Fellows, A. S. Tys, S. Petursson, S. K. Namgoong, N. G. Ramsden, P. W. Smith, J. Ch. Son, F. Wilson, D. R. Witty, G. S. Jacob and T. W. Rademacher, *FEBS Lett.*, 237 (1988) 128.
- 6 C. T. Kelly, M. Giblin and W. M. Fogarty, *Process Biochemistry*, 18 (1983) 6.
- 7 G. Antranikian, C. Herzberg and G. Gottschalk, *Appl. Environm. Microbiol.*, 53 (1987) 1668.
- 8 E. J. Shaefer and C. L. Cooney, *Appl. Environm. Microbiol.*, 43 (1982) 75.
- 9 M. Yamamoto and K. Horikochi, *Jpn. Starch Sci.*, 34 (1987) 292.
- 10 C. T. Kelly, M. Giblin and W. M. Fogarty, *Can. J. Microbiol.*, 32 (1986) 342.
- 11 M. Thyrunavukkarasu and F. G. Priest, *J. Gen. Microbiol.*, 130 (1984) 3135.
- 12 C. T. Kelly, M. E. Moriarty and W. M. Fogarty, *Appl. Microbiol. Biotechnol.*, 22 (1985) 352.
- 13 E. Martin-Rendon, J. Jimenez and T. Benitez, *Curr. Genet.*, 15 (1989) 7.
- 14 J. Behan, C. T. Kelly and W. M. Fogarty, *Biochem. Soc. Trans.*, 16 (1988) 180.
- 15 M. Kujawski and M. Wegrzyn, *Starch/Staerke*, 32 (1980) 63.
- 16 H. M. Kalikar, *J. Biol. Chem.*, 167 (1947) 461.
- 17 V. K. Laemmli, *Nature (London)*, 227 (1970) 680.
- 18 E. Beránková and B. Králová, *Sci. Papers Inst. Chem. Technol. (Prague)*, E60 (1986) 95.



# Reversed-phase high-performance liquid chromatography–thermospray mass spectrometry of radiation-induced decomposition products of thymine and thymidine

M. Berger and J. Cadet\*

*Laboratoire "Lésions des Acides Nucléiques", DRFC/SESM, Centre d'Études Nucléaires, 85X, F-38041 Grenoble (France)*

R. Berube

*Laboratoire de Spectrométrie de Masse, Faculté de Médecine, Université de Sherbrooke, Québec J1H 5N4 (Canada)*

R. Langlois and J. E. van Lier

*Groupe CRM en Sciences des Radiations, Faculté de Médecine, Université de Sherbrooke, Québec J1H 5N4 (Canada)*

---

## ABSTRACT

High-performance liquid chromatography–thermospray mass spectrometry was applied to the analysis of various radiation-induced decomposition products of thymidine including N-(2-deoxy- $\beta$ -D-*erythro*-pentofuranosyl)formamide and the various diastereomers of 5,6-dihydroxy-5,6-dihydrothymidine, 5-hydroxy-5,6-dihydrothymidine and 5,6-dihydrothymidine. This method combines high sensitivity and product resolution, rendering it particularly useful for monitoring the formation of radiation-induced base damage within DNA.

---

## INTRODUCTION

Measurement of individual base damage within DNA on exposure to radical agents such as ionizing radiation and hydroxyl radicals still remains a challenging analytical problem. Various methods involving either high-performance liquid chromatography (HPLC) or gas chromatography (GC) have been developed for the separation of the complex mixture of modified DNA components (for recent reviews, see refs. 1–3). Sensitive detection of DNA lesions can be achieved by using various methods, including amperometry [4,5] as well as colorimetric [6], fluorescent [7] and radioactive [8] post-labellings. Mass spectrometry (MS) is mostly used in combination with GC analysis [9,10]. On the other hand, this accurate method of detection has not often been associated with HPLC, only two examples

of the application of HPLC–MS to measuring radiation-induced DNA base damage being available in the literature [11,12].

The main objective of this study was to explore the possibility of using the on-line HPLC–MS technique for monitoring the formation of radiation-mediated decomposition products of the base moieties of nucleic acids. We report here the HPLC–thermospray (TSP) MS analysis of the main radiation-induced decomposition products of thymine and its 2'-deoxyribonucleoside obtained in both aerated and oxygen-free aqueous solutions. The choice of both base and nucleoside decomposition products of the same DNA component (thymine) was dictated by the fact that these compounds may be obtained either by mild acidic hydrolysis [13] or by enzymic digestion of modified DNA [1]. This allows a comparative study of the thermospray mass

spectrometric features of the two classes of compounds with emphasis on the sensitivity of detection.

## EXPERIMENTAL

### Chemicals

Thymine and 5,6-dihydrothymine were obtained from Sigma (St. Louis, MO, USA). Thymidine was purchased from Genofit (Geneva, Switzerland) and was used without further purification.

5-Hydroxy-5,6-dihydrothymine was synthesized according to Nofre *et al.* [14]. The four *cis* and *trans* diastereomers of 5,6-dihydroxy-5,6-dihydrothymidine were prepared by mild alkaline hydrolysis of *trans*-(5*R*,6*R*)- and -(5*S*,6*S*)-5-bromo-6-hydroxy-5,6-dihydrothymidine [15]. The 5*R* and 5*S* diastereomers of 5,6-dihydrothymidine and 5-hydroxy-5,6-dihydrothymidine were obtained by gamma radiolysis of thymidine in oxygen-free aqueous solutions containing cysteine [16]. N-(2-Deoxy- $\beta$ -D-erythro-pentofuranosyl)formamide was prepared by menadione photooxidation of thymidine and purified by HPLC [17].

### High-performance liquid chromatography

The HPLC separations of the various radiation-induced decomposition products of thymine and thymidine were performed using an HP 1090 system (Hewlett-Packard). Octadecylsilyl silica gel ODS 1 (100 mm  $\times$  4.6 mm I.D.) and/or ODS-2 (50  $\times$  4.6 mm I.D.) reversed-phase analytical columns were packed with 3- and 5- $\mu$ m particles, respectively (Whatman, Hillsboro, OR, USA). Samples were introduced using a Rheodyne (Berkeley, CA, USA) Model 7125 injection valve equipped with a 100- $\mu$ l loop. The isocratic mobile phase was 0.1 M ammonium acetate (pH 6) at a flow-rate of 0.8 ml/min.

### Thermospray mass spectrometry

The HPLC-TSP-MS system consisted of an HP 5988A quadrupole mass analyser (Hewlett-Packard) and a Vestec (Houston, TX, USA) thermospray interface equipped with a CC 100 Cryocool immersion cooler. Acquisition and treatment of the spectrometric data were achieved with an HP 9000 Model 216 computer. The conditions used for the TSP-MS analysis were as follows: filament, "mode on"; stem temperature, 140°C with a tip temper-

ature of 220°C; electron multiplier voltage, 2500; temperature of the source, 300°C; and calibration of the spectra was achieved by using polypropylene glycol.

## RESULTS AND DISCUSSION

The thymidine decomposition products which were analysed include the 5*R* and 5*S* diastereomers of 5,6-dihydrothymidine and 5-hydroxy-5,6-dihydrothymidine, the four *cis* and *trans* diastereomers of 5,6-dihydroxy-5,6-dihydrothymidine and N-(2-deoxy- $\beta$ -D-erythro-pentofuranosyl)formamide. In addition, 5,6-dihydrothymine, 5-hydroxy-5,6-dihydrothymine and *cis*-5,6-dihydroxy-5,6-dihydrothymine, the corresponding racemic 5,6-saturated thymine derivatives and thymidine were also included. It is worth noting that N-(2-deoxy- $\beta$ -D-erythro-pentofuranosyl)formamide and the four diastereoisomeric thymidine glycols are two of the three main classes of decomposition products of thymidine arising from both hydroxyl radical reactions [18–20] and electron transfer processes [21,22]. The latter oxidation reaction, which may be initiated by both high-intensity laser pulses and photosensitization [22], involves the transient formation of a pyrimidine radical cation [21,22]. It is also interesting that the 5*R* and 5*S* diastereomers of 5,6-dihydrothymidine and 5-hydroxy-5,6-dihydrothymidine were found to be the main radiation-induced decomposition products of thymidine in deaerated aqueous solutions when cysteine, a known radioprotector agent, was present [14].

### HPLC-TSP-MS of thymidine

HPLC-TSP-MS was performed in either the positive or negative-ion mode (Figs. 1 and 2). It is interesting to note an almost complete lack of fragmentation in the negative-ion spectrum with a predominant quasi-molecular ion at  $m/z$  301 ( $M + \text{CH}_3\text{COO}$ )<sup>−</sup> and a relatively minor fragment at  $m/z$  125 (thymine-H)<sup>−</sup>. In the positive-ion mode the fragment corresponding to the cleavage of the N-glycosidic bond at  $m/z$  127 (thymine + H)<sup>+</sup> is the base peak. However, a significant quasi-molecular ion at  $m/z$  243 ( $M + \text{H}$ )<sup>+</sup> is also observed.

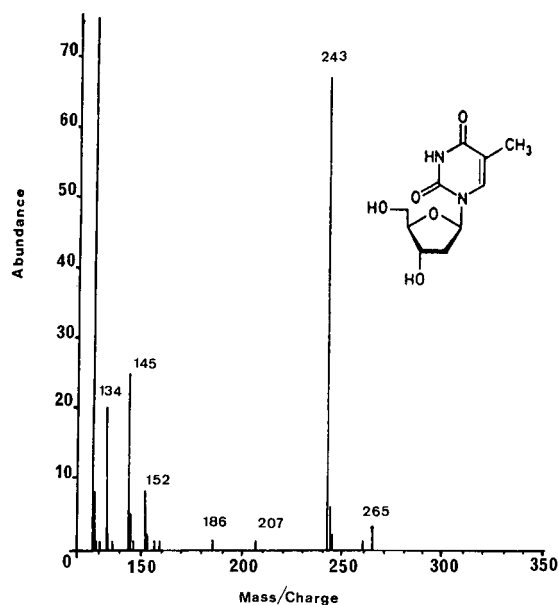


Fig. 1. Scale corrected thermospray mass spectrum in the positive-ion mode of thymidine. HPLC and TSP conditions as described under Experimental.

*Comparative HPLC-TSP-MS analysis of the 5R and 5S diastereomers of 5-hydroxy-5,6-dihydrothymidine and 5,6-dihydrothymidine*

The positive-ion thermospray mass spectra of the 5R and 5S diastereomers of 5-hydroxy-5,6-dihydrothymidine are presented in Figs. 3 and 4. The two spectra are almost identical, indicating that the stereochemistry at C-5 does not exert any signif-

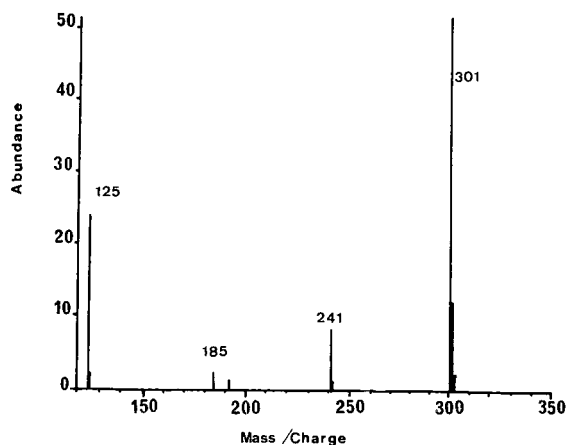


Fig. 2. Scale corrected thermospray mass spectrum in the negative-ion mode of thymidine.

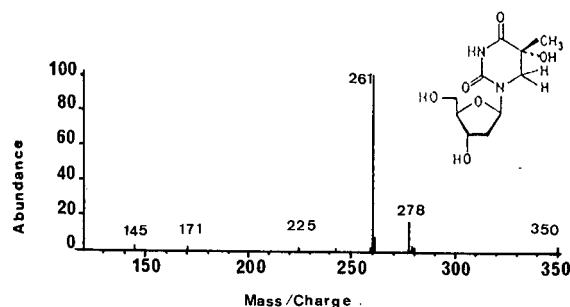


Fig. 3. Scale thermospray mass spectrum (positive-ion mode) obtained from (5R)-5-hydroxy-5,6-dihydrothymidine.

icant influence on the fragmentation pattern. Both molecules show little fragmentation with characteristic quasi-molecular ions at  $m/z$  261 ( $M + H$ )<sup>+</sup> (base peak) and  $m/z$  278 ( $M + NH_4$ )<sup>+</sup>.

It is of interest that the positive- and negative-ion spectra of the 5R and 5S diastereomers of 5,6-dihydrothymidine exhibit a predominant quasi-molecular ion at  $m/z$  245 ( $M + H$ )<sup>+</sup> and  $m/z$  303 ( $M + CH_3COO$ )<sup>-</sup>, respectively (data not shown). No fragmentation of the pyrimidine ring is observed. In addition, we note a complete lack of any fragment corresponding to the release of the free base subsequent to the cleavage of the N-glycosidic bond. The only additional significant peaks which were detected are the ions at  $m/z$  262 ( $M + NH_4$ )<sup>+</sup> and  $m/z$  243 ( $M - H$ )<sup>-</sup>, which exhibit relative intensities of 17–25% and 5–8% in the positive- and negative-ion spectra, respectively. Again, the mass spectra of the 5R and 5S diastereomers are identical.

The thermospray mass spectra of the racemic 5,6-dihydrothymine and 5-hydroxy-5,6-dihydrothymine exhibit two major peaks, which correspond to the quasi-molecular ions ( $M + H$ )<sup>+</sup> and ( $M +$

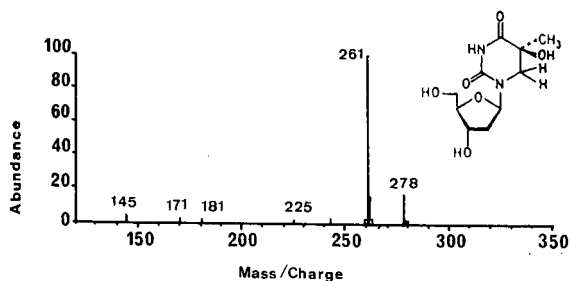


Fig. 4. Scale thermospray mass spectrum (positive-ion mode) obtained from (5S)-5-hydroxy-5,6-dihydrothymidine.

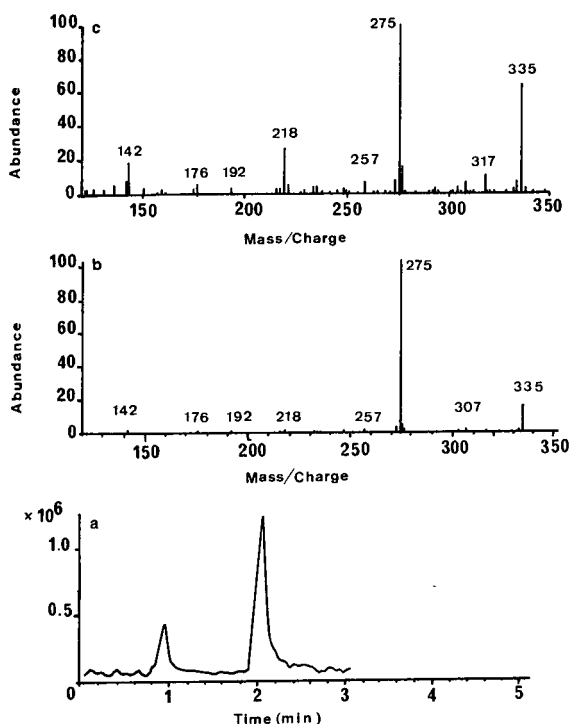


Fig. 5. (a) Total ion chromatogram (TIC) profile of (-)-*trans*-(5*S*,6*S*)- and (+)-*cis*-(5*S*,6*R*)-5,6-dihydroxy-5,6-dihydrothymidine. (b) Scale corrected thermospray mass spectrum (negative-ion mode) of (+)-*cis*-(5*R*,6*S*)-5,6-dihydroxy-5,6-dihydrothymidine. (c) Scale corrected thermospray mass spectrum (negative-ion mode) of (-)-*trans*-(5*S*,6*S*)-5,6-dihydroxy-5,6-dihydrothymidine.

$\text{NH}_4^+$  in the positive-ion mode and  $(\text{M} - \text{H})^-$  and  $(\text{M} + \text{CH}_3\text{COO})^-$  in the negative-ion mode.

#### HPLC-TSP-MS analysis of the *cis* and *trans* diastereomers of 5,6-dihydroxy-5,6-dihydrothymidine

Fig. 5a shows the total ion chromatogram obtained from the HPLC-TSP-MS analysis of a mixture of the (-)-*trans*-(5*S*,6*S*)- and (+)-*cis*-(5*S*,6*R*)-5,6-dihydroxy-5,6-dihydrothymidine in the negative-ion mode. The two modified nucleosides are well separated ( $\alpha = 2.9$ ), the *trans* diastereomer being eluted faster than the corresponding C-6 epimer [6]. The fragmentation pattern of each of the two diastereomers is similar. We note in particular the presence of the two characteristic pseudo-molecular ions at  $m/z$  275 ( $\text{M} - \text{H})^-$  and  $m/z$  335 ( $\text{M} + \text{CH}_3\text{COO})^-$  (Fig. 5b and c). The main difference

between the two spectra concerns the intensity of the fragment  $m/z$  218, which corresponds to the cleavage of the N-glycosidic bond ( $\text{base} - \text{H} + \text{CH}_3\text{COO})^-$ . Under these conditions, the *trans*-(6*S*)-diol appears to be more thermally unstable than the *cis*-(6*R*)-diol. Similarly, the dehydration process ( $m/z$  257) which is likely to involve the loss of the hydroxyl group at C-6 [23] is higher for the *trans*-diol. Intense pseudo-molecular ions at  $m/z$  277 ( $\text{M} + \text{H})^+$  and  $m/z$  294 ( $\text{M} + \text{NH}_4^+$ ) were observed when the two thymidine glycols were analysed in the positive-ion mode (data not shown).

#### HPLC-TSP-MS analysis of N-(2-deoxy-2-β-D-erythro-pentofuranosyl)formamide

The positive-ion mass spectrum of N(2-deoxy-β-D-erythro-pentofuranosyl)formamide is shown in Fig. 6. Very little fragmentation occurs, the relative intensity of the ion at  $m/z$  134 (1-amino-2-D-erythro-pentose) being only 10%. The two main frag-

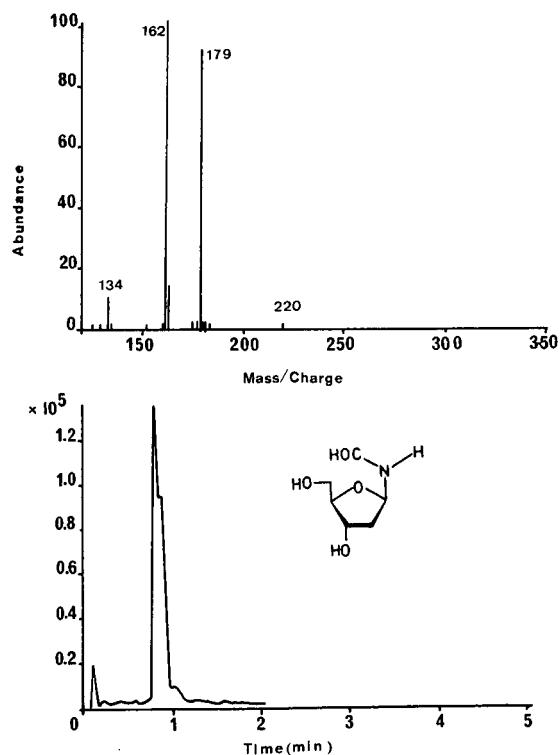


Fig. 6. Scaled thermospray mass spectrum (positive-ion mode) and total ion chromatogram (TIC) profile of N-(2-deoxy-β-D-erythro-pentofuranosyl)formamide.



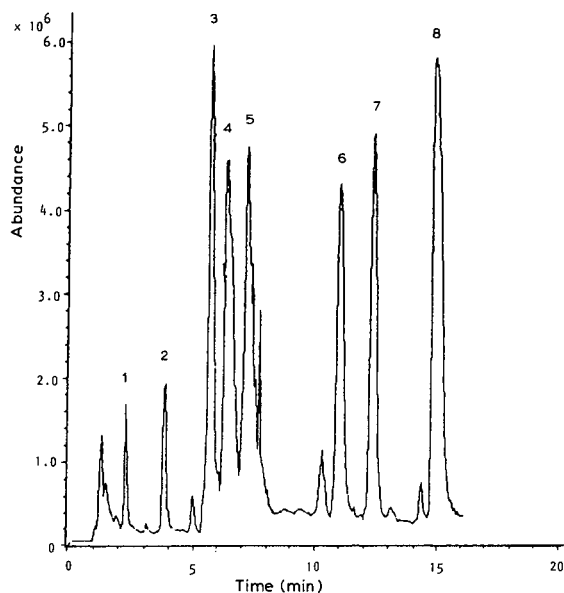


Fig. 7. Total ion chromatogram (TIC) profile of a mixture of nucleobases and nucleosides: (1) 5-hydroxy-5,6-dihydrothymine, (2) (5*R*)-5-hydroxy-5,6-dihydrothymidine, (3) (5*S*)-5-hydroxy-5,6-dihydrothymidine, (4) 5,6-dihydrothymine, (5) thymine, (6) (5*R*)-5,6-dihydrothymidine, (7) (5*S*)-5,6-dihydrothymidine and (8) thymidine.

ments correspond to the characteristic quasi-molecular ions at  $m/z$  162 ( $M + H$ )<sup>+</sup> and  $m/z$  179 ( $M + NH_4$ )<sup>+</sup>. It is also interesting that the base peak in the negative-ion spectrum is the quasi-molecular ion at  $m/z$  220 ( $M + CH_3COO$ )<sup>-</sup> (data not shown).

#### *Analysis of a complex mixture of radiation-induced decomposition products of thymine and thymidine by thermospray mass spectrometry in line with reversed-phase HPLC*

Fig. 7 shows the total ion chromatogram obtained by reversed-phase HPLC-TSP-MS analysis of a complex mixture of eight radiation-induced decomposition products of thymine and thymidine. A complete separation of the modified bases and nucleosides was achieved on the ODS-3 column [24] in less than 16 min by using 0.1 *M* ammonium acetate as the mobile phase. The following compounds were separated in decreasing order of elution: 5-hydroxy-5,6-dihydrothymine (1) > (5*R*)-5-hydroxy-5,6-dihydrothymidine (2) > (5*S*)-5-hydroxy-5,6-dihydrothymidine (3) > 5,6-dihydrothymine (4) >

TABLE I

DETECTION LIMITS OF BASES AND NUCLEOSIDES IN THE POSITIVE- AND NEGATIVE-ION MODES

Compound	Amount (ng)
Thymidine	0.1–0.3
5,6-Dihydroxy-5,6-dihydrothymidines	5
5-Hydroxy-5,6-dihydrothymidines	0.1
5,6-Dihydrothymidine	0.2
Thymine	0.1

thymine (5) > (5*R*)-5,6-dihydrothymidine (6) > (5*S*)-5,6-dihydrothymidine (7) > thymidine (8).

#### *Quantitative aspects and sensitivity: selective ion monitoring measurements*

The sensitivity of detection of the modified bases and nucleosides analysed by the HPLC-TSP-MS method is significantly increased by using the selective ion monitoring (SIM) technique under optimized conditions of measurement (source temperature varying from 275 to 300°C according to the compounds analysed, mode "on"). The detection limits of several compounds were determined by measuring the predominant pseudo-molecular ion by using the SIM technique and are listed in Table I. The detector response was linear with the amount of the compounds being analysed, as illustrated for the 5*R* diastereomer of 5-hydroxy-5,6-dihydrothymidine.

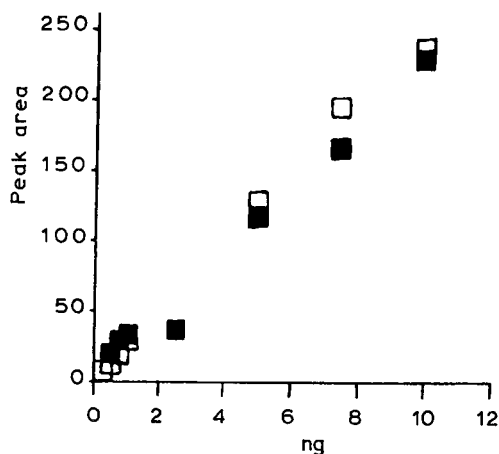


Fig. 8. Relationship between peak area on the SIM chromatogram and amount of (5*R*)-5-hydroxy-5,6-dihydrothymidine in the (□) positive- and (■) negative-ion modes.

midine (Fig. 8). Similar behaviour was observed for the other radiation-induced decomposition products of thymine and thymidine.

## CONCLUSIONS

Reversed-phase HPLC–TSP–MS is a powerful technique, combining efficient product separation with detection sensitivity, for the accurate detection of radiation-induced decomposition products of thymine and thymidine. The method is an interesting alternative (and probably a complementary tool) to the GC–MS method [7], which requires a derivatization step prior to the analysis. It is likely that a similar range of sensitivity is provided by both techniques, depending, however, on the nature of the compounds to be analysed. In this respect, it is worth noting that the sensitivity of detection of the thymine glycol is relatively poor, irrespective of the HPLC–MS or GC–MS approach used. On the other hand, HPLC–TSP–MS has the potential to detect one 5,6-dihydrothymine or 5-hydroxy-5,6-dihydrothymine residue per  $10^5$  nucleobases within 20–30  $\mu\text{g}$  of DNA, which is similar to the sensitivity offered by the HPLC–amperometric assay [4,5]. It should be mentioned that accurate determination of modified nucleobases and nucleosides would require, for both methods, the use of internal isotopically enriched standards.

Interesting and useful applications of the HPLC–TSP–MS assay involve DNA repair studies (determination of substrate specificity for repair enzymes) and the search for modified bases within cellular DNA. This complements the array of existing methods, including the specific HPLC–electrochemical assay [4,5] and the HPLC– $^{32}\text{P}$  post-labelling method [8].

## ACKNOWLEDGEMENTS

This work was supported in part by grants from the Centre National d'Études Spatiales (90/312), the France–Québec Exchange Programme and the Medical Research Council of Canada.

## REFERENCES

- 1 P. Vigny and J. Cadet, in A. Favre, R. M. Tyrrell and J. Cadet (Editors) *From Photophysics to Photobiology*, Elsevier, Amsterdam, 1987, p. 123.
- 2 J. Cadet and P. Vigny, in H. Morrison (Editor), *Bioorganic Photochemistry*, Vol. 1, Wiley, New York, 1990, p. 1.
- 3 M. Dizdaroglu, *Free Rad. Biol. Med.*, 10 (1991) 222.
- 4 R. A. Floyd, J. J. Watson, P. K. Wong, D. H. Atmiller and R. C. Rickard, *Free Rad. Res. Commun.*, 1 (1986) 163.
- 5 M. Berger, C. Anselmino, J.-F. Mouret and J. Cadet, *J. Liq. Chromatogr.*, 13 (1990) 199.
- 6 J. R. Wagner, M. Berger, J. Cadet and J. E. van Lier, *J. Chromatogr.*, 504 (1990) 191.
- 7 M. Sharma, H. C. Box and D. J. Kelman, *Chem.-Biol. Interact.*, 74 (1990) 107.
- 8 J.-F. Mouret, F. Odin, M. Polverelli and J. Cadet, *Chem. Res. Toxicol.*, 3 (1990) 102.
- 9 A. F. Fuciarelli, B. J. Wegher, E. Gajewski, M. Dizdaroglu and W. F. Blakely, *Radiat. Res.*, 119 (1989) 219.
- 10 W. G. Stillwell, H.-X. Xu, J. A. Adkins, J. S. Wishnol and S. R. Tannenbaum, *Chem. Res. Toxicol.*, 2 (1989) 94.
- 11 A. J. Alexander, P. Kebarle, A. F. Fuciarelli and J. A. Raleigh, *Anal. Chem.*, 59 (1987) 2484.
- 12 J. Cadet, M. Berger, C. Decarroz, A. Shaw, J. R. Wagner, E. Keskinova and D. Angelov, in A. Y. Spasov (Editor), *Lasers and Applications*, World Scientific, Singapore, 1987, p. 508.
- 13 M. Polverelli, M. Berger, J.-F. Mouret, F. Odin and J. Cadet, *Nucleosides Nucleotides*, 9 (1990) 451.
- 14 C. Nofre, A. Cier, R. Chapurlat and J.-P. Mareschi, *Bull. Soc. Chim. Fr.*, (1965) 332.
- 15 J. Cadet, J. Ulrich and R. Téoule, *Tetrahedron*, 31 (1975) 2657.
- 16 J. Cadet, M. Berger, P. Demonchaux and J. Lhomme, *Radiat. Phys. Chem.*, 32 (1988) 197.
- 17 R. J. Wagner, J. E. van Lier, C. Decarroz, M. Berger and J. Cadet, *Methods Enzymol.*, 186 (1990) 502.
- 18 R. Téoule, *Int. J. Radiat. Biol.*, 51 (1987) 573.
- 19 C. von Sonntag, *The Chemical Basis of Radiation Biology*, Taylor and Francis, London, 1987.
- 20 G. W. Teebor, R. J. Boorstein and J. Cadet, *Int. J. Radiat. Biol.*, 54 (1988) 131.
- 21 D. J. Deeble, M. N. Schuchmann, S. Steenken and C. von Sonntag, *J. Phys. Chem.*, 94 (1990) 8186.
- 22 J. Cadet, M. Berger, C. Decarroz, J.-F. Mouret, J. E. van Lier and R. J. Wagner, *J. Chim. Phys.*, 88 (1991) 1021.
- 23 J. R. Wagner, J. E. van Lier, C. Decarroz and J. Cadet, *Bioelectron. Bionerg.*, 18 (1987) 155.
- 24 J. Cadet, M. Berger and L. Voituriez, *J. Chromatogr.*, 238 (1982) 488.

# Improved determination of individual molecular species of phosphatidylcholine in biological samples by high-performance liquid chromatography with internal standards

Alfredo Cantafora\* and Roberta Masella

*Laboratory of Metabolism and Pathological Biochemistry, Istituto Superiore di Sanità, Viale Regina Elena 299, 00161 Rome (Italy)*

---

## ABSTRACT

Phosphatidylcholine isolated from samples of bile, liver and plasma was converted into 1,2-diradylglycerobenzoate molecular species by hydrolysis with phospholipase C and reaction with benzoic anhydride. Up to seventeen molecular species were separated and determined by reversed-phase high-performance liquid chromatography with detection at 230 nm. The major improvement introduced here was the use of distearoylphosphatidylcholine as the internal standard, which corrected the results for incomplete hydrolysis and benzylation. Other improvements concerned the clean-up of benzoyl derivatives and the chromatographic separation. The analytical results obtained were validated by comparison with the results of either lipid phosphorus or gas chromatographic determinations.

---

## INTRODUCTION

There are three different approaches to the high-performance liquid chromatographic (HPLC) determination of the molecular species profile of biologically relevant phospholipids, namely the separation of intact phospholipids, both unmodified [1–8] and modified [9–12], and UV-absorbing derivatives of partially hydrolysed phospholipids (*i.e.*, the 1,2-diradylglycerols) [13–19].

The determination of unmodified intact phospholipids, in spite of its simplicity, has not gained wide acceptance because of problems relating to the detection of the molecular species with a low degree of acyl unsaturation, as pointed out in previous reports on the determination of molecular species in bile phosphatidylcholine [7,8].

The determination of intact phospholipids based on postcolumn fluorescence derivatization with 1,6-diphenyl-1,3,5-hexatriene is attractive [12]. However, a particular apparatus is required and the determination is likely to be affected by molecular spe-

cies-related changes in interaction between the fluorescent probe and the phosphatidylcholine micelles formed by the water enrichment due to the post-column flow. Consequently, methods in which the phospholipids are converted into diradylglycerols tagged with a UV chromophore have been often preferred in practical applications [20,21], in spite of the more complex and critical analytical procedure required. Further, it is claimed that the UV-tagged diradylglycerol subclasses (*i.e.*, the alk-1-enylacyl, alkylacyl and diacyl species) are more easily separated by thin-layer chromatography (TLC) and determined [15] than the diradylglycerol acetates described by Nakagawa and Horrocks [14].

In this study, we introduced various improvements to existing methods for the determination of the diradylglycerobenzoates derived from biological phosphatidylcholines. The major improvement was the introduction of an internal standard (the distearoylphosphatidylcholine) that gave quantitative results corrected for partial hydrolysis and benzylation. Other improvements concerned the pro-

cedure of derivative purification and the chromatographic conditions used for obtaining a chromatographic profile of the molecular species well suited for the analysis of bile, plasma and liver phosphatidylcholines.

#### EXPERIMENTAL

The molecular species of phosphatidylcholine, dipalmitoyl (16:0–16:0), distearoyl (18:0–18:0), palmitoyloleoyl (16:0–18:1), palmitoylinooleoyl (16:0–18:2) and palmitoylarachidonoyl (16:0–20:4), the diarachidine and the phospholipase C (from *Bacillus cereus*) were purchased from Sigma (St. Louis, MO, USA). The species oleoylinooleoyl (18:1–18:2), stearoylinooleoyl (18:0–18:2) and stearoyl arachidonoyl (18:0–20:4) were isolated by preparative column chromatography from purified soy and egg lecithins as described previously [7]. The 1,2-diarachidine isomer was isolated from diarachidine using borate-impregnated TLC plates as described by Christie [22]. Methylheptadecanoate and silica gel 60 TLC plates were purchased from E. Merck (Darmstadt, Germany) and benzoic anhydride and 4-pyrrolidinopyridine from Fluka (Buchs, Switzerland). Other chemicals of analytical-reagent grade and solvents of HPLC grade were purchased from Carlo Erba (Milan, Italy).

Bile samples were mixed with isopropanol (1:5, v/v) and centrifuged to remove proteins. Phosphatidylcholine was isolated from this alcoholic solution by TLC with the solvent system chloroform–methanol–acetic acid–water (65:25:15:4, v/v). The band of phosphatidylcholine was scraped from the silica gel and eluted with 10 ml of chloroform–methanol–water (60:40:6, v/v/v).

Lipid extracts from liver and plasma samples were prepared with chloroform–methanol (2:1, v/v) according to Folch *et al.* [23]. Phosphatidylcholine was isolated by TLC as described above.

Phosphatidylcholine was converted into the corresponding diradylglycerol by enzymatic hydrolysis with phospholipase C as described previously [24]. Briefly, the sample of bile phosphatidylcholine was mixed with 100  $\mu$ g of distearoylphosphatidylcholine. The solvent was evaporated under nitrogen and the residue was dissolved in 0.5 ml of 4-(2-hydroxyethyl)-1-piperazineethanesulphonic acid (HEPES) buffer (pH 7.3) containing 0.4 mM zinc

chloride, 1 mM mercaptoethanol and 20 units of phospholipase C (from *B. cereus*). The mixture was maintained under continuous stirring in a shaking water-bath for 3 h at 37°C. The diradylglycerol was extracted three times with 2-ml portions of diethyl ether. The extracts were combined and mixed with 100  $\mu$ g of 1,2-diarachidine and the solvent was evaporated under nitrogen. The benzoate derivative of diradylglycerol molecular species was prepared by a modification of the method described by Blank *et al.* [19]. Briefly, 0.3 ml of reaction mixture (10 mg of benzoic anhydride and 25  $\mu$ g of 4-pyrrolidinopyridine dissolved in 1 ml of anhydrous benzene) was added to the sample and allowed to stand for 90 min at room temperature. The reaction was stopped by adding 1 ml of concentrated ammonia solution. The benzoate derivative was extracted with three 2 ml portions of *n*-hexane to eliminate the excess of benzoic acid. The pooled extracts were passed through a cartridge filled with 1.5 g of diatomaceous earth (Extrelut, E. Merck), which was wetted prior to use with 2 ml of 1 M hydrochloric acid. The cartridge was washed with 3 ml of *n*-hexane. The *n*-hexane was collected and evaporated under nitrogen. The residue was dissolved in 100  $\mu$ l of the mobile phase for HPLC.

HPLC analysis was performed with an apparatus produced by Gilson Medical Electronics (Middleton, WI, USA), equipped with an UV detector set at 230 nm. The column used was a Spherisorb ODS-2, 5  $\mu$ m (250  $\times$  4.6 mm I.D.) (Phase Separations, Queensferry, Clwyd, UK), maintained at 38  $\pm$  0.1°C by an electronic thermostat. The mobile phases tested during the study contained methanol, ethanol, isopropanol, water and acetonitrile in different proportions. For bile samples the best results were obtained with methanol–acetonitrile–ethanol–water (29:21:47:2.8, v/v) at a flow-rate of 1 ml/min.

The relative retention times (RRT) of molecular species contained in mixtures of authentic standards were calculated by dividing the retention time of each peak by that of the peak given by 1,2-diarachidine benzoate. A linear graph was constructed between log RRT and the total number of hydrophobic carbon atoms in the fatty acid side-chains of the disaturated molecular species of diacylglycerobenzoate tested [5]. The total hydrophobic carbon number (HCN) for the unsaturated molecular species was calculated by interpolation of the linear

graph using its log RRT value. The unsaturated species showed, in comparison with their saturated parent compounds, a reduction in the HCN values that were used for the prediction of the elution sequence of molecular species [5,7].

The identity of unknown peaks and the validation of the results obtained by the HPLC determination were made by the gaschromatographic (GC) determination of the fatty acid methyl esters prepared from either phosphatidylcholine or diradylglycerobenzoate fractions, as described previously [7].

## RESULTS AND DISCUSSION

The HPLC of molecular species of diradylglycerobenzoates derived from biological phosphatidylcholines suffered from both qualitative and quantitative problems due to the complexity of natural mixtures and the analytical procedures applied, respectively.

The study of the qualitative problems started from an attempt to separate the complex mixture of 1,2-diradylglycerobenzoates derived from bile phosphatidylcholine in a manner comparable to

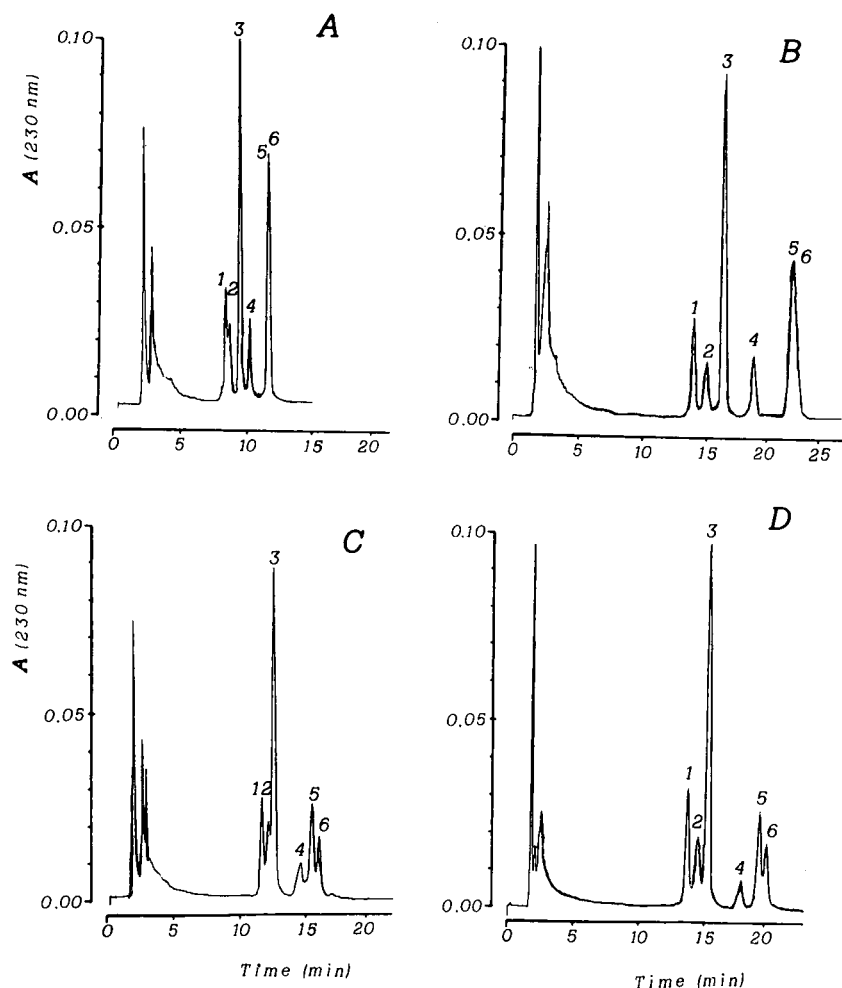


Fig. 1. Chromatographic separations of the six molecular species of diradylglycerobenzoates derived from the major molecular species of bile phosphatidylcholine with four different mobile phases: (A) acetonitrile-isopropanol (80:20, v/v); (B) acetonitrile-methanol-ethanol (70:12:18, v/v/v); (C) acetonitrile-methanol-ethanol (15:34:51, v/v/v) with 2.8% of water added; (D) acetonitrile-methanol-ethanol (30:28:42, v/v/v) with 3.0% of water added. Peaks: 1 = 16:0-20:4; 2 = 18:1-18:2; 3 = 16:0-18:2; 4 = 18:0-20:4; 5 = 16:0-18:1; 6 = 18:0-18:2.

that described previously for intact molecular species of human and rat bile [7,8]. This was done by studying the effects of modifications of the mobile phase described previously for the separation of 1,2-diradylglycerobenzoates derived from liver phospholipids [16] [acetonitrile–2-propanol (80:20, v/v)] on the separation of the major molecular species of bile phosphatidylcholine. Some significant steps in the optimization process are illustrated in the four chromatograms shown in Fig. 1. This sequence showed that acetonitrile improved the resolution between 2-arachidonoyl and 2-linoleoyl species while water and methanol are required for the

separation between the pairs of species 18:1–18:2/16:0–18:2 and 16:0–18:1/18:0–18:2.

HPLC under the final chromatographic conditions of the diradylglycerobenzoates derived from either human or rat bile phosphatidylcholines gave the results shown in Fig. 2. The same conditions also allowed good separations of liver and plasma phosphatidylcholines whose molecular species distributions were considered to be metabolically related to that of bile (Fig. 3).

The RRTs and the capacity factors ( $k'$ ) measured with standard mixtures of molecular species with different degrees of acyl unsaturation are reported

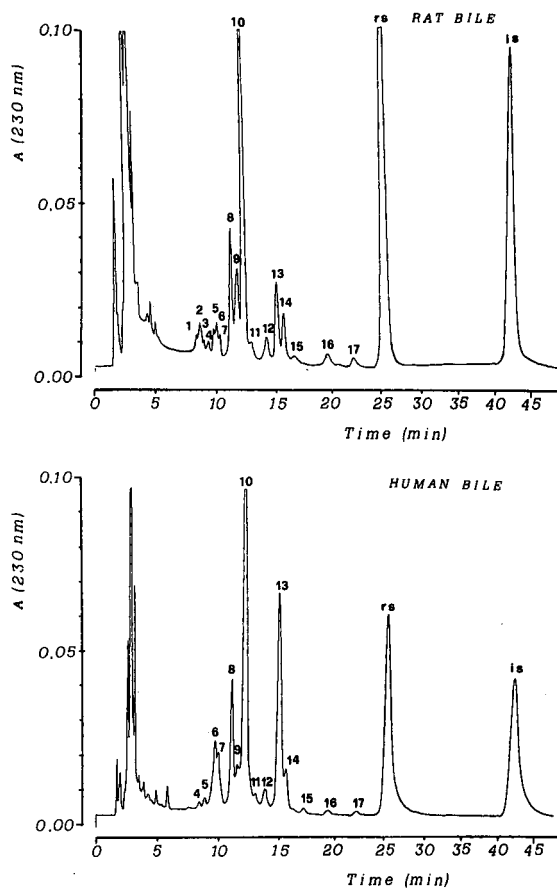


Fig. 2. HPLC separation of the molecular species of 1,2-diradylglycerobenzoates derived from phosphatidylcholine of rat bile and human bile under the analytical conditions described under Experimental. The identification of the molecular species corresponding to each peak is reported in Table II; rs is the peak relative to distearoylphosphatidylcholine and is that relative to 1,2-diarachidine.

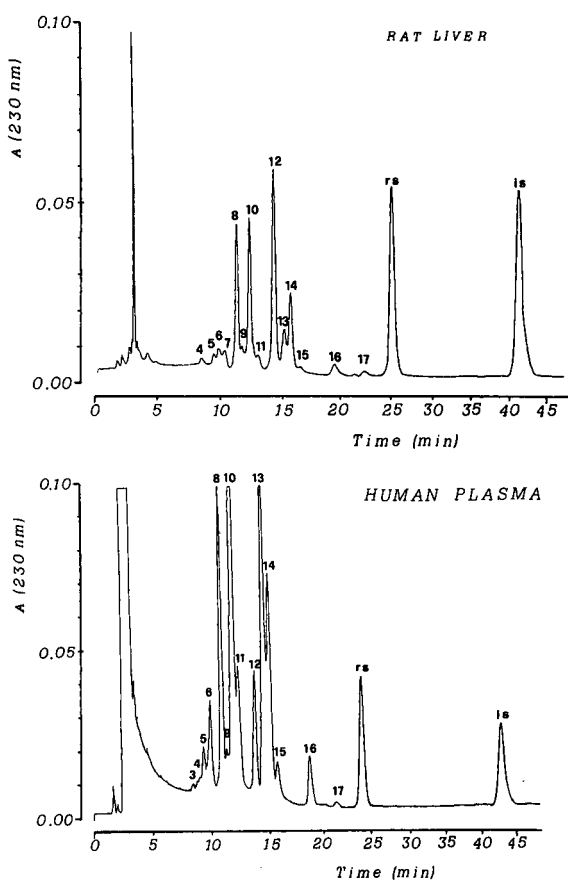


Fig. 3. HPLC separation of the molecular species of the 1,2-diradylglycerobenzoates derived from phosphatidylcholine of rat liver and human plasma under the analytical conditions described under Experimental. The identification of the molecular species corresponding to each peak is reported in Table II; rs is the peak relative to distearoylphosphatidylcholine and is that relative to 1,2-diarachidine.

TABLE I

CAPACITY FACTORS ( $k'$ ), RELATIVE RETENTION TIMES (RRT) AND HYDROPHOBIC CARBON NUMBERS (HCN) OBTAINED WITH STANDARD MIXTURES OF PHOSPHATIDYLCHOLINE MOLECULAR SPECIES

Molecular species	Degree of unsaturation	$k'$	RRT <sup>a</sup>	HCN
14:0-14:0	0	5.395	0.220	28.00 <sup>b</sup>
16:0-16:0	0	9.581	0.364	32.00 <sup>b</sup>
18:0-18:0	0	16.674	0.608	36.00 <sup>b</sup>
20:0-20:0	0	27.868	1.000	40.00 <sup>b</sup>
16:0-18:1	1	9.450	0.362	31.96 <sup>c</sup>
18:0-18:1	1	12.604	0.468	33.96 <sup>c</sup>
16:0-18:2	2	7.516	0.295	30.39 <sup>c</sup>
18:0-18:2	2	9.901	0.375	32.39 <sup>c</sup>
18:1-18:2	3	7.170	0.283	30.02 <sup>c</sup>
16:0-20:4	4	6.849	0.270	29.61 <sup>c</sup>
18:0-20:4	4	8.844	0.341	31.61 <sup>c</sup>

<sup>a</sup> RRT was calculated by dividing the retention time of each species by the retention time of the 20:0-20:0 species (41.8 ± 0.87 min).

<sup>b</sup> Total number of hydrophobic carbon atoms in the fatty acyl side-chains.

<sup>c</sup> Calculated by the relationship  $HCN = 18.218 \log RRT + 39.978$ , which was obtained by the linear regression of  $\log RRT$  vs. the total number of hydrophobic carbon atoms in the fatty acyl side-chains of the disaturated molecular species.

in Table I. Table I also shows the HCN values for unsaturated molecular species as calculated by the linear regression of HCN vs.  $\log RRT$  reported in the footnote.

The quantitative aspects of this method were studied without assumptions about the yield of either enzymatic hydrolysis or the benzoylation reaction. The objective evaluation of the quantitative results was realized by the addition of two analytical standards during the preparation of the diacylglycerobenzoate derivatives. Specifically, at the beginning of the procedure, to the phospholipid sample was added a known amount of the molecular species distearoylphosphatidylcholine that had the characteristics of an internal standard. This standard was virtually absent in the samples under consideration (below 0.2% of the molecular species distribution in many unspiked samples analysed) and gave a completely resolved chromatographic peak. The distearoylphosphatidylcholine produced

an amount of 1,2-distearine related to the yield of enzymatic hydrolysis. However, its peak area was proportional to the amount of phosphatidylcholine converted into diacylglycerobenzoate throughout the procedure. To calculate the yield of the enzymatic hydrolysis, we added, after the hydrolysis a known amount of 1,2-diarachidine, a diacylglycerol species that could not be derived from the sample. Indeed, 1,2-diarachidine was used as an internal standard for calculating the amount of 1,2-distearine formed. This allowed us to verify that the yield of enzymatic hydrolysis, which had been reported to proceed near to completion (yield 98.6%) [25], was actually much lower ( $88.0 \pm 6.7\%$ , as determined in twelve separate experiments). This difference, which was probably explained by changes in the quality of the enzyme or the purity of the substrate, demonstrated the importance in the use of distearoylphosphatidylcholine as internal standard of taking into account the actual degree of hydrolysis. Another observation that emphasized the importance of the internal standard was derived from a comparison of replicate samples. In many instances, even if the amounts of phospholipids calculated with the internal standard (distearoylphosphatidylcholine) were in good agreement, the absolute areas of the peaks were clearly different. A possible explanation was provided by experiments with mixtures of pure molecular species of diacylglycerols. In these experiments, the yield of benzoylation, which had been reported to be quantitative [26], was found to be affected by the presence of moisture, alcohols and salts in the reaction medium (data not shown).

The possibility that differences in the degree of unsaturation of the molecular species affected the determination was ruled out by comparing the calibration graphs (peak area vs. amount of molecular species) of three species with different degrees of unsaturation (dipalmitoyl-, palmitoyloleoyl- and palmitoyllinoleoylphosphatidylcholine). These graphs were linear over a wide range of amounts and had similar slopes (data not shown). This was in agreement with the findings of Snyder and Kirkland [27], who reported similar molar absorptivity values for saturated and unsaturated diacylglycerol derivatives. These facts indicated that the peak areas did not need any specific correction for calculating either the distribution or amount of molecular species.

TABLE II  
PERCENTAGE DISTRIBUTION OF MOLECULAR SPECIES OF PHOSPHATIDYLCHOLINE IN HUMAN BILE AND IN SAMPLES OF RAT BILE, LIVER AND PLASMA SAMPLES

The values reported represent the mean  $\pm$  S.D. of three separate determinations on each sample.

No.	Molecular species	Human bile	Rat bile	Rat liver	Human plasma
1	16:1-20:4	n.d. <sup>a</sup>	0.7 $\pm$ 0.24	n.d.	n.d.
2	16:1-16:1	n.d.	2.8 $\pm$ 0.38	n.d.	n.d.
3	14:0-20:4	n.d.	0.7 $\pm$ 0.17	n.d.	n.d.
4	16:1-18:2	0.5 $\pm$ 0.12	0.7 $\pm$ 0.18	n.d.	0.4 $\pm$ 0.12
5	14:0-18:2	0.7 $\pm$ 0.09	1.8 $\pm$ 0.11	1.3 $\pm$ 0.10	2.7 $\pm$ 0.16
6	16:0-22:6	9.7 $\pm$ 0.61	3.4 $\pm$ 0.21	2.2 $\pm$ 0.14	4.6 $\pm$ 0.22
	16:0-18:3				
7	18:1-20:4	3.2 $\pm$ 0.34	1.0 $\pm$ 0.22	0.6 $\pm$ 0.16	n.d.
8	16:0-20:4	9.9 $\pm$ 0.57	10.1 $\pm$ 0.79	17.1 $\pm$ 1.01	12.7 $\pm$ 0.86
9	18:1-18:2	3.8 $\pm$ 0.25	8.1 $\pm$ 0.51	1.3 $\pm$ 0.16	0.5 $\pm$ 0.12
10	16:0-18:2	44.1 $\pm$ 2.88	46.9 $\pm$ 3.23	19.9 $\pm$ 1.28	28.1 $\pm$ 1.43
11	16:0-20:3	0.5 $\pm$ 0.09	0.3 $\pm$ 0.10	1.1 $\pm$ 0.10	8.4 $\pm$ 0.72
12	18:0-20:4	1.4 $\pm$ 0.12	4.1 $\pm$ 0.18	29.8 $\pm$ 1.52	6.3 $\pm$ 0.42
13	16:0-18:1	20.6 $\pm$ 1.06	11.3 $\pm$ 0.77	8.3 $\pm$ 0.46	18.9 $\pm$ 0.95
14	18:0-18:2	3.7 $\pm$ 0.14	4.6 $\pm$ 0.21	14.3 $\pm$ 0.77	12.1 $\pm$ 0.99
15	18:0-20:3	0.3 $\pm$ 0.10	0.3 $\pm$ 0.10	0.6 $\pm$ 0.10	1.8 $\pm$ 0.10
16	18:0-18:1	0.8 $\pm$ 0.12	1.5 $\pm$ 0.20	2.6 $\pm$ 0.18	3.7 $\pm$ 0.24
17	20:0-18:2	0.6 $\pm$ 0.10	1.7 $\pm$ 0.12	1.1 $\pm$ 0.08	n.d.

<sup>a</sup> n.d. = < 0.2%.

Table II reports the distribution of molecular species obtained for samples of rat bile and liver and human bile and plasma by HPLC determination (run in triplicate). The average relative standard deviation (R.S.D.) was *ca.* 11%. However, if

we excluded the contribution given by species which represented less than 1% of the distribution, the R.S. D. had a more acceptable value of 6%, without appreciable differences due to the type of sample.

The molecular species distributions determined

TABLE III  
COMPARISON BETWEEN MEAN FATTY ACID DISTRIBUTION DEDUCED FROM MOLECULAR SPECIES COMPOSITION DETERMINED BY HPLC AND THAT FOUND BY GC ANALYSIS OF FATTY ACID METHYL ESTERS

Fatty acid	Rat bile		Human bile		Rat liver		Human plasma	
	HPLC	GC	HPLC	GC	HPLC	GC	HPLC	GC
14:0	1.2	1.1	0.4	0.4	0.6	1.2	1.4	1.0
16:0	36.3	36.9	42.4	44.2	24.3	21.9	36.3	36.3
16:1	3.4	2.9	0.2	1.2	n.d. <sup>a</sup>	0.5	0.2	0.8
18:0	5.3	6.0	3.1	3.6	23.5	22.9	11.9	13.2
18:1	11.0	10.9	14.3	15.8	6.4	7.2	11.5	13.5
18:2	31.9	32.4	26.3	24.7	18.8	17.3	21.9	19.9
18:3	0.8	1.0	2.4	0.5	0.6	0.4	1.1	0.9
20:0	0.8	0.2	0.3	0.3	0.5	0.3	n.d.	0.2
20:3	0.3	0.2	0.4	0.9	0.9	0.7	5.1	4.6
20:4	8.2	7.9	7.3	6.8	23.7	26.6	9.5	8.8
22:6	0.8	0.5	2.4	1.6	0.6	1.0	1.1	1.0

<sup>a</sup> n.d. = < 0.2%.



TABLE IV

COMPARISON BETWEEN QUANTITATIVE RESULTS FOR PHOSPHATIDYLCHOLINE BY HPLC (SUM OF ALL MOLECULAR SPECIES) AND GC OR LIPID PHOSPHORUS DETERMINATIONS

Results are reported as mean  $\pm$  S.D. of three separate determinations on each sample.

Sample	Units	HPLC	GC	Lipid phosphorus
Human bile	mg/ml	4.0 $\pm$ 0.25	3.9 $\pm$ 0.22	3.8 $\pm$ 0.23
Rat bile	mg/ml	0.4 $\pm$ 0.03	0.4 $\pm$ 0.02	0.4 $\pm$ 0.02
Rat liver	mg/g	9.9 $\pm$ 0.87	10.5 $\pm$ 0.54	9.5 $\pm$ 0.39
Human plasma	mg/ml	0.7 $\pm$ 0.04	0.7 $\pm$ 0.03	0.7 $\pm$ 0.03

by the present HPLC method were validated by comparison between the fatty acyl composition deduced from the HPLC distribution and that found by GC determination of fatty acid methyl esters. The results of this comparison, shown in Table III, indicate that, for the major fatty acids, the difference between the theoretical and experimental proportions is 7.2% of the value found by GC. This value can be considered acceptable as it is only slightly higher than the average R.S.D. found in replicate analyses.

The quantitative results were validated by comparison of the amounts determined by HPLC with either GC or lipid phosphorus determinations. These results, reported in Table IV, did not show significant differences. The quantitative result was also verified by the use of standard mixtures of molecular species, which indicated agreement between the theoretical and found values to within  $\pm$  5.5%.

The clean-up of the derivative with a diatomaceous earth cartridge also contributed to obtaining these results. This step eliminated any residue of reagents and gave chromatograms with a stable baseline and without spurious peaks.

In conclusion, the use of the analytical standard but also with modifications of both sample preparation and chromatographic separation of benzoate derivatives of diradylglycerobenzoate allowed a reliable determination of both the qualitative and quantitative compositions of molecular species of phosphatidylcholines derived from liver, bile and plasma extracts.

#### ACKNOWLEDGEMENTS

The expert technical assistance of Mrs. Tiziana Marinelli is gratefully acknowledged. This investi-

gation was partially supported by the Progetto Finalizzato Invecchiamento of the National Research Council of Italy (Grant No. 91.00466.PF40).

#### REFERENCES

- 1 N. A. Porter, R. A. Wolf and J. R. Nixon, *Lipids*, 14 (1979) 20–24.
- 2 F. B. Jungalwala, V. Hayssen, J. M. Pasquini and R. H. McCluer, *J. Lipid Res.*, 20 (1979) 579–587.
- 3 B. J. Compton and W. C. Purdy, *J. Liq. Chromatogr.*, 3 (1980) 1183–1194.
- 4 C. G. Crawford, R. D. Plattner, D. J. Sessa and J. J. Rackis, *Lipids*, 15 (1980) 91–94.
- 5 M. Smith and F. B. Jungalwala, *J. Lipid Res.*, 22 (1981) 697–704.
- 6 G. M. Patton, J. M. Fasulo and S. J. Robins, *J. Lipid Res.*, 23 (1982) 190–196.
- 7 A. Cantafora, A. Di Biase, D. Alvaro, M. Angelico, M. Marin and A. F. Attili, *Clin. Chim. Acta*, 134 (1983) 281–295.
- 8 A. Cantafora, M. Cardelli and R. Masella, *J. Chromatogr.*, 507 (1990) 339–349.
- 9 M. Smith, P. Monchamp and F. B. Jungalwala, *J. Lipid Res.*, 22 (1981) 714–719.
- 10 J. Y.-K. Hsieh, D. K. Welch and J. C. Turcotte, *Lipids*, 16 (1981) 761–763.
- 11 J. Y.-K. Hsieh, D. K. Welch and J. G. Turcotte, *J. Chromatogr.*, 208 (1981) 398–403.
- 12 A. D. Postle, *J. Chromatogr.*, 415 (1987) 241–251.
- 13 M. Batley, N. H. Packer and J. W. Redmond, *J. Chromatogr.*, 198 (1980) 520–525.
- 14 Y. Nakagawa and L. A. Horrocks, *J. Lipid Res.*, 24 (1983) 1268–1275.
- 15 M. L. Blank, M. Robinson, V. Fitzgerald and F. Snyder, *J. Chromatogr.*, 298 (1984) 473–482.
- 16 H. Takamura, H. Narita, R. Urade and M. Kito, *Lipids*, 21 (1986) 356–361.
- 17 M. Schlame, H. Rabe, B. Rustow and D. Kunze, *Biochim. Biophys. Acta*, 958 (1988) 493–496.
- 18 P. V. Subbaiah and H. Monshizadegan, *Biochim. Biophys. Acta*, 963 (1988) 445–455.
- 19 M. L. Blank, E. A. Cress, V. Fitzgerald and F. Snyder, *J. Chromatogr.*, 508 (1990) 382–385.

- 20 P. V. Subbaiah and P. H. Pritchard, *Biochim. Biophys. Acta*, 1003 (1989) 145–150.
- 21 C. C. Akoh and R. S. Chapkin, *Lipids*, 25 (1990) 613–617.
- 22 W. W. Christie, *Lipid Analysis*, Pergamon Press, Oxford 2nd ed., 1982, p. 101.
- 23 J. Folch, M. Lees and G. M. Stanley *J. Biol. Chem.*, 226 (1957) 497–509.
- 24 E. L. Krug and C. Kent, *Methods Enzymol.*, 72 (1981) 347–351.
- 25 J. J. Myher and A. Kuksis. *Can. J. Biochem. Cell. Biol.*, 62 (1984) 352–362.
- 26 M. L. Blank, E. A. Cress, T.-C. Lee, N. Stephens, C. Piantadosi and F. Snyder, *Anal. Biochem.*, 133 (1983) 433–436.
- 27 L. R. Snyder and J. J. Kirkland, *Introduction to Modern Liquid Chromatography*, Wiley, New York, 2nd ed., 1979, pp. 733–734.

# Determination of benzene metabolites in urine of mice by solid-phase extraction and high-performance liquid chromatography

Harald Schad\*, Freya Schäfer, Lothar Weber and Hans Joachim Seidel

*Institut für Arbeits- und Sozialmedizin, Universität Ulm, Albert-Einstein-Allee 11, D-7900 Ulm (Germany)*

---

## ABSTRACT

A method was developed for quantitative measurement of *trans,trans*-muconic acid, catechol, hydroquinone and phenol in urine. Hydrolysis of esterified and glucuronized phenolic compounds was effected by specific enzymes. The hydrolysed mixture was purified and separated by solid-phase extraction with an anion exchanger, followed by extraction with diethyl ether. By using a clean-up procedure the natural background from mouse urine could be reduced, so that the detection limit of the metabolites was in the range 3–60 mg/l. Optimization of the chromatographic conditions resulted in a short high-performance liquid chromatography analysis time. Phenol had the longest retention time of about 10 min. The clean-up procedure could also be used for phenylmercapturic acid, an additional benzene metabolite, but for sensitive high-performance liquid chromatographic detection of phenylmercapturic acid other conditions are necessary.

---

## INTRODUCTION

Benzene is an important organic chemical, widely used in industry. Chronic exposure to benzene can cause leukaemia in humans, and it is a carcinogen at many organs in animals [1,2]. In the body, benzene is metabolized by the microsomal cytochrome P-450 monooxygenase system into benzene epoxide. This benzene epoxide is metabolized in three different pathways which end in excretion of *trans,trans*-muconic acid, phenylmercapturic acid and different phenols. Various techniques have been reported for the separation, quantitation and identification of benzene metabolites to elucidate the chemical pathogenesis of benzene toxicity. Most of the described procedures could detect only single metabolites. Gad El-Karim *et al.* [3] found a high-performance liquid chromatography (HPLC) method able to analyse the four benzene metabolites in the urine of mice, but the retention times were quite long. Sabourin *et al.* [4] used HPLC too, but worked with radiolabelled benzene. This is not possible in most laboratory environments. In partic-

ular, it is not suitable for analyses in human monitoring (which is important for occupational medicine). This publication describes a procedure for the identification of *trans,trans*-muconic acid, catechol, hydroquinone and phenol from the urine of mice. Using solid-phase extraction the background of the chromatograms was reduced and therefore the analysis time was considerable shorter.

## MATERIALS AND METHODS

### Chemicals

Methanol was supplied by LAB-SCAN and *trans,trans*-muconic acid by Fluka. All other chemicals were from Merck. All chemicals were of the highest purity available. For hydrolysis, three enzymes were used:  $\beta$ -glucuronidase/arylsulphatase (Merck, 4114), arylsulphatase (Sigma, S 1629) and  $\beta$ -glucuronidase (Boehringer, 127051).

Phosphate solutions were prepared from an aqueous 5 mmol/l  $K_3PO_4$  solution which was treated with concentrated phosphoric acid to pH 3.4 and pH 7.

### Urine source

Groups of 16 female BDF-1 mice weighing 20–25 g were housed in metabolism cages designed for urine collection. Animal rooms were maintained at 24°C with a relative humidity of 50%. Rooms were on a 12-h light–dark cycle. Water was provided *ad libitum*. During the inhalation period no food was present in the cages. The mice were exposed to 300 ppm benzene for 6 h a day, 5 days a week. The urine (300 ppm urine) was collected for 24 h in phycoerythrin (PE)-coated vials containing 30 mg of ascorbic acid to avoid oxidation of urine. Urine was stored at –20°C until analysis.

### Determination of urinary benzene metabolites

**Hydrolysis.** A 0.125-ml aliquot of mice urine was diluted with water to 4 ml and adjusted to pH 4.5 with ascorbic acid. The diluted urine was treated with three enzymes:

Sample 1: 0.0125 ml of  $\beta$ -glucuronidase/arylsulphatase (Merck, 4114).

Sample 2: 0.0125 ml of arylsulphatase (Sigma, S 1629).

Sample 3: 0.0125 ml of  $\beta$ -glucuronidase, prediluted with water (1:6, v/v) (Boehringer, 127051).

Hydrolysis was performed at 37°C for 48 h. This hydrolysis procedure is not necessary for unconjugated metabolites.

Sample 4: urine was thawed at room temperature, diluted, acidified and applied to the anion exchanger.

### Separation by anion exchanger

After hydrolysis of urine, 4 ml of the samples were applied to an anion exchanger. The anion exchanger was a Bond Elut extraction cartridge filled with 500 mg of SAX sorbent (Analytichem International) previously conditioned with 3 ml of methanol and 3 ml of distilled water. After application of the urinary samples, the cartridge was washed with 3 ml phosphate solution (pH 7) to elute the fraction of phenols (I). The next eluent was 3 ml of 0.5 M aqueous sulphuric acid for the *trans,trans*-muconic acid fraction (II).

### Ether extraction

Ether extraction was performed at a pH less than 3 after acidification of the phenol fraction (I) with concentrated hydrochloric acid. Each fraction was treated separately. The fractions were vortexed

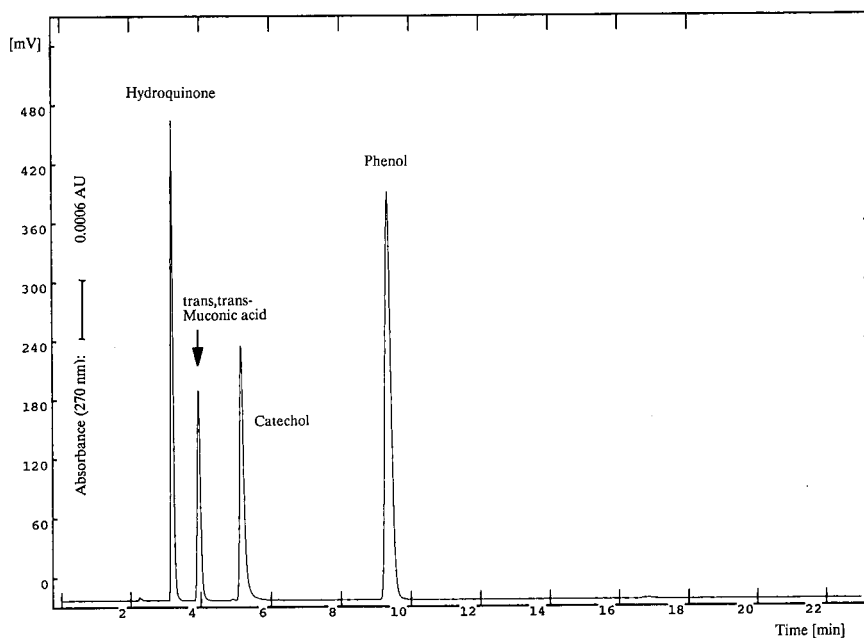


Fig. 1. Chromatogram of a standard solution of catechol (90 mg/l), hydroquinone (186 mg/l), phenol (300 mg/l) and muconic acid (7.5 mg/l).

three times with 5 ml of diethyl ether. The ether layers were removed, combined and evaporated to dryness at 30°C and 400 hPa and the residue dissolved in 1 ml of 1% aqueous phosphoric acid. A 20- $\mu$ l volume was injected for HPLC analysis.

#### Chromatographic conditions

Analysis was carried out by HPLC with an ODS column (250  $\times$  4.6 mm I.D.) filled with Nucleosil ODS, 5  $\mu$ m particle size (Bischoff). The detector (SM 4000, LDC Analytical) was set at 270 nm and

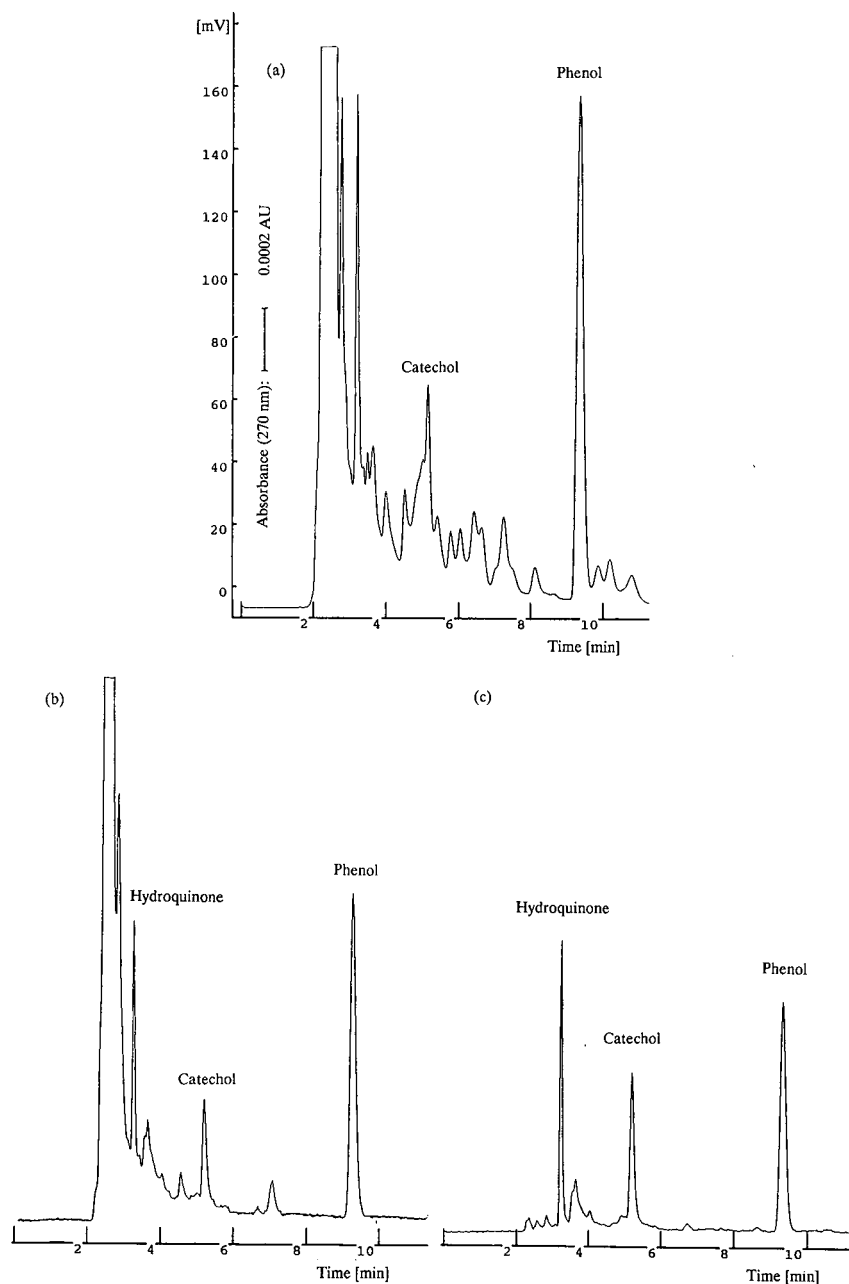


Fig. 2. Chromatograms of 300 ppm urine (a) after hydrolyzation, (b) after solid-phase extraction (fraction I), and (c) after evaporation (fraction I).

0.01 AUFS. The eluent was a solution of pH 3.4 phosphate solution–methanol (70:30, v/v). The detector was connected to AXXIOM integrating software.

With a flow-rate of 1 ml/min the retention time of hydroquinone was 3.2 min, of *trans,trans*-muconic acid 3.9 min, of catechol 5.2 min, and of phenol 9.3 min. The duration of an analytical cycle was 45 min.

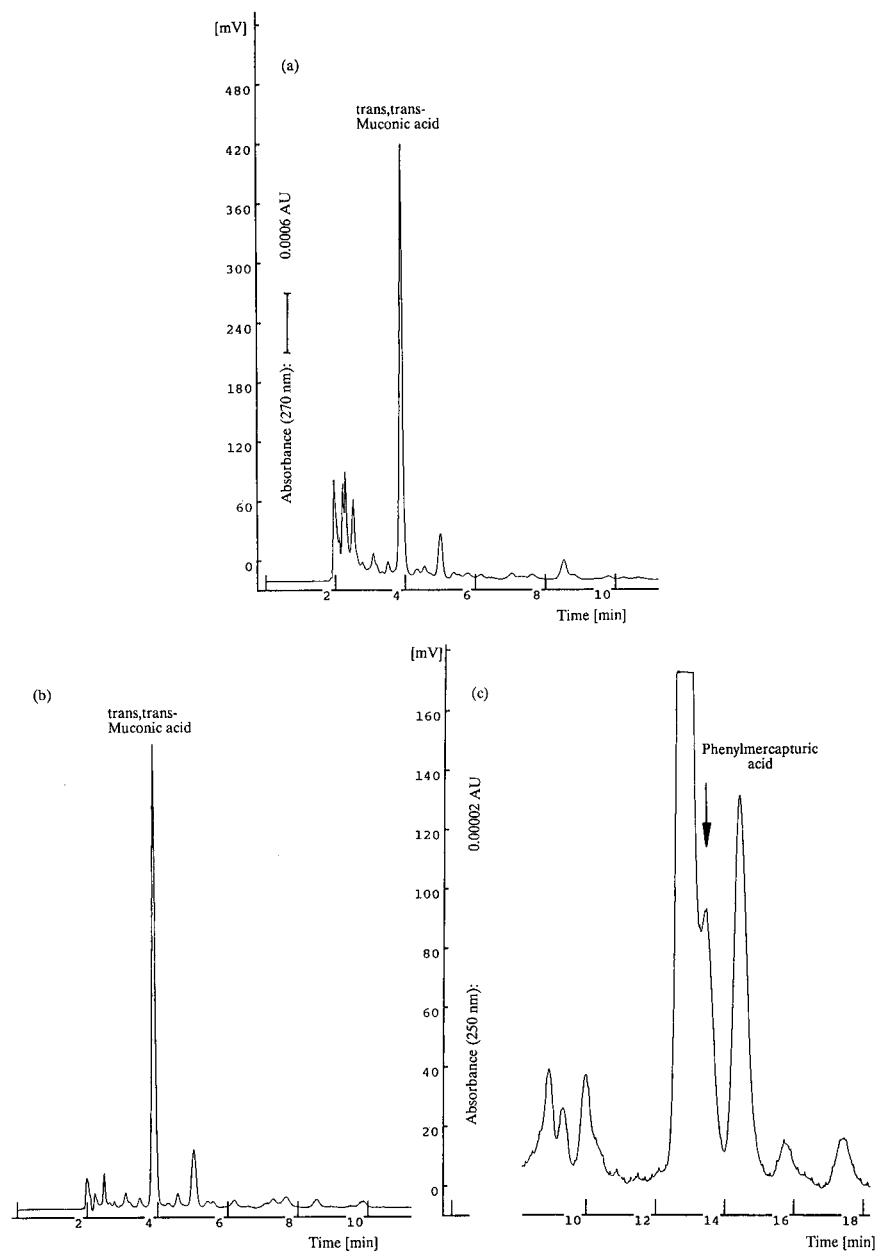


Fig. 3. Chromatograms of 300 ppm urine (a) after solid-phase extraction (fraction II), (b) after evaporation (fraction II) and (c) after evaporation at a wavelength of 250 nm for detection of phenylmercapturic acid.

## RESULTS AND DISCUSSION

We tried to establish an HPLC method which enables the simultaneous identification of four benzene metabolites in urine. We found the optimum HPLC conditions to be an ODS column and an isocratic solvent of methanol and phosphate solution. The retention time of *trans,trans*-muconic acid could be influenced by changing the pH of the solvent. An increase in the pH from 1 to 7 reduces the retention time from 7 to 2 min. Under the conditions mentioned in the Materials and Methods section separation of the four metabolites was optimized (Fig. 1). The advantage was that the retention time of phenol, the last metabolite in the chromatogram, was around 10 min and this therefore guaranteed a short analysis time [3].

For the isolation of benzene metabolites from urine, a clean-up procedure was necessary to discriminate sufficiently between natural background and metabolite signals (Fig. 2a). The purification embraced a solid-phase extraction (anion exchanger) and a liquid-liquid extraction with diethyl ether. The SAX column separated *trans,trans*-muconic acid from phenols. The *trans,trans*-muconic acid fraction could be injected directly into the HPLC system, because ether extraction does not significantly improve the chromatogram (Fig. 3a and b). However extraction with diethyl ether had the advantage that the *trans,trans*-muconic acid fraction could be concentrated if necessary. For the phenol fraction (I) the ether extraction was indispensable, because there was an important background reduction, especially in the neighbourhood of the hydroquinone signal (Fig. 2b and c).

The detection limits ( $3 \times$  signal-to-noise ratio) of the benzene metabolites are: catechol 7 mg/l, hydro-

quinone 60 mg/l, phenol 36 mg/l and *trans,trans*-muconic acid 3 mg/l.

By using enzymes it was possible to differentiate between conjugated (glucuronides and sulphate esters) and unconjugated metabolites. Nevertheless, the *trans,trans*-muconic acid peak was depressed when using enzymes and the rate of recovery was reduced below 50%. Since *trans,trans*-muconic acid in the urine of mice is not conjugated [3], the acid could be detected using a non-enzymatic method. Overloading of the 500-mg SAX column occurred when using 1 ml of 300 ppm urine, because *trans,trans*-muconic acid was then also found in the phenol fraction (I).

Using different amounts of native mice urine (1, 0.5, 0.25 ml) the recovery rates for benzene metabolites showed considerable variations. This problem needs further investigation.

In addition to the four benzene metabolites, phenylmercapturic acid has a remarkable role in benzene metabolism. This acid from the glutathione pathway could be isolated using the same clean-up procedure as for *trans,trans*-muconic acid. However, the HPLC method used was not sensitive enough, because there was an unknown signal in the chromatogram which interfered with the phenylmercapturic acid signal (Fig. 3c). There will be a further publication dealing with this problem.

## REFERENCES

- 1 M. Aksoy, *Am. J. Ind. Med.*, 7 (1985) 395-402.
- 2 C. Maltoni, A. Ciliberti, G. Cotti, B. Conti and F. Belpoggi, *Environ. Health Perspect.*, 82 (1989) 109-124.
- 3 M. M. Gad El-Karim, V. M. Sadagopa Ramanujam and M. S. Legator, *Xenobiotica*, 15 (1985) 211-220.
- 4 P. J. Sabourin, W. E. Bechtold, L. S. Birnbaum, G. Lucier and R. F. Henderson, *Toxicol. Appl. Pharmacol.*, 94 (1988) 128-140.





## Short Communication

# Determination of 5-hydroxymethylfurfural by ion-exclusion chromatography with UV detection

Hie-Joon Kim\* and Michelle Richardson

Food Engineering Directorate, US Army Natick Research, Development and Engineering Center, Kansas Street, Natick, MA 01760 (USA)

### ABSTRACT

5-Hydroxymethylfurfural (HMF) was determined without interferences in juices, honey, syrup, tomato paste, grape juice concentrate and dehydrated pear by anion-exclusion chromatographic separation and UV detection at 285 nm. The samples were mixed with water, filtered and injected without extensive sample treatment, which is normally required in conventional spectrophotometric or reversed-phase high-performance liquid chromatographic methods. HMF at the 50 ppb level was determined with a signal-to-noise ratio of 6. The recovery of HMF added to honey was 98% at the 10 ppm level and 91% at 30 ppm.

### INTRODUCTION

5-Hydroxymethylfurfural (HMF) is the end product of acid-catalyzed hexose dehydration [1] and is often used as an index of deteriorative changes in tomato paste [2], honey [3] and fruit products [4–6]. Its accurate determination in fruit products is therefore important. In honey, HMF is used as an indicator of adulteration with acid-converted invert syrups [7] or of a heating history.

Spectrophotometric methods have been used for many years for HMF [8–11]. The original Winkler method [8] involves toxic *p*-toluidine, and is complicated by uncertainty in the color measurement [10]. The AOAC method for honey relies on the reaction of hydrogensulphite with HMF and has not been applied to other foods or citrus products. Experimental errors are expected if other compounds that absorb at 284 nm and react with hydrogensulphite are present at appreciable concentrations.

Recently, several reversed-phase (RP) high-performance liquid chromatographic (HPLC) methods

have been published [12–14] using UV detection at 280–285 nm. Jeuring and Koppers [12] determined HMF in spirits and honey with minimum sample treatment. Extensive sample treatment [precipitation with potassium hexacyanoferrate(III), Carrez I, and zinc sulphate, Carrez II, centrifugation, and filtration] was needed for citrus juices [13] and tomato products [14]. Lee *et al.* [13] added another step, namely elution with ethyl acetate from a C-18 cartridge following washing with hexane, to remove contaminants in orange juice, and reported a detection limit of 50 ppb<sup>a</sup>.

We have been using ion-exclusion chromatography (IEC) with photodiode-array (PDA) detection to monitor changes in food constituents taking place as a result of high-temperature/short-time processing. We noticed that HMF is eluted late from the anion-exclusion column, free from any interference, even if a complex food extract is injected without the precipitation step. Consequently, we

<sup>a</sup> Throughout the article the American billion (10<sup>9</sup>) is meant.

describe in this paper the advantages of the IEC method over the RP-HPLC method, and demonstrate that HMF in complex foods and beverages can be determined by IEC with a high specificity and sensitivity without extensive sample clean-up.

## EXPERIMENTAL

### *Sample treatment*

All juice, juice drink, honey, syrup and tomato paste samples were purchased from a local store. Grape juice concentrate was obtained from a manufacturer. Freeze-dried pears are a component of Meal, Ready-to-Eat (MRE), a military ration.

Aseptically processed juice, honey or syrup samples were diluted tenfold with deionized water, filtered through a 0.45- $\mu$ m nylon 66 membrane filter (Alltech, Deerfield, IL, USA) and injected into either an IEC or a RP-HPLC system without further treatment. Tomato juice, orange juice and grape juice concentrate were diluted ten- or twentyfold with water, centrifuged for 2 min in a Brinkmann (Westbury, NY, USA) Model 5414 Eppendorf centrifuge if necessary, filtered and injected. Freeze-dried pears were homogenized with a twentyfold excess of water using Polytron (Brinkmann) and filtered as above.

### *Chromatographic analysis*

For IEC, an Alltech Model 325 metal-free pump was used to deliver 10 mM sulphuric acid eluent at a flow-rate of 0.8 ml/min. A Wescan anion-exclusion HS (sulphonated polystyrene-divinylbenzene) column (100  $\times$  4.6 mm I.D.) and an anion-exclusion guard cartridge (Wescan Instruments, Deerfield, IL, USA) were used. The sample was injected through a 20- $\mu$ l loop of a Rheodyne injector. The UV detector was either a Waters (Milford, MA, USA) Model 990 PDA detector or a Schoeffel Model SF770 variable-wavelength UV detector. When the PDA detector was used, the UV spectra were obtained in the wavelength range 190–350 nm every 6 s. The three-dimensional (3-D) data were stored in a NEC PowerMate 2 computer and manipulated to obtain a 3-D plot, a contour diagram, a chromatogram at 285 nm or a UV spectrum of a chromatographic peak. The wavelength of the Schoeffel detector was set at 285 nm. The signal obtained at the 0–0.01 absorbance range setting was fed into a Spectra-Physics Model 4270 integrator.

A Waters  $\mu$ Bondapak C<sub>18</sub> column (250  $\times$  4.6 mm I.D.) and an RP guard cartridge were used for RP-HPLC. A Rheodyne injector with a 50- $\mu$ l loop was used. The Waters Model 510 pump delivered acetonitrile–water (3:97) at a flow-rate of 1.6 ml/min. The Schoeffel detector was used at 285 nm.

A standard solution of HMF (Aldrich, Milwaukee, WI, USA) in deionized water was injected alternately with the samples and the peak heights were compared.

### *Recovery study*

Recovery of 10 and 30 ppm of HMF from honey was studied by both IEC and RP-HPLC. Six 2-g aliquots of honey were weighed into six 50-ml beakers. To two of these beakers 2.0 ml of deionized water were added (control). A 2.0-ml volume of 10 ppm HMF solution was added to two other beakers and 2.0 ml of 30 ppm HMF solution to the two remaining beakers. The contents were mixed with a spatula and left at room temperature for 5 min. Water (16 ml) was added to each beaker and the contents were mixed and filtered. The filtrate from the 30 ppm spiked sample was further diluted twofold before injection. Each filtrate was injected twice. The height of the HMF peak was compared with that of a 2 ppm standard HMF solution. The recovery experiment by the IEC method was repeated with honey a few days later. The recovery of 30 ppm HMF from orange juice was studied by the IEC method on another day.

## RESULTS AND DISCUSSION

We first observed elution of HMF from the IEC column, using a PDA detector, while analyzing heat-processed fruit samples. The spectrum of the compound that eluted relatively late from the column (4 min from a high-speed column) showed the characteristic double maxima (230 and 285 nm) of HMF. The compound was collected after the detector and analyzed by gas chromatography–mass spectrometry (GC–MS). The parent molecular weight of 126 and the typical electron impact fragments with  $m/z$  of 109, 97 and 69 for HMF were observed [15]. When authentic HMF was injected, it was eluted at the same retention time. Subsequently, IEC with fixed-wavelength detection at 285 nm was routinely used.

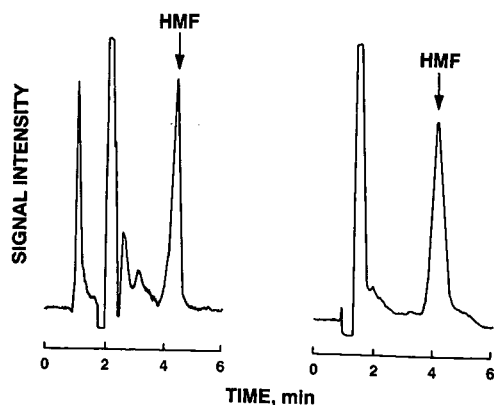


Fig. 1. Chromatograms of *ca.* 2 ppm of HMF in diluted honey (tenfold), obtained by (left) the RP-HPLC and (right) the IEC method. RP-HPLC: Waters  $\mu$ Bondapak  $C_{18}$  column ( $250 \times 4.6$  mm I.D.), acetonitrile–water (3:97) as eluent at a flow-rate of 1.6 ml/min. IEC: Wescan anion-exclusion/HS column ( $100 \times 4.6$  mm I.D.), 10 mM  $H_2SO_4$  as eluent at a flow-rate of 0.8 ml/min. UV detection at 285 nm.

HMF was eluted at *ca.* 4 min after injection in both RP-HPLC (long column, 1.6 ml/min) and IEC (short column, 0.8 ml/min). Fig. 1 shows HMF peaks corresponding to *ca.* 2 ppm in honey, diluted tenfold and injected without Carrez precipitation. Even though the chromatogram given by the IEC method is cleaner, there is also no interference in the

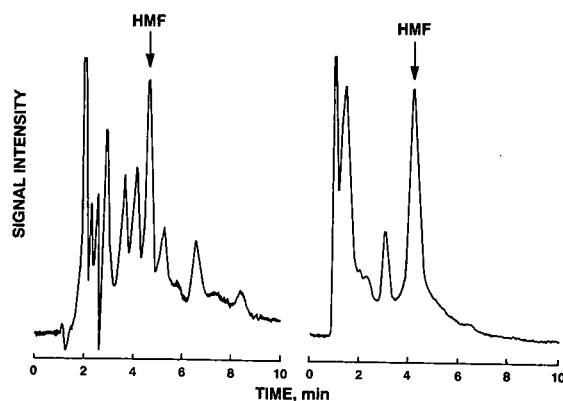


Fig. 2. Chromatograms of 10 ppm of HMF added to tomato juice and diluted tenfold, obtained by (left) the RP-HPLC and (right) the IEC method.

RP-HPLC method. On average, 21.5 and 19.4 ppm of HMF were obtained by the RP-HPLC and IEC methods, respectively (Table I, control). The recovery results in Table I show that the recovery of 10 and 30 ppm of HMF added to honey is satisfactory by both methods. The relative standard deviation of the recovery during the day was *ca.* 2% by the IEC method. When 30 ppm of HMF were added to the orange juice, 29.7 ppm were recovered by the IEC method. The recovery of 30 ppm of HMF on three different days, two from honey and one from orange juice, ranged from 91 to 99%.

The chromatogram for tomato juice obtained by the RP-HPLC method was much more complex, and quantitation of HMF was subject to an uncertainty because of the interfering peaks. Approximately 1 ppm of HMF in the juice was measured by the IEC method. Fig. 2 shows results obtained by both methods for tomato juice spiked with 10 ppm of HMF and diluted tenfold before injection. It appears that further sample treatment, such as Carrez precipitation, is needed for the RP-HPLC analysis [14]. The chromatogram on the right demonstrates that accurate determination of HMF without precipitation is possible by the IEC method. A similar chromatogram was obtained for tomato paste and 102 ppm of HMF was measured.

Lee *et al.* [13] noted that orange juice contains compounds that are eluted with the HMF by the RP-HPLC method. They used Carrez precipitation and elution with ethyl acetate from a  $C_{18}$  cartridge,

TABLE I

RECOVERY OF ADDED HMF FROM HONEY BY REVERSED-PHASE AND ION-EXCLUSION CHROMATOGRAPHY

Sample	RP-HPLC <sup>a</sup>		IEC <sup>b</sup>	
	Observed (ppm)	Recovered (ppm)	Observed (ppm)	Recovered (ppm)
Honey, control	21.5 (0.6)	—	19.4 (0.3)	—
Honey, 10 ppm spike	31.2 (0.6)	9.7 (0.3)	28.6 (0.4)	9.2 (0.2)
Honey, 30 ppm spike	50.0 (2.0)	28.5 (1.4)	47.6 (0.9)	28.2 (0.7)

<sup>a</sup> Average of four determinations with standard deviation in parentheses.

<sup>b</sup> Average of eight determinations with standard deviation in parentheses.

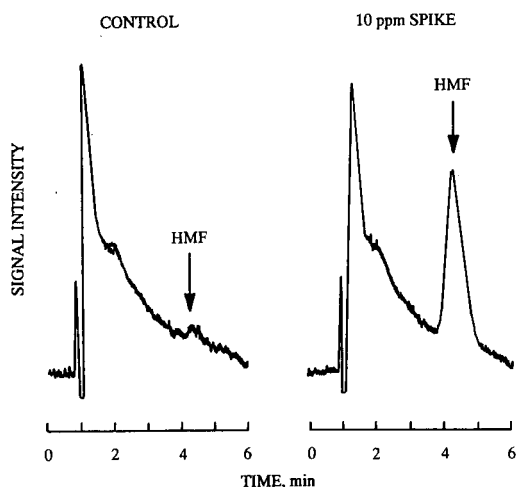


Fig. 3. Chromatograms of orange juice with (right) and without (left) addition of 10 ppm of HMF after twentyfold dilution, obtained by the IEC method.

following a hexane wash. The ethyl acetate had to be dried before chromatography. When orange juice (reconstituted from frozen juice) was diluted twentyfold with water, filtered and injected, the chromatogram shown on the left in Fig. 3 was obtained by the IEC method. The chromatogram was relatively clean around 4 min, and a small peak corresponding to about 0.05 ppm of HMF was observed (1 ppm in the juice). When the juice was spiked with 10 ppm of HMF and diluted twentyfold, a peak corresponding to 0.55 ppm, shown on the right, was obtained as expected. When the orange juice filtrate was analyzed by the RP-HPLC method using acetonitrile-water (3:97) as eluent, no significant interference was observed.

The method was applied to a variety of aseptically processed juice drinks, and HMF concentrations ranging from 2.0 to 19.4 ppm were obtained. The chromatograms were very clean, and no interference was observed with any samples tested. HMF was also observed without interference in syrup (12 ppm), grape juice concentrate (22 ppm) and dehydrated pears stored at 38°C for 1 year (34 ppm).

At the highest sensitivity setting of the UV detector (0–0.01 absorbance range), a signal-to-noise ratio of 6 was observed when 50 ppb HMF solution was injected. The peak height between 0 and 10 ppm was linear with a correlation coefficient of 0.99. The HMF solution was stable in water for

several hours at room temperature. The detector response was also very stable; therefore, automated analysis should be possible.

The IEC separation has been successfully used for the determination of weak acid anions, such as sulphite [16,17], nitrite [18–20] and ascorbic acid [21]. The polymeric resin of the IEC column is also widely used for carbohydrates. This paper demonstrates that a rapid and accurate determination of HMF, which is an important carbohydrate degradation product and a useful quality indicator in food and beverage products, is possible without extensive sample treatment when IEC is used with UV detection.

#### ACKNOWLEDGEMENTS

We thank Drs. Irwin Taub and Tom Yang for support and valuable discussions.

#### REFERENCES

- 1 P. E. Shaw, J. H. Tatum and R. E. Berry, *Carbohydr. Res.*, 5 (1967) 266.
- 2 B. S. Luh, S. Leonard and G. L. Marsh, *Food Technol.*, 12B (1958) 347.
- 3 B. S. Luh and P. J. Kamber, *Food Technol.*, 17 (1963) 105.
- 4 R. E. Berry and J. H. Tatum, *J. Agric. Food Chem.*, 13 (1965) 588.
- 5 H. S. Lee and S. Nagy, *Food Technol.*, 42, No. 11 (1988) 91.
- 6 J. W. White, Jr., I. Kushnir and M. H. Subers, *Food Technol.*, 18 (1964) 153.
- 7 J. W. White, Jr. and J. Siciliano, *J. Assoc. Off. Anal. Chem.*, 63 (1980) 7.
- 8 O. Winkler, *Z. Lebensm.-Unters.-Forsch.*, 102 (1955) 161.
- 9 S. Meydavi and Z. Berk, *J. Agric. Food Chem.*, 26 (1978) 282.
- 10 J. W. White, Jr., *J. Assoc. Off. Anal. Chem.*, 62 (1979) 509.
- 11 J. W. White, Jr., I. Kushnir and L. W. Doner, *J. Assoc. Off. Anal. Chem.*, 62 (1979) 921.
- 12 H. J. Jeuring and F. J. E. M. Kupperts, *J. Assoc. Off. Anal. Chem.*, 63 (1980) 1215.
- 13 H. S. Lee, R. L. Rouseff and S. Nagy, *J. Food Sci.*, 51 (1986) 1075.
- 14 S. Porretta and L. Sandei, *Food Chem.*, 39 (1991) 51.
- 15 W. Yeomans, personal communication.
- 16 H.-J. Kim, G. Y. Park and Y.-K. Kim, *Food Technol.*, 41, No. 11 (1987) 85.
- 17 H.-J. Kim, *J. Assoc. Off. Anal. Chem.*, 73 (1990) 216.
- 18 H.-J. Kim and Y.-K. Kim, *Anal. Chem.*, 61 (1989) 1485.
- 19 H.-J. Kim, *J. Chromatogr.*, 503 (1990) 466.
- 20 H.-J. Kim and K. R. Conca, *J. Assoc. Off. Anal. Chem.*, 73 (1990) 561.
- 21 H.-J. Kim, *J. Assoc. Off. Anal. Chem.*, 72 (1989) 681.

# Determination of inositol polyphosphates from human T-lymphocyte cell lines by anion-exchange high-performance liquid chromatography and post-column derivatization

Andreas H. Guse\* and Frank Emmrich

*Max-Planck-Society, Clinical Research Unit for Rheumatology/Immunology at the Institute for Clinical Immunology of the University, Schwabachanlage 10, D-8520 Erlangen (Germany)*

## ABSTRACT

The intracellular amounts of several inositol tris-, tetrakis- and pentakisphosphates and inositol hexakisphosphate were determined in resting and stimulated cells from human T-lymphocyte lines. The inositol polyphosphates were separated by anion-exchange high-performance liquid chromatography and were detected on-line by a recently developed post-column dye system. In the human T-lymphocyte cell line Jurkat, basal intracellular concentrations ranged between  $25 \pm 10$  pmol per  $10^9$  cells for inositol 1,4,5-trisphosphate to  $6380 \pm 355$  pmol per  $10^9$  cells for inositol hexakisphosphate. Similar basal concentrations were observed in the human T-lymphocyte cell line HPB.ALL, with the exception that inositol hexakisphosphate was approximately  $665 \pm 10$  pmol per  $10^9$  cells. Stimulation of the human T-lymphocyte cell line Jurkat via the T-cell receptor by a monoclonal antibody directed against the T-cell receptor-CD3 complex induced time-dependent changes in the intracellular concentrations of multiple inositol polyphosphate isomers, including inositol 1,3,4-trisphosphate, inositol 1,3,4,5-tetrakisphosphate, inositol 1,3,4,6-tetrakisphosphate, an as yet unidentified inositol tetrakisphosphate isomer, inositol 1,3,4,5,6-pentakisphosphate, inositol 1,2,3,4,6-pentakisphosphate and DL-inositol 1,2,4,5,6-pentakisphosphate. Inositol 1,4,5-trisphosphate increased only transiently after 5 min, whereas DL-inositol 1,4,5,6-tetrakisphosphate (determined as the enantiomeric mixture) increased after 20 min.

## INTRODUCTION

It is now widely accepted that inositol polyphosphates play an important role in the process of transmembrane signalling [1,2]. In particular, inositol 1,4,5-trisphosphate [ $\text{Ins}(1,4,5)\text{P}_3$ ] causes the release of  $\text{Ca}^{2+}$  from intracellular stores and the increased cytosolic  $\text{Ca}^{2+}$  concentration initiates a number of cell-type specific physiological responses. In this paper,  $\text{InsP}_2$ ,  $\text{InsP}_3$ ,  $\text{InsP}_4$ ,  $\text{InsP}_5$ ,  $\text{InsP}_6$  represent *myo*-inositol bis-, tris-, tetrakis-, pentakis- and hexakisphosphate with isomeric positioning of phosphate groups as indicated and assumed to be D-isomers.

$\text{Ins}(1,4,5)\text{P}_3$  has been described as playing a key part in the activation of T-lymphocytes [3]. These cells act as effector cells and are an important regu-

latory element directing the function of the immune system.

To measure changes in  $\text{Ins}(1,4,5)\text{P}_3$  and other inositol polyphosphate, most workers have used conventional anion-exchange separation and radioactive detection in samples from cells previously labelled with *myo*-[ $^3\text{H}$ ]inositol [4–6]. The disadvantages of these systems are: (i) the inability to measure real intracellular concentrations as labelling to isotopic equilibrium is not achieved in most systems; (ii) the discontinuous detection system (collecting of fractions, liquid scintillation counting) limits the separation efficiency; (iii) the lack of sensitivity for the on-line detection of *myo*-[ $^3\text{H}$ ]inositol phosphates by radioactivity detectors.

Two post-column systems for the detection of non-radioactively labelled phosphorylated com-

pounds have been published [7–10]. Although the first system was not sensitive enough for the determination of trace amounts of inositol phosphates (detection limit approximately 800 pmol InsP<sub>3</sub> per sample) [7,8], the second, the so-called “metal–dye detection” system [9,10] has already proved to be useful for the determination of the intracellular concentrations of inositol phosphates in HL-60 cells [11]. This post-column dye system, first described by Mayr [9], is based on the competition between anionic compounds eluting from the column and the dye 2-(4-pyridylazo)resorcinol for complex formation with Y<sup>3+</sup>. Although the dye–Y<sup>3+</sup> complex absorbs strongly at 520 nm, there is diminished absorption when the eluting anionic compounds compete for Y<sup>3+</sup> binding. Inverting the analogue signal from the detector then leads to chromatogram with “positive” peaks.

This paper reports the determination of basal intracellular concentrations of inositol polyphosphates in the human T-cell lines Jurkat and HPB.ALL using the metal–dye detection system. In response to stimulation of the T-cell receptor–CD3 complex, increases were observed in the intracellular concentrations of Ins(1,4,5)P<sub>3</sub>, Ins(1,3,4)P<sub>3</sub>, Ins(1,3,4,5)P<sub>4</sub>, Ins(1,3,4,6)P<sub>4</sub>, Ins(1,4,5,6)P<sub>4</sub> and/or Ins(3,4,5,6)P<sub>4</sub> (determined as the enantiomeric mixture), an additional undefined InsP<sub>4</sub> isomer, Ins(1,2,3,4,6)P<sub>5</sub> and Ins(1,3,4,5,6)P<sub>5</sub>. In contrast, the intracellular concentration of Ins(1,2,4,5,6)P<sub>5</sub> decreased with stimulation.

## EXPERIMENTAL

### Materials

Ins(1,3,4)P<sub>3</sub> was purchased from Calbiochem (Frankfurt, Germany). Ins(1)P<sub>1</sub>, Ins(1,4)P<sub>2</sub>, Ins(1,4,5)P<sub>3</sub>, Ins(1,3,4,5)P<sub>4</sub>, Ins(1,2,5,6)P<sub>4</sub>, Ins(1,4,5,6)P<sub>4</sub> and Ins(1,3,4,5,6)P<sub>5</sub> were from Boehringer Mannheim (Mannheim, Germany). InsP<sub>6</sub> and alkaline phosphatase were from Sigma (Taufkirchen, Germany). YCl<sub>3</sub> · 6H<sub>2</sub>O was purchased from Janssen (Nettetal, Germany). Hydrochloric acid and triethanolamine, both of analytical–reagent grade, were from Merck (Darmstadt, Germany). 2-(4-Pyridylazo)resorcinol was from Serva (Heidelberg, Germany). Doubly distilled water or Milli-Q water (Millipore–Waters, Eschborn, Germany) was used throughout the experiments. The monoclonal

antibody to CD3, OKT3, was purified from hybridoma supernatant on protein A–Sepharose. Ins(1,3,4,6)P<sub>4</sub> was obtained by phosphorylation of Ins(1,3,4)P<sub>3</sub> in a rat liver homogenate [12].

### *Culture of the human T-lymphocyte cell lines Jurkat and HPB.ALL*

The cells were cultured in RPMI-1640 medium (Gibco-BRL, Eggenstein, Germany) supplemented with 10% fetal calf serum, penicillin (100 U/ml), streptomycin (50 µg/ml), L-glutamine (300 mg/ml) and 4-(2-hydroxyethyl)-1-piperazineethanesulphonic acid (HEPES) (20 mM) at 37°C with 5% carbon dioxide in air. The cell density in flasks containing 200 ml of medium was between  $1.5 \cdot 10^5$  cells per ml of fresh culture and  $1.5 \cdot 10^6$  cells per ml of culture ready to be harvested.

### *Stimulation protocol and extraction of inositol phosphates*

The cells (approximately  $2 \cdot 10^8$ – $4 \cdot 10^8$  cells per 200 ml of medium) were harvested by centrifugation (6 min, 18°C, 450 g) and resuspended in 10 ml of fresh RPMI-1640 medium (as above) and were kept at 37°C for 10 min. Buffer (for control values) or OKT3 (final concentration 10 µg/ml) was then added for different periods of time. Two minutes before the end of the incubation period, the cells were pelleted (2 min, 450 g). The supernatant was decanted and the cells were lysed by the addition of 1 ml of ice-cold perchloric acid (10%, v/v). The perchloric acid extract was immediately vortex-mixed and freeze–thawed twice in liquid nitrogen. The perchloric acid extracts were left on ice for 30 min to extract the soluble inositol phosphates. Then the precipitated protein was removed by centrifugation (10 min, 8800 g) and the supernatant was titrated to pH 4–5 by the addition of potassium hydroxide solution (small volumes of the following concentrations were added successively: 7, 3.5, 1.75 and 0.875 M). The samples were left on ice for 30 min and then centrifuged to remove the potassium perchlorate precipitate (10 min, 8800 g).

### *Sample preparation for determination by high-performance liquid chromatography (HPLC)*

Nucleotides were removed from the samples by extraction with charcoal as described previously [11]. Directly before injection into the HPLC sys-

tem, the samples were filtered through disposable filters (0.45  $\mu\text{m}$ ; Schleicher and Schüll, Dassel, Germany). The solid-phase extraction method that was originally introduced with the metal-dye detection system [9] was not used for two reasons: (i) the inositol phosphates were extracted from the cell pellet so that no interference from salts or buffers from the medium was expected; (ii) to avoid the acid-catalysed migration of phosphate groups on the inositol ring [11].

#### *HPLC separation and determination by the metal-dye detection system*

The determination of the inositol phosphates was carried out with a Kontron Instruments HPLC system consisting of two pumps (Model 420), two micro-mixing chambers (Model 494) and a UV-visible detector (Model 430) equipped with two MonoQ columns (5  $\times$  0.5 cm; Pharmacia, Freiburg, Germany) in line. System control and data acquisition were performed with the computerized MT1-system/D450-software from Kontron Instruments (Munich, Germany).

The separation of inositol phosphates was achieved by an upward concave gradient as described previously [9]. The composition of the eluents was: A, 0.02 mM HCl–13.5  $\mu\text{M}$   $\text{YCl}_3$ ; B, 0.4 M HCl–21  $\mu\text{M}$   $\text{YCl}_3$ . The dye solution, C [350  $\mu\text{M}$  2-(4-pyridylazo)resorcinol, 1.6 M triethanolamine, pH 9.1], was pumped by a third HPLC pump (Beckman 110B, Munich, Germany) and mixed with the column eluate in a ratio of 1:2 by a micro-mixing chamber with a dead volume of 800  $\mu\text{l}$  (Model 494, Kontron Instruments). This modification was introduced to reduce the baseline noise and resulted in a better sensitivity than with a T-junction and a knitted coil. The detector was auto-zeroed at the start of each chromatogram. The absorbance was measured at 520 nm and the analogue signal inverted, baseline-subtracted and integrated by the MT1/D450-system.

#### *Semi-preparative isolation of $\text{InsP}_5$ isomers*

Phytic acid (0.2 g; Fluka, Buchs, Switzerland) was hydrolysed in 1.5 ml of sodium acetate solution (0.2 M, pH 4.0 with acetic acid) at 100°C for 6 h. Then a 50- $\mu\text{l}$  portion was diluted with 1 ml of doubly distilled water and separated by anion-exchange HPLC as described above. Peak 7 (Fig. 1A) was

collected, lyophilized and dissolved in 4.5 ml of doubly distilled water and a 100- $\mu\text{l}$  aliquot was rechromatographed (Fig. 1B). A 1.5-ml portion was then separated as above. Peaks 4–8 were collected, lyophilized and dissolved in 300  $\mu\text{l}$  of doubly distilled water. Aliquots (30  $\mu\text{l}$  diluted with 1 ml of doubly distilled water) were rechromatographed (Fig. 1C–G). The yields of purified  $\text{InsP}_5$  isomers were 1.2–2.4  $\mu\text{mol}$ .

## RESULTS

#### *Evaluation of the analytical system*

When carrying out the sample preparation procedure with a standard mixture of inositol pentakisphosphates and  $\text{InsP}_6$ , the recovery of all isomers was greater than 88% [mean  $94 \pm 5.2\%$  ( $n = 8$ )]. These experiments also confirmed published data [11] that there is no acid-catalysed migration of phosphate groups under such conditions. In addition, some samples from cells were spiked with DL- $\text{Ins}(1,2,3,4,5)\text{P}_5$  as an internal standard. Recoveries of about 96% indicate no loss due to catabolism of the sample, *e.g.* by acid-stable phosphatase activities.

By monitoring the column eluate at 260 nm without using the post-column dye system, three charcoal extractions were necessary to remove the nucleotides from cell samples. To rule out that any of the peaks were due to elution of nucleotides or other polyanionic compounds (*e.g.* polysulphated substances), control samples were treated as follows. First, HPLC separation with a wavelength setting of 260 nm without using the post-column dye system was used to detect the remaining nucleotides. It was found that the nucleotides were eluted before  $\text{Ins}(1,3,4)\text{P}_3$  and did not interfere with the detection of later eluting compounds. Secondly, control samples were treated with alkaline phosphatase. After adjusting the pH to 8 with triethanolamine, the samples were reacted with 12 U of alkaline phosphatase at 37°C for 24 h. Alkaline phosphatase treatment led to the disappearance of all peaks designated as inositol polyphosphates.

The linear regression analysis of the calibration graphs for several inositol polyphosphate isomers revealed  $r$  values  $> 0.99$  in the range of 50 pmol to 1.5 nmol (Table I). When relating the slope of the calibration graphs to the number of phosphate

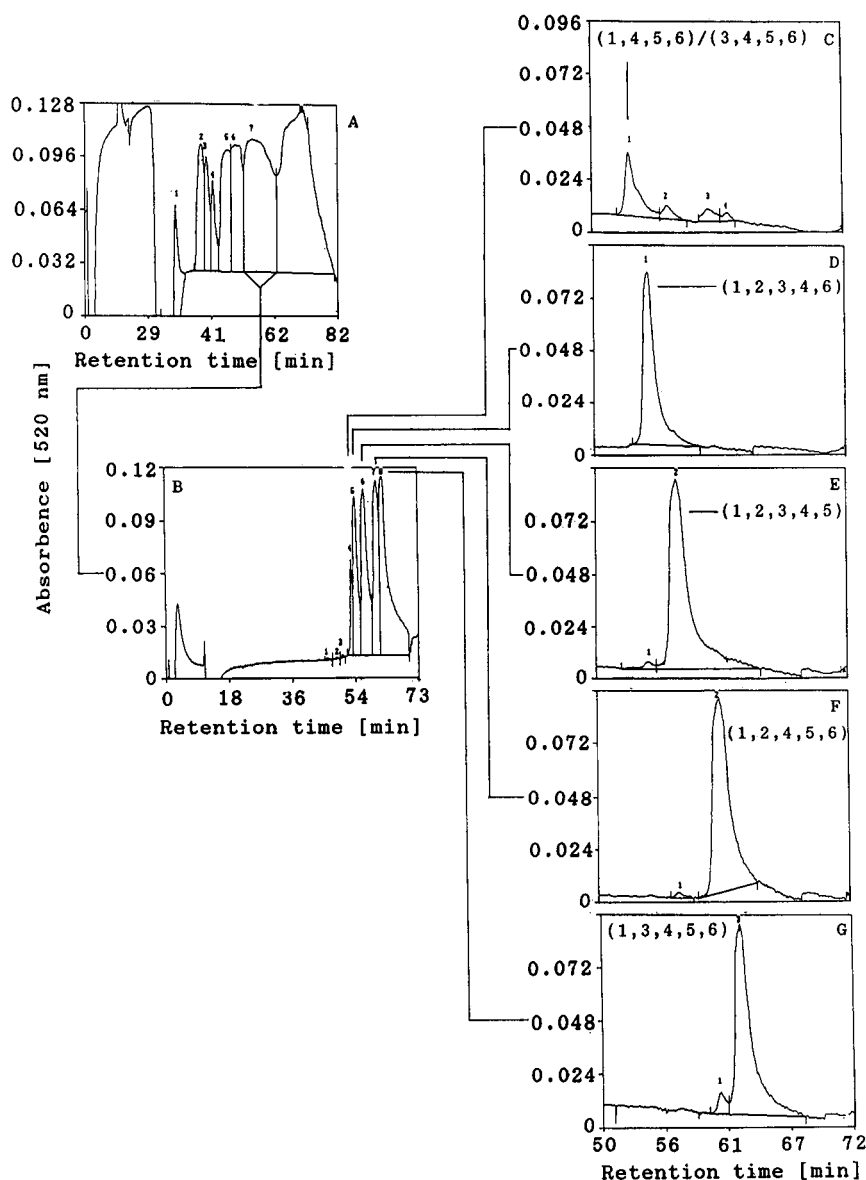


Fig. 1. Semi-preparative isolation of  $\text{InsP}_5$  isomers. Samples were separated by anion-exchange HPLC on MonoQ columns ( $50 \times 5$  mm, two columns in-line; Pharmacia) by an upward concave gradient from  $0.02 \text{ M HCl}$ – $13.5 \mu\text{M YCl}_3$  to  $0.4 \text{ M HCl}$ – $21 \mu\text{M YCl}_3$ . The flow-rate through the columns was  $1.2 \text{ ml/min}$  whereas the dye solution [ $350 \mu\text{M}$  2-(4-pyridylazo)resorcinol,  $1.6 \text{ M}$  triethanolamine,  $\text{pH } 9.1$ ] was pumped at  $0.6 \text{ ml/min}$ . The absorbance of the mixture was measured on-line at  $520 \text{ nm}$ . A  $50\text{-}\mu\text{l}$  aliquot of an  $\text{InsP}_6$  hydrolysate containing  $\text{InsP}_1$  to  $\text{InsP}_6$  was separated (A), peak 7 was collected (A), lyophilized and dissolved in  $4.5 \text{ ml}$  of doubly distilled water and a  $100\text{-}\mu\text{l}$  aliquot was rechromatographed (B), resulting in the resolution of  $\text{DL-Ins}(1,4,5,6)\text{P}_4$  (B, peak 4),  $\text{Ins}(1,2,3,4,6)\text{P}_5$  (B, peak 5),  $\text{DL-Ins}(1,2,3,4,5)\text{P}_5$  (B, peak 6),  $\text{DL-Ins}(1,2,4,5,6)\text{P}_5$  (B, peak 7) and  $\text{Ins}(1,3,4,5,6)\text{P}_5$  (B, peak 8). A  $1.5\text{-ml}$  portion was then separated as above. Peaks 4–8 were collected, lyophilized and dissolved in  $300\text{-}\mu\text{l}$  of doubly distilled water. Aliquots of  $30 \mu\text{l}$  diluted with  $1 \text{ ml}$  of doubly distilled water were then rechromatographed (C–G).



TABLE I

CALIBRATION GRAPHS FOR INOSITOL POLYPHOSPHATES DETERMINED BY THE METAL-DYE DETECTION SYSTEM

Mixtures of standard Ins(1,4)P<sub>2</sub>, Ins(1,4,5)P<sub>3</sub>, Ins(1,3,4,5)P<sub>4</sub>, Ins(1,4,5,6)P<sub>4</sub>, Ins(1,3,4,5,6)P<sub>5</sub> and InsP<sub>6</sub> in the range 50–1500 pmol were determined on a MonoQ column (100 × 5 mm, Pharmacia) as described under Experimental. Linear regression analysis of the signal (mV min) as a function of the amount (pmol) gave the values in this table.

Inositol polyphosphate	Slope	Intercept	<i>r</i>
Ins(1,4)P <sub>2</sub>	0.0319	0.1321	0.9995
Ins(1,4,5)P <sub>3</sub>	0.0549	0.0893	0.9995
Ins(1,3,4,5)P <sub>4</sub>	0.0670	-0.5710	0.9998
Ins(1,4,5,6)P <sub>4</sub>	0.0687	-0.1460	0.9990
Ins(1,3,4,5,6)P <sub>5</sub>	0.0819	-0.6000	0.9929
InsP <sub>6</sub>	0.0943	-0.0850	0.9999

groups on the inositol ring, a linear correlation was found ( $s_c = 0.01518n_p + 0.00573$ ,  $r = 0.9909$ , where  $s_c$  is the slope of the calibration graphs and  $n_p$  is the number of phosphate groups).

#### Determination of multiple inositol polyphosphates in human T-cell lines

In the human T-cell line Jurkat at least eleven inositol polyphosphates could be separated by HPLC and on-line metal-dye detection (Fig. 2). The isomeric identity of several compounds was determined by (i) comparing the retention times with commercially available standards and (ii) by the addition of the commercially available compounds to cell extracts before analysis. Ins(1,4)P<sub>2</sub>, Ins(1,3,4)-P<sub>3</sub>, Ins(1,4,5)P<sub>3</sub>, Ins(1,3,4,5)P<sub>4</sub>, the enantiomeric pair Ins(1,4,5,6)P<sub>4</sub>–Ins(3,4,5,6)P<sub>4</sub>, Ins(1,3,4,5,6)P<sub>5</sub> and InsP<sub>6</sub> were clearly identified by this method. In addition, two further InsP<sub>4</sub> isomers and two InsP<sub>5</sub> isomers were found (Fig. 2, peaks 8, 10, 12, 13). One of the InsP<sub>4</sub> isomers (Fig. 2, peak 8) was identified as Ins(1,3,4,6)P<sub>4</sub> as it had an identical retention time to the standard compound that was prepared by phosphorylation of Ins(1,3,4)P<sub>3</sub> in rat liver extracts [12]. The second peak (Fig. 2, peak 10) eluted between Ins(1,3,4,5)P<sub>4</sub> and Ins(1,4,5,6)P<sub>4</sub>–Ins(3,4,5,6)P<sub>4</sub>. As no standard substance with the same retention time was available, the isomeric identity could not be determined.

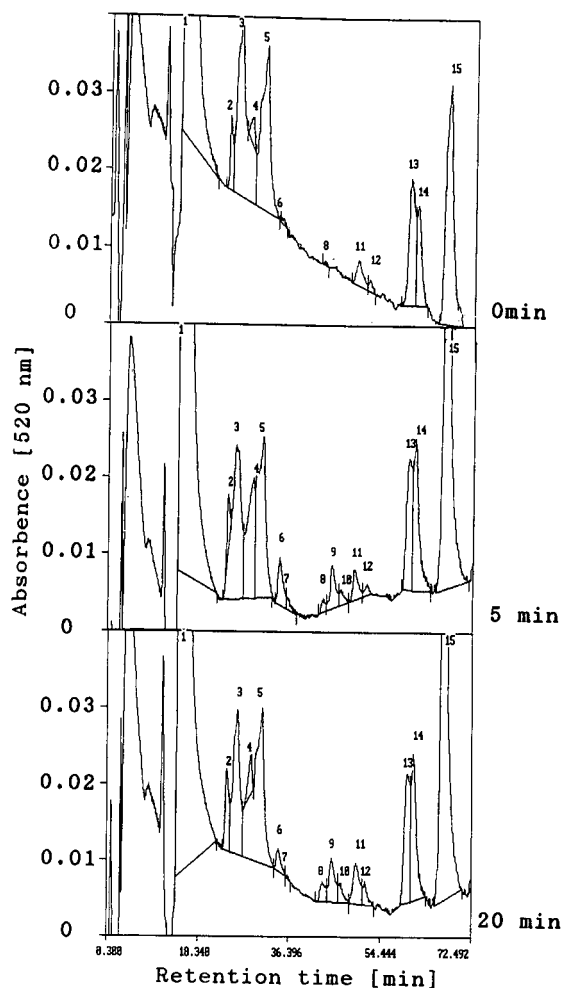


Fig. 2. HPLC determination of inositol polyphosphates from Jurkat T-lymphocytes. Samples from resting and stimulated cells (stimulation time is given on the right-hand side) were processed and analysed using the same conditions as in Fig. 1. Mixing of the column eluate and the dye solution was carried out in a micro-mixing chamber. The absorbance was measured at 520 nm and the inverted analogue signal was transferred to the computerized data system D450/MT1. Peaks were identified by co-chromatography with commercially available standards. Peaks: 1 = InsP<sub>1</sub> + P<sub>i</sub>; 2 = Ins(1,4)P<sub>2</sub>; 3–5 = ?; 6 = Ins(1,3,4)P<sub>3</sub>; 7 = Ins(1,4,5)P<sub>3</sub>; 8 = Ins(1,3,4,6)P<sub>4</sub>; 9 = Ins(1,3,4,5)P<sub>4</sub>; 10 = InsP<sub>4</sub> with unclear isomeric identity; 11 = Ins(1,4,5,6)P<sub>4</sub>–Ins(3,4,5,6)P<sub>4</sub>; 12 = Ins(1,2,3,4,6)P<sub>5</sub>; 13 = Ins(1,2,4,5,6)P<sub>5</sub>; 14 = Ins(1,3,4,5,6)P<sub>5</sub> and 15 = InsP<sub>6</sub>.

Two additional peaks (Fig. 2, peaks 12 and 13) were detected between the standards Ins(1,4,5,6)P<sub>4</sub> and Ins(1,3,4,5,6)P<sub>5</sub>. The first of these (Fig. 2, peak 12) eluted 1.4 min behind Ins(1,4,5,6)P<sub>4</sub>, whereas the second (Fig. 2, peak 13) eluted 2 min before

Ins(1,3,4,5,6)P<sub>5</sub>. The two compounds are probably InsP<sub>5</sub> isomers for several reasons: (i) in the original system [9,10] Ins(1,4,5,6)P<sub>4</sub> was shown to be the slowest eluting InsP<sub>4</sub> isomer followed by Ins-(1,2,3,4,6)P<sub>5</sub>; (ii) InsP<sub>5</sub> isomers prepared by the acid hydrolysis of phytic acid (see under Experimental) eluted between standard Ins(1,4,5,6)P<sub>5</sub> and standard InsP<sub>6</sub> and were identified according to their elution positions as Ins(1,2,3,4,6)P<sub>5</sub>, DL-Ins(1,2,3,4,5)P<sub>5</sub>, DL-Ins(1,2,4,5,6)P<sub>5</sub> and Ins(1,3,4,5,6)-P<sub>5</sub> [10]; (iii) the first compound from Jurkat samples co-eluted with the Ins(1,2,3,4,6)P<sub>5</sub> standard while the second co-eluted with standard DL-Ins-(1,2,4,5,6)P<sub>5</sub>. According to these results the compounds found in Jurkat extracts are probably Ins-(1,2,3,4,6)P<sub>5</sub> and DL-Ins(1,2,4,5,6)P<sub>5</sub>.

The basal concentrations of individual inositol polyphosphates from Jurkat T-cells varied over more than 2 orders of magnitude from 25 ± 10 pmol per 10<sup>9</sup> cells (*n* = 4) for Ins(1,4,5)P<sub>3</sub> to 6380 ± 355 pmol per 10<sup>9</sup> cells (*n* = 4) for InsP<sub>6</sub> (Table I). In unstimulated cells Ins(1,3,4,5)P<sub>4</sub> was not detected under the conditions used. Ins(1,4,5,6)P<sub>4</sub>-Ins(3,4,5,6)P<sub>4</sub> was predominant among the InsP<sub>3</sub> and InsP<sub>4</sub> isomers in resting cells at 525 ± 50 pmol per 10<sup>9</sup> cells (*n* = 4), whereas the concentration of each of the other InsP<sub>3</sub> and InsP<sub>4</sub> isomers was less than

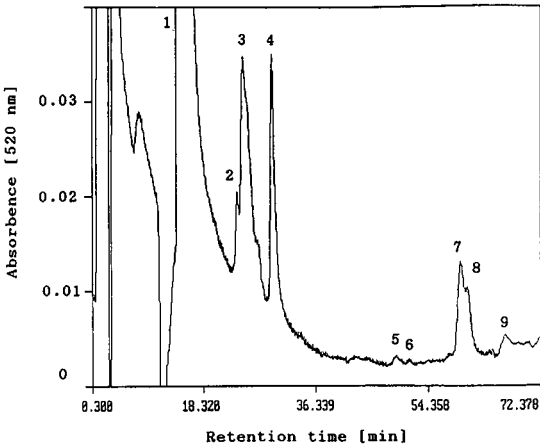


Fig. 3. HPLC determination of inositol polyphosphates from HPB.ALL T-lymphocytes. A sample from unstimulated HPB.ALL T-lymphocytes was analysed using the same conditions as in Fig. 2. Peaks: 1 = InsP<sub>1</sub> + P<sub>i</sub>; 2 = Ins(1,4)P<sub>2</sub>, 3,4 = ?; 5 = Ins(1,4,5,6)P<sub>4</sub>-Ins(3,4,5,6)P<sub>4</sub>; 6 = Ins(1,2,3,4,6)P<sub>5</sub>; 7 = Ins(1,2,4,5,6)P<sub>5</sub>; 8 = Ins(1,3,4,5,6)P<sub>5</sub>; 9 = InsP<sub>6</sub>.

100 pmol per 10<sup>9</sup> cells. Interestingly, of the InsP<sub>5</sub> isomers, the putative DL-Ins(1,2,4,5,6)P<sub>5</sub> and Ins-(1,3,4,5,6)P<sub>5</sub> were approximately 24- and 16-fold higher than the amount of the putative Ins-(1,2,3,4,6)P<sub>5</sub> isomer.

TABLE II  
TIME COURSE OF INOSITOL POLYPHOSPHATES IN JURKAT T-LYMPHOCYTES STIMULATED BY THE MONOCLONAL ANTIBODY OKT3 VIA THE T-CELL RECEPTOR-CD3 COMPLEX

The analysis of inositol polyphosphates was carried out as described in Fig. 2 and under Experimental.

Inositol polyphosphate	Concentration (mean ± S.D., <i>n</i> = 4) (pmol per 10 <sup>9</sup> cells)		
	0 min	5 min	20 min
Ins(1,3,4)P <sub>3</sub>	70 ± 10	460 ± 115 <sup>a</sup>	340 ± 30 <sup>a</sup>
Ins(1,4,5)P <sub>3</sub>	25 ± 10	170 ± 15 <sup>a</sup>	25 ± 5
Ins(1,3,4,6)P <sub>4</sub>	35 ± 20	240 ± 30 <sup>a</sup>	250 ± 20 <sup>a</sup>
Ins(1,3,4,5)P <sub>4</sub>	—	570 ± 105 <sup>a</sup>	850 ± 15 <sup>a</sup>
InsP <sub>4</sub> (?)	10 ± 5	185 ± 50 <sup>a</sup>	190 ± 15 <sup>a</sup>
Ins(1,4,5,6)P <sub>4</sub> -Ins(3,4,5,6)P <sub>4</sub>	525 ± 50	525 ± 70	850 ± 25 <sup>a</sup>
Ins(1,2,3,4,6)P <sub>5</sub>	115 ± 30	355 ± 30 <sup>a</sup>	305 ± 20 <sup>a</sup>
Ins(1,2,4,5,6)P <sub>5</sub>	2740 ± 125	1790 ± 155 <sup>a</sup>	1865 ± 85 <sup>a</sup>
Ins(1,3,4,5,6)P <sub>5</sub>	1855 ± 90	2190 ± 165 <sup>b</sup>	2090 ± 115 <sup>b</sup>
InsP <sub>6</sub>	6380 ± 355	6860 ± 255	6680 ± 320

<sup>a</sup> *p* ≤ 0.01 (Student's *t*-test).

<sup>b</sup> *p* ≤ 0.05 (Student's *t*-test).

In the human T-lymphocyte cell line HPB.ALL similar basal concentrations of inositol phosphates were seen. The intracellular concentration of InsP<sub>6</sub> was about ten-fold lower in this cell line (Fig. 3).

Stimulation of Jurkat T-lymphocytes by the monoclonal antibody to CD3, OKT3 (10 µg/ml), revealed a complex pattern of mass changes in the different inositol polyphosphates (Fig. 2, Table II). The intracellular concentrations of Ins(1,3,4)P<sub>3</sub> and Ins(1,4,5)P<sub>3</sub> were increased transiently (Fig. 2), whereas the concentrations of the InsP<sub>4</sub> isomers [Ins(1,3,4,6)P<sub>4</sub>, Ins(1,3,4,5)P<sub>4</sub> and the unidentified isomer] remained raised for 20 min. In contrast, Ins(1,4,5,6)P<sub>4</sub> and/or Ins(3,4,5,6)P<sub>4</sub> (identified as the enantiomeric mixture) remained at the control level for 5 min, but increased within 20 min (Fig. 2). Of the InsP<sub>5</sub> isomers, an increase in Ins(1,2,3,4,6)P<sub>5</sub> and Ins(1,3,4,5,6)P<sub>5</sub> within 5 min was noticed, which remained raised for 20 min also (Fig. 2). The very high level of InsP<sub>6</sub> also increased after stimulation. However, a significant effect could be observed only transiently after 3 min (data not shown). In contrast, Ins(1,2,4,5,6)P<sub>5</sub> did not increase, but decreased continuously for 20 min in response to stimulation by the antibody to CD3.

## DISCUSSION

These results clearly show that the anion-exchange HPLC separation and post-column dye system [9,10] are suitable for the determination of intracellular concentrations of inositol polyphosphates in human T-lymphocyte cell lines. It could be shown that T-cell receptor-CD3 stimulation in intact Jurkat T-lymphocytes results in changes of the intracellular concentration not only of Ins(1,4,5)P<sub>3</sub> and Ins(1,3,4,5)P<sub>4</sub> but of numerous inositol polyphosphates. Whereas the basal concentration or the receptor-mediated formation of some inositol polyphosphates was observed in other cell types [13–16], a novel finding is that an InsP<sub>5</sub> isomer, probably Ins(1,2,3,4,6)P<sub>5</sub>, is formed in response to stimulation in the human T-cell line Jurkat. Also, the receptor-mediated decrease of Ins(1,2,4,5,6)P<sub>5</sub> in response to stimulation is a novel observation. Ins(1,2,4,5,6)P<sub>5</sub> probably serves as a source for InsP<sub>6</sub> as it has been observed that Ins(1,2,4,5,6)P<sub>5</sub> rather than the other InsP<sub>5</sub> isomers is

phosphorylated to InsP<sub>6</sub> by a cytosolic extract from Jurkat T-lymphocytes [17].

A receptor-mediated increase of the intracellular concentration of Ins(1,3,4,5)P<sub>4</sub>, Ins(1,3,4,6)P<sub>4</sub>, Ins(3,4,5,6)P<sub>4</sub>, Ins(1,3,4,5,6)P<sub>5</sub> and InsP<sub>6</sub> has been described in the human myeloid cell line HL-60 [11]. However, the time courses of the intracellular concentrations of these individual isomers in HL-60 cells on stimulation with formyl-Met-Leu-Phe were very different from those observed in Jurkat T-cells, indicating different regulatory mechanisms. In particular, in HL-60 cells there was a significantly faster synthesis of Ins(1,3,4,5)P<sub>4</sub>, Ins(1,3,4,6)P<sub>4</sub> and Ins(3,4,5,6)P<sub>4</sub>, with a peak value at 1–2 min and a rapid decrease to control values within 5 min [11].

## ACKNOWLEDGEMENT

The Max-Planck Research Unit for Rheumatology/Immunology is funded by the German Ministry for Research and Technology (BMFT) by grant No. 01 VM 8702.

## REFERENCES

- 1 M. J. Berridge, *Annu. Rev. Biochem.*, 56 (1987) 159.
- 2 M. J. Berridge and R. F. Irvine, *Nature (London)*, 341 (1989) 197.
- 3 A. Goldsmith and A. Weiss, *Science*, 240 (1988) 1029.
- 4 C. Grado and C. E. Ballou, *J. Biol. Chem.*, 236 (1961) 54.
- 5 M. J. Berridge, R. M. C. Dawson, C. P. Downes, J. P. Heslop and R. F. Irvine, *Biochem. J.*, 212 (1983) 473.
- 6 R. F. Irvine, A. J. Letcher, D. J. Lander and C. P. Downes, *Biochem. J.*, 223 (1984) 237.
- 7 J. L. Meek, *Proc. Natl. Acad. Sci., U.S.A.*, 83 (1986) 4162.
- 8 J. L. Meek and F. Nicoletti, *J. Chromatogr.*, 351 (1986) 303.
- 9 G. W. Mayr, *Biochem. J.*, 254 (1988) 585.
- 10 G. W. Mayr, in R. F. Irvine (Editor), *Methods in Inositide Research*, Raven Press, New York, 1990, p. 83.
- 11 D. Pittet, W. Schlegel, D. P. Lew, A. Monod and G. W. Mayr, *J. Biol. Chem.*, 264 (1989) 18489.
- 12 S. B. Shears, *J. Biol. Chem.*, 264 (1989) 19879.
- 13 S. B. Shears, J. B. Parry, E. K. Y. Tang, R. F. Irvine, R. H. Michell and C. J. Kirk, *Biochem. J.*, 246 (1987) 139.
- 14 C. A. Hansen, S. von Dahl, B. Huddel and J. R. Williamson, *FEBS Lett.*, 236 (1988) 53.
- 15 T. Balla, L. Hunyadi, A. C. Baukal and K. J. Catt, *J. Biol. Chem.*, 264 (1989) 9386.
- 16 F. S. Menniti, K. G. Oliver, K. Nogimori, J. F. Obie, S. B. Shears and J. W. Putney, Jr., *J. Biol. Chem.*, 265 (1990) 11167.
- 17 A. H. Guse and F. Emmrich, unpublished results.



# Separation of flavonol-2-O-glycosides from *Calendula officinalis* and *Sambucus nigra* by high-performance liquid and micellar electrokinetic capillary chromatography

Piergiorgio Pietta\* and Annamaria Bruno

Università degli Studi di Milano, Via Celoria 2, 20133 Milan (Italy)

Pierluigi Mauri

Istituto Tecnologie Biomediche Avanzate, Via Ampere 56, 20131 Milan (Italy)

Angelo Rava

Istituto Biochimico Pavese, Viale Certosa 10, 27100 Pavia (Italy)

---

## ABSTRACT

*Calendula officinalis* and *Sambucus nigra* flowers were analysed by reversed-phase high-performance liquid chromatography (RP-HPLC) and micellar electrokinetic capillary chromatography (MECC). RP-HPLC was performed on C<sub>8</sub> Aquapore RP 300 columns with eluents containing 2-propanol and tetrahydrofuran. MECC was carried out on a 72-cm fused-silica capillary using sodium dodecyl sulphate and sodium borate (pH 8.3) as the running buffer. The results obtained by these techniques are compared.

---

## INTRODUCTION

Flavonoids are a widespread group of natural products and in recent years different investigations on their biochemical and pharmacological properties have been reported [1].

Flavonoids are mainly described for their ability to inhibit a variety of enzymes [2] and for their radical scavenging [3] and anti-inflammatory [4] activity. Their analysis is therefore of prime importance, and so far high-performance liquid chromatography (HPLC) has been the main method used.

According to our strategy [5], flavonoids from *Betula folium*, *Ononis spinosa*, *Helichrysum italicum*, *Ginkgo biloba*, *Anthemis nobilis*, *Equisetum arvense*, *Orthosiphon spicatus* and *Solidago virgaurea* can be sharply separated by elution on C<sub>8</sub> columns with systems containing 2-propanol and tetra-

hydrofuran. Recently [6], we reported the separation of flavonol-3-O-glycosides from *Ginkgo biloba* by micellar electrokinetic capillary chromatography (MECC). Extending this investigation, in this work *Calendula officinalis* and *Sambucus nigra* flowers were analysed by RP-HPLC and MECC.

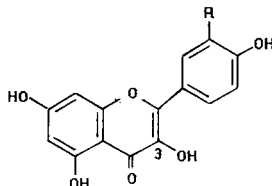
## EXPERIMENTAL

### Materials

The reference compounds a, b, e and h (Table I) were purchased from Extrasynthese (Genay, France). Astragalin (i) was already available in this laboratory [7]. *Calendula officinalis* and *Sambucus nigra* flowers were obtained from Milanfarma (Milan, Italy). All other chemicals were of HPLC grade.

TABLE I

FLAVONOL-3-O-GLYCOSIDES FROM *CALENDULA OFFICINALIS* AND *SAMBUCUS NIGRA*

	
R = H	Keempferol [K]
R = OH	Quercetin [Q]
R = OCH <sub>3</sub>	Isorhamnetin [I]
Compound	Peak
I-3-O-glucoside	a
I-3-O-6-rhamnosylglucoside (I-3-O-rutinoside)	b
I-3-O-2-rhamnosylglucoside (I-3-O-neohesperidoside)	c
I-3-O-2 <sup>G</sup> -rhamnosylrutinoside	d
Q-3-O-6-rhamnosylglucoside (rutin)	e
Q-3-O-2-rhamnosylglucoside (Q-3-O-neohesperidoside)	f
Q-3-O-2 <sup>G</sup> -rhamnosylrutinoside	g
Q-3-O-glucoside (isoquercitrin)	h
K-3-O-glucoside (astragalin)	i

### Equipment

**HPLC.** HPLC analyses were performed on a Waters Assoc. (Milford, MA, USA) liquid chromatograph equipped with a Model U6K universal injector and a Model 510 pump connected to a Model HP 1040A photodiode-array detector (Hewlett-Packard, Waldbronn, Germany). The analytical column was a 7- $\mu$ m C<sub>8</sub> Aquapore RP 300 cartridge (220  $\times$  2.1 mm) and the semi-preparative column was a 7- $\mu$ m C<sub>8</sub> Aquapore RP 300 (250  $\times$  7 mm I.D.) (Applied Biosystems, San Jose, CA, USA).

The eluent for *Calendula officinalis* flowers was 2-propanol–tetrahydrofuran–water (10:5:85) at a flow-rate of 0.4 ml/min [in semi-preparative runs, the flow-rate was 4 ml/min and the peaks were collected by means of a Gilson Model 201 fraction collector (Biolabo Instruments, Milan, Italy)]. The eluent for *Sambucus nigra* flowers was 2-propanol–tetrahydrofuran–water (12:4:84) at a flow-rate of 0.4 ml/min.

**MECC.** The separations were performed using a Applied Biosystems Model 270A capillary electrophoresis apparatus equipped with a 72 cm  $\times$  50  $\mu$ m I.D. fused-silica capillary. The buffer was 20–25 mM sodium borate (pH 8.3) and 40–60 mM sodium dodecyl sulphate (SDS). The other conditions were voltage 277 V/cm, temperature 27°C, injection 1-s

aspiration (4 nl) and detection at 260 and 320 nm. The data were analysed on a Shimadzu (Kyoto, Japan) CR3A data processor.

### Sample preparation

***Calendula officinalis.*** Dried flowers (2 g) were extracted with 20 ml of 50% methanol at room temperature for 24 h. The clear filtrate was evaporated to dryness under vacuum and the residue was dissolved in 3 ml of methanol. A 1-ml volume of this solution was diluted with 2 ml of water and applied to a previously activated (5 ml of methanol followed by 5 ml of water) Sep-Pak C<sub>18</sub> cartridge. After washing with 3 ml of water and 3 ml of 30% methanol, the flavonoid fraction was eluted with 5 ml of 70% methanol. The eluate was evaporated to dryness and the residue was dissolved in 1 ml of 30% methanol.

***Sambucus nigra.*** Dried flowers (2.5 g) were extracted with 50 ml of 50% methanol at room temperature for 48 h. After filtration, the solution was evaporated to dryness under vacuum and the residue was dissolved in 2 ml of methanol. A 0.5-ml volume of this solution was processed as described above.

### Hydrolysis

Acid hydrolysis was carried out in sealed tubes at 100°C for 45 min with 0.5 mg of d glycoside dis-

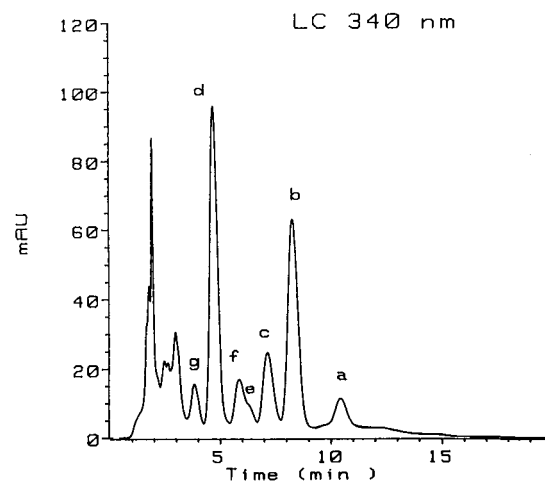


Fig. 1. Typical chromatogram of *Calendula officinalis* flower extract. Column, 7- $\mu$ m C<sub>8</sub> Aquapore RP 300 cartridge (220  $\times$  2.1 mm I.D.); eluent, 2-propanol–tetrahydrofuran–water (10:5:85); flow-rate, 0.4 ml/min. For peaks, see Table I.

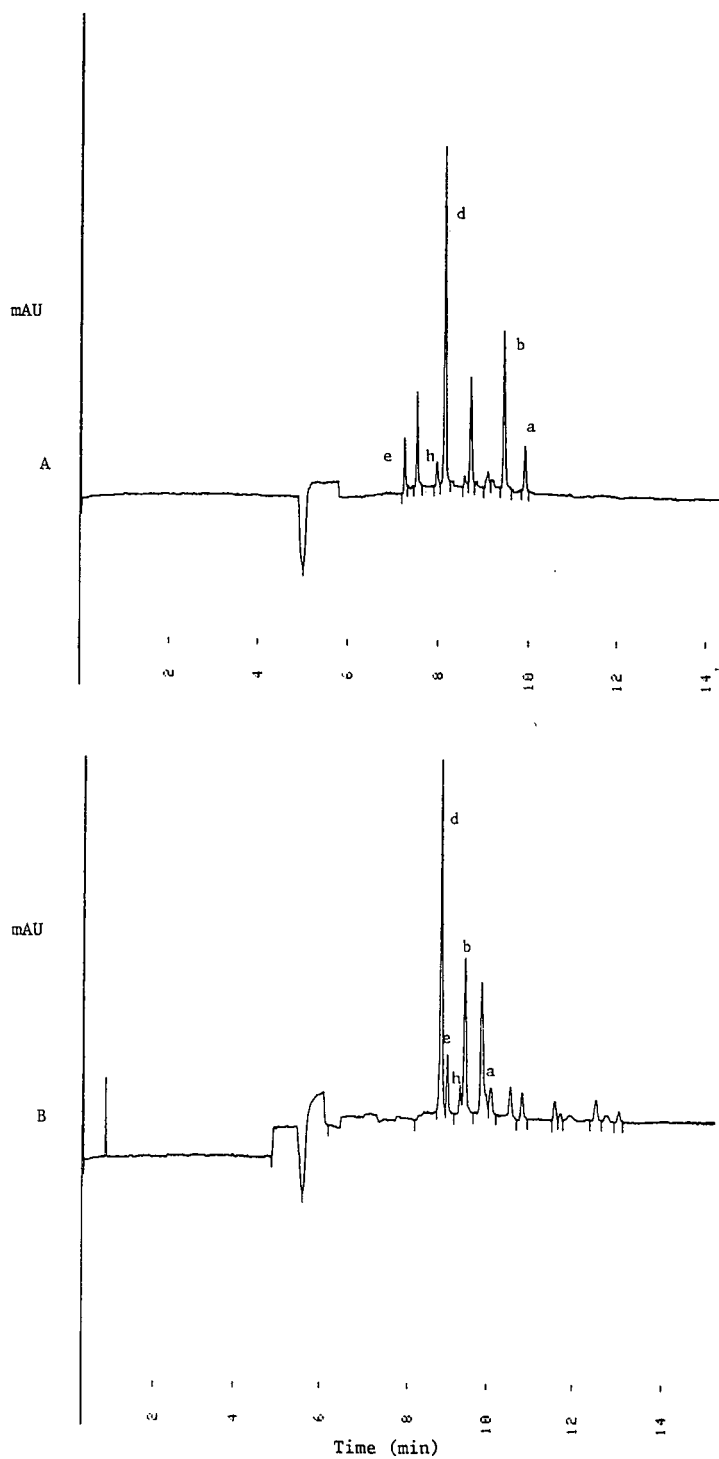


Fig. 2. Typical electropherograms of *Calendula officinalis* flower extract. Conditions: capillary 72 cm  $\times$  50  $\mu$ m I.D. fused silica; voltage, 277 V/cm; buffer, (A) 60 mM SDS–20 mM borate (pH 8.3) and (B) 40 mM SDS–25 mM borate (pH 8.3); detection, 260 nm; attenuation, 16 mV full-scale. For peaks, see Table I.

solved in 0.2 ml of *M* HCl and 0.8 ml of methanol. Isorhamnetin was detected by HPLC [8], whereas glucose and rhamnose were detected as acetyl derivatives by gas chromatography [9].

## RESULTS AND DISCUSSION

### *Calendula officinalis*

Different flavonol-3-O-glycosides have recently been identified in *Calendula officinalis* flowers [10], and their structures elucidated by NMR and mass spectrometry (Table I). A typical chromatogram of an extract is shown in Fig. 1. Peaks a and b were identified as isorhamnetin-3-O-glucoside and isorhamnetin-3-O-rutinoside, respectively, by co-chromatography with authentic specimens; moreover, the identity was confirmed by comparing their on-line UV spectra with those of corresponding standards. Also the peaks c and d gave spectra typical of isorhamnetin glycosides. The major peak d was isolated and on acid hydrolysis isorhamnetin and rhamnose and glucose (in the ratio 2:1) were detected, thus indicating that this peak was the previously reported isorhamnetin-3-O-2<sup>G</sup>-rhamnosylrutinoside [10].

Owing to its chromatographic and spectrophotometric characteristics, peak c can be considered as the fourth described isorhamnetin derivative, *i.e.*,

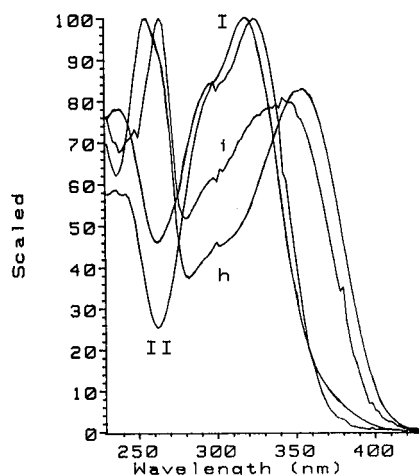


Fig. 4. UV spectra of isoquercitrin (h), astragalín (i) and peaks I and II in Fig. 3.

isorhamnetin-3-O-neohesperidoside. Peaks e, f and g gave one-line UV spectra typical of quercetin. Of these peaks, the low and partially resolved peak e was identified as rutin by co-chromatography with a standard. Peaks f and g can be assigned as the previously reported quercetin-3-O-neohesperidoside and quercetin-3-O-2<sup>G</sup>-rhamnosylrutinoside on the basis of their chromatographic behaviour and UV spectra.

Typical electropherograms obtained from *Calendula officinalis* flower extract using two different running buffers are shown in Fig. 2. MECC allowed confirmation of the presence of rutin (peak e) and the detection of isoquercitrin (peak h). Analogously, peak a, b and d were identified by comparison with authentic specimens. Owing to the lack of on-line spectral information, the identification of the other three peaks was not possible.

### *Sambucus nigra*

Rutin and isoquercitrin (Table I) are the main flavonolglycosides of *Sambucus nigra* flowers [11]. These compounds were sharply separated by isocratic elution (Fig. 3) and their identities were confirmed by co-chromatography and on-line UV spectral comparison with rutin and isoquercitrin standards. A small peak due to astragalín was also identified. As shown in Fig. 4, peaks I and II gave UV

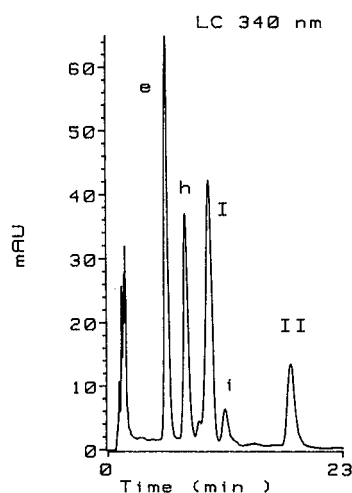


Fig. 3. Typical chromatogram of a *Sambucus nigra* flower extract. Column as in Fig. 1; eluent, 2-propanol-tetrahydrofuran, water (12:4:84); flow-rate, 0.4 ml/min. For peaks, see Table I.



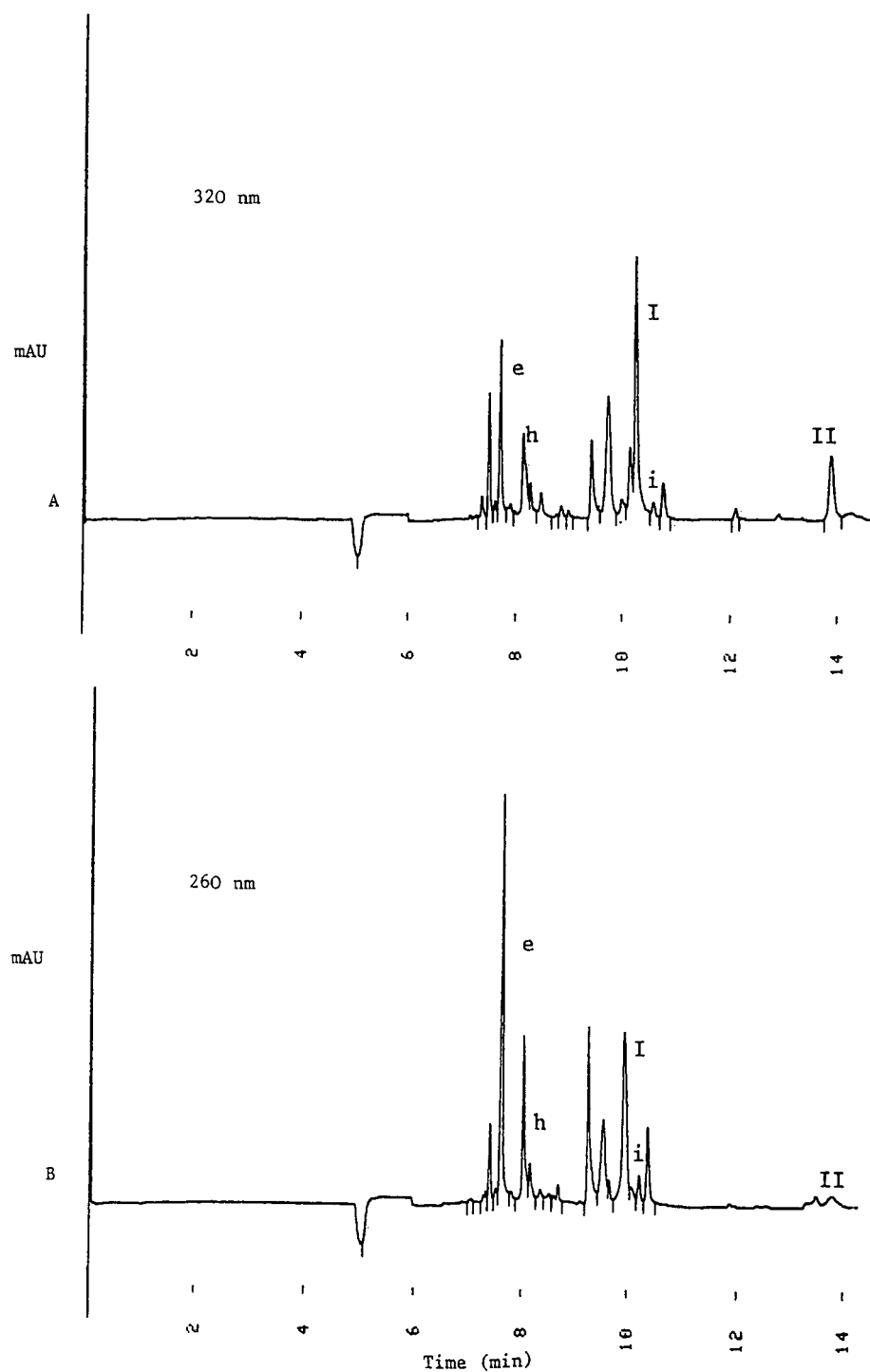


Fig. 5. Typical electropherograms of *Sambucus nigra* flower extract, with detection at (A) 320 and (B) 260 nm. Conditions as in Fig. 2A. For peaks, see Table I.

spectra with a minimum at 260 nm and a maximum near 320 nm, thus excluding a flavonol structure.

MECC of *Sambucus nigra* flowers extracts yielded a baseline separation within 12 min (Fig. 5). Peaks e, h and i were assigned by comparison with standards, whereas peaks I and II were identified by differential UV absorption at 260 and 320 nm.

From these results, it can be concluded that MECC can be used as a complementary technique with HPLC for the analysis of flavonol-3-O-glycosides from *Calendula officinalis* and *Sambucus nigra* flowers. However, technological improvement of capillary electrophoresis apparatus for on-line UV spectra is needed to achieve the same analytical data as HPLC.

#### ACKNOWLEDGEMENT

The authors are grateful to CNR-P.S. "Innovazione Produttiva nella P&MI" for providing funds.

#### REFERENCES

- 1 E. Middleton, Jr., and P. Feriola, in V. Cody, E. Middleton, Jr., J. B. Harborne and A. Beretz (Editors), *Plant Flavonoids in Biology and Medicine: Biomedical Cellular and Medicinal Properties*, Alan R. Liss, New York, 1989, p. 251.
- 2 O. Schimmer, *Dtsch. Apoth.-Ztg.*, 35 (1986) 1881.
- 3 W. Bors, W. Heller, C. Michel and M. Saran, *Methods Enzymol.* 186 (1990) 343.
- 4 T. Brasseur, *J. Pharm. Belg.*, 44 (1989) 235.
- 5 P. Pietta, P. Mauri, A. Bruno, A. Rava, E. Manera and P. Ceva, *J. Chromatogr.*, 553 (1991) 223.
- 6 P. Pietta, P. Mauri, A. Rava and G. Sabbatini, *J. Chromatogr.*, 549 (1991) 367.
- 7 P. Pietta, P. Mauri, C. Gardana, R. Maffei and M. Carini, *J. Chromatogr.*, 537 (1991) 459.
- 8 P. Pietta, C. Gardana, P. Mauri and L. Zecca, *J. Chromatogr.*, 558 (1991) 296.
- 9 D. J. Nevins, P. D. English and A. Karr, *Carbohydr. Res.*, 5 (1967) 340.
- 10 E. Vical-Ollivier, R. Elias, F. Faure, A. Babadjamamian, F. Crespín, G. Balansard and G. Bondon, *Planta Med.*, 55 (1989) 73.
- 11 H. Wagner, S. Blodt and E. M. Zgainski, *Plant Drug Analysis*, Springer, Berlin, 1984, p. 178.

# High-performance liquid chromatographic method with fluorescence detection for the determination of total homocyst(e)ine in plasma

I. Fermo, C. Arcelloni, E. De Vecchi, S. Vigano' and R. Paroni\*

*Istituto Scientifico, Hosp. San Raffaele, Via Olgettina 60, 20132 Milan (Italy)*

---

## ABSTRACT

A high-performance liquid chromatographic method for the determination of total plasma homocyst(e)ine [H(e)] after reduction with sodium tetrahydroborate and precolumn derivatization with *o*-phthalaldehyde is described. The analyses, carried out on a reversed-phase C<sub>18</sub> column, were based on spectrofluorimetric detection. The sensitivity was 1 pmol per injection and the intra- and inter-assay relative standard deviations were 1.8% and 5%, respectively. The plasma H(e) concentration determined in 40 healthy volunteers (20–60 years old) was  $12.4 \pm 2.9 \mu\text{M}$  (mean  $\pm$  S.D.), in good agreement with reference values.

---

## INTRODUCTION

Homocysteine [HCys] is a thiol-containing amino acid produced during the transsulphuration pathway of methionine [1,2]. In the last decade attention has been focused on a possible role of H(e) metabolism in the pathogenesis of atherosclerosis. The possibility that mild impairments of homocyst(e)ine [H(e)] levels may be a risk factor for vascular diseases in some patients has been suggested by studies on homocystinuria. This disease, due to cystathionine  $\beta$ -synthase (EC 4.2.1.22) deficiency in the homozygous form, or to defects in the remethylation of HCys to methionine for vitamin B<sub>12</sub> or folate deficiency, was shown to be frequently associated with several vascular diseases in infancy and childhood [1–7]. Experimental studies [8,9] demonstrated that the abnormal accumulation of this amino acid in tissues and blood has injurious effects on the endothelial cells, inducing vascular damage.

One of the major problems encountered in studies on the potential atherogenic role of H(e) was the development of an accurate and simple assay, able to screen, in a normal population, subjects having a

congenital predisposition to occlusive vascular disease. Several approaches to the analysis of H(e) have been described, including gas chromatography-mass spectrometry (GC-MS) [10], radioenzymic assay [11] and high-performance liquid chromatography (HPLC). The last technique, which is the most widely applied, may be combined with different detectors such as post-column ninhydrin derivatization and spectrophotometric detection in the visible range [12–14], electrochemical detection [15–18] or precolumn derivatization and spectrofluorimetric detection [19–23].

The most recently described precolumn labelling agent is monobromobimane (mBrB), a fluorogenic thiol-specific reagent [19–22]. However this derivatization, characterized by the formation of interfering adducts, requires different clean-up steps to remove the mBrB hydrolysis products [20,22]. In view of this fact we tested *o*-phthalaldehyde (OPA) as derivatizing agent, already used previously for amino acid analyses [24,25]. The OPA fluorophore rapidly links the primary amino groups of amino acids, giving derivatized products that could be detected with high sensitivity, and was previous-

ly found to be suitable for the determination of particular amino acids present in very low concentrations in the urinary matrix [25].

This paper describes a simple and sensitive HPLC method with OPA precolumn derivatization for the determination of total homocyst(e)ine in plasma.

## EXPERIMENTAL

### *Chemicals*

Homocysteine, OPA, sodium tetrahydroborate ( $\text{NaBH}_4$ ) and 2-mercaptoethanol (2-MCE) were obtained from Fluka (Buchs, Switzerland) and homocysteic acid from Sigma (St. Louis, MO, USA). Iodoacetic acid, propionic acid and dimethyl sulfoxide (DMSO) were purchased from Janssen Chimica (Beerse, Belgium). All chemicals and solvents were of analytical-reagent grade and were obtained from BDH (Poole, UK). Doubly distilled water and solvents were filtered, prior to use, through a 0.45- or 0.22- $\mu\text{m}$  filter Millipore (Bedford, MA, USA).

### *Reagents and solutions*

$\text{NaBH}_4$  (3 M) was dissolved in NaOH (0.1 M), then mixed with DMSO (2:1, v/v) and stored in a glass vial at 4°C. The solution was prepared freshly every week. Iodoacetic acid solution (9.3 mg/ml) was prepared every day in boric acid (0.1 M, pH 9.5). The derivatization solution was made by dissolving 5 mg of OPA in 100  $\mu\text{l}$  of methanol and then adding 0.9 ml of sodium borate buffer (400 mM, pH 9.5) and 3  $\mu\text{l}$  of 2-MCE. The concentrations of homocysteine and homocysteic acid standard solutions in 0.1 M HCl were 0.4 and 1.2 mM, respectively. For the preparation of stock sodium propionate buffer, propionic acid (15.68 ml) and anhydrous disodium hydrogenphosphate (49.6 g) were dissolved in water with stirring. The solution was titrated exactly to pH 6.5 with a few drops of NaOH (2 M), diluted to 1 l with water and stored at room temperature.

### *Apparatus*

The HPLC System Gold (Beckman, Palo Alto, CA, USA) consisted of a Model 126 pump connected through a Model 406 analog interface with a Model LS-3 fluorescence detector (Perkin-Elmer,

Norwalk, CT, USA). The spectrofluorimeter was set at a fixed scale of 10 and operated at excitation and emission wavelengths of 230 and 417 nm, respectively.

### *Chromatographic conditions*

The Beckman Ultrasphere ODS analytical (5  $\mu\text{m}$ ) column (250  $\times$  4.6 mm I.D.) was protected by a Brownlee (Santa Clara, CA, USA) Spheri 5-ODS (5  $\mu\text{m}$ ) guard column (30  $\times$  4.6 mm I.D.). The mobile phase consisted of two eluents: A [water–stock sodium propionate buffer–acetonitrile (60:30:10)] and B [water–acetonitrile–methanol (45:30:25)]. The flow-rate was 1.4 ml/min. The analysis was carried out with 100% solvent A. After the elution of HCys (about 22 min), the proportion of solvent B was increased to 90% over 2 min and held for 10 min, then decreased to 0% in 2 min and after 5 min the HPLC system was ready for next run. The total analysis time was 35 min.

### *Derivatization procedure*

For the determination of homocyst(e)inemia, the reduction and cleavage of protein-bound HCys were performed by adding to 200  $\mu\text{l}$  of plasma 300  $\mu\text{l}$  of water, 300  $\mu\text{l}$  of 9 M urea (pH 9.0), 10  $\mu\text{l}$  of homocysteic acid solution as internal standard, 30  $\mu\text{l}$  of *n*-amyl alcohol antifoaming agent and 45  $\mu\text{l}$  of  $\text{NaBH}_4$ –DMSO solution. The samples were incubated at 50°C for 30 min and deproteinized with 500  $\mu\text{l}$  of 6% perchloric acid. After centrifugation, 500  $\mu\text{l}$  of the supernatant were mixed with 100  $\mu\text{l}$  of 40 mM iodoacetic acid and 100  $\mu\text{l}$  3 M NaOH and then 200  $\mu\text{l}$  were derivatized with 100  $\mu\text{l}$  of OPA solution. After exactly 1 min, because of the instability of the derivatives [25], 20  $\mu\text{l}$  were injected into the column.

### *Plasma sample preparation*

Whole blood specimens were collected in sterile Vacutainer tubes containing sodium citrate. After centrifugation at 1500 g for 15 min, the plasma samples were immediately frozen and stored at –20°C until analysis.

Plasma samples were not reduced with  $\text{NaBH}_4$  prior to the derivatization step, to quantify the non-protein-bound homocysteine.

## RESULTS

*Sample preparation*

In order to obtain the maximum yield of the OPA-H(e) derivative, the optimum  $\text{NaBH}_4$  concentration was initially determined. The reducing agent, in fact, is necessary for cleavage of the protein-bound sulphur-containing amino acids and to keep the thiols in a reduced form. Testing various  $\text{NaBH}_4$  concentrations (34–408 mM in the reduction step) with normal (15  $\mu\text{M}$ ) and above-normal (35  $\mu\text{M}$ ) H(e) plasma samples, a plateau in the yield of H(e) between 103 and 204 mM (Fig. 1) was observed. When concentrated homocystine solution (200  $\mu\text{M}$  homocysteine equivalents) was used, the plateau was reached with 204 mM  $\text{NaBH}_4$ . To avoid the formation of interfering adducts  $\text{NABH}_4$  solution was usually prepared freshly every week.

Different excitation and emission wavelengths were chosen, compared to our previous work on amino acid analysis [24,25], because the HCys-OPA derivative shows a higher fluorescence intensity. Under these conditions a very large interfering peak in the initial part of the chromatogram due to 5-sulphosalicylic acid was observed, so we preferred to use 6%  $\text{HClO}_4$  for deproteinization.

An essential condition for the formation of a thio-substituted isoindole is the reinstatement of a basic pH (pH > 9) [26], so addition of 3 M NaOH is necessary to buffer the acidity of the samples.

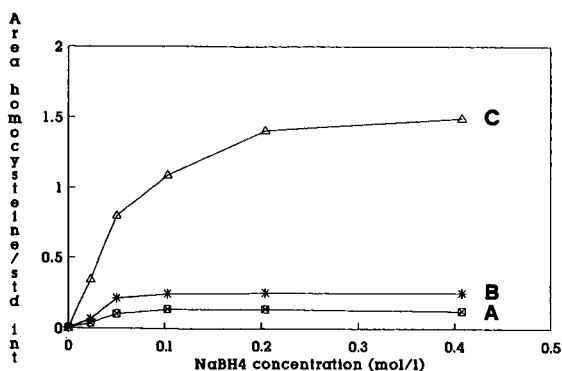


Fig. 1. Influence of  $\text{NaBH}_4$  in homocyst(e)ine determination. Increased concentrations of  $\text{NaBH}_4$  were used to analyse A = a normal plasma sample (15  $\mu\text{M}$ ); B = a plasma sample containing an above normal concentration of H(e) (35  $\mu\text{M}$ ); C = homocystine standard solution (200  $\mu\text{M}$  homocysteine equivalents). The concentration of  $\text{NaBH}_4$  on the abscissa refers to the amount present in the reduction step.

To stabilize OPA derivatives, which can produce non-fluorescent adducts by intermolecular sulphur-oxygen rearrangement [27], 2-MCE was added to OPA solution. The low volume of 2-MCE used (3:1000, v/v) in the last step of sample derivatization precluded its possible contribution to a reduction of plasma disulphide bonds, allowing the application of this method also for the determination of free homocysteine (Fig. 2D).

To prevent the subsequent reoxidation of the thiols and above all to strengthen the weak OPA-H(e) bond, the reaction mixture, immediately after deproteinization, was treated with iodoacetic acid (50 mM) for S-carboxymethylation.

*HPLC analysis*

The determination of HCys was initially performed by an isocratic run, using a mixture of 50 mM disodium hydrogenphosphate buffer (pH 7.4) and acetonitrile (89:11) as described by Cooper and Turnell [28] for plasma cystine analysis. As HCys eluted very close to the surrounding peaks, to improve the separation, different percentages of acetonitrile (ranging from 8% to 12%) and various pH values and ionic strengths were tested (data not shown).

The best resolution of HCys was observed by using a buffer (pH 6.5) containing sodium hydrogenphosphate (105 mM), propionic acid (75 mM) and 10% of acetonitrile. Applying these conditions, HCys eluted at 22 min and was well separated from the asparagine and serine peaks (Fig. 2).

*Linearity, precision and sensitivity*

Quantitative assay was performed by means of calibration graphs, obtained from an aqueous solution of homocysteine in the range 0–320  $\mu\text{M}$ . The relative fluorescence intensities of OPA-homocysteine/internal standard were plotted as a function of homocysteine concentration (Fig. 3). The response of the detector was linear in the tested range and linear regression analysis yielded  $y = 0.0061x + 0.030$  with a correlation coefficient of 0.999. When increased amounts of HCys were added to normal plasma samples, and immediately processed according to the present method, a linear relationship ( $r = 0.999$ ,  $y = 0.007x + 0.17$ ) was observed between the peak area of OPA-H(e) and the concentration of HCys added to human plasma (Fig. 3).

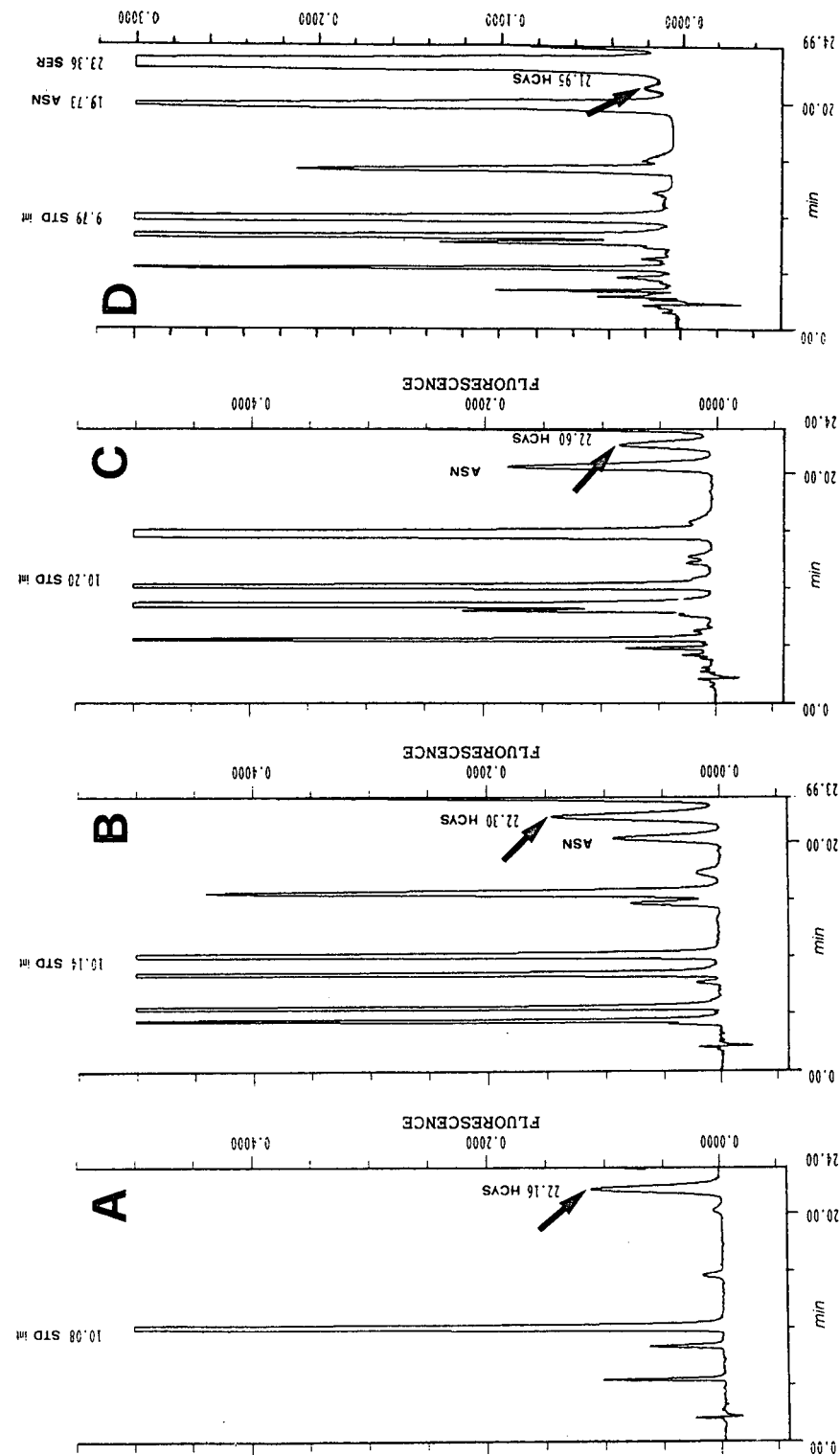


Fig. 2. HPLC determination of plasma homocyst(e)ine. Eluent, acetonitrile–sodium propionate buffer–water (10:30:60). The analysis was carried out on a Beckman Ultrasphere C<sub>18</sub> (5  $\mu$ m) column (250  $\times$  4.6 mm I.D.). Flow-rate 1.4 ml/min. Excitation at 230 nm and emission at 418 nm. Fixed scale = 10. (A) Chromatogram of a solution of homocysteine (20  $\mu$ M) with internal standard homocysteic acid. (B) Partial reproduction of the chromatogram of a Sigma standard physiological amino acid mixture [26] enriched with homocysteine standard. (C) Analysis of a plasma sample not reduced with NaBH<sub>4</sub>. Fixed scale of detector = 20.

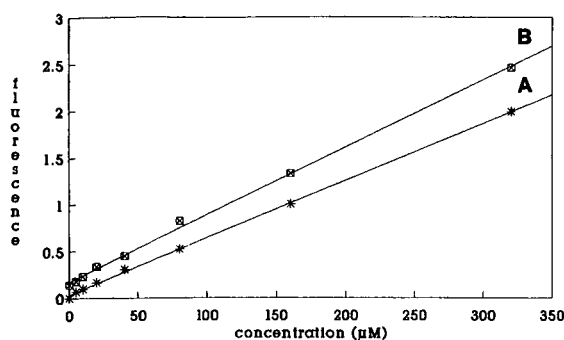


Fig. 3. Linearity of the assay for OPA-homocyst(e)ine in (A) a standard mixture and (B) a normal plasma sample. The integrated peak areas, normalized to the internal standard, were plotted versus the amount of homocysteine standard added.

The within-day reproducibility of the assay for total H(e) was determined by injecting aliquots ( $n = 8$ ) of the same plasma sample, and the between-day reproducibility was calculated from the analysis of the same plasma sample for seven consecutive days. The relative standard deviations (R.S.D.) were 1.8% and 5%, respectively.

To determine the recovery of the method, different amounts of HCys (1–64 nmol) were added to 200- $\mu$ l aliquots of the same pooled plasma. The average recovery was  $94 \pm 17\%$  (mean  $\pm$  S.D.). The lower limit of sensitivity was 1 pmol injected, equivalent to a plasma concentration of 0.7  $\mu$ M.

#### *Influence of anticoagulants*

In order to study the possible interference of anticoagulants on plasma H(e) determination, whole blood specimens, withdrawn by venipuncture from five healthy donors, were collected in different Vacutainer tubes containing EDTA, heparin and sodium citrate. The mean levels found were  $12.24 \pm 0.70$ ,  $11.86 \pm 1.11$  and  $11.84 \pm 1.36$   $\mu$ M for EDTA, heparin and sodium citrate, respectively, showing no statistical differences among the three different treatments ( $p > 0.05$ , Student's *t*-test). We adopted sodium citrate as anti-coagulant, as it is commonly used in the coagulation laboratory of our Institute.

#### *Plasma reference values*

In order to define the physiological plasma H(e) levels, we determined this amino acid in plasma samples withdrawn by venipuncture from 40 fasting

healthy subjects (20–60 years old). The mean H(e) concentration was  $12.4 \pm 2.9$   $\mu$ M (S.D.), which was consistent with literature values [2,10,18,21].

#### DISCUSSION

A sensitive and reproducible assay for total plasma homocyst(e)ine with OPA derivatization and HPLC analysis has been developed. As HCys, in normal human plasma, is predominantly bound with proteins (particularly to albumin) [11], we employed  $\text{NaBH}_4$  as a disulphide reducing agent. After deproteinization with  $\text{HClO}_4$ , plasma samples were treated with 50 mM iodoacetic acid for S-carboxymethylation. The blocking of the sulphhydryl groups, in fact, involves the formation of a very stable fluorescent isoindole product [28], providing reproducible analytical values.

The OPA reaction is highly pH dependent and at  $\text{pH} < 9.0$  no reaction occurs [26], therefore the addition of 3 M NaOH after the deproteinization step is necessary to ensure a high derivatization yield (more than 94%).

The OPA derivatization method shows a very good sensitivity (1 pmol per injection), similar to other HPLC procedures [17,20,21]. No problems of interference from the reducing agent and a great saving of time over mBrB derivatization [21] were observed. In addition, the fluorescence intensity of the OPA-HCys derivative is sufficiently high to determine the free form also. H(e) determination was carried out on a commercial reversed-phase column at room temperature without requiring the utilization of special and expensive chromatographic apparatus or column heating [20]. The use of an internal standard with respect to other procedures [20,21,23] contributed to improving the precision of the method.

The average concentration of total plasma H(e) determined with our method was  $12.4 \pm 2.9$   $\mu$ M ( $n = 40$ ). This value was in good agreement with H(e) levels obtained applying different other analytical techniques including GC-MS (7–22  $\mu$ M) [10], a reference analyser ( $11.5 \pm 0.9$   $\mu$ M) [2] or HPLC in combination with either mBrB derivatization ( $16.15 \pm 5.4$   $\mu$ M) [21] or electrochemical detection ( $10.0 \pm 3.2$   $\mu$ M) [18].

These data confirm the validity of this specific and reproducible method, allowing its accurate ap-

plication in clinical research. The evaluation of the potential atherogenic properties of H(e), made possible by the present method, will be investigated by an accurate definition of normal plasma H(e) range and by the determination of H(e) levels in patients afflicted with different cardiovascular diseases. This study will allow us to evaluate the potential atherogenic properties of H(e).

#### ACKNOWLEDGEMENTS

This research was partially supported by CNR (Consiglio Nazionale delle Ricerche). We thank Miss Marilena Lomartire for valuable technical assistance.

#### REFERENCES

- 1 P. M. Ueland and H. Refsum, *J. Lab. Clin. Med.*, 114 (1989) 473.
- 2 A. Andersson, L. Brattstrom, B. Israelsson, A. Isaksson and B. Hultberg, *Clin. Chim. Acta*, 192 (1990) 69.
- 3 D. E. L. Wilcken and B. Wilcken, *J. Clin. Invest.*, 57 (1976) 1079.
- 4 L. E. Brattstrom, J. E. Hardebo and B. L. Hultberg, *Stroke*, 15 (1984) 1012.
- 5 G. H. J. Boers, A. G. H. Smals, F. J. M. Trijbels, B. Fowler, J. A. Bakkeren, W. J. Kleijer and P. W. C. Kloppenborg, *N. Engl. J. Med.*, 313 (1985) 709.
- 6 S. S. Kang, P. W. K. Wong, H. J. Cook, M. Norusis and J. V. Messer, *J. Clin. Invest.*, 77 (1986) 1482.
- 7 M. R. Malinow, *Circulation*, 81 (1988) 466.
- 8 G. M. Rodgers and W. H. Kane, *J. Clin. Invest.*, 77 (1986) 1909.
- 9 P. G. de Groot, C. Willems, G. H. J. Boers, M. D. Gonsalves, W. G. van Aken and J. A. van Mourik, *Eur. J. Clin. Invest.*, 13 (1983) 405.
- 10 S. P. Stabler, P. D. Marcell, E. R. Padell, R. H. Allen, D. S. Savage and J. Lindenbaum, *J. Clin. Invest.*, 81 (1988) 466.
- 11 H. Refsum, S. Helland and P. M. Ueland, *Clin. Chem.*, 31 (1985) 624.
- 12 V. C. Wiley, N. P. B. Dudman and D. E. L. Wilcken, *Metabolism*, 38 (1989) 734.
- 13 A. J. Olszewski and W. B. Szoskak, *Atherosclerosis*, 69 (1988) 109.
- 14 A. Andersson, L. Brattstrom, A. Isaksson, B. Israelsson and B. Hultberg, *Scand. J. Clin. Lab. Invest.*, 49 (1989) 445.
- 15 R. Saetre and D. L. Rabenstein, *Anal. Biochem.*, 90 (1978) 684.
- 16 S. B. Thomson and D. J. Tucker, *J. Chromatogr.*, 382 (1986) 247.
- 17 D. L. Rabenstein and G. T. Yamashita, *Anal. Biochem.*, 180 (1989) 259.
- 18 M. R. Malinow, S. S. Kang, L. M. Taylor, P. W. K. Wong, B. Coull, T. Inahara, D. Mukerjee, G. Sexton and B. Upson, *Circulation*, 79 (1989) 1181.
- 19 S. Velury and S. B. Howell, *J. Chromatogr.*, 424 (1988) 141.
- 20 H. Refsum, P. M. Ueland and A. M. Svardal, *Clin. Chem.*, 35 (1989) 1921.
- 21 D. W. Jacobsen, V. J. Gatautis and R. Green, *Anal. Biochem.*, 178 (1989) 208.
- 22 R. C. Fahey, G. L. Newton, R. Dorian and E. M. Kosower, *Anal. Biochem.*, 111 (1981) 357.
- 23 A. Araki and Y. Sako, *J. Chromatogr.*, 422 (1987) 43.
- 24 I. Fermo, E. De Vecchi, L. Diomedea and R. Paroni, *J. Chromatogr.*, 534 (1990) 23.
- 25 I. Fermo, E. De Vecchi, C. Arcelloni, P. Brambilla, A. Pastoris and R. Paroni, *J. Liq. Chromatogr.*, 14 (1991) 1715.
- 26 V. J. K. Svedas, I. J. Galaev, I. L. Borisov and I. V. Berezin, *Anal. Biochem.*, 101 (1980) 188.
- 27 W. A. Jacobs, M. W. Leburg and E. J. Maday, *Anal. Biochem.*, 156 (1986) 334.
- 28 J. D. H. Cooper and D. C. Turnell, *J. Chromatogr.*, 227 (1982) 158.



# High-performance liquid chromatographic analysis of the pigments of blood-red prickly pear (*Opuntia ficus indica*)

Elisabetta Forni, Andrea Polesello, Dario Montefiori and Andrea Maestrelli

Istituto per la Valorizzazione Tecnologica dei Prodotti Agricoli, Via Venezian 26, 20133 Milan (Italy)

## ABSTRACT

A method for the extraction, separation and evaluation of betalaines, the pigments of blood-red *Opuntia ficus indica* grown in Sicily, was studied. Tests with different solvent systems showed that extraction of the pigments with water–ethanol was the most complete. For the preparative separation of the betalaines, reversed-phase low-pressure column chromatography on an octadecylsilica bonded phase (RP-18) was the most suitable. Using phosphate buffer (pH 5)–methanol (85:15) the major yellow and red-violet pigments were sharply separated and recovered in good purity. Elution with the same mixture in the ratio 70:30 separated three minor yellow and red-violet components. The amounts of the yellow pigment were evaluated spectrophotometrically at 475 nm and of the red-violet pigment at 538 nm. For the evaluation of the purity of the recovered pigments, a reversed-phase high-performance liquid chromatographic method was applied using a LiChrosorb Select B column eluted with 0.1 M phosphate buffer (pH 5)–methanol (85:15), with spectrophotometric detection at 538 nm for the red pigments and 475 nm for the yellow pigment. The yellow pigment obtained was pure indicaxanthin, whereas in the red-violet pigments betanin and isobetanin were identified with another not yet characterized betalainic glucoside.

## INTRODUCTION

Since the official EEC regulations have restricted the use of synthetic red colorants as additives in food, and the harmful ones have been banned, there has been a growth of interest in the application of natural pigments.

Betanin, also called “beetroot red”, is accepted, among the natural pigments, by EEC and Italian regulations in force with the Sigle E162. It is used mainly to colour foods not requiring thermal treatment, such as yoghurt, confectionery, ice-cream, syrups and sausages. Betanin is the major compound of a group of glucosides called betacyanins whose aglycones are the enantiomers betanidin and isobetanidin, as shown in Fig. 1. The structures were elucidated by Wyler's group [1,2].

Betacyanins are the pigments of plants of the order Centrospermae, where they represent a taxonomic chemical constituent, like anthocyanins in some other plants. Betacyanins are frequently associated with yellow betaxanthins of similar biogen-

esis; the term betalaines includes the two classes of pigments. Various workers [3–5] have listed 44 betacyanins, which represent 37 plants in seven families; other new betacyanins were identified by surveying further 34 species of Cactaceae [6]. In *Opuntia ficus indica*, Piatelli and co-workers [7,8] identified and characterized two main pigments: a red-violet betanin, usually accompanied by minor amounts of its C-15 diastereoisomer isobetanin [7], and a yellow indicaxanthin [8] (Fig. 1).

Our studies of new sources of betanin colorant started with *Phytolacca decandra* berries, grown in Italy [9]. Extraction of the pigment was very simple, but it was necessary to remove a toxic saponin. The product obtained was tested for its pigmenting power and for its stability in model soft and alcoholic drinks [10].

Within a research programme of the Italian Ministry of Agriculture and Forestry for the development of tropical fruit cultivation and utilization in southern Italy, the pigments of blood-red prickly pear (*Opuntia ficus indica*) were of interest. We have

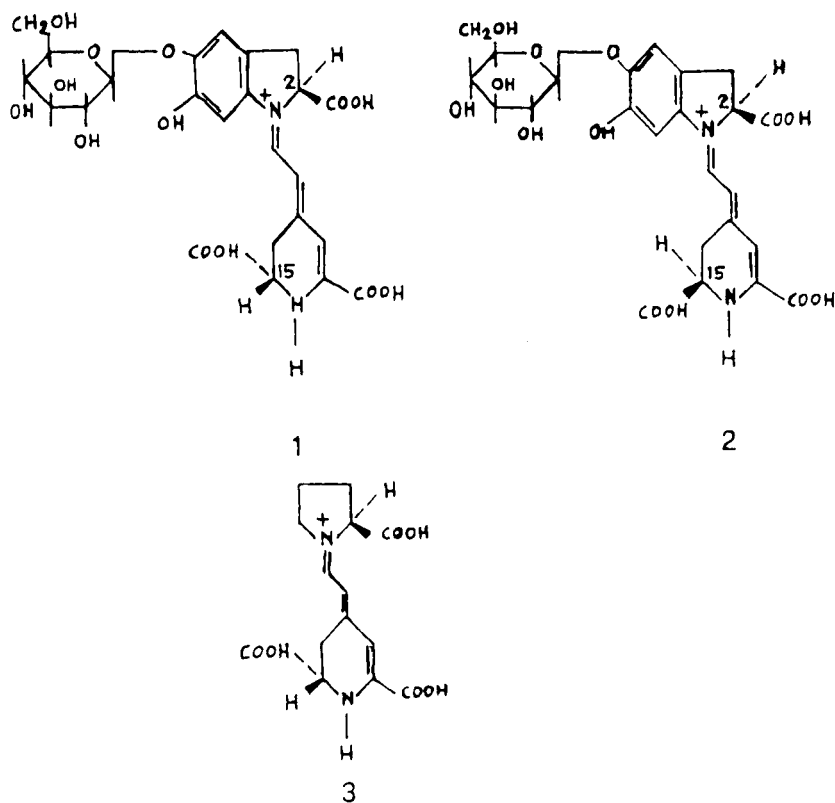


Fig. 1. Prickly pear major pigments: 1 = betanin; 2 = isobetanin; 3 = indicaxanthin.

therefore studied the modes of extraction and the evaluation of these pigments by using solid-phase techniques and high-performance liquid chromatographic (HPLC) analysis.

#### EXPERIMENTAL

Prickly pear Sanguigno fruits (*Opuntia ficus indica* L.) grown in Sicily were used. They were post-harvest ripened until the maximum colour values of the surface were reached:  $L^* = 43.12 \pm 1.03$ ,  $a^* = 22.16 \pm 1.55$ ,  $b^* = 9.07 \pm 1.22$  (CIE 1976  $L^*$ ,  $a^*$ ,  $b^*$  system). The fruits were peeled before homogenization.

#### Extraction of pigments

A 50-g amount of homogenized pulp was shaken with 100 ml of the following extracting solutions: (1) water; (2) dilute citric acid (pH 4.5); (3) ethanol-water (80:20); and (4) ethanol-dilute citric acid (pH

4.5) (80:20). After 5 min of magnetic stirring, the suspensions were centrifuged for 15 min at 1200 g. The extractions were repeated three times until there was total decolorization of the residue. The aqueous extracts were diluted to 500 ml in volumetric flasks. Before dilution of the aqueous-alcoholic extracts, the ethanol was removed by vacuum evaporation at 50°C in a rotary evaporator.

The spectra of the extracts were scanned in the visible range with a Philips PU 8800 spectrophotometer and the concentration of the pigments was estimated using  $A_{538}$  (1%) = 1120 for betanin [1,2] and  $A_{475}$  (1%) = 650 calculated from  $\log A = 4.63$  for indicaxanthin [8].

#### Thin-layer chromatography (TLC)

Preparative silica gel 60 plates (E. Merck, code 13895), 20 × 20 cm, 1 mm layer thickness, and cellulose plates (E. Merck, code 15275), 20 × 20 cm, 0.5 mm layer thickness, were used with two mobile

phases: acetic acid-methanol (40:60) and acetic acid-propanol-water (20:60:20),  $\text{NH}_2$  F<sub>254</sub> analytical HPTLC plates (F. Merck, code 15647) were used with the following mobile phases: 0.1 M phosphate buffer (pH 4 and 5) and 0.1 M phosphate buffer (pH 5)-acetonitrile (50:50, 60:40, 70:30, 80:20 and 90:10).

#### *Low-pressure column chromatography (LPLC)*

Preliminary tests were made with glass columns (10 cm × 2 cm I.D.), eluting by applying nitrogen pressure at the top in darkness. With LiChroprep  $\text{NH}_2$  (E. Merck, code 13974), the mobile phases tested were 0.1 M phosphate buffer (pH 5)-acetonitrile (60:40, 70:30 and 80:20). With ICN Silica RP-8 and RP-18 (32-63) 60A (ICN Biochemicals, code 05010), the mobile phases tested were 0.1 M phosphate buffer (pH 5)-methanol (75:25, 80:20, 85:15 and 90:10).

#### *Reversed-phase preparative column chromatography of the pigments*

The above RP-18 phase was packed in a 50 cm × 5 cm I.D. column, then eluted by applying nitrogen pressure in dim light. Elution was performed in two steps, first with 0.1 M phosphate buffer (pH 5)-methanol (85:15) and second with 0.1 M phosphate buffer (pH 5)-methanol (70:30). The column was then flushed with isopropanol and conditioned again with the first eluent for a new separation.

#### *HPLC of pigments*

A Jasco HPLC system consisting of a Jasco Model 880 Pu pump, a Rheodyne Model 7125 injector and a Jasco Model 870 UV-VIS spectrophotometric detector was used. A Hibar RT 250-4, LiChrosorb RP-Select B (25 cm × 5  $\mu\text{m}$  I.D.). (E. Merck, art. 19608) column was used, eluting with 0.1 M phosphate buffer (pH 5)-methanol (85:15) at a flow-rate of 0.5 ml/min.

For each sample the detection was applied at 475 and 538 nm (0.08 a.u.f.s.) using two runs to identify the yellow (Y) and red-violet (V) constituents at their particular absorption maxima.

#### *Preparation of purified standards from a commercial red beet betanin concentrate*

A commercial red beet betanin concentrate (IFF code 6200), purified by the already described pre-

parative techniques, was used as a standard for betanin and isobetanin. The fractions obtained were subjected to HPLC using the above method.

#### *Enzymatic hydrolysis of glucosides in the pigments*

To distinguish aglycones from glucosides, the violet pigments were treated with  $\beta$ -glucosidase according to Piattelli and Minale [7] and Schwartz and Von Elbe [11]. Volumes of 10 ml of violet fraction V and of red beet extract were incubated at 37°C with 5 ml 0.001%  $\beta$ -glucosidase (Boehringer Mannheim, code 105422). Samples were removed immediately and at 30-min intervals and injected into the HPLC system to follow the disappearance of the glucoside peaks.

## RESULTS AND DISCUSSION

#### *Extraction of pigments*

The visible absorption spectrum of the aqueous-alcoholic extract of the prickly pear was the same as that of the pressed juice. The presence of both yellow pigments absorbing at 475 nm and red-violet pigments absorbing at 538 nm was observed. The average amount obtained for the yellow pigments was about 40 mg per 100 g of fresh pulp and for the red-violet pigments, about 14 mg per 100 g, i.e., with a ratio of about 3:1. The yields of the pigments extracted using the solvents tried were not significantly different. Ethanol-water (80:20) extraction was chosen, because this solvent can recover the pigments completely from the pulp without co-extracting polysaccharides and other alcohol-insoluble solids. This simplifies the further purification of the coloured extracts.

#### *Preparative chromatography of pigments*

*TLC.* Preliminary tests were carried out by TLC on different adsorption layers using several solvent systems. The  $R_F$  values are given in Table I. The visible spectra of the red bands eluted both on silica gel and on cellulose indicated that this band was a mixture of violet and yellow compounds. The amino-bonded silica phase showed the best separation of the violet and yellow pigments in a shorter time than the other two phases. TLC was not considered for preparative purposes, because the coloured bands quickly faded after evaporation of the solvent even when protected from light and oxygen.

TABLE I  
TLC RESULTS

Stationary phase	Eluent	$R_f$			Development time (min)
		Violet	Red	Yellow	
Silica gel	Acetic acid-methanol (40:60)	0.88	0.42	0.23	40
Cellulose	Acetic acid-propanol-water (20:60:20)	0.22	0.80	1.00	60
NH <sub>2</sub> -silica gel	0.1 M phosphate buffer (pH 5)-acetonitrile (70:30)	0.80	—	0.06	20

*Preparative liquid chromatography.* As the weak anion-exchange capacity of amino-bonded silica gave the best results for the TLC separation of the yellow from violet pigments, this phase was tried in a column for preparative purposes. RP-8 and RP-18 phases, already utilized in the preparative HPLC of beetroot betanins [11], were also tested. All the solvent systems were at pH 5 because betanin has its maximum absorption and its highest stability at this pH. The results of these trials are given in Table II. With RP-18 the total elution of pigments was obtained by using two eluents with different concentrations of the organic modifier. The first eluent eluted the two major components, the yellow-orange fraction Y and the violet fraction V, successively. The less polar pigments that remained at the top of the column were eluted with the second eluent.

According to the absorption spectra reported in Fig. 2, fractions Y and V appeared as single coloured substances, whereas fractions FR, FV and

FO appeared as mixtures of minor yellow and red violet pigments in different proportions (Fig. 3).

As the minor components were considered to be unimportant for utilization purposes, our research was developed to recover and to study the major fractions Y and V, choosing chromatography on an RP-18 column and single elution with 0.1 M phosphate buffer (pH 5)-methanol (80:15) for preparative purposes. The best means of removing the residual substances from the column was by flushing with isopropanol.

#### HPLC of Y and V fractions

*Yellow fraction Y.* HPLC separation on an end-capped RP-8 phase (LiChrosorb RP Select B) with detection at 475 nm displayed a single peak for this fraction. According to Piattelli *et al.* [8], this compound should be identified as indicaxanthin from the retention time and the absorption spectrum.

*Red-violet fraction V.* HPLC separation under the same conditions as above, with detection at 538

TABLE II  
PREPARATIVE LIQUID CHROMATOGRAPHIC RESULTS

Stationary phase	Eluent	Order of elution
NH <sub>2</sub> -silica	0.1 M phosphate buffer (pH 5)-acetonitrile (80:20)	Poorly separated
RP-8 silica	As above	Two band: yellow and red violet (mixture of violet and yellow).
RP-18 silica	1st eluent: 0.1 M phosphate buffer (pH 5)-methanol (85:15)	Two bands: Y = yellow-orange; V = violet
	2nd eluent: 0.1 M phosphate buffer (pH 5)-methanol (70:30)	Three minor bands: FR = rose; FV = red-violet; FO = orange

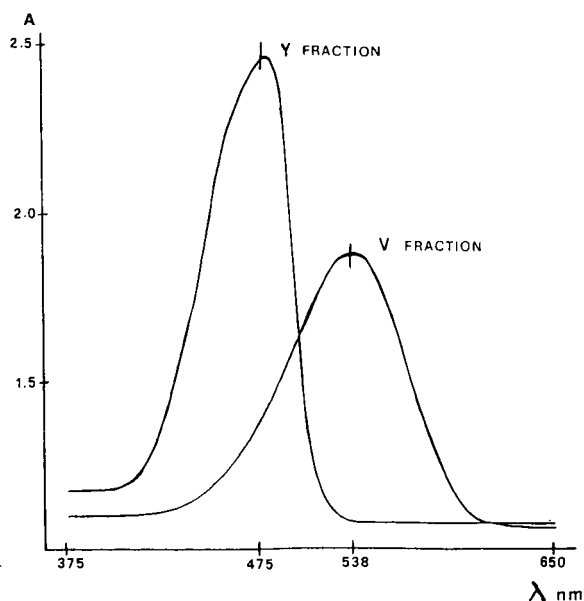


Fig. 2. Absorption spectra of yellow (Y) and violet (V) bands eluted from the RP-18 column with 0.1 M phosphate buffer (pH 5)-methanol (80:15).

nm, showed three major peaks eluting at 6.47 min (peak A), 11.05 min (peak B) and 28.30 min; other smaller peaks present are believed to be degradation products. The same HPLC procedure was also applied to a previously purified commercial betanin concentrate. Comparing the retention times of the peaks of the two chromatograms of the prickly pear

pigments and that of red beet, we can identify peak A as betanin and peak B as isobetanin, while the peak at 28.30 min is not present in the beetroot extract.

Evidence in support of this identification was provided by treatment of both the betanin extracts, *Opuntia ficus indica* (V) and beetroot, with  $\beta$ -glucosidase. According to Schwartz and Von Elbe [11], the enzymatic hydrolysis of betanin and isobetanin gives rise to aglycone peaks that have higher retention values than to their parent compounds. As shown in Fig. 4, enzymatic hydrolysis of the beetroot extract yields betanidin and isobetanidin exclusively (peaks A1 and B1). A same trend is observed in Fig. 5 for the hydrolysed fraction V: peaks A and B, which diminished, are the betacyanin glucosides, whereas the peaks A1 and B1 are the corresponding less polar aglycones. Hence the compounds present in that red-violet fraction V were identified as A = betanin (6.47 min), A1 = betanidin (10.05 min), B = isobetanin (11.05 min) and B1 = isobetanidin (18.64 min). The different order of elution of betanins and betanidins compared with the reported

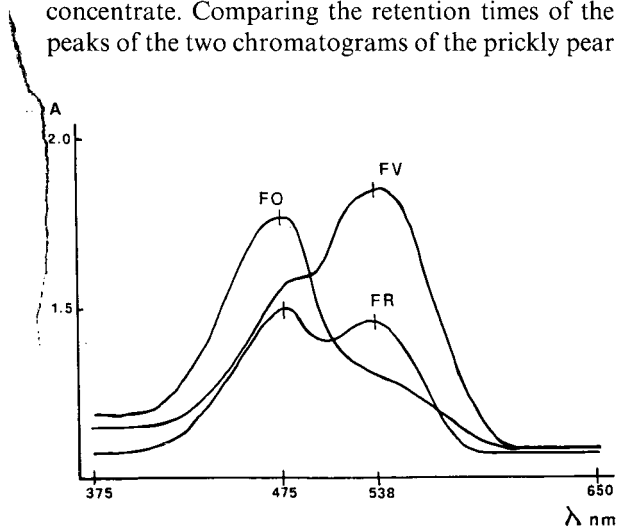


Fig. 3. Absorption spectra of the less polar bands FR = rose, FV = red violet and FO = orange, eluted from the RP-18 column with 0.1 M phosphate buffer (pH 5)-methanol (70:30).

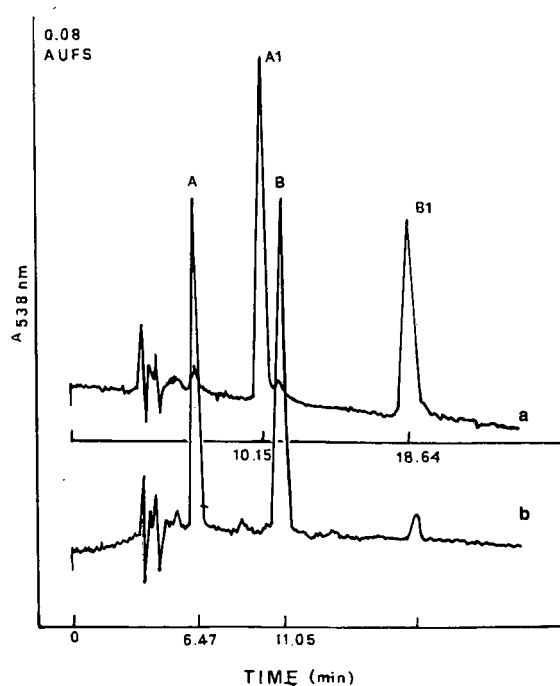


Fig. 4. HPLC of beetroot extract before (b) and after (a) treatment with  $\beta$ -glycosidase: A = betanin; B = isobetanin; A1 = betanidin; B1 = isobetanidin.

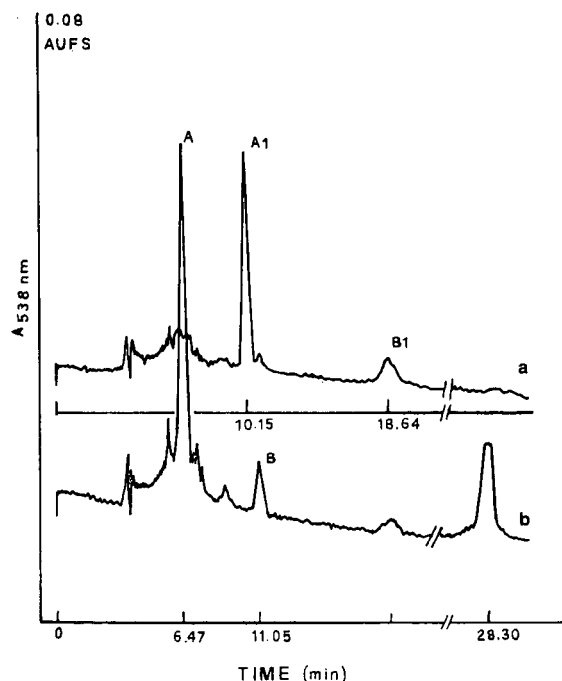


Fig. 5. HPLC of the V fraction before (b) and after (a) treatment with  $\beta$ -glucosidase: A = betain; B = isobetanin; A1 = betanidin; B1 = isobetanidin; peak at 28.30 min = a not previously quoted betain glucoside.

[11] can be attributed to the difference in polarity between RP-8 used here and RP-18 used previously [11]. Hence the interactions of these compounds with the stationary phase may change.

For the red-violet compounds with a retention time of 28.30 min, we could not find any information in the literature. It was less polar than the other betanins, it absorbed between 538 and 540 nm at pH 5 and it was hydrolysable by  $\beta$ -glucosidase. The absorption spectrum and the RP-HPLC analysis exclude the identification of this peak as neobetanin, an orange compound claimed by Strack *et al.* [12] as a major constituent of *Opuntia ficus indica* pigments. That this substance could be a glucoside of a low-polarity betacyanin is the only possible suggestion at present.

## CONCLUSIONS

The red-violet major pigment extracted from blood-red prickly pear presented some differences from the red beet betanin concentrate. It is constituted mainly of betanin and of another betacyanin glucoside, with traces of isobetanin and isobetanidin, while the red beet colorant concentrate contains mainly betanin and isobetanin, in about equal amounts.

The selected techniques of extraction with an aqueous-alcoholic solvent and preparative column chromatography on RP-18; allowed us to recover the two major yellow and red violet pigments from blood-red prickly pears. By using an aqueous-alcoholic extraction medium, the enzymatic activity can be hampered, and also polysaccharides and other alcohol-insoluble compounds are left behind in the residue pulp. Moreover, this method avoided the formation of artifacts. In fact, only traces of isobetanin and isobetanidin were found, indicating that the epimerization was minimized during the preparative process [5,7,11]. Hence reversed-phase low-pressure chromatography can be used for both practical and research purposes without causing alterations.

The developed isocratic RP-HPLC method was suitable for monitoring the composition of both the yellow and red-violet compounds. With this method, in the red-violet fraction a so far uncharacterized betacyanin glucoside was observed. According to our results (not shown), the optimum stability of the pigments was at pH 5. This pH proved to be efficient for the separation of the compounds with an end-capped fine particle size, slightly polar RP-8 phase, such as the LiChrosorb Select B column used here.

The purity of the peaks was also checked using diode-array spectrophotometric detection, confirming the high resolution of this column. The extension of this method to the determination of the detected compounds is being developed.

## ACKNOWLEDGEMENTS

This research was supported by a Italian Ministry of Agriculture and Forestry grant. Project Tropical and Subtropical Fruit. Paper No. 410.

## REFERENCES

- 1 M. Wyler, T. J. Mabry and A. S. Dreiding, *Helv. Chim. Acta*, 46 (1963) 1745.
- 2 M. E. Wilcox, M. Wyler, T. J. Mabry and A. S. Dreiding, *Helv. Chim. Acta*, 48 (1965) 252.
- 3 M. Piattelli, in E. E. Corm (Editor), *Biochemistry of Plants*, Vol 7, Academic Press, New York, 1981, p. 557.
- 4 R. A. Harmer, *Food Chem.*, 5 (1980) 81.
- 5 M. Piattelli and L. Minale, *Phytochemistry*, 3 (1964) 547.
- 6 M. Piattelli and F. Imperato, *Phytochemistry*, 8 (1969) 1503.
- 7 M. Piattelli and L. Minale, *Phytochemistry*, 3 (1964) 307.
- 8 M. Piattelli, L. Minale and G. Prota, *Tetrahedron*, 20 (1964) 2325.
- 9 E. Forni, A. Trifilò and A. Polesello, *Food Chem.*, 10 (1983) 35.
- 10 E. Forni, A. Trifilò and A. Polesello, *Food Chem.*, 13 (1984) 149.
- 11 S. J. Schwartz and J. M. von Elbe, *J. Agric. Food Chem.*, 28 (1980) 540.
- 12 D. Strack, V. Engel and V. Wray, *Phytochemistry*, 26 (1987) 2399.





# Determination of catecholamines in urine by liquid chromatography and electrochemical detection after on-line sample purification on immobilized boronic acid

Britt-Marie Eriksson\* and Margareta Wikström

*Bioanalytical Chemistry, Astra Hässle AB, S-431 83 Mölndal (Sweden)*

---

## ABSTRACT

Norepinephrine, epinephrine and dopamine in urine were measured by an automated liquid chromatographic method. After sample purification on a column containing silica-immobilized boronic acid, which showed great affinity for catecholamines at neutral pH, the catecholamines were eluted by backflushing with an acidic mobile phase and transferred to a cation exchanger for separation. Detection was performed electrochemically and the relative standard deviation was 2% for the analysis of endogenous concentrations in human urine.

---

## INTRODUCTION

Liquid chromatography with electrochemical or fluorimetric detection has attained wide acceptance for assay of catecholamines in urine. Most often extensive purification of the complex urine sample is required prior to the chromatographic separation. Extraction methods utilizing organic solvents [1,2], cation-exchange resin [3–5], aluminium oxide [6–9], immobilized boronic acid [10,11] or combinations of these techniques [12–14] have been used. Automated methods have also been applied, using ASPEC (automatic sample preparation with extraction columns, Gilson) or coupled-column systems [15–20]. In this paper we have adapted the same approach for determination of catecholamines as previously demonstrated for vanilmandelic acid (VMA) in urine [21].  $\alpha$ -Hydroxycarboxylic acids, like VMA, bind to boronic acid at a low pH, while catechol compounds containing vicinal *cis*-diols form cyclic boronate esters at neutral pH. By combining affinity to boronate and cation-exchange chromatography a highly selective chromatographic system was obtained, enabling a simple analysis by direct injection of urine samples.

## EXPERIMENTAL

### *Chemicals and reagents*

Hydrochloric acid, ethylenediaminetetraacetic acid (EDTA) and all buffer substances were of analytical-reagent grade (Merck, Darmstadt, Germany) and methanol was of high-performance liquid chromatography (HPLC) grade (Rathburn, Walk-erburn, UK). Epinephrine (E) bitartrate, norepinephrine (NE) bitartrate, dopamine (DA) hydrochloride, metanephrine (MN) hydrochloride and VMA were obtained from Sigma (St. Louis, MO, USA),  $\alpha$ -methyldopamine (MDA) hydrochloride from Merck Sharp and Dohme (Rahway, NJ, USA) and dihydroxyphenylethylene glycol (DOPEG) and 3-methoxy-4-hydroxyphenylethylene glycol (MOPEG) piperazine salt from Regis (Morton Grove, IL, USA).

### *Chromatographic system*

A scheme of the chromatographic system is presented in Fig. 1. It comprised three Model 2150 pumps (LKB, Bromma, Sweden), a Model 465 autosampler with a refrigerated sample tray (Kontron, Zürich, Switzerland) and 0.75-ml injection

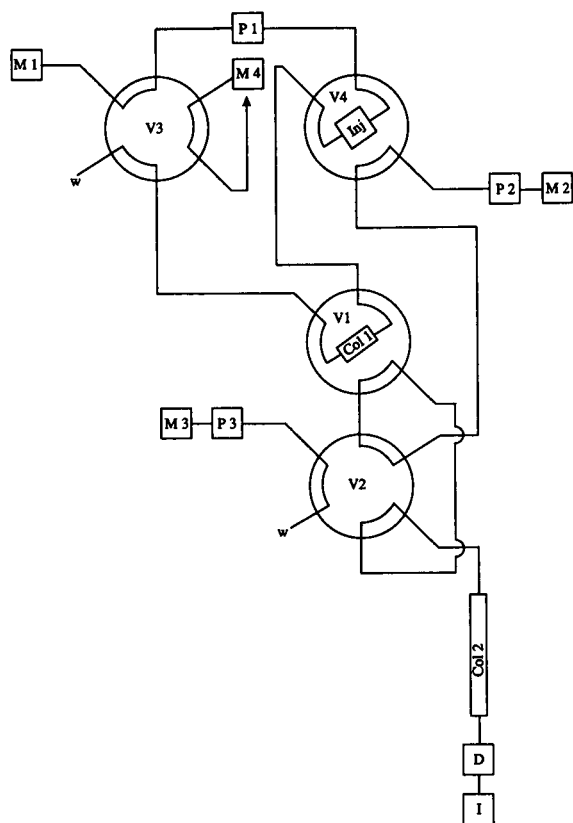


Fig. 1. Coupled-column liquid chromatographic system. P1, P2 and P3 = pumps; M1, M2, M3 and M4 = mobile phases 1 (phosphate buffer pH 7.0,  $I=0.01$ ), 2 (phosphate buffer pH 3.0–3.5,  $I=0.1$ , containing 0.3 mM EDTA and 5–25% methanol), 3 and 4 (phosphate buffer pH 3.2,  $I=0.01$ ); Inj = autoinjector; Col 1 = SelectiSpher-10 Boronate; Col 2 = Nucleosil 5SA; V1, V2, V3 and V4 = six-port valves; D = detector; I = integrator; w = waste. For further details, see text.

vials of polypropylene with attached stoppers (Milian Instruments, Geneva, Switzerland), a Model 4270 integrator (Spectra-Physics, San Jose, CA, USA), a Model 7010 six-port valve (Rheodyne, Berkeley, CA, USA) and three Model C6W six-port valves with a high-speed switching unit mounted on an air actuator (Valco, Schenkon, Switzerland). Two of the valves, V1 and V2, were controlled by the integrator and the switching times were 12 and 17.5 min for valve 1 and 13.5 and 25 min for valve 2 (Table I). Valve V3 was controlled by the autosampler and switched after the last set of samples had been injected. The fourth valve, V4, was switched

TABLE I  
SCHEME OF COLUMN-SWITCHING EVENTS

Time after injection (min)	Switch valve No.	Event
0.0		The sample is injected onto column 1
12.0	1	Columns 1 and 2 are connected. Column 1 is backflushed with an acidic mobile phase and the analytes are transferred to column 2
13.5	2	Columns 1 and 2 are disconnected from each other Column 1 is washed
17.5	1 reset	Column 1 is reconditioned until the next injection
25	2 reset	After the chromatogram is completed the next sample is injected

manually to enable direct injection onto the separation column in recovery studies. The columns were packed with SelectiSpher-10 Boronate ( $35 \times 2.1$  mm I.D.) (Skandinaviska GeneTec, Kungsbäcka, Sweden) and Nucleosil 5SA ( $100 \times 4.6$  mm I.D.) (Machery-Nagel, Düren, Germany).

The neutral mobile phase (pH 7.0; ionic strength,  $I=0.01$ ) contained disodium hydrogenphosphate (2.65 mM) and sodium dihydrogenphosphate (2.10 mM) and the acidic phase (pH 3.2;  $I=0.1$ ) contained sodium dihydrogenphosphate (100 mM), phosphoric acid (15 mM), EDTA (0.3 mM) and methanol (5–25%). For washing of the boronate column a phosphate buffer solution (pH 3.2;  $I=0.01$ ) was used. The water was deionized and filtered through a Milli-Q system (Millipore, Molsheim, France), and prior to use the mobile phases were degassed and filtered through a  $0.45\text{-}\mu\text{m}$  MF Millipore filter. The flow-rates were 1.0 ml/min and the eluent from the cation-exchange column was monitored with an ESA Model 5100A Coulochem electrochemical detector (Environmental Sciences, Bedford, MA, USA), with a Model 5011 analytical cell operated at +0.00 V and +0.30 V and a Model 5020 guard cell operated at +0.35 V.

#### Analytical procedure

Urine samples were acidified with 5 M hydrochloric acid to pH 4 before storage at  $-20^\circ\text{C}$ . After

thawing, the urine samples were mixed and centrifuged for 2 min at 1000 g. A 150- $\mu$ l volume of a urine sample or a reference solution of the catecholamines (200 nM) in 1 mM hydrochloric acid was transferred to an injection vial and placed in the autosampler. Addition of a 20- $\mu$ l volume of an internal standard solution of MDA (10  $\mu$ M) in 1 mM hydrochloric acid was performed by the autosampler. It was also programmed to adjust the pH of the sample to 7 by adding 80  $\mu$ l of a solution of 250 mM disodium hydrogenphosphate containing 10 mM EDTA (pH 8) and then mixing the sample by three repetitive pipettings. The injection volume was 20–200  $\mu$ l.

## RESULTS AND DISCUSSION

### Retention capacity of boronic acid-substituted silica

In a previous study [21] we used immobilized boronic acid to isolate VMA from urine samples. A complex between the boronate matrix and the  $\alpha$ -hydroxycarboxylic acid was formed at low pH. We also studied the retention of related compounds on the boronic acid packing material at pH between 2.1 and 7.7. The results of some representative compounds and of the catecholamines are shown in Figs. 2 and 3. The catecholamines were strongly retained at neutral pH, while the 3-O-methylated amines (MN) and the neutral catechol compounds (DOPEG) were less retarded. The acids (VMA) and the O-methylated neutral compounds (MOPEG) were practically unretained at a neutral pH.

### Column switching

For purification and concentration of the urine sample, we utilized the ability of the boronate matrix to strongly retain the catecholamines at pH 7. After injection of the sample, the boronate column was washed for 12 min with a neutral mobile phase. Valve V1 was then switched and the column backflushed with an acidic phase, which rapidly desorbed the catecholamines and transferred them to the cation exchanger, where separation was performed. The time schedule for switching of the valves is reported in Table I. After 0.5–1.5 min of backflushing, the boronate column was disconnected from the separation column by switching of valve V2. While the catecholamines were separated on the cation exchanger and detected, the boronate

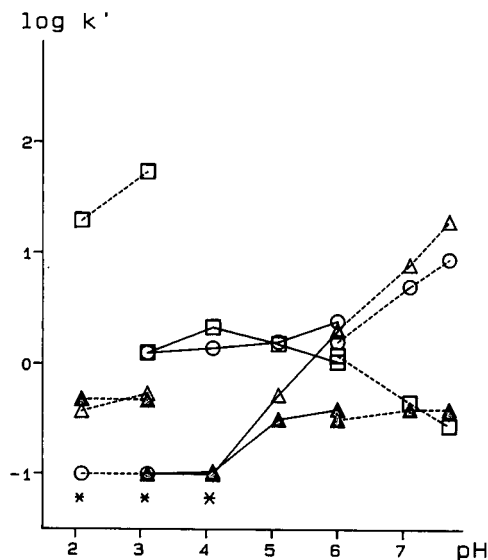


Fig. 2. Influence of pH of the mobile phase on the retention of some catechol derivatives. Stationary phase: SelectiSpher-10 Boronate. Mobile phase: phosphate buffer ( $I=0.01$ ) pH 2.1, 3.1, 6.0, 7.1, 7.7 (----) and citrate buffer ( $I=0.01$ ) pH 3.1, 4.1, 5.1, 6.0 (—); \* =  $\log k'$  values lower than  $-1$ . Key: ○ = MN; △ = DOPEG; □ = VMA; ▲ = MOPEG.

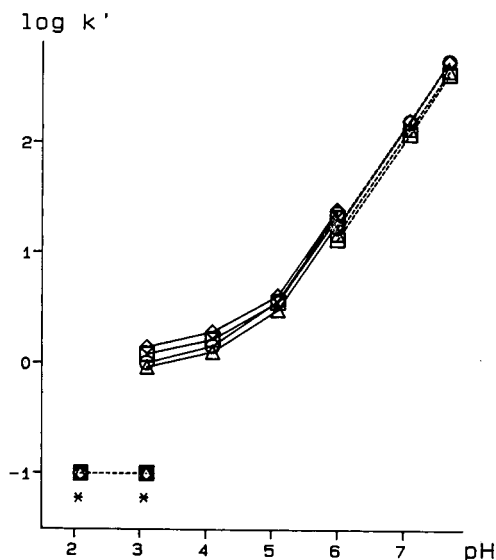


Fig. 3. Influence of pH of the mobile phase on the retention of catecholamines. Conditions as in Fig. 2. Key: ○ = E; △ = NE; □ = DA; ◇ = MDA.

column was washed backwards for 4 min with a buffer solution of pH 3 and, after resetting of valve V1, reconditioned with the neutral mobile phase until the next injection. When the chromatogram was completed, valve V2 was reset and the next sample was injected. When all the samples had been chromatographed valve V3 was switched in order to flush the boronate column with a buffer solution of pH 3, until the next set of samples was to be analyzed. This was done to promote a long lifetime of the boronate column. It seems as if the column in the long run tolerated the buffer solution of pH 3 better than the buffer solution of pH 7.

### Chromatography

The retention capacity of the boronate phase was tested by coupling the column outlet directly to the detector. Owing to the high affinity of the catecholamines for the boronic acid material at pH 7, the column could be washed for more than 12 min without any loss of analyte. The catecholamines were then desorbed at an acidic pH and eluted onto the cation exchanger. For analysis of catecholamines in biological samples, cation-exchange chromatography has proved to be more selective than reversed-phase chromatography [6,7,14]. Owing to variations in the retention capability between different batches of cation-exchange material, the pH of the mobile phase was varied between 3.0 and 3.5 and the content of methanol used was 5–25%. A more acidic pH of the mobile phase promoted the desorption of the catecholamines from the boronate matrix, but then an interfering peak appeared in the chromatogram. Its capacity factor ( $k'$ ) at pH 1.8 was 10.6 but only 1.9 at pH 2.9. The retention times of the catecholamines were practically unchanged in this pH range. In order to avoid contamination of subsequent chromatograms, owing to incomplete desorption of the boronate column, a 4-min washing step using a buffer solution of pH 3 was introduced after each injection. A chromatogram of a human urine sample obtained after column switching is shown in Fig. 4. The peak eluting between NE and E could easily be moved by adjusting the methanol content of the mobile phase. After a couple of months the cell response of the electrochemical detector had declined, but it was restored by washing with 6 *M* nitric acid.

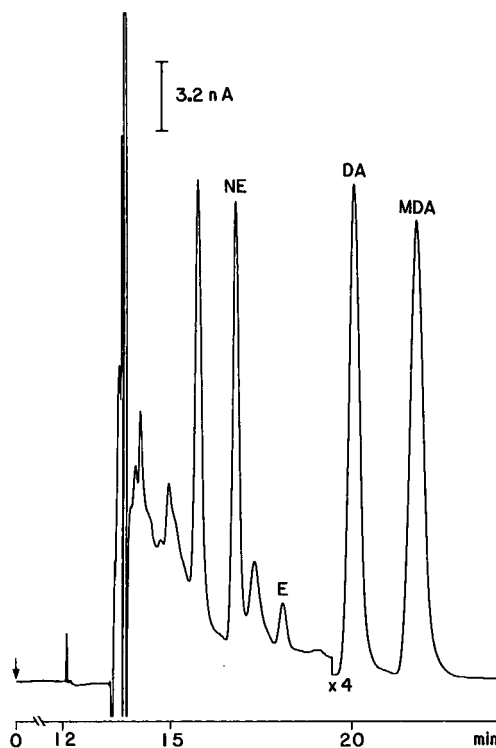


Fig. 4. Chromatogram of a human urine sample containing 220 nM NE, 34.3 nM E and 960 nM DA. Injected sample 120  $\mu$ l; potential +0.30 V. Mobile phase 2: phosphate buffer pH = 3.2,  $I$  = 0.1, containing 0.3 mM EDTA and 21% methanol. Other chromatographic conditions as in Fig. 1.

### Stability

It was important that the adjustment of the samples to pH 7 was performed just before injection of the 20- to 200- $\mu$ l volume, owing to instability of the catecholamines at this pH. By adding 10 mM EDTA to the 250 mM disodium hydrogenphosphate solution (pH 8.0), the catecholamines were kept stable at pH 7 for at least 30 min. The urine samples and the standard solutions in 1 mM hydrochloric acid were stable for more than 24 h in the cold injection vials.

### Recovery and precision

Peak areas of standard solutions recorded after injection into the coupled-column system were compared with those recorded after direct injection onto the cation-exchange column. The recoveries ob-

TABLE II

DETERMINATION OF NOREPINEPHRINE, EPINEPHRINE AND DOPAMINE IN URINE SAMPLES BY THE AUTOMATED COUPLED-COLUMN METHOD (I) AND BY THE EARLIER PRESENTED LIQUID CHROMATOGRAPHIC METHOD (II) [6]

The values are expressed as nmol/mmol creatinine; R.S.D. = relative standard deviation.

Sample	Norepinephrine			Epinephrine			Dopamine		
	I	II	R.S.D. (%)	I	II	R.S.D. (%)	I	II	R.S.D. (%)
1	28.4	27.9	1.2	3.43	3.52	1.8	179	181	0.8
2	23.9	22.4	4.6	4.65	4.55	1.5	137	135	1.0
3	29.8	29.6	0.5	5.29	5.45	2.1	187	187	0.0
4	20.0	20.6	2.1	4.70	3.84	14.2	147	150	1.4
5	28.1	29.4	3.2	3.76	2.95	17.0	106	108	1.3
6	42.6	42.5	0.2	6.15	5.75	4.8	278	276	0.5
7	24.4	24.4	0.0	3.88	3.56	6.1	185	189	1.5
8	14.8	13.9	4.4	2.38	2.29	2.7	104	99	3.5
9	27.7	29.4	4.2	15.4	15.9	2.3	137	146	4.5
10	30.2	30.5	0.7	6.95	6.42	5.6	187	202	5.5
11	21.3	20.9	1.3	4.83	3.96	14.0	172	180	3.2
12	19.0	22.1	10.7	1.37	1.66	13.5	116	132	9.1
13	30.4	30.8	0.9	5.39	5.16	3.1	152	153	0.5
14	19.8	19.8	0.0	3.30	2.90	9.1	163	162	0.4

tained were  $98.3 \pm 4.1$ ,  $97.4 \pm 4.7$ ,  $100.0 \pm 2.7$  and  $105.0 \pm 2.8\%$  for NE, E, DA and MDA, respectively ( $n=15$ ). The recovery from urine samples determined by standard addition of 55–220 nM was  $100.0 \pm 4.2\%$  for all three catecholamines ( $n=9$ ). The ratios of the peak height of the analyte to that of the internal standard, MDA, in the reference samples were measured and the median value was used for calculation of the urine concentration. The relative standard deviations for human urine samples containing 220 nM NE, 34.3 nM E and 960 nM DA were 2.0, 2.1 and 1.3%, respectively ( $n=15$ ), and for aqueous standard samples, at concentrations of 220 nM, the values were 1.9, 1.6 and 0.71% ( $n=15$ ). The limit of quantitation for epinephrine in human urine was 5 nM with a relative standard deviation of 10% ( $n=10$ ), and the method was linear up to at least ten times the concentration of the reference solution used in the analytical procedure. The accuracy of the method was tested by analysing some of the samples using our earlier published method [6], which is based on purification by alumina before cation-exchange liquid chromatography. Good agreement between the two methods was found, as shown in Table II.

#### ACKNOWLEDGEMENT

We thank Dr. Bengt-Arne Persson for valuable discussions of the manuscript and Mr. Bengt Kull for performing the creatinine analyses.

#### REFERENCES

- 1 F. Smedes, J. C. Kraak and H. Poppe, *J. Chromatogr.*, 231 (1982) 25.
- 2 F. A. J. van der Hoorn, F. Boomsma, A. J. Man in 't Veld and M. A. D. H. Schalekamp, *J. Chromatogr.*, 563 (1991) 348.
- 3 J. Odink, H. Sandman and W. H. P. Schreurs, *J. Chromatogr.*, 377 (1986) 145.
- 4 J. B. Nair, M. N. Munk and J. D. McLean, *J. Chromatogr.*, 416 (1987) 340.
- 5 H. Nohta, E. Yamaguchi, Y. Ohkura and H. Watanabe, *J. Chromatogr.*, 493 (1989) 15.
- 6 B.-M. Eriksson, S. Gustafsson and B.-A. Persson, *J. Chromatogr.*, 278 (1983) 255.
- 7 M. Beschi, M. Castellano, E. Agabiti-Rosei, D. Rizzoni, P. Rossini and G. Muiesan, *Chromatographia*, 24 (1987) 455.
- 8 G. M. Anderson, T. A. Durkin, J. B. Morton and D. J. Cohen, *J. Chromatogr.*, 424 (1988) 373.
- 9 H. Tsuchiya, T. Koike and T. Hayashi, *Anal. Chim. Acta*, 218 (1989) 119.
- 10 L. Hansson, M. Glad and C. Hansson, *J. Chromatogr.*, 265 (1983) 37.

- 11 R. T. Peaston, *J. Chromatogr.*, 424 (1988) 263.
- 12 T. Huang, J. Wall and P. Kabra, *J. Chromatogr.*, 452 (1988) 409.
- 13 M. Claeys, A. Schepers, L. Dillen and W. P. de Potter, *J. Pharm. Biomed. Anal.*, 6 (1988) 895.
- 14 P. Hjemdahl, P. T. Larsson, T. Bradley, T. Åkerstedt, I. Anderzén, K. Sigurdsson, M. Gillberg and U. Lundberg, *J. Chromatogr.*, 494 (1989) 53.
- 15 M. Goto, T. Nakamura and D. Ishii, *J. Chromatogr.*, 226 (1981) 33.
- 16 P. O. Edlund and D. Westerlund, *J. Pharm. Biomed. Anal.*, 2 (1984) 315.
- 17 J. de Jong, A. J. F. Point, U. R. Tjaden, S. Beeksmā and J. C. Kraak, *J. Chromatogr.*, 414 (1987) 285.
- 18 K.-S. Boos, B. Wilmers, R. Sauerbrey and E. Schlimme, *Chromatographia*, 24 (1987) 363.
- 19 G. Grossi, A. Bargossi, A. Lippi and R. Battistoni, *Chromatographia*, 24 (1987) 842.
- 20 R. Said, D. Robinet, C. Barbier, J. Sartre and C. Huguet, *J. Chromatogr.*, 530 (1990) 11.
- 21 B.-M. Eriksson and M. Wikström, *J. Chromatogr.*, 567 (1991) 1.

# Determination of cinnamic acid and paeoniflorin in traditional chinese medicinal preparations by high-performance liquid chromatography

Kuo-Ching Wen, Cheng-Yu Huang and Fang-Su Liu

National Laboratories of Foods and Drugs, Department of Health, Executive Yuan, 161–2 Kuen-Yang Street, Nankang, Taipei (Taiwan)

## ABSTRACT

A high-performance liquid chromatographic method for the determination of cinnamic acid in *Cinnamomi ramulus* and paeoniflorin in *Paeoniae radix* was established. The samples were separated by a LiChrospher RP-18 column with water–acetonitrile–methanol–acetic acid (61:34:5:0.1 or 80:15:5:0.1, v/v) as the mobile phase at a flow-rate of 1.0 ml/min. Cinnamic acid and paeoniflorin were determined by UV detection at 280 and 250 nm, respectively. The method was applied to determine the optimum conditions for the extraction of the traditional Chinese medicinal preparation Huang Chi Chien Chung Tong, which contains *Cinnamomi ramulus* and *Paeoniae radix*. The results indicate that the best extraction conditions involved the use of an ultrasonic bath at 60°C for 30 min. In this experiment, butyl paraben and methyl paraben were used as the internal standards for cinnamic acid and paeoniflorin, respectively. A good and reproducible separation of cinnamic acid and paeoniflorin was obtained within 15 min. The method was also applicable to other preparations that contain *Cinnamomi ramulus* and *Paeoniae radix* such as Guey Chi Chia Long Ku Muu Li Tong, Kuei Chi Chien Chung Tong and Tang Kuei Chien Chung Tong.

## INTRODUCTION

Traditional Chinese medicines, especially the concentrated type, are widely used and suitable assay methods are therefore needed for quality control purposes. In Japan, since 1985, the Ministry of Health and Welfare has required that all concentrated herbal preparations submitted for inspection and registration should include a content analysis with at least two chemical components as markers [1]. It has also regulated that all concentrated herbal preparations produced by pharmaceutical factories should be compared with the standard decoction<sup>a</sup> and the resulting difference in content of their marker components should be within  $\pm 30\%$ . How-

ever, as our knowledge of the effective components of traditional Chinese medicines is still limited and the chemical compositions are very complicate, to determine accurately the contents of traditional Chinese medicine is very difficult. Research in this area is progressing in order that the process of Chinese medicine manufacture can be established on a scientific basis.

Huang Chi Chen Chung Tong is a prescription often used to treat physical weakness, and was studied in this work. Two components, cinnamic acid (present in *Cinnamomi ramulus*) and paeoniflorin (present in *Paeoniae radix*) were selected for analysis; their structural formulae are shown in Fig. 1. High-performance liquid chromatography (HPLC) was employed to establish the optimum conditions for determination [2–8], which hopefully would serve as a reference for determining the contents of other prescriptions containing *Cinnamomi ramulus* and *Paeoniae radix*. In this experi-

<sup>a</sup> Standard decoction: to raw herb materials representing 1-day's dosage add a twentyfold weight excess of water and boil for more than 30 min until the liquid has reduced to half of the original volume. Filter the liquid to obtain the preparation.

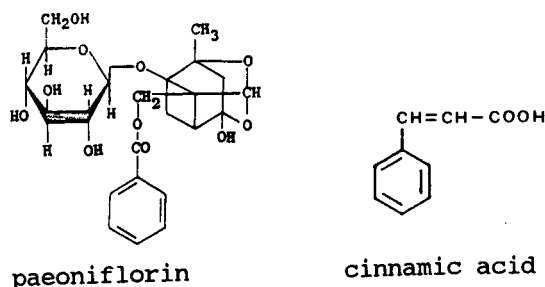


Fig. 1. Structures of marker components.

ment, we also examined the effects of different extraction times and temperatures on the extracted amounts of cinnamic acid and paeoniflorin. The effects of various processes of concentration, drying and the addition of other excipients are also discussed.

## EXPERIMENTAL

### Materials

According to ref. 9, the following materials are needed to prepare Huang Chi Chen Chung Tong: *Cinnamomi ramulus*, 3 g; *Paeoniae radix*, 6 g; *Zingiberis rhizoma*, 3 g; *Zizyphi fructus*, 3 g; *Glycyrrhizae radix*, 3 g; *Astragali radix*, 1.5 g; and *Saccharum granorum*, 20 g. Other Chinese concentrated herbal preparations containing *Cinnamomi ramulus* and *Paeoniae radix* include Huang Chi Chen Chung Tong, Guey Chi Chia Long Ku Mum Li Tong and Kuei Chi Chen Chung Tong.

### Chemicals and reagents

Reference standards of *trans*-cinnamic acid and paeoniflorin were purchased from Nacalai Tesque (Kyoto, Japan). The internal standards butyl paraben and methyl paraben were obtained from Sigma (St. Louis, MO, USA). Methanol and acetonitrile (HPLC grade) were purchased from ALPS (Taiwan) and all other reagents were of analytical-reagent grade.

### Liquid chromatography

A Waters–Millipore LC system with a U6K injector and a Model 990 photodiode-array detector was used. For reversed-phase HPLC, a LiChrospher RP-18 (5- $\mu$ m) column (125  $\times$  4 mm I.D.) (Merck) with water–acetonitrile–methanol–acetic acid

(61:34:5:0.1, v/v, for cinnamic acid and 80:15:5:0.1, v/v, for paeoniflorin) as the mobile phase at a flow-rate of 1.0 ml/min was adopted, with UV absorbance detection at 280 nm for cinnamic acid and 250 nm for paeoniflorin. Pretreatment of the solvents with a vacuum filter for degassing was applied.

### Sample preparation for HPLC

**Calibration graph.** Cinnamic acid and paeoniflorin were accurately weighed and dissolved in methanol to give various concentrations within the range 0.001–0.01 and 0.025–0.3 mg/ml, respectively. An appropriate amount of internal standard was added to each solution to give concentrations of 0.1 mg/ml of butyl paraben or 0.02 mg/ml of methyl paraben. Calibration graphs were plotted based on linear regression analysis of the peak-area ratios.

**Standard decoction.** Amounts of crude drug equivalent to a daily dose of Huang Chi Chen Chung Tong were weighed and pulverized. A twentyfold weight excess of water was added and the mixture was boiled for more than 30 min to halve the original volume. A suitable amount of internal standard was added to the solution to give concentrations of 0.1 mg/ml of butyl paraben or 0.02 mg/ml of methyl paraben.

**Concentrated herbal preparations.** An amount equivalent to 1 g of *Cinnamomi ramulus* (or *Paeoniae radix*) was weighed and pulverized if necessary. Extraction was carried out by vibrating with an ultrasonic bath in 90 ml of 50% methanol for 30 min. After extraction, the sample was filtered and diluted to 100 ml with the addition of internal standard to give concentrations of 0.1 mg/ml of butyl paraben or 0.02 mg/ml of methyl paraben.

**Recovery.** Amounts of crude drugs equivalent to 50 doses of Huang Chi Chen Chung Tong without *Cinnamomi ramulus* were weighed and pulverized together. Then four doses of these powders were weighed precisely and separately, each 36.5 g. To these four doses were added 1, 2, 3 and 4 g of *Cinnamomi ramulus* with known cinnamic acid contents of 7.21, 14.42, 21.63 and 28.84 mg, respectively. A twentyfold weight excess of water was added and the mixture was boiled for more than 30 min to halve the original volume. A suitable amount of internal standard was added to the solution to give a concentration of 0.1 mg/ml of butyl paraben.



Amounts of crude drugs equivalent to 50 doses of Huang Chi Chen Chung Tong without *Paeoniae radix* were weighed and pulverized together. Then four doses of these powder were weighed precisely and separately, each 33.5 g. To these four doses were added 2, 4, 6 and 8 g of *Paeoniae radix* with known paeoniflorin contents of 25.26, 50.52, 75.78 and 101.04 mg, respectively. A twentyfold weight excess of water was added and the mixture was boiled for more than 30 min to halve the original volume. A suitable amount of internal standard was added to the solution to give a concentration of 0.02 mg/ml of methyl paraben.

All samples were filtered through a Millipore filter and 10 µl of filtrate were injected for HPLC analysis to calculate the concentration of cinnamic acid or paeoniflorin from their calibration graphs.

RESULTS AND DISCUSSION

The calibration graph for cinnamic acid and methyl paraben was obtained over the range 0.001–0.01 mg/ml. The results, through linear regression analysis, showed a good linear relationship between the peak-area ratio and concentration. Table I gives the results and the regression equation. A similar good linear relationship was obtained from the calibration graph for paeoniflorin and butyl paraben (Table II).

Cinnamic acid present in *Cinnamomi ramulus* and paeoniflorin in *Paeoniae radix* were determined by HPLC under the established conditions. The retention times for cinnamic acid and butyl paraben were 4.2 and 14.5 min, respectively (Fig. 2); retention

TABLE I  
RELATIONSHIP BETWEEN CONCENTRATION OF CINNAMIC ACID AND THE PEAK-AREA RATIO

Regression equation:  $y = -0.001 + 0.042x$  ( $r = 0.9996$ ).

Concentration (mg/ml)	Peak-area ratio <sup>a</sup>
0.001	0.025 (1.48)
0.003	0.071 (1.12)
0.005	0.120 (0.78)
0.010	0.240 (0.90)

<sup>a</sup> Peak area of cinnamic acid/peak area of butyl paraben, with relative standard deviation (%) in parentheses ( $n = 6$ ).

TABLE II  
RELATIONSHIP BETWEEN CONCENTRATION OF PAEONIFLORIN AND PEAK-AREA RATIO

Regression equation:  $y = -0.00005 + 0.297x$  ( $r = 0.9998$ ).

Concentration (mg/ml)	Peak-area ratio <sup>a</sup>
0.025	0.087 (0.94)
0.050	0.176 (1.27)
0.100	0.339 (1.61)
0.300	1.016 (0.69)

<sup>a</sup> Peak area of paeoniflorin/peak area of methyl paraben, with relative standard deviation (%) in parentheses ( $n = 6$ ).

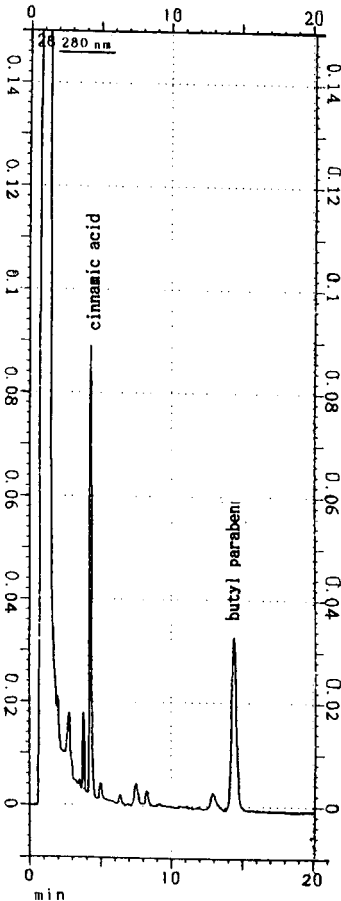


Fig. 2. Chromatogram of cinnamic acid in Huang Chi Chen Chung Tong. Column, LiChrospher RP-18; mobile phase, water–acetonitrile–methanol–acetic acid (61:34:5:0.1, v/v); flow-rate, 1 ml/min.

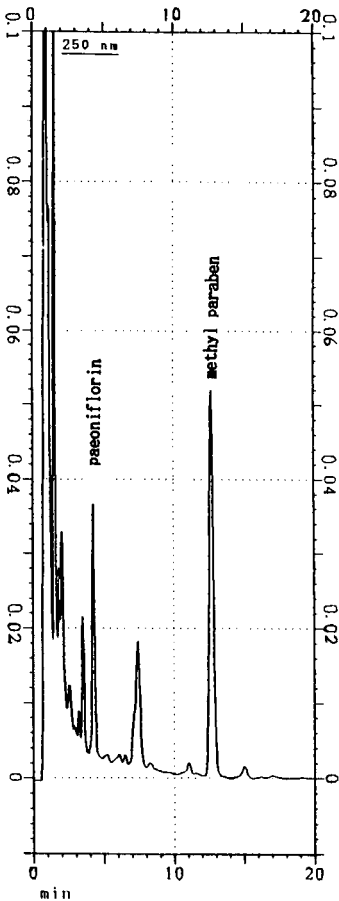


Fig. 3. Chromatogram of paeoniflorin in Huang Chi Chen Chung Tong. Column, LiChrospher RP-18; mobile phase, water–acetonitrile–methanol–acetic acid (80:15:5:0.1, v/v); flow-rate, 1 ml/min.

times for paeoniflorin and methyl paraben are 4.2 and 12.5 min, respectively (Fig. 3). The assay method used has the following advantages that it is easy and convenient to operate, is rapid and the accuracy of the determination is improved by the addition of an internal standard.

Traditional Chinese medicines are usually prepared by boiling with water. However, extraction of components with water from preparations tends to cause problems during the experiment, *e.g.*, the extracted materials may block the column. For this reason, four solvents were tried for extraction: water, methanol, methanol–water (30:70) and methanol–water (50:50). Two methods, refluxing and using an ultrasonic bath, were used to extract cinnamic acid from *Cinnamomi ramulus* and paeoniflorin from *Paeoniae radix*. The largest extracted amount was assigned an arbitrary value 100 to compare the efficiencies of the various extraction methods. The results are given in Tables III and IV ( $n = 6$ ) and it indicate that both methods have similar effects on the determination of cinnamic acid and paeoniflorin. They also show that methanol, methanol–water (30:70) and methanol–water (50:50) are the best solvents for cinnamic acid extraction whereas water, methanol–water (30:70) and methanol–water (50:50) are best for paeoniflorin.

We also studied the optimum temperature and time for extracting cinnamic acid and paeoniflorin. The samples were vibrated with an ultrasonic bath for 30 and 60 min at 30, 60 and 80°C. The results are shown in Tables V and VI. As can be seen, the

TABLE III  
YIELDS OF CINNAMIC ACID EXTRACTED FROM *CINNAMOMI RAMULUS* BY VARIOUS SOLVENTS

Method	Yield (%)			
	Methanol	Methanol–water (30:70)	Methanol–water (50:50)	Water
Reflux (30 min)	100	98.0	98.3	81.8
Agitation with ultrasonic bath	100	98.9	99.7	84.3

TABLE IV  
YIELDS OF PAEONIFLORIN EXTRACTED FROM *PAEONIAE RADIX* BY VARIOUS SOLVENTS

Method	Yield (%)			
	Methanol	Methanol– water (30:70)	Methanol– water (50:50)	Water
Reflux (30 min)	46.4	99.0	99.2	100
Agitation with ultrasonic bath	48.9	99.2	99.5	100

TABLE V  
YIELDS OF CINNAMIC ACID EXTRACTED WITH  
METHANOL–WATER (50:50) FROM HUANG CHI CHIEN  
CHUNG TONG AT VARIOUS TEMPERATURES

Time (min)	Yield (%)		
	30°C	60°C	80°C
30	82.7	100	99.6
60	87.5	99.8	99.5

TABLE VI  
YIELDS OF PAEONIFLORIN EXTRACTED WITH  
METHANOL–WATER (50:50) FROM HUANG CHI CHIEN  
CHUNG TONG AT VARIOUS TEMPERATURES

Time (min)	Yield (%)		
	30°C	60°C	60°C
30	79.3	100	99.9
60	84.7	99.3	99.1

amounts of the two components extracted did not increase with time or elevated temperature after extraction at 60°C for 30 min.

After comparing the various extraction methods with respect to solvent, temperature and time, and considering the conditions that might be applied during the manufacture of Chinese medicines, we conclude that the best way to extract cinnamic acid

and paeoniflorin is to vibrate the sample with an ultrasonic bath for 30 min at 60°C with methanol–water (50:50) as solvent.

The accuracy of the HPLC assay method was determined by recovery tests and the precision was evaluated by measuring the reproducibility [relative standard deviation (R.S.D.)]. The recoveries were 95.3% for cinnamic acid and 95.9% for paeoniflorin

TABLE VII  
RECOVERY OF CINNAMIC ACID IN HUANG CHI CHIEN CHUNG TONG

Amount of <i>Cinnamomi</i> <i>ramulus</i> taken (g)	Content of cinnmic acid in <i>Cinnmomi</i> <i>ramulus</i> (mg)	No. of injections ( <i>n</i> )	Amount measured (mg)	Recovery (%)	Mean ± S.D. (%)	R.S.D. (%)
1	7.21	6	6.73	93.3	95.3 ± 1.58	1.66
2	14.42	6	13.70	95.0		
3	21.63	6	20.76	96.0		
4	28.84	6	27.97	97.0		

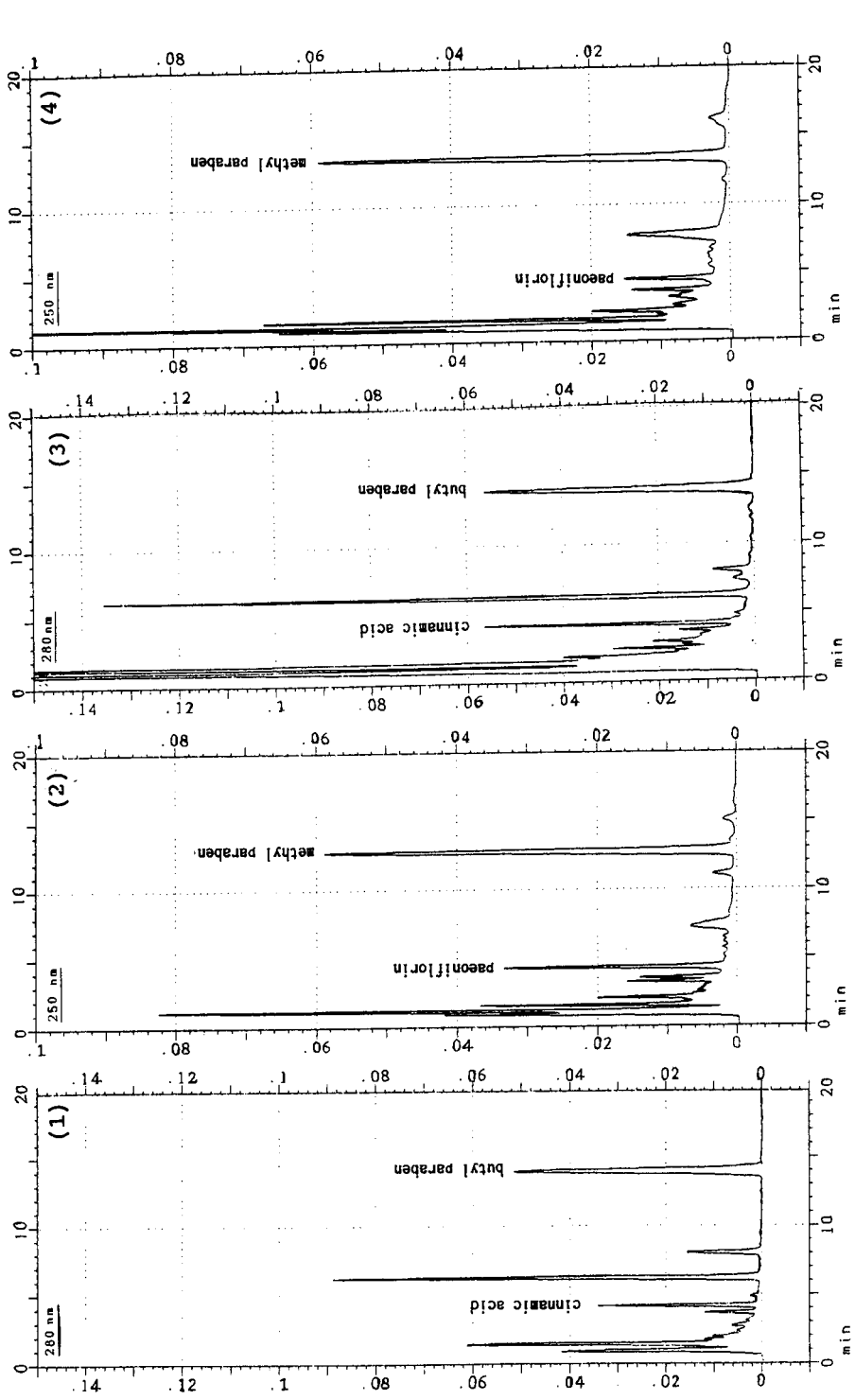


Fig. 4. Chromatograms of different samples: (1) and (2) Guey Chi Chia Long Ku Mum Li Tong; (3) and (4) Kuei Chi Chien Chung Tong. HPLC conditions: (1) and (3) as in Fig. 2; (2) and (4) as in Fig. 3.

TABLE VIII  
RECOVERY OF PAEONIFLORIN IN HUANG CHI CHIEN CHUNG TONG

Amount of <i>Paoniae radix</i> taken (g)	Content of paeoniflorin in <i>Paoniae radix</i> (mg)	No. of injections (n)	Amount measured (mg)	Recovery (%)	Mean $\pm$ S.D. (%)	R.S.D. (%)
2	25.26	6	24.05	95.2	95.9 $\pm$ 2.07	2.16
4	50.52	6	48.80	96.6		
6	75.78	6	73.81	97.4		
8	101.04	6	92.27	91.3		

TABLE IX  
REPRODUCIBILITY OF THE DETERMINATION OF CINNAMIC ACID IN HUANG CHI CHIEN CHUNG TONG

Injection No.	Amount measured (mg/g)	Mean $\pm$ S.D. (%)	R.S.D. (%)
1	7.24	7.212 $\pm$ 0.017	0.23
2	7.22		
3	7.19		
4	7.21		
5	7.20		
6	7.21		

TABLE X  
REPRODUCIBILITY OF THE DETERMINATION OF PAEONIFLORIN IN HUANG CHI CHIEN CHUNG TONG

Injection No.	Amount measured (mg/g)	Mean $\pm$ S.D. (%)	R.S.D. (%)
1	12.73	12.625 $\pm$ 0.183	1.45
2	12.28		
3	12.62		
4	12.81		
5	12.67		
6	12.64		

TABLE XI  
CONTENTS OF CINNAMIC ACID IN COMMERCIAL PREPARATIONS CONTAINING *CINNAMOMI RAMULUS* AND *PAEONIAE RADIX*

Sample	No. <sup>a</sup>	Loss on drying (%)	Content of cinnamic acid in <i>Cinnamomi ramulus</i> -containing preparations (%)
Huang Chi Chen Chung Tong	1g	2.67	0.26
	2p	3.01	0.77
	3p	2.73	0.40
Guey Chi Chia Long Ku Mum Li Tong	1p	3.52	0.32
	2p	2.44	0.66
	3g	3.79	1.87
Kuei Chi Chien Chung Tong	1p	2.83	0.54

<sup>a</sup> p = Powder; g = granules.

TABLE XII  
CONTENTS OF PAEONIFLORIN IN COMMERCIAL PREPARATIONS CONTAINING *CINNAMOMI RAMULUS* AND *PAEONIAE RADIX*

Sample	No. <sup>a</sup>	Loss on drying (%)	Content of paeoniflorin in <i>Paeoniae radix</i> -containing preparations (%)
Huang Chi Chen Chung Tong	1g	2.67	0.26
	2p	3.01	0.77
	3p	2.73	0.40
Guey Chi Chia Long Ku Mum Li Tong	1p	3.52	0.32
	2p	2.44	0.66
	3g	3.79	1.87
Kuei Chi Chien Chung Tong	1p	2.83	0.54

<sup>a</sup> p = Powder; g = granules.

(*n* = 6), and R.S.D.s were 0.23% for cinnamic acid and 1.45% for paeoniflorin. The results of these tests are given in Tables VII–X. We conclude that the method is precise and accurate for the determination of cinnamic acid and paeoniflorin in commercial preparations.

Three different commercial brands of Huang Chi Chen Chung Tong were extracted with the above method and their contents of cinnamic acid and paeoniflorin were determined as described. The results were satisfactory. Other preparations containing *Cinnamomi ramulus* and *Paeoniae radix*, such as Guey Chi Chia Long Ku Mum Li Tong and Kuei Chi Chien Chung Tong, were also analysed with the same method and the results were satisfactory (Fig. 4). The contents of cinnamic acid and

paeoniflorin determined in the different preparations are given in Tables XI and XII.

To elucidate the effects of the concentration process and starch excipient on the determination of cinnamic acid and paeoflorin, the process was applied under reduced pressure at 50°C and with lypholization, as adopted in pharmaceutical factories. The results indicated that the process conditions and starch content did not significantly affect the determination of the two components. The results are given in Tables XIII and Table XIV.

The cinnamaldehyde, which is also present in *Cinnamomi ramulus*, was chosen as a marker [10]. However, the content of cinnamaldehyde tends to decrease with increase in boiling time and temperature. Taking into account the possibility than the

TABLE XIII  
EFFECTS OF CONCENTRATION BY REDUCED PRESSURE AND LYOPHILIZATION ON CONTENTS OF CINNAMIC ACID AND PAEONIFLORIN IN HUANG CHI CHIEN CHUNG TONG

Method	Content (%)	
	Cinnamic acid	Paeoniflorin
Decoction without concentration	0.72	1.26
Concentrated by reduced pressure at 50°C	0.70	1.26
Lyophilization	0.68	1.20

TABLE XIV  
EFFECT OF STARCH ON CONTENTS OF CINNAMIC ACID AND PAEONIFLORIN IN HUANG CHI CHIEN CHUNG TONG

Excipient	Content (%)	
	Cinnamic acid	Paeoniflorin
Without starch	0.72	1.26
With starch	0.69	1.21

method used here might be applied to the analysis of concentrated preparations, cinnamic acid is to be preferred as a marker because it is not affected by time and temperature. The chromatogram of the standard decoction shows that the cinnamaldehyde content decreased with prolonged boiling and because so low that it was difficult to measure. However, the chromatogram of the commercial preparations showed highly concentrated cinnamaldehyde. More research on this aspect needs to be done.

## REFERENCES

- 1 M. Harada, Y. Ogihara, Y. Kano, A. Akahori, Y. Ichio, O. Hiura and H. Suzuki, *Iyakuhin Kenkyu*, 19 (1988) 852.
- 2 M. Harada, Y. Ogihara, Y. Kano, A. Akahori, Y. Ichio, O. Miura, K. Yamamoto and H. Suzuki, *Iyakuhin Kenkyu*, A20 (1989) 1300.
- 3 H. Suzuki, *Shoyakugaku Zasshi*, 38 (1984) 144.
- 4 Y. Akada, S. Kawano and Y. Tanase, *Yakugaku Zasshi*, 99 (1979) 858.
- 5 K. Asakawa, T. Hattori, M. Ueyama, A. Shinoda and Y. Miyake, *Yakugaku Zasshi*, 99 (1979) 598.
- 6 S.-J. Sheu, C.-H. Yu, Y.-P. Chen and H.-Y. Hsu, *J. Chin. Agric. Chem. Soc.*, 19 (1981) 46.
- 7 A. Akahori and K. Kagawa, *Shoyakugaku Zasshi*, 32 (1978) 24.
- 8 K. Sagara, T. Oshima and T. Yoshida, *J. Chromatogr.*, 409 (1987) 365.
- 9 H.-Y. Hsu and C.-S. Hsu, *Commonly Used Chinese Herb Formulas with Illustrations*, Oriental Healing Arts Institute, Taiwan, 1980.
- 10 Y. Yokota, C. Eziri and H. Saito, *Research on Home Medicines*, 8 (1989) 14.





# Analysis and isolation of indole alkaloids of fungi by high-performance liquid chromatography

Milan Wurst\*

*Institute of Microbiology, Czechoslovak Academy of Sciences, Videnska 1083, CS-142 20 Prague 4 (Czechoslovakia)*

Roman Kysilka

*Watrex Institute, Hostalkova 117, CS-169 00 Prague 6 (Czechoslovakia)*

Tomas Koza

*Institute of Microbiology, Czechoslovak Academy of Sciences, Videnska 1083, CS-142 20 Prague 4 (Czechoslovakia)*

---

## ABSTRACT

An efficient analytical and isolation method was elaborated for biologically active tryptamines using a computer-aided liquid chromatographic–gas chromatographic system. The separation method includes a new efficient extraction procedure, optimization programme for high-performance liquid chromatographic separation, identification by diode-array detection and a spectrometric and electrochemical assay. The identification of indole alkaloids was confirmed by thin-layer and gas chromatography and mass spectrometry. The method was used for analysis and isolation of psychotropic substances in extracts from the fruit bodies of hallucinogenic fungi of genera *Psilocybe*, *Inocybe* and *Amanita* and in mycelial extracts from the species *Psilocybe bohemica*.

---

## INTRODUCTION

Three decades after their discovery in fungi of the genus *Psilocybe* in Mexico, indole alkaloids of the tryptamine type [1,2] have become biochemically important drugs in psychotherapy and psychodiagnostics. Chromatographic methods are widely used in studies of these psychotropic compounds found in biological materials. Special attention is paid to fungi of the genera *Psilocybe*, containing psilocybin and psilocin. Gas chromatography (GC) has been widely used for this purpose [3]; prior to analysis, however, poorly volatile and heat-labile tryptamines have to be chemically converted into acetate [4], enamine [5], isothiocyanate [6] or trimethylsilyl (TMS) derivatives [7]. A GC–mass spectrometric (MS) system has been used for the analysis of TMS derivatives of bufotenin [6], psilocybin and psilocin

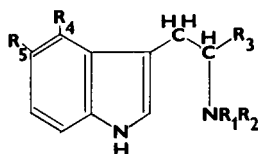
[8]. Tryptamine compounds are often separated and assayed by high-performance liquid chromatography (HPLC) with UV spectrophotometric [9–23], electrochemical (ED) [16,19–21] or fluorimetric [11,12,15,16,18] detection, and sometimes with MS identification [10,14,18].

Studies of indole alkaloids form part of research into the metabolism of aromatic amino acids in microorganisms and include a search for new efficient extraction and separation procedures, optimization of HPLC analysis, high identification fidelity and computer-aided evaluation of results. Some studies in this direction are reported in this paper.

## EXPERIMENTAL

### *Chemicals*

Analytical standards of indole alkaloids were ob-



	R <sub>1</sub>	R <sub>2</sub>	R <sub>3</sub>	R <sub>4</sub>	R <sub>5</sub>
Tryptamine	H	H	H	H	H
Tryptophan	H	H	COOH	H	H
Serotonin	H	H	H	H	OH
5-Hydroxy-N-methyltryptamine	Me	H	H	H	OH
5-Hydroxytryptophan	H	H	COOH	H	OH
Bufotenin	Me	Me	H	H	OH
Psilocin	Me	Me	H	OH	H
Psilocybin	Me	Me	H	H <sub>2</sub> PO <sub>4</sub>	H

tained from Sigma (St. Louis, MO, USA), except psilocybin and psilocin, which were obtained from Sandoz (Basle, Switzerland).

The silylation reagent N-(methyl-N-(*tert*.-butyldimethylsilyl) trifluoroacetamide (MTBSTFA) was purchased from Pierce Eurochemie (Oud-Beijerland, Netherlands). Other chemicals were of analytical-reagent grade from Lachema (Brno, Czechoslovakia).

#### Microbiological materials

Species of fungi of the genera *Psilocybe* and *Amanita* were collected at various places in Czechoslovakia and of the genus *Inocybe* in Germany. The fungus *Psilocybe bohemica* from our laboratory collection was cultivated at 24°C in a 300-ml flask containing 100 ml of complex medium on a reciprocal shaker (3 Hz, amplitude 50 mm).

#### Sample preparation

The dried fruit bodies of fungi of the genera *Psilocybe*, *Inocybe* or *Amanita* were cut and then completely homogenized in a glass mortar, whereas the samples of mycelium were only homogenized. Extraction was performed in 20-ml vials at a constant sample weight of 10 mg on a reciprocal shaker (1.2 Hz, amplitude 15 mm).

Psilocybin was extracted for 10 min with 0.50 ml of 70% methanol (saturated with potassium nitrate), whereas psilocin and bufotenin were extracted with water-ethanol (75:25) for 160 min. The crude extract was filtered through a 1- $\mu$ m PTFE filter before injection into the HPLC apparatus.

#### Derivatization

Silylation was modified for derivatization of samples or standard compounds of the tryptamine type: a dried sample of standard indole alkaloids (about 0.3 mg) was placed in a glass ampoule, dissolved in a mixture of 0.1 ml of acetonitrile and 0.1 ml of MTBSTFA and heated in the sealed ampoule for 10 min at 90°C. The procedure yielded samples converted completely into *tert*.-butyldimethylsilyl (TBDMS) derivatives. After cooling, the samples were used directly for GC analysis.

#### Gas chromatography

GC analyses were performed on Sigma 3B gas chromatograph (Perkin-Elmer, Norwalk, CT, USA) with flame ionization detection (FID). TBDMS derivatives of indole alkaloids were separated on a 30 m  $\times$  0.25 mm I.D. SPB-1 fused-silica column (Supelco, Gland, Switzerland) with temperature programming from 250 to 300°C at 3°C/min. The injection port (split injector, splitting ratio 1:70) and detector were maintained at 300°C. Hydrogen was employed as the carrier gas at a flow-rate of 42 cm/s. Samples of 0.2–0.5  $\mu$ l were introduced with a 1- $\mu$ l Hamilton (Bonaduz, Switzerland) microsyringe.

Identification of the TBDMS derivatives of individual components of a mixture was carried out by comparing their retention characteristics with those of the standards. Detector signals were processed by Baseline 810 chromatographic software (Waters, Milford, MA, USA).

### High-performance liquid chromatography

The liquid chromatograph consisted of a Model 3B high-pressure pump, which ensures programming of the mobile phase concentration and flow-rate, a Model 7105 injection valve (Perkin-Elmer) and a Waters model 990+ photodiode-array detector. A model 641 VA voltammetric detector (Metrohm, Herisau, Switzerland) was connected in series with a UV detector. The separations were performed on a 300 mm  $\times$  3.9 mm I.D. column (A) packed with  $\mu$ Bondapak C<sub>18</sub> (7  $\mu$ m) and Guard Pak C<sub>18</sub> (Waters), on a 250 mm  $\times$  4 mm I.D. column (B) packed with Silasorb SPH C<sub>18</sub> (7.5  $\mu$ m) (Lachema, Brno, Czechoslovakia) or on a 250 mm  $\times$  8 mm I.D. semi-preparative column (C) packed with Separon SGX C<sub>18</sub> (7  $\mu$ m) (Tessek, Prague, Czechoslovakia). The columns were eluted isocratically with 0.1 M citrate-phosphate buffer (pH 2.8)-ethanol (95:5) (column A) or methanol-water-acetic acid (5:95:1) (column B) or (10:90:1) (column C). The flow-rate was 1.0 ml/min and the columns were maintained at 25°C.

Sample doses were 1–5  $\mu$ l of methanolic solution (concentration about 1 mg/ml) in the analytical column and 100–200  $\mu$ l in the semi-preparative column. Samples of 200  $\mu$ l were repeatedly injected on to the semi-preparative column and the fraction containing the analyte compound was collected in a 5-ml flask during elution. It was then evaporated under vacuum and the residue was used for identification by GC, MS and UV spectrometry. Standard compounds and samples were used for thin-layer chromatography (TLC) in 0.1-ml aliquots (about 20  $\mu$ g of the compounds).

Qualitative analysis of psychotropic indole compounds was performed by comparing their elution volumes with those of reference samples. The results were confirmed by TLC, GC, MS and UV spectrometry. Indole alkaloids were determined by means of the internal normalization and external standard method. Detector signals were processed by the Baseline 810 software (Waters).

### Thin-layer chromatography

Psilocybin, psilocin, bufotenin, etc., were identified on Silufol UV 254 foils eluted with *n*-butanol-water-acetic acid (24:10:10). Tryptamines were detected with Ehrlich reagent (2% *p*-dimethylaminobenzaldehyde in 1 M hydrochloric acid) and yielded red-violet spots after completion of the reaction.

### Mass spectrometry

Mass spectra were measured with a Varian MAT model 311 instrument with ionization energy 70 eV, current 1 mA, ion source temperature 200°C and inlet temperature 35°C for psilocin, bufotenin and 140°C for psilocybin. The high-resolution peak-matching technique employed gave errors of  $\pm 5$  ppm.

## RESULTS AND DISCUSSION

### Extraction

Extraction of psychotropic indole compounds from biological material (*Psilocybe bohemica*) has received scant attention in the literature on the analysis of these substances. The extraction is performed with mixtures of lower alcohols and water, sometimes with adjusted ionic strength or pH. The yield of psilocybin extraction by the commonly used methanol is only 80% of the amount obtained by extraction into 75% (v/v) methanol saturated with potassium nitrate (Fig. 1). Aqueous ethanol solutions are unsuitable for psilocybin extraction (maximum yield 36%). A 90% yield can be attained with 1% acetic acid in methanol. This system is suitable especially for preparative purposes as both solvents can be evaporated.

The best extraction results with psilocin were obtained with 75% (v/v) aqueous ethanol, whereas

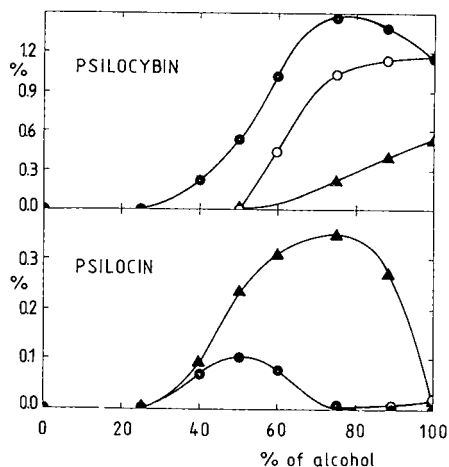


Fig. 1. Dependence of the determined amount of psilocybin and psilocin on the composition of the extracting agent: ● = methanol-water-saturated KNO<sub>3</sub>; ○ = methanol-water; ▲ = ethanol-water.

methanol gave less than 10% of the amount recovered with 75% ethanol (Fig. 1). The optimum extraction systems for psilocybin and psilocin therefore differ.

A kinetic equation was used to calculate the time necessary for extraction of 99.9% of both psilocybin and psilocin. In contrast to literature data, complete recovery of psilocybin was found to require only 10 min and of psilocin 160 min [24].

### Separation

The optimum composition of the mobile phase (amount of ethanol) for the chromatographic separation of tryptamines was determined by computer processing of experimental data on retention and on column efficiency, using an optimization and simulation program based on application of the so-called chromatographic optimization function (COF) [20]. Fig. 2 gives the conditions for the HPLC separation of individual tryptamines. Optimum separation of key tryptamines was achieved on the Silasorb SPH C<sub>18</sub> column (B) with citrate-phosphate buffer containing 10% ethanol as mobile phase (Table I). Separation of indole alkaloids from *Amanita* fungus was done on a  $\mu$ Bondapak C<sub>18</sub> + Guard Pak column (A) with citrate-phosphate buffer containing 5% ethanol as mobile phase.

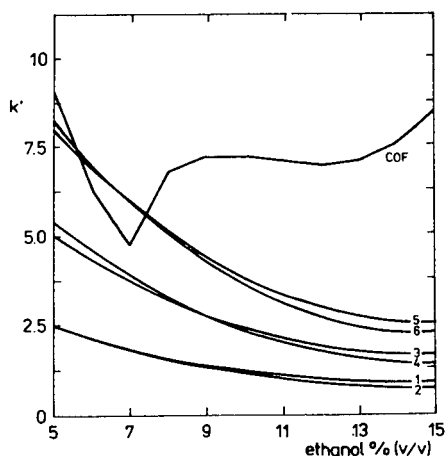


Fig. 2. Dependence of the capacity factor ( $k'$ ) and the chromatographic optimization function (COF) on the ethanol content in the mobile phase. 1 = Psilocybin; 2 = serotonin; 3 = tryptophan; 4 = bufotenin; 5 = tryptamine; 6 = psilocin.

### Identification

The separation and identification of a mixture of indole alkaloids in extracts from fungi of genera *Psilocybe*, *Inocybe* and *Amanita* were first verified by TLC. The purity of individual compounds was demonstrated chromatographically ( $R_F$ ) based on red-violet spots typical of tryptamines. Identifica-

TABLE I

RETENTION AND DETECTION DATA FOR THE INDOLE ALKALOIDS

Substance	Retention data		Detection limit (ng)		Relative standard deviation (%) <sup>b</sup>	
	GC (°C) <sup>a</sup>	HPLC ( $k'$ )	UV	ED	UV	ED
5-Hydroxytryptophan	294.0	1.004	20	0.5	3.2	3.2
Psilocybin	—	1.004	20	1.0	2.8	3.5
5-Hydroxytryptamin (serotonin)	273.5	1.253	64	2.6	3.2	3.2
Bufotenin	263.5	1.931	34	1.0	3.1	3.5
Tryptophan	273.0	2.721	88	2.8	2.0	2.4
Tryptamine	260.	4.043	30	1.0	2.7	2.5
Psilocin	263.5	3.979	22	0.7	3.0	2.9
5-Hydroxy-N-methyltryptamine	277.0	—	—	—	—	—

<sup>a</sup> Temperature programmed from 200 to 300°C.

<sup>b</sup> Six parallel determinations.

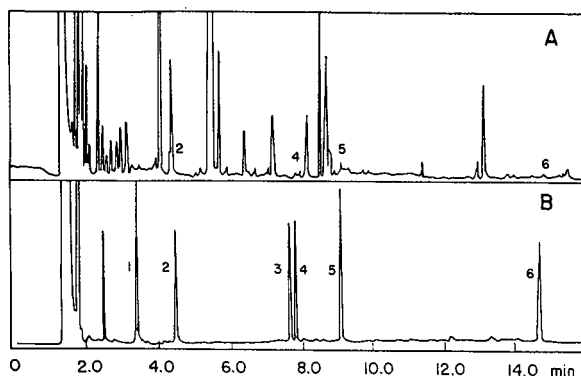


Fig. 3. GC of (A) the extract from fruit bodies of the fungus *Amanita citrina* (A) and (B) a mixture of the hallucinogen standards (TBDMS derivatives). 1 = Tryptamine; 2 = bufotenin; 3 = tryptophan; 4 = serotonin; 5 = 5-hydroxy-N-methyltryptamine; 6 = 5-hydroxytryptophan.

tion of a mixture of indole alkaloids from *Amanita* fungi was further confirmed by GC of their TBDMS derivatives, together with customary indole standards. The separation was performed on an SPB-1 capillary column with temperature programming from 250 to 300°C at 3°C/min. Chromatographic verification of their purity (Fig. 3, Table I) showed no separation of isomeric compounds (bufotenin and psilocin). This does not complicate the identification of the two compounds, however, as the probability of their mutual presence in any biological material is negligible.

The HPLC-separated mixture of indole alkaloids was then identified by recording the UV spectra of

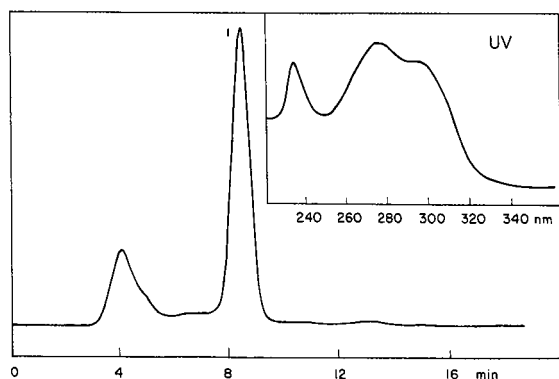


Fig. 4. HPLC of the extract from fruit bodies of the fungus *Amanita citrina* (Vestec, 1987). 1 = Bufotenin. Inset, UV spectrum of bufotenin.

individual compounds during the separation process itself using a diode-array detector (Table I). Fig. 4 shows a chromatogram of bufotenin with the UV spectrum of bufotenin obtained from the computer.

The UV spectra of psychotropic substances agree fully with literature data [25].

#### Determination

The rapid HPLC screening method on Silasorb SPH C<sub>18</sub> (B) with citrate-phosphate buffer (pH 2.8)–ethanol (90:10) mobile phase does not ensure complete separation in all instances. A combination of chromatographic separation with selective ED can separate all components of a mixture of indole alkaloids. Hydroxylated tryptamines and tryptophan can be selectively detected at a working electrode potential of +0.60 V (vs. Ag–AgCl), whereas the half-wave potential of other substances are higher than +0.80 V [21]. The detection limits with the UV photometric detector are of the order of units to tens of nanograms, and with the electrochemical detector units to tenths of nanograms in the inlet (Table I). Quantification of the mixture components was done by the external standard method and evaluation of peak heights. As indicated by the relative standard deviation ( $s_r$ ), this screening method is less exact than common direct methods ( $s_{r, uv} = 3.4\text{--}6.3\%$ ;  $s_{r, ED} = 7.2\text{--}9.1\%$ ).

Differences in the chromatographic behaviours of psilocybin and psilocin make it necessary to use two different mobile phases for the assay of either substance. The preparative application dictates that the mobile phase must be easy to evaporate completely. Its pH cannot be adjusted with a buffer but with an easy-to-evaporate organic acid. The indole alkaloids in extracts from genera *Amanita*, *Psilocybe* and *Inocybe* were analysed by an exact HPLC method on column A ( $\mu$ Bondapak C<sub>18</sub>) with citrate-phosphate buffer (pH 2.8)–ethanol (90:10 or 95:5) as the mobile phase, and psilocybin and psilocin on column B (Silasorb SPH C<sub>18</sub>) with methanol–water–acetic acid (5:95:1 or 10:90:1) as the mobile phase.

A series combination of spectrophotometric and electrochemical detection was also used. Psilocybin was determined from the UV detector (267 nm) recording and psilocin from the electrochemical detector trace (Fig. 5). Table I show that this method

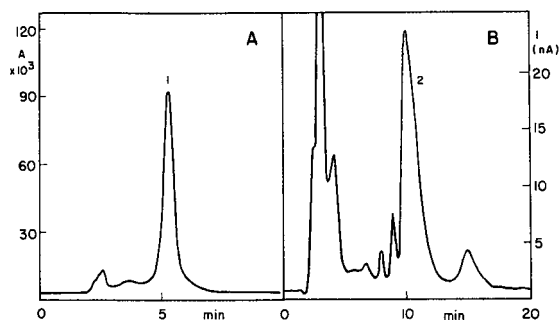


Fig. 5. HPLC of indole alkaloids with (A) UV photometric and (B) electrochemical detection. 1 = Psilocybin; 2 = psilocin.

yields substantially better relative standard deviations than the screening method.

### Isolation

The lipophilic fraction of biological material was removed by extraction into light petroleum (b.p. 40–60°C) (psilocin, bufotenin) or a mixture of light petroleum and chloroform (psilocybin). Psilocin was extracted with 75% aqueous ethanol whereas psilocybin was extracted with 1% acetic acid in methanol.

Isolation of tryptamines was done on a semi-preparative chromatographic column. Psilocybin was

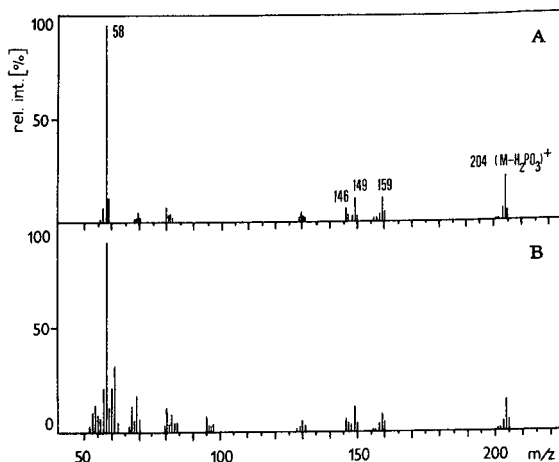


Fig. 6. Mass spectra of an extract of *Psilocybe bohemica*. (A) Psilocybin standard; (B) indole alkaloid isolated from the extract.

chromatographed on a column of Separon SGX C<sub>18</sub> (C) with methanol–water–acetic acid (5:95:1) as the mobile phase. Psilocin and bufotenin were separated under analogous conditions on the same column but with methanol–water–acetic acid (10:90:1) as the mobile phase. Isolated psilocybin, psilocin and bufotenin were identified by MS. Fig. 6 shows the mass spectrum of an extract from biological material.

TABLE II

### CONTENTS OF PSYCHOTROPIC COMPONENTS IN FRUIT BODIES OF THE GENUS *AMANITA*

Species	Locality	Year	Compound <sup>a</sup> (%)				
			OH-MeTPA	OH-TRP	BUF	TPA	TRP
<i>A. citrina</i>	Pribram	1987				0.06	
<i>A. citrina</i>	Vestec	1987			1.058		
<i>A. citrina</i>	Helfenburg	1988			0.593		
<i>A. citrina</i>	Vestec	1988			1.424		
<i>A. citrina</i>	Talin	1889	0.039		1.899		0.025
<i>A. citrina</i>	Krenicna	1989		0.033	0.678		
<i>A. citrina</i>		1989		0.593	1.693		
<i>A. citrina</i>	Neveklov	1989		0.099	0.332		
<i>A. citrina</i>	Vestec	1989			0.414		0.007
<i>A. porphyria</i>	Lounovice	1987			0.374		
<i>A. porphyria</i>	Vestec	1989	0.072		0.617		
<i>A. rubescens</i>	Vestec	1989			0.018		
<i>A. rubescens</i>	Krenicna	1989			0.020		

<sup>a</sup> TRP = Tryptophan; TPA = tryptamine; BUF = bufotenin; OH-MeTPA = 5-hydroxy-N-methyltryptamine; OH-TRP = 5-hydroxytryptophan.

TABLE III

CONTENTS OF PSYCHOTROPIC COMPOUNDS IN FRUIT BODIES OF THE GENERA *PSILOCYBE* AND *INOCYBE*

Species	Locality	Year	Psilocybin (%)	Psilocin (%)
<i>P. bohemica</i>	Frenstat	1981	0.46	0.02
<i>P. bohemica</i>	Sazava	1982	1.14	0.07
<i>P. bohemica</i>	Sazava	1983	0.64	0.48
<i>P. semilanceata</i>	Praha	1980	1.05	0.12
<i>P. semilanceata</i>	Krasna Lipa	1982	0.91	0.09
<i>P. semilanceata</i>	Spiska N. Ves	1986	0.76	0.09
<i>P. cyanescens</i>	Mason County, WA, USA	1984	0.00	0.45
<i>P. cyanescens</i>	Horni Bradlo	1986	0.10	0.47
<i>I. aeruginascens</i>	Potsdam, Germany	1982	0.33	—
<i>I. aeruginascens</i>	Potsdam	1983	0.34	—
<i>I. aeruginascens</i>	Potsdam	1984	0.38	—
<i>I. aeruginascens</i>	Potsdam	1986	0.03	0.02

### Application

The above procedures were used for the separation, identification, isolation and determination of indole alkaloids in extracts from the fruit bodies of fungi from the genera *Psilocybe*, *Inocybe* and *Amanita* and mycelial extracts from the fungus *Psilocybe bohemica*. Table II summarizes the results of analysis of three *Amanita* species collected recently (1987–89) at various localities in Czechoslovakia and Estonia. Two species, *A. citrina* and *A. porphyria*, contain bufotenin (0.3–1.9%) as the major component whereas other tryptamines and tryptophan are present at trace levels. *A. porphyria* has a lower bufotenin content (0.3–0.7%), *A. citrina* from Estonia has a high bufotenin level (1.9%). *A. rubescens* contains no bufotenin, similar to one finding in *A. citrina*.

Comparison of *Amanita* and *Psilocybe* fungi collected in the 1980s in Czechoslovakia and in the USA (Table III) showed similar contents of the major component psilocybin (0.1–1.4%) but psilocin levels in *Psilocybe* are considerably lower (0.02–0.5%). Species of the genus *Inocybe* (collected in Germany) exhibit low psilocybin levels (0.03–0.4%) and negligible psilocin contents (0.02%). The extract from *Inocybe aeruginascens* (1986) contained another compound with a retention time shorter

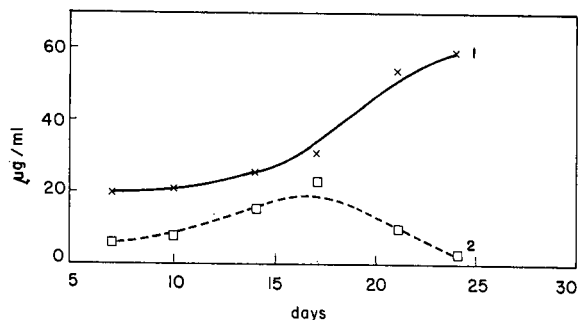


Fig. 7. Production of indole alkaloids during submerged cultivation of *Psilocybe bohemica*. 1 = Psilocybin; 2 = psilocin.

than that of psilocybin but with an essentially identical UV spectrum. It was probably baeocystin, in accordance with the data of Gartz [26].

Chromatographic analysis of psilocybin and psilocin was used during the culturing of the fungus *Psilocybe bohemica* (Fig. 7). Isolation of both compounds from fruit bodies and mycelia was verified by HPLC. The psilocybin recovery was 75–80% of the original amount and with psilocin it was 80–90%.

## REFERENCES

- 1 V. P. Wasson and R. G. Wasson, *Mushrooms, Russia and History*, Pantheon Books, New York, 1957.
- 2 R. G. Wasson, *Trans. N.Y. Acad. Sci.*, 21 (1959) 325.
- 3 H. M. Fales and J. J. Pisano, *Anal. Biochem.*, 3 (1962) 337.
- 4 C. J. W. Brooks and E. C. Horning, *Anal. Chem.*, 36 (1964) 1540.
- 5 E. C. Horning, M. G. Horning, W. J. A. Vandenheuvel, K. L. Knox, B. Holmstedt and C. J. W. Brooks, *Anal. Chem.*, 36 (1964) 1546.
- 6 N. Narasimhachari, J. Spaide and B. Heller, *J. Chromatogr. Sci.*, 9 (1971) 502.
- 7 B. Holmstedt, W. J. A. Vandenheuvel, W. L. Gardiner and E. C. Horning, *Anal. Biochem.*, 8 (1964) 151.
- 8 D. B. Repke, D. T. Leslie and G. Guzman, *Lloydia*, 40 (1977) 566.
- 9 M. F. Balandrin, A. D. Kinghorn, S. J. Smolenski and R. H. Dobberstein, *J. Chromatogr.*, 157 (1978) 365.
- 10 P. C. White, *J. Chromatogr.*, 169 (1979) 453.
- 11 M. Perkal, G. L. Blackman, A. L. Ottrey and L. K. Turner, *J. Chromatogr.*, 196 (1980) 180.
- 12 A. L. Christiansen, K. E. Rasmussen and F. Tonnesen, *J. Chromatogr.*, 210 (1981) 163.
- 13 M. W. Beug and J. Bigwood, *J. Chromatogr.*, 207 (1981) 379.
- 14 A. L. Christiansen and K. E. Rasmussen, *J. Chromatogr.*, 244 (1982) 357.
- 15 B. R. Sitaram, R. Talomsin, G. L. Blackman, W. R. McLeod and G. N. Vaughan, *J. Chromatogr.*, 275 (1983) 21.
- 16 A. L. Christiansen and K. E. Rasmussen, *J. Chromatogr.*, 270 (1983) 293.
- 17 S. M. Sottolano and I. S. Lurie, *J. Forensic Sci.*, 28 (1983) 929.
- 18 M. Wurst, M. Semerdzieva and J. Vokoun, *J. Chromatogr.*, 286 (1984) 229.
- 19 R. Kysilka, M. Wurst, V. Pacakova, K. Stulik and L. Haskovec, *J. Chromatogr.*, 320 (1985) 414.
- 20 R. Kysilka and M. Wurst, *J. Chromatogr.*, 446 (1988) 315.
- 21 R. Kysilka and M. Wurst, *J. Chromatogr.*, 464 (1989) 434.
- 22 S. Borner and R. Brenneisen, *J. Chromatogr.*, 408 (1987) 402.
- 23 T. Stijve and T. W. Kuyper, *Planta Med.*, 51 (1985) 385.
- 24 R. Kysilka and M. Wurst, *Planta Med.*, 56 (1990) 327.
- 25 *The Merck Index*, Merck, Rahway, NJ, 9th ed., 1976, p. 1027.
- 26 J. Gartz, *Planta Med.*, 53 (1987) 539.



# Use of high-performance liquid chromatographic peak deconvolution and peak labelling to identify antiparasitic components in plant extracts

Nestor Perez-Souto

CENIC Quimica, Avenida 25 Y158, Playa Ciudad, Havana (Cuba)

Roderick J. Lynch\*, Gregory Measures and John T. Hann

Unicam Ltd.\*, York Street, Cambridge (UK)

---

## ABSTRACT

*Artemisia absinthium* L. is a commonly used medicinal plant for parasitic diseases all over the world. By means of high-performance liquid chromatography with diode-array detection and the PU6100 solvent optimization system, two sesquiterpene lactones,  $\alpha$ -santonin and ketopelenolid-A, were tentatively identified in methanolic extracts of this plant.  $\alpha$ -Santonin is a well known antiparasitic compound and could be one of the active principles of this plant species. Reconstructed spectra are potentially useful in scanning a complex chromatogram for pharmacologically active compounds.

---

## INTRODUCTION

For many years, the isolation and identification of natural products from plants widely used in folk medicine, or with a clearly demonstrated pharmacological activity, have been intensively studied. A major role in this kind of research is played by chromatographic methods, in particular liquid chromatography.

Many species of the large genus *Artemisia* (family Asteraceae) have been used in folk medicine all over the world, and the antiparasitic activity of several species is well known [1–3]. The Asteraceae family is characterized by structurally diverse sesquiterpene lactones (a large class of terpenes). Reports dealing with the isolation and structure elucidation of sesquiterpene lactones have increased during the last decade for two main reasons: first, these components have been used as chemical markers in chemo-

taxonomy, and second, a number of compounds received considerable attention owing to their various biological activities [4,5]. A detailed review of the sesquiterpene lactones of the *Artemisia* genus has been published [6] and many more compounds have since been isolated.

The species *Artemisia absinthium* L., growing in different regions of the world, has been intensively studied because of several reports on its antiparasitic medicinal properties and because of its use in the preparation of wines and beverages. Many terpenes have been identified in the essential oil, in addition to sesquiterpene lactones, coumarins and other compounds. Toxic effects have also been reported [4,5,7–10]. In recent years, this species, and many others of the genus *Artemisia*, have been investigated to find the sesquiterpene lactone artemisinin (Qinghaosu), which so far has been isolated only from *Artemisia annua* L. from China, and which has unique clinical properties against malaria [11–14].

Aqueous, aqueous alcoholic and methanolic ex-

---

\* Formerly Philips Analytical Chromatography.

tracts of *Artemisia absinthium* growing in Havana, Cuba, showed consistent and reproducible antiparasitic activity against three different parasites in tests carried out at the Institute of Tropical Medicine (IPK) in Havana. We considered it of interest to develop some phytochemical work-up of this plant material, to establish some of the active principles elaborated by this Cuban plant. One important approach was the chromatographic comparison of some standards with extracts, or fractions, of this plant by means of high-performance liquid chromatography (HPLC) with diode-array detection (DAD), and the use of software for data handling, solvent optimization and peak comparison.

## EXPERIMENTAL

### *Plant extraction and fractionation*

Aerial parts of *Artemisia absinthium* growing in Guira de Melena, Havana, were collected in July 1990, air dried and finely ground. The plant species was determined by comparison with authentic herbarium specimens and voucher samples are deposited in the Herbarium of the Botany Institute of the Cuban Academy of Sciences. A 5-g amount of fine powdered material was extracted first with water (50 ml) at 50°C for 8 h, filtered, dried and extracted with methanol (50 ml) at 50°C for 8 h. Both water and methanolic extracts were used for chromatographic studies.

### *Standards*

$\alpha$ -Santonin, ketopelenolid-A, absynthin and artemisin, four sesquiterpene lactones isolated from different species of the genus *Artemisia* growing in Europe, were kindly provided by Dr. J. Harmatha (Terpenes Department, Institute of Organic Chemistry and Biochemistry of the Czechoslovak Academy of Sciences). Chemical structures of these lactones were determined by spectroscopic methods (infrared, nuclear magnetic resonance, mass, circular dichroism, optical rotatory dispersion, ultra violet, etc.) and chemical correlation [5]. The standards were dissolved in methanol at concentrations of 1 and 0.1 mg/ml.

### *HPLC equipment and conditions*

The liquid chromatograph consisted of an HPLC pumping system with quaternary solvent capability

(Unicam Analytical, Cambridge, UK), an injection valve fitted with a 20- $\mu$ l sample loop (Rheodyne) and a 250  $\times$  4.0 mm I.D. column (Superspher Spherisorb 100 RP-18, 4  $\mu$ m; Merck). Diode-array data were collected on a PU6003 diode-array system, which consists of a PU4120 detector and a P3202 IBM PC-compatible computer (Unicam Analytical). This computer was also used for the data handling and processing with a PU6100 solvent optimizer (Unicam Analytical). Helium degassing was used and all injected samples were filtered through Anotop 10 plus 0.2- $\mu$ m disposable filters.

## RESULTS AND DISCUSSION

Previous work on the extraction and fractionation of fresh and dried aerial parts of *A. absinthium* with solvents such as water, water-methanol and methanol, partitioning with immiscible solvents such as chloroform, ethyl acetate, *n*-butanol, etc., and even open-column chromatography with several stationary phases was not very successful in isolating and identifying active compounds in this plant. This was due mainly to the presence of high-polarity compounds and a lack of resolution. On the other hand, the biological testing of fractions against three types of parasites indicated that the methanolic fraction was the most active, but activity was also present in other polar fractions. The availability of some sesquiterpene lactone standards isolated from the same genus species growing in Europe, and the possibility of working with HPLC coupled to a DAD system and PU6100 software for solvent optimization and peak comparison, provided a good opportunity to investigate the chemical composition of this medicinal plant. Dried plant powder was first extracted with water to eliminate very polar compounds with short retention times on reversed-phase columns, and then extracted with pure methanol. This methanolic extract was used for HPLC without further preparation.

The standards were prepared at a concentration of 1 mg/ml for artemisin, santonin and ketopelenolid-A and 2 mg/ml for absynthin because of its lower absorption at 210 nm. The mixture of standards at this concentration, or diluted tenfold, was used for the solvent optimization software and peak comparison as described [15,16]. The first experiment for optimization was a gradient from meth-

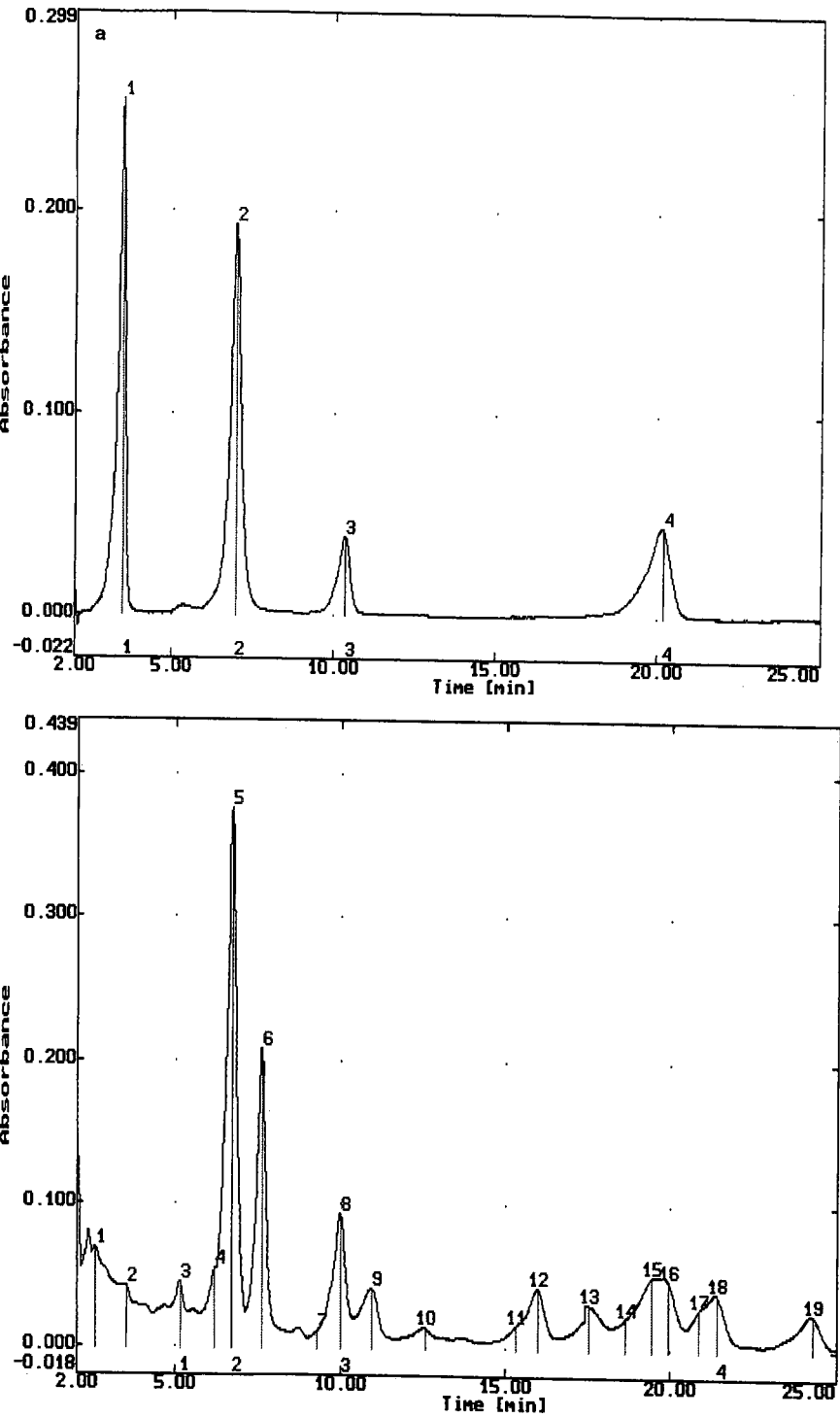


Fig. 1. (a) Chromatogram of the four standards, (1) artemisin, (2) santonin, (3) ketopelenolid-A and (4) absynthin in methanol-water (53:47). (b) Chromatogram of the methanolic extract from *Artemisia absynthium*, methanol-water (53:47). Wavelength: maximum absorbance above 210 nm.

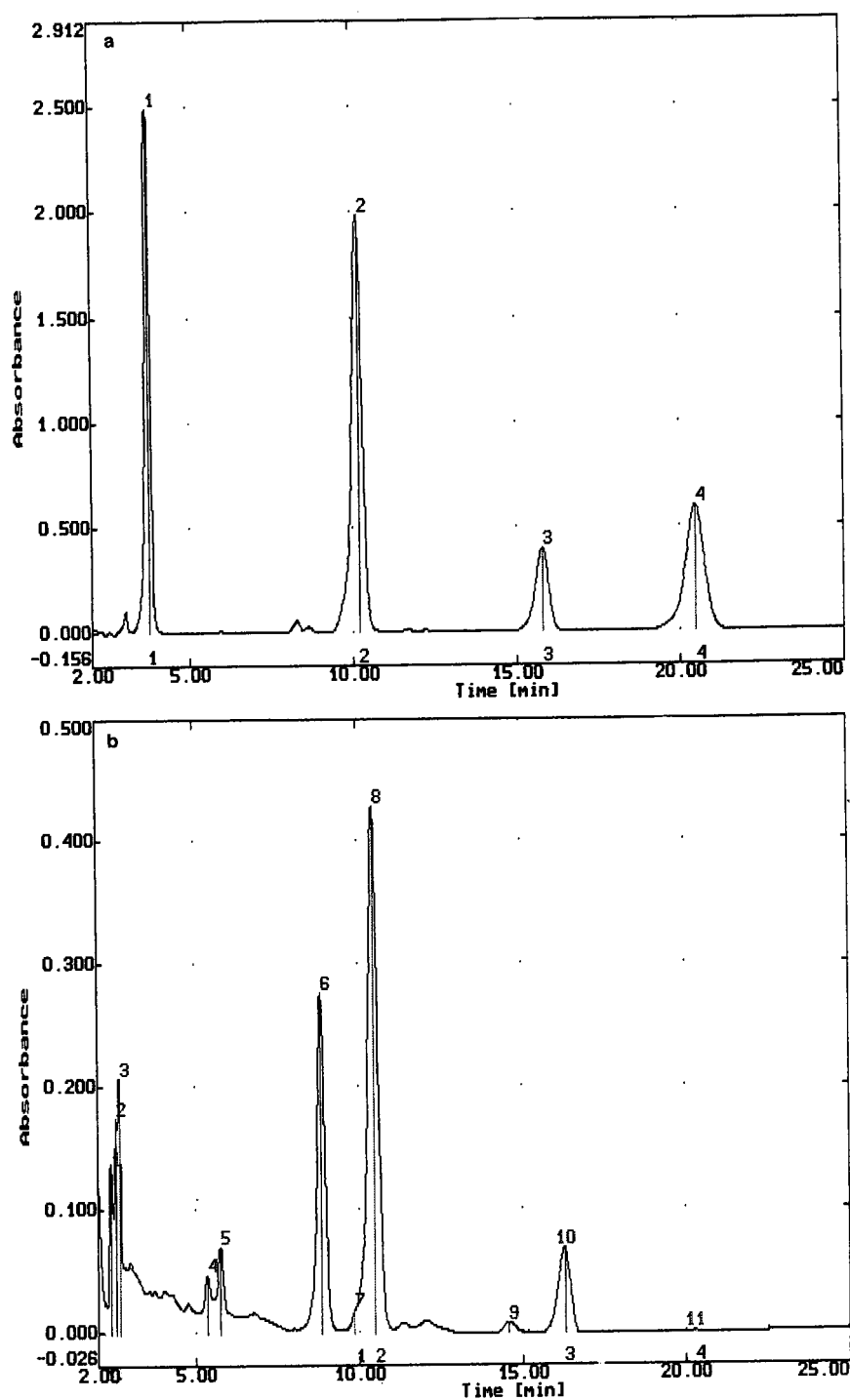


Fig. 2. As Fig. 1, but with the solvent acetonitrile-water (40:60).

anol–water (40:60) to pure methanol in 20 min at a flow-rate of 1 ml/min. Retention times from this run were used by the software to predict the methanol–water composition; after some updating we obtained a good separation with methanol–water (53:47). The order of elution was artemisin (3 min 19 s), santonin (6 min 37 s), ketopelenolid-A (9 min 55 s) and absynthin (18 min 50 s) (Fig. 1a).

After program prediction and some updating, a solvent composition of acetonitrile–water (40:60) proved to be convenient for the standards: artemisin (3 min 37 s), santonin (10 min 13 s), ketopelenolid-A (15 min 37 s) and absynthin (20 min 25 s) (Fig. 2a). With this acetonitrile–water composition we obtained almost the same retention times for the first- and last-eluting compounds, and a convenient spacing for the second and third. The prediction for the tetrahydrofuran (THF)–water composition according to the PU6100 was THF–water (25:75). In this experiment we obtained the following retention times: artemisin 5 min 43 s, santonin 9 min 37 s, ketopelenolid-A 14 min 25 s and absynthin 17 min 43 s. This was also a good separation but the

presence of THF in the solvent is less appropriate for the detection of ketopelenolid-A and absynthin, lactones with only a low UV end absorption. Because of this we tried a ternary mixture of water–methanol–acetonitrile and after some updates of the program data we obtained a satisfactory composition of water–methanol–acetonitrile (50:30:20) with the following retention times: artemisin 3 min 37 s, santonin 8 min 43 s, ketopelenolid-A 13 min 58 s and absynthin 26 min 16 s.

The next step was to separate the plant methanolic extract using these solvents and to use the PU6100 to match the labelled standard peaks and spectra with those present in the plant extract.

The solvent optimization software contains peak identification, or labelling functions, which enable the correct assignments to be made as the solvents change. In this instance we are using the peak-labelling functions as a peak identification tool. The procedure is first to deconvolute the three-dimensional chromatogram and to obtain the “pure” spectra of the peaks by iterative target transformation factor analysis (ITTFA) [15]. These spectra and

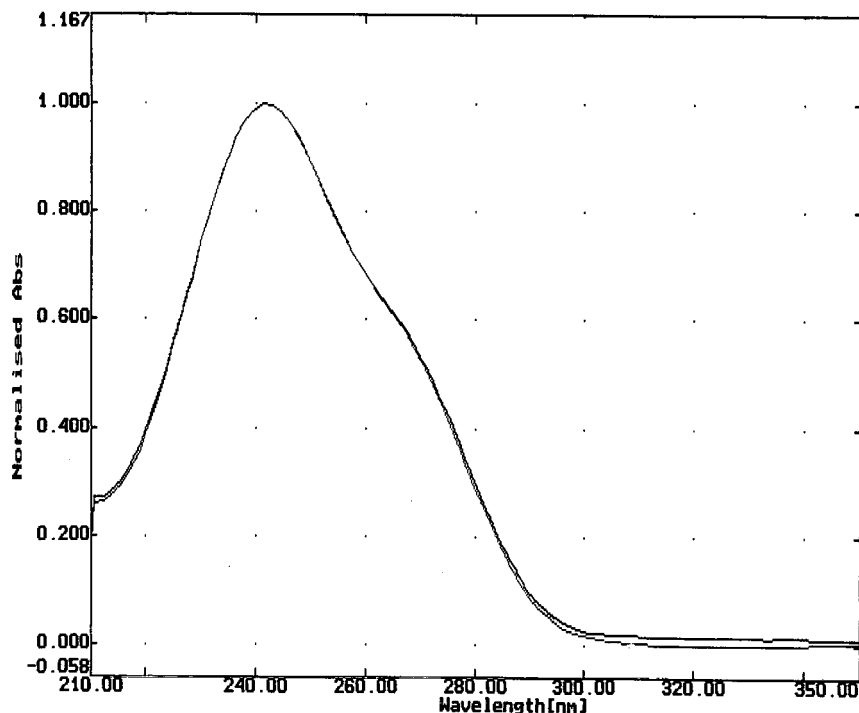


Fig. 3. Comparison of the spectrum of santonin (bottom trace) with that of peak 5 of the extract in methanol–water (53:47).

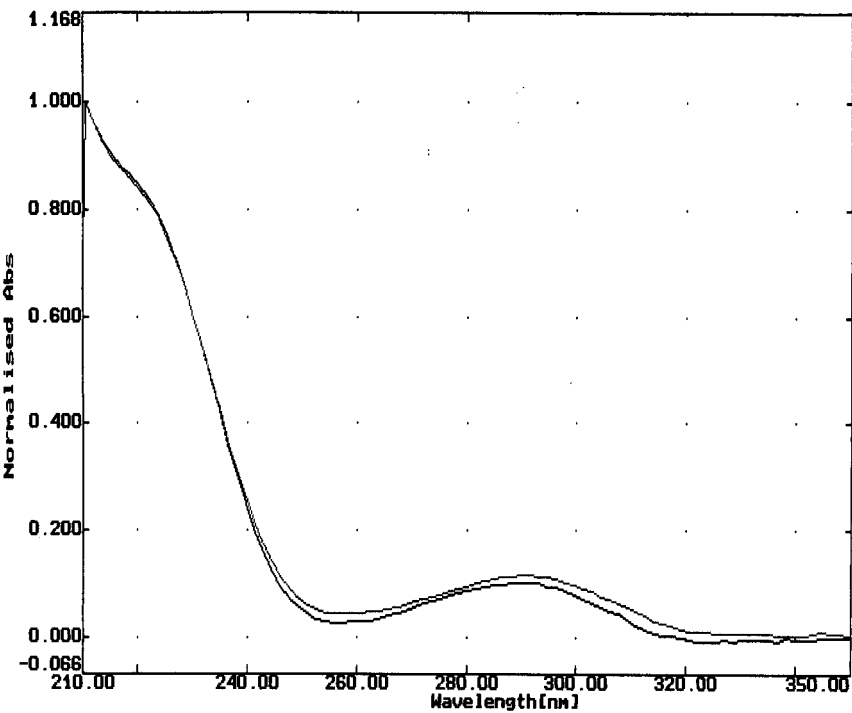


Fig. 4. Comparison of the spectrum of ketopelenolid-A (top trace) with that of peak 8 of the extract in methanol–water (53:47).

Peak Labelling								
<hr/>								
Data name : NESTOR_NMET53-3.CSN								
Solvent : 53.0% MeOH 47.0% Water								
REF	POSITION	SIZE	WIDTH	SPEC	CONC	TIME	MATCH	NAME
<hr/>								
1	0.000	0.000	0.000	0.00	0.00	0.00	0.00	ARTEMIS
2	6.670	247.980	0.187	1.00	1.00	0.96	0.95	SANTONI
3	9.956	38.837	0.239	0.98	1.00	0.96	0.94	KETOPEL
4	21.362	14.482	0.441	0.88	1.00	0.93	0.82	ABSYNTH
<hr/>								
Data name : NESTOR_NMETAC40.CSN								
Solvent : 40.0% ACN 60.0% Water								
REF	POSITION	SIZE	WIDTH	SPEC	CONC	TIME	MATCH	NAME
<hr/>								
1	0.000	0.000	0.000	0.00	0.00	0.00	0.00	ARTEMIS
2	10.439	285.820	0.263	1.00	1.00	0.90	0.90	SANTONI
3	16.242	34.915	0.346	0.96	1.00	0.88	0.85	KETOPEL
4	20.261	1.595	0.641	0.71	1.00	1.00	0.71	ABSYNTH
<hr/>								
Size : peak volume (Abs * nm * Time)								

Fig. 5. The peak labelling information from the PU6100 solvent optimizer, showing the spectral matching factors and retention matching factors for each peak of interest. Reference 1 was not assigned.

peak areas are then matched. More details of this process are given in ref. 15. In Fig. 1a and b chromatograms of the standard mixture (top) and methanolic extract from the plant (bottom) in the same solvent, methanol–water (53:47), are compared. Fig. 2a and b show a similar comparison using acetonitrile–water (40:60). Standard 2 ( $\alpha$ -santonin) seems to be present in the methanol extract as peak 5 and standard 3 (ketopelenolid-A) as peak 8 in the same extract. UV spectra of the compounds in peaks 2 and 5, and 3 and 8, are almost completely superimposable (Figs. 3 and 4) and the retention times agree within 3.9% and 3.5%, respectively. The same situation was found when the mixture of standards was compared with methanolic extracts in the other two solvent systems, acetonitrile–water (40:60) and water–methanol–acetonitrile (50:30:20); the spectrum matching factors for standards 2 and 3 were close to unity with corresponding peaks in the plant extract. The retention times agreed within 2.8% (santonin) and 3.0% (ketopelenolid-A).

Fig. 5 shows the peak labelling output of the PU6100 with the solvents methanol–water (53:47) and acetonitrile–water (40:60). There are high matching factors for both santonin and ketopelenolid-A in both solvents. However, the matching factor for peak 4 is lower and its identity is inconclusive. Absynthin has a spectrum which is very different from those of peaks 15–17 in Fig. 1b. The spectrum of peak 18 is similar, and has an intermediate matching factor of 0.88 in Table I. However, the retention times are substantially different and its presence cannot be confirmed.

## CONCLUSIONS

Using the described equipment and software we developed chromatographic methods for the analysis and preparation of four sesquiterpene lactones and for the analysis of the methanolic extract of *Artemisia absinthium*. The results suggest that  $\alpha$ -

santonin and ketopelenolid-A are present in these extracts. The presence of santonin in Cuban *Artemisia absinthium* aerial parts is a possible explanation for the antiparasitic properties of this medicinal plant, because  $\alpha$ -santonin has been used for many years as a medicine for parasitic diseases.

The spectral reconstruction algorithms are potentially useful in highlighting compounds with known or similar chromophores in a complex chromatogram. The use of the algorithms in this way avoids lengthy and unnecessary method development in the search for pharmacologically active compounds.

## REFERENCES

- 1 E. Rodriguez, G. H. N. Towers and J. C. Mitchell, *Phytochemistry*, 15 (1976) 1573.
- 2 Qinghaosu Antimalarial Co-ordinating Research Group, *Chin. Med. J.*, 92 (1979) 811.
- 3 N. Katz, presented at the *Simposio Brasil-China de Quimica e Farmacologia de Produtos Naturais*, Rio de Janeiro, December 14, 1989, paper L-44.
- 4 F. C. Seaman, *Bot. Rev.*, 48, No. 2 (1982) 121.
- 5 N. H. Fischer, E. J. Olivier and H. D. Fischer, *Prog. Chem. Org. Nat. Prod.*, 38 (1979) 49.
- 6 R. G. Kelsey and F. Shafizadeh, *Phytochemistry*, 18 (1979) 1591.
- 7 T. Sacco and F. Chialva, *Planta Med.*, 54 (1988) 93.
- 8 M. C. Delahaye, in *Artemisie, Ricerca ed Applicazione, Supplemento al Quaderno Agricolo*, Federagrario, Turin, 1985, p. 233.
- 9 R. Truhaut, in *Artemisie, Ricerca ed Applicazione, Supplemento al Quaderno Agricolo*, Federagrario, Turin, 1985, p. 181.
- 10 J. Volak and J. Stodola, *Plantae Medicinales*, Artia, Prague, and Grund, Paris, 1983.
- 11 J. M. Liu *et al.*, *Acta Chim. Sinica*, 37 (1979) 129.
- 12 4th Meeting of the Scientific Working Group on the Chemotherapy of Malaria, Beijing, 1981, WHO Report, TDR Chemal SWG (4) QHS/813, p. 5.
- 13 D. L. Klayman, J. L. Ai and N. Acton, *J. Nat. Prod.*, 47 (1984) 715.
- 14 J. E. F. Reynolds (Editor), *Martindale. The Extra Pharmacopeia*, Pharmaceutical Press, London, 29th ed., 1989.
- 15 R. Lynch and G. Measures, *Lab. Pract.*, 39, No. 1 (1990) 61.
- 16 R. Lynch, S. D. Patterson and R. E. A. Escott, *LC · GC Int.*, 3, No. 9 (1990) 54.





# Improved high-performance liquid chromatographic method for the determination of coenzyme Q<sub>10</sub> in plasma

G. Grossi\*, A. M. Bargossi, P. L. Fiorella and S. Piazzì

*Laboratorio Centralizzato, Policlinico S. Orsola, Via Massarenti 9, I-40138 Bologna (Italy)*

M. Battino

*Istituto di Biochimica, University of Ancona, Ancona (Italy)*

G. P. Bianchi

*Istituto di Clinica e Terapia Medica, University of Bologna, Bologna (Italy)*

## ABSTRACT

Coenzyme (Co) Q<sub>10</sub> was dissociated from lipoproteins in plasma by treatment with methanol and extraction with *n*-hexane. Subsequent clean-up on silica gel and C<sub>18</sub> solid-phase extraction cartridges with complete recovery ( $99 \pm 1.2\%$ ) produced a clean extract. High-performance liquid chromatographic (HPLC) separation was performed on a C<sub>18</sub> reversed-phase column. Three simple, rapid procedures are presented: HPLC with final UV (275 nm) detection, a microanalysis utilizing a three-electrode electrochemical detector and a microanalysis with column-switching HPLC and electrochemical detection. The methods correlate very well with classical ethanol-*n*-hexane extraction with UV detection. The identity and purity of the Co Q<sub>10</sub> peak were investigated and the resulting methods were concluded to be suitable for total plasma Co Q<sub>10</sub> determination. The average level in healthy subjects was  $0.80 \pm 0.20$  mg/l; the minimum detectable Co Q<sub>10</sub> plasma level was 0.05 and 0.005 mg/l for UV and electrochemical detection, respectively. The methods were applied to many samples and the plasma Co Q<sub>10</sub> reference values for healthy subjects, athletes, hyperthyroid, hypothyroid and hypercholesterolaemic patients are given.

## INTRODUCTION

Coenzyme (Co) Q<sub>10</sub> (2,3-dimethoxy-5-methyl-6-decaprenylbenzoquinone; Fig. 1), also known as ubiquinone, is classed as a fat-soluble quinone and is an essential component of the mitochondrial respiratory chain, where it acts as an electron shuttle, controlling the efficiency of oxidative phosphorylation [1]. Moreover, it has a function as a membrane stabilizing agent, for avoiding lipid peroxidation and regulating lipid fluidity.

It may occur that the Co Q<sub>10</sub> mitochondrial content gives a functional limiting effect, particularly in cases of increased respiratory demand [2]. A low Co Q<sub>10</sub> plasma level may indicate an impaired cellular

energetic function. It is important to emphasize how this possibility affects, in the same way, both muscular and myocardial performances. Co Q<sub>10</sub> administration can counteract and improve functions in patients affected by several kinds of encephalomyopathy due to Co Q<sub>10</sub> inhibition of biosynthesis or stimulation of degradation [3–5] and in patients affected by heart failure [6].

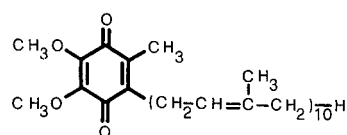


Fig. 1. Coenzyme Q<sub>10</sub>, oxidized form.

For all these reasons, plasma Co Q<sub>10</sub> determination has been included in the routine activity of clinical chemistry laboratories.

Co Q<sub>10</sub> has been determined in plasma by liquid chromatography (LC) with UV detection after liquid-liquid extraction [7]. Electrochemical detection (ED) gave the possibility of monitoring also the reduced form [8]. For total plasma Co Q<sub>10</sub> determination, the sample is usually converted into the corresponding reduced form by treatment with sodium tetrahydroborate and subsequently determined by high-performance liquid chromatography (HPLC) with ED [9,10].

All these procedures are too time consuming and unsuitable for routine determinations, particularly when total Co Q<sub>10</sub> is required, as, from the clinical point of view, this is the most significant value.

We have systematically examined the advantages and limitations of solid-phase extraction (SPE), the ED and automation for the determination of Co Q<sub>10</sub> by HPLC.

A coulometric detector is able to give a 100% yield of the electrochemical reaction and can detect the oxidized form [10]. The reduced form is unstable at room temperature and quickly becomes oxidized [8,10], so SPE, when performed utilizing a vacuum manifold and subjecting the sample to prolonged air flushing, can cause total conversion of Co Q<sub>10</sub> into the oxidized form, allowing the determination of total Co Q<sub>10</sub>.

The column-switching technique improves the automation of the analytical procedures, greatly increasing the laboratory productivity.

An HPLC procedure that is to be applied in clinical chemistry must consider the kind of instrumentation currently available in the laboratory and must allow the method to be run without being obliged to apply a sophisticated technique such as column switching utilizing a UV detector must be sufficient.

In this paper, three very simple and rapid procedures are presented. They have an increasing level of difficulty in utilizing the instrumentation, but can be fully automated, correlate very well and are interchangeable.

## EXPERIMENTAL

### *Chemical and reagents*

Co Q<sub>10</sub> and the internal standard (I.S.), Co Q<sub>6</sub>

were kindly supplied by Eisai (Tokyo, Japan). Methanol, *n*-hexane and 2-propanol, all of HPLC grade, and glacial acetic acid, of INSTRA grade, were obtained from J. T. Baker (Deventer, Netherlands). Sodium acetate, of analytical-reagent grade, was purchased from E. Merck (Darmstadt, Germany).

Venous blood was drawn in tubes containing 50  $\mu$ l of 0.01 *M* tripotassium ethylenediaminetetraacetate.

SPE extraction cartridges containing silica (100 mg) (Analytichem Bond Elut Si) or octadecyl-bonded silica (50 mg) (Analytichem Bond Elut C<sub>18</sub>) and the column-switching disposable precolumn containing octadecyl-bonded silica (50 mg; 40  $\mu$ m), 20 mm  $\times$  2 mm I.D. (Analytichem AASP Cassette C<sub>18</sub>), were obtained from Varian Sample Preparation Products (Harbor City, CA, USA).

The analytical columns were protected with a Model 7315 on-line filter Rheodyne (Cotati, CA, USA).

The reversed-phase (RP) analytical column, Ultrasphere XL C<sub>18</sub>, 3  $\mu$ m (70 mm  $\times$  4.6 mm I.D.) with a C<sub>18</sub> guard column, 3  $\mu$ m (5 mm  $\times$  4.6 mm I.D.) were supplied by Beckman (San Ramon, CA, USA). The normal-phase (NP) analytical column, Si 60 Supersphere, 4  $\mu$ m (50 mm  $\times$  4 mm I.D.) was from E. Merck.

### *Instrumentation*

The SPE clean-ups were performed using a Model SPE-21 vacuum manifold (J. T. Baker). The Model 2510 HPLC pump and the Model 2050 UV detector (set at 275 nm, 0.02 a.u.f.s.) were obtained from Varian (Walnut Creek, CA, USA). For manual injection, a Model 7125 valve (Rheodyne) fitted with a 50- $\mu$ l loop was used.

For ED a multi-electrode Coulochem 5100 A electrochemical detector fitted with a Model 5021 conditioning cell and a Model 5011 analytical cell, all from Environmental Sciences Assoc. (ESA) (Bedford, MA, USA), was employed. To oxidize Co Q<sub>10</sub> before HPLC separation, a Model 5020 guard cell (ESA) was added.

For applying the column-switching technique, a Model 222 autosampler, a Model 401 diluter, an Anachem interface, all from Gilson (Villiers-le-Bel, France), an AASP solid-phase autosampler and a ten-port valve, all from Varian, were utilized, jointly with the HPLC pump and the electrochemical detector.

### Preparation of standards

Stock solutions (100 mg/l) of Co Q<sub>10</sub> and Co Q<sub>9</sub> (I.S.) were prepared in *n*-hexane and stored at 4°C.

To obtain standard solutions, Co Q<sub>10</sub>-free plasma was fortified with Co Q<sub>10</sub> to give concentrations of 0, 0.625, 1.25, 2.50 and 5.0 mg/l. These standards were prepared fresh daily.

### HPLC mobile phases

For normal-phase separation, degassed *n*-hexane was used as the mobile phase at a flow-rate of 1 ml/min; for reversed-phase (RP) separation with UV detection, 2-propanol-methanol (1:4) was employed at a flow-rate of 2 ml/min; for RP separation with ED and for column-switching HPLC, 50 mM sodium acetate in glacial acetic acid-2-propanol-methanol (24:450:1435) was used at a flow-rate of 2 ml/min.

### Electrode connections

The cells were assembled as follows: analytical column → Model 5021 conditioning cell (set at -0.60 V) → Model 5011 analytical cell (set at detector 1 -0.15 V, detector 2 +0.45 V, response 4, gain 10 × 30). Only for the Co Q<sub>10</sub>H<sub>2</sub> study an additional Model 5020 guard cell (set at +0.50 V) was installed between the injection valve and the analytical column.

### Column-switching HPLC conditions

The column-switching instrumentation was assembled as reported previously [11,12].

### Samples

Samples of 5 ml of venous blood were taken in the morning by venepuncture from the forearm of subjects who had fasted for at least 8 h. The samples were immediately centrifuged at 2000 *g* for 15 min at room temperature. The plasma was separated and kept at -20°C in polypropylene tubes. On the day assigned for analysis the samples were thawed for 2 h at room temperature.

### Method A

Plasma (1 ml) was subjected to liquid-liquid extraction according to Takada *et al.* [7] and subsequently to RP-HPLC with UV detection.

### Method B: plasma Co Q<sub>10</sub> determination with UV detection

In a 100 × 16 mm polypropylene tube, 1 ml of plasma was deproteinized with 1 ml of methanol, then 0.1 ml of I.S. (Co Q<sub>9</sub>, 25 mg/l in *n*-hexane) and 3.9 ml of *n*-hexane were added. The tube was vortex mixed and centrifuged at 2000 *g* for 10 min. A 3-ml portion of the *n*-hexane phase was transferred into another tube, 4 ml of *n*-hexane were added to the aqueous phase and the extraction was repeated. A 7-ml volume of the *n*-hexane phase was passed through a 100-mg silica SPE cartridge, previously activated with 2 ml of *n*-hexane; the cartridge was then washed with 2 ml of *n*-hexane and dried under a 380-mmHg vacuum for 1 min. Co Qs were eluted with 2 × 0.5 ml of methanol and the collected methanol was then purified on a 50 mg C<sub>18</sub> SPE cartridge, previously activated with 2 ml of methanol and equilibrated with 2 ml of water. After a washing step with 1.5 ml of methanol, Co Qs were eluted with 2 × 0.15 ml of 2-propanol and 50 µl of the eluted fraction were injected into the RP-HPLC column for separation and UV detection.

### Method C: plasma Co Q<sub>10</sub> determination with electrochemical detection

In a 100 × 16 mm I.D. polypropylene tube, 0.1 ml of plasma was deproteinized with 0.2 ml of methanol, then 10 µl of I.S. (Co Q<sub>9</sub>, 25 mg/l in *n*-hexane) and 1 ml of *n*-hexane were added. The tube was vortex mixed, 1.5 ml of *n*-hexane were added and the tube was vortex mixed again and centrifuged at 2000 *g* for 10 min. A 2-ml volume of the *n*-hexane phase was passed through a 100-mg silica SPE cartridge and all the steps were performed as above but, unlike in method B, the C<sub>18</sub> cartridge was eluted with 2 × 0.2 ml of 2-propanol and 50 µl of the eluted fraction were injected into the RP-HPLC column for separation and ED.

### Method D: plasma Co Q<sub>10</sub> determination with column-switching HPLC

Plasma (0.1 ml) was extracted and purified on a silica cartridge as in method C. The 1-ml methanol fraction eluted from silica was collected in a 75 × 12 mm I.D. polypropylene tube and placed on a Gilson 222 autosampler. The disposable precolumn utilized was C<sub>18</sub>, 40 µm, 50 mg (20 mm × 2 mm I.D.) and, using the dilute syringe as a pump, was

activated with 0.5 ml of methanol, equilibrated with 0.5 ml of water, loaded with 0.2 ml of the sample and washed with 1.5 ml of methanol. The AASP ten-port valve then connected the precolumn to the analytical column for 0.5 min, the Co Qs were transferred to the analytical column by 1.0 ml of the HPLC mobile phase, the separation was performed on the C<sub>18</sub> analytical column and the effluent was monitored by ED. As soon as the ten-port valve had returned to the load position, the precolumn was replaced with a new one. The 5-ml loop was washed with 25 ml of 2-propanol and the clean-up of the next sample then took place.

## RESULTS AND DISCUSSION

Co Q<sub>10</sub> is a lipophilic molecule, freely soluble in hydrocarbons, insoluble in water, almost insoluble in methanol and soluble in hot ethanol, 2-propanol and 1-propanol.

The liquid-liquid extraction method (A) was taken as a reference method to compare the improvements obtained by applying the SPE sample clean-up. In Fig. 2, a typical chromatographic profile obtained applying method A is shown.

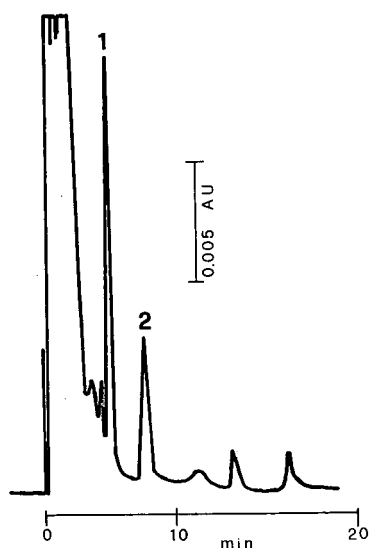


Fig. 2. Analytical profile obtained on applying method A to a plasma containing (1) Co Q<sub>9</sub> (I.S.), 2.50 mg/l, and (2) Co Q<sub>10</sub>, 0.92 mg/l. Column, C<sub>18</sub>, 3  $\mu$ m (75 mm  $\times$  4.6 mm I.D.) (Beckman); mobile phase, 2-propanol-methanol (1:4); flow-rate, 2 ml/min; detection, UV, 275 nm, 0.02 a.u.f.s.; chart speed, 5 mm/min.

This method was found to be unsuitable for routine determinations owing to the following problems: a high solvent front; some later-eluting peaks causing a long run time; an interfering peak close to that of the I.S.; the injected sample was not clean and caused frit clogging; the precolumn lifetime was short owing to strongly retained substances; there was a large volume of *n*-hexane to be evaporated and the extraction was too time consuming; and automatic sampler injection was impossible owing to the presence of precipitate.

To improve the clean-up, we tried to load the plasma directly on to RP cartridges, but unfortunately the plasma proteins, to which Co Q<sub>10</sub> is bonded, were not retained and the recovery was zero.

In Table I, the Co Q<sub>10</sub> breakthrough volumes obtained on various SPE cartridges are reported. For eluate monitoring, RP-HPLC with UV detection and NP-HPLC [UV detector set at 275 nm,  $k'$  (Co Q<sub>10</sub>) = 3.3] were used. The silica cartridge showed a high breakthrough volume in *n*-hexane and was suitable for sample concentration from large solvent volumes, but unsuitable for sample clean-up, because any solvent that was able to wash out interfering substances had also eluted the analyte.

It must be emphasized that methanol, which was almost unable to solubilize crystalline Co Q<sub>10</sub>, could solubilize and elute it when Co Q<sub>10</sub> was loaded on silica, probably because molecule-stationary phase interactions are weaker than molecule-molecule interactions, typical of the crystalline state. Co

TABLE I

Co Q<sub>10</sub> BREAKTHROUGH VOLUME (ml) ON DIFFERENT BOND-ELUT EXTRACTION CARTRIDGES

Solvent	Cartridge		
	Si 100 mg	NH <sub>2</sub> 100 mg	C 18 50 mg
<i>n</i> -Hexane	>> 14	12	< 1
Light petroleum (b.p. 40–60°C)	>> 12		
Chloroform	< 1	< 1	< 1
Methanol	0.2	0.2	3
2-Propanol	0.3	0.3	0.15
1-Propanol	0.3	0.3	< 0.3

TABLE II

RECOVERY OF Co Q<sub>10</sub> APPLYING *n*-HEXANE FROM LIQUID-LIQUID EXTRACTION TO SILICA CARTRIDGE

Sample (ml)		Solvents (ml)				Recovery after elution with 1 ml of methanol (%)
Plasma <sup>a</sup>	Water <sup>a</sup>	Methanol	Ethanol	Acetonitrile	<i>n</i> -Hexane	
	1				4	98
	1		1		4	1.5
	1			1	4	3
	1	1			4	97
1	1 <sup>b</sup>				4	1
1		1			4	80
1		1			4 + 4	98

<sup>a</sup> Spiked with Co Q<sub>10</sub> to give 100 mg/l.<sup>b</sup> Unspiked.

Q<sub>10</sub> solution in methanol remained stable for several days at room temperature.

In conclusion, the silica cartridge, is useful for replacing the original solution of Co Q<sub>10</sub> in a large volume of *n*-hexane with a Co Q<sub>10</sub> solution in a small volume of methanol, whereas the C<sub>18</sub> cartridge is suitable for clean-up and concentration steps.

Utilizing the C<sub>18</sub> cartridge, it is possible to load a methanol solution of Co Q<sub>10</sub> and perform the subsequent washing step with methanol; moreover, of the elution cartridge with 2-propanol represents a quantitative concentration step.

In contrast to what was reported by some authors [10], 1-propanol was not a good solvent for the Co Q<sub>10</sub> loading step on the C<sub>18</sub> cartridge.

A reliable clean-up flow-scheme is plasma Co Q<sub>10</sub> liquid-liquid extraction in *n*-hexane, solvent replacement with methanol performed on a silica cartridge and final clean-up performed on a C<sub>18</sub> cartridge. First the plasma has to be deproteinized to break the Co Q<sub>10</sub>-protein bonds; *n*-hexane alone is unable to perform this step, whereas methanol, ethanol and acetonitrile are effective.

Table II shows the recoveries obtained by coupling liquid-liquid extraction with silica cartridge treatment.

Ethanol and acetonitrile were partially miscible with *n*-hexane, so the subsequent loading step on silica was adversely influenced.

In Fig. 3 a typical chromatographic profile obtained on applying method B is shown, and it is

clear that no late-eluting peak is detected and the solvent front is very low.

The theoretical plate number, calculated for the Co Q<sub>10</sub> peak, was  $N = 1629$ . This low efficiency is due to the high eluting power of 2-propanol in the analytical HPLC system; in fact, injecting Co Q<sub>10</sub> solubilized in methanol, we obtained  $N = 3559$ . Reduction of the injection volume to 10  $\mu$ l eliminated

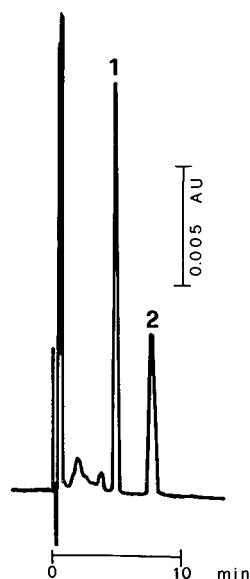


Fig. 3. Analytical profile obtained on applying method B to a plasma containing (1) Co Q<sub>9</sub> (I.S.), 2.50 mg/l, and (2) Co Q<sub>10</sub>, 0.92 mg/l. Conditions as in Fig. 2.

TABLE III  
SPE EXTRACTION OPTIMIZATION STUDY

Co Q <sub>10</sub> recovery from silica cartridge by elution with methnaol (%)		Co Q <sub>10</sub> released from C <sub>18</sub> cartridge when the breakthrough volume is exceeded (loading + washing step)		Co Q <sub>10</sub> recovery from C <sub>18</sub> cartridge by elution with 2-propanol	
Volume of methanol employed (ml)	Co Q <sub>10</sub> recovery (%)	Volume of methanol (ml)	Co Q <sub>10</sub> released (%)	Volume of 2-propanol employed (ml)	Co Q <sub>10</sub> recovery (%)
0.25	83.8	3.0	0.0	0.25	93.5
0.50	99.3	3.5	0.2	0.30	97.7
0.75	99.9	4.0	0.9	0.40	98.5
1.00	100.0	4.5	2.5	0.50	99.0
		5.0	4.0		
		5.5	5.6		

TABLE IV  
PLASMA Co Q<sub>10</sub> RECOVERIES (% ± R.S.D., *n* = 10) WITH DIFFERENT METHODS

Plasma Co Q <sub>10</sub> (mg/l)	Method			
	A	B	C	D
1.21	92.1 ± 6.5	97.7 ± 3.9	98.5 ± 2.2	98.3 ± 2.5
0.32	87.3 ± 7.1	93.4 ± 4.2	96.2 ± 3.4	95.1 ± 3.7

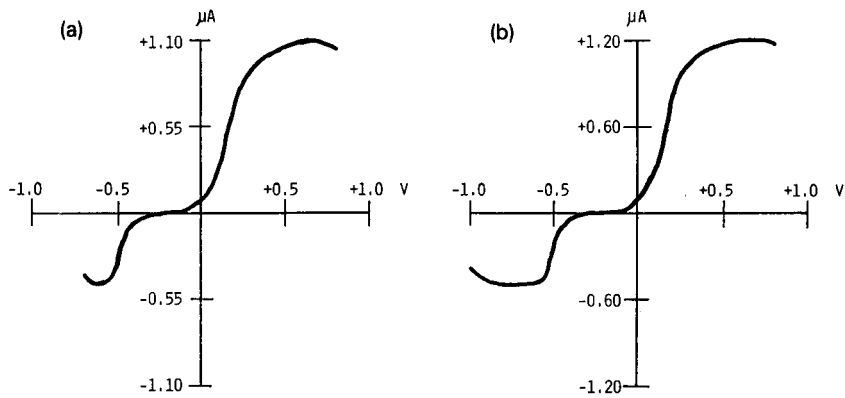


Fig. 4. Hydrodynamic voltammograms obtained for (a) Co Q<sub>9</sub> and (b) Co Q<sub>10</sub>. Abscissa, applied voltage; ordinate, detector response (μA).

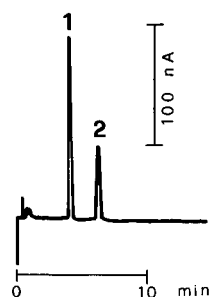


Fig. 5. Analytical profile obtained on applying method C to a plasma containing (1) Co Q<sub>9</sub> (I.S.), 2.50 mg/l, and (2) Co Q<sub>10</sub>, 0.92 mg/l. Column, C<sub>18</sub>, 3  $\mu$ m (75 mm  $\times$  4.6 mm I.D.) (Beckman); mobile phase, 50 mM sodium acetate in glacial acetic acid-2-propanol-methanol (24:450:1435); flow-rate, 2 ml/min; electrochemical detector, conditioning cell, -0.60 V; detector 1, -0.15 V; detector 2, +0.45 V; gain, 10  $\times$  30; integrator attenuation, 10; chart speed, 5 mm/min.

this difference and a high efficiency was obtained for both the solvents, but the sensitivity was inadequate for monitoring low Co Q<sub>10</sub> plasma levels.

In Table III, the data obtained for the SPE extraction optimization study are reported.

In Table IV, Co Q<sub>10</sub> recoveries and relative standard deviations (R.S.D.s) for method B are given. The I.S. recovery was  $95.1 \pm 3.8\%$  and no peak was found in unspiked plasma at the retention time of the I.S. The calibration graph was linear ( $y = 31.2x$ , where  $x$  = Co Q<sub>10</sub> concentration in plasma in mg/l and  $y$  = Co Q<sub>10</sub> peak height in mm), also without using the I.S. peak height for calculations, and the minimum detectable Co Q<sub>10</sub> level in plasma was 0.05 mg/l.

#### ELECTROCHEMICAL DETECTION

Sodium acetate and acetic acid were added to the

mobile phase employed for ED to ensure the conductivity necessary for electrochemical reactions.

In Fig. 4, the hydrodynamic voltammograms for Co Q<sub>9</sub> and Co Q<sub>10</sub> are reported. They were obtained by repeated injections into the HPLC system of a 4.2 mg/l solution of standards in 2-propanol, increasing the detector potential by 0.05 V in each subsequent run.

Our electrochemical cells have a coulometric (100%) yield and can be considered as electrochemical reactors; consequently, the detector response being higher in oxidation, the best results were obtained by reducing Co Q<sub>10</sub> in the conditioning cell (-0.60 V) and monitoring with the analytical cell operating in the oxidation mode (+0.45 V).

In Fig. 5, a typical analytical profile obtained by applying method C to a plasma sample is shown. No solvent peak appears; the only peaks detected were those of the I.S. and Co Q<sub>10</sub>. The sensitivity was very high, the detector was set at medium gain and was useless to operate with a higher plasma volume.

In Table IV, the Co Q<sub>10</sub> recoveries and R.S.D.s for method C are given. The time necessary to complete a run was 7 min and the calibration graph was linear ( $y = 15.5x$ , where  $x$  = Co Q<sub>10</sub> concentration in plasma in mg/l and  $y$  = Co Q<sub>10</sub> peak height in mm), also without using the I.S. peak height for calculations, and the minimum detectable Co Q<sub>10</sub> level in plasma was 0.01 mg/l.

The identity and purity of the Co Q<sub>10</sub> and Co Q<sub>9</sub> peaks were confirmed for methods B and C: the Co Q<sub>10</sub> UV spectrum was characterized by an absorbance maximum at 275 nm and two half-waves at 292 and 259 nm, while the hydrodynamic voltammogram (Fig. 4) showed a maximum of response at +0.60 V and a half-wave at +0.18 V. Pure stan-

TABLE V

RESULTS OF PURITY AND IDENTITY STUDIES ( $\pm$  R.S.D.,  $n = 5$ ) FOR Co Q<sub>10</sub> AND Co Q<sub>9</sub> PEAKS

HPLC detection	Ratio of peak heights obtained at	Co Q <sub>10</sub> peak		Co Q <sub>9</sub> peak	
		Standard	Sample	Standard	Sample
UV	292/275 nm	0.52 $\pm$ 0.02	0.51 $\pm$ 0.02	0.59 $\pm$ 0.02	0.57 $\pm$ 0.02
UV	259/275 nm	0.52 $\pm$ 0.02	0.53 $\pm$ 0.02	0.51 $\pm$ 0.02	0.50 $\pm$ 0.02
ED	+0.15/+0.45 V	0.438 $\pm$ 0.010	0.444 $\pm$ 0.011	0.454 $\pm$ 0.010	0.458 $\pm$ 0.010
ED	+0.60/+0.45 V	1.041 $\pm$ 0.025	1.064 $\pm$ 0.025	1.086 $\pm$ 0.026	1.075 $\pm$ 0.027

TABLE VI  
COLUMN-SWITCHING HPLC OPTIMIZATION

Precolumn	Optimized valve reset time (min)	Breakthrough volume (ml of methanol)	
		Passed through the precolumn	Total
C <sub>2</sub>	0.1	<0.2	0.825
C <sub>8</sub>	0.1	0.3	0.925
C <sub>18</sub>	0.5	1.475	2.100

dards and real plasma samples ( $n = 5$ ) were extracted with method B and injected three times into the HPLC system, with the UV detector set at 275, 292 and 259 nm. Then extraction method C was applied with the electrochemical detector 2 set at +0.45, +0.15 and +0.60 V.

The results are given in Table V. Comparison of the values obtained for the Co Q<sub>10</sub> peak for the standard with those obtained for the samples showed out that they were very close, indicating that the peaks referred to the same substance and

there were no co-eluted substances in the same peak.

#### Column switching

In Table VI, the results obtained by employing different precolumns are shown. As the dead volume between the injection port of the Model 222 autosampler and the precolumn was 0.625 ml, the amount of methanol employed in the final washing step was always increased by this volume. In previous column-switching methods for determining other analytes [11,12], we used a final washing step with water before switching the valve. For Co Q<sub>10</sub> this step must be avoided, because water causes precipitation of the analyte in the precolumn and the HPLC mobile phase volume, necessary for precolumn elution, would be increased excessively.

In Fig. 6 a typical chromatogram, obtained from plasma samples applying method D, is shown and in Table IV Co Q<sub>10</sub> recoveries and R.S.D.s from plasma are given. The I.S. recovery was  $95.2 \pm 3.7\%$  and no peak was found in unspiked plasma at the retention time of the I.S.

The calibration graph was linear ( $y = 46.0x$ , where  $x$  = Co Q<sub>10</sub> concentration in plasma in mg/l and  $y$  = Co Q<sub>10</sub> peak height in mm) and the minimum detectable Co Q<sub>10</sub> level in plasma was 0.005 mg/l.

As, from the second sample on, the preparation of the sample takes place simultaneously with HPLC separation of the previous sample, the total analysis time is 8 min, even though the preparation time is 4 min and the HPLC separation time is 8 min.

#### Total plasma Co Q<sub>10</sub> determination

The clinical requirement is to determine total plasma Co Q<sub>10</sub>, the single oxidized or reduced fraction being irrelevant [2] owing to Co Q<sub>10</sub> functioning as a homogeneous pool [13].

As reported, ubiquinol is rapidly oxidized even at  $-20^\circ\text{C}$  [8,10]; powerful antioxidants cannot be used, as they would reduce the oxidized form [10]; during storage the percentage of the reduced form with respect to the total decreases, but the total content remains unchanged [9]. Powerful reducing agents, such as sodium tetrahydroborate or dithionite, are needed to effect the quantitative reduction of Co Q<sub>10</sub>, even though tetrahydroborate absorbed



Fig. 6. Analytical profile obtained on applying method D to a plasma containing (1) Co Q<sub>9</sub> (I.S.), 2.50 mg/l, and (2) Co Q<sub>10</sub>, 0.92 mg/l. Column-switching precolumn, C<sub>18</sub>, 40–60  $\mu\text{m}$  (20 mm  $\times$  2 mm I.D.). Analytical column, mobile phase and detector as in Fig. 5. Integrator attenuation, 512; chart speed, 5 mm/min.



on the injector and/or the analytical column can reduce the oxidized form in next runs [10]. Moreover, the Co Q<sub>10</sub>H<sub>2</sub> level in 2-propanol or ethanol gradually decreases [7,9]. A glass column is necessary for original Co Q<sub>10</sub>H<sub>2</sub> determination [10].

For all these reasons, for total Co Q<sub>10</sub> determination (*i.e.*, Co Q<sub>10</sub> plus Co Q<sub>10</sub>H<sub>2</sub>), we avoided both the direct original Co Q<sub>10</sub>H<sub>2</sub> determination and the utilization of reducing agents and preferred to employ an electrochemical reactor to convert the injected Co Q<sub>10</sub>H<sub>2</sub> into the oxidized form.

After liquid-liquid extraction of plasma using method A, samples were injected into the RP-HPLC system equipped with an electrochemical detector and Co Q<sub>10</sub>H<sub>2</sub> was oxidized in the guard cell installed between the injection valve and the analytical column. As a 100% yield of the oxidation reaction in the guard cell was obtained, we could determine the total amount of Co Q<sub>10</sub> in plasma samples ( $n = 12$ ). The same samples were injected without the guard cell and only the oxidized fraction was determined. No difference was observed in the values obtained, indicating that only oxidized Co Q<sub>10</sub> was present in our samples.

For determining the retention time of Co Q<sub>10</sub>H<sub>2</sub>, a solution containing the I.S. + Co Q<sub>10</sub> was injected into the HPLC system with the guard cell set at  $-0.60$  V, in this way reducing Co Q before HPLC separation. The retention times were Co Q<sub>9</sub>H<sub>2</sub> 2.46, Co Q<sub>10</sub>H<sub>2</sub> 3.63, Co Q<sub>9</sub> 4.40 and Co Q<sub>10</sub> 6.64 min. Applying method C, no peak with a retention time around 3.6 min was detected and none was detected before the oxidized I.S.

As method A also extracts the reduced form [7], these results confirm that in our samples Co Q<sub>10</sub> was present only in the oxidized form. The same electrochemical reactor was applied by injecting plasma samples stored and extracted with methods B, C and D ( $n = 12$ ) and fresh samples ( $n = 12$ ), extracted immediately after the sampling, and the same results were obtained. This confirms that our extraction procedures fully oxidize the Co Q<sub>10</sub>H<sub>2</sub> and the proposed methods are suitable for total Co Q<sub>10</sub> determination.

In Table VII, the results of the correlation study among the proposed methods are reported. The methods were applied to many real samples and in Table VIII the data obtained for a group of healthy subjects and some patients not submitted to any pharmacological treatment are given.

TABLE VII

## CORRELATION STUDY AMONG THE METHODS

Plasma samples,  $n = 34$ . Co Q<sub>10</sub> range: 0.20–1.21 mg/l.

Y = method	X = method	Correlation coefficient, $r$
B	A	0.985
C	A	0.993
D	A	0.994

In endurance athletes a low plasma Co Q<sub>10</sub> level has been found, which correlates with the high aerobic power that they developed [14–16]. A similar study on patients with thyroid diseases showed the connection between thyroid hormones and Co Q<sub>10</sub>, as reported by other authors [17].

Finally, a study on hypercholesterolaemic patients, under pharmacological treatment with HMGCoA-reductase inhibitors, was useful for investigating the effect of these drugs on cholesterol and Co Q<sub>10</sub>, which follow the same mevalonate pathway [18]. Our data correlated well with those obtained by other authors, both for healthy subjects [19] and various groups of patients [14–18].

## CONCLUSIONS

Utilizing the proposed methods, cleaner and more replicable chromatographic profiles were obtained, in addition to simplifying the extraction and analytical procedures considerably. The reduction

TABLE VIII

## SUMMARY OF RESULTS OF APPLICATION TO SAMPLES FROM PATIENTS

Subjects <sup>a</sup>	Plasma Co Q <sub>10</sub> (mg/l) <sup>b</sup>	$n$
Healthy subjects, 20–60 years (m. and f.)	$0.80 \pm 0.20$	50
Endurance athletes (m.)	$0.58 \pm 0.17$	40
Hyperthyroid patients (f.)	$0.27 \pm 0.13$	21
Hypothyroid patients (f.)	$0.62 \pm 0.11$	11
Hypercholesterolaemic patients (m. and f.)	$1.15 \pm 0.15$	30

<sup>a</sup> m. = Male; f. = female.

<sup>b</sup> Mean value  $\pm$  2 S.D.

in the volumes of *n*-hexane employed allowed the elimination of glass-tubes with blind nipples and simplified the mixing, vortex mixing being adequate.

The utilization of silica SPE cartridges for solvent replacement, instead of the traditional evaporation under a stream of nitrogen, produced a substantial shortening of the preparation time, a decrease in the analytical errors (less product was lost on the tube walls) and a cost reduction (saving of nitrogen); moreover, it allowed efficient solubilization in methanol, essential for the subsequent clean-up on a C<sub>18</sub> cartridge.

The very good correlation among the methods enables them to be utilized without distinction: the choice depends on the availability of the instruments in the laboratory. The reduction in the analytical time generates a 2.2-fold increase in the productivity of the instruments. For preparing 40 samples utilizing method A it would take 4 h over two days, whereas applying our methods 1 h 20 min is sufficient and the preparation can be done in a real time of less than 2 h, including centrifugations.

If an automatic sampler is available, 160 samples per day can be analysed, with an instrumental utilization of 24 h and an operator availability of 8 h per day. Further advantages of the methods are that the total Co Q<sub>10</sub> is determined directly and the data obtained routinely in various laboratories are comparable and suitable for statistical studies.

#### ACKNOWLEDGEMENTS

The authors are grateful to Master Pharma, Parma, Italy, for the support given.

#### REFERENCES

- 1 M. Battino, R. Fato, G. Parenti Castelli and G. Lenaz, *Int. Rev. Conn. Tiss. Res.*, 12 (1990) 137.
- 2 G. Lenaz, in G. Lenaz (Editor), *Coenzyme Q, a Biochemical Rationale for the Therapeutic Effects of Coenzyme Q*, Wiley, Chichester, 1985, pp. 435–439.
- 3 S. Ogasahara and A. G. Engel, *Neurology*, 38, Suppl. 1 (1988) 269.
- 4 S. Ogasahara, Y. Nishikawa, S. Yorifuji, F. Soga, Y. Nakamura, M. Takahashi, S. Hashimoto, N. Kono and N. Tarm, *Neurology*, 36 (1986) 45.
- 5 S. Zierz, G. Jahns and F. Jerusalem, *J. Neurol.*, 236 (1989) 97.
- 6 H. Langsjoen, P. H. Langsjoen, K. Folkers, *Am. J. Cardiol.*, 65 (1990) 521.
- 7 M. Takada, S. Ikenoya, T. Yuzuriha and K. Katayama, *Biochim. Biophys. Acta*, 679 (1982) 308.
- 8 J. K. Lang and L. Packer, *J. Chromatogr.*, 385 (1987) 109.
- 9 T. Okamoto, Y. Fukunaga, Y. Ida and T. Kishi, *J. Chromatogr.*, 430 (1988) 11.
- 10 P. O. Edlund, *J. Chromatogr.*, 425 (1988) 87.
- 11 G. Grossi, A. Bargossi, R. Battistoni and G. Sprovieri, *J. Chromatogr.*, 465 (1989) 113.
- 12 G. Grossi, A. M. Bargossi, C. Lucarelli, R. Paradisi, C. Sprovieri and G. Sprovieri, *J. Chromatogr.*, 541 (1991) 273.
- 13 A. Kroger, *Methods Enzymol.*, 53 (1978) 579.
- 14 J. Karlsson, in G. Benzi (Editor), *Advances in Myochemistry I*, Libbey, London, 1987, pp. 305–321.
- 15 P. L. Fiorella, A. M. Bargossi, G. Grossi, R. Motta, R. Senaldi, M. Battino, S. Sassi, G. Sprovieri and T. Lubich, in K. Folkers, G. P. Littarru and T. Yamagami (Editors), *Biomedical and Clinical Aspects of Coenzyme Q*, Vol. 6, Elsevier, Amsterdam, 1991, pp. 513–520.
- 16 M. Battino, A. M. Bargossi, P. L. Fiorella and G. Lenaz, *G. Ital. Chim. Clin.*, 15 (1990) 347.
- 17 A. Mancini, L. De Marinis, F. Calabrò, R. Sciuto, A. Oradei, S. Lippa, S. Sandric, G. P. Littarru and A. Barbarino, *J. Endocrinol. Invest.*, 12 (1989) 511.
- 18 K. Folkers, P. Langsjoen, R. Willis, P. Richardson, L. J. Xia, C. Q. Ye and H. Tamagawa, *Proc. Natl. Acad. Sci. U.S.A.*, (1990) 8931.
- 19 Y. Tomono, J. Hasegawa, T. Seki, K. Motegi and N. Morishita, *Int. J. Clin. Pharmacol. Ther. Toxicol.*, 24 (1986) 536.

# Reversed-phase high-performance liquid chromatography of anionic and ethoxylated non-ionic surfactants and pesticides in liquid pesticide formulations

Tamás Bán\*

*Chinoin Pharmaceutical and Chemical Works Ltd., Department Agrovet, P.O. Box 49, H-1780 Budapest (Hungary)*

Elisabeth Papp and János Inczédy

*Research Group for Analytical Chemistry of the Hungarian Academy of Sciences, P.O. Box 158, H-8201 Veszprém (Hungary)*

---

## ABSTRACT

A procedure has been developed for the chromatographic separation of anionic (linear alkylbenzene sulphonates) and non-ionic (ethoxylated nonylphenols, ethoxylated fatty acids and ethoxylated fatty amines) surfactants and a pesticide (cypermethrine) in liquid pesticide formulations using a reversed-phase high-performance liquid chromatographic system.

---

## INTRODUCTION

The type and ratio of ionic and non-ionic surfactants used in liquid pesticide formulations have a great effect on the quality and stability of emulsions and on the biological activity of the pesticide. The analysis of these emulsifiers and their separation from the active component is therefore an important analytical task.

The analysis of products containing several types of surfactants is complicated, as the materials used are complex mixtures of various homologues, isomers and oligomers. Thus the number of components is large and can vary depending on the origin and on the quality of the materials used.

In practice, an octylsilica stationary phase, gradient elution of an aqueous acetonitrile mobile phase and UV detection are used for the simultaneous chromatographic determination of ionic and non-ionic surfactants [1–5]. These separations are also suitable for the quantitation of these compounds.

The separation and analysis of mixtures containing fatty acid- and fatty amine-based surfactants is more complicated, as the UV absorption of these materials is much less than that of benzene derivatives in the usual wavelength range used. Ethoxylated fatty acids contain at least four types of components, *i.e.* free fatty acids, free polyethylene glycols (PEGs), PEG monoesters and PEG diesters [6]. The simultaneous separation of all four types of surfactants has not yet been reported.

Components of ethoxylated fatty acids were separated according to the length of the hydrocarbon chain and the chemical structure (free acid, PEG monoester, PEG diester) on a reversed-phase column [7,8]. Oligomers of ethoxylated fatty acids were separated on a normal-phase column [7,9–11].

Separation of the components of the ethoxylated fatty amines in liquid pesticide formulations was achieved based on the homologues and the degree of ethoxylation (EO) using reversed-phase and normal-phase separation techniques, respectively [12]. The detection system used was suitable for the sen-

sitive and selective detection of amine-type surfactants as the detection system did not respond to alkylphenols, alcohols and esters.

Schreuder and Martijn [13] reported the simultaneous determination of alkylbenzene sulphonates (ABSs) and ethoxylated alkylphenols in liquid pesticide formulations. The separation of the two surfactant types was achieved in reversed-phase high-performance liquid chromatography (RP-HPLC) after the preliminary separation of the solvent and the active component of the formulation using cartridges filled with silica gel and aminoalkyl-modified silica gel.

#### EXPERIMENTAL

The chromatographic system used consisted of a pump (Model Liquopump 312, Labor MIM, Hungary), a variable-wavelength UV detector (Model OE-308, Labor MIM) and a six-port injection valve (Model 7125, Rheodyne) with a 20- $\mu$ l loop and a recorder. The analytical column used contained octylsilica (Nucleosil C<sub>8</sub>) and had dimensions of 150  $\times$  4.0 mm I.D., 5  $\mu$ m particle size. The column was maintained at ambient temperature (24  $\pm$  1°C).

The eluents were methanol–aqueous phosphate buffers. The eluents were prepared by weighing (to  $\pm$  0.01 g) the calculated amount of methanol yielding the pre-selected percentage composition (density 0.796 mg/ml) into a calibrated flask. H<sub>3</sub>PO<sub>4</sub> and NaH<sub>2</sub>PO<sub>4</sub> were then added from stock solutions. Distilled water was slowly added while keeping the temperature at 25.0°C. After careful equilibration, the last few drops of water were added. This eluent preparation procedure was very reproducible.

The pH of the filtered and degassed eluents was measured by a combined glass electrode and a digital pH meter (Model OP-208, Radelkis, Hungary), calibrated with aqueous buffers at pH 4.0 and 7.0.

Selective elution of the four optical isomer pairs of the active component of the pesticide (cypermethrine) was achieved using a normal-phase HPLC system with a silica gel column (Bio-Separation Technologies, Budapest, Hungary; 150  $\times$  4.0 mm I.D., 5  $\mu$ m particle size), and an eluent of *n*-hexane–dichloro methane (85:15) containing 0.26% dioxane. The system used was a Spectra Physics gradient pump, a Rheodyne 7125 injector with a 20- $\mu$ l loop, a Linear Instruments UV detector set at

233 nm, with data acquisition and integration on an IBM PS/2 Model 30 computer. Complete separation of the four isomer pairs was achieved within 12 min using this system at a flow-rate of 2.0 ml/min.

The macroporous, strongly basic ion-exchange resin used (Type Duolite IMAC HP 555, Rohm and Haas; capacity 3.00 mequiv./g) was cleaned by washing with aqueous methanol solutions of various methanol concentrations (25, 50 75%) and with 100% methanol.

#### RESULTS AND DISCUSSION

The retention behaviour of ABSs (C<sub>8</sub>–C<sub>14</sub> homologues), ethoxylated nonylphenols (average EO 2–30), ethoxylated fatty acids (non-specified fatty acid EO 6, oleic acid EO 7) and ethoxylated fatty amines (oleylamine EO 2 and EO 6, tallowamine EO 15 and EO 30 tallowamine hydrogenated EO 15 and EO 30) was studied as a function of the methanol concentration (65–85%) and pH (2.7–6.5) of the eluent. The alkyl chain composition of the non-specified fatty acid (EO 6) was not given by the manufacturer, but the main component of this sample was assumed to be C<sub>18</sub> on the basis of retention volumes.

Selective separation of these four types of surfactants was not achieved by varying the methanol concentration of the eluent as the retention behaviour of all the surfactants examined was similar.

Table I shows the effect of eluent pH on the capacity factors (*k'*) of the surfactants at a methanol concentration of 80%. The retention of the amines was greatly influenced by the eluent pH; the *k'* values increase with increasing eluent pH. However, the eluent pH does not appreciably affect the retention of the ethoxylated nonylphenols and the ethoxylated fatty acids. The ionic strength of eluents of pH 3.8 and 6.5 was different: the concentration of NaH<sub>2</sub>PO<sub>4</sub> in the eluents was 0 and 25 mM, respectively. Therefore the decrease in the retention of the sulphonates is due to an increase in the concentration of the phosphate salt [14]. The retention of the sulphonates between pH 3.8 and 6.5 is approximately the same, as the concentration of the phosphate salt in the eluent is unchanged (25 mM NaH<sub>2</sub>PO<sub>4</sub>).

At pH 2.7 (80% methanol–60 mM H<sub>3</sub>PO<sub>4</sub>), peaks of homologues of the ABSs overlapped with

TABLE I

EFFECT OF ELUENT pH ON THE RETENTION OF COMPONENTS OF IONIC AND NON-IONIC SURFACTANTS IN METHANOL-AQUEOUS PHOSPHATE BUFFER ELUENTS CONTAINING 80% METHANOL

Eluent composition: pH 2.7, 80% methanol (MeOH)–60 mM  $\text{H}_3\text{PO}_4$ ; pH 3.8, 80% MeOH–40 mM  $\text{H}_3\text{PO}_4$ –25 mM  $\text{NaH}_2\text{PO}_4$ ; pH 4.4, 80% MeOH–10 mM  $\text{H}_3\text{PO}_4$ –25 mM  $\text{NaH}_2\text{PO}_4$ ; pH 6.5, 80% MeOH–25 mM  $\text{NaH}_2\text{PO}_4$ . Column, Nucleosil  $\text{C}_{18}$ , 150  $\times$  4.0 mm I.D., 5  $\mu\text{m}$  particle size.

Component	$k'$			
	pH 2.7	pH 3.8	pH 4.4	pH 6.5
<i>Alkylbenzene sulphonates</i>				
$\text{C}_{10}$ ABS	0.89	0.45	0.42	0.40
$\text{C}_{11}$ ABS	1.13	0.59	0.56	0.56
$\text{C}_{12}$ ABS	1.42	0.80	0.75	0.73
$\text{C}_{13}$ ABS	1.80	0.95	0.94	0.93
<i>Ethoxylated nonylphenols (NP)</i>				
NP 1, 2, 3 EO	1.34	1.16	1.19	1.41
NP 23 EO	1.59	1.38	1.38	1.83
<i>Ethoxylated fatty acids</i>				
Oleylamine 2 EO	0.45	0.75	0.86	2.66
	0.53	0.94	1.08	2.81
Oleylamine 6 EO	0.60	1.00	1.12	3.00
Tallowamine 15 EO	0.81	1.31	1.38	3.28
Tallowamine 30 EO	0.91	1.39	1.47	3.40
<i>Ethoxylated fatty amines</i>				
Fatty acid 6 EO <sup>a</sup>	2.88	2.44	2.50	3.80
Oleic acid 7 EO	2.84	2.44	2.45	3.38

<sup>a</sup> The alkyl chain composition of fatty acid 6 EO was not given by the manufacturer, but the main component of this sample was assumed to be  $\text{C}_{18}$  on the basis of retention volumes.

peaks of ethoxylated amines and alkylphenols, thus selective separation was not achieved. However; complete separation of ABSs and ethoxylated fatty acids, or all three types of ethoxylated non-ionic surfactants, was achieved at this pH. At pH values between 3.8 and 4.4 (80% methanol–40 mM  $\text{H}_3\text{PO}_4$ –10–25 mM  $\text{NaH}_2\text{PO}_4$ ), complete separation of ABSs, ethoxylated tallowamines and ethoxylated fatty acids, or the selective elution of ethoxylated nonylphenols and fatty acids, was obtained. The simultaneous separation of all four types of surfactants was achieved when ethoxylated oleylamine was present in the mixture at pH 6.5 (80% methanol–25 mM  $\text{NaH}_2\text{PO}_4$ ) [15].

The selective separation of ethoxylated tallowamines and ethoxylated fatty acids was not possible because their retention was similar at pH 6.5 (Table I). The selective separation of ethoxylated tallowamines from ethoxylated fatty acids and ethoxylated nonylphenols was obtained only after the prelim-

inary separation of ABSs from the mixture containing all four types of surfactants by ion exchange.

A 2-ml volume of a mixture containing 1.75–20.0 g/l ABS, 2.0–40.0 g/l ethoxylated nonylphenol, 20.0–62.5 g/l ethoxylated fatty amine and 7.5–40.0 g/l ethoxylated fatty acid was pipetted onto an ion-exchange column containing 10 ml of resin ( $\text{Cl}^-$ ). The non-ionic surfactants were eluted quantitatively with 25 ml of methanol and were separated chromatographically with the pH 2.7 eluent (Fig. 1). Regeneration of the anion-exchange resin and the quantitative elution of ABSs was achieved with 50 ml of a mixture containing 80% methanol–0.5 M hydrochloric acid. Selective separation of ABS homologues was achieved with the eluent containing 65–70% methanol (65–70% methanol–40 mM  $\text{H}_3\text{PO}_4$ –25 mM  $\text{NaH}_2\text{PO}_4$ , pH  $\approx$  3.5) (Fig. 2). Note that if  $\text{C}_8$ ,  $\text{C}_9$  and  $\text{C}_{14}$  homologues are present in the mixture of the four types of surfactants, selective separation can be achieved using the separa-

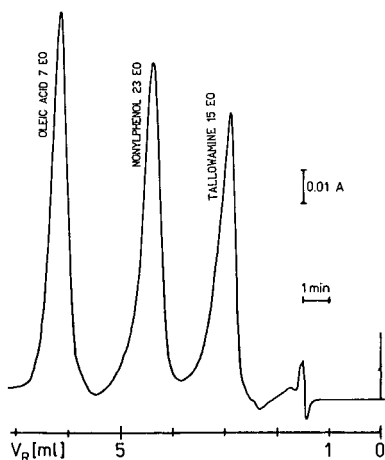


Fig. 1. Simultaneous separation of nonylphenol, tallowamine and oleic acid ethoxylates. Column, Nucleosil  $C_8$  ( $150 \times 4.0$  mm I.D.,  $5 \mu\text{m}$  particle size); eluent, 80% methanol–60 mM  $\text{H}_3\text{PO}_4$ , pH 2.7; eluent flow-rate, 0.5 ml/min;  $\lambda = 220$  nm; sample, 20  $\mu\text{l}$  of 9.1 g/l tallowamine 15 EO–170 mg/l NP 23 EO–4.5 g/l oleic acid 7 EO.

tions described above (ion exchange, elution with hydrochloric acid–aqueous methanol, RP-HPLC separation).

Using RP-HPLC, selective separation of all the eight isomers of the pesticide (cypermethrine) was not achieved; all the isomers eluted as one symmetrical peak with the methanol–aqueous phosphate buffer eluent containing 80% methanol. Selective

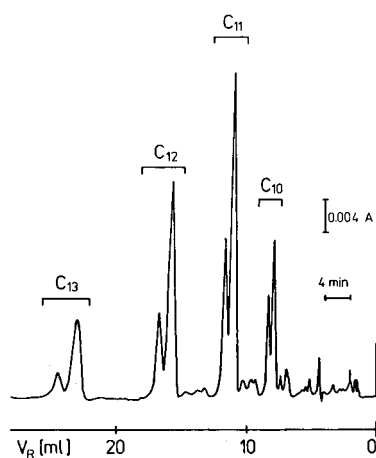


Fig. 2. Complete separation of ABS homologues and partial separation of positional isomers of homologues. Column as in Fig. 1. Eluent, 70% methanol–25 mM  $\text{NaH}_2\text{PO}_4$ –40 mM  $\text{H}_3\text{PO}_4$ , pH 3.5; eluent flow-rate, 0.5 ml/min;  $\lambda = 224$  nm; sample, 20  $\mu\text{l}$  of 115 mg/l ABSs.

elution of the four optical isomer pairs was achieved using a normal-phase HPLC system (see under Experimental).

Such a good separation of the isomers was not achieved in the RP-HPLC system used, even with water–acetonitrile as the eluent. All the isomers of cypermethrine were eluted as one peak with the eluent containing 80% methanol. The retention of the components eluted as this peak was about the same ( $k' = 1.28$ ) as that of nonylphenols of low EO (see Table I and Smedes *et al.* [15]). The retention of the isomers of cypermethrine was unaffected by eluent pH in the range 2.7–6.5.

Cypermethrine is stable in apolar solvents but is unstable in polar solvents, *e.g.* in aqueous methanol eluents. The active matter can be hydrolysed by even trace amounts of water in technical-grade xylene, which is the solvent in the pesticide formulation. The rate of hydrolysis is relatively low, and is about 1% per day (Antal Gajáry, Chinoin, Hungary, unpublished results). Several molecules, such as amines, can react with cypermethrine with the formation of new esters and amides. These reactions are fast enough to occur within a couple of minutes while dissolving the active component and the surfactants (ethoxylated fatty amines first) in methanol or in the eluent. The simultaneous separation of ABSs, cypermethrine, ethoxylated oleylamine and ethoxylated oleic acid is shown in Fig.

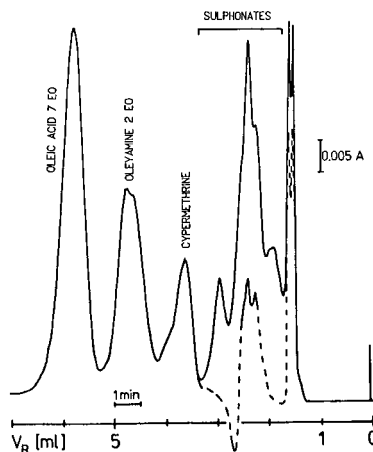


Fig. 3. Simultaneous separation of ABSs, cypermethrine, ethoxylated oleylamine and ethoxylated oleic acid before (solid line) and after (broken line) the separation of ionic compounds from the mixture using an ion-exchange resin. Column as in Fig. 1. Eluent, 80% methanol–25 mM  $\text{NaH}_2\text{PO}_4$ , pH 6.5; eluent flow-rate, 0.5 ml/min;  $\lambda = 220$  nm.

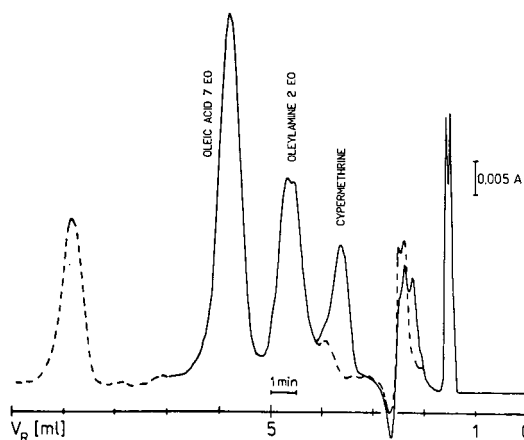


Fig. 4. Reaction of cypermethrine in the presence of ethoxylated oleylamine before (solid line) and after (broken line) the reaction between amine and cypermethrine. Column as in Fig. 1. Eluent, 80% methanol–25 mM  $\text{NaH}_2\text{PO}_4$ , pH 6.5; eluent flow-rate, 0.5 ml/min;  $\lambda = 220$  nm.

3. The shapes of the peaks of the homologues of ABSs are assymetric, which shows the presence of the products of the reactions described above. The chromatogram marked with the broken line was obtained after the preliminary separation of sulphonates from the mixture by the anion-exchange resin. Besides this reaction, other reactions occur which produce compounds with long retention times. As a consequence of this reaction, cypermethrine disappears from the mixture (Fig. 4, broken line). Fig. 4 shows that the area and shape of the peak of the ethoxylated oleylamine does not vary while cypermethrine is reacting, so, although the amines do not react with cypermethrine, they act as catalysts. It is not surprising that oleylamine (EO 2) is divided into two peaks, as the technical-grade sample analysed contained isomers and several ethoxylated oligomers.

Cypermethrine is stable in weakly acidic solvents at about pH 4 [16]. In acidic solvents, however, ethoxylated fatty amines rapidly react with the acid and the absorbances of the products of this reaction differ strongly from those of the amines; quantitation of them is therefore impossible. Cypermethrine itself remains unchanged and can be quantified.

## CONCLUSIONS

It is concluded that the simultaneous and isocratic separation of components of mixtures containing

ionic (ABSs) and non-ionic (nonylphenol, fatty acid and fatty amine ethoxylates) surfactants can be achieved using a RP-HPLC technique with an octylsilica stationary phase and methanol–aqueous phosphate buffer eluents. Separation of the four types of surfactants when ethoxylated tallowamines were present in the mixture was achieved only after the preliminary separation of ionic compounds on an anion-exchange resin. The quantitative elution of non-ionic surfactants from the resin was carried out with methanol; regeneration of the resin, *i.e.* the quantitative elution of ionic components, was obtained with a methanol–hydrochloric acid mixture. The simultaneous separation of non-ionic compounds of the first fraction containing the ethoxylates was achieved in the described RP-HPLC system. Complete separation of the homologues and even partial separation of the positional isomers of homologues of the second fraction was also achieved.

In the presence of cypermethrine the separation of ABSs, ethoxylated fatty amines, ethoxylated fatty acids and the active component of the pesticide was achieved after the preliminary separation of ionic surfactants on an anion-exchange resin.

## REFERENCES

- 1 A. Marcomini and W. Giger, *Anal. Chem.*, 59 (1987) 1709.
- 2 A. Marcomini, S. Capri and W. Giger, *J. Chromatogr.*, 403 (1987) 243.
- 3 A. Marcomini, F. Filpuzzi and W. Giger, *Chemosphere*, 17 (1988) 853.
- 4 A. Marcomini and W. Giger, *Tenside Surfactants Deterg.*, 25 (1988) 226.
- 5 A. Marcomini, P. D. Capel and W. Giger, *Naturwissenschaften*, 75 (1988) 460.
- 6 Th. F. Tadros, *Surfactants*, Academic Press, London, 1984.
- 7 R. M. Cassidy, *J. Liq. Chromatogr.*, 1 (1978) 241.
- 8 M. Kudoh, M. Kotsuji, S. Fudano and K. Tsuji, *J. Chromatogr.*, 295 (1984) 187.
- 9 A. Aserin, N. Garti and M. Frenkel, *J. Liq. Chromatogr.*, 7 (1984) 1545.
- 10 I. Zeman, *J. Chromatogr.*, 363 (1986) 223.
- 11 I. Zeman and M. Bareš, *Tenside Deterg.*, 23 (1986) 181.
- 12 R. H. Schreuder, A. Martijn, H. Hoppe and J. C. Kraak, *J. Chromatogr.*, 368 (1988) 339.
- 13 R. H. Schreuder and A. Martijn, *J. Chromatogr.*, 435 (1988) 73.
- 14 F. Smedes, J. C. Kraak, C. F. Werkhoven-Goewie, U. A. Th. Brinkmann and R. W. Frei, *J. Chromatogr.*, 247 (1982) 123.
- 15 T. Bán, E. Papp and J. Inczédy, *Magyar Kémiai Folyóirat*, 6 (1991) 246.
- 16 C. R. Worthing, *The Pesticide Manual: A World Compendium*, The Lavenham Press, Lavenham, 9th ed., 1990.





# Analysis of block copolymers by high-performance liquid chromatography under critical conditions

T. M. Zimina\*,☆

*Department of Pharmaceutical Chemistry, University of Bradford, Bradford BD7 1DP (UK)*

J. J. Kever and E. Yu. Melenevskaya

*Institute of Macromolecular Compounds, Academy of Sciences, St. Petersburg 199004 (Russia)*

A. F. Fell

*Department of Pharmaceutical Chemistry, University of Bradford, Bradford BD7 1DP (UK)*

---

## ABSTRACT

The complete chromatographic characterization of block copolymers (molecular weight *versus* chemical composition) is an important problem in polymer chemistry. The experimental validity of the concept of so-called “chromatographic invisibility”, predicted theoretically by Gorbunov and Skvortsov on the basis of the phenomenon of critical conditions known in liquid chromatography, was examined. The theoretical approach predicts the possibility of one component of an A–B block copolymer being eluted under gel permeation chromatographic conditions, whereas the size of the alternate “invisible” component exerts no effect on the overall elution profile of the block copolymer. This applies only when special thermodynamic conditions, *i.e.*, eluent composition and temperature, are fulfilled, where the distribution coefficient  $K$  is unity, regardless of molecular weight. Block copolymers of poly(styrene–methyl methacrylate) and poly(styrene–*tert.*-butyl methacrylate) were used as examples with binary and ternary mixtures of acetonitrile–dichloromethane, methanol–chloroform, tetrahydrofuran–dichloromethane and tetrahydrofuran–dichloromethane–hexane as eluents for chromatography under critical conditions on wide-pore silica gel in narrow-bore columns.

---

## INTRODUCTION

Compositional and molecular weight distributions in block copolymers are strongly correlated with the mechanical and hydrodynamic properties of these macromolecular compounds. The evaluation of these data is an important problem in polymer chemistry, for which chromatographic methods can be used. The most advantageous chromatographic approach available at present is so-called orthogonal chromatography [1–3], or the combination of separations in different dimensions,

*i.e.*, size and composition. An example is the combination of gel permeation chromatography (GPC) and gradient (normal- or reversed-phase) chromatography, where the gradient step is used for evaluating the compositional distribution.

However, the application of isocratic chromatography in evaluating compositional heterogeneity data may be more advantageous than the gradient mode, primarily owing to the better reproducibility of retention time data in equilibrated systems without the recovery stage. Another problem in gradient separations is the variation of the background absorption in the ultraviolet region, commonly used for detection, of the eluents most frequently used in polymer analysis [1]. The “invisibilities” concept [4] is useful in that it allows the molecular weight of the

---

\* Address for correspondence: Institute of Macromolecular Compounds, Academy of Sciences, St. Petersburg 199004, Russia.

structural units in block copolymers to be evaluated directly, which is not possible with other chromatographic methods.

Taking these considerations into account, the approach developed theoretically [4] and presented here as an experimental methodology seems to have inherent advantages. The method enables steric exclusion effects in chromatography to be suppressed for some defined parts of a copolymer, so that they become invisible, thus enabling another, visible part of the molecule to be evaluated under GPC conditions, as if it were being chromatographed separately. This approach is based on a theoretical treatment described elsewhere [4,5]. Some earlier experimental results assessing the validity of the concept of invisibility have been presented previously [6].

The objectives of this present study were to explore this concept under a variety of chromatographic conditions and to examine the influence of different factors (such as mobile phase composition, temperature and molecular weight of the sample) on the chromatographic zone profile of poly(methyl methacrylate) (PMMA) and poly(*tert.*-butyl methacrylate) (PtBMA). It was hoped to evaluate the mechanism of adsorption over the range of conditions examined.

#### THEORETICAL BACKGROUND

Critical conditions in the liquid chromatography of polymers represent the thermodynamic state where the distribution coefficient of a polymer becomes unity ( $K = 1$ ), regardless of its molecular weight. This phenomenon has been examined by some workers [7–9] in the context of the concept of a universal mechanism in chromatography and it was shown that the most important parameter that defines the chromatographic behaviour of a polymer is the energy,  $-\varepsilon$ , of interaction of a polymer segment and the sorbent. This parameter depends on the thermodynamic state of the system and assumes a specific value when the chromatographic state of the system undergoes a transfer from exclusion to adsorption conditions. The data obtained were interpreted as a phase transfer, and exclusion–adsorption was considered as a manifestation of the universal law of chromatography. The range of thermodynamic conditions over which this

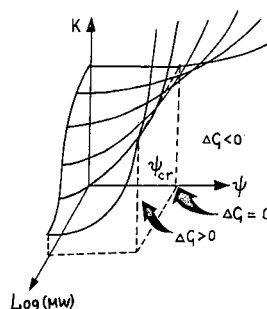


Fig. 1. Distribution coefficient,  $K$ , versus logarithm of molecular weight,  $\log(MW)$ , and volume fraction of eluent modifier,  $\psi$ .  $\Delta G = -kT \ln K$ , where  $k$  is Boltzmann's constant and  $T$  is absolute temperature.

phase transfer occurred were defined as the critical conditions, for which the appropriate energy was  $-\varepsilon_{cr}$ . Thus the range corresponding to GPC can be defined as that where  $-\varepsilon < -\varepsilon_{cr}$  ( $\Delta G > 0$ ), while the range of adsorption corresponds to  $-\varepsilon > -\varepsilon_{cr}$  ( $\Delta G < 0$ ), as illustrated in Fig. 1. Under critical conditions, where ( $\Delta G = 0$ ) a homopolymer elutes with the total volume of the column, regardless of its molecular weight.  $\Delta G$  is the change in conformational free energy of the macromolecule when it enters the pore.

This phenomenon has been confirmed experimentally for different types of polymers and sorbents [7,9]. A theoretical approach has been developed by Gorbunov and Skvortsov [4,5] on the basis of Cassasa's theory of the chromatography of macromolecules [10]. They proposed the term "chromatographic invisibility" to describe the insensitivity of a chromatographic system to the molecular weight of a polymer under these particular conditions. They applied the idea of chromatographic invisibility in developing a theory for the separation of block copolymers of the A–B type, according to the lengths of the "visible" blocks only, in some types of copolymers with complicated architecture in pores of arbitrary diameter. They have also shown that the theory is valid in general for cases when the invisible blocks possess a free terminus on the chains. This approach was developed theoretically for flexible-chain macromolecules, assuming no excluded volume effects in slit-like pores.

The main statements of the theory developed by Gorbunov and Skvortsov [4] are as follows. According to the basic approach of Cassasa [10] under the

above conditions, the distribution coefficient of the macromolecule,  $K$ , is equal to the ratio of the free energies of a macromolecule in and out of the pore, which in general can be written as

$$K = D^{-1} \int_0^D Z(x) dx \quad (1)$$

where  $Z(x)$  is the statistical sum of the chain, one end of which is at a distance  $x$  from the pore wall, and  $D$  is the width of the slit-like pore.

On this basis, and after introducing the appropriate value of the energy of interaction of the chain segment with the pore wall, it was shown that under critical conditions the statistical sum of the chain is  $Z_{cr}(x) = 1$ , for any size of macromolecule and  $D$  and for all  $x$ , and consequently  $K_{cr} = 1$ . On the same basis, for a block copolymer of the A-B type, the expression for  $K$  can be defined as

$$K_{AB} = D^{-1} \int_0^D Z_A(x) Z_B(x) dx \quad (2)$$

where  $Z_A(x)$  and  $Z_B(x)$  are the statistical sums of the appropriate blocks. Hence, if critical conditions are established for block B, then  $Z_B(x) = 1$ , so that  $K_{ABcr}$  of the total block copolymer molecule is given by the following expression:

$$K_{ABcr} = D^{-1} \int_0^D Z_A(x) dx = K_A \quad (3)$$

which means that block B becomes chromatographically invisible.

It was of interest to check the validity of this concept experimentally with real block copolymers. For this purpose, the simplest block copolymers of the A-B type were chosen. Eqn. 3 as developed by Gorbunov and Skvortsov [4] was taken as the basic concept of this work in developing a method to determine the polydispersity and compositional heterogeneity in block copolymers.

## EXPERIMENTAL

### Equipment

Standard chromatographic equipment used in-

cluded a Model 3000 spectrophotometer (LDC Analytical, Riviera Beach, FL, USA) with cell volume 1.5  $\mu$ l, two LKB model 2150 pumps (Pharmacia, Uppsala, Sweden) with a PU404 solvent mixer (Philips Analytical, Cambridge, UK) for regulation of the binary mixed mobile phase composition, a Rheodyne (Cotati, CA, USA) Model 7125 injection valve with a 1- $\mu$ l loop and a TC 931 column heater (Applied Chromatography Systems, Macclesfield, UK).

### Columns

Normal-phase S5X silica gel of 5- $\mu$ m particle size and 300-Å pore diameter (Phase Separations, Clwyd, UK). was packed in a stainless-steel column (250 mm  $\times$  2 mm I.D.). The column was calibrated with polystyrene (PS) and PMMA standards over the molecular weight range 1700–1 950 000 obtained from Polymer Labs. (Church Stretton, UK). The column efficiency for benzene was 28 000 theoretical plates/m.

Another type of silica gel, LiChrospher Si-300, also of 5- $\mu$ m particle size and 300-Å pore diameter (Merck, Darmstadt, Germany), was packed in a fluoroplastic column (350 mm  $\times$  0.5 mm I.D.) [6]. The calibration procedure was the same as that for the S5X silica gel and the column efficiency for benzene was 29 000 theoretical plates/m.

### Calculation procedures

The peak asymmetry was calculated according to the standard procedure. A perpendicular was drawn from the peak maximum to the baseline. At a point 10% from the baseline the segments to the leading and tailing edges (A and B, respectively) were measured. The asymmetry was obtained by dividing of length of the tailing segment, B, by that for the leading segment, A.

The equilibrium distribution of the split zones, defined here as the apparent distribution coefficient,  $\langle K \rangle$ , was measured as the ratio of the peak areas of the two zones observed for PtBMA under near-critical conditions. The range of the  $\langle K \rangle$  value was the same as that for the conventional distribution coefficient,  $K$ .

### Eluents

The eluent components used were dichloromethane (DCM), chloroform (CHL), acetonitrile (ACN),

TABLE I  
CHARACTERISTICS OF BLOCK COPOLYMERS

Sample	Molecular weight	PS weight fraction (%)
P(S- <i>t</i> BMA)		
No. 53	70 000	19.0
No. 41	95 000	5.0
No. 11	100 000	2.5
No. 31	130 000	50.0
P(S-MMA) <sup>a</sup>		
No. 1	14 000	50.0
No. 2	35 000	50.0
No. 3	58 000	50.0
No. 4	107 800	50.0

<sup>a</sup> Manufacturer's data based on NMR.

methanol (MET), tetrahydrofuran (THF) and *n*-hexane (HEX), all of high-performance liquid chromatographic grade. Mixed mobile phases were made by volume mixing and then their compositions were regulated precisely by the two pumps.

#### Samples

A-B-type block copolymers of poly(styrene-*tert*-butyl methacrylate) P(S-*t*BMA) were obtained by successive anionic polymerization at the Institute of Macromolecular Compounds Academy of Sciences (St. Petersburg, Russia) according to the procedure described previously [11,12], which permits the preparation of linear narrow-disperse polymers. PS precursors were collected directly from the reactor after the first stage of the process; hence it was possible to obtain the molecular weight characteristics of the PS blocks of the block copolymers.

Block copolymers of poly(styrene-methyl methacrylate) P(S-MMA) were obtained from Polymer Labs. The molecular characteristics of the samples are described in Table I. All the samples of homopolymers and block copolymers were dissolved in the mobile phase at a concentration of *ca.* 0.1% (w/v) and aliquots of 1  $\mu$ l were injected.

Samples of isobutyl methyl ketone, methyl ethyl ketone and acetone were all of analytical-reagent grade and were injected into the column without dilution.

## RESULTS AND DISCUSSION

### Chromatography of polymers under critical conditions

The eluent required to give critical conditions for polar blocks (PMMA, PtBMA) of block copolymers on silica gel sorbent was found by varying the percentage of the polar component. For non-polar blocks (PS), GPC conditions were expected. However, it is necessary to bear in mind the dependence of the thermodynamic properties of an eluent, as determined by its composition and temperature, in order to avoid a shift of the retention time of PS as a result of changes in the Mark-Kuhn constants, *i.e.*, owing to a change in the size of the macromolecule. These conditions were established using the eluent system DCM-ACN with restricted amount of ACN owing to the problems of solute solubility. DCM is a good solvent for all the samples, whereas for PS it creates size-exclusion conditions in chromatography. On the other hand, PMMA and PtBMA are totally adsorbed. ACN as a desorption component

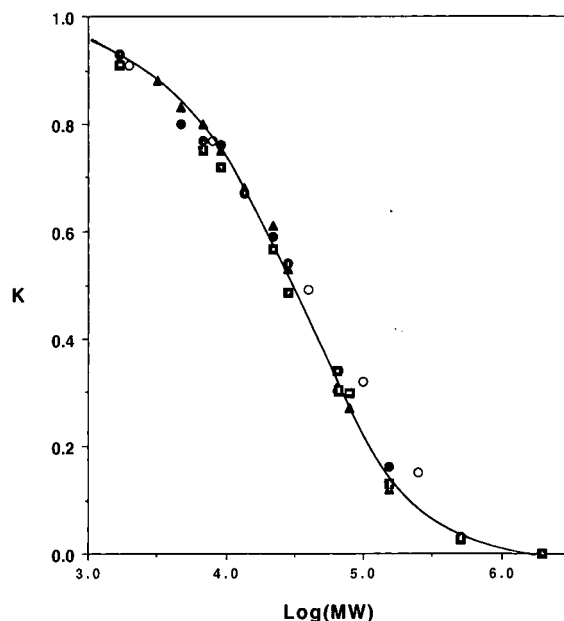


Fig. 2. Calibration graphs of distribution coefficient, *K*, versus logarithm of molecular weight, log (MW), for PS standards in different eluents: ( $\blacktriangle$ ) THF; ( $\bullet$ ) ACN-CHL (47:53, v/v); ( $\blacksquare$ ) MET-CHL (20:80, v/v); and ( $\circ$ ) ACN-DCM (1:1, v/v). Column: 350  $\times$  2 mm I.D., packed with silica gel S5X (this column was used in all the experiments except as noted in the text).

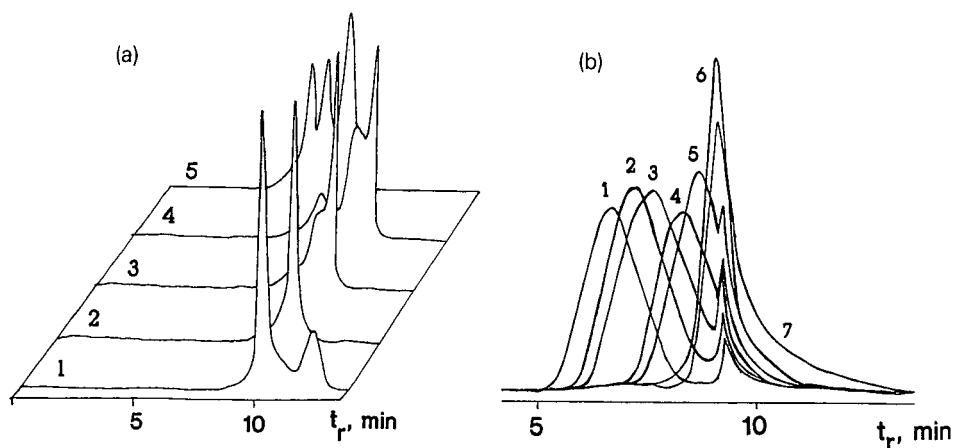


Fig. 3. Chromatographic zone shift under near-critical conditions. Column:  $350 \times 0.5$  mm I.D., packed with LiChrospher Si-300. (A) PMMA (MW 27 700, 60 000, 107 000). Eluent, ACN–DCM: (1) 42.8:57.2; (2) 43.0:57.0; (3) 43.1:56.9; (4) 43.3:56.7; (5) 46.0:54.0 (v/v). (5) GPC, (2) critical and (1, 3 and 4) near-critical conditions. (B) PtBMA (MW 80 000). Eluent, ACN–DCM: (1) 11.2:88.8; (2) 10.6:89.4; (3) 10.3:89.7; (4) 9.9:90.1; (5) 9.6:90.4; (6) 9.3:90.7; (7) 9.0:91.0 (v/v). (1) GPC, (6) critical and (2, 3, 4, 5 and 7) near-critical conditions.

of the eluent is appropriate for PtBMA because small amounts (less than 10%) are sufficient, with no problem with solubility. However, ACN is less successful for PMMA, because considerable concentrations of ACN are necessary for its desorption, and these are near the limits of solute solubility. As a result, a slight shift of the calibration dependence was observed for PS under the critical conditions for PMMA. However, this shift was considered to be negligible, because it did not exceed a value of 5% in different eluents over the range of molecular weights of interest (Fig. 2). On the basis of these data, it may be assumed that PS elutes by a GPC mechanism.

Another desorptive component used in the binary mixed mobile phase with DCM was THF, which did not lead to any problems with solubility, but did influence the shape of the calibration dependence under critical conditions. However, this shift was not substantial and was not taken into account (Fig. 2).

As has been shown previously for other polymers [7–9], critical conditions exist for a particular eluent composition and sorbent. In this work they have been found for PMMA and for PtBMA in eluent systems containing two or three components of different polarity. These systems were ACN–DCM, ACN–CHL, MET–CHL, THF–DCM and THF–HEX–DCM. In the range of molecular weights from 20 000 to 100 000, a shift of peak position and a change in elution order, as described earlier for other

polymers, was observed under adsorption conditions (Fig. 3).

For higher molecular weight samples, a splitting of zones and reversible pumping of samples from the GPC zone to critical conditions was observed for both PMMA and PtBMA. The results for PMMA standards in the system MET–CHL, shown in Fig. 4, indicate the strong dependence of peak shape on the molecular weight of PMMA, which manifested itself in splitting of the chromatographic zone followed by considerable peak tailing. For the PtBMA sample in the THF–DCM system, peak splitting indicates another mechanism of sorption with division of the zone into two zones, one of which elutes under GPC conditions and another under critical conditions, where the fraction of the zones changes in accordance with the thermodynamic state of the chromatographic system. However, both zones have a regular shape without any tailing.

The data on the influence of temperature on the distribution coefficients of the PMMA standards in the binary eluent system ACN–CHL (1:1, v/v) are shown in Fig. 5. The relationships have a regular character and the distribution coefficients gradually shift to unity when the temperature increases. These data are in qualitative agreement with those obtained for PS in the system CHL–tetrachloromethane [7].

An investigation of the relationship between

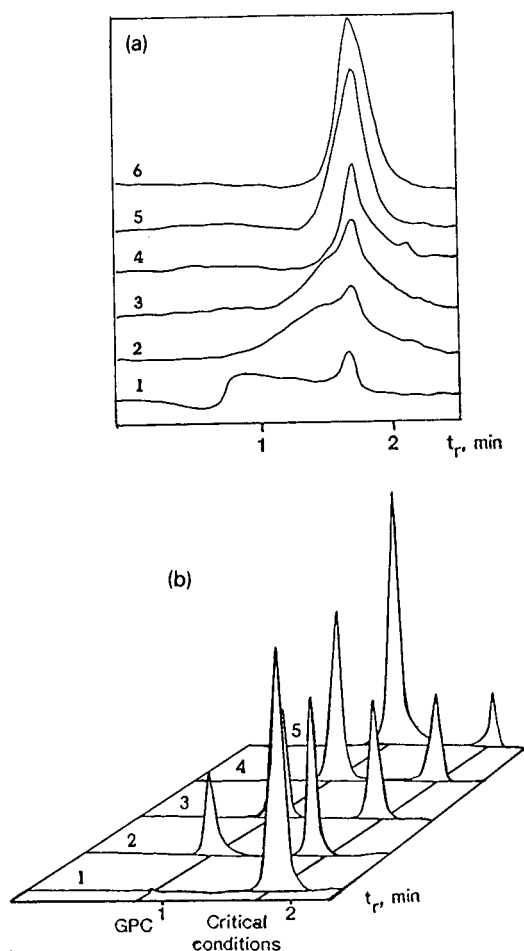


Fig. 4. Influence of molecular weight of the samples on (A) chromatographic zone profiles under near-critical conditions for PMMA (A) and (B) zone splitting for high-molecular-weight PtBMA. (A) PMMA MW: (1) 400 000; (2) 265 000; (3) 185 000; (4) 107 000; (5) 82 000; (6) 60 000. Eluent: MET-CHL (20:80, v/v). (B) PtBMA MW: 200 000. Eluent, THF-DCM: (1) 5.0:95.0; (2) 5.4:94.6; (3) 5.85:94.15; (4) 6.5:93.5; (5) 9.0:91.0 (v/v).

the thermodynamic state of the chromatographic system, *i.e.*, mobile phase composition, and the retention characteristics in the range of near-critical conditions was performed on the basis of approaches developed by Scott and Kucera [13,14] by comparing the behaviours of related substances with polarity values close to those of PMMA and PtBMA. The relationships between the reciprocal of the corrected retention volume,  $1/V_R$ , and the volume fraction of solvent modifier were obtained for

isobutyl methyl ketone, methyl ethyl ketone and acetone (Fig. 6). The retention behaviour of each of these substances was then compared with those of PMMA and PtBMA. For both eluent systems, ACN-DCM and THF-DCM, the relationships show a non-linear character over a wide range of eluent composition. This behaviour was of the type observed previously by McCann *et al.* [15] and designated a "type VI" system. These relationships can be approximated by two linear regions with different slopes. According to data obtained by Scott and Kucera [14], these areas could possibly be interpreted as the areas of monolayer formation and slow double-layer formation, respectively. Comparison of these relationships with the graphs of the distribution coefficient of PMMA,  $K$ , and the apparent distribution coefficient for PtBMA,  $\langle K \rangle$ , shows that critical conditions may exist in the range of mobile phase composition of THF-DCM, corresponding to the completion of monolayer formation (Fig. 6) and where retention has a displacement character. All the values are plotted on the same numerical scale. Analogous relationships were obtained for the eluent ACN-DCM.

These data are in agreement with those obtained

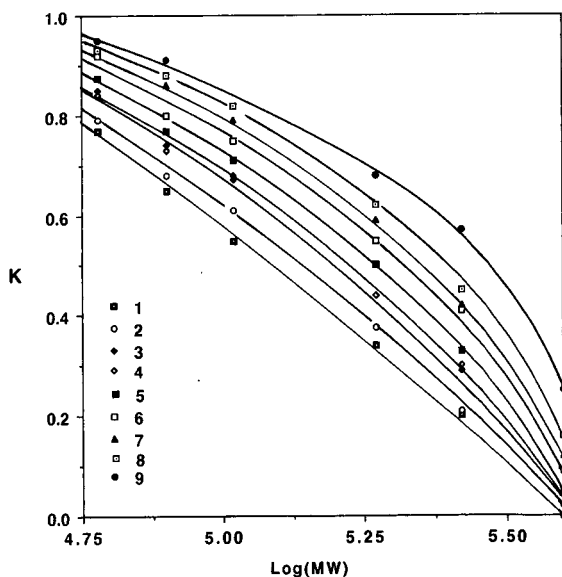


Fig. 5. Relationships between the distribution coefficients and  $\log(MW)$  for PMMA standards at different temperatures. Eluent: CHL-ACN (1:1, v/v). (1) 25; (2) 30; (3) 35; (4) 37; (5) 40; (6) 42; (7) 45; (8) 47.2; (9) 50.2°C.

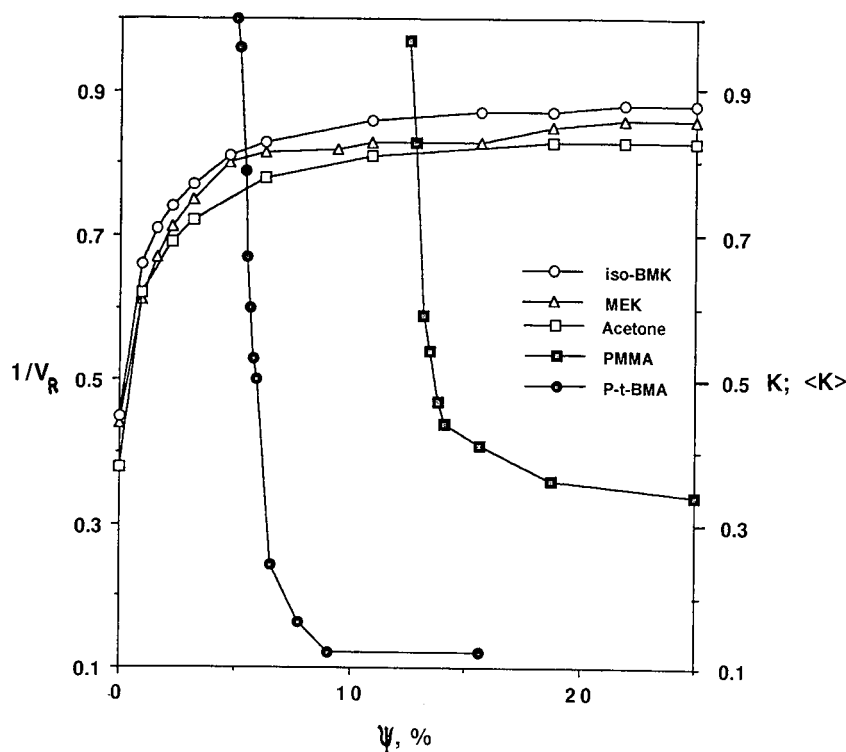


Fig. 6. Comparison of the relationships between the reciprocal of retention volume,  $1/V_R$ , for (○) isobutyl methyl ketone, (△) methyl ethyl ketone and (□) acetone and the volume fraction of THF in the eluent (THF–DCM), and that of the distribution coefficient,  $K$ , for (■) PMMA (MW 82 000) and the apparent distribution coefficient,  $\langle K \rangle$ , for (●) PtBMA (MW 200 000) (see text) under the same conditions.

by Tennikov *et al.* [7] for PS in the system tetra-chloromethane–chloroform. The nature of the monolayer formed on the surface of silica gel apparently plays an important role in the mechanism of retention of polymers under near-critical conditions. The addition of a non-polar component, *n*-hexane, which may, according to Scott and Kucera's data [13,14], lead to dense bilayer formation, changes the shapes of the chromatographic zones considerably. In Fig. 7, the relationship between the asymmetry of the chromatographic zone profiles for PtBMA and the volume fraction of the eluent modifier is shown for the systems HEX–THF and HEX–DCM–THF. In the former system, where bilayer formation can be expected, considerable asymmetry and peak tailing were observed, whereas addition of DCM led to a considerable decrease in asymmetry. These data show the significance of the nature of the polar component layer as regards the chromatographic behaviour of polymers

under near-critical conditions, an observation which needs further systematic investigation.

#### *Chromatography of block copolymers under critical conditions*

The next step was to examine the validity of the theoretical concept of chromatographic invisibility for evaluating the molecular characteristics of block copolymers.

When critical conditions apply for one of the blocks of a block copolymer of the A–B type, so that according to theory [4] it becomes chromatographically invisible, it can be expected that the chromatogram of the block copolymer will coincide with that for the visible block (PS block), at least so far as the positions of their peaks are concerned. Prediction is limited to peak positions, as the theoretical basis for this effect is developed only in terms of equilibrium distribution coefficients, and does not take into account the dynamics and kinetics of the

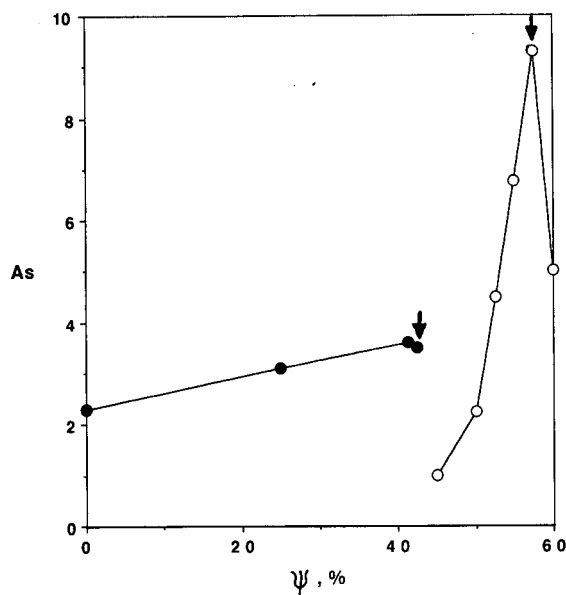


Fig. 7. Relationships between asymmetry,  $A_s$ , and volume fraction of eluent modifier,  $\psi$ , for PtBMA (MW 200 000) in different eluents: (○) HEX-THF and (●) HEX-THF-DCM (THF-DCM constant at 1:1, v/v; variable HEX,  $\psi$ ). Arrows indicate the critical conditions for PtBMA.

processes that are responsible for the shape of the peak profiles. The experimental results obtained confirm this prediction.

Hence the values of retention times,  $t_r$ , in the chromatograms of P(S-tBMA) samples (Table I) and their PS precursors coincide in the eluent system ACN-DCM (9.3:90.7, v/v; 25°C) (Fig. 8). In the

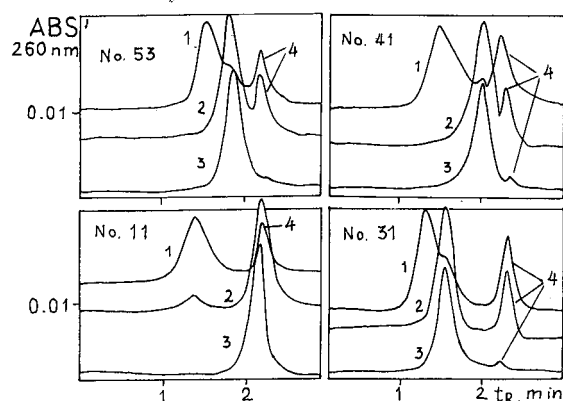


Fig. 8. Chromatograms of P(S-tBMA) and PS precursors with ACN-DCM as eluent. (1) GPC; (2) critical conditions; (3) PS precursor; (4) impurity.

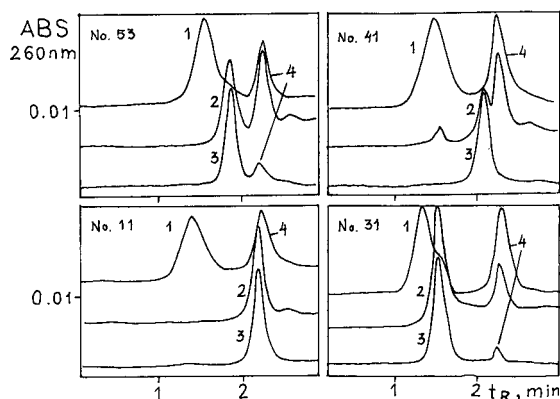


Fig. 9. As Fig. 8 with THF-DCM as eluent.

system THF-DCM, good coincidence of the chromatograms of PS and of the related block copolymers under critical conditions (5.5:94.5, v/v; 28°C) was clearly achieved (Fig. 9).

It should be noted that the absolute value of the eluent composition can vary in the range 5–10%, depending on the water content of the solvent and on the state of the silica gel. It is likely that the validity of this concept is limited to visible blocks whose size exceeds a certain minimum, as implicated in Table I.

## APPLICATIONS

The methodology described above was applied to the analysis of block copolymers of P(S-MMA) (Table I). The data presented in Table II show the

TABLE II

PS WEIGHT FRACTIONS IN BLOCK COPOLYMERS OF P(S-MMA) EVALUATED BY MEANS OF CHROMATOGRAPHY UNDER CRITICAL CONDITIONS

Molecular weight of block copolymer	Apparent molecular weight of block copolymer under critical conditions <sup>a</sup>	Weight fraction of PS (%)
107 800	49 000	46
58 500	24 000	42
35 000	15 000	43
14 000	7000	50

<sup>a</sup> Apparent molecular weight was evaluated with the help of a calibration graph with respect to PS standards.



values of the PS fraction in block copolymers obtained by means of chromatography under critical conditions, where block copolymers are eluted as pure PS blocks in GPC. The data can be considered as reasonable and accepted as one of the first examples showing the additional possibility of evaluating of block copolymer heterogeneity.

## CONCLUSIONS

The theoretical prediction of the chromatographic invisibility of individual blocks in block copolymers under critical conditions has been confirmed experimentally for the case of A-B block copolymers of P(S-MMA) and P(S-tBMA) with molecular weights up to 100 000 in wide-pore silica gel. Under these conditions, block copolymer macromolecules elute according to the size of the visible block.

It was found that critical thermodynamic conditions are feasible when the monolayer formation on the silica gel surface is complete. The shape of the zone profile under near-critical conditions is influenced by the molecular weight of the polymer (*i.e.*, by the ratio of the size of the molecule to that of the pore) and by the nature of the polar component layer on the surface of the silica gel.

The data obtained suggest possibilities for the direct, non-destructive analysis of individual components of complex macromolecules.

## ACKNOWLEDGEMENTS

The authors are grateful to Dr. Vladimir N.

Zgonnik (Institute of Macromolecular Compounds, St. Petersburg, Russia) for this cooperation in providing the samples of synthesized P(S-tBMA) and valuable discussions. The valuable technical assistance of Alan Holmes (Department of Pharmaceutical Chemistry, University of Bradford, UK) is acknowledged with thanks. Dr. Peter Myers (Phase Separations) is thanked for kindly providing some of the columns for this work.

## REFERENCES

- 1 S. T. Balke and R. D. Pathel, *Adv. Chem. Ser.*, No. 203 (1983) 281.
- 2 G. Glokner and H. G. Barth, *J. Chromatogr.*, 499 (199 ) 645.
- 3 S. Mori, *J. Appl. Polym. Sci.*, 38 (1989) 95.
- 4 A. A. Gorbunov and A. M. Skvortsov, *Vysokomol. Soedin., Ser. A*, 30 (1988) 895.
- 5 A. A. Gorbunov and A. M. Skvortsov, *Vysokomol. Soedin., Ser. A*, 30 (1988) 453.
- 6 T. M. Zimina, J. J. Kever, E. Yu. Melenevskaya and B. G. Belenkii, *Vysokomol. Soedin., Ser. A*, 33 (1991) 1349.
- 7 M. B. Tennikov, P. P. Nefedov, M. A. Lasareva and S. Ya. Frenkel, *Vysokomol. Soedin., Ser. A*, 19 (1977) 657.
- 8 A. M. Skvortsov, B. G. Belenkii, E. S. Gankina and M. B. Tennikov, *Vysokomol. Soedin., Ser. A*, 20 (1978) 678.
- 9 S. G. Entelis, V. V. Evreinov and A. I. Kusaev, *Reaktsionnosposobnie Oligomeri*, Nauka, Moscow, 1985.
- 10 E. F. Cassasa, *J. Polym. Sci., Part B*, 5 (1967) 773.
- 11 A. E. Muller, in T. E. Hogen-Esch (Editor), *Recent Advances in Anionic Polymerisation*, Elsevier, New York, 1986.
- 12 M. E. Eremina, V. N. Erenburg, V. N. Zgonnik, E. Yu. Melenevskaya, E. N. Levenagen and R. I. Palchik, *Vysokomol. Soedin., Ser. A*, 27 (1985) 1308.
- 13 B. Scott and P. Kucera, *J. Chromatogr.*, 171 (1979) 37.
- 14 B. Scott and P. Kucera, *J. Chromatogr.*, 149 (1978) 93.
- 15 M. McCann, S. Madden, J. H. Purnell and C. A. Ellington, *J. Chromatogr.*, 294 (1984) 349.



# Comparison of several methods for the determination of trace amounts of polar aliphatic monocarboxylic acids by high-performance liquid chromatography

A. J. J. M. Coenen, M. J. G. Kerkhoff, R. M. Heringa and S. van der Wal\*

*DSM Research, P.O. Box 18, 6160 MD Geleen (Netherlands)*

## ABSTRACT

Reversed-phase high-performance liquid chromatography followed by direct detection by UV absorbance at 200 nm is a convenient method for the determination of polar aliphatic carboxylic acids. It can only be used for “clean” samples, except for formic and acetic acid, owing to a lack of retention. Up to butyric acid, ion-exclusion chromatography with conductimetric detection is generally preferred, allowing the detection of less than 120 µg/l. Each ion-exclusion column has its own selectivity and efficiency; interfering compounds are another problem. The precision at the 1 ppm level is about 2% ( $n = 10$ ). Pre-column derivatization of carboxylic acids with 4-bromomethyl-6,7-dimethoxycoumarin has been fully automated but is not recommended; limitation of the water content, internal standardization and carry-over correction are necessary. Pre-column derivatization with 2-nitrophenylhydrazine is a better way to obtain detection limits of one nanogram (or 50 µg/l) of  $C_4$ – $C_9$  carboxylic acid. The analyses are fully automated, can be performed in an aqueous environment and give a precision better than 4% at levels of 1 mg/l of analyte.

## INTRODUCTION

In the chemical and polymer industries there is an increasing demand for the determination of trace amounts of polar aliphatic carboxylic acids in aqueous extracts of process fluids.

In this work, four high-performance liquid chromatography (HPLC) methods were compared with respect to the concentration and mass detection limit, precision and ease of use. Selectivity was only considered in general terms as the targeted analyte matrices were of diverse origins.

The four methods studied were: (1) ion-suppression reversed-phase HPLC (RP-HPLC) with UV absorbance detection; (2) a high performance ion-exclusion chromatography (HPICE) method with conductimetric detection; (3) the BMMC method, pre-column derivatization with 4-bromomethyl-6,7-dimethoxycoumarin (BMMC) and RP-HPLC with fluorescence detection; and (4) the NPH method, pre-column derivatization with 2-nitrophenylhydrazine (NPH) and RP-HPLC with absorbance detection at 400 nm.

## EXPERIMENTAL

The four methods are summarized in Table I. The pre-column derivatization of the BMMC method was performed in a Promis (Spark, Emmen, Netherlands) unit, which is shown schematically in Fig. 1. All the tubing of the peristaltic pump was poly (vinyl chloride). During the load cycle the reagent flow-rate was 0.1 ml/min and the waste flow-rate was 0.32 ml/min. The sample was differentially aspirated at 0.12 ml/min. Reagent 1 (75 mg of potassium carbonate and 21 µl of water) was added to 7.5 ml of a 10 mM 18-crown-6 solution in acetonitrile. The mixture was sonicated for 15 min, diluted with 3.75 ml of acetonitrile, filtered through a 0.2-µm filter and diluted with 0.5 ml of acetonitrile. Reagent 2 was 1 mg/ml of BMMC (Kodak, Rochester, NY, USA) in acetonitrile.

The pre-column derivatization unit of an HP-1090 liquid chromatograph (Hewlett-Packard, Waldbronn, Germany) was used for the NPH reaction (see Fig. 2). The NPH reagent consisted of 0.04 M NPH hydrochloride (Janssen, Beerse, Belgium)

TABLE I  
SUMMARY OF METHODS

	Method			
	UV	HPICE	NPH	BMMC
Sample acids R-COOH	R = C2, C3, C5, C7, C9	R = C0, C1, C2, C3	R = C5, C6, C7, C8, C9	R = C4, C5, C6, C7, C8
Liquid chromatography	Gilson	Dionex 20001	HP-1090	HP-1050
Column	250 × 4 mm; Nucleosil 120-5 C <sub>18</sub>	250 × 10 mm; HPICE-AS1	100 × 4 mm; Nucleosil 120-5 C <sub>18</sub>	100 × 3 mm; Nucleosil 102-5 C <sub>18</sub>
Eluent A	10 mM H <sub>3</sub> PO <sub>4</sub> , pH 2.5	1 mM octanesulphonic acid	Water, pH 4.5 with HCl	10 mM H <sub>3</sub> PO <sub>4</sub> , pH 6.5 with NaOH
Eluent B	Acetonitrile	–	Acetonitrile	Acetonitrile
Gradient	20 → 100% B in 10 min	–	30 → 75% B in 15 min	5 → 100% B in 30 min
Temperature (reaction)	Ambient	Ambient	60°C	Ambient
Temperature (column)	Ambient	Ambient	50°C	Ambient
Flow-rate	1 ml/min	1.2 ml/min	1 ml/min	2 ml/min
Pre-column derivatization unit	Gilson 231-401	–	HP-1090	Promis, Spark
Injection volume	1000 µl	500 µl	26 µl	20 µl
Detector	Linear UV 204 nm	Waters 431 conductivity	Diode array (HP-1090)	HP-1046 A fluorescence
Wavelength(s)	λ = 200 nm	–	λ = 400 nm	λ <sub>ex</sub> = 340 nm; λ <sub>em</sub> = 417 nm
Pre-column derivatization reagents	–	–	2-nitrophenylhydrazine hydrochloride	4-bromomethyl-6,7-dimethoxy coumarine
Reaction time	–	–	20 min	15 min
Suppressor	–	AMMS-ICE (Dionex)	–	–
Suppressor fluid	–	10 mM tetrabutylammoniumhydroxide, 2 ml/min	–	–

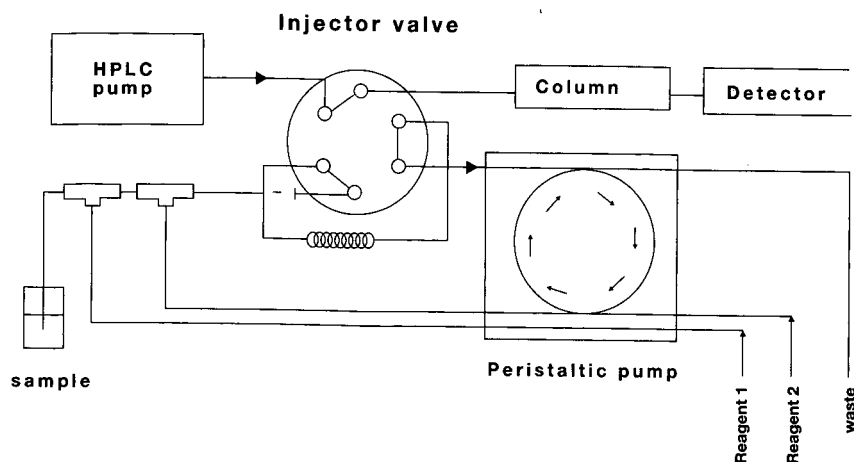


Fig. 1. Schematic diagram of the Promis pre-column derivatization unit.

in 50% aqueous ethanol; the EDC reagent solution (see Table II) contained 3% pyridine, 47% ethanol and 0.25 *M* 1-ethyl-3-(3-dimethylaminopropyl)carbodiimide hydrochloride (Polysciences, Warrington, PA, USA) in water.

The liquid chromatograph for the UV detection method consisted of a Gilson 305/302 gradient pumping system with an 805 monometric module, an 811 gradient mixer and a Model 231-401 auto-

sampler. Detection at 200 nm was performed on a Linear UV-204 detector (Linear, Reno, NY, USA).

For the HPICE method a Dionex 2000i or 4000i ion chromatograph (Dionex, Sunnyvale, CA, USA) was used, equipped with an anion micromembrane suppressor and a Waters 431 conductivity detector (Waters, Milford, MA, USA).

An HP-1050 gradient solvent delivery system with an HP-1046A fluorescence detector was used

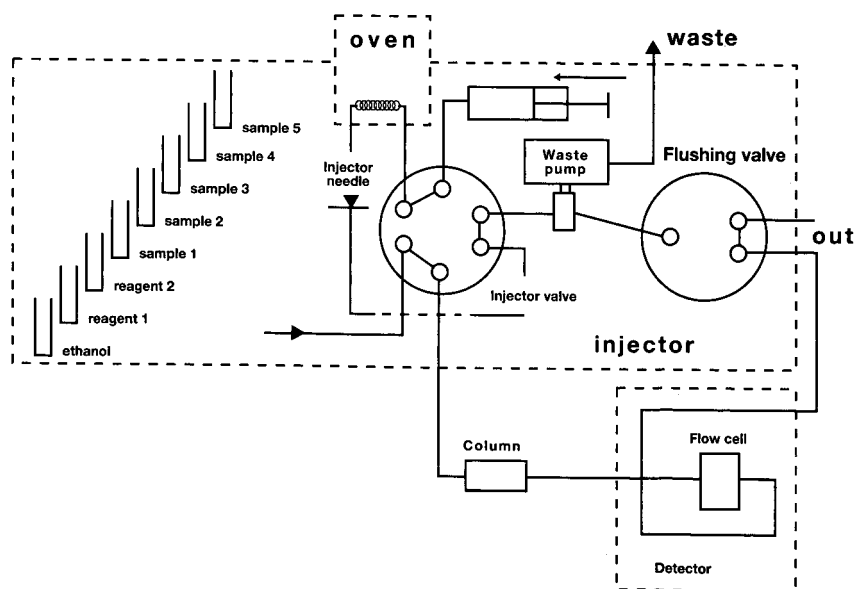


Fig. 2. Schematic diagram of the HP-1090 liquid chromatograph used for the NPH method.

for the BMMC method and an HP-1090 system with a built-in diode-array detector for the NPH method (all from Hewlett-Packard).

All reversed-phase columns were Nucleosil 120-5C<sub>18</sub> (Macherey-Nagel, Düren, Germany); all solvents were of P.A. quality (Merck, Darmstadt, Germany).

## RESULTS AND DISCUSSION

### UV method

Many monocarboxylic acids show enough retention to be detected by HPLC at a mobile phase pH lower than the  $pK_a$  value of their carboxylic acid groups.

Direct UV absorbance detection at short wavelengths is often problematic because of its lack of selectivity and sensitivity. Most organic compounds with a polar group have an absorbance in the region 180–205 nm, comparable with or larger than that of carboxylic acids [1].

The problem with the sensitivity can be partly overcome by using on-column concentration [2]. A signal-to-noise ratio of 3 is obtained at about 100 ng of analyte injected onto the column. By introducing the largest possible volume of aqueous sample into the column, the detection limit, expressed as the concentration in the original sample, is reduced.

This method is applicable to the determination of carboxylic acids with a higher retention than acetic acid (*cf.* Fig. 3).

Disturbances from the injection plug in the elution region of formic and acetic acids and interferences from impurities in the solvents used do not allow the extension of this method to more polar carboxylic acids or larger injection volumes.

### HPICE method

Formic acid, acetic acid and the more polar carboxylic acids such as diglycolic acid and monochloroacetic acid can be determined by separation on a low-capacity ion exchanger, such as Dionex AS-4A, followed by suppressed conductivity detection. Monocarboxylic acids containing a longer aliphatic chain are not sufficiently retained for determination by this method. An alternative method uses a combination of adsorption and ion-exclusion chromatography on a sulphonated polystyrene-divinylbenzene resin [3].

In applying this method, striking differences in the selectivities among the HPICE AS-1 columns were observed (compare Fig. 4A and B). At concentrations compatible with UV detection (see under *UV method*) the ratio of the absorbance to the conductimetric signal of the method, the low selectivity and the variability of the columns stress the need for

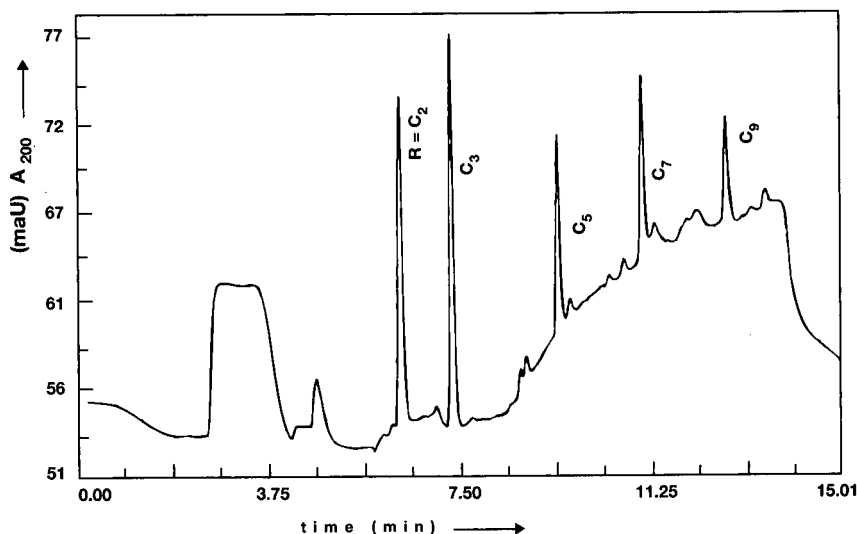


Fig. 3. Chromatogram of five aliphatic carboxylic acids, obtained by RP-HPLC and direct UV detection at 200 nm. See under Experimental and Table I for details. Injection: 10 mg/l of each acid in water.

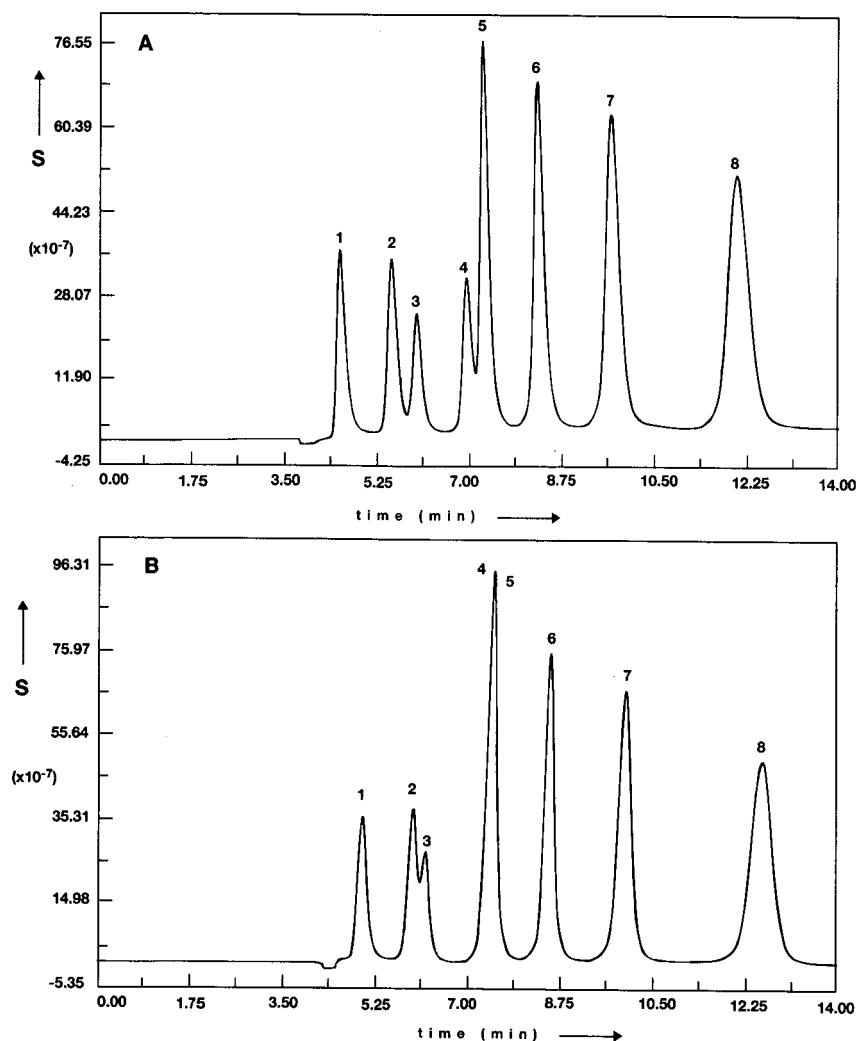


Fig. 4. Chromatograms of a test mixture of carboxylic acids on HPICE-AS1 columns. Signal-to-noise ratios: column A, 2612; B, 5098. For conditions see Table I. Injection: 40  $\mu$ l of test mixture consisting of (1) 30 mg/l citric acid, (2) 34 mg/l diglycolic acid, (3) 38 mg/l monochloroacetic acid, (4) 37 mg/l hydroxyacetic acid, (5) 47 mg/l formic acid, (6) 81 mg/l acetic acid, (7) 127 mg/l propionic acid and (8) 198 mg/l butyric acid.

high efficiency to avoid the use of a corroborative analysis method at lower analyte concentrations. The Van Deemter curve (Fig. 5) indicates that the optimum flow-rate for resolution per unit time, at  $(H/u)$  min (where  $H$  = theoretical plate height and  $u$  = linear velocity) [4], is about 1.2 ml/min at 80 atm. The HPLC equipment allows operation at 275 atm, so four columns could be coupled. The result is given in Fig. 6. A much better resolution of the first

five components can only be obtained by changing the selectivity of the system, *e.g.* by modifying the octanesulphonic acid concentration.

The detection limits for formate and butyrate in water with octanesulphonic acid added to give a 1 mM solution, using a 500- $\mu$ l loop for injection, are 20 and 120  $\mu$ g/l, respectively. The maximum loop volume is dependent on the analyte to be determined and its matrix.

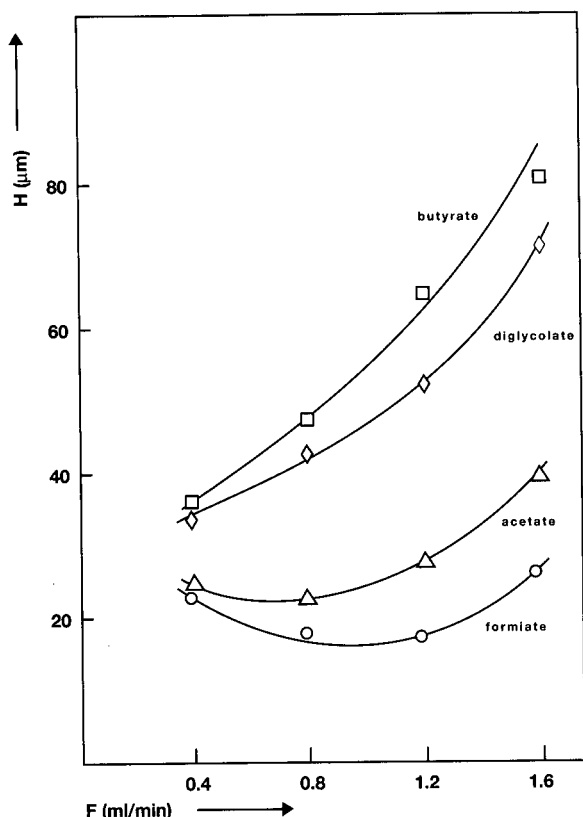


Fig. 5. Theoretical plate height ( $H$ ) as a function of flow-rate ( $F$ ) for different analytes on a Dionex system with two HPICE-AS1 columns in series. For conditions see Table 1.

### BMMC method

In the first two methods discussed the main drawbacks are the low selectivity and the large injection volumes necessary for acceptable limits of detection.

Pre-column derivatization with BMMC seems attractive as a result of its high selectivity, the improvement in sensitivity for carboxylic acids, the short reaction time and availability of reagents. The reaction is represented schematically in Fig. 7. The potassium counter-ion of the carboxylic anion is selectively complexed by 18-crown-6, allowing the "naked" carboxylic anion to substitute for a bromine atom of the reagent.

The resulting ester can be detected fluorimetrically. It is resistant to light and stable in an aqueous environment, in contrast to the reagent. Automated on-line pre-column derivatization, even at room temperature, using BMMC was possible with the introduction of an 18-crown-6-potassium carbonate suspension [5]. BMMC is slightly more polar than 4-bromomethyl-methoxycoumarin and its derivative has a higher intrinsic fluorescent sensitivity [6].

Base-catalysed solvolysis to coumaric acid is a problem for all coumarin reagents [7]. This problem manifests itself as a ghost peak which competes with the analyte for the reagent. The product of the analyte may also be solvolysed, which will lead to

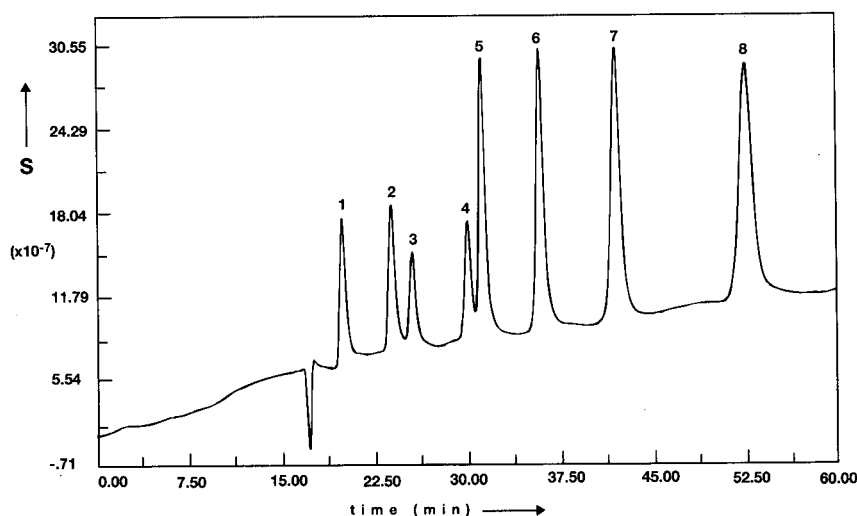


Fig. 6. Chromatogram at optimum conditions for resolution per unit time. Columns: four  $250 \times 10$  mm HPICE-AS1 columns in series. Flow-rate: 1.2 ml/min 1 mM octanesulphonic acid, 220 atm. Injection as in Fig. 4.



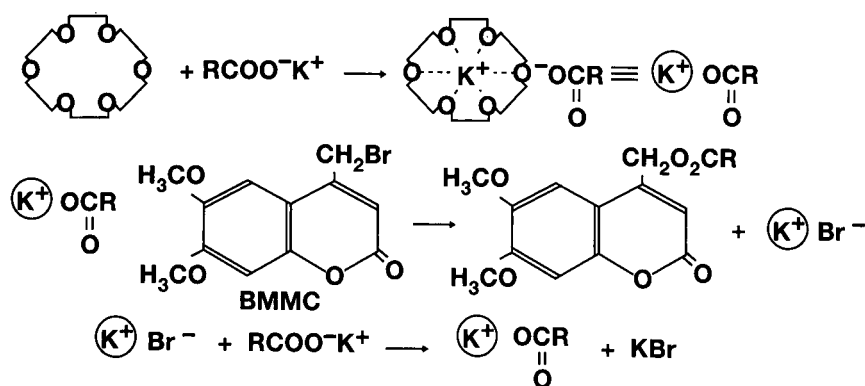


Fig. 7. Schematic representation of the BMMC reaction.

multiple derivatives and irreproducible results. The exclusion of water and limiting the concentration of the base to a stoichiometric amount cannot be carried out in practice, so internal standardization has to be used.

The pre-column derivatization was carried out as in Wolf and Korf [5], but the dimethoxy reagent and a filtered suspension were used to prevent clogging of the derivatization unit. A chromatogram of an acetonitrile sample containing 1.4 mg/l of each the carboxylic acids indicated is shown in Fig. 8.

An injected blank sample of acetonitrile indicat-

ed the presence of carboxylic acids, which could not be traced to any of the reagents or solvents used and thus has to be attributed mainly to carry-over from the previous injection, in spite of extensive rinsing with ethanol, the most effective solvent except for formic acid (which will carry-over and compete for the reagent). This percentage of carry-over (PCO) is determined as a function of the analyte concentration in the sample,  $A$ , from the first and the fifth consecutive blank,  $B$ , respectively:

$$\text{PCO}(\%) = (B_1 - B_5/A - B_5) \times 100$$

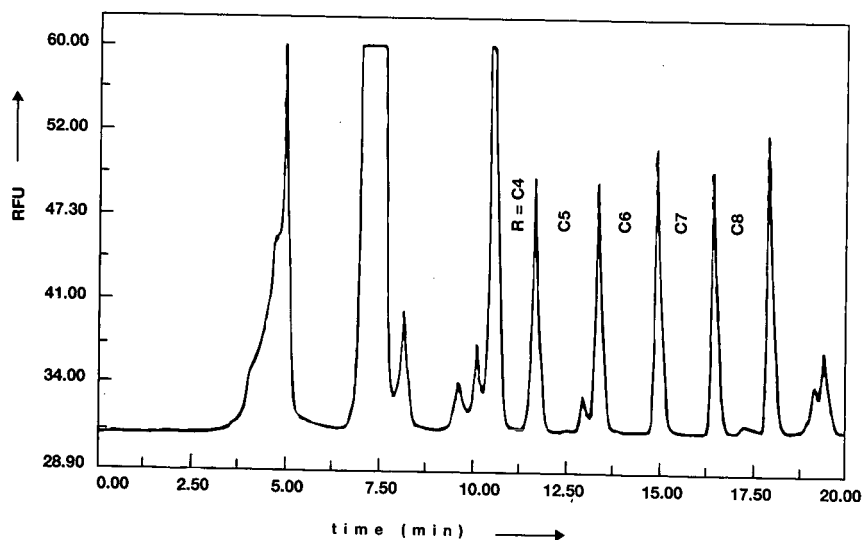


Fig. 8. Separation of BMMC derivatives of pentanoic to nonanoic acid. For conditions see Table I. Injection: 1.4 mg/l of each carboxylic acid in acetonitrile. RFU are relative fluorescence units.

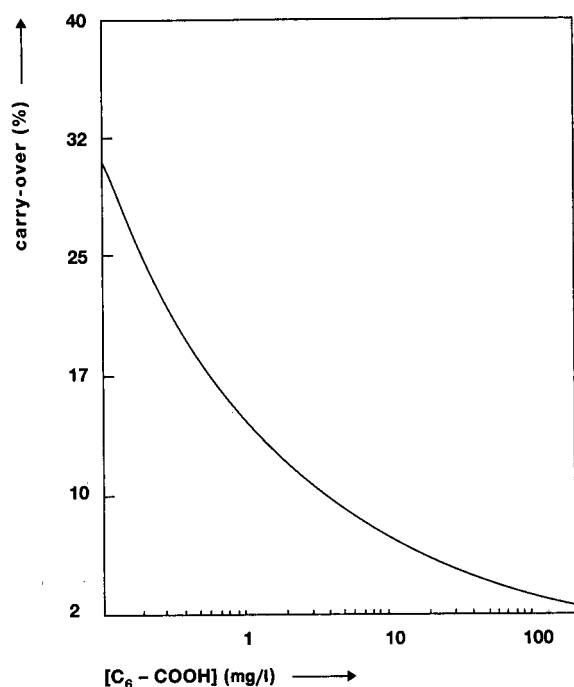


Fig. 9. Percentage of carry-over as a function of heptanoic acid.

The result is given in Fig. 9.

By subtracting the carry-over of the previous sample and adding that of the sample itself, the corrected concentrations can be reconstructed from the measured data.

Calibration graphs show a linear dynamic range of approximately  $10^3$ . The system appeared to be contaminated with the analytes at about 100 ppb after three months of intermittent use and was abandoned in favour of the following method.

#### NPH method

Aliphatic as well as aromatic carboxylic acids react with NPH to form acid hydrazides when 1-eth-

yl-3-(3-dimethylaminopropyl)carbodiimide hydrochloride is added as a coupling agent (see Fig. 10). Derivatization with NPH has as an advantage over almost all published carboxylic acid derivatization methods in that the reaction can be carried out in an aqueous environment [8].

The reaction product can be detected by its absorbance at 230 or 400 nm (see Fig. 11). Reaction by-products which may interfere when detecting at 230 nm can be removed by a second reaction stage after the addition of potassium hydroxide. At 400 nm the acid hydrazides are detected with a four-fold less sensitivity ( $\epsilon_m \approx 5 \cdot 10^3$ ) than at 230 nm, but only one reaction step is necessary as the main interferences do not absorb at this wavelength. At mg/l levels the derivatives could not be determined by fluorescence detection.

Without a second reaction stage and extraction the derivatization was optimized for the concentration of HCl and NPH, reaction temperature and reaction time in a fully automated HP-1090 pre-

TABLE II

NPH DERIVATIZATION PROTOCOL

Line	Function
1	Draw 0.0 $\mu$ l from Vial 0 Ethanol
2	Draw 1.0 $\mu$ l from Vial 1 2NPH · HCl
3	Draw 0.0 $\mu$ l from Vial 0
4	Draw 2.0 $\mu$ l from Vial 2 1EDC · HCl
5	Draw 0.0 $\mu$ l from Vial 0
6	Draw 20.0 $\mu$ l from Sample
7	Draw 0.0 $\mu$ l from Vial 0
8	Draw 2.0 $\mu$ l from Vial 2
9	Draw 0.0 $\mu$ l from Vial 0
10	Draw 1.0 $\mu$ l from Vial 1
11	Draw 0.0 $\mu$ l from Vial 0
12	Mix 30.0 $\mu$ l cycles 10
13	Wait 20.0 min
14	Inject

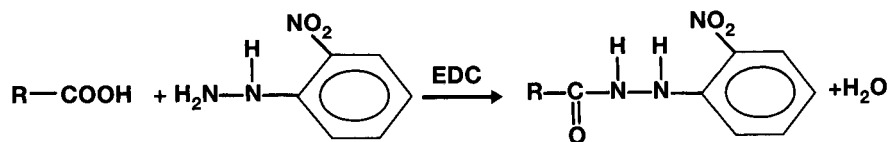


Fig. 10. Schematic representation of the NPH reaction.

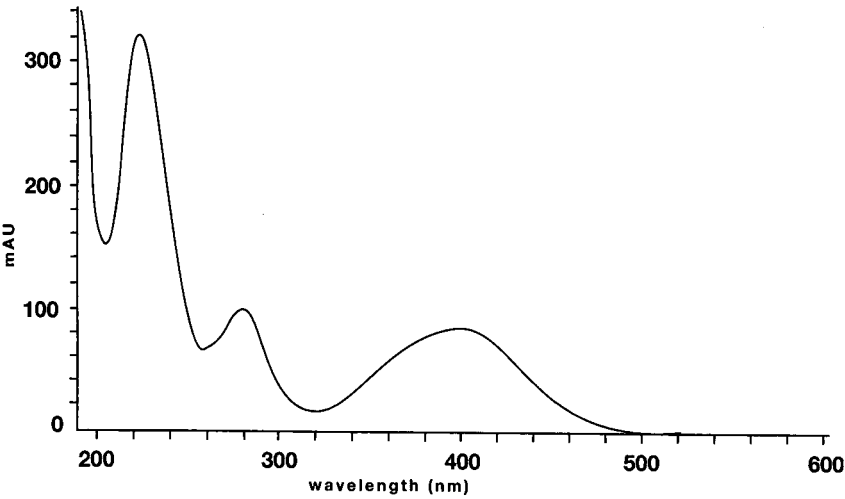


Fig. 11. Absorbance spectrum of the NPH derivative of hexanoic acid in the mobile phase used. For conditions see Table I.

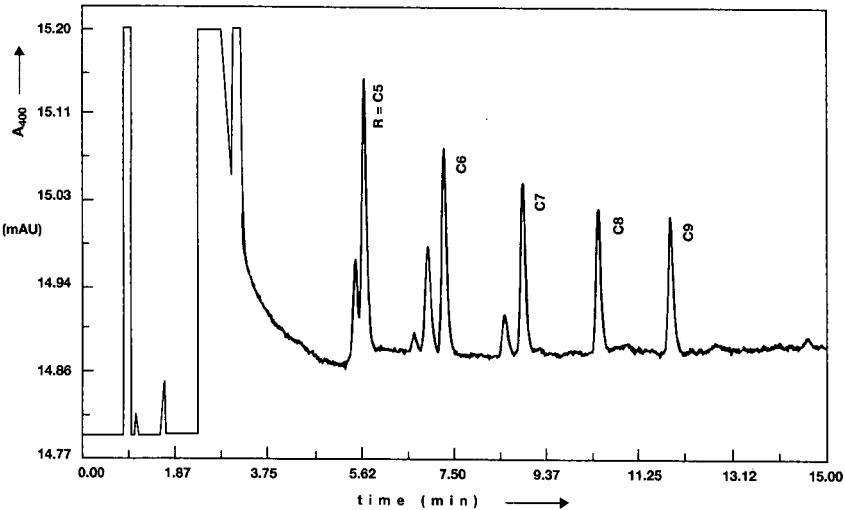


Fig. 12 Separation of NPH derivatives of hexanoic to decanoic acid. For conditions see Table I. Injection: 1.3 mg/l of each carboxylic acid in water.

TABLE III  
COMPARISON OF THE FOUR METHODS

R.S.D. = Relative standard deviation; I.S. = internal standard

Method	Injection volume ( $\mu$ l)	R-COOH: R =	Detection limit		R.S.D. (%)	I.S.
			$\mu$ g/l	ng		
UV	1000	C <sub>6</sub>	100	100	—	—
HPICE	500	C <sub>1</sub>	40	20	1.9	—
NPH	26	C <sub>6</sub>	50	1.3	3.2	C <sub>7</sub>
BMMC	20	C <sub>6</sub>	60	1.2	7.6	C <sub>7</sub>

column derivatization unit (see Fig. 2). The optimum protocol for determining analytes at a concentration of less than 10 mg/l is given in Table II. At higher concentrations the volume of sample should be decreased or the calibration graphs will not be linear as there will not be sufficient excess reagent. Sample volumes larger than 20  $\mu$ l have not yet been used successfully. A different protocol may improve incomplete mixing for larger sample volumes. Some ethanol (1–10%) was added to the test sample to ensure the complete dissolution of the less polar carboxylic acids. A chromatogram of 1.3 mg/l of each of the five aliphatic carboxylic acids is shown in Fig. 12. The coefficient of variation of the peak areas is 7.0 (R = C<sub>5</sub>), 5.6 (C<sub>6</sub>), 8.2 (C<sub>7</sub>), 9.2 (C<sub>8</sub>) and 8.7% (C<sub>9</sub>), respectively, and 3.2, 2.6, 2.6 and 3.9% when using the C<sub>7</sub>–COOH peak as an internal standard ( $n = 10$ ).

## COMPARISON AND CONCLUSIONS

An overall comparison of the four methods studied here is given in Table III. At the 1 mg/l level HPICE can be recommended for carboxylic acids at least as polar as butyric acid, whereas the fully automated NPH method can be most effectively used for less polar carboxylic acids.

## REFERENCES

- 1 S. van der Wal and L. R. Snyder, *J. Chromatogr.*, 255 (1983) 463.
- 2 J. Lankelma and H. Poppe, *J. Chromatogr.*, 149 (1978) 587.
- 3 J. Weiss, *Handbook of Ion Chromatography*, Dionex, Sunnyvale, CA, 1986.
- 4 S. van der Wal and J. F. K. Huber, *J. Chromatogr.*, 149 (1978) 431.
- 5 J. H. Wolf and J. Korf, *J. Chromatogr.*, 436 (1988) 437.
- 6 R. Farinotti, Ph. Siard, J. Bourson, S. Kirkiacharian, B. Valeur and G. Mahuzier, *J. Chromatogr.*, 269 (1983) 81.
- 7 K. D. Ertel and J. T. Carstensen, *J. Chromatogr.*, 411 (1987) 297.
- 8 H. Miwa, C. Hiyama and M. Yamamoto, *J. Chromatogr.*, 321 (1985) 165.

# Planar chips technology for miniaturization and integration of separation techniques into monitoring systems

## Capillary electrophoresis on a chip

Andreas Manz\*, D. Jed Harrison<sup>☆</sup>, Elisabeth M. J. Verpoorte, James C. Fettingner, Aran Paulus, Hans Lüdi<sup>☆☆</sup> and H. Michael Widmer

*Central Analytical Research, Ciba-Geigy Ltd., CH-4002 Basle (Switzerland)*

---

### ABSTRACT

Miniaturization of already existing techniques in on-line analytical chemistry is an alternative to compound-selective chemical sensors. Theory on separation science predicts higher efficiency, faster analysis time and lower reagent consumption for microsystems. Micromachining, a well known photolithographic technique for structures in the micrometer range, is introduced. A first capillary electrophoresis experiment using a chip-like structure is presented.

---

### INTRODUCTION

The continuous monitoring of a chemical parameter, usually the concentration of a chemical species, is gaining increasing attention in biotechnology, process control, and the environmental and medical sciences. Chemical sensors exhibit only a minimal number of applications for measurements of combustion gases, certain ions and enzyme substrates. The state-of-the-art strategy is called “total chemical analysis system” (TAS), which periodically transforms chemical information into electronic information. In such a system, sampling, sample transport, necessary chemical reactions, chromatographic or electrophoretic separations and detec-

tion are performed automatically. Some examples of TAS, such as a gas chromatographic monitor [1] and an on-line glucose analyser [2], have been reported. Recently, we proposed a general concept for a miniaturized TAS [3–6].

As far as separation techniques are concerned, miniaturization has been heavily discussed for many years. Improved separation performance at shorter retention times is predicted by theory. Miniaturization has been experimentally realized using small-diameter particles or open capillaries. Deviations from theoretical predictions have usually been caused by inhomogeneity in column packings or capillary diameters, inappropriate injections or large detection volumes. At least two publications have been presented in the literature on the use of photolithographically fabricated microstructures for gas [7] and liquid chromatography [8]. Recently, we proposed a 15-nl detector cell for absorption measurements (optical pathlength 1 mm [4–6]). This

---

<sup>☆</sup> Permanent address: University of Alberta, Edmonton, Canada.

<sup>☆☆</sup> Present address: Ciba-Corning Diagnostic Corp., Medfield, MA, USA.

paper presents a technique for the manufacture of entire microchannel systems with very high precision. Such systems allow injections in the pl or nl range, dilutions, pre- or post-column reactions and sophisticated small-volume detections to be combined with, for example, capillary electrophoresis (CE).

#### THEORY AND MINIATURIZATION

Two approaches provide information on the behaviour of a simple flow system when it is miniaturized: (1) a set of numerical values can be calculated, using standard formulae to give the order of magnitude for a specific parameter; and (2) consideration of the proportionalities, *i.e.* the parameter of interest as a function of the variables to be miniaturized (space and time), shows the major trends of a parameter during its down-scale. In the case of capillary separation systems, the two approaches are equally interesting.

Table I depicts the results of an analysis carried out according to approach 1. Choice of the desired

number of theoretical plates at a given retention time, as well as the heating power per length (in the case of CE), allows comparison of the resulting capillary dimensions and operation conditions for CE, liquid chromatographic (LC) and supercritical fluid chromatographic (SFC) separation experiments. The microchannels must be a few micrometers in diameter (2.8–24  $\mu\text{m}$ ), a few centimeters in length (6.5–20 cm) and need small-volume detectors (3.3–94 pl). Although these values cannot replace experimental results, they give an indication of values forbidden by theory. Approach 1 is very meaningful if the values of the given parameters are clear and if the optimum performance is well defined, as is the case with the Golay equation for capillary LC and SFC.

In the case of CE, the optimum performance is basically determined by the maximum voltage applied to the system. The higher the voltage, the better the separation performance and, at the same time, the faster the analysis. The limitation is usually given by the heat produced in the capillary. Three parameters may be relevant: the power per

TABLE I

CALCULATED PARAMETER SETS FOR A GIVEN SEPARATION PERFORMANCE OBTAINED WITH CE, LC AND SFC

Assumed constants are: diffusion coefficients of the sample in the mobile phase,  $1.6 \cdot 10^{-9} \text{ m}^2/\text{s}$  (CE, LC) and  $10^{-8} \text{ m}^2/\text{s}$  (SFC); viscosities of the mobile phase,  $10^{-3} \text{ Ns/m}^2$  (CE, LC) and  $5 \cdot 10^{-5} \text{ Ns/m}^2$  (SFC); electrical conductivity of the mobile phase,  $0.3 \text{ S/m}$  (CE); electrical permittivity  $\times$  zeta potential  $5.6 \cdot 10^{-11} \text{ N/V}$  (CE)

Parameter	Symbol (unit)	CE (micellar)	Capillary LC	Capillary SFC
Number of theoretical plates	$N$	100 000	100 000	100 000
Analysis time	$t(k' = 5)$ (min)	1	1	1
Heating power	$P/L$ (W/m)	1.1	—	—
Capillary inner diameter	$d$ ( $\mu\text{m}$ )	24	2.8	6.9
Capillary length	$L$ (cm)	6.5	8.1	20
Pressure drop	$\Delta p$ (atm)	—	26	1.4 <sup>a</sup>
Voltage	$\Delta U$ (kV)	5.8	—	—
Signal bandwidth	$\sigma_x$ (mm)	0.21	0.56	1.4
Signal bandwidth	$\sigma_t$ (ms)	42	70	70
Signal bandwidth	$\sigma_v$ (pl)	94	3.3	52
Ratio length/diameter of an eluting peak	$\sigma_x/d$	<i>ca.</i> 10	<i>ca.</i> 200	<i>ca.</i> 200
Detection volume requirements	$\sigma_v/2$ (pl)	<47	<1.6	<26
Optical pathlength parallel to flow	$\sigma_x/2$ ( $\mu\text{m}$ )	<105	<280	<700
Optical pathlength perpendicular to flow	$d$ ( $\mu\text{m}$ )	<24	<2.8	<6.9
Response time requirements	$\sigma_t/2$ (ms)	<21	<35	<35

<sup>a</sup> The pressure needed to maintain the mobile phase in the supercritical state may exceed this value, *e.g.* for carbon dioxide the inlet and outlet pressure could be 75.4 and 74 bar, respectively.

TABLE II

## EXAMPLE OF A PROPORTIONALITY ANALYSIS FOR CE

The given miniaturization factors are  $d$  and  $L$ . Three arbitrarily chosen time dependencies are shown here. The remaining parameters are then calculated using the basic definition of  $d$ ,  $L$  and time

Parameter	Symbol	$L$ system	$d \cdot L$ system	$d^2 \cdot L$ system
Diameter of capillary	$d$	$d$	$d$	$d$
Length of capillary	$L$	$L$	$L$	$L$
Time	$t$	$L$	$d \cdot L$	$d^2 \cdot L$
Linear flow-rate	$u = L/t$	Constant	$1/d$	$1/d^2$
Péclet number	$v \propto u \cdot d$	$d$	Constant	$1/d$
Reduced plate height	$h = 2/v$	$1/d$	Constant	$d$
Number of theoretical plates	$N = L/(d \cdot h)$	$L$	$L/d$	$L/d^2$
Electric field	$E \propto u$	Constant	$1/d$	$1/d^2$
Applied voltage	$U = E \cdot L$	$L$	$L/d$	$L/d^2$
Electric current	$I \propto U \cdot d^2/L$	$d^2$	$d$	Constant
Power per volume	$\propto U \cdot I/(d^2 \cdot L)$	Constant	$1/d^2$	$1/d^4$
Power per length	$= U \cdot I/L$	$d^2$	Constant	$1/d^2$
Temperature difference	$\Delta T \propto I^2$	$d^4$	$d^2$	Constant

unit volume, the power per unit length, and the temperature difference generated in a steady-state thermal diffusion system. An example of a proportionality analysis according to approach 2 is shown in Table II. The miniaturization of a CE system is characterized by the inner diameter  $d$  of the capillary, by its length  $L$  and by the time  $t$ . Time cannot be set into a well defined relation with  $d$  or  $L$ , which means that we have one degree of freedom. Out of the numerous possible dependencies, a set of three have been chosen: time proportional to  $L$  (length), to  $d \cdot L$  (area) and to  $d^2 \cdot L$  (volume), with power per unit volume, power per unit length and temperature difference as a constant, respectively. All of the remaining parameters of interest are then strictly based on  $d$  and  $L$ .

The  $L$  system is characterized by a time scale forced into proportionality with  $L$ . For example, a ten-fold shorter capillary implies a ten-fold shorter retention time if the electric field strength (and the linear flow-rate) are kept constant. The number of theoretical plates must decrease. The influence of  $d$  is restricted to the current flow and the power generated in the capillary.

In the  $d \cdot L$  system, the time scale depends on  $d$  multiplied by  $L$ . This implies that all the reduced

variables used in capillary LC, e.g. Péclet number or reduced plate height [9], are kept constant. In the same way the power per unit length, which is often used as a measure of thermal effects [10], remains constant. In this case, an improvement of both separation performance and analysis time can be achieved if  $d$  is miniaturized more drastically than  $L$ . For example, a ten-fold decrease in  $d$  and a five-fold decrease in  $L$  would double the number of theoretical plates in 1/50th of the retention time. Starting from a known CE experiment ( $d = 70 \mu\text{m}$ ,  $L = 1 \text{ m}$ ,  $n = 10^6$  and  $t = 30 \text{ min}$ ), we would obtain  $2 \cdot 10^6$  theoretical plates within 36 s using a capillary of  $20 \text{ cm} \times 7 \mu\text{m}$  I.D. The increase in plate number can be understood as arising from the increased electric field and from the decreased migration times, since longitudinal diffusion plays a major role. This system has been experimentally proven to be true by Monnig and Jorgenson [10].

The  $d^2 \cdot L$  system is based on a constant temperature difference in the capillary when steady temperature diffusion is taken into account [11]. It is far more optimistic than the  $d \cdot L$  system. Experimentally, it has not yet been possible to prove this system to be valid at all.

## MICROMACHINING

Originated by the microelectronics industry, the photolithographic patterning of layer structures on the surface of silicon wafers has become a well known and high-tech standard procedure. In addition to its semiconductor qualities, monocrystalline silicon is abundant and inexpensive, can be produced and processed controllably to extremely high standards of purity and perfection, has excellent mechanical and chemical properties (yield strength better than steel, Young's modulus identical to steel, Knoop hardness comparable to quartz, chemical inertness comparable to glass) and is highly amenable to miniaturization (down into the micrometer range). The surface treatment to obtain mechanical structures is called micromachining [12]

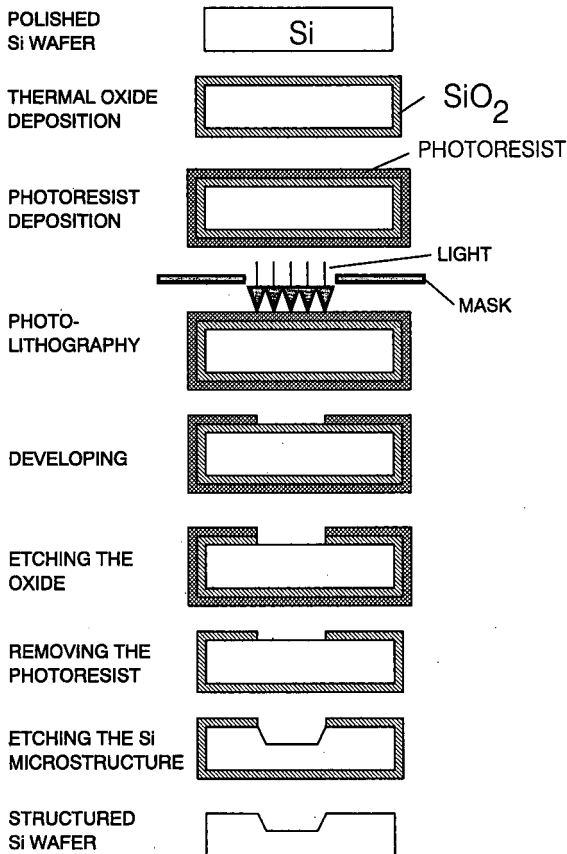


Fig. 1. Process steps of a standard one-mask micromachining procedure to etch a channel structure into silicon.

and includes fabrication steps such as film deposition, photolithography, etching and bonding. A simple process for obtaining a channel in silicon is shown in Fig. 1. It is obvious that the two-dimensional shape of the channel layout is given by the photomask, but the particular pattern does not affect the complexity of the process at all. As soon as a variation in depth (third dimension) or material (*e.g.* a metal layer) is needed, additional processes must be added to the sequence.

There are mainly four different groups of processes:

(1) Film deposition includes spin coating, thermal oxidation, physical vapour deposition (PVD) and chemical vapour deposition (CVD), low-pressure CVD, plasma-enhanced CVD, sputtering, etc. A large variety of metals, inorganic oxides, polymers and other materials can be deposited using these techniques.

(2) Photolithography, a technique used to transfer a layout pattern from a mask onto a photosensitive film, can be done using visible light for structures larger than 1  $\mu\text{m}$ . For special applications such as submicron patterning, UV, X-ray or electron beam lithography is used.

(3) Etching is performed either as a wet chemical process or as a plasma process. Isotropic as well as anisotropic processes are known.

(4) Bonding means the assembly of pieces of silicon onto silicon, glass or other substrates. The subject of micromachining has been dealt with in great detail in many sources in the literature. For more information, see for instance ref. 13, which gives a good review of this huge field.

Silicon-, quartz- and glass-based physical and chemical sensors and actuators are currently a focus of interest [14]. Compared with conventional machining, photolithographic processes allow cheap mass fabrication of complicated microstructures. Hundreds to thousands of structures may be fabricated in the same batch. The precision and reproducibility of the structure elements are excellent. Silicon allows monolithic integration of electronics, sensors and actuators, but micromachining has to be done under clean-room conditions and needs high-tech instrumentation. However, in the last few years, the number of companies offering custom-made silicon, quartz and glass microstructures has significantly increased.



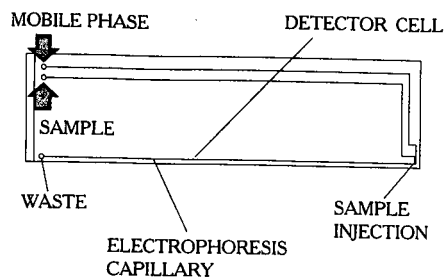


Fig. 2. Glass microstructure for injection and CE. Size  $15 \times 4$  cm. Electrophoresis channel  $30 \times 10 \mu\text{m}$ . The external laser fluorescence detector was positioned 6.5 cm from the point of injection.

### CAPILLARY ELECTROPHORESIS ON A CHIP

We have made six different structures in silicon (covered by Pyrex glass) [15] and one in amorphous glass [16]. The silicon structures, even with state-of-the-art insulating films ( $\text{SiO}_2$  and  $\text{Si}_3\text{N}_4$ ), exhibited poor voltage breakdown characteristics. In the best case, 950 V could be applied on a single device for a few minutes. Better results have been obtained with amorphous glass or quartz.

The photolithographically fabricated glass device shown in Fig. 2 was used to perform a first CE experiment "on a chip". The overall size of the structure is  $150 \times 40 \times 10$  mm. It consists of two glass plates, one of them containing the etched channels and the other serving as a cover. The three channels, two of them being  $10 \mu\text{m}$  deep and  $30 \mu\text{m}$  wide, the

other  $10 \mu\text{m}$  by 1 mm, meet at one point. The intersection has a volume of 9 pl, which means that no extra dead volume exists. The cross-section of the channels is not exactly rectangular, but rounded at the corners (compare with refs. 17–19). Detection was done using a laser fluorescence set-up similar to the one described previously [20,21] located somewhere downstream from the electrophoresis capillary (0–135 mm after the point of injection). The buffer reservoirs containing the platinum electrodes were pipette tips mounted directly into the drilled holes at the ends of the channels.

To set the experiment up, the background electrolyte and the fluorescent sample mixture were both driven past the injection and detection points by externally applied voltages, allowing positioning of the detector. The carrier electrolyte was then driven through the electrophoresis channel to flush it out. A 30-s pulse of 500 V applied to the sample channel provided the injection. To run the electropherogram, 3000 V were applied to the carrier electrolyte and the separation capillary (200 V/cm). The resulting separation of two fluorescent dyes is shown in Fig. 3. For calcein, a performance of 18 000 theoretical plates has been obtained. The height equivalent to a theoretical plate is  $3.6 \mu\text{m}$ , which is comparable to a non-optimized standard CE experiment. The standard deviation of the peak in terms of time, length and volume was 1.4 s, 0.49 mm and 145 pl, respectively.

### CONCLUSIONS

Consideration of hydrodynamics and diffusion processes indicates faster and more efficient chromatographic separations, faster electrophoretic separations and shorter transport times for miniaturized TAS. The consumption of carrier, reagent or electrophoresis buffer is dramatically reduced. Micromachining, especially photolithographic processes, offers access to novel analytical microstructures such as branched-channel systems having no dead volume.

The access to electrophoretic separations within a planar glass structure shown here is a first step towards an integrated microflow system using CE together with injection, sample pretreatment and post-column reactions, etc. We anticipate that higher voltages can be applied to the structure to speed

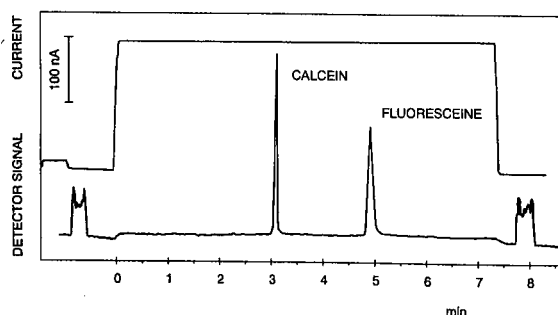


Fig. 3. CE separation of two fluorescent dyes. Sample:  $20 \mu\text{M}$  calcein,  $20 \mu\text{M}$  fluorescein. Background electrolyte: 50 mM borate, 50 mM Tris, pH 8.5, 3000 V on 13 cm. Detection at 6.5 cm, fluorescence, excitation 490 nm, collection 520 nm, injection through side channel, 500 V for 30 s.

up the separation and to increase its performance. Silicon structures would show a problem at high applied voltages. The reasonable range might be up to 200 V. This, of course, implies a poor efficiency (small number of theoretical plates), but relatively short retention times.

## REFERENCES

- 1 H. M. Widmer, J. F. Erard and C. Grass, *Int. J. Environ. Anal. Chem.*, 18 (1984) 1.
- 2 M. Garn, P. Cevey, M. Gisin and C. Thommen, *Biotechnol. Bioeng.*, 34 (1989) 423.
- 3 A. Manz, N. Graber and H. M. Widmer, *Sens. Actuators*, B1 (1990) 244.
- 4 E. Verpoorte, A. Manz, H. Lüdi and H. M. Widmer, in *Transducers '91, Digest of Technical Papers*, IEEE, Piscataway, NJ, 1991, p. 796.
- 5 A. Manz, J. C. Fetting, E. Verpoorte, H. Lüdi, H. M. Widmer and D. J. Harrison, *Trends Anal. Chem.*, 10 (1991) 144.
- 6 E. Verpoorte, A. Manz, H. Lüdi, A. E. Bruno, F. Maystre, B. Krattiger, H. M. Widmer, B. H. van der Schoot and N. F. de Rooij, *Sens. Actuators*, submitted for publication.
- 7 S. C. Terry, J. H. Jerman and J. B. Angell, *IEEE Trans. Electron. Devices*, ED-26 (1979) 1880.
- 8 A. Manz, Y. Miyahara, J. Miura, Y. Watanabe, H. Miyagi and K. Sato, *Sens. Actuators*, B1 (1990) 249.
- 9 A. Manz and W. Simon, *Anal. Chem.*, 59 (1987) 74.
- 10 C. A. Monnig and J. W. Jorgenson, *Anal. Chem.*, 63 (1991) 802.
- 11 R. B. Bird, W. E. Stewart and E. N. Lightfoot, *Transport Phenomena*, Wiley, New York, 1960, pp. 267–271.
- 12 K. E. Petersen, *Proc. IEEE*, 70 (1982) 420.
- 13 W. H. Ko and J. T. Suminto, in W. Göpel, J. Hesse and J. N. Zemel (Editors), *Sensors, a Comprehensive Survey*, Vol. 1, VCH Weinheim, 1989, pp. 107–168.
- 14 *Proceedings of Transducers '89; Sens. Actuators*, A21–A23 (1990) and *Sens. Actuators*, B1 (1990); *Proceedings of Transducers '91, Digest of Technical Papers*, IEEE, Piscataway, NJ, 1991.
- 15 D. J. Harrison, A. Manz and P. G. Glavina, in *Transducers '91; Digest of Technical Papers*, IEEE, Piscataway, NJ, 1991, p. 792.
- 16 A. Manz, D. J. Harrison, J. C. Fetting, E. Verpoorte, H. Lüdi and H. M. Widmer, in *Transducers '91; Digest of Technical Papers*, IEEE, Piscataway NJ, 1991, p. 939.
- 17 T. Tsuda, J. V. Sweedler and R. N. Zare, *Anal. Chem.*, 62 (1990) 2149.
- 18 M. Jansson, Å. Emmer and J. Roeraade, *J. High Resolut. Chromatogr. Chromatogr. Commun.*, 12 (1989) 797.
- 19 J. F. Brown and J. O. N. Hinckley, *J. Chromatogr.*, 109 (1975) 225.
- 20 J. W. Jorgenson and K. D. Lukacs, *Science (Washington, D.C.)*, 222 (1983) 266.
- 21 E. Gassmann, J. E. Kuo and R. N. Zare, *Science (Washington, D.C.)*, 230 (1985) 813.

# Separation of leucinostatins by capillary zone electrophoresis

M. G. Quaglia\*

*Dipartimento Studi Farmaceutici, Università degli Studi "La Sapienza", P. le A. Moro 5, 00185 Rome (Italy)*

S. Fanali and A. Nardi

*Istituto di Cromatografia del CNR, Area di Ricerca di Roma, Casella Postale 10, 00016 Monterotondo Scalo, Rome (Italy)*

C. Rossi and M. Ricci

*Istituto di Chimica Farmaceutica e di Tecnica Farmaceutica, Università degli Studi di Perugia, Via del Liceo, 60100 Perugia (Italy)*

---

## ABSTRACT

A capillary zone electrophoretic method was used to separate some leucinostatins, the nonapeptides obtained by submerged cultures of *Paecilomyces marquandii* or *Paecilomyces lilacinus*. These compounds are of pharmaceutical interest for their remarkable antibiotic, cytotoxic and phytotoxic activities. The proposed method allows the separation of leucinostatins from very complex mixtures and shows high efficiency, good resolution and a very short analysis time.

---

## INTRODUCTION

Recently we reported the isolation and structural elucidation of several components of a new family of peptides, named leucinostatins followed by alphabetical letters (Fig. 1), produced by submerged cultures of *Paecilomyces marquandii* [1–6]. Leucinostatins A, B and D have been independently found by Japanese workers in the cultural broth of *Paecilomyces lilacinus* A-257 [7,8]. These peculiar nonapeptides show very interesting antibiotic, cytotoxic and phytotoxic properties.

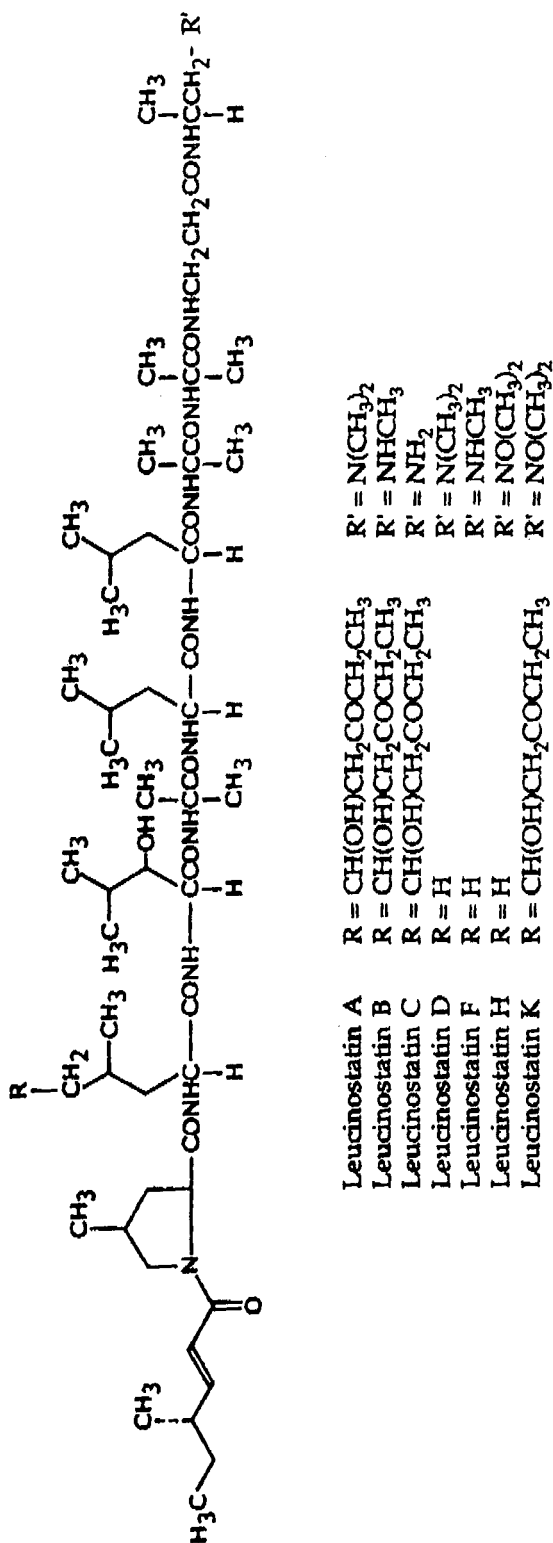
As the separation of these compounds presented some difficulties because of their very similar  $R_F$  values (Leucinostatin F could in fact only be obtained by preparative thin-layer chromatography [6], we tried to improve their separation by applying capillary zone electrophoresis (CZE), as this technique has already been successfully applied in protein and peptide analyses [9–15] and to charged

and/or uncharged molecules [16]. This paper describes the use of CZE to separate leucinostatins in very complex mixtures with excellent efficiency, high resolution and a short analysis time.

## EXPERIMENTAL

The leucinostatins were kindly provided by the Institute of Medicinal Chemistry and Pharmaceutical Techniques of Perugia University. Other reagents and solvents were supplied by Carlo Erba.

A Bio-Rad Labs. (Richmond, CA, USA) HPE 100 apparatus equipped with a UV detector with a deuterium lamp (190–380 nm) was used. The apparatus was equipped with a power supply able to deliver up to 12 kV. Sampling and electrophoresis were controlled by a microprocessor. Separation of the leucinostatins was performed in a Bio-Rad Labs. Model 148-3002 HPE capillary cartridge (20 cm × 0.025 mm, coated).



The electrophoretic experiments were carried out at 8 kV (constant) and 15  $\mu$ A. Sampling was performed by using the electrophoretic application method at 7 kV for 6 s. The capillary was filled with the background electrolyte (BGE) of 0.1 *M* phosphate buffer (pH 2.5) by using a 100- $\mu$ l Hamilton microsyringe. Electropherograms were recorded with an LKB Model 2210 line recorder at a chart speed of 10 mm/min. UV detection was carried out at 206 nm.

Separate acetonitrile–water (1:1, v/v) solutions of leucinostatin A, B, D, F, H and K (1 mg/ml) were prepared. The samples for analysis were obtained by transferring 1 ml of each solution into a 30-ml volumetric flask and diluting to volume with the same solvent mixture.

N-Methylation by phase-transfer catalysis of leucinostatin A was applied to give the methylammonium salt [Fig. 1,  $R' = N^+(\text{CH}_3)_3$ ]. The reaction was carried out by using an equivalent amount of iodomethane in dry dichloromethane in the pres-

ence of powdered potassium hydroxide and tetrabutylammonium bromide as catalyst with stirring at room temperature.

## RESULTS AND DISCUSSION

Several electrolyte systems were tested in order to optimize the separation conditions. As the leucinostatins considered have very similar structures they therefore need specific methods for their separation. The best conditions were realized using phosphate buffer (pH 2.5). With this BGE all leucinostatins moved as cations with a relative high velocity.

Working standard solutions were prepared with leucinostatins in order to verify the specificity of the proposed method. Fig. 2 shows the electropherogram of a mixture containing leucinostatin A, B, D and K. Whereas leucinostatin D and K are well separated, A and B are unresolved. The separation of the latter two leucinostatins is possible only when the methylammonium salt of leucinostatin A is formed (Fig. 3).

The electropherogram of a mixture of several leucinostatins (Fig. 4) shows partial overlapping of the peaks of leucinostatin F and K; however this partial separation can be considered satisfactory for the detection of such a complex mixture of compounds.

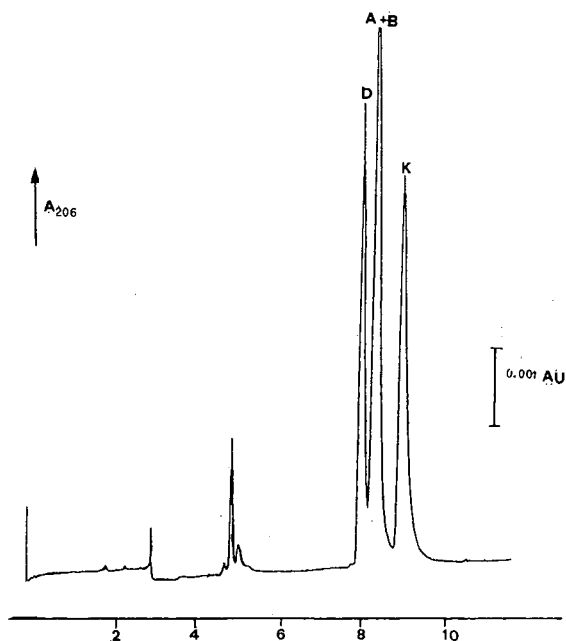


Fig. 2. Electropherogram of the separation of leucinostatin A, B, D and K. BGE: 0.1 *M* phosphate buffer (pH 2.5). Sampling: electrophoresis at 7 kV for 6 s. The mixture contained  $3.33 \cdot 10^{-2}$  mg/ml of each leucinostatin. Electrophoretic experiment: 8 kV; 15  $\mu$ A. Time scale in min.

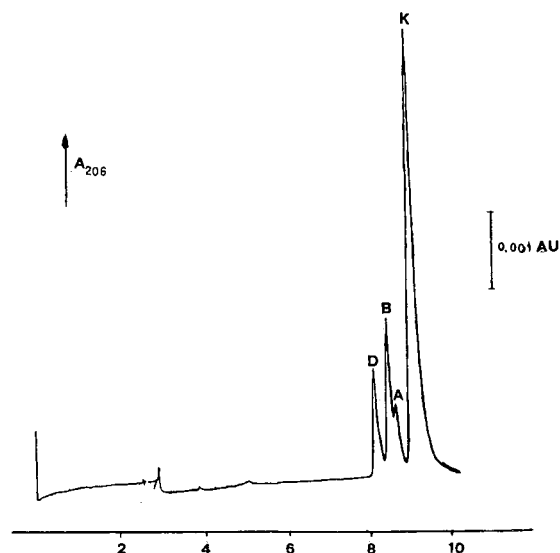


Fig. 3. Electropherogram of the separation of leucinostatin A (methylammonium salt), B, D and K. Conditions as in Fig. 2.

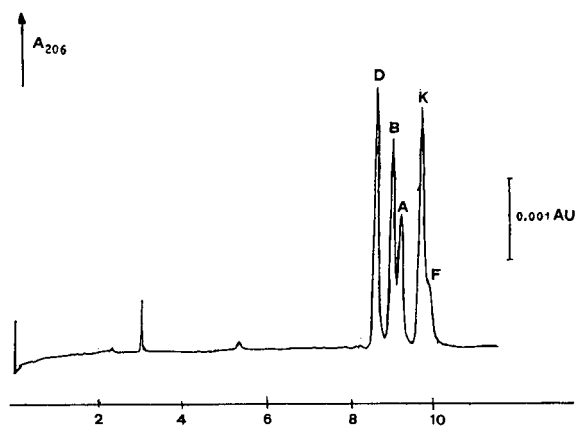


Fig. 4. Electropherogram obtained from a mixture of leucinostatin D, B, A (methylammonium salt), K and F. Conditions as in Fig. 2.

Using the same working conditions, a good separation of leucinostatin A, D, H and K was achieved (Fig. 5).

Additionally the proposed CZE method allows the purity control of leucinostatins extracted from culture broth. The electropherogram for to a crude sample of leucinostatin B (Fig. 6) shows very clearly that other compounds are also present. The latter

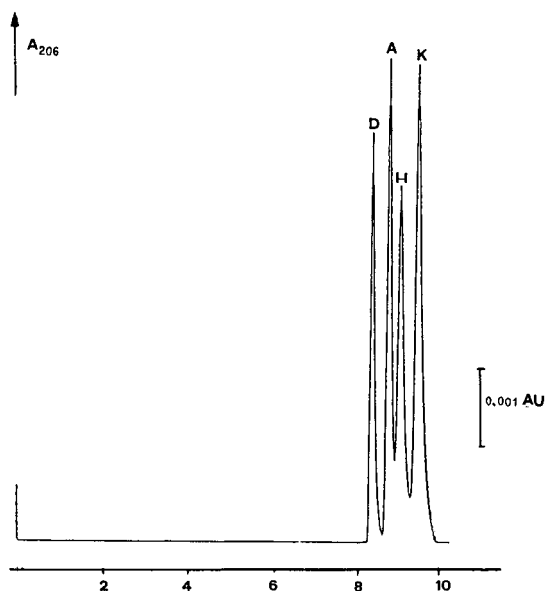


Fig. 5. Separation of leucinostatin D, A, H and K. Conditions as in Fig. 2.

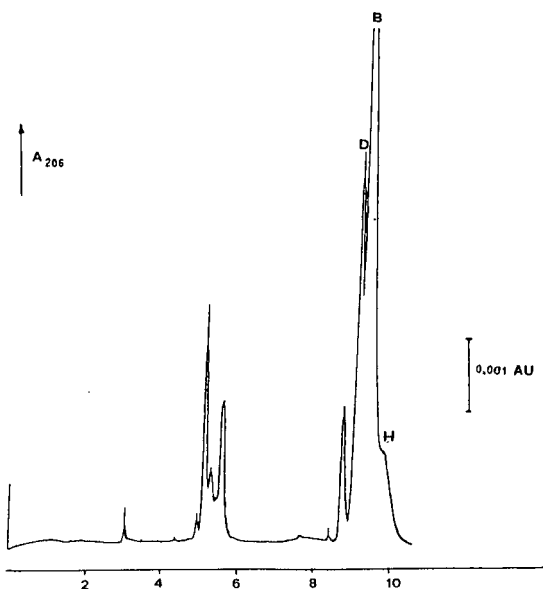


Fig. 6. CZE analysis of a crude leucinostatin B sample. Leucinostatin D and H are also present. Conditions as in Fig. 2.

were characterized by enrichment with leucinostatin standards. In this way it was possible to identify leucinostatins D and H; the peak at 8.8 min is probably due to an unknown leucinostatin, whereas the remaining peaks between 3 and 6 min are not leucinostatins.

The results demonstrate CZE is a sensitive, specific and rapid method which allows the identification, with good resolution, of leucinostatin A, B, D, H, K and partially F in only 10 min. The possibility of distinguishing between leucinostatin A and B using their ammonium salt formation probably would not be easy in a crude sample where other leucinostatin ammonium salts could form.

Leucinostatins have been shown to be very toxic [17] and as these compounds are produced by a microorganism which may also grow on stored food-stuffs [18], the detection of these peptides is very important.

#### ACKNOWLEDGEMENTS

This research was supported by a grant from CNR, "Piano Finalizzato-Chimica Fine e Secondaria II" and a grant from the Ministero dell'Uni-

versità e della Ricerca Scientifica e Tecnologica (40%).

## REFERENCES

- 1 C. G. Casinovi, L. Tuttobello, C. Rossi and Z. Benciari, *Phytopathol. Mediterr.*, 22 (1983) 103.
- 2 C. Rossi, Z. Benciari, C. G. Casinovi and L. Tuttobello, *Phytopathol. Mediterr.*, 22 (1983) 209.
- 3 C. G. Casinovi, C. Rossi, L. Tuttobello and M. Ricci, *Eur. J. Med. Chem. Chim. Ther.*, 21 (1986) 527.
- 4 C. Rossi, L. Tuttobello, M. Ricci, C. G. Casinovi and L. Radics, *J. Antibiot.*, 40 (1987) 130.
- 5 C. Rossi, L. Tuttobello, M. Ricci, C. G. Casinovi and L. Radics, *J. Antibiot.*, 40 (1987) 714.
- 6 C. Rossi, M. Ricci, L. Tuttobello, S. Cerrini, A. Scatturin, G. Vertuani, V. Ambrogi and L. Perioli, *Acta Technol. Legis Med.*, 1 (1990) 109.
- 7 K. Fukushima, T. Arai, Y. Mori, M. Tsuboi and M. Suzuki, *J. Antibiot.*, 36 (1983) 1613.
- 8 A. Isogal, A. Suzuki, S. Tamura, S. Higashikawa and S. Kuyama, *J. Chem. Soc., Perkin Trans. I*, (1984) 1405.
- 9 P.D. Grossmann, K. J. Wilson, G. Petrie and H. H. Lauer, *Anal. Biochem.*, 173 (1988) 265.
- 10 B. L. Karger, A. S. Cohen and A. Guttman, *J. Chromatogr.*, 492 (1989) 585.
- 11 S. Hjertén and M. D. Zhu, *Protides Biol. Fluids Proc. Colloq.*, 33 (1985) 537.
- 12 V. Rohlicek and Z. Deyl, *J. Chromatogr.*, 494 (1989) 87.
- 13 A. Pessi, E. Bianchi, L. Chappinelli, A. Nardi and S. Fanali, *J. Chromatogr.*, 557 (1991) 307.
- 14 F. Foret, S. Fanali and P. Bocek, *J. Chromatogr.*, 516 (1990) 219.
- 15 P. Ferranti, A. Malorni, P. Pucci, S. Fanali, A. Nardi and L. Ossicini, *Anal. Biochem.*, 194 (1991) 1.
- 16 F. Foret and P. Bocek, in A. Chrambach, M. J. Dunn and B. J. Radola (Editors), *Advances in Electrophoresis*, VCH, Weinheim, 1983, 273.
- 17 L. Tuttobello, F. De Bernardis, R. Lorenzini, M. Ricci, C. Rossi and R. Vertecchio, *Atti Soc. Ital. Sci. Vet.*, 41 (1987) 1103.
- 18 C. Rossi, unpublished results.





CHROMSYMP. 2456

# Separation of naphthalene-2,3-dicarboxaldehyde-labeled amino acids by high-performance capillary electrophoresis with laser-induced fluorescence detection

Teruhisa Ueda<sup>\*,☆</sup>, Rosalind Mitchell, Fumito Kitamura<sup>☆</sup> and Timothy Metcalf

*Shimadzu-Kansas Research Laboratory in the Center for Bioanalytical Research, University of Kansas, 2095 Constant Avenue, Lawrence, KS 66047 (USA)*

Theodore Kuwana

*Center for Bioanalytical Research and Department of Chemistry, University of Kansas, 2095 Constant Avenue, Lawrence, KS 66047 (USA)*

Akira Nakamoto

*Analytical Instruments Division, Shimadzu Corporation, 1 Nishinokyo-Kuwabaracho, Nakagyo-ku, Kyoto 604 (Japan)*

---

## ABSTRACT

Analysis of amino acids derivatized by reaction with naphthalene-2,3-dicarboxaldehyde (NDA) was investigated using high-performance capillary electrophoresis (HPCE) combined with laser-induced fluorescence detection. Of the HPCE modes, capillary zone electrophoresis, micellar electrokinetic chromatography and cyclodextrin (CD)-modified micellar electrokinetic chromatography (CD-MEKC) were applied to the separation of these amino acid derivatives. CD-MEKC allowed separation in less than 30 min and proved to be effective for chiral separation in some cases. A detection limit of 0.8 amol was obtained for NDA-labelled leucine at a signal-to-noise ratio of 2.

---

## INTRODUCTION

Recent advances in biotechnology require highly sensitive analytical methods for the determination of biological compounds such as amino acids and polypeptides. This has led to the development of a variety of analytical instrumentation, including high-performance liquid chromatography (HPLC) and high-performance capillary electrophoresis (HPCE) with high resolving power. Compared with

HPLC, HPCE seems to be more attractive in terms of the high column efficiency and the possibility of improved mass sensitivities for sample components due to smaller injection volumes [1]. Unfortunately, currently available commercial detectors limit the sensitivities actually obtainable.

Recently, several detection schemes including electrochemical [2,3], radiometric [4], mass spectrometric [5], indirect fluorescence [6] and laser-induced fluorescence [7–10] have been investigated to achieve improved sensitivity. To date, the most sensitive detector investigated for the capillary zone electrophoresis (CZE) of amino acids was based on the laser-induced fluorescence after precolumn deri-

---

<sup>☆</sup> Present address: R&D Engineering Department, Analytical Instruments Division, Shimadzu Corporation, 1 Nishinokyo-Kuwabaracho, Nakagyo-ku, Kyoto 604, Japan.

vatization with fluorescein isothiocyanate (FITC) [7]. Nickerson and Jorgenson [8] also demonstrated the utility of laser-induced fluorescence (LIF) detection for CZE by employing several tagging reagents, such as *o*-phthalaldehyde (OPA), naphthalene-2,3-dicarboxaldehyde (NDA) and FITC, for the pre-column derivatization of amino acids. The detection limits are at the attomole level, but the neutral amino acids migrate at similar velocities in the CZE mode, thereby resulting in poor separation of these amino acids.

Although lower detection limits can be obtained with LIF detection, it is necessary to find a greater variety of tagging reagents which favor the use of a laser, and whose derivatization product is compatible with the methods of separation in HPCE. Liu *et al.* [9] reported a new tagging reagent, 3-(4-carboxybenzoyl)-2-quinolinecarboxaldehyde (CBQCA), which gave isoindole derivatives of amino acids and peptides detectable in the low attomole range. CBQCA exhibited some desirable properties regarding the peak excitation wavelength coincidence of the derivatized compounds with the output wavelength of the helium-cadmium (He-Cd) laser (442 nm), the migration behavior of those compounds in HPCE and the reactivity with a variety of compounds such as peptides. However, the reagent is not yet commercially available. Therefore, we decided to examine NDA derivatization further, as only a limited exploration of HPCE has been made with this reagent, yet it is readily available commercially.

NDA reacts with primary amines in the presence of cyanide to form 1-cyano-2-substituted-benz[*l*]isoindole (CBI) derivatives, which exhibit improved stability compared with OPA derivatives and high quantum efficiencies [11,12], even in the aqueous buffer solutions usually required in HPCE. Further, the excitation maxima of these compounds are well matched to the output wavelength of the He-Cd laser. Although some of the CBI-amino acids have been used to reveal the advantages of LIF detection in CZE [7,13], the separation of these compounds has not been pursued by other electrophoretic methods, such as micellar electrokinetic chromatography (MEKC) or cyclodextrin (CD)-modified MEKC. In this study, the separation of CBI-amino acids was investigated using several modes of HPCE to characterize the migration profiles of these compounds within each mode. LIF detection of these compounds was performed to demonstrate the capability of the HPCE-LIF system as an analytical tool which can exhibit high resolving power and high sensitivity.

## EXPERIMENTAL

### Apparatus

Fig. 1 shows a schematic diagram of the optical configuration of the LIF detector used. The laser is a Model 4207NB He-Cd laser (Liconix, Santa Clara, CA, USA), which can produce 7 mW of output power at 442 nm. The emitted light from the laser

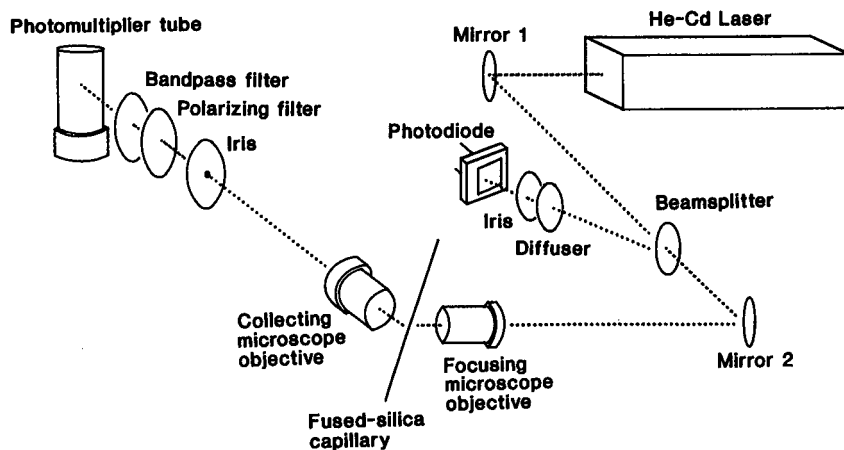


Fig. 1. Schematic diagram of laser-induced fluorescence detector for HPCE.

was reflected from a dielectric mirror (Model DM.6, 99% reflectivity at 442 nm) (Newport, Fountain Valley, CA, USA) and divided into two beams with a Model 44920 beam splitter (Oriel, Stratford, CT, USA). The laser output was monitored with a silicon photodiode (Hamamatsu, Bridgewater, NJ, USA) after passing the split portion of the laser beam through an optical diffuser (Oriel) and an iris diaphragm (Oriel). The output of the photodiode was converted to voltage and used as a reference voltage to compensate for the laser source noise with an analogue ratio circuit designed and constructed in this laboratory. The portion of the laser beam transmitted directly through the splitter was reflected from a second mirror and focused with a  $10\times$  microscope objective (Oriel) on the bared surface of a fused-silica capillary from which a 2-mm portion of the polyimide coating was removed at a point 50 cm from the inlet end. The capillary tubing of 50  $\mu\text{m}$  I.D. and 290  $\mu\text{m}$  O.D. (Code No. 062464; Scientific Glass Engineering, Ringwood, Victoria, Australia) was mounted axially at  $45^\circ$  to the laser beam in order to reduce the collection of scattered excitation light. The emitted fluorescence from the sample was collected with a  $20\times$  microscope objective (Oriel) at right-angles to the incident beam and passed through an iris diaphragm, a polarizing filter (Code No. 65.5050; Rolyn Optics, Covina, CA, USA) and a Model 490DF20 bandpass filter with a center wavelength of 490 nm and a half-bandwidth of 20 nm (Omega Optical, Brattleboro, VT, USA). As the numerical aperture of the microscope objective used in this study was 0.4, the calculated efficiency of collection of the emitted fluorescence from the analyte was *ca.* 4% [7]. A Model R1527 photomultiplier tube (Hamamatsu) operated at 900 V with a Model 227 high-voltage power supply (Pacific Instruments, Concord, CA, USA) was used to detect fluorescence. The current output from the photomultiplier was converted to voltage and divided by the reference voltage with the analogue ratio circuit. The resulting voltage ratio was displayed on a Model CR501 data processor (Shimadzu, Columbia, MD, USA).

Capillary electrophoresis was performed with an in-house designed instrument. A Model EH30R3 high-voltage power supply (Glassman High Voltage, Whitehouse Station, NJ, USA) was used to generate the electric field across a capillary of 70 cm

total and 50 cm separation length. Each end of the capillary was immersed in a separate glass bottle filled with buffer solution. Platinum wire electrodes were inserted in the buffer solutions for electrical connection. The high-voltage end of the capillary was enclosed in a Plexiglas box with a safety interlock. For temperature control, the capillary was inserted in 40 cm  $\times$  0.8 mm I.D. Teflon tube, which was connected to two PEEK T-joints so that water could be circulated outside the capillary.

### Reagents

The amino acid standard solution (A2161) used as a stock solution was purchased from Sigma (St. Louis, MO, USA). According to the manufacturer, it is prepared as a standard for the fluorescence detection of amino acids from protein hydrolysates, and contains  $2.5 \cdot 10^{-5} M$  of each amino acid, except L-cystine at  $1.25 \cdot 10^{-5} M$ . The standard solution was tested to ensure that each component was within 4% of its stated concentration. Individual L-amino acids for spiking for peak identification and DL-amino acids for chiral separation were also purchased from Sigma (Code No. LAA-21 and DLAA). NDA (Code No. A5594) was obtained from Tokyo Kasei (Tokyo, Japan). Sodium cyanide from Fluka Chemical (Ronkonkoma, NY, USA) was used as received. Sodium hydroxide of semiconductor grade, boric acid, sodium dodecyl sulfate (SDS), CDs (Code No. 85608-8 for  $\beta$ -CD and 86141-3 for  $\gamma$ -CD) were purchased from Aldrich (Milwaukee, WI, USA). All solutions were prepared in NANOpure (Sybron Barnstead, Boston, MA, USA) and filtered through a 0.2- $\mu\text{m}$  pore size membrane filter before use.

### Stock solutions

Stock solutions of 100 mM borate buffer were prepared weekly by dissolving 1.316 g of boric acid and an appropriate amount of sodium hydroxide in 200 ml of NANOpure water. NDA was dissolved in HPLC-grade acetonitrile (Fisher Scientific, Pittsburgh, PA, USA) at 4.6 mg per 25 ml to give a 1 mM solution every month. Stock solutions of 10 mM cyanide were prepared every 2 weeks by dissolving 49 mg of sodium cyanide in 100 ml of NANOpure water. For the preparation of amino acid solutions, serial dilutions with 0.1 M hydrochloric acid were made on a weekly basis from the stock solution to

give the desired concentration. All the solutions were stored at 4°C. For the experiments in which samples of less than 2.5  $\mu\text{M}$  of each amino acid were used, all glassware was well rinsed with fresh NANOpure water just before use.

#### Derivatization procedure

To 700  $\mu\text{l}$  of borate buffer solution (100 mM, pH 9.5) in a 1.5-ml vial, 100  $\mu\text{l}$  of sodium cyanide solution (10 mM) and 100  $\mu\text{l}$  of amino acid solution were added and mixed. Next, 100  $\mu\text{l}$  of NDA solution (1 mM) were added to the vial and the vial was capped. After gentle shaking, the reaction was allowed to proceed at 25°C for 30 min. The standard sample solutions were prepared in concentrations ranging from 1 nM to 1  $\mu\text{M}$  for each amino acid (except for L-cystine at half those concentrations).

#### Procedure

Sample solutions were introduced into the capillary with a hydrodynamic injection method. The injection volume was calculated according to the equation described by Rose and Jorgenson [14]. After the introduction of sample solution, 15 kV were applied across the capillary. Peak identification was performed by spiking the mixture with the individual amino acids (internal addition method).

#### RESULTS AND DISCUSSION

##### Separation of CBI-amino acids

Although the sample solutions used in this study contained sixteen amino acids with primary amine groups, multi-derivatized compounds, such as lysine and cystine, cannot be detected with this method

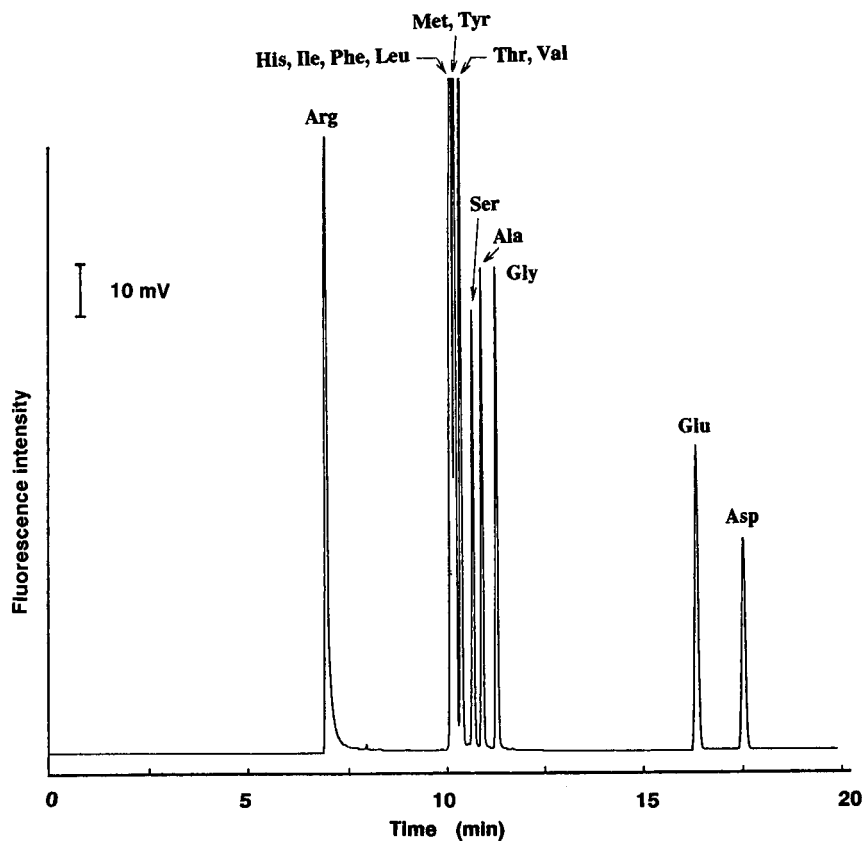


Fig. 2. Electropherogram of CBI-amino acids obtained by CZE. Electrolyte, 100 mM borate buffer (pH 9.0); capillary, 50  $\mu\text{m}$  I.D. (290  $\mu\text{m}$  O.D.), 70 cm in total length (50 cm to the detector); applied voltage, 15 kV; current, 27  $\mu\text{A}$ ; estimated injection volume, 2.9 nL; concentration for each CBI-amino acid,  $2.5 \cdot 10^{-7}$  M.

because of fluorescence quenching [15]. The quantum efficiency of the di-derivatized lysine is only 0.02, compared with 0.5–0.8 for other amino acids. Even though NDA and OPA display common functionalities, *i.e.*, dicarboxaldehyde, it was reported that the addition of a surfactant such as Brij did not reduce the fluorescence quenching as it did with the OPA system [15]. However, it may be possible to enhance the fluorescence intensity for di-derivatized compounds with the addition of SDS or CDs to the electrolyte which worked well in the OPA system [16]. Therefore, three modes of HPCE, *i.e.*, CZE, MEKC and CD-MEKC, were applied to the separation of these CBI-amino acids with LIF detection.

In CZE, migration of each component in the sample is dependent of the ionic nature of the component. Usually, electroosmotic mobility through a fused-silica capillary at a neutral pH is larger than the electrophoretic mobility of the sample component. Hence the CBI-amino acids, which are negatively charged at pH 9.0 because of the remaining carboxylate, would migrate toward the detector. As shown in Fig. 2, these compounds are not well resolved in the CZE mode owing to the similarity of the molecular structure. However, the migration order of these compounds can be explained on the

basis of the theory of CZE; CBI-Arg appeared first, then the CBI derivatives of neutral amino acids and finally CBI-Glu and CBI-Asp. As the isoelectric points ( $pI$ ) are 10.76 for Arg, 3.08 for Glu and 2.98 for Asp, the observed migration order seems reasonable at least for these amino acids. The separation of other derivatives seemed to be difficult in the CZE mode because of their close  $pI$  values.

MEKC, which was first proposed by Terabe *et al.* [17], has been investigated by many researchers as a separation technique for both neutral and ionic compounds while retaining the high resolving power of HPCE. In this separation mode, an ionic surfactant such as SDS is added to the electrolyte at concentrations exceeding the critical micellar concentration. The separation of the solutes occurs on the basis of the partition mechanism between an aqueous buffer and a micelle. Therefore, MEKC would be expected to expand the application of HPCE to a variety of compounds. Fig. 3 illustrates the electropherogram of the CBI-amino acids obtained by MEKC. Compared with Fig. 2, the separation of the amino acids was dramatically improved by the addition of SDS to the electrolyte. CBI-Ser and CBI-Thr migrated faster than other amino acids, presumably owing to their hydrophilic

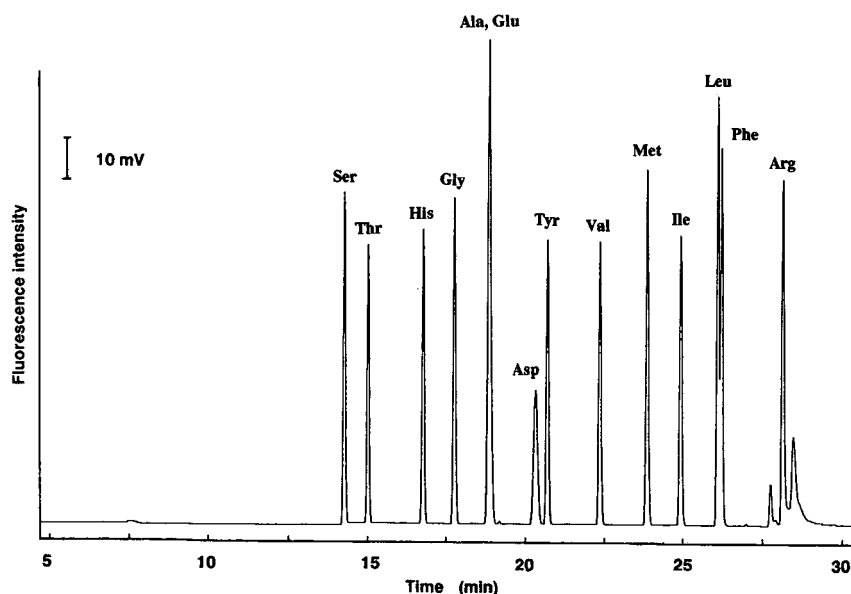


Fig. 3. Electropherogram of CBI-amino acids obtained by MEKC. Electrolyte, 50 mM SDS–100 mM borate buffer (pH 9.0); applied voltage, 15 kV; current, 35  $\mu$ A; estimated injection volume, 2.5 nL; other conditions as in Fig. 2.

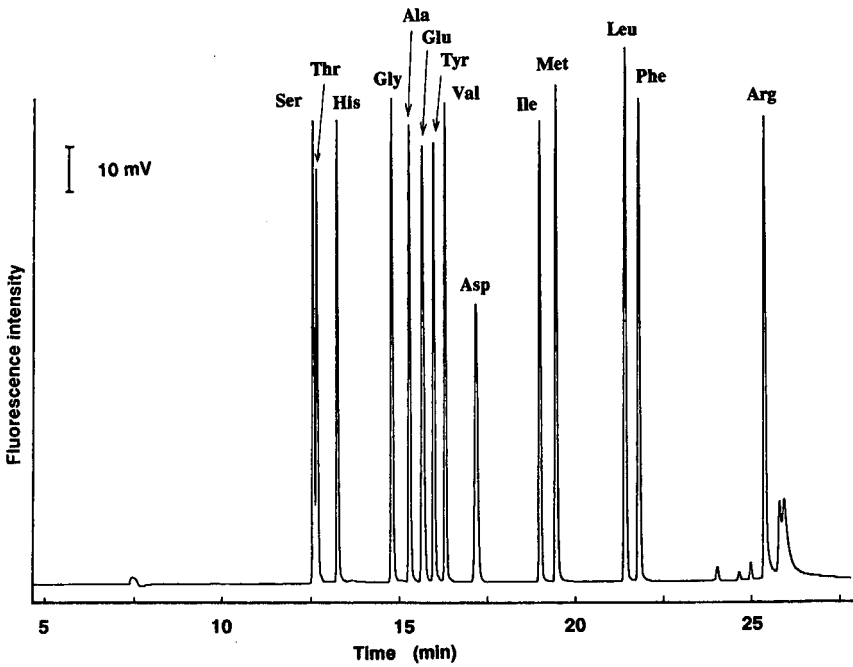


Fig. 4. Electropherogram of CBI-amino acids obtained by  $\beta$ -CD-MEKC. Electrolyte, 10 mM  $\beta$ -CD–50 mM SDS–100 mM borate buffer (pH 9.0); applied voltage, 15 kV; current, 36  $\mu$ A; estimated injection volume, 2.5 nl; other conditions as in Fig. 2.

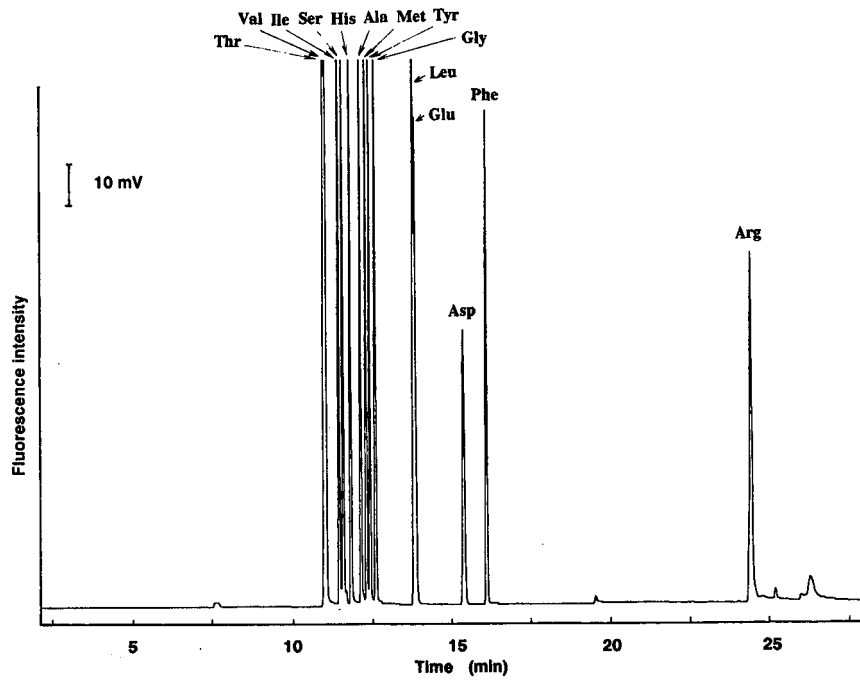


Fig. 5. Electropherogram of CBI-amino acids obtained by  $\gamma$ -CD-MEKC. Electrolyte, 10 mM  $\gamma$ -CD–50 mM SDS–100 mM borate buffer (pH 9.0), applied voltage, 15 kV; current, 36  $\mu$ A; estimated injection volume, 2.5 nl; other conditions as in Fig. 2.

residues. Under these analytical conditions, CBI-Ala and CBI-Glu co-eluted, and the separation of CBI-Leu and CBI-Phe was incomplete by MEKC even at different pH values and/or higher concentrations of SDS. Manipulation of the migration time of CBI-Glu, which was possible by changing pH of the buffer solution, led to an improved separation of CBI-Glu and CBI-Ala at pH 7.0. Unfortunately, the sensitivity towards lysine and cystine was still poor. In Fig. 3, the small peak just before the CBI-Arg corresponded to di-derivatized cystine, and the peak just after the CBI-Arg contained di-derivatized lysine together with by-products of the NDA reaction. Although a cationic surfactant is available for MEKC, CBI-amino acids did not separate satisfactorily in the presence of cetyltrimethylammonium bromide, presumably owing to the ion-pair formation between this cationic surfactant and the negatively charged CBI-amino acids.

A more successful approach was to add CDs to the MEKC system. This technique has already been reported by Terabe *et al.* [18] for the separation of highly hydrophobic compounds. In this study, addition of CDs to the electrolyte was expected to improve the separation of derivatized amino acids as it did in reversed-phase chromatography by introducing another partition mechanism [19]. CD itself will migrate at a velocity identical with the electroosmotic flow. When a solute interacts with a CD through the formation of an inclusion complex, its migration time becomes shorter. The difference in migration time for a solute with CD is strongly dependent on the degree of complexation of the solute with CD. Therefore, addition of CD to the micellar solution can change the migration selectivity for the solutes in MEKC. This method, named CD-MEKC by Terabe *et al.* [18], was applied to the separation of CBI-amino acids in this study.

Fig. 4 shows the electropherogram of the CBI-amino acids obtained by  $\beta$ -CD-MEKC. Compared with Fig. 3, the separation of CBI-Leu and CBI-Phe was dramatically improved. CBI-Ala now migrated substantially faster than CBI-Glu and the migration times were all reduced. Other conditions being equal, the addition of  $\beta$ -CD reversed the elution order of CBI-Met–CBI-Ile and CBI-Asp–CBI-Val.

Fig. 5 shows the different elution profile obtained when  $\beta$ -CD was replaced with  $\gamma$ -CD. Table I lists the migration orders of the CBI-amino acids in MEKC,

TABLE I

ELUTION ORDER OF CBI-AMINO ACIDS IN MEKC AND CD-MEKC

Analytical conditions are given in Fig. 3 for MEKC, in Fig. 4 for  $\beta$ -CD-MEKC and in Fig. 5 for  $\gamma$ -CD-MEKC.

Elution order	MEKC	$\beta$ -CD-MEKC	$\gamma$ -CD-MEKC
1	Ser	Ser	Thr
2	Thr	Thr	Val
3	His	His	Ile
4	Gly	Gly	Ser
5	Ala, Glu	Ala	His
6	—	Glu	Ala
7	Asp	Tyr	Met
8	Tyr	Val	Tyr
9	Val	Asp	Gly
10	Met	Ile	Leu
11	Ile	Met	Glu
12	Leu	Leu	Asp
13	Phe	Phe	Phe
14	Arg	Arg	Arg

$\beta$ -CD-MEKC, and  $\gamma$ -CD-MEKC. The reproducibility of migration times for CBI-amino acids was less than 2% relative standard deviation ( $n = 5$ ) in these modes. It was obvious that even though this separation system contained the same concentration of SDS in the operating buffer solutions, addition of CDs produced different selectivities in terms of solute migration characteristics. It can be concluded that CDs are effective for separations where manipulation of selectivity is necessary in MEKC.

#### Chiral separation of CBI-DL-amino acids

During the course of this study, we found that the chiral separation of some CBI-DL-amino acids could be performed by CD-MEKC. This is not surprising, because CD or CD derivatives have been successfully applied to the enantiomeric separation of dansylated DL-amino acids in both HPLC [20,21] and other modes of HPCE [22,23]. The electropherogram shown in Fig. 6 illustrates the chiral separation of CBI-DL-amino acids obtained by  $\beta$ -CD-MEKC. The electrolyte contained 10 mM  $\beta$ -CD, 50 mM SDS, and 100 mM borate buffer (pH 9.0). Even though the difference in migration times for the D- and L-forms were very small, the inherently high efficiency of HPCE allowed the separation of these

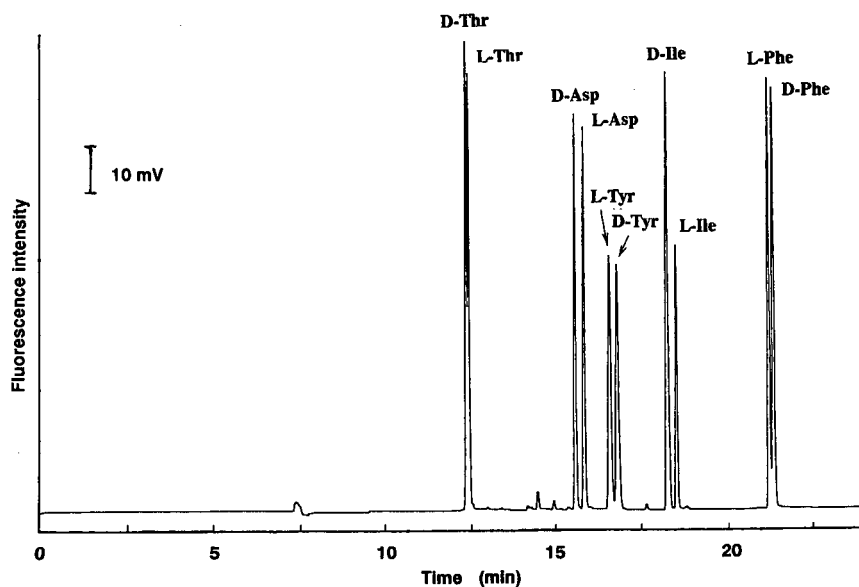


Fig. 6. Electropherogram of a mixture of five CBI-DL-amino acids obtained by  $\beta$ -CD-MEKC. Concentration of each pair of CBI-DL-amino acids,  $4.0 \cdot 10^{-7}$  M; other conditions as in Fig. 4.

enantiomers, provided that the electrolyte contained SDS. The elution order of D- and L-enantiomers seemed to be dependent on the structure of the amino acids. As shown in Fig. 6, the D-enantiomers migrated faster than the L-enantiomers for deriva-

tized aliphatic amino acids (Thr, Asp and Ile), whereas the reverse occurred for aromatic amino acids (Tyr and Phe). Even though all CBI-amino acids contain naphthalene rings in their structures, the functional group on each amino acid residue

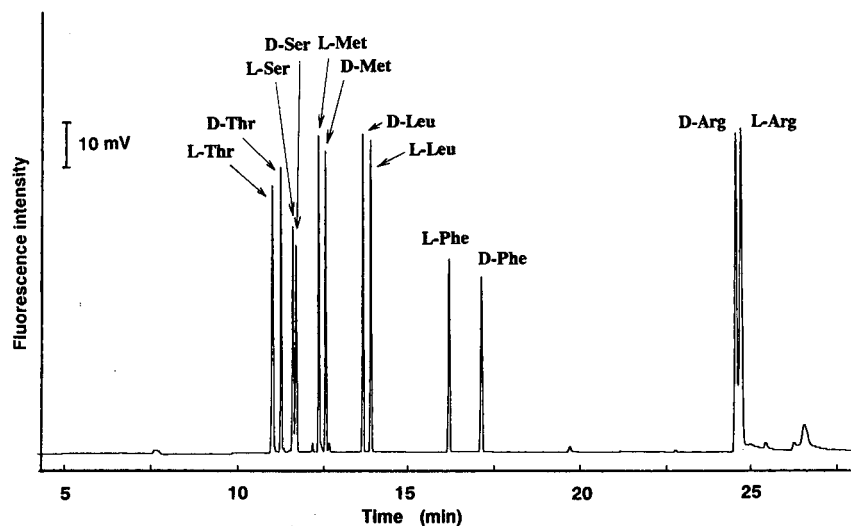


Fig. 7. Electropherogram of a mixture of six CBI-DL-amino acids obtained by  $\gamma$ -CD-MEKC. Concentration of each pair of CBI-DL-amino acids,  $2.0 \cdot 10^{-7}$  M; other conditions as in Fig. 5.



might be important for their chiral recognition as these functional groups govern the degree of the formation of an inclusion complex.

To investigate further the nature of the chiral separation in CD-MEKC,  $\gamma$ -CD was employed with the same micellar solution. Fig. 7 shows the chiral separation of the CBI-DL-amino acids by  $\gamma$ -CD-MEKC. Here, the L-form of CBI-Phe still migrated faster than the D-form, whereas the elution order of the enantiomers of CBI-DL-Thr was reversed: the resolution of both pairs was enhanced. Indeed, all the D/L-forms shown in Fig. 7 were better separated than by  $\beta$ -CD-MEKC, with the exception of D- and L-Asp, which could not be separated (not shown). In the future, optimization of analytical conditions such as pH, concentration of SDS and CD, addition of organic solvent and buffer species will be necessary to understand the mechanism of the chiral separation of amino acids in CD-MEKC.

#### Detection limits

To assess the limits of detection (LOD) for the CBI-amino acids in HPCE, mixtures of the derivatives were injected at a concentration of  $2.5 \cdot 10^{-7}$  M for each amino acid (corresponding to  $2.5 \cdot 10^{-6}$

M before derivatization). The estimated injection volumes were 2.9 nl for CZE and 2.5 nl for MEKC. Table II lists the mass detection limits for the amino acids obtained by CZE, MEKC and  $\beta$ -CD-MEKC. The sensitivity varied little, the estimated detection limits ranging from 0.7 amol ( $2.4 \cdot 10^{-10}$  M) to 2.3 amol ( $9.2 \cdot 10^{-10}$  M). The detector produced a linear response over the range of  $10^{-9}$ – $10^{-6}$  M using the derivatized sample solutions serially diluted with the electrolytes.

As the spot diameter of the laser beam is *ca.* 25  $\mu$ m on the capillary surface, a "detection cell" volume of *ca.* 35 pl can be estimated. As a medium detection limit of  $5.0 \cdot 10^{-10}$  M of a CBI-amino acid in 35 pl corresponds to 0.018 amol (10 500 molecules) of the analyte, and the collection efficiency of the microscope objective used in this study was considered to be 4%, the observed fluorescence is emitted from about 420 molecules of the analyte. This calculation was made to assess the theoretical limits of detection in the present system and the results indicate that there is still room for improvement. Further increases in sensitivity could be achieved by increasing the cell volume, so far as this can be done without losing resolution, increasing the collection efficiency of the emitted fluorescence and increasing the laser power. A new tagging reagent, having a high molar absorptivity at the excitation wavelength of the laser and high quantum efficiency, would also improve the detection limits. Investigations involving both these aspects of LIF detection are being continued.

#### CONCLUSIONS

The results of this work demonstrate (1) the improvement of the selectivities for CBI-amino acids by MEKC and CD-MEKC compared with CZE, (2) the chiral separation of CBI-DL-amino acids by CD-MEKC and (3) the high sensitivity obtained for these derivatives by using an LIF detector. Overall, the HPCE-LIF system can provide a powerful microanalytical method for biological molecules such as amino acids and peptides.

#### ACKNOWLEDGEMENTS

This work was funded by the Shimadzu Corporation and by the Kansas Technology Enterprise Corporation. The authors thank Dr. Susan Lunte

TABLE II

#### LIMITS OF DETECTION FOR CBI-AMINO ACIDS IN HPCE-LIF

Limits of detection were calculated based on a signal-to-noise ratio of 2.

Amino acid	LOD (amol)		
	CZE	MEKC	$\beta$ -CD-MEKC
Ser	0.7	1.0	0.9
Thr	—	1.1	1.1
His	—	1.1	1.0
Gly	0.7	1.0	0.9
Ala	0.7	—	1.0
Glu	1.1	—	1.0
Tyr	—	1.1	1.0
Val	—	1.1	0.9
Asp	1.5	2.3	1.6
Ile	—	1.1	1.0
Met	—	0.9	0.9
Leu	—	—	0.8
Phe	—	—	0.9
Arg	—	0.9	0.9

for her helpful suggestions on the procedure for the derivatization of the amino acids.

## REFERENCES

- 1 A. G. Ewing, R. A. Wallingford and T. M. Olefirowicz, *Anal. Chem.*, 61 (1989) 292A.
- 2 R. A. Wallingford and A. G. Ewing, *Anal. Chem.*, 60 (1988) 258.
- 3 X. Huang, T. K. Pang, M. J. Gordon and R. N. Zare, *Anal. Chem.*, 59 (1987) 2747.
- 4 M. J. Gordon, X. Huang, S. L. Pentoney and R. N. Zare, *Science*, 242 (1988) 224.
- 5 R. D. Smith, J. A. Olivares, N. T. Nguyen and H. R. Udseth, *Anal. Chem.*, 60 (1988) 436.
- 6 W. G. Kuhr and E. S. Yeung, *Anal. Chem.*, 60 (1988) 1832.
- 7 Y. F. Cheng and N. J. Dovichi, *Science*, 242 (1988) 562.
- 8 B. Nickerson and J. W. Jorgenson, *J. High Resolut. Chromatogr. Chromatogr. Commun.*, 11 (1988) 878.
- 9 J. Liu, Y.-Z. Hsieh, D. Wiesler and M. Novotny, *Anal. Chem.*, 63 (1991) 408.
- 10 A. S. Cohen, D. R. Najarian and B. L. Karger, *J. Chromatogr.*, 516 (1990) 49.
- 11 B. K. Matuszewski, R. S. Givens, K. Srinivasachar, R. G. Carlson and T. Higuchi, *Anal. Chem.*, 59 (1987) 1102.
- 12 P. de Montigny, J. F. Stobaugh, R. S. Givens, R. G. Carlson, K. Srinivasachar, L. A. Sternson and T. Higuchi, *Anal. Chem.*, 59 (1987) 1096.
- 13 B. Nickerson and J. W. Jorgenson, *J. High Resolut. Chromatogr. Chromatogr. Commun.*, 11 (1988) 533.
- 14 D. J. Rose and J. W. Jorgenson, *Anal. Chem.*, 60 (1988) 642.
- 15 S. M. Lunte and O. S. Wong, *LC GC*, 7 (1989) 908.
- 16 H. N. Shingh and W. L. Hinze, *Analyst (London)*, 107 (1982) 1073.
- 17 S. Terabe, K. Otsuka, K. Ichikawa, A. Tsuchiya and T. Ando, *Anal. Chem.*, 56 (1984) 111.
- 18 S. Terabe, Y. Miyashita, O. Shibata, E. R. Barnhart, L. R. Alexander, D. G. Patterson, B. L. Karger, K. Hosoya and N. Tanaka, *J. Chromatogr.*, 516 (1990) 23.
- 19 K. Fujimura, T. Ueda, M. Kitagawa, H. Takayanagi and T. Ando, *Anal. Chem.*, 58 (1986) 2668.
- 20 D. W. Armstrong, Y. I. Han, S. M. Han and R. A. Menges, *Anal. Chem.*, 59 (1987) 2594.
- 21 K. Fujimura, S. Suzuki, K. Hayashi and S. Masuda, *Anal. Chem.*, 62 (1990) 2198.
- 22 S. Terabe, *Trends Anal. Chem.*, 8 (1989) 129.
- 23 A. S. Cohen and B. L. Karger, *J. Chromatogr.*, 397 (1987) 409.

# Determination of substituted purines in body fluids by micellar electrokinetic capillary chromatography with direct sample injection

Wolfgang Thormann\*, Andrea Minger, Sarah Molteni, Jitka Caslavská and Petr Gebauer<sup>☆</sup>

*Department of Clinical Pharmacology, University of Bern, Murtenstrasse 35, CH-3010 Bern (Switzerland)*

---

## ABSTRACT

Many substituted purines (theobromine, caffeine, paraxanthine, theophylline and uric acid, as well as other methylated xanthines and uric acids) can easily be separated and analysed in one run using micellar electrokinetic capillary chromatography with a borate-phosphate buffer containing 75 mM sodium dodecyl sulphate (pH  $\approx$  9). Serum, saliva and urine samples collected after the self-administration of caffeine and serum samples from patients receiving theophylline or caffeine pharmacotherapy were screened for substituted purines. The data presented show the ease of using on-column multi-wavelength detection for investigating the feasibility of direct sample application, the characterization of sample pretreatment procedures and peak confirmation by comparing absorption spectra. It is shown that the determination of purines in serum and saliva samples, including therapeutic concentrations of caffeine and theophylline, can be accomplished without any sample pretreatment, whereas sample extraction is required for the determination of purines in urine. Quantitative data for the determination of micromolar amounts of theophylline (samples from adult patients) and caffeine (samples from infants born prematurely) in serum samples compare well with data obtained by non-isotopic immunoassays. Micellar electrokinetic capillary chromatography with the direct injection of serum or saliva samples requires only microlitre volumes of sample and several different compounds can be determined within a few minutes.

---

## INTRODUCTION

Theophylline is a potent bronchodilator and respiratory stimulant and is widely used in the treatment of asthma [1]. Both theophylline and caffeine are used for the treatment of apnoea in infants born prematurely [2,3]. As a consequence of the variation of pharmacokinetics between patients, it is widely recognized that it is necessary to monitor concentrations of drugs in individual patients to ensure the maximum clinical response and to avoid undesirable side-effects associated with overdoses of these compounds. Caffeine clearance is also used as a liv-

er function test, which requires the determination of caffeine concentrations in serum or saliva samples [4]. Non-isotopic immunoassays [3,5] and many chromatographic methods [3,5–7] have been developed as instrumental approaches for the determination of theophylline and caffeine in body fluids.

High-performance capillary electrophoresis (HPCE) and micellar electrokinetic capillary chromatography (MECC, an interface between electrophoresis and chromatography) are attractive approaches for the determination of pharmaceuticals in body fluids [8–16]. In MECC two distinct phases are used, an aqueous and a micellar or pseudo-stationary phase. These two phases are established by buffers containing surfactants [*e.g.* sodium dodecyl sulphate (SDS)] above their critical micellar concentration. An MECC analysis is performed in equip-

---

\* Permanent address: Institute of Analytical Chemistry, Czechoslovak Academy of Sciences, CS-611 42 Brno, Czechoslovakia.

ment designed for HPCE, *i.e.* in an open-tubular capillary of very small internal diameter. A high-voltage d.c. electric field is applied along the column, causing a movement of the entire liquid (the so-called electro-osmotic flow) and migration of the charged micelles. Non-ionic solutes partition between the two phases and elute with zone velocities between those of the two phases. Their elution order is essentially based on the degree of partitioning [14]. In such a system several substituted purines of very similar structure can be well separated with a buffer of about pH 8 containing 50 mM SDS [17].

In a previous investigation [15] the advantages of using fast-scanning, multi-wavelength detection for the HPCE-MECC determination of barbiturates in serum samples and urine was shown. This approach allowed peak confirmation and peak purity to be evaluated by comparing the absorption spectra. The objectives of the work described in this paper were to investigate (i) the suitability of direct sample introduction and various extraction procedures for the determination of caffeine, theophylline, paraxanthine, uric acid and related compounds in human serum, saliva and urine samples by MECC using on-column, fast-scanning polychrome detection, and (ii) the determination of theophylline and caffeine in serum samples by MECC compared with non-isotopic immunoassays.

## EXPERIMENTAL

### *Chemicals and origin of samples*

All chemicals used were of analytical-reagent or research grade. The purines were obtained from Fluka (Buchs, Switzerland), except uric acid, which was purchased from Merck (Darmstadt, Germany). Bovine plasma was prepared by centrifugation of bovine blood (from the local slaughterhouse) and blank human serum samples were obtained by centrifugation of the authors' blood (1500 *g* for 10 min). Blank saliva samples were obtained from a subject who does not drink any beverages containing caffeine or other methylxanthines. Serum samples were collected in the routine drug assay laboratory where they were received for therapeutic drug monitoring of patients receiving theophylline pharmacotherapy and of infants born prematurely and receiving treatment with caffeine or theophylline. After centrifugation, all samples were assayed

for theophylline or caffeine by an automated enzyme immunoassay and stored at  $-20^{\circ}\text{C}$  until required.

### *Self-administration of caffeine*

Coffee was prepared from disposable bags of instant coffee packaged for the study of the overnight clearance of caffeine from saliva [4]. A bag containing 2 g of instant decaffeinated coffee powder spiked with 140 mg of caffeine was used to prepare a cup of coffee. One or two cups were administered.

### *Immunoassays*

Caffeine concentrations were determined in serum and saliva samples by an automated enzyme-multiplied immunoassay technique (EMIT; Syva, Palo Alto, CA, USA) using a Cobas Bio centrifugal analyser (F. Hoffmann-La Roche, Diagnostica, Basle, Switzerland) as previously described by Zysset *et al.* [3]. Theophylline concentrations were measured using an EMIT (Syva) procedure similar to that for caffeine and by an automated fluorescence polarization immunoassay (FPIA) on a TDx analyzer (Abbott Laboratories, Irving, TX, USA). The FPIA assays were performed according to the manufacturer's instructions. The EMIT assays for caffeine and theophylline are designed to determine caffeine and theophylline concentrations from 5.2 to 155  $\mu\text{M}$  (1–30  $\mu\text{g/ml}$ ) and 13.9 to 222  $\mu\text{M}$  (2.5–40  $\mu\text{g/ml}$ ), respectively. The FPIA assay operates between 2.8 and 222  $\mu\text{M}$  (0.51–40  $\mu\text{g/ml}$ ).

### *Electrophoretic instrumentation and running conditions*

The instrument with multi-wavelength detection used in this work has been described previously [15]. Briefly, it features a 75  $\mu\text{m}$  I.D. fused-silica capillary of about 90 cm length (Product TSP/075/375, Polymicro Technologies, Phoenix, AZ, USA) and a fast-scanning multi-wavelength detector (Model UVIS 206 PHD) with an on-column capillary detector cell (No. 9550-0155; both from Linear Instruments, Reno, NV, USA) towards the capillary end. The effective separation distance was 70 cm. A constant voltage of 20 kV was applied. The cathode was on the detector side. Sample application occurred manually through dipping the anodic capillary end into the sample vial and lifting it 34 cm for a specified time interval (typically 5 s). Multi-wavelength data were

read, evaluated and stored by a Mandax AT 286 computer system using the 206 detector software package version 2.0 (Linear Instruments), with windows 286 version 2.1 (Microsoft, Redmont, WA, USA). Conditioning for each experiment was performed by rinsing the capillary with 0.1 M sodium hydroxide solution for 3 min and with buffer for 5 min. Throughout this work the 206 detector was used in the high-speed polychrome mode by scanning from 195 to 320 nm at 5-nm intervals (26 wavelengths). With these settings the sampling rate was 3.69 data points per second and wavelength unit.

For quantitation the model 270A capillary electrophoresis system (Applied Biosystems, San Jose, CA, USA) was used. This apparatus features automated capillary rinsing, sampling and execution of the electrokinetic run. For these experiments it was equipped with a 50  $\mu\text{m}$  I.D. fused-silica capillary with an effective separation length of 35 to 45 cm. A Model D-2000 chromato-integrator (Merck-Hitachi, Darmstadt, Germany) was used for recording the pherograms and for quantitation by peak-area measurements. The integrator sampling period was set to one data point per 200 ms throughout this work. Unless otherwise stated, before each run the capillary was rinsed with 0.1 M sodium hydroxide solution (1 min) and with buffer (2 min). The injection of the sample was achieved by vacuum suction for 1–2 s. A constant voltage of 15–30 kV was applied and the temperature was set at 40°C.

#### *Electrophoresis buffers and standard solutions*

For monitoring the purines a buffer of 75 mM SDS, 6 mM  $\text{Na}_2\text{B}_4\text{O}_7$  and 10 mM  $\text{Na}_2\text{HPO}_4$  (pH  $\approx$  9) was used. All standard solutions of purines were prepared in buffer or methanol at concentrations of 100–360  $\mu\text{g}/\text{ml}$ . The blank and patient samples were spiked by adding known aliquots of these standard solutions to the body fluids prior to sample injection or extraction. For quantitation, aliquots of the methanolic standard solutions were added to a glass test-tube with a conical bottom, evaporated to dryness under a stream of nitrogen (40°C) and reconstituted with either 0.5 ml of bovine plasma, blank human serum or patient serum.

#### *Direct injection of body fluids*

Serum, saliva and urine samples were either injected as received or, prior to injection, filtered us-

ing 0.2- $\mu\text{m}$  Nalgene (25 mm diameter) disposable syringe filters (Nalge Company, Rochester, NY, USA).

#### *Extraction of purines*

The rapid extraction of substituted purines from serum (or bovine plasma) and saliva samples was achieved using Sep-Pak  $\text{C}_{18}$  cartridges (Waters, Division of Millipore, Milford, MA, USA), which are reversed-phase octadecylsilane-bonded silica columns. These were conditioned immediately before use by drawing 2 ml of methanol followed by an equal volume of water through the column with a plastic syringe. The columns were loaded by the application of a mixture of 0.5 ml of serum (bovine plasma) or saliva sample and 0.5 ml of 20 mM phosphate buffer (pH 7), then rinsed with 2 ml of water and dried with an equal volume of air. The columns were eluted into a test-tube with 0.6 ml of methanol before evaporation to dryness under a gentle stream of nitrogen at 30–40°C. The residue was dissolved in 200  $\mu\text{l}$  of running buffer.

Liquid-liquid extraction for the determination of substituted purines in serum (bovine plasma) and saliva samples by MECC was performed using a modification of the method of Zysset *et al.* [3]. Into an 11-ml screw-capped Sovirel test-tube, 0.5 ml of serum (bovine plasma) or saliva sample, 0.2 g of ammonium sulphate and 8 ml of chloroform-isopropanol (1:1, v/v) were added. After vigorous shaking for 30 min and centrifugation at 1500 g for 10 min the organic layer was transferred into a test-tube with a conical bottom and evaporated to dryness under a gentle stream of nitrogen at 70°C. The residue was dissolved in 200  $\mu\text{l}$  of running buffer, shaken for 30 s, taken up by a 2-ml plastic syringe and filtered through a Nalgene syringe filter (0.2  $\mu\text{m}$ , 25 mm diameter).

The purines were extracted from urine using Bond Elut Certify cartridges and the Vac Elut set-up (both from Analytichem International, Harbor City, CA, USA). With minor alterations, the manufacturer's instructions for acidic and neutral drugs were used, as described previously for the determination of barbiturates [15]. After extraction the dried residue was dissolved in 100–200  $\mu\text{l}$  of running buffer.

## RESULTS AND DISCUSSION

*MECC of substituted purines in serum, saliva and urine samples*

The three-dimensional electropherogram shown in Fig. 1A represents the absorbance *versus* retention time *versus* wavelength relationship for a model mixture consisting of ten substituted purines. These compounds are found in the metabolic pathways of caffeine and theophylline in humans [18]. Each component is characterized by its retention and migration behaviour, with theobromine (compound 1) being the fastest (the least interaction with the micelles) and uric acid (compound 10) the slowest. Fig. 1B shows the data at three wavelengths only, indicating that these purines are readily detected at 280 nm and that there is baseline resolution except between 1-methyluric acid (compound 8) and 7-methyluric acid (compound 9). Under the

investigated experimental conditions, several other purines were found to co-elute with one of these compounds. 3,7-Dimethyluric acid formed a mixed zone with 7-methylxanthine, 1-methylxanthine with 1-methyluric acid, and 1,3- and 1,7-dimethyluric acid with 3-methylxanthine. The absorbance spectrum of each compound can be extracted from the data points as so-called time slices. When the background absorption was subtracted, the spectra compared well with those measured on a standard spectrophotometer. Background-subtracted, normalized spectra are used to aid comparisons (see below).

Two extraction methods were investigated to monitor caffeine and theophylline in serum samples. Fig. 2 shows three-dimensional pherograms of theobromine, caffeine and theophylline extracted from spiked bovine plasma using the liquid-liquid extraction (panel A) and the Sep-Pak C<sub>18</sub> (panel B)

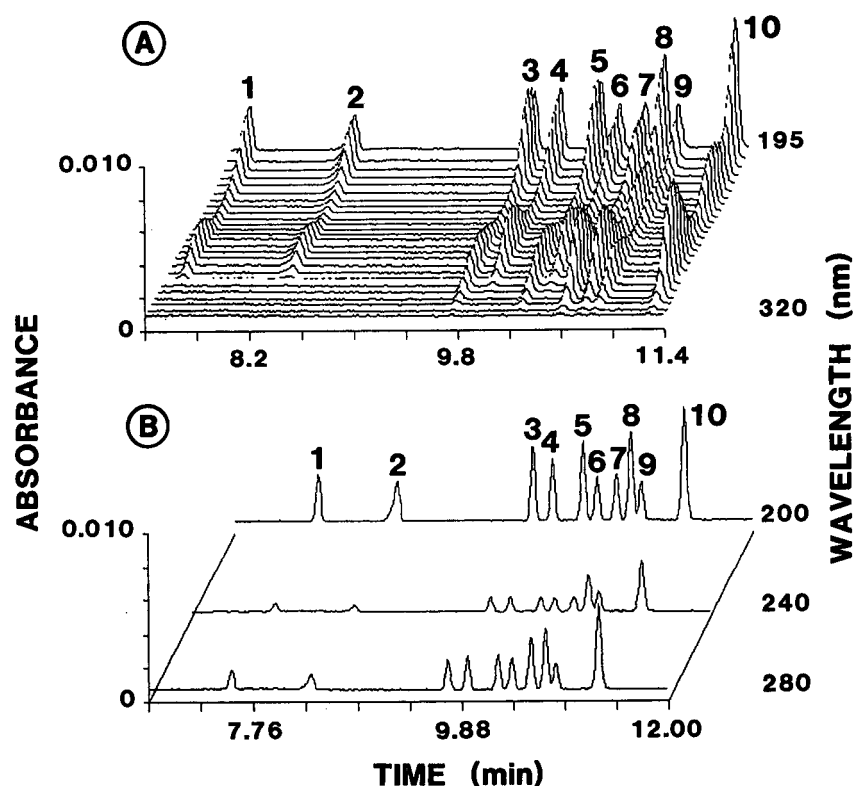


Fig. 1. Three-dimensional electropherograms of a model mixture of ten substituted purines (A) and pherograms at three wavelengths of the same run (B). The applied voltage was a constant 20 kV and the current was 75  $\mu$ A. Peaks: 1 = theobromine (3,7-dimethylxanthine); 2 = caffeine (1,3,7-trimethylxanthine); 3 = paraxanthine (1,7-dimethylxanthine); 4 = theophylline (1,3-dimethylxanthine); 5 = 7-methylxanthine; 6 = 3-methylxanthine; 7 = 3-methyl uric acid; 8 = 1-methyl uric acid; 9 = 7-methyl uric acid; 10 = uric acid.

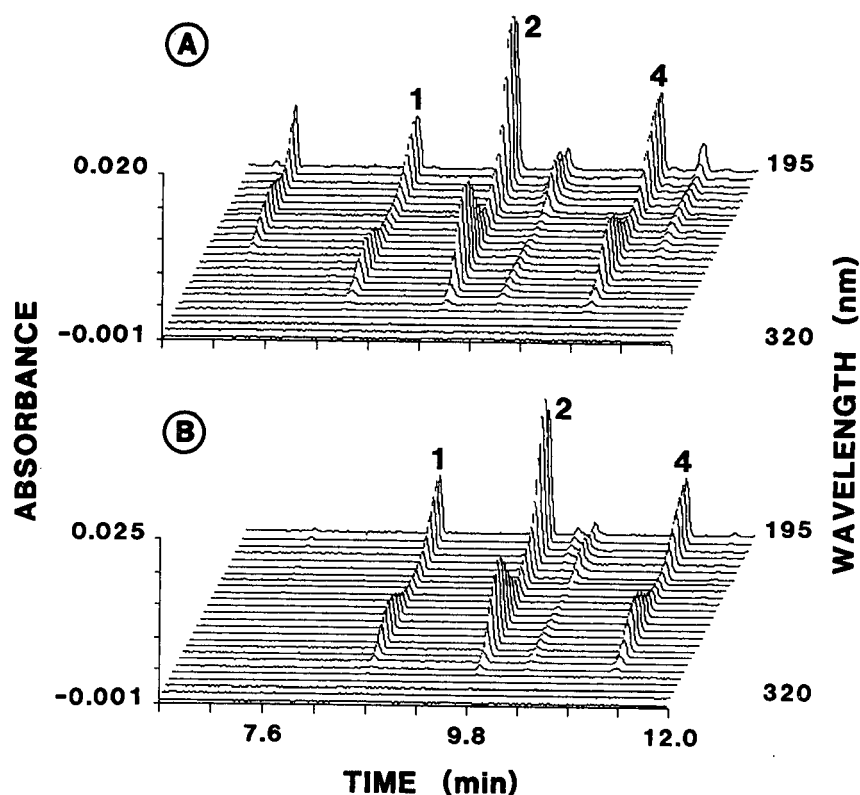


Fig. 2. Three-dimensional data plot obtained after liquid-liquid (A) and Sep-Pak (B) extraction of bovine plasma spiked with theobromine (*ca.*  $140 \mu\text{M}$ ), caffeine (*ca.*  $250 \mu\text{M}$ ) and theophylline (*ca.*  $140 \mu\text{M}$ ). The applied voltage was a constant 20 kV and the current was  $74 \mu\text{A}$ .

pretreatment procedures. The three purines could easily be identified by comparing their spectra with those obtained from Fig. 1 (data not shown), as well as by their retention behaviour, *i.e.* time of detection relative to a known compound such as theobromine. With both procedures, the three compounds extracted well and provided well resolved pherograms when detected at or close to 280 nm. With the solid-phase method, however, a lower number of components was extracted from the serum matrix.

The data presented in Fig. 3A and B were obtained with a human serum sample which was only passed through a  $0.2\text{-}\mu\text{m}$  syringe filter before sample injection. This serum sample was prepared 1 h after the self-administration of 140 mg of caffeine. It represents the same sample previously investigated as a blank probe for the determination of

barbiturates in another buffer system [15]. As in this previous investigation, the data shown in panel B show that components eluting between caffeine (peak 2) and uric acid (peak 10) can be analysed with direct sample injection, *i.e.* without extraction. Analysis by an EMIT gave a caffeine concentration of  $22.8 \mu\text{M}$ . Serum proteins are dissolved by SDS and elute (as a very broad zone) after uric acid. For comparison, the three-dimensional pherogram of a serum sample collected 2.5 h after caffeine self-administration (EMIT  $21.3 \mu\text{M}$  caffeine) and extracted using the liquid-liquid extraction procedure is presented in Fig. 3C. In both instances, the spectral information allowed the positive identification of caffeine (peak 2), its metabolite paraxanthine (peak 3) and uric acid (peak 10), as is illustrated by the normalized spectra of panels D, E and F, respectively.

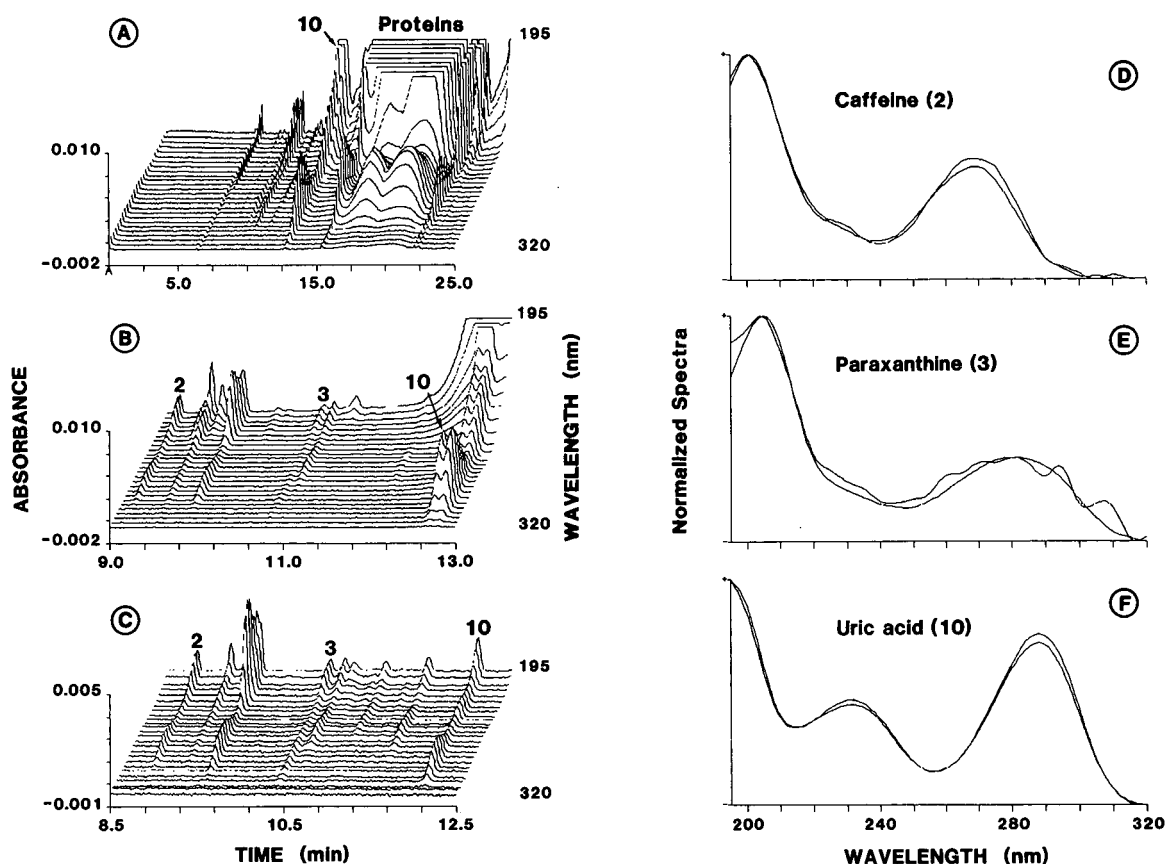


Fig. 3. Three dimensional data plots of a directly injected serum sample (complete pherogram in A and expanded section in B) and after liquid-liquid extraction (C). Power conditions as in Fig. 1. Spectral identity proof of eluting caffeine (D), paraxanthine (E) and uric acid (F) zones are presented as a comparison of the background corrected time slices with computer-stored, normalized spectra.

The data shown in Fig. 4 were obtained with a serum sample from a patient receiving theophylline pharmacotherapy (EMIT 95  $\mu M$ ). The suitability of direct sample introduction for drug monitoring is shown with the example of panel A. A clear theophylline zone is produced within the analytical window. Fig. 4B shows the three-dimensional pherogram after Sep-Pak extraction and Fig. 4C the spectral proof of identity for the theophylline zone. The corresponding single-wavelength data for 200 and 280 nm are presented in Fig. 5. These data clearly show that well resolved theophylline peaks are obtained with either method when monitored at 280 nm. The serum concentration of theophylline was determined as 87  $\mu M$  using Sep-Pak clean-up and

detection at 280 nm (see below) and 96  $\mu M$  using FPIA. Thus, MECC has the potential to determine serum theophylline at concentrations of pharmacological interest (the therapeutic range of this compound is 55–110  $\mu M$ ) and without elaborate sample pretreatment.

The direct injection of serum samples in MECC allows rapid analysis which can be performed on very small sample volumes (a few microlitres), such as those from infants born prematurely, samples which are typically too small to be pretreated. The three-dimensional pherograms presented in Fig. 6 were obtained with two unfiltered serum samples from infants. All the assigned peaks could be verified by comparing normalized time slices, and well



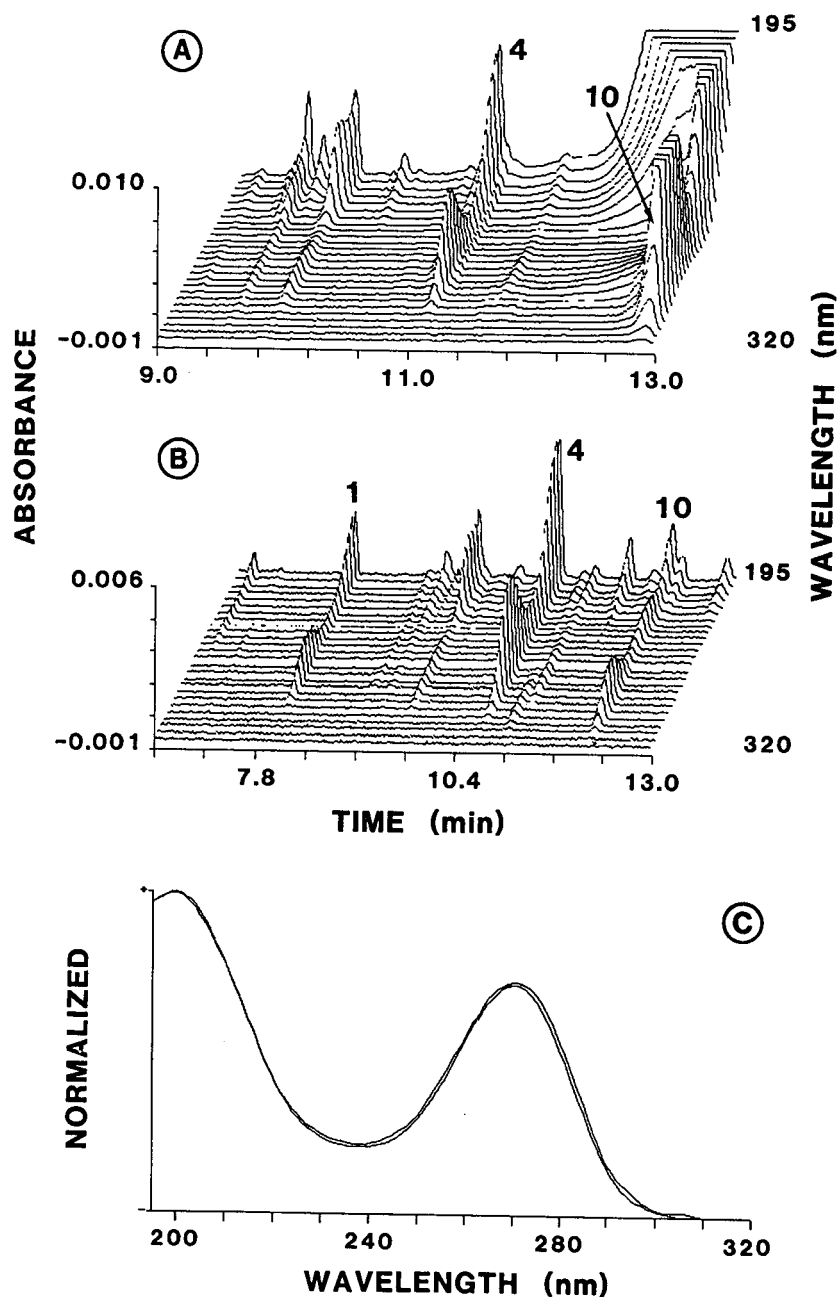


Fig. 4. Data for a directly injected (A) and a Sep-Pak-extracted (B) serum sample of a patient receiving theophylline pharmacotherapy. For the extraction, theobromine ( $40 \mu\text{M}$ ; peak 1 in panel B) was added as an internal standard. Power conditions as in Fig. 1. Panel C shows a background corrected time slice of the theophylline zone of panel B compared with that of a computer-stored reference spectrum.

resolved pherograms were obtained at 280 nm (data not shown), indicating that the direct injection of serum samples from infants could be used for the

determination of purines. Serum concentrations of caffeine, determined by EMIT, were 14 (Fig. 6A) and 107 (Fig. 6B)  $\mu\text{M}$ . The theophylline concentra-

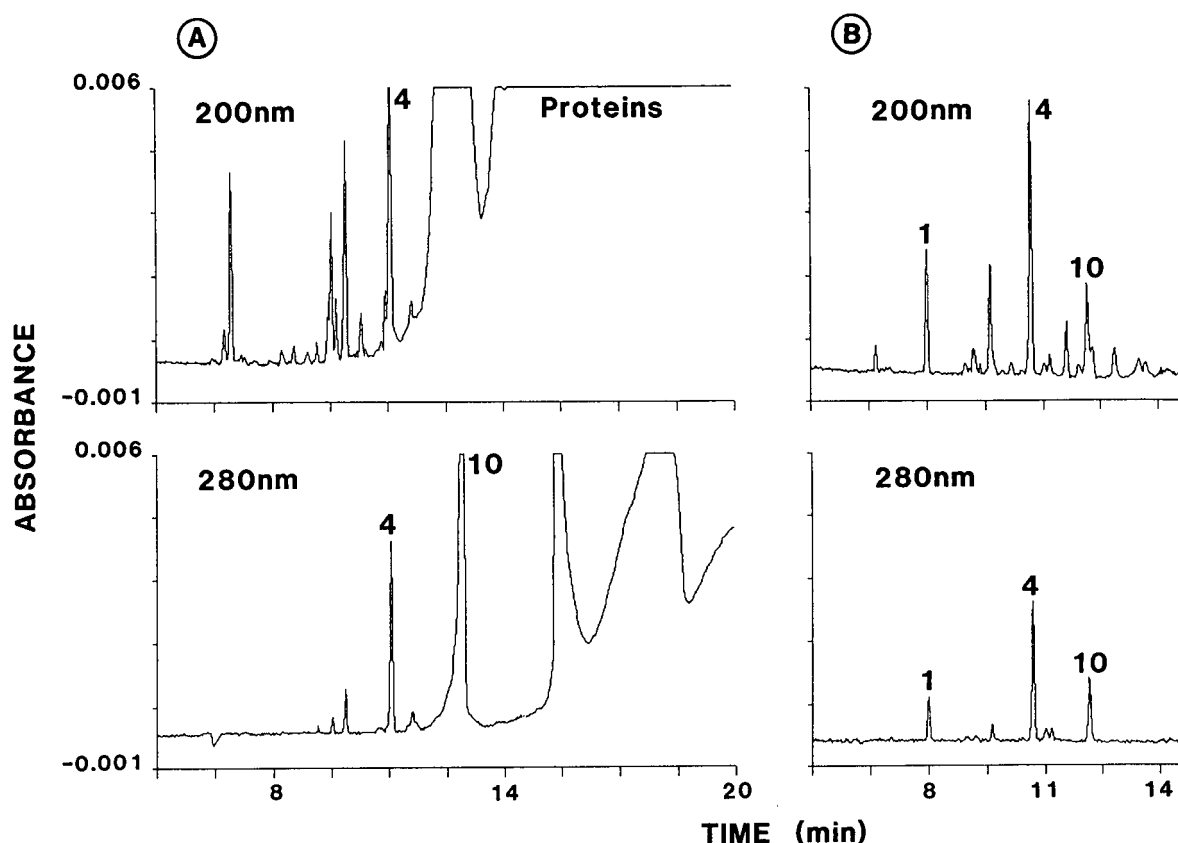


Fig. 5. Single-wavelength pherograms (200 and 280 nm) of the data presented in Fig. 4A and B.

tions were 35.7 and 3.5  $\mu\text{M}$ , respectively, using FPIA. An analysis of the sample shown in Fig. 6A, but filtered prior to injection, gave no change in the caffeine and theophylline peaks. The two serum samples are interesting because they show metabolic differences in the drugs given. Theophylline was given in the sample of Fig. 6A and caffeine in the sample of Fig. 6B. Not surprisingly, caffeine is clearly detected as a metabolite of theophylline in infants born prematurely [18] using MECC (Fig. 6A), whereas no substantial amount of theophylline is found during caffeine pharmacotherapy (Fig. 6B).

The determination of caffeine [4] and theophylline [19] in saliva has been reported as being a useful alternative to the monitoring of these compounds in serum samples. This non-invasive method has great potential, particularly for children, as it avoids the potential trauma associated with venipuncture. As

with the serum samples, it was of interest to elucidate the possibilities of direct injection of saliva compared with different sample extraction procedures. Fig. 7A and B shows multi-dimensional pherograms obtained after the direct injection of a filtered saliva sample which was collected about 1 h after the self-administration of 280 mg of caffeine. For that sample, concentrations of caffeine and theophylline in saliva were determined to be 29.8 (EMIT) and <2  $\mu\text{M}$  (FPIA), respectively. Fig. 7A shows the pattern measured between 0 and 25 min, showing a much reduced protein content of saliva compared with that of serum samples. The expanded caffeine-uric acid window of the same data is presented in Fig. 7B and the corresponding data from a blank saliva sample from a subject who did not take any caffeine-containing beverages nor food is given in Fig. 7C. Fig. 7D shows the pherogram obtained with the saliva sample of Fig. 7A and B

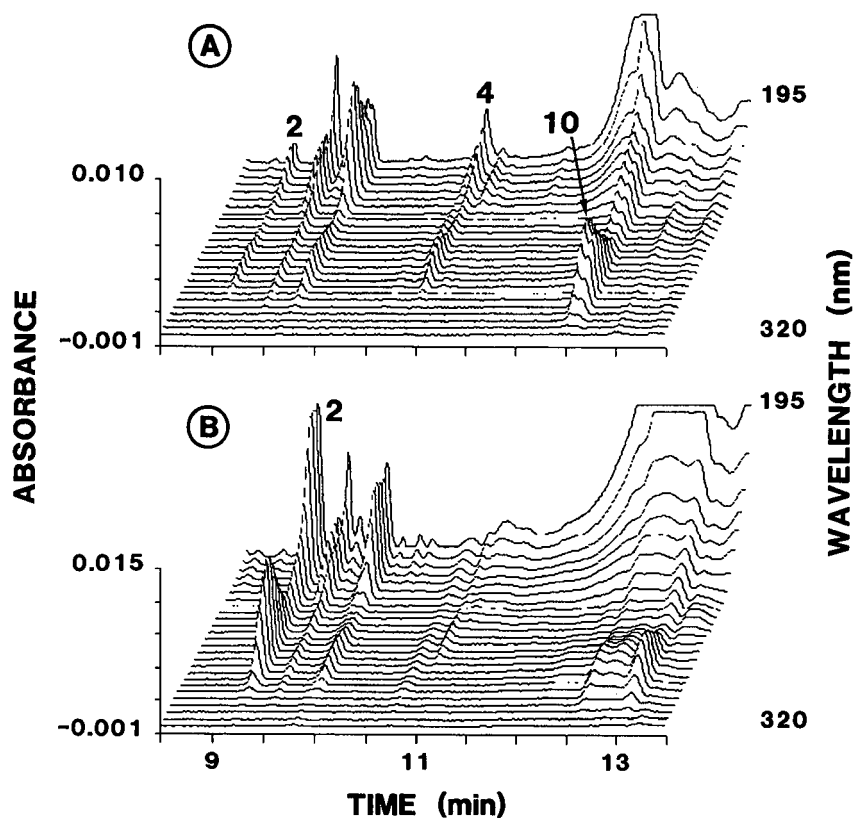


Fig. 6. Multi-wavelength data obtained by the direct injection of serum samples from two infants born prematurely. (A) Infant with theophylline treatment; (B) with caffeine pharmacotherapy. Power conditions as in Fig. 1.

but after liquid-liquid extraction as a clean-up procedure. The assigned peaks of caffeine, paraxanthine and uric acid could easily be verified by comparing normalized, background corrected time slices (data not shown).

The analysis of urine from a subject with regular coffee consumption by direct injection reveals the presence of many highly concentrated compounds (Fig. 8A and B). With this approach, only uric acid could be reliably assigned. Thus, for the determination of caffeine and other purines, sample clean-up is necessary, as is shown by the pherograms presented in Fig. 8C-E. With the liquid-liquid extraction method developed for serum and saliva samples (Fig. 8C), many compounds became even more concentrated than in urine alone, whereas with the Sep-Pak procedure (Fig. 8D) the urine matrix could be simplified, but the determination of caffeine was not possible. However, the Bond Elut Certify method allowed the unambiguous determination of caf-

feine and paraxanthine in this urine sample (Fig. 8E).

#### *Theophylline and caffeine concentrations in serum samples from patients*

The determination of theophylline in human serum samples by MECC was performed by the external and internal standard methods using theobromine as the reference compound. All measurements were made on an ABI instrument. Peak areas of single injections were used as the basis for data evaluation. Two approaches were investigated, the direct injection of serum samples and simplification of the sample matrix by Sep-Pak extraction prior to sample analysis. With direct sample injection calibration graphs were constructed with spiked human serum samples in the concentration range 10–120  $\mu\text{M}$  (five data points) and with 60  $\mu\text{M}$  theobromine as an internal standard. Detection was at 280 nm. A typical pherogram is shown in Fig. 9B. The cali-

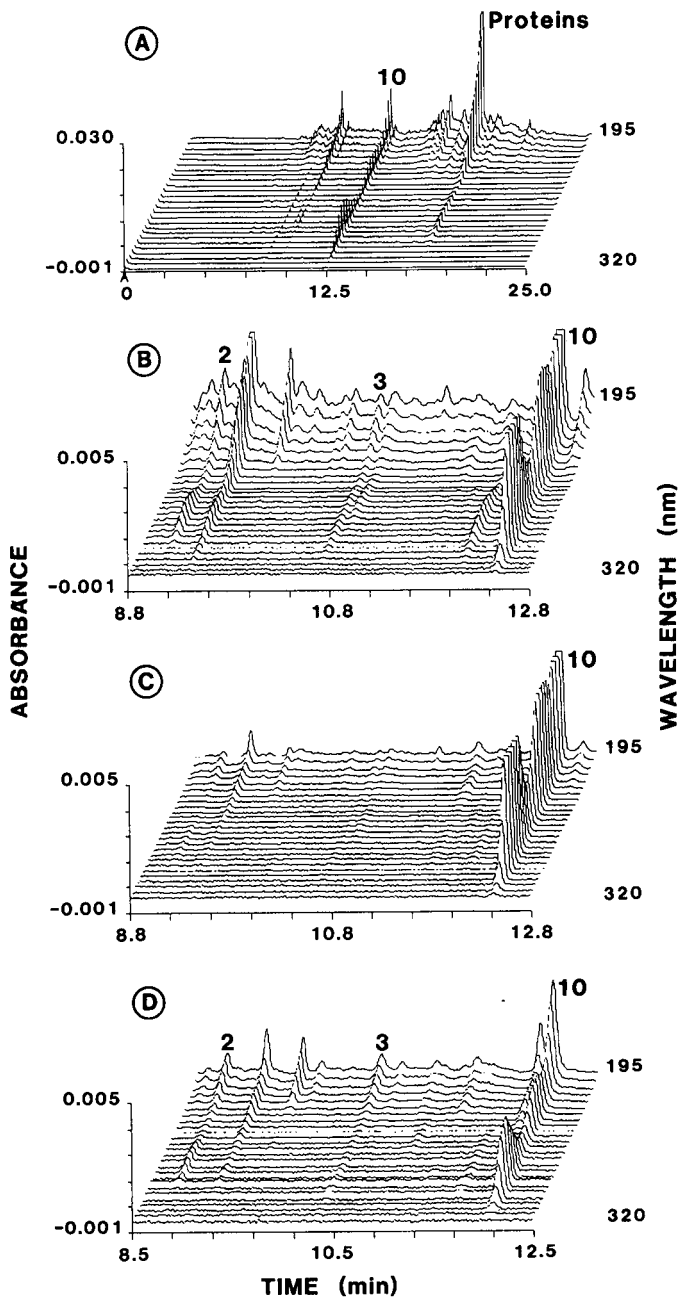


Fig. 7. Pherograms of saliva samples. (A) Complete data plot between 0 and 25 min and (B) expanded section of the same run with direct injection of a saliva sample which was collected 1 h after the self-administration of 280 mg of caffeine. (C) Data obtained after the direct injection of a saliva sample from a subject who does not consume any caffeine. (D) Data plot of the saliva sample of panels A and B but after liquid-liquid extraction. Power conditions as in Fig. 1.

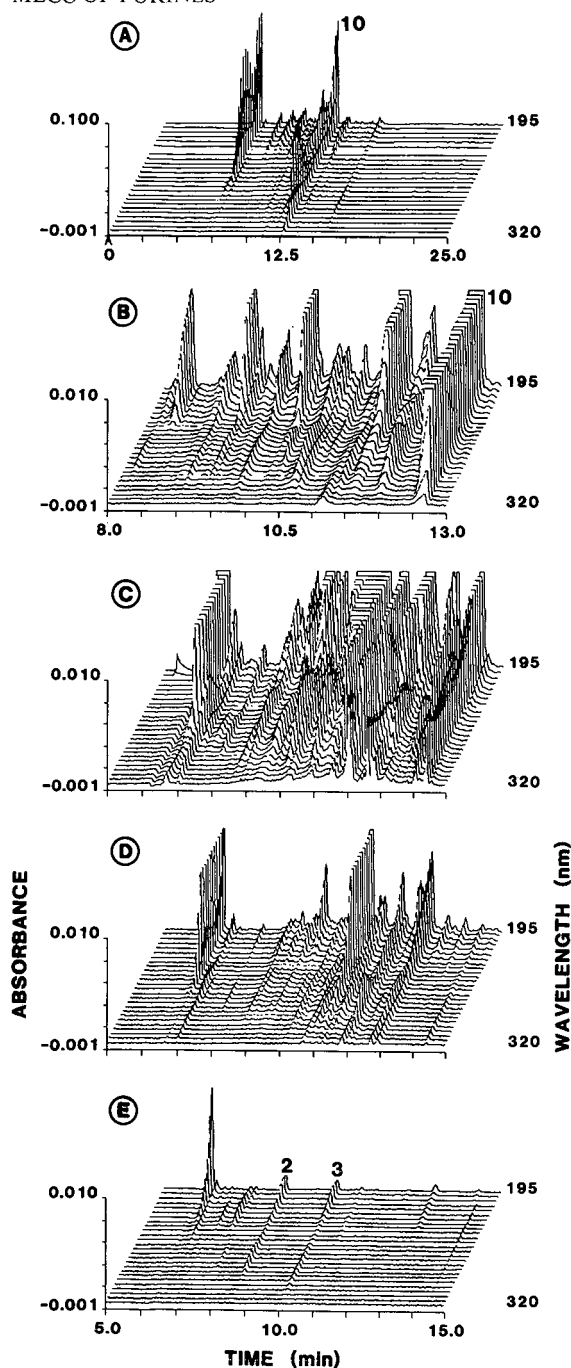


Fig. 8. Three-dimensional pherograms of a urine sample. The complete data plot of a directly injected urine sample is presented in panel A and part of the data on a ten-fold more sensitive absorbance scale in panel B. Three-dimensional data plots of the same urine sample obtained after (C) liquid-liquid, (D) Sep-Pak and (E) Bond Elut Certify extraction are also shown. Power conditions as in Fig. 1.

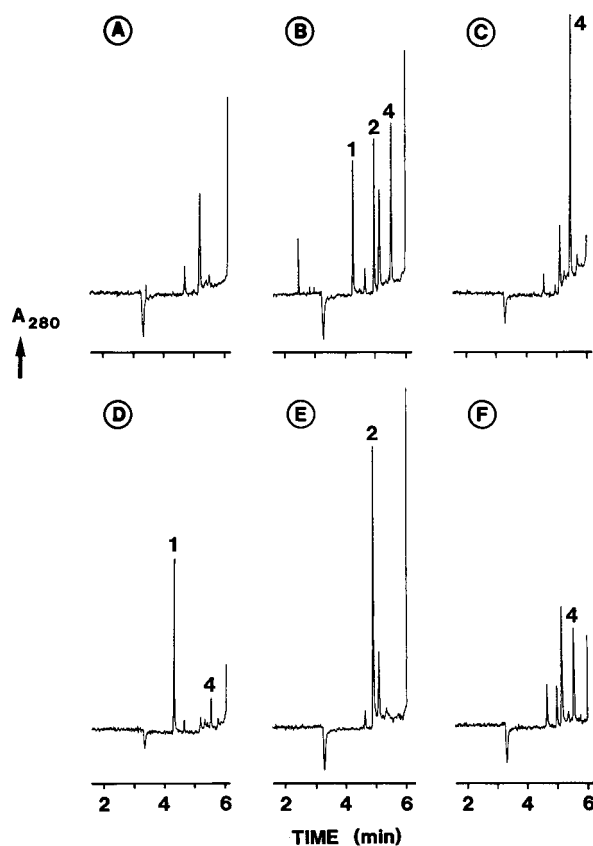


Fig. 9. Single-wavelength electropherograms (280 nm) obtained with direct injection of serum samples using the automated instrument. The injection time was 1 s, the effective capillary length was 37 cm and the applied voltage was a constant 15 kV (32  $\mu$ A current) in all instances. (A) Blank serum sample; (B) blank serum sample spiked with theobromine, caffeine and theophylline (60  $\mu$ M each); (C) sample from patient receiving theophylline; (D) sample from patient receiving theophylline spiked with theobromine (60  $\mu$ M); (E) sample from infant (caffeine treatment); (F) sample from infant (theophylline treatment).

bration graphs were linear (typical correlation coefficient 0.995; slope 37.7;  $y$ -intercept 5.2  $\mu$ M). Similar correlations were obtained with external data evaluation, *i.e.*, without the incorporation of the internal standard. It was interesting to find that bovine plasma could not be used as a calibration matrix for the direct sample injection because of interfering peaks. For Sep-Pak extraction calibration graphs were constructed with bovine plasma spiked with theophylline in the concentration range 5–160  $\mu$ M (six data points) and with 40  $\mu$ M theobromine as an internal standard. Detection was at 200 and 280 nm. The graphs showed good linearities with

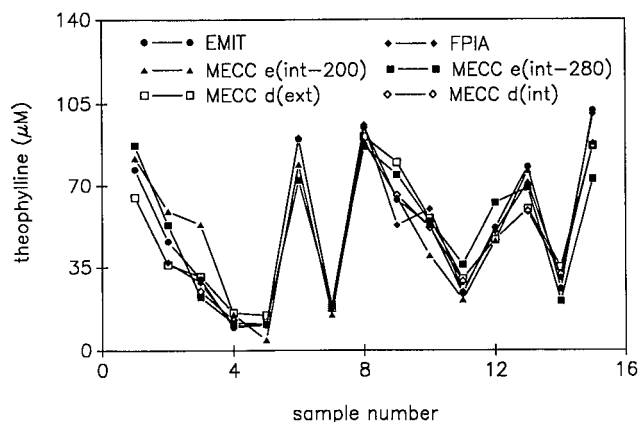


Fig. 10. Theophylline concentrations in serum samples from fifteen patients determined by MECC with direct injection (evaluated with and without internal standard and denoted by d(int) and d(ext), respectively), MECC after solid-phase extraction and with detection at 200 and 280 nm (both evaluated with internal standard and denoted by e(int-200) and e(int-280), respectively), EMIT and FPIA.

correlation coefficients of 0.998 and 0.995, slopes of 35.05 and 24.04 and  $y$ -intercepts of  $-10.6$  and  $-3.21 \mu\text{M}$  for the two sets of data, respectively. Slightly lower correlations were obtained using the external standard method.

Fifteen serum samples from patients receiving theophylline treatment were analysed by MECC and their theophylline concentrations compared with those obtained by two non-isotopic immunological techniques, EMIT and FPIA. All the data correlated well (Fig. 10 and Table I). It is interesting to note that the data from the two immunological procedures correlate better (coefficient 0.988, see Table I) than the MECC data evaluated with different approaches (coefficients between 0.895 and 0.984). The MECC data were slightly lower than those obtained by EMIT (Fig. 11A), indicating the presence of cross-reactivity of other purines in the immunoassays. The data summarized in Table I show that with direct sample injection better correlations with the EMIT data were obtained compared with Sep-Pak extraction. This suggests that more reliable theophylline concentrations are determined without extraction. Furthermore, after extraction, more reliable data were obtained when monitored at 280 than when monitored at 200 nm, this difference being attributed to the difference in the number of detected peaks at the two wave-

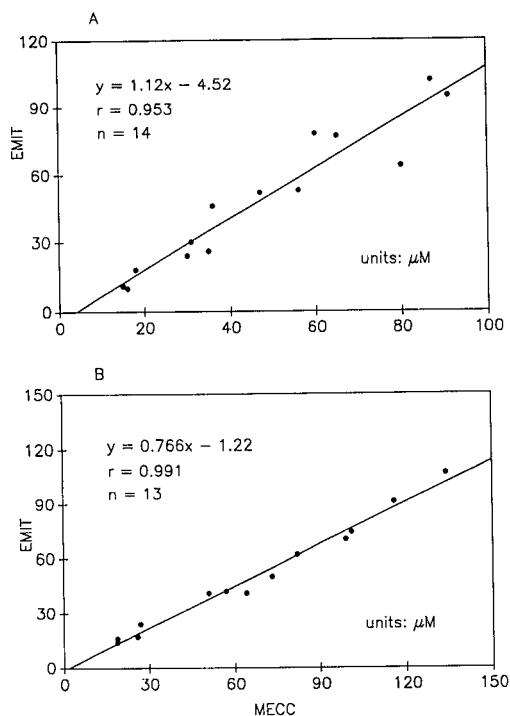


Fig. 11. Comparison of drug concentrations determined by EMIT and MECC (obtained with direct injection of serum sample and without incorporation of an internal standard). (A) Theophylline concentration in serum samples from adult patients; (B) caffeine concentrations in serum samples from infants born prematurely.

lengths (Fig. 5). Several serum samples also showed distortions of the theophylline peaks, which were not seen in longer capillary columns. The deviations, however, are insignificant with respect to the relatively wide treatment range used for theophylline. With direct sample injection good reproducibility was obtained. The mean retention time (relative standard deviation; R.S.D.) for theophylline of ten consecutively injected samples was 5.47 min (0.6%). The R.S.D. of peak areas was 5–7%. The theophylline concentrations determined with and without the inclusion of the internal standard were essentially equal. This is in contrast to the results with purines (data not shown) and barbiturates [15,16] using sample extraction prior to analysis.

The determination of caffeine in serum samples from infants born prematurely was performed by the external standard method using peak areas of single injections as the basis for data evaluation.

TABLE I

## LINEAR REGRESSION ANALYSIS DATA OF COMPARATIVE SERUM THEOPHYLLINE CONCENTRATIONS

The acronyms d(int) and d(ext) represent data obtained with direct injection of serum samples and data evaluation based on internal and external calibration, respectively. e(int-280) and e(int-200) refer to Sep-Pak extraction and detection at 280 and 200 nm, respectively.

Assay 1 (x-axis)	Assay 2 (y-axis)	<i>n</i>	Slope	y-Intercept ( $\mu M$ )	<i>r</i>
MECC d(int)	MECC d(ext)	8	1.01	3.44	0.984
MECC d(ext)	EMIT	14	1.12	-4.52	0.953
MECC d(int)	EMIT	8	1.23	-7.62	0.972
MECC d(ext)	MECC e(int-280)	14	0.976	2.36	0.913
MECC d(int)	MECC e(int-280)	8	0.969	1.37	0.936
MECC e(int-280)	EMIT	15	1.06	-1.79	0.930
MECC e(int-200)	EMIT	14	1.03	-0.213	0.947
MECC e(int-200)	MECC e(int-280)	14	0.964	1.89	0.895
FPIA	EMIT	15	1.01	0.503	0.988

Samples were directly injected and pherograms were measured at 280 nm. Typical pherograms are depicted in Fig. 9E and F. Calibration graphs were constructed with spiked human serum samples in the concentration range 10–120  $\mu M$  (five data points). Linear relationships with correlation coefficients between 0.995 and 0.999, slopes of 0.0117 to 0.0135 and y-intercepts ranging from 0.9 to 3.2  $\mu M$  caffeine were obtained. Fifteen samples from infants receiving either theophylline or caffeine treatment were analysed and the caffeine concentrations compared with those obtained by EMIT. The data correlated well (Fig. 11B), but the MECC data were consistently higher than the caffeine concentrations determined by EMIT. No explanation could be found for this deviation. In fact, higher EMIT concentrations were expected because of cross reactivity with other substituted purines, including paraxanthine and theophylline. To gain an insight into this problem further investigations are required. The average retention time was 4.93 min with an R.S.D. of 1.7% ( $n = 10$ ). Occasionally, a sudden increase in elution time to values between 5.2 and 6.7 min was observed. If this occurred a 15-min wash with 1 *M* sodium hydroxide solution had to be used to restore the correct measuring conditions. Reproducibility was improved by rinsing with 0.1 *M* sodium hydroxide solution and buffer for 3 and 5 min, respectively, between each run.

It is interesting to add that caffeine concentrations greater than 50  $\mu M$  originated from caffeine

pharmacotherapy, whereas caffeine concentrations less than 40  $\mu M$  were found during treatment with theophylline, when caffeine is produced as metabolite. The conclusion is reached that MECC with direct sample injection and without the inclusion of an internal standard produces pharmacologically meaningful data which can be used for monitoring caffeine in serum samples of infants during treatment with theophylline or caffeine.

## CONCLUSIONS

Using body fluids as samples, fast-scanning polychrome detection is an interesting approach for the characterization and identification of eluting zones in MECC. The multi-wavelength data reveal the suitability of the direct injection of serum or saliva samples (no protein removal required) for the determination of micromolar amounts of caffeine, theophylline, paraxanthine and uric acid by MECC. The direct injection of urine is not possible for the determination of methylated xanthines at these concentrations.

The determination of theophylline and caffeine in serum samples by MECC with on-column UV adsorption detection can be used for concentrations of pharmacological interest, *i.e.*, covering the therapeutic ranges of the two drugs (55–110 and 25–100  $\mu M$ , respectively). The results correlate well with those obtained by homogeneous immunoassays. No sample pretreatment of any sort, including pre-

column treatment as in high-performance liquid chromatography [20], nor internal standard is required. Measurements can be performed on serum samples as small as a few microlitres and with a detection limit in the low micromolar range. Hence MECC is an attractive method for therapeutic drug monitoring, particularly for small sample volumes such as body fluids from infants. It is a rapid assay which is easy to perform. With MECC as described here, it is assumed that total drug concentrations are determined (but not proven) as a result of the release of the protein-bound portion of the drug by SDS (direct sample injection) or the extraction procedure. Free drug concentrations would be obtained if the proteins were removed (*e.g.*, with ultrafiltration) prior to sample injection or extraction.

#### ACKNOWLEDGEMENTS

The authors acknowledge helpful discussions with Dr. Thomas Zysset and the valuable technical assistance of Mr. Frank Binder and the laboratory technicians of the departmental drug assay laboratory. The generous loan of the 206 UVIS detector by its manufacturer, Linear Instruments (Reno, NV, USA), is gratefully acknowledged. The disposable bags of instant coffee were kindly provided by Haco (Gümligen, Switzerland). This work was sponsored partly by the Research Foundation of the University of Bern and the Swiss National Science Foundation.

#### REFERENCES

- 1 A. Herxheimer, *Drug Ther. Bull.*, 17 (1979) 91.
- 2 M.C. Nahata, D. A. Powell and T. G. Franko, *Ther. Drug Monit.*, 5 (1983) 269.
- 3 T. Zysset, A. Wahlländer and R. Preisig, *Ther. Drug Monit.*, 6 (1984) 348, and references cited therein.
- 4 G. Jost, A. Wahlländer, U. von Mandach and R. Preisig, *Hepatology*, 7 (1987) 338.
- 5 R. L. Boeckx, E. M. Frith and F. E. Simons, *Ther. Drug Monit.*, 1 (1979) 65.
- 6 J. L. Cohen, C. Cheng, J. P. Henry and Y. L. Chan, *J. Pharm. Sci.*, 67 (1978) 1093.
- 7 K. K. Midha, S. S. Sved, R. D. Hossie and I. J. McGilveray, *Biomed. Mass Spectrom.*, 4 (1977) 172.
- 8 M. C. Roach, P. Gozel and R. N. Zare, *J. Chromatogr.*, 426 (1988) 129.
- 9 Y. Tanaka and W. Thormann, *Electrophoresis*, 11 (1990) 760.
- 10 T. Nakagawa, Y. Oda, A. Shibukawa and H. Tanaka, *Chem. Pharm. Bull.*, 36 (1988) 1622.
- 11 T. Nakagawa, Y. Oda, A. Shibukawa, H. Fukuda and H. Tanaka, *Chem. Pharm. Bull.*, 37 (1989) 707.
- 12 D. E. Burton, M. J. Sepaniak and M. P. Maskarinec, *J. Chromatogr. Sci.*, 24 (1986) 347.
- 13 H. Nishi, T. Fukuyama and M. Matsuo, *J. Chromatogr.*, 515 (1990) 245.
- 14 H. Nishi and S. Terabe, *Electrophoresis*, 11 (1990) 691.
- 15 W. Thormann, P. Meier, C. Marcolli and F. Binder, *J. Chromatogr.*, 545 (1991) 445.
- 16 P. Meier and W. Thormann, *J. Chromatogr.*, 559 (1991) 505.
- 17 D. E. Burton, M. J. Sepaniak and M. P. Maskarinec, *Chromatographia*, 21 (1986) 583.
- 18 M. J. Arnaud, in P. B. Dews (Editor), *Caffeine*, Springer, Berlin, 1984, pp. 3–38.
- 19 I. A. Siegel, H. Ben-Aryeh, D. Gozal, A. A. Colin, R. Szargel and D. Laufer, *Ther. Drug Monit.*, 12 (1990) 460.
- 20 Y. Kouno, C. Ishikura, N. Takahashi, M. Homma and K. Oka, *J. Chromatogr.*, 515 (1990) 321.



# Factors affecting the separation of inorganic metal cations by capillary electrophoresis

Andrea Weston and Phyllis R. Brown\*

*Department of Chemistry, University of Rhode Island, Kingston, RI 02881 (USA)*

Petr Jandik, William R. Jones and Allan L. Heckenberg

*Ion Analysis Department, Waters Chromatography Division of Millipore, 34 Maple St., Milford, MA 01757 (USA)*

---

## ABSTRACT

Various alkali metals, alkaline earth metals, transition metals and lanthanides were separated by capillary electrophoresis, and factors influencing the separations were studied. The reproducible separation of fifteen metal cations was completed in 8 min. The detection system showed a linear relationship between peak area and analyte concentration. To permit the use of indirect photometric detection and to ensure symmetrical peak shapes, a highly UV-absorbing amine having an electrophoretic mobility similar to those of the analyte cations was chosen as the major component of the electrolyte. Complexing compounds were added to the electrolyte to maximize selectively the differences in the apparent mobilities of the cations and enhance the separations.

---

## INTRODUCTION

In recent years, capillary electrophoresis (CE) has been used mainly for the separation of biological macromolecules [1–3]. Fewer papers have been published relating to inorganic compounds. Of these papers, the majority report separations of inorganic anions. The separations of anions by CE have been shown to be highly sensitive (nanomolar limits of detection) and highly efficient (20 000–1 000 000 theoretical plates) [4–7]. They offer a selectivity which is complementary to existing techniques such as ion chromatography. Although the first published application of CE for inorganic cations was reported in 1967 by Hjerten [8], few applications of CE for inorganic cations have since been published [9–11].

A recent paper on cation separations was published by Foret *et al.* [12]. In this method, indirect UV detection was utilized for the separation of a group of lanthanide cations. Complexing agents were added to the electrolyte to effect a highly efficient separation in under 5 min. A different

complexing agent was employed by Swaile and Sepaniak [13] for the laser-based fluorescence detection of three common metal ions. The effect of pH and complexing agent concentration on the separation of the three metal cations was described.

We report here several successful separations of Group IA, Group IIA, transition metal and lanthanide cation mixtures by CE, with indirect UV detection, and some method development rules unique to the separation of inorganic cations.

## EXPERIMENTAL

A Waters (Milford, MA, USA) Quanta 4000 capillary electrophoresis system, equipped with a positive power supply, was used. Fused-silica capillaries, 75  $\mu\text{m}$  I.D. and 52 cm from the point of sample introduction to the detector window, were obtained from Waters (AccuSep capillaries). Indirect UV detection was achieved with the use of a zinc lamp and a 214-nm optical filter. The samples were introduced into the capillary by 20- or 30-second hydrostatic injections from a height of 10 cm.

Standard 2-ml polyethylene sample vials (Sun Brokers, Wilmington, NC, USA) were used as containers for the carrier electrolyte and for all the standards and samples. A Waters 860 Data Station and Waters SIM interface were used to record and evaluate the electropherograms, the subsequent statistical processing being performed using Cricket-Graph (Cricket Software, Malvern, PA, USA) with a Macintosh SE personal computer (Apple Computers, Cupertino, CA, USA).

All solutions, electrolytes and standards were prepared using 18-M $\Omega$  water generated by a Milli-Q laboratory water purification system (Millipore, Bedford, MA, USA). The transition metal standards were prepared by the dilution of standards obtained from Sigma (St. Louis, MO, USA), and the alkali and alkaline earth metal standards were prepared from salts obtained from Aldrich Chemical (Milwaukee, WI, USA), as was the analytical reagent-grade  $\alpha$ -hydroxyisobutyric acid (HIBA). The UV background-providing component of the electrolyte, UVCat 1, was obtained from Waters.

## RESULTS AND DISCUSSION

The selectivity of ion separations in CE can be predicted from the tabulated values of the equivalent ionic conductivities [14],  $\lambda_i$ , which are directly related to the electrophoretic mobilities,  $\mu_i$ , of the ions:

$$\mu_i = \lambda_i/F \quad (1)$$

where  $F$  is the Faraday constant. The electrophoretic mobilities, in turn, determine the velocity of the analyte under a given set of CE conditions. The resulting velocity of the ion is a sum of two contributions, the velocity of the ion and the velocity of the electroosmotic flow (EOF). The EOF is the bulk flow of liquid due to the effect of the electric field on the electrical double layer adjacent to the capillary wall. Hence it is the apparent mobility of the ions, which includes an electroosmotic component in addition to an electrophoretic component, that is measured in CE.

The velocity of migration in CE,  $v_{app}$ , is given in its simplest form by

$$v_{app} = (\mu_i + \mu_{EOF}) E \quad (2)$$

where  $\mu_i$  is the electrophoretic mobility of the ion,

$\mu_{EOF}$  is the electroosmotic flow mobility and  $E$  is the electric field, or, in more detail, by [15]

$$v_{app} = \frac{L_d}{t} \cdot \frac{L_t}{V} \cdot E = \frac{L_d}{t} \quad (3)$$

where  $v_{app}$  is the measured migration velocity of the solute peak,  $E$  is the electric field strength,  $L_d$  is the length of the capillary from the injection end to the detector,  $L_t$  is the total length of the capillary,  $t$  is the measured migration time of the solute and  $V$  is the voltage across the capillary.

The velocity of the EOF is dependent on the charge of the capillary wall. The polarity of the charge on the wall determines the direction of the flow, while the amount of charge (zeta potential) determines the magnitude of the flow. For the anions, the differences in the equivalent ionic conductivities are sufficiently large that selective separations of large numbers of anions are possible [16] simply by modifying the velocity of the EOF. On the other hand, the equivalent ionic conductivities of the cations, and consequently their mobilities, are too close in many instances to expect selective separations based solely on the migration behavior of free cations. However, the apparent mobilities of cations may be affected by altering the charge on the analytes, by modifying the pH of the electrolyte or by the addition of complexing agents to the electrolyte.

An example of the effect of pH on the separation of inorganic cations is given by the separation of the alkali metals from the ammonium ion. In the separation of inorganic cations by CE, the positively charged ions migrate away from the positive power supply towards the detector, in the direction of the EOF. Smaller ions with higher equivalent ionic conductivities migrate the fastest (Fig. 1). In the separation in Fig. 2a, the cations elute in the order predicted by their equivalent ionic conductivities. As expected, potassium and ammonium co-elute at pH 6.15 owing to their identical equivalent ionic conductivities. By altering the pH of the electrolyte, the ionization of the alkali metal cations and their mobilities will be essentially unaffected. However, as the pH of the electrolyte is increased, the  $\text{NH}_4^+$  becomes progressively less protonated ( $\text{p}K_b$  of  $\text{NH}_4^+ = 4.75$ ) and its apparent mobility decreases. At pH 8.5, the apparent mobilities of  $\text{K}^+$  and  $\text{NH}_4^+$  become sufficiently different to permit an effective separa-

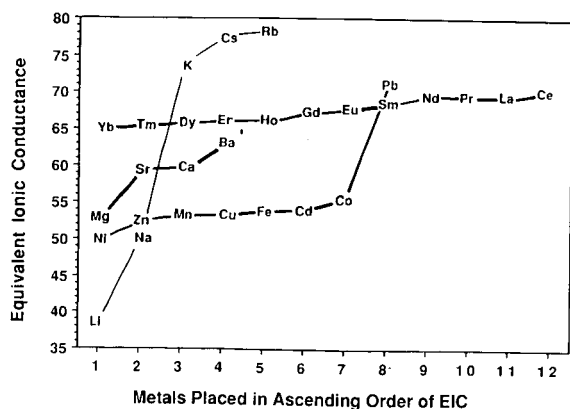


Fig. 1. Plot of equivalent ionic conductivities (EIC) of the Group IA, Group IIA, transition metal and lanthanide metal cations, placed in ascending order of EIC. The closer the values, the more challenging the separation. It can be seen that the Group IA cations are more readily separated than the transition metals or the lanthanides.

tion (Fig. 2b). In addition to its effect on the mobility of the ammonium ion, the pH also affects the EOF. As the silanol groups on the capillary wall are weakly acidic ( $pK = 7-8$ ) [17], the degree of their ionization is also dependent on the pH of the electrolyte. The higher the pH, the faster is the EOF. Thus, at high pH (*ca.* 8), in addition to the separation of  $K^+$  from  $NH_4^+$ , the total analysis time also decreases (Fig. 2b).

The separation of the alkali metals from the alkaline metals provides another example where poor resolution may be predicted from the equivalent ionic conductivities. As the equivalent ionic conductivities of strontium and calcium and also of sodium and magnesium are close, strontium and calcium co-migrate as do sodium and magnesium. In this instance, however, the addition of a weak complexing agent alters the apparent mobilities of the

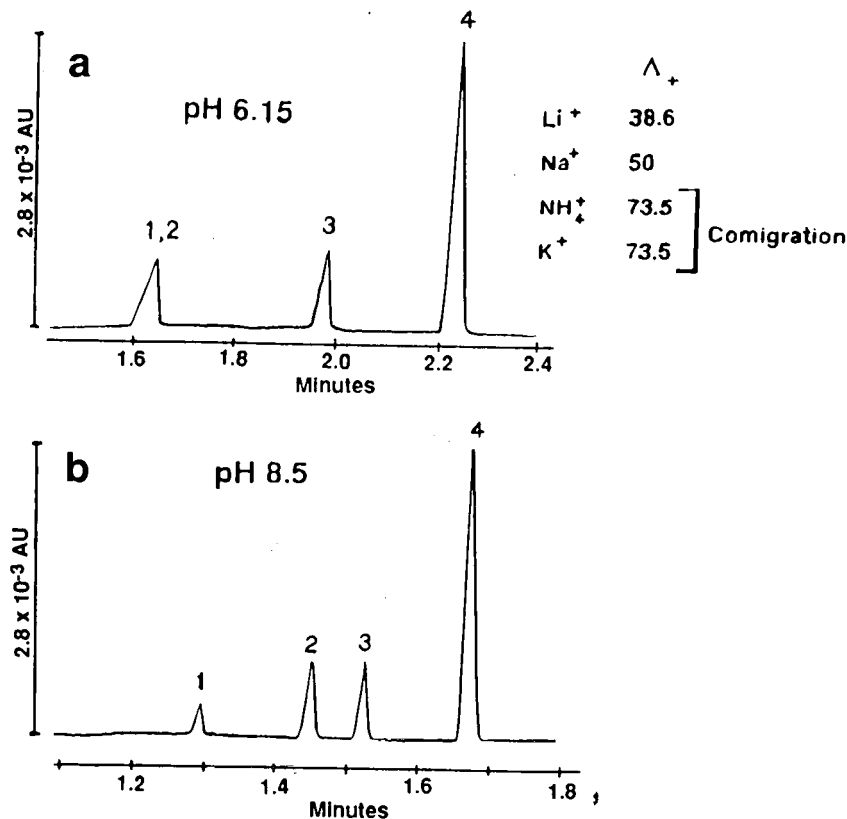


Fig. 2. (a) Separation of the Group IA metal cations in the presence of ammonia, using indirect photometric detection at 214 nm. Carrier electrolyte contains 5 mM morpholinoethanesulphonate adjusted to pH 6.15. A fused-silica capillary ( $75 \mu m$  I.D., 52 cm from the point of injection to the detector) was used for the separation and a positive voltage of 25 kV was employed. The sample was introduced into the capillary by hydrostatic injection, from a height of 10 cm, for 30 s. Potassium and ammonium have identical equivalent ionic conductivities and therefore co-elute. Peaks: 1 = potassium; 2 = ammonium; 3 = sodium; 4 = lithium. (b) CE separation of the Group IA metal cations at pH 8.5 in the presence of ammonia. CE conditions as in (a) except for pH. By altering the pH, the apparent mobilities of the analytes can be selectively modified. Peaks as in (a).

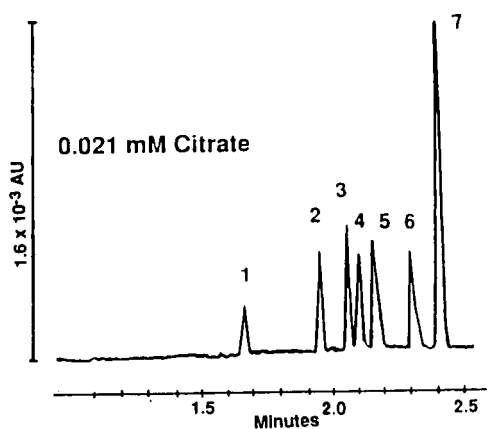


Fig. 3. Complete separation of Group IA and IIA metal cations due to the addition of a complexing agent (citrate) to the electrolyte. Carrier electrolyte, 5 mM Waters UVCat-1 (pH 5.5); capillary, 60 cm  $\times$  75  $\mu$ m I.D. fused silica; voltage, 25 kV (positive); hydrostatic injection, 30 s from 10 cm height; indirect UV detection at 214 nm. Peaks: 1 = potassium; 2 = barium; 3 = strontium; 4 = sodium; 5 = calcium; 6 = magnesium; 7 = lithium.

cations sufficiently to permit a separation. An equilibrium, described by the stability constant  $K$ , is formed between the more mobile free cation and the slower, complexed form of the cation.

The interaction between the metal ion, M, and the

complexing agent, CA, is described by the following equilibrium expression [13]:

$$K = \frac{[M(CA^-)_n]}{[M][CA^-]^n} \quad (4)$$

where  $n$  is the number of ligands. The apparent (observed) electrophoretic mobilities of the metal ions are then a combination of the mobilities of the free metal and the various complexes:

$$\mu_{app} = \alpha \mu_{M^+} + \beta \mu_{ML} + \dots + \mu_{EOF}$$

where  $\alpha + \beta = 1$  and are the mole fractions of each species in the capillary and  $\mu_{M^+}$  and  $\mu_{ML}$  are the mobilities of the free ion and a metal complex, respectively.

Although the equivalent ionic conductivities of the co-migrating cations are close, they are not identical. The addition of citrate at pH 5.5, a weakly complexing agent, is sufficient to effect a separation (Fig. 3). The additional benefit of the complexing agent is its effect on peak symmetry. The uncomplexed metals have a higher mobility than the co-ion in the background electrolyte and the peaks show various degrees of fronting [18,19]. The complexed cations possess lower apparent mobilities, which more closely match the mobility of the electrolyte. The peak shapes in Fig. 3, therefore, exhibit better peak symmetry.

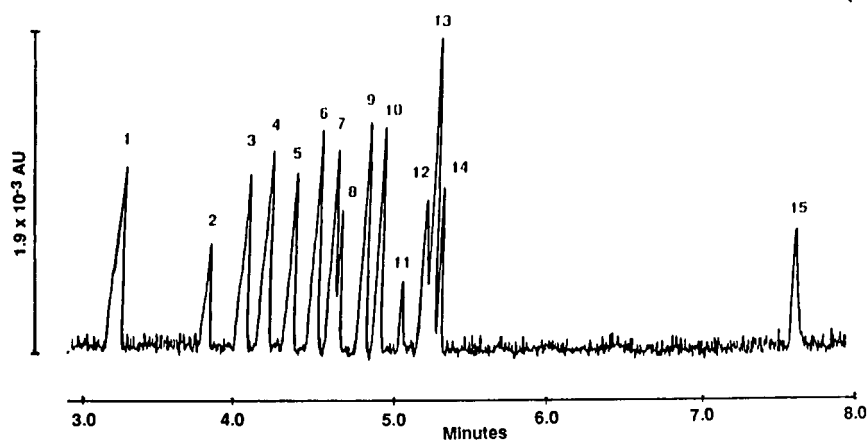


Fig. 4. Separation of alkali, alkaline earth and transition metal cations with the aid of an alternative complexing agent, HIBA. Carrier electrolyte, 5 mM Waters UVCat-1–6.5 mM HIBA (pH 4.4); capillary as described previously; voltage, 20 kV (positive); hydrostatic injection, as before; indirect UV detection at 214 nm. Peaks: 1 = potassium (0.8 ppm); 2 = barium (1.5 ppm); 3 = strontium (1.5 ppm); 4 = calcium (0.7 ppm); 5 = sodium (0.6 ppm); 6 = magnesium (0.4 ppm); 7 = manganese (0.8 ppm); 8 = cadmium (0.8 ppm); 9 = iron(II) (1.0 ppm); 10 = cobalt (0.8 ppm); 11 = lead (1.0 ppm); 12 = nickel (0.6 ppm); 13 = lithium (0.2 ppm); 14 = zinc (0.4 ppm); 15 = copper (0.6 ppm).

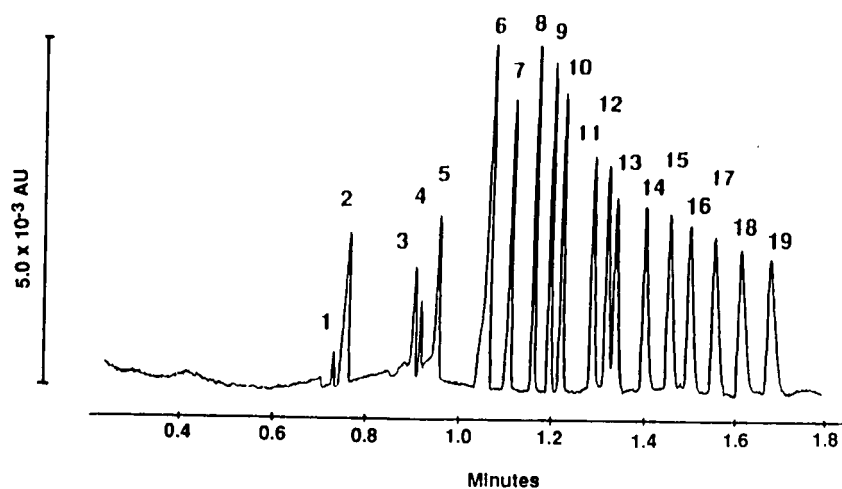


Fig. 5. Simultaneous separation of alkali, alkaline earth and lanthanide metal cations by CE. Carrier electrolyte, 10 mM Waters UVCat-1–4.0 mM HIBA (pH adjusted to 4.4 with acetic acid); capillary, 36.5 cm  $\times$  75  $\mu$ m I.D. fused silica; voltage, 30 kV (positive); hydrostatic injection, 20 s from 10 cm height; indirect UV detection at 214 nm. Peaks: 1 = rubidium (2 ppm); 2 = potassium (5 ppm); 3 = calcium (2 ppm); 4 = sodium (1 ppm); 5 = magnesium (1 ppm); 6 = lithium (1 ppm); 7 = lanthanum (5 ppm); 8 = cerium (5 ppm); 9 = praseodymium (5 ppm); 10 = neodymium (5 ppm); 11 = samarium (5 ppm); 12 = europium (5 ppm); 13 = gadolinium (5 ppm); 14 = terbium (5 ppm); 15 = dysprosium (5 ppm); 16 = holmium (5 ppm); 17 = erbium (5 ppm); 18 = thulium (5 ppm); 19 = ytterbium (5 ppm).

In addition to citrate, HIBA has also been utilized as a complexing agent applicable to the separation of metals which have mobilities similar to one another [14]. HIBA is most commonly used in

complexation reactions with the lanthanides [20], but was chosen here to aid in the separation of the alkali and alkaline earth metals from a group of transition metals (Fig. 4). The separations of 1 ppm

TABLE I

SENSITIVITIES FOR ALKALI, ALKALINE EARTH, TRANSITION AND LANTHANIDE METALS USING CAPILLARY ELECTROPHORESIS

Detection limits defined as  $2 \times$  noise in concentration units, using 10-cm hydrostatic injection and indirect UV detection at 214 nm for 30 s with the alkali, alkaline earth and transition metals and for 20 s with the lanthanide metals.

Cation	Sensitivity (ppb) <sup>a</sup>	Cation	Sensitivity (ppb) <sup>a</sup>	Cation	Sensitivity (ppb) <sup>a</sup>
Potassium	135	Manganese	120	Lanthanum	92
Barium	394	Cadmium	162	Cerium	77
Strontium	243	Iron	132	Praseodymium	81
Calcium	107	Cobalt	110	Neodymium	89
Sodium	96	Lead	388	Samarium	115
Magnesium	57	Nickel	118	Europium	120
Lithium	18	Zinc	72	Gadolinium	138
		Copper	206	Terbium	146
				Dysprosium	154
				Holmium	163
				Erbium	170
				Thulium	183
				Ytterbium	197

<sup>a</sup> The American billion ( $10^9$ ) is meant here.

TABLE II  
REPRODUCIBILITY OF CE METHOD

Cation	R.S.D. (%) ( <i>n</i> = 5)	
	Migration time	Peak area
Potassium	0.34	1.80
Sodium	0.37	2.60
Lithium	0.38	1.40
Barium	0.37	0.97
Strontium	0.38	1.07
Calcium	0.37	1.20
Magnesium	0.38	0.80

or less of each of fifteen cations was completed in 8 min with baseline resolution between the majority of the peaks. In ion chromatography, the separation of these fifteen cations requires two different separation modes and detection schemes [14].

The equivalent ionic conductivities of the lanthanides are even more similar to one another than those of the transition metals. The separation of the lanthanides from one another is therefore more chellenging than the separation of transition metals. Using HIBA as the complexing agent, a mixture containing less than 5 ppm of each of nineteen cations, including lanthanides and alkali and alka-

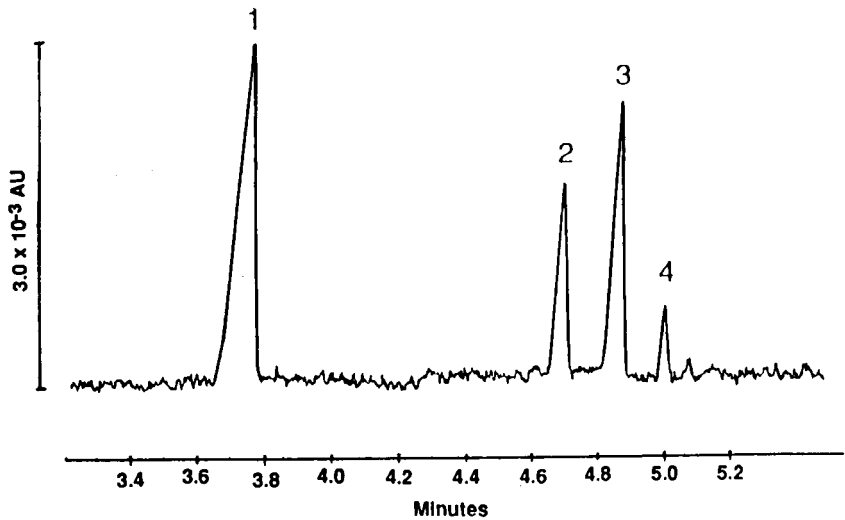


Fig. 7. CE analysis of a commercial cough syrup. CE conditions as in Fig. 6. The syrup was diluted 1:200 before analysis. Peaks: 1 = potassium; 2 = calcium; 3 = sodium; 4 = magnesium.

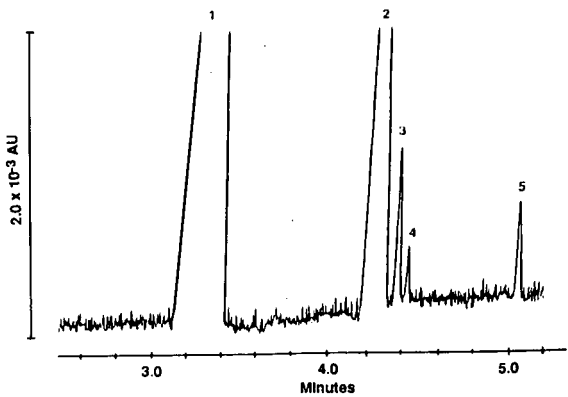


Fig. 6. CE analysis of a fermentation broth sample. Carrier electrolyte, 5 mM Waters UVCat-1–6.5 mM HIBA (pH 4.2), capillary, 60 cm × 75 μm I.D. fused silica; voltage, 20 kV (positive); hydrostatic injection, 30 s from 10 cm height; indirect UV detection at 214 nm. The original sample was diluted 1:100 before analysis. In the diluted sample, potassium and sodium are in the 100–1000 ppm range, while the other three analytes are in the 10–100 ppb range. Peaks: 1 = potassium; 2 = sodium; 3 = magnesium; 4 = manganese; 5 = zinc.

line earth metals, were separated in under 2 min (Fig. 5).

Minimum detectable injected concentrations for the metals, based on the peak height of twice the baseline noise, are given in Table I for the electrophoretic buffer containing UVCat-1 and HIBA at

pH 4.4. The relative standard deviation (R.S.D.) in migration time for each of the Group IA and IIA cations, shown in Table II, was less than 1% ( $n = 5$ ), and the R.S.D. in peak area was less than 2% (except Na = 2.6%). The linear dynamic range was almost two orders of magnitude above the detection limit ( $R > 0.997$ ), the upper limit of calibration being due to loss of resolution rather than loss of linearity.

The potential of this technique for analyses for cations in complex matrices is shown in Figs. 6 and 7. With only a dilution required for the sample preparation, a fermentation broth and various cough medicines were both successfully analyzed for metal cations. In addition, this method shows great potential for use in environmental monitoring, to determine the concentrations of major cationic components in fresh, sea and waste waters rapidly, reproducibly and with high sensitivity.

## REFERENCES

- 1 B. L. Karger, A. S. Cohen and A. Guttman, *J. Chromatogr.*, 492 (1989) 585.
- 2 F. Foret and P. Boček, *Electrophoresis*, 11 (1990) 661.
- 3 W. G. Kuhr, *Anal. Chem.*, 62 (1990) 403R.
- 4 F. E. P. Mikkers, F. M. Everaerts and T. M. P. Verheggen, *J. Chromatogr.*, 169 (1979) 11.
- 5 F. Foret, M. Deml, V. Kahle and P. Boček, *Electrophoresis*, 7 (1986) 430.
- 6 L. Gross and E. S. Yeung, *J. Chromatogr.*, 60 (1989) 169.
- 7 W. R. Jones and P. Jandik, *Am. Lab.*, 22 (1990) 51.
- 8 S. Hjertén, *Chromatogr. Rev.*, 9 (1967) 122.
- 9 T. Tsuda, K. Nomura and G. Nakagawa, *J. Chromatogr.*, 264 (1983) 385.
- 10 X. Huang, T.-K. J. Pang, M. J. Gordon and R. N. Zare, *Anal. Chem.*, 59 (1987) 2747.
- 11 J. L. Beckers, Th. P. E. M. Verheggen and F. M. Everaerts, *J. Chromatogr.*, 452 (1988) 591.
- 12 F. Foret, S. Fanali, A. Nardi and P. Boček, *Electrophoresis*, 11 (1990) 780.
- 13 D. F. Swaile and M. J. Sepaniak, *Anal. Chem.*, 63 (1991) 179.
- 14 P. R. Haddad and P. E. Jackson, *Ion Chromatography (Journal of Chromatography Library, Vol. 46)*, Elsevier, Amsterdam, 1990.
- 15 P. D. Grossman, J. C. Colburn and H. H. Lauer, *Anal. Biochem.*, 179 (1989) 28.
- 16 W. R. Jones, P. Jandik and A. Weston, *J. Chromatogr.*, 546 (1991) 445.
- 17 M. L. Hair and W. Herte, *J. Phys. Chem.*, 74 (1970) 91.
- 18 F. E. P. Mikkers, F. M. Everaerts and Th. P. E. M. Verheggen, *J. Chromatogr.*, 169 (1979) 1.
- 19 F. Foret, S. Fanali, L. Ossicini and P. Boček, *J. Chromatogr.*, 470 (1989) 299.
- 20 T. Hirokawa, N. Aoki and Y. Kiso, *J. Chromatogr.*, 312 (1984) 11.





# Prediction of migration behavior of oligonucleotides in capillary gel electrophoresis

András Guttman\*, Robert J. Nelson and Nelson Cooke

*Beckman Instruments, Inc., Palo Alto, CA 94304 (USA)*

---

## ABSTRACT

The influence of the primary structure (base composition) on the electrophoretic migration properties of single-stranded oligodeoxyribonucleotides in capillary polyacrylamide gel electrophoresis was investigated using homo- and heterooligomers under denaturing and non-denaturing conditions. Homooligodeoxyribonucleotides of equal chain lengths but of different base composition showed significant differences in mobility. In addition, the migration properties of heterooligomers were found to be highly dependent on their base composition. A simple equation is presented for predicting relative migration times using denaturing and non-denaturing polyacrylamide capillary gel electrophoresis. Orange-G was used as an internal standard and as the basis of the relative migration time calculations. Examples are presented using homo- and heterooligomers in the 10–20-mer range to show the correlation of the primary structure and their predicted and observed migration rates.

---

## INTRODUCTION

High-performance capillary electrophoresis (HPCE) is rapidly becoming an important separation tool in analytical biochemistry and molecular biology [1–5]. Capillary polyacrylamide gel electrophoresis of oligonucleotides and DNA and RNA molecules under denaturing and non-denaturing conditions have been shown to provide separations of very high efficiency [6–8]. As an instrumental approach to electrophoresis, the method offers the ability to do multiple injections on the same gel-filled capillary column, with on-column UV detection and on-line data processing [9].

In this work, the influence of the primary structure (base composition) on the migration properties of homo- and heterooligodeoxyribonucleotides in capillary polyacrylamide gel electrophoresis was studied. Previous reports have described slab [10] and capillary [11] polyacrylamide gel electrophoresis under denaturing conditions as an accurate method for the determination of the chain length and molecular weight of small DNA and RNA molecules. However, in our experiments with capillary

gel electrophoresis, the direct correlation between the chain length of the homooligomers and their migration times was found to be unreliable. It was observed that under both denaturing and non-denaturing electrophoresis conditions, oligonucleotides were not separated according to their chain lengths alone. In fact, base composition plays a significant role in oligonucleotide migration in polyacrylamide gels. A reliable model has been developed to predict the electrophoretic migration times of any oligonucleotide with a known sequence relative to homooligomers having the same chain lengths.

## EXPERIMENTAL

### *Apparatus*

In all these studies, the P/ACE System 2100 capillary electrophoresis apparatus (Beckman Instruments, Palo Alto, CA, USA) was used with reversed polarity (cathode on the injection side and anode on the detection side). The separations were monitored on-column at 254 nm. The temperature of the gel-filled capillary columns was controlled by the liquid

cooling system of the P/ACE instrument at 25°C. The electropherograms were acquired and stored on an Everex 386/33 computer using System Gold software (Beckman Instruments).

### Procedures

Polymerization of the non-denaturing linear (non-cross-linked) polyacrylamide was accomplished within fused-silica capillary tubing (Polymicro Technologies, Phoenix, AZ, USA) in 100 mM Tris-borate-2 mM EDTA (pH 8.5) buffer. Polymerization was initiated by ammonium peroxydisulfate and catalyzed by tetramethylethylenediamine (TEMED). The denaturing gel column employed was the eCAP gel U100P (Beckman Instruments). To obtain a similar pore structure, both the non-denaturing and the denaturing polyacrylamide gels were prepared at the same concentration. The samples were injected electrokinetically into the gel-filled capillary columns, typically using 0.1 W s. Samples were boiled for 5 min and then cooled for 30 s in ice-water before injection.

### Chemicals

The homodecamers of adenylic [ $p(\text{dA})_{10}$ ], cytidylic [ $p(\text{dC})_{10}$ ], guanylic [ $p(\text{dG})_{10}$ ] and thymidyl [ $p(\text{dT})_{10}$ ] acids, the homooligomer mixtures,  $p(\text{dA})_{12-18}$ ,  $p(\text{dC})_{12-18}$ ,  $p(\text{dG})_{12-18}$  and  $p(\text{dT})_{12-18}$ , and the human K-ras oncogenes (dGTTGGAGCT-G-TGGCGTAG and dGTTGGAGCT-T-GTGGCGTAG) were purchased for Pharmacia (Piscataway, NJ, USA). The samples were diluted to 0.5 absorbance unit/ml (ca. 20  $\mu\text{g}/\text{ml}$ ) with water before injection and were stored at -20°C when not in use. Ultra-pure electrophoresis-grade acrylamide, Tris, boric acid, EDTA, urea, ammonium peroxydisulfate and TEMED were employed (Schwartz/Mann Biotech, Cambridge, MA, USA). Orange G (Sigma, St. Louis, MO, USA) was used in the electrophoretic separations as an internal standard at 0.001% concentration. All buffer solutions were filtered through a 0.2- $\mu\text{m}$  pore size filter (Schleicher & Schüll, Keene, NH, USA) and carefully vacuum degassed.

## RESULTS AND DISCUSSION

Initial efforts were focused on achieving high-res-

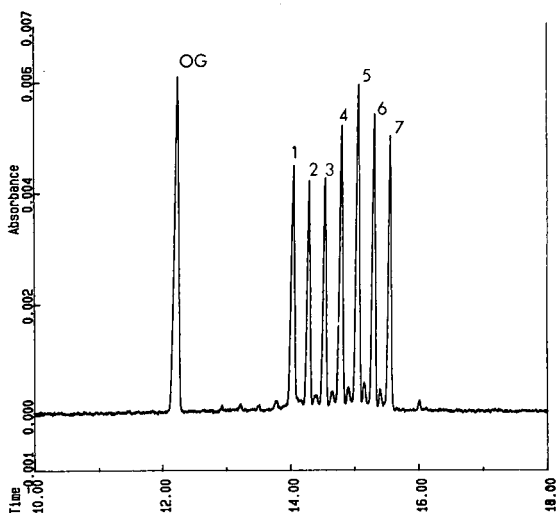


Fig. 1. Non-denaturing capillary polyacrylamide gel electrophoretic separation of  $p(\text{dT})_{12-18}$  oligodeoxythymidilic acid mixture with the internal standard Orange G. Peaks: OG = Orange G; 1 =  $p(\text{dT})_{12}$ ; 2 =  $p(\text{dT})_{13}$ ; 3 =  $p(\text{dT})_{14}$ ; 4 =  $p(\text{dT})_{15}$ ; 5 =  $p(\text{dT})_{16}$ ; 6 =  $p(\text{dT})_{17}$ ; 7 =  $p(\text{dT})_{18}$ . Conditions: isoelectrostatic (constant applied electric field), 400 V/cm; prepacked non-denaturing polyacrylamide gel column, effective length 40 cm, total length 47 cm; buffer, 100 mM Tris-boric acid-2 mM EDTA (pH 8.5); injection, 0.1 W s. Time in min.

olution separations of homooligodeoxyribonucleotides using high-performance capillary gel electrophoresis under non-denaturing and denaturing conditions. As reported earlier [12], the pH of the buffer system used in capillary gel electrophoresis has a remarkable effect on the migration properties of different homooligomers; therefore, the pH in all experiments reported (denaturing and the non-denaturing) was maintained at 8.5.

### Non-denaturing capillary polyacrylamide gel columns

Fig. 1 shows the baseline resolution of one of the four homooligomer mixtures [ $p(\text{dT})_{12-18}$ ] separated on a non-denaturing polyacrylamide gel-filled capillary column. The peak marked OG corresponds to the internal standard Orange G, which was selected because of its rapid migration relative to the short oligonucleotides. The other three homooligomer mixtures,  $p(\text{dA})_{12-18}$ ,  $p(\text{dC})_{12-18}$  and  $p(\text{dG})_{12-18}$  were also separated on the same column, again using Orange G as the internal standard. The relative migration times were calculated

from the ratio of the migration time of the actual oligomer to that of the internal standard. A linear relationship existed between the relative migration times ( $t'$ ) and the chain lengths of the homooligomers ( $n$ ) in the size range examined, as shown in Fig. 2, according to the following equations:

$$p(dA)_n: t'(A_n) = 0.0161n + 0.7979 \quad (1a)$$

(R.S.D. 0.999%)

$$p(dT)_n: t'(T_n) = 0.0205n + 0.9023 \quad (1b)$$

(R.S.D. 0.999%)

$$p(dC)_n: t'(C_n) = 0.0182n + 0.7961 \quad (1c)$$

(R.S.D. 0.998%)

$$p(dG)_n: t'(G_n) = 0.0071n + 0.9590 \quad (1d)$$

(R.S.D. 0.999%)

where  $p(dA)_n$ ,  $p(dT)_n$ ,  $p(dC)_n$  and  $p(dG)_n$  are the individual homo- $n$ -mers of adenylic, thymidylic, cytidylic and guanylic acid, respectively, and R.S.D. is the relative standard deviation.

The plots have similar slopes for the  $p(dA)_{12-18}$ ,  $p(dC)_{12-18}$  and  $p(dT)_{12-18}$  samples (eqns. 1a-c), but a different slope for  $p(dG)_{12-18}$  (eqn. 1d). This last slope is much lower, resulting in a different migration order depending on the base number for a mixture of the four homooligomers. For example, the migration order below 14 bases is  $A > C > G > T$ , between 14 and 18 bases  $A > G > C > T$  and above 18 bases  $G > A > C > T$ . This anomalous migration behavior may be due to the strong self-

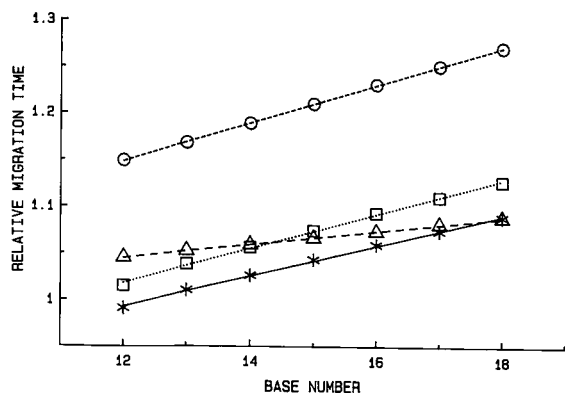


Fig. 2. Relationship between the chain length and the relative migration time of the homodeoxyribooligomer mixtures on non-denaturing polyacrylamide gel-filled capillary. Conditions as in Fig. 1. The calculation of relative migration times was based on the migration time of Orange G. \* =  $p(dA)_{12-18}$ ; ○ =  $p(dT)_{12-18}$ ; □ =  $p(dC)_{12-18}$ ; △ =  $p(dG)_{12-18}$ .

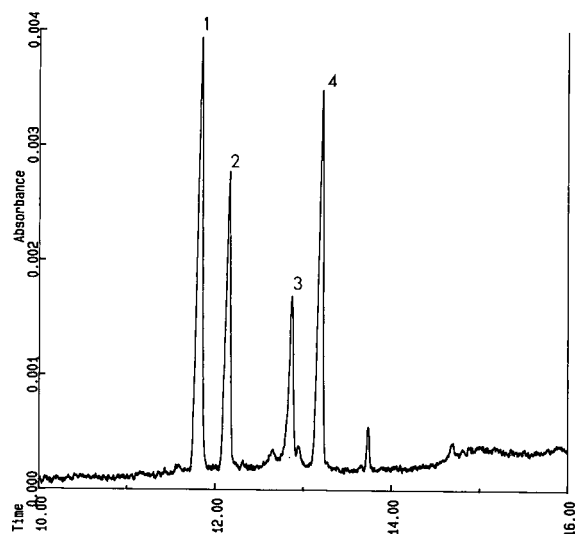


Fig. 3. Capillary polyacrylamide gel electrophoretic separation of a homodecamer mixture on non-denaturing gel. Peaks: 1 =  $p(dA)_{10}$ ; 2 =  $p(dC)_{10}$ ; 3 =  $p(dG)_{10}$ ; 4 =  $p(dT)_{10}$ . Conditions as in Fig. 1. Migration time of Orange G (determined in the immediately following run): 12.386 min.

association tendency of guanosine under non-denaturing conditions, which might cause conformational changes such as bending [10].

Also of interest in Fig. 2 is the comigration of the 14-mers of  $p(dC)$  and  $p(dG)$  and that of the 18-mers of  $p(dA)$  and  $p(dG)$ . These results indicate that the migration rate of some oligomers could be relatively insensitive to a difference in base composition resulting in co-migration in non-denaturing gels.

As the base-specific retardation of oligonucleotides is an additive effect [13], migration times can be easily predicted using linear extrapolation from the relative migration times of the homooligomers. Fig. 3 shows a non-denaturing capillary gel electrophoretic separation of a mixture of four homodecamers and Table I gives the predicted and observed relative migration times of the four sample components. As can be seen in Table I, there is excellent agreement between the extrapolated and observed relative migration time values ( $\pm 0.1\%$ ). The identification of the homooligomers was accomplished by spiking with the individual compounds. The small peak after peak 4 is an impurity from  $p(dT)_{10}$ . As Orange G migrates too close to peak 3, its migration time was determined in the immediate-

TABLE I  
OBSERVED AND PREDICTED RELATIVE MIGRATION TIMES OF VARIOUS HOMO- AND HETEROOLIGODEOXYRIBONUCLEOTIDES IN NON-DENATURING POLYACRYLAMIDE CAPILLARY GEL ELECTROPHORESIS

Relative migration times were calculated using Orange G as internal standard.

Nucleotide sequence	Relative migration time		Migration order
	Observed	Calculated	
p(dA) <sub>10</sub>	0.957	0.960	1
p(dC) <sub>10</sub>	0.983	0.981	2
p(dG) <sub>10</sub>	1.039	1.032	3
p(dT) <sub>10</sub>	1.068	1.107	4
dGTTGGAGCT-G-GTGGCGTAG	1.149	1.150	1
dGTTGGAGCT-C-GTGGCGTAG	1.156	1.155	2
dGTTGGAGCT-T-GTGGCGTAG	1.160	1.161	3

ly following run, by using peak 1 [p(dA)<sub>10</sub>] as internal standard.  
Whereas simple relative migration time extrapolation is satisfactory for homooligomers, the prediction of the relative migration time of a heterooligomer (*t'*) is improved by using the relative migration times of the four corresponding homooligomers in the following relationship:

$$t'(A_aT_tC_cG_g) = \frac{a}{n} t'(A_n) + \frac{t}{n} t'(T_n) + \frac{c}{n} t'(C_n) + \frac{g}{n} t'(G_n) \quad (2)$$

where *t'* is relative migration time vs. the internal standard, *n* is the oligonucleotide chain length (*n* = *a* + *t* + *c* + *g*) and *a*, *t*, *c* and *g* are the numbers of the individual bases in the oligonucleotide. The parameters *t'*(*A<sub>n</sub>*), *t'*(*T<sub>n</sub>*), *t'*(*C<sub>n</sub>*) and *t'*(*G<sub>n</sub>*) correspond to the relative migration times of the homooligo-*n*-mers of adenylic, thymidylic, cytidylic and guanylic acid, respectively. The most accurate calculation requires the availability of standards with chain lengths equal to the unknown. If standards are not available, the extrapolated values from linear plots such as Figs. 2 and 5 should be used. Capillary polyacrylamide gel electrophoresis of homo- and/or heterooligomers of known chain lengths and base compositions showed excellent correlation between

the observed and predicted migration times (Table I).  
We have also obtained (see Fig. 4) the separation of heterooligomers with the same chain lengths and similar sequences in order to emphasize the effectiveness of the mathematical prediction of the migration order. Fig. 4 shows the non-denaturing gel

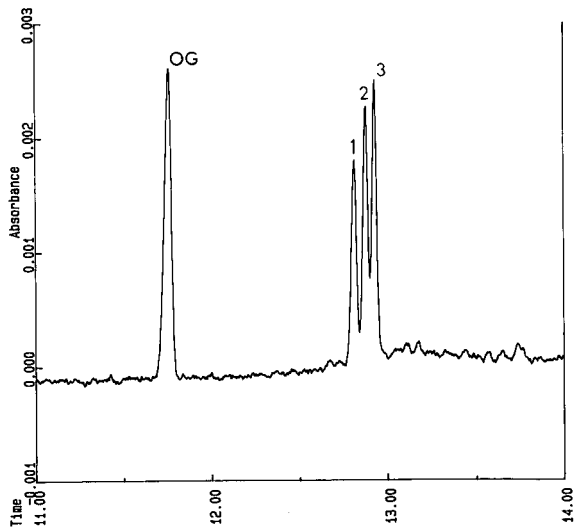


Fig. 4. Non-denaturing capillary polyacrylamide gel electrophoretic separation of a human K-ras oncogene mixture. Peaks: 1 = dGTTGGAGCT-G-GTGGCGTAG; 2 = dGTTGGAGCT-C-GTGGCGTAG; 3 = dGTTGGAGCT-T-GTGGCGTAG. Conditions as in Fig. 1.

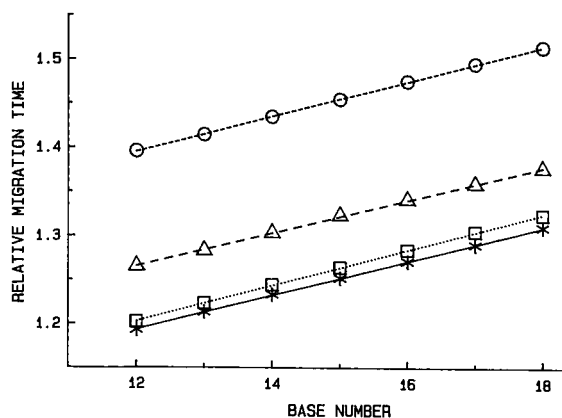


Fig. 5. Relationship between the chain length and the relative migration time of the homodeoxyribooligomer mixtures on a denaturing polyacrylamide gel-filled capillary. Conditions: iso-electrostatic (constant applied electric field), 400 V/cm; eCAP gel U100P column, effective length 40 cm, total length 47 cm; injection, 0.1 W s. The calculation of relative migration times was based on the migration time of Orange G. Symbols as in Fig. 2.

electrophoretic separation of a mixture of three human K-ras oncogenes. These oligomers have the same chain length (19-mers) and almost the same primary sequence, differing only by one base in the middle (position 10) of the chain (see primary structure in Table I). Because of the high resolving power of capillary gel electrophoresis, this method is capable of separating these closely related species. Note that the observed and predicted migration times are

very similar (see Table I). The location of guanosine in the tenth position speeds up the migration rate of the heterooligomer, relative to that of cytidine or thymidine. This migration order is consistent with the data in Fig. 2. The identity of the oligomers was confirmed by spiking the mixture with the individual compounds. As no homooligo-nanodecamers were available for these experiments, the  $t'(A_n)$ ,  $t'(T_n)$ ,  $t'(C_n)$  and  $t'(G_n)$  parameters for eqn. 2 were calculated by extrapolation of the linear plots in Fig. 2.

#### Denaturing capillary polyacrylamide gel columns

When denaturing gels (eCAP gel U100P) were used for the separation of the same oligonucleotide mixtures, different migration properties were observed. In contrast to the behavior seen in Fig. 2, all four of the homooligomer mixtures have parallel plots of relative migration time as a function of the chain lengths, as shown in Fig. 5, according to the following equations:

$$p(dA)_n: t'(A_n) = 0.0193n + 0.9609 \quad (\text{R.S.D. } 0.999\%) \quad (3a)$$

$$p(dT)_n: t'(T_n) = 0.0202n + 1.1559 \quad (\text{R.S.D. } 0.999\%) \quad (3b)$$

$$p(dC)_n: t'(C_n) = 0.0204n + 0.9590 \quad (\text{R.S.D. } 0.999\%) \quad (3c)$$

$$p(dG)_n: t'(G_n) = 0.0188n + 1.0398 \quad (\text{R.S.D. } 0.999\%) \quad (3d)$$

TABLE II

OBSERVED AND PREDICTED RELATIVE MIGRATION TIMES OF VARIOUS HOMO- AND HETEROOLIGODEOXYRIBONUCLEOTIDES IN DENATURING POLYACRYLAMIDE CAPILLARY GEL ELECTROPHORESIS

Relative migration times were calculated using Orange G as internal standard.

Nucleotide sequence	Relative migration time		Migration order
	Observed	Calculated	
p(dA)10	1.153	1.155	1
p(dC)10	1.163	1.162	2
p(dG)10	1.237	1.233	3
p(dT)10	1.356	1.355	4
dGTTGGAGCT-G-GTGGCGTAG	1.427	1.422	2
dGTTGGAGCT-C-GTGGCGTAG	1.416	1.419	1
dGTTGGAGCT-T-GTGGCGTAG	1.430	1.429	3

The non-parallel discrepancy previously observed on non-denaturing gels does not occur in this instance, probably owing to the denaturing effect of the 7 *M* urea in the gel [14]. By means of eqn. 2, relative migration times can be calculated in a similar way as above. The relative migration data for the samples are summarized in Table II, which shows the observed and calculated migration times of the homo- and heterooligonucleotide mixtures separated on denaturing gel. Referring back to the migration behavior of the oligonucleotides on non-denaturing gels, it is important to note that the migration order has been changed among the three human K-ras oncogenes (Tables I and II). Again, this was confirmed by spiking the mixture with the individual oncogenes. As in this instance the increasing guanosine content does not have the same accelerating effect as was observed on the non-denaturing gel, the migration order is the same as that observed for the homooligomers (Table II,  $A > C > G > T$ ). The accelerating effect of A- and C-rich oligomers and the retarding effect of G- and T-rich oligomers can be predicted for the chain-length range examined.

## CONCLUSIONS

Investigations of the electrophoretic migration behavior of various homo- and heterooligomers of known nucleotide sequences have been presented. Using non-denaturing gels, we found that the relative migration order is not constant for homooligomers of the same chain length, but is dependent on the base number: for base numbers less than 14, it is  $A > C > G > T$ , and for base numbers larger than 18, it is  $G > A > C > T$ . This discrepancy is probably caused by the strong self-association tendency of guanosine (conformation changes such as bending). Employing denaturing gels, however, the migration order of the homooligomers is the same for the entire chain-length range examined, namely  $A > C > G > T$ . In this instance, the self-association effect of the guanosine is assumed to be negligible owing to the presence of urea, a denaturing agent, in the gel. The denaturing gel has a much higher sensitivity to guanosine content than the non-denaturing gel. There is, however, an increased ability of the non-denaturing gel to resolve A and C over the denaturing gel (compare Figs. 2 and 5).

Because of the parallel slopes achieved using denaturing gels, we believe that the migration times of heterooligonucleotides are more predictable in this instance. In addition, it can be demonstrated using eqn. 2 that several combinations of sequences might be resolved in one system and not in another. Therefore, in order to increase the confidence in oligomer identity, one might need to utilize both denaturing and non-denaturing conditions.

Oligonucleotides of different sequences, but with the same chain length, are more likely to show different migration times. With respect to base composition, an equation was derived in order to predict the migration time of a known oligonucleotide sequence. Reproducibility and additivity of base-specific retardation are the basis of the calculation procedure for the relative migration times. It should be emphasized that eqn. 2 is considered to be valid only for primer-sized oligonucleotides ( $n < 25$ ), and it should be further evaluated for longer ones.

The method opens up a new feature of capillary polyacrylamide gel electrophoresis in the identification of, and discrimination between, oligonucleotides by their mobility shift relative to an internal standard. This can be easily computed by an automated capillary electrophoretic system, such as the P/ACE 2100. A further interesting application of this equation is to calculate the migration time differences between oligonucleotides, and to design appropriate electrophoresis conditions, such as column length, necessary for their separation. This can be important for separations of oligonucleotides of the same chain length but different base composition, such as two strands of double-stranded DNA (denaturing gel), or in point mutation studies (non-denaturing gel). Whereas denaturing conditions are necessary to reduce guanosine self-association and solve compression problems, non-denaturing gels might also offer different selectivity in certain instances.

## ACKNOWLEDGEMENT

The authors thank Professor B. L. Karger and Drs. Aran Paulus and László Králik for stimulating discussions. The help of Phyllis Browning in the preparation of the manuscript is also greatly appreciated.

## REFERENCES

- 1 J. W. Jorgenson and K. D. Lukacs, *Science (Washington, D.C.)*, 222 (1983) 266.
- 2 S. Hjerten and M. D. Zhu, *J. Chromatogr.*, 347 (1985) 191.
- 3 R. A. Wallingford and A. G. Ewing, *Anal. Chem.*, 60 (1988) 258.
- 4 M. J. Gordon, X. Huang, S. L. Pentoney and R. N. Zare, *Science (Washington, D.C.)*, 242 (1988) 224.
- 5 B. L. Karger, *Nature (London)*, 339 (1989) 641.
- 6 J. A. Lux, H. F. Yin and G. Schomburg, *J. High Resolut. Chromatogr.*, 13 (1990) 436.
- 7 A. Guttman, A. S. Cohen, D. N. Heiger and B. L. Karger, *Anal. Chem.*, 62 (1990) 137.
- 8 D. N. Heiger, A. S. Cohen and B. L. Karger, *J. Chromatogr.*, 516 (1990) 33.
- 9 B. L. Karger, A. S. Cohen and A. Guttman, *J. Chromatogr.*, 492 (1989) 585.
- 10 T. Maniatis, E. F. Fritsch and J. Sambrook, *Molecular Cloning: a Laboratory Manual*. Cold Spring Harbor Laboratory, Cold Spring Harbor, NY, 1982.
- 11 A. Paulus, E. Gassmann and M. G. Field, *Electrophoresis*, 11 (1990) 702.
- 12 A. Guttman, A. Arai, A. S. Cohen, E. Uhlmann and B. L. Karger, presented at the 14th International Symposium on Column Liquid Chromatography, Boston, MA, May 20-25, 1990, paper P414.
- 13 R. Frank and H. Koester, *Nucleic Acids Res.*, 6 (1979) 2069.
- 14 A. Guttman and N. Cooke, *Am. Biotech. Lab.*, 9, No. 4 (1991) 10.





# Capillary electrophoresis with electrochemical detection employing an on-column Nafion joint

Thomas J. O'Shea<sup>☆</sup>, Robin D. Greenhagen, Susan M. Lunte\* and Craig E. Lunte

*Center for Bioanalytical Research, University of Kansas, Lawrence, KS 66046 (USA)*

Malcolm R. Smyth

*School of Chemical Sciences, Dublin City University, Dublin (Ireland)*

Donna M. Radzik

*Marion Merrell Dow, Kansas City, MO 64134 (USA)*

Nori Watanabe

*Department of Industrial Chemistry, Faculty of Engineering, University of Tokyo, Tokyo (Japan)*

---

## ABSTRACT

The construction and evaluation of an on-column joint utilizing Nafion tubing for the isolation of the electrical circuit from the detection end of a capillary zone electrophoresis system is described. The joint enables electrochemical detection to be performed without adverse effects from the applied high voltage. The joint is both simple to construct and durable. The electrochemical detector employing a carbon fiber working electrode exhibited high coulometric efficiencies and a detection limit of  $6 \cdot 10^{-9} M$  or 34.8 amol for hydroquinone. A high efficiency, of the order of 185 000 theoretical plates, was achieved for this compound. This system was evaluated for the detection of phenolic acids in apple juice and for the determination of naphthalene-2,3-dicarboxaldehyde derivatized amino acids in a brain homogenate. The use of voltammetry as a method of compound verification was also demonstrated.

---

## INTRODUCTION

Since its introduction over a decade ago, capillary electrophoresis (CE) has become established as a powerful analytical tool for the separation of complex mixtures [1]. Capillaries with small diameter are advantageous over conventional slab gel electrophoresis for separations owing to the higher efficiency, lower joule heating effect and faster analysis times. One of the main areas of research is the development of sensitive detection systems. Because

of the small sample volumes involved, high-sensitivity and small-volume detectors are necessary for the analysis of many real samples. Much of the work on CE and most commercial instruments use UV detection. However, as this is an optical technique and is path-length dependent, the sensitivity is limited when using small-diameter capillaries. Laser-based fluorescence detectors are more sensitive, but are expensive and limited to certain wavelengths. Electrochemical detection has an advantage over these methods in that the response is not dependent on path-length; therefore, very small capillary diameters can be used without a sacrifice in signal. It also utilizes relatively inexpensive instrumentation [2,3].

---

<sup>☆</sup> Permanent address: School of Chemical Sciences, Dublin City University, Dublin, Ireland.

Wallingford and Ewing [2,3] developed an off-column electrochemical detector and have reported  $10^{-8}$  M detection limits for several catechol compounds. In their system, two pieces of capillary column are coupled inside a piece of porous glass capillary. This joint permits the flow of ions but not bulk electrolytic flow, enabling the detection end of the capillary to be held at ground. The fabrication of this joint assembly is difficult and intricate. Unless perfect alignment of both sections of the capillary is achieved, considerable band broadening can occur. The joint does not appear to be durable as the porous glass is extremely fragile and must be kept submerged in solution. Another limitation of this design is that the porous glass capillary is not readily available. Huang and Zare [4] designed an on-column frit which also served to isolate the final section of the capillary column from the applied electrical field. However, they reported the drawbacks of this design, including lack of capillary-to-capillary reproducibility, leakage of the frit and difficulty of fabrication (requiring the use of a carbon dioxide laser). Recently, Huang *et al.* [5] reported that it is not necessary to isolate the microelectrode from the high voltage if capillaries with very small inside diameter ( $5\text{ }\mu\text{m}$ ) are employed. In such small capillaries, the current generated by

the CE separation is low enough that it does not adversely affect the electrochemical detection. However, as a consequence of the small size, the concentration detection limits are not as low as those reported with larger inside diameter capillary columns.

This paper describes an alternative construction procedure in which the detection end of the capillary column is isolated from the high applied voltage. We believe this system to be simpler and more durable than those previously published. The capacity of the system for the analysis of real samples is explored, in addition to the use of voltammetric characterization as a method of compound identification.

## EXPERIMENTAL

### *Construction of the joint assembly*

Fused-silica capillaries (65–70 cm) with an I.D. of  $50\text{ }\mu\text{m}$  and an O.D. of  $360\text{ }\mu\text{m}$  were obtained from Polymicro Technologies (Phoenix, AZ, USA). A capillary cutter (Supelco, Bellfonte, PA, USA) was used to score the polyimide coating *ca.* 1.5 cm from the end of the capillary column. A 1-cm length of Nafion tubing (I.D.  $0.33\text{ mm}$ , O.D.  $0.51\text{ mm}$ ) (Perma Pure Products, Tom's River, NJ, USA) was then carefully threaded over the score mark. Both

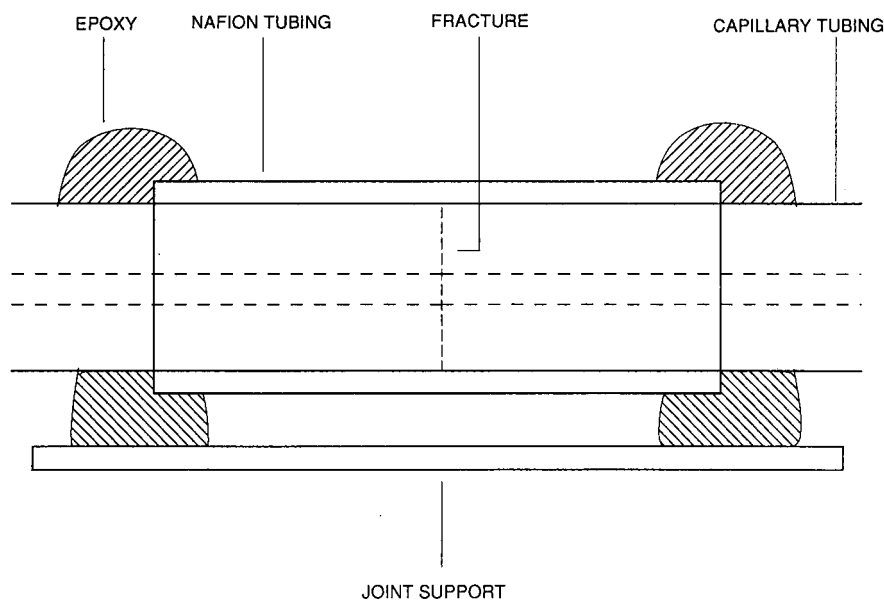


Fig. 1. Schematic diagram of Nafion joint.

ends of the Nafion tubing were sealed to the capillary tubing using 815 epoxy resin (Mid-Con Plastics, Wichita, KS, USA) with 20% (v/v) triethylenetetramine. This was cured overnight. Once cured, gentle pressure was applied to either end of the Nafion tubing, causing the capillary to fracture at the score. The Nafion tube holds the capillary joint securely in place and insures correct alignment. For additional support, the joint was epoxied to a small section of glass. A schematic diagram of the joint is illustrated in Fig. 1. We have completed the construction with a 100% success rate.

### CE apparatus

Electrophoresis in the capillary was driven by a high-voltage d.c. (0–30 kV) power supply (Glassman High Voltage, Whitehouse Station, NJ, USA). The anodic high-voltage end of the capillary was isolated in a Plexiglas box fitted with an interlock for operator safety. A digital microampere current meter was positioned between the platinum wire ground cathode and ground. Experiments were performed at ambient air temperature (24°C). For UV work a CV<sup>4</sup> absorbance detector (ISCO, Lincoln, NE, USA) was employed. Sample introduction was performed using pressure injection, which was found to be reproducible and avoided bias associated with electrokinetic injection. The injection volume was calculated in a continuous-fill mode by recording the time required for the sample to reach the detector.

The Nafion joint was manipulated through two openings in opposite sides of a plastic beaker and

subsequently sealed in place with epoxy. The joint was immersed in buffer solution and this assembly served as the cathodic buffer reservoir. The detection capillary section was then inserted into the electrochemical detection cell. An illustration of the complete system is shown in Fig. 2.

Previous investigations by Wallingford and Ewing [2] reported that back-pressure in the detection capillary section is a significant contributor to zone broadening. However, they demonstrated that if the length is shorter than 2 cm, peak distortion is negligible. Accordingly, we positioned the Nafion joint *ca.* 1.5 cm from the detection end of the column. A small section of polyimide was removed from the end of the detection capillary to provide better visualization of the insertion of the micro-electrode.

### Electrochemical detection

The electrochemical cell is similar in design to those described previously [2,6]. Cylindrical carbon fiber microelectrodes were constructed by aspiration of a 33- $\mu$ m diameter fiber (Avco Specialty Products, Lowell, MA, USA) into a 1.0 mm I.D. capillary tube. The capillary tube was then pulled with a List-Medical Model 3A vertical pipet puller (Medical Systems, Greenvale, NY, USA). Silicone rubber adhesive (General Electric, Waterford, NY, USA) was applied to the tip of the capillary where the fiber protruded. Once cured, the sealant formed an intact seal around the fiber which was found to be resistant to all buffer solutions used. In addition, owing to the nature of the sealant, added flexibility was imparted

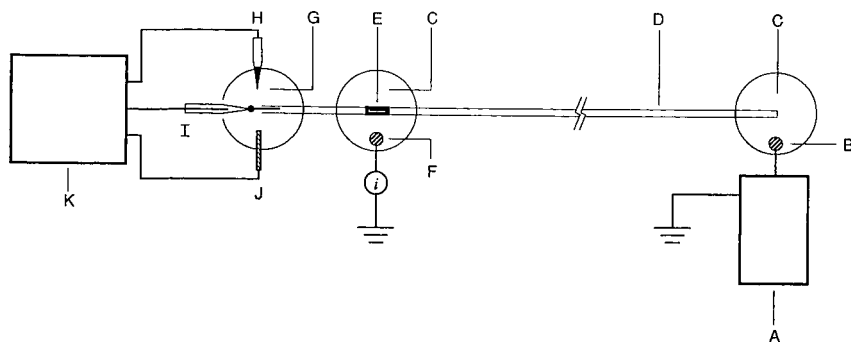


Fig. 2. Schematic diagram of CE system. A, High-voltage power supply; B, anode; C, buffer reservoirs; D, capillary column; E, Nafion joint; F, cathode; G, detection cell; H, reference electrode; I, carbon fiber microelectrode; J, auxiliary electrode; K, amperometric detector.

to the fiber, which aided in the insertion of the fiber into the capillary column. The fiber was then cut to the required length, 150–250  $\mu\text{m}$ , using surgical scissors. Electrical contact was established via a copper wire cemented to the carbon fiber using silver epoxy (Ted Pella, Redding, CA, USA).

The microelectrode was then mounted on an X–Y–Z micromanipulator (Newport, Fountain Valley, CA, USA) and positioned in the electrochemical detection cell. With the aid of an optical microscope, the microelectrode was aligned and inserted into the capillary column. The cell was operated in a three-electrode configuration, with platinum wire auxiliary and a laboratory-built Ag/AgCl reference electrode.

Electrode connections were made to a BAS LC-4C (Bioanalytical Systems, West Lafayette, IN, USA) amperometric detector. The low currents generated at the microelectrode required the electrochemical cell to be shielded in a Faraday cage to reduce noise contributions from external sources.

Electrochemical pretreatment of the microelectrode was performed using a 50-Hz square-wave waveform of 2 V amplitude for 1 min. This was accomplished using a function generator (Exact Electronics, Hillsboro, OR, USA) connected to the external input of the BAS LC-4C. An oscilloscope was used to monitor the applied waveform. Using this arrangement, pretreatment could be performed without removing the microelectrode from the capillary column.

#### *Chemicals*

Hydroquinone, glutamic acid, aspartic acid, *p*-chlorogenic acid, caffeic acid, *p*-coumaric acid and sinapic acid were purchased from Sigma (St. Louis, MO, USA) and used as received. Naphthalene-2,3-dicarboxaldehyde (NDA) was supplied by Oread Labs. (Lawrence, KS, USA). Sodium cyanide was obtained from Fisher Scientific (Fair Lawn, NJ, USA).

All other chemicals were of analytical-reagent grade. All solutions were prepared in NANOpure water (Sybron-Barnstead, Boston, MA, USA) and filtered through a 0.45- $\mu\text{m}$  pore size membrane filter before use.

#### *Apple juice preparation*

The phenolic acids present in apple juice (Tree

Top, Selah, WA, USA) were separated from possible interferents by passing 4 ml of juice through a Sep-Pak C<sub>18</sub> cartridge and washing the column with 10 ml of NANOpure water. A 2-ml volume of 0.01 M sodium borate solution (pH 9.25) was used to elute the phenolic acids. Neutral phenols remained on the column. This extract was injected directly onto the capillary.

#### *Brain homogenate preparation*

A rat was killed by cervical dislocation and the brain removed. Approximately 1.7 g of brain was homogenized in 10 ml of 50 mM borate buffer (pH 9.0) for 15 min. A 1-ml volume of homogenate was then removed and acidified with 80  $\mu\text{l}$  of concentrated perchloric acid and centrifuged at 16 000 *g* for 10 min. The supernatant was filtered with a 2- $\mu\text{m}$  filter. A 50- $\mu\text{l}$  aliquot of the supernatant was derivatized in a final volume of 1 ml. The derivatization procedure was carried out as described previously [7].

## RESULTS AND DISCUSSION

Several tests were performed to evaluate the Nafion joint and to characterize the effects of this modification. No substantial difference (<1%) in the current measurement was observed between capillaries that did not contain the joint and those that had been modified when the same applied field strength and buffer were used.

No difference in electroosmotic flow was obtained when grounding was conducted either through the joint or at the detection end of the capillary column. As this experiment could not be carried out with the electrochemical detector, a UV–VIS detector was employed. Current measurements taken at both of these grounded positions were essentially the same. Reproducibility of joint-to-joint construction was examined based on the measurement of electroosmotic flow for six modified columns. The relative standard deviation was calculated to be 6.8%. No deterioration of the operation of a modified column was apparent following daily use over a 2-month period.

Although the Nafion joint completes the electrical circuit, the detection end of the column does not appear to be at “true” ground, as the noise levels were found to be proportional to the applied

voltage. Further, when buffers were used which exhibited higher electrophoretic currents (*i.e.*, buffers of a lower resistance), detector noise was observed to increase. This has also been reported by Wallingford and Ewing [2]. In order to minimize this effect, buffers of high resistance should be employed.

#### Linearity and detection limit for hydroquinone

To ascertain the detector response using the described system, hydroquinone was chosen as the test analyte. Using 0.01 *M* sodium acetate buffer (pH 6.0) and a separation voltage of 425 V/cm, linear regression analysis for concentrations ranging from  $7 \cdot 10^{-8}$  to  $1 \cdot 10^{-4}$  *M* provided a calibration graph with a correlation coefficient of 0.998 ( $n = 10$ ). The high separation efficiency achievable with CE was apparent, with the number of theoretical plates calculated from the peak half-width for hydroquinone being of the order of 185 000. The detection limit for this compound was calculated from the electropherogram shown in Fig. 3 and was determined to be  $6 \cdot 10^{-9}$  *M* based on a signal-to-noise ratio of 2. Using 5.8 nl as the injection volume, the detection limit corresponds to 34.8 amol. From a review of literature, this is the lowest concentration limit of detection reported using CE with electrochemical detection. Relative standard deviations for the reproducibility of the migration time and the detector response for hydroquinone were 0.7% and 1.8%, respectively ( $n = 8$ ).

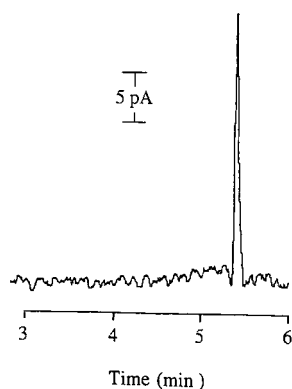


Fig. 3. Electropherogram of  $7 \cdot 10^{-8}$  *M* hydroquinone. 0.01 *M* sodium acetate (pH 6.0); separation voltage, 425 V/cm; detection potential, 750 mV vs. Ag/AgCl.

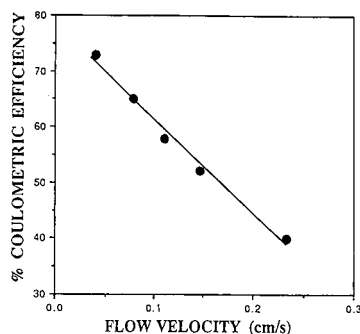


Fig. 4. Coulometric efficiency as a function of flow velocity for  $1 \cdot 10^{-4}$  *M* hydroquinone. Conditions as in Fig. 3.

The coulometric efficiency of the detector was also examined. Insertion of a 33  $\mu\text{m}$  O.D. carbon fiber into a 50  $\mu\text{m}$  I.D. capillary column produces an annular flow width of *ca.* 8.5  $\mu\text{m}$ . This, and the high sensitivity, are indicative of a thin-layer flow cell of high coulometric efficiency. To measure the coulometric efficiency as a function of flow velocity, a known volume of  $1 \cdot 10^{-4}$  *M* hydroquinone was injected. Different flow velocities were achieved by adjustment of the applied electrophoretic voltage between 65 and 400 V/cm. The coulometric efficiency could be determined by knowing the number of moles, current sensitivity and chart speed, and that the oxidation of hydroquinone involves 2 F/mol. The coulometric efficiency was determined at several flow velocities. Fig. 4 illustrates the data

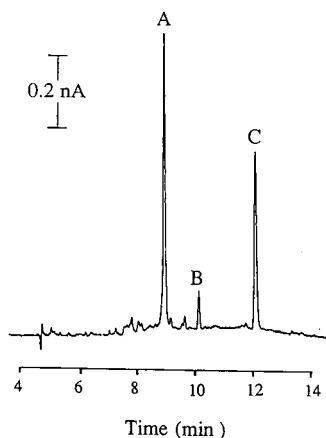


Fig. 5. Electropherograms of apple juice extract. 0.01 *M* sodium borate (pH 9.5); separation voltage, 425 V/cm; detection potential, 650 mV vs. Ag/AgCl.

obtained in this study and, as expected, demonstrates the high efficiencies for flow velocities typically utilized in CE separations.

#### *Analysis of apple juice*

The application of this system to real sample matrices was examined. The electropherogram obtained for the apple juice extract is shown in Fig. 5. Based on the migration times, peaks A, B and C were identified as chlorogenic acid, *p*-coumaric acid and caffeic acid, respectively. However, migration time is not always a reliable indicator of peak identity, particularly in CE where the sample matrix can have a considerable effect on the mobility of the sample constituents. For further verification of peak identity and purity assessment, voltammetric characterization was utilized. The combination of voltammetric characterization and migration time provides peak identity assignments with a high degree of certainty.

It has been shown that it is not necessary to obtain the entire voltammogram of the analyte in order to characterize sample components; the comparison of current response in the region where it changes most rapidly is sufficient [8]. To do this, the current response obtained at a potential near  $E_{1/2}$  (where the current is most dependent on potential) was ratioed to the current response at a potential where the current is no longer dependent on potential (mass transport-limited value). As each phenolic acid has a different hydrodynamic response curve in terms of voltage and shape, the ratio is unique to each compound. Current ratios have been employed extensively for the voltammetric characterization of compounds in complex samples [9–11]. In this

system, the current responses for both standards and sample peaks were measured at 550, 750 and 950 mV. Current ratios (ratioed to 950 mV) recorded are given in Table I. The ratios for *p*-coumaric acid and caffeic acid were virtually identical with those of the sample components eluting at the same time. However, peak A and chlorogenic acid did not exhibit similar voltammetric behavior, indicating impurity. This was further verified when sinapic acid, another phenolic constituent of apple juice, was found to co-elute with chlorogenic acid.

#### *Analysis of brain tissue homogenate*

The detection of glutamic and aspartic acid in a rat brain homogenate was investigated. These are important excitatory amino acids that can play a role as neurotransmitters in the brain [12]. Both amino acids lack electrochemically active moieties; therefore, derivatization is necessary for their detection. NDA reacts with primary amines in the presence of cyanide to produce cyano[*f*]benzoisindole (CBI) derivatives. These have been shown to be electroactive at moderate oxidation potentials [13]. Fig. 6 illustrates electropherograms of a standard mixture of  $1 \times 10^{-5}$  M of both CBI-amino acids. Fig. 7 shows the electropherogram recorded for the derivatized brain tissue homogenate in which both glutamic and aspartic acid were detected. This is the first reported use of a derivatizing agent to enhance detection in CE with amperometric detection.

It was found that the carbon fiber had to be pretreated between successive injections of brain homogenate samples in order to maintain current sensitivity. It is presumed that fouling of the electrode surface occurs owing to the formation of

TABLE I  
VOLTAMMETRIC CHARACTERIZATION OF APPLE JUICE COMPONENTS

Conditions as in Fig. 5.

Sample components	Retention time (min)		Current ratio			
	Sample	Standard	550 mV/950 mV		750 mV/950 mV	
			Sample	Standard	Sample	Standard
(A) Chlorogenic acid	8.0	8.0	0.011	0.053	0.171	0.263
(B) <i>p</i> -Coumaric acid	9.1	9.0	0.025	0.026	0.254	0.246
(C) Caffeic acid	10.5	10.4	0.313	0.306	0.543	0.523

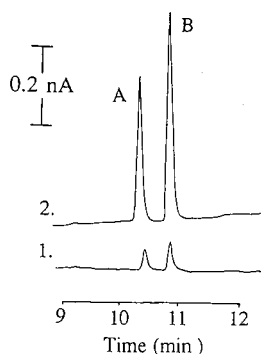


Fig. 6. Electropherograms of CBI derivatives of  $1 \times 10^{-5} M$  (A) glutamic acid and (B) aspartic acid. (1) Response of untreated carbon fiber microelectrode; (2) response for pretreated carbon fiber microelectrode.  $0.01 M$  sodium borate (pH 9.25); separation voltage, 425 V/cm; detection potential, 900 mV vs. Ag/AgCl.

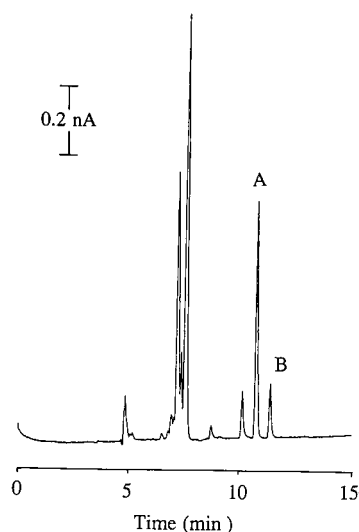


Fig. 7. Electropherograms of CBI-derivatized rat brain tissue homogenate. (A) CBI-glutamic acid; (B) CBI-aspartic acid. Conditions as in Fig. 6.

insoluble reaction products and the pretreatment "cleans" these from the surface. Electrochemical pretreatment has been shown previously to have a dramatic effect on the response of carbon fiber microelectrodes [14–16]. This is demonstrated in Fig. 6. Application of a square-wave waveform to the microelectrode increased the current sensitivity nearly ten-fold over that of the untreated electrode. The detector response was also found to be very reproducible when the electrode was pretreated between injections [17].

## CONCLUSIONS

An electrochemical detection system for CE has been developed that is more easily constructed than those previously reported. The design was evaluated and found to be extremely durable with no adverse effects on the CE separation. The resulting system has detection limits for hydroquinone in the low attomole range. In addition, voltammetry was used to verify peak identity and purity.

We believe that the simplicity of construction of this system should make electrochemical detection for CE more accessible to other investigators. This design also lends itself to sample collection and coupling to other end-column detectors. Future studies will be focused on the analysis of brain dialysate, which requires the high sensitivity for small sample volumes provided by the system.

## ACKNOWLEDGEMENTS

This work was supported by the Kansas Technology Enterprise Corporation. The LC-4C was donated by Bioanalytical Systems. T.O'S. gratefully acknowledges an Eolas scholarship. The authors thank Nancy Harmony and Garrity Repta for their contributions to this project.

## REFERENCES

- 1 J. W. Jorgenson and K. D. Lukacs, *Anal. Chem.*, 53 (1981) 1298.
- 2 R. A. Wallingford and A. G. Ewing, *Anal. Chem.*, 59 (1987) 1762.
- 3 R. A. Wallingford and A. G. Ewing, *Anal. Chem.*, 61 (1989) 98.
- 4 X. Huang and R. N. Zare, *Anal. Chem.*, 62 (1990) 443.
- 5 X. Huang, R. N. Zare, S. Sloss and A. G. Ewing, *Anal. Chem.*, 63 (1991) 189.
- 6 L. A. Knecht, E. J. Guthrie and J. W. Jorgenson, *Anal. Chem.*, 56 (1984) 479.
- 7 P. de Montigny, J. F. Stobaugh, R. S. Givens, R. G. Carlson, K. Srinivasachar, L. A. Sternson and T. Higuchi, *Anal. Chem.*, 59 (1987) 1096.
- 8 D. A. Roston and P. T. Kissinger, *Anal. Chem.*, 53 (1981) 1695.
- 9 S. M. Lunte, K. D. Blankenship and S. A. Read *Analyst (London)*, 113 (1988) 99.
- 10 D. A. Roston, R. E. Shoup and P. T. Kissinger, *Anal. Chem.*, 54 (1982) 1417A.

- 11 C. E. Lunte and P. T. Kissinger, *Anal. Chem.*, 55 (1983) 1458.
- 12 A. M. Palmer, P. H. Hutson, S. L. Lowe and D. M. Bowen, *Exp. Brain Res.*, 75 (1989) 659.
- 13 S. M. Lunte, T. Mohabbat, O. S. Wong and T. Kuwana, *Anal. Biochem.*, 178 (1989) 202.
- 14 F. G. Gonon, C. M. Fombarlet, M. J. Buda and J.-F. Pujol, *Anal. Chem.*, 53 (1981) 1386.
- 15 T. J. O'Shea, A. Costa Garcia, P. Tunon Blanco and M. R. Smyth, *J. Electroanal. Chem.*, 307 (1991) 63.
- 16 J. Wang, P. Tuzhi and V. Villa, *J. Electroanal. Chem.*, 234 (1987) 119.
- 17 T. O'Shea, M. R. W. Telting-Diaz, S. M. Lunte, C. E. Lunte and M. R. Smyth, *Electroanalysis*, in press.



# Electrokinetic reversed-phase chromatography with packed capillaries

Hideko Yamamoto, Joseph Baumann and Fritz Erni\*

*Analytical Research and Development, Shandoz Pharma Ltd., 4002 Basle (Switzerland)*

---

## ABSTRACT

Possibilities and limitations for the applicability of electroendosmotic flow as an elution system in reversed-phase chromatography with packed capillaries were investigated. By using electroendosmotic elution, very high performance could be achieved. No loss of column efficiency was observed up to linear electroendosmotic flows of *ca.* 3 mm/s. With 50- $\mu$ m I.D. fused-silica capillaries, packed with 3- $\mu$ m ODS, reduced plate heights of 1.7–2.2 were obtained for test compounds ( $k' = 0$ –4.8) at a linear velocity of 2.6 mm/s. Electroendosmotic elution systems allowed the use of very small-particle packing materials. With 1.6- $\mu$ m Monospher ODS, an extremely high chromatographic efficiency of up to 790 theoretical plates/s was obtained.

---

## INTRODUCTION

Capillary liquid chromatography has been investigated by several groups because of its potential to increase the performance of chromatography for high-resolution analysis and for the analysis of extremely small samples [1]. Packed [2,3], drawn packed [4,5] and open-tubular [6,7] capillary columns have been employed and high efficiency in chromatographic performance has been demonstrated. Capillary electrokinetic separation techniques such as capillary zone electrophoresis [8–12], capillary micellar electrokinetic chromatography [13,14], capillary gel electrophoresis [15] and capillary isoelectric focusing [16] have stimulated further developments of capillary liquid chromatography. In these techniques (except capillary gel electrophoresis and capillary isoelectric focusing), the transport of solutes, both uncharged and charged, is based mainly on electroendosmotic flow induced by the electrical field. Electroendosmotic flow originates from the electrical double layer on the surface and this phenomenon has been fully described [17,18]. The flow profile of electroendosmotic flow is nearly flat compared with the parabolic flow pro-

file of pressure pumping. This feature offers high plate efficiency in capillary electrokinetic separation techniques.

Electroendosmotic elution systems have been used in open-tubular [19–21] and drawn packed reversed-phase capillary chromatography [22] as an alternative to pressure elution systems. Jorgenson and Lukacs [23] discussed the applicability of electroendosmotic elution systems in packed capillary reversed-phase chromatography and reduced plate heights of 1.9 were obtained for a peak eluting at *ca.* 30 min using a 65 cm  $\times$  0.17 mm I.D. capillary packed with 10- $\mu$ m ODS packing. However, they pointed out some difficulties in working with these systems.

For the analysis of very complex samples, it is necessary to increase the chromatographic performance. It is expected that electrokinetic reversed-phase chromatography with packed systems will allow the achievement of this goal and it also has the advantages of packed capillaries (higher capacity than open-tubular and drawn packed capillaries). In this paper, we describe the possibilities and limitations of applying electrokinetic elution systems in packed capillary reversed-phase chromatography.

## EXPERIMENTAL

*Preparation of packed capillaries*

Fused-silica capillaries (50  $\mu\text{m}$  I.D., 365  $\mu\text{m}$  O.D.) (Polymicro Technologies, Phoenix, AZ, USA) were used as column materials. First, 4- $\mu\text{m}$  spherical silica packings were packed into the capillaries in order to sinter the end-frit as follows. The end of the capillary was firmly tapped downwards into a tightly compacted pile of 4- $\mu\text{m}$  spherical silica wetted with sodium silicate solution and deionized water. The packing was sintered at the end of the capillary by gently heating with a small microtorch flame for *ca.* 15 s. A slurry of 4- $\mu\text{m}$  spherical silica packing (Superspher Si 60; Merck, Darmstadt, Germany) in acetonitrile (1:10, w/v) was prepared with ultrasonication (5 min) and pumped into the capillary at 5000 p.s.i. using a liquid chromatographic pump (Model 100 solvent metering system; Altex Scientific, Berkeley, CA, USA) and a stainless-steel tubing reservoir (350 mm  $\times$  2 mm I.D.). The base of the reservoir connected to the inlet of the capillary was placed in an ultrasonic bath during packing.

After packing, the mobile phase was replaced with distilled water and the capillary was equilibrated. The end-frit was sintered in *ca.* 19 cm from the outlet frit by very gentle heating. First the packing was dried and the polyimide coating was incinerated in the lower part of the flame, then the end-frit (3–5 mm) was sintered by heating in the middle of the flame for 20 s. During heating the capillary should be rotated slowly and the heating should be concentrated on the required position. The outlet frit was cut off and the capillary was emptied of the 4- $\mu\text{m}$  spherical silica packings by pumping distilled water from each side. The polyimide coating was burned away to make a detection window. The capillary was flushed with acetonitrile and packed up to the inlet with a reversed-phase packing material (3- $\mu\text{m}$  ODS-Hypersil, Shandon Southern Products, Runcom, UK) as described above at 6000 p.s.i. In order to pack 1.6- $\mu\text{m}$  Monospher ODS (Merck), the pressure was set at 9000 p.s.i. After the equilibration with distilled water, the length of the packed section and non-packed section was arranged by cutting the capillary ends. In electrokinetic reversed-phase chromatography, ODS silica packings are negatively charged, and the electro-

phoretic mobility is higher than the elektroendosmotic mobility. Therefore, it was necessary to sinter a frit at the inlet to prevent the packing from migrating out. The frit was sintered in the same way as the outlet frit.

*Chromatographic system*

Chromatographic runs were carried out with a laboratory-made apparatus similar to that used for capillary zone electrophoresis. The inlet of the capillary was connected to a stainless-steel six-port rotary valve including an injection port (Model 7010; Rheodyne, Cotati, CA, USA), in order to use high-pressure pumping to eliminate air bubbles from the capillaries. A carbon electrode from a positive polarity high-voltage power supply (Alpha MK II, Model 2907P, 0–60 kV; Brandenburg, Surrey, UK) and a stainless-steel tube from the valve were inserted in an anode chamber filled with the mobile phase. The outlet was inserted in a capped cathode vial. On-column detection was carried out with a Model 783A ultraviolet detector (Applied Biosystems, Foster City, CA, USA), which was modified to separate the detection unit from the apparatus by using optical fibres (600  $\mu\text{m}$  I.D., 1 mm O.D.; Laaber Rüsselsheim, Germany). The samples were injected electrokinetically.

*Reagents*

Sodium tetraborate (Merck) was used to increase the pH of the mobile phase. Acetonitrile, benzyl alcohol, benzaldehyde, benzene and toluene were obtained from Merck, 1,2-dichlorobenzene, 1,2,3-trichlorobenzene, 1,2,3,4-tetrachlorobenzene, pentachlorobenzene and hexachlorobenzene from Aldrich-Chemie (Steinheim, Germany) and 1-naphthol and 2-naphthol from Fluka (Buchs, Switzerland). Distilled water was used to prepare the mobile phase. The mobile phase was filtered through a nylon 66 membrane (0.2- $\mu\text{m}$  pore size). Isradipin [isopropyl methyl 4-(benzofurazanyl)-1,4-dihydro-2,6-dimethyl-3,5-pyridinedicarboxylate] and its neutral by-products were obtained from Sandoz Pharma (Basle, Switzerland).

## RESULTS AND DISCUSSION

*Electroendosmotic flow in packed capillaries*

The properties of electroendosmotic flow in

packed capillaries have been discussed [23,24] and are considered to be the same as in open-tubular capillaries, except that an electrical double layer exists on the surface of each silica-based particle in contact with the electrolyte. Several factors regulate electroosmotic flow ( $F_{OS}$ ). Field strength, pH and ionic strength of the mobile phase, organic modifiers and ionic modifiers have been investigated in open-tubular capillaries [9,19,25–27]. Therefore, these factors were also investigated in packed capillaries. The flow velocity was measured by monitoring the retention time of an unretained peak (thiourea).  $F_{OS}$  increased with decreasing molarity of sodium tetraborate. The highest  $F_{OS}$  was observed at concentrations of 2–4 mM. A curve similar to that in open-tubular systems was obtained for the pH of sodium tetraborate buffer adjusted with phosphoric acid *vs.*  $F_{OS}$ .  $F_{OS}$  increased between pH 6 and 8. No increase in  $F_{OS}$  was observed above pH 8–9. It was important to investigate the dependence on the concentration of organic modifiers, especially acetonitrile, in electrokinetic reversed-phase chromatography. As shown in Fig. 1,  $F_{OS}$  decreased on increasing the concentration of acetonitrile. The decrease in  $F_{OS}$  was only *ca.* 33% at 60% acetonitrile. This phenomenon was considered to be due to the decrease in dielectric constant and the magnitude of the zeta potential.

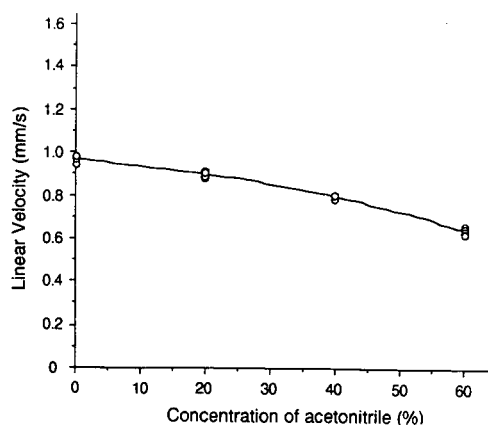


Fig. 1. Dependence of electroosmotic flow linear velocity on the concentration of acetonitrile. Capillary, 640 mm  $\times$  50  $\mu$ m I.D.  $\times$  365  $\mu$ m O.D. packed with Monospher ODS (1.6  $\mu$ m); applied voltage, 15 kV; mobile phase, 4 mM sodium tetraborate (pH 9.2)–acetonitrile.

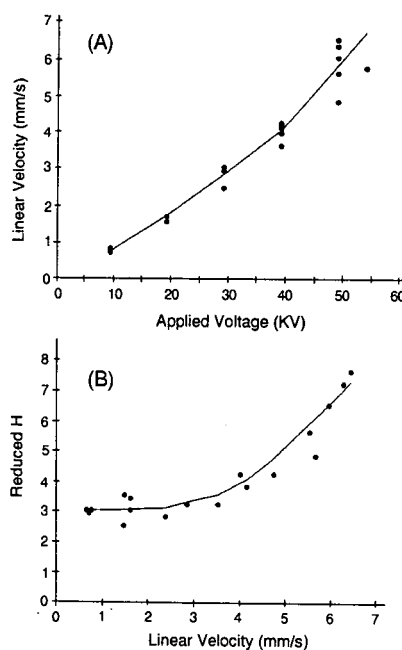


Fig. 2. (A) Dependence of electroosmotic flow velocity on applied voltage; (B) reduced plate height *vs.* electroosmotic flow velocity. Capillary, 143 mm; packing, Hypersil ODS (3  $\mu$ m); mobile phase, 2 mM sodium tetraborate (pH 8.7)–80% acetonitrile; sampling, 1.5 kV for 4 s; sample, thiourea.

#### Dependence of theoretical plate numbers on linear velocity

In order to evaluate the electroosmotic elution system in packed capillary chromatography, the maximum applicable field strength and the dependence of plate numbers on linear flow velocity were investigated. For this purpose, a short capillary (143 mm) packed with Hypersil ODS (3  $\mu$ m) was employed, so that it was possible to apply very high field strengths to the capillary. No formation of bubbles was observed up to 55 kV across the capillary (field strength *ca.* 2 kV/cm in the packed section) and a *ca.* 6 mm/s electroosmotic flow was obtained. However,  $F_{OS}$  was unstable above 50 kV applied voltage and higher than the expected velocity, as shown by the curve of  $F_{OS}$  *vs.* applied voltage (Fig. 2A). This could be considered to be the result of heating effects. No decrease in plate efficiency was observed until  $F_{OS}$  = 3 mm/s (below *ca.* 30 kV, field strength *ca.* 1.1 kV/cm) (Fig. 2B). This means that it is possible to perform rapid anal-

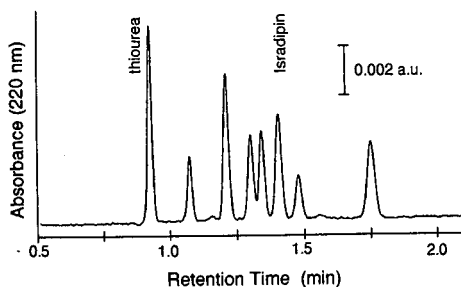


Fig. 3. Example of chromatograms obtained by electrokinetic reversed-phase chromatography with packed capillaries. A mixture of Isradipin, its by-products and thiourea was analysed. Applied voltage, 30 kV; other conditions as in Fig. 2.  $F_{OS} = 2.6$  mm/s (current 1.8  $\mu$ A).

yses without a decrease in plate numbers. An example of the chromatograms obtained with this capillary at  $F_{OS} = 2.6$  mm/s is shown in Fig. 3. Isradipin and its six different by-products ( $k' = 0.17$ – $0.90$ ) were separated in 1.6 min. With longer capillaries (285 mm), better reduced plate heights were obtained, e.g., 1.8–2.2 for thiourea and benzene derivatives ( $k' = 0$ – $4.8$ ), as shown in Fig. 4. The decrease in the plate numbers at very high  $F_{OS}$  seems to be due to band broadening caused by the heating. This phenomenon has been observed in open-tubular electrokinetic chromatography [9,21] and discussed by Knox [24]. However, the peak shape was very

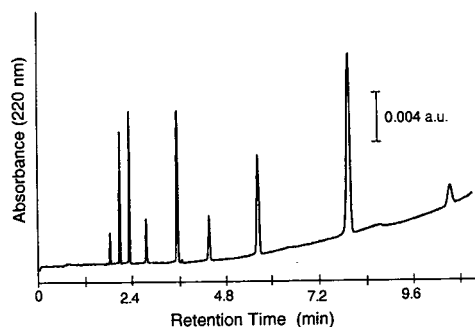


Fig. 4. High-resolution analysis of benzene derivatives. Peaks, from left to right: thiourea [ $N = 46\,000$ , reduced plate height ( $h$ ) = 2.0], benzyl alcohol ( $N = 54\,000$ ,  $h = 1.8$ ), benzaldehyde ( $N = 56\,000$ ,  $h = 1.7$ ), benzene ( $N = 47\,000$ ,  $h = 2.0$ ), 1,2-dichlorobenzene ( $N = 54\,000$ ,  $h = 1.8$ ), 1,2,3-trichlorobenzene ( $N = 52\,000$ ,  $h = 1.8$ ), 1,2,3,4-tetrachlorobenzene ( $N = 49\,000$ ,  $h = 2.0$ ), pentachlorobenzene ( $N = 43\,000$ ,  $h = 2.2$ ) and hexachlorobenzene ( $N = 43\,000$ ,  $h = 2.2$ ). Capillary, 285 mm; packing, Hypersil ODS (3  $\mu$ m); mobile phase, 2 mM sodium tetraborate–80% acetonitrile; applied voltage, 45 kV (current 2.0  $\mu$ A); sampling, 2.5 kV for 5 s.  $F_{OS} = 2.6$  mm/s.

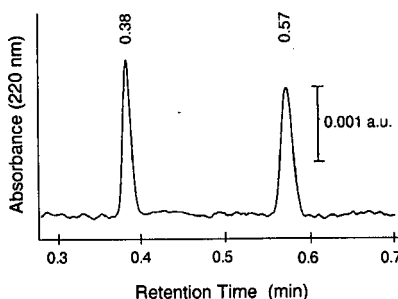


Fig. 5. Example of rapid analysis. Linear velocity of electroosmotic flow, 6.3 mm/s; applied voltage, 50 kV (current 2.9  $\mu$ A). Peaks: left, thiourea ( $N = 6600$ ,  $N/s = 290$ ,  $h = 7.2$ ); right, Isradipin ( $N = 8000$ ,  $N/s = 230$ ,  $h = 6.0$ ). Other conditions as in Fig. 2.

symmetrical even at *ca.*  $F_{OS} \approx 6$  mm/s, as shown in Fig. 5.

Curves of plate numbers vs. linear velocity for electrokinetic chromatography and pressure-driven chromatography were compared by using the same capillary (Table I). Pressure-driven chromatography was performed with the same procedure as electrokinetic chromatography and the sample solution was injected electrokinetically. With pressure elution, the highest plate number was obtained at *ca.* 0.9 mm/s and the value decreased subsequently with increasing linear velocity. With electroosmotic elution, however, no changes in the plate numbers were observed from 0.8 to 2.6 mm/s, as shown in Table I and Fig. 2B, and improved plate numbers were observed at any velocity owing to the plug profile of electroosmotic flow.

#### Stability and reproducibility of chromatographic performance

An expected problem with this technique was the stability of ODS silica packings at high pH. A high pH is necessary to obtain high electroosmotic flow. In fact, it took some time to obtain stable conditions of  $F_{OS}$ , UV baseline and current with newly packed capillaries. Once stable conditions had been obtained, however, chromatography could be performed with some daily initial equilibration procedures as in conventional high-performance liquid chromatography.  $F_{OS}$  and the retention times of the test mixture containing Isradipin, its by-products and thiourea ( $k' = 0$ – $0.9$ ) were reproducible with relative standard deviation 1.6–2.2% in ten continuous runs at 40 kV with a capillary 285 mm  $\times$  50

TABLE I

## COMPARISON OF PLATE EFFICIENCY BETWEEN ELECTROENDSMOTIC ELUTION AND HYDROSTATIC PRESSURE ELUTION

Values of reduced plate heights for nine components ( $k' = 0-4.8$ ) were averaged. The chromatogram obtained at an electroendosmotic flow of 2.6 mm/s is shown in Fig. 4.

Linear velocity (mm/s)	Reduced plate height	
	Electroendosmotic	Hydrostatic pressure
1.1 (0.9) <sup>a</sup>	2.0	3.0
2.6 (2.2)	1.9	3.6

<sup>a</sup> Value in parentheses: linear velocity of hydrostatic pressure flow.

$\mu\text{m I.D.} \times 365 \mu\text{m O.D.}$ ) packed with Hypersil ODS ( $3 \mu\text{m}$ ), and stable results were obtained for longer than 1 month.

The reproducibility of this technique between capillaries was also examined. Three capillaries of the same size packed with Hypersil ODS ( $3 \mu\text{m}$ ) were prepared, and  $F_{\text{os}}$  and  $k'$  of seven components were compared (Fig. 6). The deviation of  $k'$  values was about 9% in spite of good reproducibility of  $F_{\text{os}}$  (3% deviation). This result may be due to differences in the packing conditions of the capillaries.

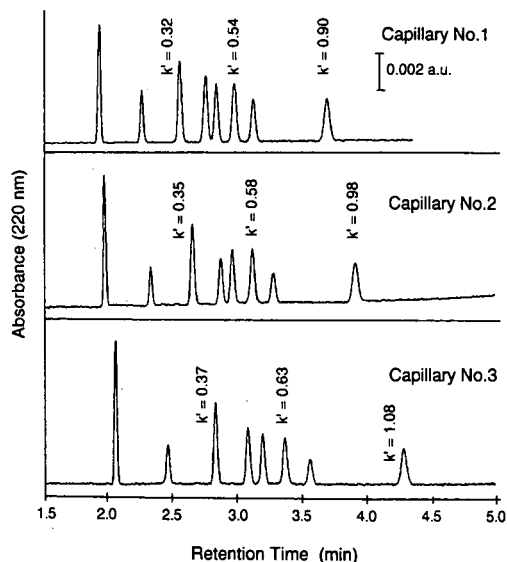


Fig. 6. Reproducibility of chromatographic performance between three capillaries. Three capillaries of the same size packed with Hypersil ODS were prepared and employed for electrokinetic reversed-phase chromatography. Applied voltage, 40 kV; other conditions as in Fig. 4. Sample as in Fig. 3.

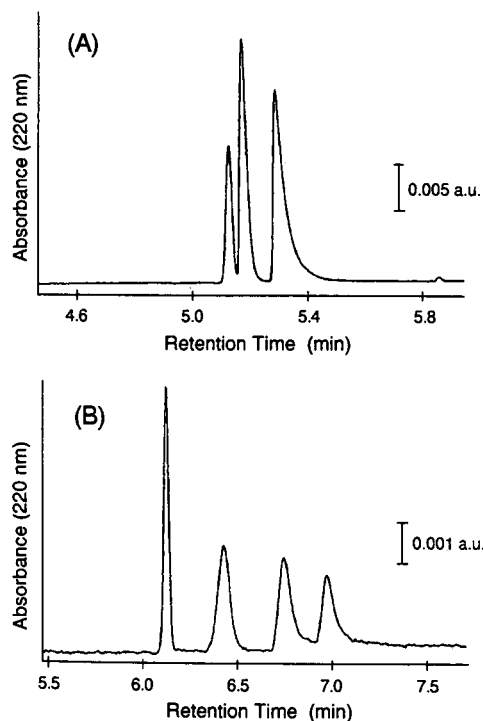


Fig. 7. Two examples of chromatograms obtained with  $1.6\text{-}\mu\text{m}$  Monospher ODS. (A) Capillary,  $680 \text{ mm} \times 50 \mu\text{m I.D.}$ ; mobile phase,  $4 \text{ mM}$  sodium tetraborate ( $\text{pH } 9.2$ ).  $F_{\text{os}} = 2.2 \text{ mm/s}$ . Peaks, from left to right: thiourea ( $N = 243\,000$ ,  $N/s = 790$ ), benzyl alcohol ( $N = 220\,000$ ,  $N/s = 710$ ), benzaldehyde ( $N = 108\,000$ ,  $N/s = 340$ ). (B) Capillary,  $675 \text{ mm}$ ; mobile phase,  $4 \text{ mM}$  sodium tetraborate- $20\%$  acetonitrile.  $F_{\text{os}} = 1.8 \text{ mm/s}$ . Peaks, from left to right: thiourea ( $N = 248\,000$ ,  $N/s = 670$ ), toluene ( $N = 47\,000$ ,  $N/s = 120$ ), 2-naphthol ( $N = 52\,000$ ,  $N/s = 130$ ), 1-naphthol ( $N = 62\,000$ ,  $N/s = 150$ ). Applied voltage,  $35 \text{ kV}$  (current  $1.3 \mu\text{A}$ ,  $1.1 \mu\text{A}$ ); sampling,  $5 \text{ kV}$  for  $5 \text{ s}$ .

### Electrokinetic reversed-phase chromatography with small-particle packing material

It is of interest to use very small particles in capillary chromatography in order to increase the efficiency. Thus 1.6- $\mu\text{m}$  Monospher ODS was used as the column packing. Two of the chromatograms are shown in Fig. 7. For the unretained compound (thiourea) more than 240 000 theoretical plates per 680 mm (the reduced plate height of 1.9) were obtained in 5.2 min (Fig. 7A). This leads to 790 theoretical plates/s, which is extremely high. From the curve of reduced plate height vs. linear velocity (Fig. 8), it can be expected to obtain an even higher efficiency than 800 theoretical plates/s when higher field strengths are applied. With pressure elution, a *ca.* 0.24 mm/s linear velocity was obtained with the same capillaries at *ca.* 6000 p.s.i., and it would necessary to apply *ca.* 25 000 p.s.i. to the system to obtain even a 1 mm/s linear velocity. With 1.6- $\mu\text{m}$  Monospher ODS, however, a significant decrease in plate numbers for retained compounds was observed. Toluene ( $k' = 0.05$ ) showed gave about one fifth of the theoretical plates, as shown in Fig. 7B. The reason for this phenomenon is unclear, but similar results were observed with pressure elution. It might be due to the small capacity of the Monospher packing and the limitations of mass transfer.

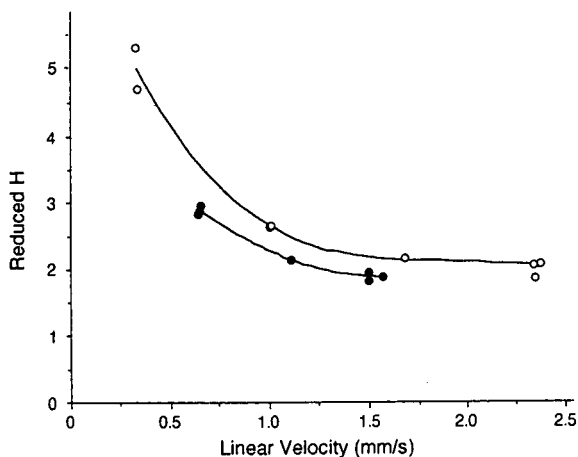


Fig. 8. Curves of reduced plate height vs. electroendosmotic flow velocity in a capillary packed with 1.6- $\mu\text{m}$  Monospher ODS. Capillary, 620 mm; (O) applied voltage 5–35 kV with 4 mM sodium tetraborate mobile phase; (●) applied voltage 15–35 kV with 4 mM sodium tetraborate–60% acetonitrile mobile phase; sample, thiourea.

### Wide-bore capillaries

This technique offers other possibilities. One is the use of capillaries of larger inside diameter without a decrease in plate efficiency and in order to improve the detection sensitivity. The sensitivity of detection was improved about threefold without any decrease in efficiency with 100  $\mu\text{m}$  I.D. capillaries compared with 50  $\mu\text{m}$  I.D. capillaries. Preliminary experiments indicated that the use of capillaries larger than 200  $\mu\text{m}$  I.D. is possible.

### CONCLUSIONS

The advantage of the application of electroendosmotic elution in liquid chromatography is the possibility of achieving high plate efficiencies (plates/s) without limitation of the particle sizes (specially for very small particles). This is due to the lack of pressure restrictions and the advantages of the plug profile of electroendosmotic flow. As shown here, electroendosmotic elution systems could be applied successfully in packed capillary reversed-phase chromatography. Very high performance (plates generated per unit time) could be achieved. There was no limitation to the use of a 1.6- $\mu\text{m}$  packing, where 790 theoretical plates/s were obtained. This technique is very useful for rapid and high-resolution analyses and also in trace analysis because of the high capacity of packed capillaries.

### REFERENCES

1. R. T. Kennedy and J. W. Jorgenson, *Anal. Chem.*, **61** (1989) 436.
2. K. E. Karlsson and M. Novotny, *Anal. Chem.*, **60** (1988) 1662.
3. R. T. Kennedy and J. W. Jorgenson, *Anal. Chem.*, **61** (1989) 1128.
4. V. L. McGuffin and M. Novotny, *J. Chromatogr.*, **255** (1983) 381.
5. T. Tsuda, I. Tanaka and G. Nakagawa, *Anal. Chem.*, **56** (1984) 1249.
6. D. Ishii and T. Takeuchi, *J. Chromatogr. Sci.*, **18** (1980) 462.
7. P. R. Dluznieski and J. W. Jorgenson, *J. High Resolut. Chromatogr. Chromatogr. Commun.*, **11** (1988) 332.
8. F. E. P. Mikkers, F. M. Everaerts and Th. P. E. M. Verheggen, *J. Chromatogr.*, **169** (1979) 11.
9. J. W. Jorgenson and K. D. Lukacs, *Anal. Chem.*, **53** (1981) 1298.
10. S. Hjertén, *J. Chromatogr.*, **270** (1983) 1.
11. R. T. Kennedy, M. D. Oates, B. R. Cooper, B. Nickerson and J. W. Jorgenson, *Science*, **246** (1989) 57.

- 12 T. M. Olefirowicz and A. G. Ewing, *Anal. Chem.*, 62 (1990) 1872.
- 13 S. Terabe, K. Otsuka and T. Ando, *Anal. Chem.*, 57 (1985) 834.
- 14 D. E. Burton, M. J. Sepaniak and M. P. Maskarinec, *J. Chromatogr. Sci.*, 24 (1986) 347.
- 15 A. S. Cohen, D. R. Najarian, A. Paulus, A. Guttman, J. A. Smith and B. L. Karger, *Proc. Natl. Acad. Sci. U.S.A.*, 85 (1988) 9660.
- 16 S. Hjertén, J. L. Liao and K. Yao, *J. Chromatogr.*, 387 (1987) 127.
- 17 A. W. Adamson, *Physical Chemistry of Surfaces*, Wiley-Interscience, New York, 3rd ed., 1976, Ch. 4.
- 18 V. Pretorius, B. J. Hopkins and J. D. Schieke, *J. Chromatogr.*, 99 (1974) 23.
- 19 T. Tsuda, K. Nomura and G. Nakagawa, *J. Chromatogr.*, 248 (1982) 241.
- 20 W. D. Pfeffer and E. S. Yeung, *Anal. Chem.*, 62 (1990) 2178.
- 21 G. J. M. Bruin, P. P. H. Tock, J. C. Kraak and H. Poppe, *J. Chromatogr.*, 517 (1990) 557.
- 22 J. H. Knox and I. H. Grant, *Chromatographia*, 24 (1987) 135.
- 23 J. W. Jorgenson and K. D. Lukacs, *J. Chromatogr.*, 218 (1981) 209.
- 24 J. K. Knox, *Chromatographia*, 26 (1988) 329.
- 25 J. C. Reijenga, G. V. A. Aben, Th. P. E. M. Verheggen and F. M. Everaerts, *J. Chromatogr.*, 260 (1983) 241.
- 26 S. Fujiwara and S. Honda, *Anal. Chem.*, 59 (1987) 487.
- 27 T. Tsuda, *J. High Resolut. Chromatogr. Chromatogr. Commun.*, 10 (1987) 622.





# Analytical study of heavy crude oil fractions by coupling of the transalkylation reaction with supercritical fluid chromatography

P.-L. Desbène\* and A. Abderrezag

*L.A.S.O.C., Institut Universitaire de Technologie, Université de Rouen, 43 Rue Saint Germain, 27000 Evreux (France)*

B. Desmazières

*Laboratoire de Chimie Organique Structurale, Université P. et M. Curie, URA 455, 4 Place Jussieu, 75005 Paris (France)*

---

## ABSTRACT

Previous work involved the utilization of the transalkylation reaction (retro-Friedel-Crafts reaction to transfer alkyl-substituting chains from the asphaltenes aromatic matrix to a light aromatic acceptor) in the analysis of heavy crude oil fractions by coupling it with capillary gas chromatography (GC). In such conditions, a mapping of alkyl chains substituting the complex aromatic matrix of heavy crude oil fractions can be set up. However, it appears from NMR data and quantitative measurements of alkyl chains detected in GC that only about 50% of the transferable chains are effectively involved. This result poses the questions of whether heavy fractions of crude oil contain alkyl chains longer than those evidenced by GC and whether the partial transalkylation is due to an equilibrium. In order to answer these questions, supercritical fluid chromatography (SFC) was used instead of GC. An efficient transfer from model molecules (*n*-alkylnaphthalenes) substituted by alkyl chains up to C<sub>31</sub> was observed, whereas GC did not show evidence for chains longer than C<sub>24</sub>. However, in with various petroleum asphaltenes (Boscan, Arabian Light, Maya) no transfer of chains longer than C<sub>21</sub>–C<sub>28</sub> was observed. Moreover, better quantitative results were obtained by SFC, as the analysis limit is well above C<sub>21</sub>. For instance, the global transfer yield of alkyl chains from Boscan asphaltenes was 5.2% *versus* 4.6% in GC. The transalkylation yields were significantly increased when successive transalkylations were performed.

---

## INTRODUCTION

Structural studies of heavy crude oils and heavy oil residues are difficult because of the extreme complexity of these mixtures [1]. Methods for separating such materials according to chemical classes have been reported but, even within each separate group, one still finds a complex mixture of compounds [1]. For many of these mixtures, spectroscopic measurements, especially <sup>1</sup>H and <sup>13</sup>C NMR, indicate the presence of alkyl groups and of aromatic and heterocyclic rings [2]. However, obtaining more detailed structural information from NMR is difficult owing to the wide variety of compounds and to the overlapping of peaks corresponding to different chemical structures [3–6].

In order to obtain some information about the nature and abundance of alkyl chains substituting the aromatic matrix of these complex mixtures, we previously used the reversibility of the Friedel-Crafts reaction combined with capillary gas chromatography–mass spectrometry (GC–MS) [7]. After optimizing the operating conditions in order to allow analytical studies, using model molecules and a Boscan atmospheric residue, we found that a satisfactory compromise between an efficient transfer of alkyl chains and the minimum degradation of these chains is possible [8,9]. This result is obtained when benzene is used as an acceptor of alkyl chains, with slightly hydrated aluminium bromide as Lewis acid, and a 4-h reaction time at 60°C. Under these conditions, it becomes possible to obtain relatively

precise mapping of the alkyl chains substituting the aromatic matrix. However, with atmospheric residues, a rough comparison between transfer yields and data resulting from NMR measurements indicates that only about 50% of potentially transferable chains are effectively transferred to the light aromatic acceptor. Hence, in spite of its efficiency, the transalkylation reaction is not quantitative. This relative lack of efficiency was recently confirmed by a comparative study by pyrolysis—GC—MS of various asphaltenes before and after transalkylation [10].

The lack of quantitiveness can originate partly from the limitation of GC analysis because of the low volatility of some compounds such as phenylalkanes possessing  $C_{23}$ – $C_{24}$  or longer alkyl chains, for which GC analysis is difficult or impossible, partly from insufficient reversibility of the Friedel–Crafts reaction, although this phenomenon should be limited under our operating conditions as benzene is used in large excess (solvent), and partly from the poor accessibility of reaction sites in these complex organic matrixes.

In order to answer these questions and to improve the method, we considered the possibility of replacing capillary GC with capillary supercritical fluid chromatography (SFC). We report in this paper an analytical study by SFC of the reaction media obtained after transalkylation of four asphaltenes of various origins but of the same type (type II) according to the classification of Tissot and Welte [11].

## EXPERIMENTAL

### SFC analyses

SFC analyses were performed using a Carlo Erba (Milan, Italy) SFC 3000 supercritical fluid chromatograph fitted with a 10 m  $\times$  100  $\mu$ m I.D. fused-silica column coated with SE-52 stationary phase and a flame ionization detector.

Samples were obtained from the mixing of the products obtained from three parallel transalkylations of 150 mg of asphaltenes each time, under the operating conditions reported below. The solution was concentrated to about 5% of the initial volume by evaporating benzene under nitrogen. The residue was weighed, 0.25 wt. % of *n*-hexadecane was added as an internal standard and the mixture was then injected.

The analytical conditions were as follows: eluent, supercritical carbon dioxide (medical grade; Carboxyque Française, Paris, France); oven temperature, 110°C; detector temperature, 310°C; conical restrictor (giving a mobile phase linear flow-rate of 2.0–2.5 cm s<sup>-1</sup>); and pressure programming, isobaric at 100 atm for 10 min, then a linear gradient at 5 atm/min to 280 atm and isobaric at 280 atm for 30 min.

### Calibration

The response factors of the series phenylalkanes possessing alkyl chain lengths from  $C_2$  to  $C_{31}$ , naphthylalkanes substituted by alkyl chains from  $C_2$  to  $C_{31}$  and 1, $\omega$ -dinaphthylalkanes with alkyl chain lengths from  $C_3$  to  $C_{10}$  were measured in a concentration range 0.05–0.15 wt. % using *n*-hexadecane as internal standard at a fixed concentration (0.25 vol. %).

### Transalkylation reaction

In a typical experiment, 150  $\pm$  1 mg of asphaltenes were dissolved in 10 ml of dry benzene in a 20 ml SVL screw-capped tube (Prolabo). Benzene was used both as a solvent and as a light acceptor of alkyl chains. Then 10  $\mu$ l of distilled water were added using a syringe. A 300-mg amount of aluminium bromide was quickly dissolved in 5 ml of dry benzene and the solution was immediately poured into the benzenic solution of asphaltenes. The tube was sealed and placed in an ultrasonic bath thermostated at 60°C. This last operation represents the zero time of reaction.

After 4 h in the ultrasonic bath, the reaction medium, after addition of 3 ml of benzene to rinse the reactor, was centrifuged at 23 000 g for 10 min. The solid phase was treated with 5 ml of benzene and the suspension was again centrifuged. This second organic phase was combined with the first and hydrolysis and neutralization were performed by adding a 5% aqueous solution of sodium carbonate (15 ml). The organic phase was decanted, washed twice with distilled water and stored in a sealed flask.

### Samples and reagents

Asphaltenes were prepared by precipitation with *n*-heptane, according to the NFT 6011S standard [12] from atmospheric residues (340°C+) of Arabian Light (Algeria), Boscan (Venezuela), Kirkouk

(Iraq) and Maya (Mexico) furnished by the IFP-Elf-Total sample bank (Solaize, France).

Anhydrous 98% aluminium bromide from Janssen (Puteaux, France) was used without any further treatment. Benzene (analytical-reagent grade) from Merck (Darmstadt, Germany) was purified by 3–4 successive crystallisations in a deep freezer, until a constant melting point of 4°C was reached and a gas chromatogram showed only the benzene peak. This purification procedure allows for the elimination of impurities such as toluene, and *o*- and *m*-xylene, which are undesirable in analytical transalkylation.

Water was purified by double distillation or by filtration and reversed osmosis using a Milli-Q + Milli-Ro system from Millipore (Molsheim, France).

Calibration graphs were established using either commercial compounds, *viz.*, *n*-alkanes ( $C_{18}$  and  $C_{20}$ ), *n*-alkylbenzenes (alkyl chains from  $C_2$  to  $C_{12}$ ) and ethylnaphthalenes of analytical-reagent grade from Janssen, or compounds synthesized as described previously [9], *viz.*, *n*-alkylbenzenes possessing  $C_{16}$ ,  $C_{20}$ ,  $C_{26}$  and  $C_{31}$  alkyl chains, *n*-alkylnaphthalenes with  $C_{10}$ ,  $C_{16}$ ,  $C_{22}$ ,  $C_{26}$  and  $C_{31}$  alkyl chains and 1, $\omega$ -dinaphthylalkanes with  $\omega = 3, 4, 5, 6, 10$ .

## RESULTS AND DISCUSSION

Using our previous analytical procedure [7,10] it was difficult to obtain evidence for the transfer of alkyl chains longer than  $C_{21}$ – $C_{22}$ . In particular, it was impossible to model the transfer of chains longer than  $C_{22}$  from alkylnaphthalenes, used as models of the oil aromatic matrix, as these compounds were not eluted by GC beyond  $C_{22}$ . We used capillary SFC to solve this problem. Effectively this technique should allow the analysis in reaction media obtained after transalkylation of non-volatile compounds possessing alkyl chains of length clearly longer than  $C_{22}$ , and also a sufficient efficiency to analyse these complex reaction media in a reasonable time.

As a first step we optimized the chromatographic conditions with a mixture of compounds modelling the reaction medium resulting from the transalkylation of an oil aromatic matrix. This model mixture contained alkylbenzenes (from  $C_2$  to  $C_{31}$ ) corresponding to the potential products of transalkyla-

tion and alkylnaphthalenes ( $C_{22}$ ,  $C_{26}$  and  $C_{31}$ ) used as models of the oil aromatic matrix. As the aim of this study was to obtain both qualitative and quantitative information about the transalkylation products, we added an internal standard to the model mixture at the beginning of optimization. As alkanes are stable in the reaction medium [9], we searched for one that did not interfere with phenylalkanes under our conditions, and *n*-hexadecane was adopted.

As shown in Fig. 1, it is possible to analyse the model mixture in less than 1 h with our SE-52 column (10 m  $\times$  100  $\mu$ m I.D.) at 110°C and with a pressure gradient.

The analysis, under the same conditions, of the reaction medium obtained after transalkylation of a heavy oil fraction is reported in Fig. 2. It must be noted that capillary SFC is less sensitive than capillary GC and we had to concentrate the initial reaction medium to 5% of its initial volume in order to perform this analysis. Using the co-elution technique and extrapolation, it appears that this oil fraction does not contain alkyl chains longer than  $C_{27}$ – $C_{28}$ .

However, as already mentioned, our aim was not only to obtain qualitative information about the composition of heavy crude oil fractions, so we measured the response factors of the main products

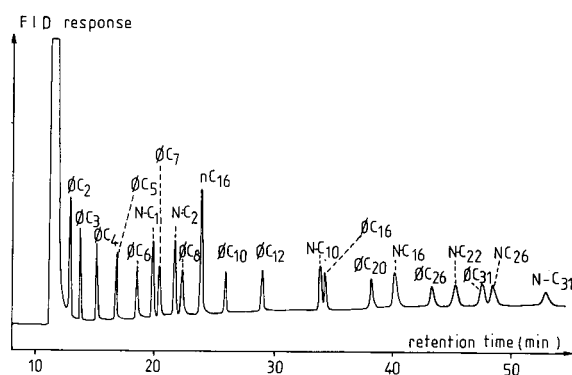


Fig. 1. SFC analysis of a mixture of alkyaromatics modelling the reaction media resulting from the transalkylation of oil heavy fractions. Conditions: SE-52 column (10 m  $\times$  100  $\mu$ m I.D.); eluent,  $CO_2$ , linear flow-rate 2 cm  $s^{-1}$ ; injection volume, 60 nl; split, *ca.* 1:20; temperature 110°C; pressure programme, isobaric at 100 atm for 10 min, linear gradient of 5 atm  $min^{-1}$  to 280 atm, isobaric at 280 atm for 60 min.  $\Phi C_n$  = Alkylbenzenes;  $N-C_n$  = alkylnaphthalenes;  $nC_{16}$  = internal standard.

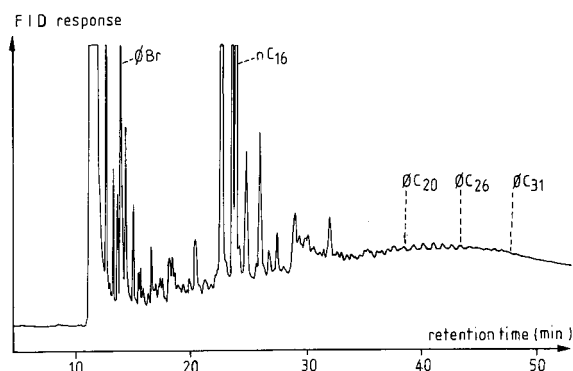


Fig. 2. SFC analysis of the reaction medium resulting from the transalkylation of Kirkouk asphaltenes. Conditions as in Fig. 1.

resulting from the transalkylation prior to the study of asphaltenes from various origins. The response coefficients obtained for a series of phenylalkanes and for the same naphthylalkanes, normalized to those of ethylbenzene and methylnaphthalene, respectively, are reported in Table I. The results shows that under the conditions used, alkylben-

zenes substituted by alkyl chains from  $C_2$  to  $C_{16}$  give similar responses, regardless of concentration (in the range 0.05–0.25%, v/v), the responses of alkylbenzenes possessing longer chains decrease when the chain length increases and the detector response is linear in the concentration range 0.05–0.1% (v/v), regardless of the alkyl chain length. At higher concentrations, a deviation from linearity is observed for both short and long alkyl chains. This relatively limited range of linearity is not a problem because the individual concentrations of the transalkylation products remain below 0.1% (v/v) under the conditions used and according to our previous studies [7,10].

From these response factors, it was possible to calculate the overall yield of transalkylation as 7.5% ( $\sigma = 0.8\%$ ) for Kirkouk asphaltenes. This yield is only slightly greater than that obtained by capillary GC for the same asphaltenes (7%,  $\sigma = 0.8\%$ ) [10]. Qualitatively, the comparison of the SFC analysis reported here and of the GC analysis described previously [10] shows that the phenylalkanes found in the reaction media are only slightly

TABLE I

RESPONSE FACTORS OF ALKYL BENZENES AND ALKYL NAPHTHALENES

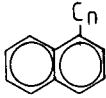
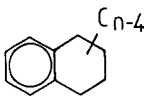
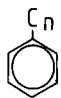
Internal standard: *n*-hexadecane (0.25%, v/v).

Length of alkyl chain	Alkylbenzene concentration (% v/v, $n < 16$ ; % w/v, $n \geq 16$ )						Alkyl naphthalenes (concentration 0.10%, w/v)	
	0.05		0.10		0.25		$R/R_{Na-C_1^a}$	$R/R_{n-C_{16}}$
	$R/R_{\phi C_2}$	$R/R_{n-C_{16}}$	$R/R_{\phi C_2}$	$R/R_{n-C_{16}}$	$R/R_{\phi C_2}$	$R/R_{n-C_{16}}$		
$C_1$							1.00	0.346
$C_2$	1.00	0.190	1.00	0.370	1.00	0.755	1.04	0.361
$C_3$	1.01	0.191	0.99	0.369	1.09	0.820		
$C_4$	1.01	0.191	1.01	0.375	1.22	0.922		
$C_5$	1.00	0.190	0.98	0.364	1.29	0.973		
$C_6$	1.01	0.191	0.94	0.349	1.34	1.02		
$C_7$	0.95	0.181	0.92	0.340	1.29	0.971		
$C_8$	0.89	0.179	0.93	0.343	1.34	1.01		
$C_{10}$	0.94	0.178	0.97	0.359	1.33	1.00	0.83	0.287
$C_{12}$	0.91	0.173	0.98	0.363	1.38	1.04		
$C_{16}$	0.94	0.179	1.01	0.373	0.63	0.477	0.78	0.270
$C_{20}$	0.79	0.150	0.86	0.319	0.52	0.393		
$C_{22}$							0.68	0.234
$C_{26}$	0.64	0.121	0.69	0.255	0.360	0.272	0.63	0.218
$C_{31}$							0.56	0.194
<i>n</i> - $C_{16}$	5.26	1.00	2.70	1.00	1.32	1.00	2.89	1.00

<sup>a</sup> Na- $C_1$  is 1-methylnaphthalene.

TABLE II

TRANSALKYLATION YIELDS OF ALKYLNAPHTHALENES USED AS MODEL COMPOUNDS OF ASPHALTENES AROMATIC MATRIX

Alkyl-naphthalene transalkylated	% of alkyl chain transferred as:	
		
$n = 22$	10	22
$n = 26$	8	32.5
$n = 31$	12.5	32

longer than those previously identified ( $C_{27}$ – $C_{28}$  by SFC *versus*  $C_{22}$ – $C_{23}$  by GC).

Some questions arise from these observations: are aromatic matrices of oil substituted by alkyl chains no longer than  $C_{27}$ – $C_{28}$ , or is transalkylation inefficient in the case of long alkyl chains? In order to solve this problem, we analysed by SFC reaction media obtained after transalkylation of alkyl-naphthalenes substituted by  $C_{22}$ ,  $C_{26}$  and  $C_{31}$  alkyl chains. These compounds were used as model molecules of the asphaltene matrices and the analytical conditions were the same as those for Kirkouk asphaltene.

The results of these transalkylations are given in Table II, and the chromatogram obtained by SFC for the transalkylation reaction media of  $n$ - $C_{31}$ -alkyl-naphthalene is reported in Fig. 3.

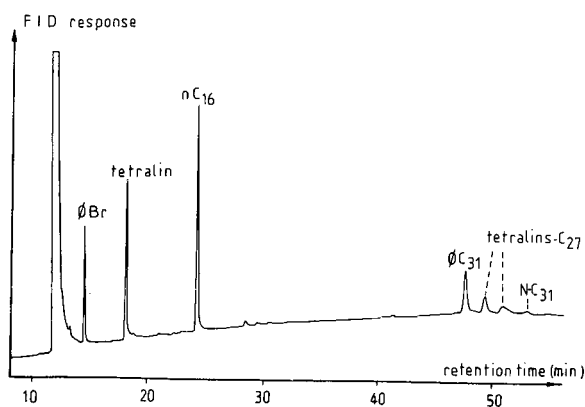


Fig. 3. SFC analysis of the reaction medium resulting from the transalkylation of  $n$ - $C_{31}$ -alkyl-naphthalene. Conditions as in Fig. 1.

These results indicate some of the main features of the aptitude of long alkyl chains to undergo transalkylation and the stability of the reaction products. As previously observed with shorter alkyl chains ( $C_{10}$  and  $C_{12}$  [9]),  $C_{22}$ -,  $C_{26}$ - and  $C_{31}$ -alkyl-naphthalenes are transalkylated. The percentage of chains transferred (between 30 and 45%) is close to the values obtained with  $C_{10}$ - and  $C_{12}$ -alkyl-naphthalenes (about 40%). As with the shorter chains, the alkyl chain is partly rearranged by cyclization during the transfer, producing tetralins substituted by  $C_{n-4}$  alkyl chains. Hence, in the transalkylation of  $C_{22}$ -alkyl-naphthalene, the reaction media can still be analysed by GC–MS, allowing the identification of the transalkylation product. The transalkylation yield is in fact greater for the transalkylation of model molecules [9], indicating that the stability of alkylbenzenes in the reaction media decreases when the chain length increases. It was concluded that the aromatic matrix of Kirkouk asphaltene does not possess  $n$ -alkyl chains longer than  $C_{27}$ – $C_{28}$  in detectable amounts.

We verified this conclusion by the SFC analysis of reaction media from the transalkylation of various asphaltene. The chromatograms obtained for Arabian Light, Boscan and Maya asphaltene are reported in Fig. 4.

Comparison of Fig. 2 and 4 shows that slightly longer chains are transferred from the Kirkouk asphaltene aromatic matrix to the light acceptor (benzene) than from the other asphaltene. In Kirkouk asphaltene, the longest alkyl chain transferred is  $C_{27}$ – $C_{28}$ , *versus*  $C_{23}$ – $C_{24}$  for Boscan, Maya and Arabian Light asphaltene. As SFC provides evidence for the transfer of alkyl chains appreciably longer than those previously detected by GC, we can now confirm that the length of alkyl chains substituting the aromatic matrix of asphaltene is not greater than  $C_{23}$ – $C_{28}$ , depending on the origin of the oil.

Consequently, the lack of quantitiveness of the transalkylation reaction results from some cause other than the inadequacy of the technique used to analyse the reaction media obtained after the transfer of alkyl chains from the oil aromatic matrix to benzene. The comparison of the overall yields of transalkylation obtained by SFC and in GC for various asphaltene, reported in Table III, clearly proves this point.

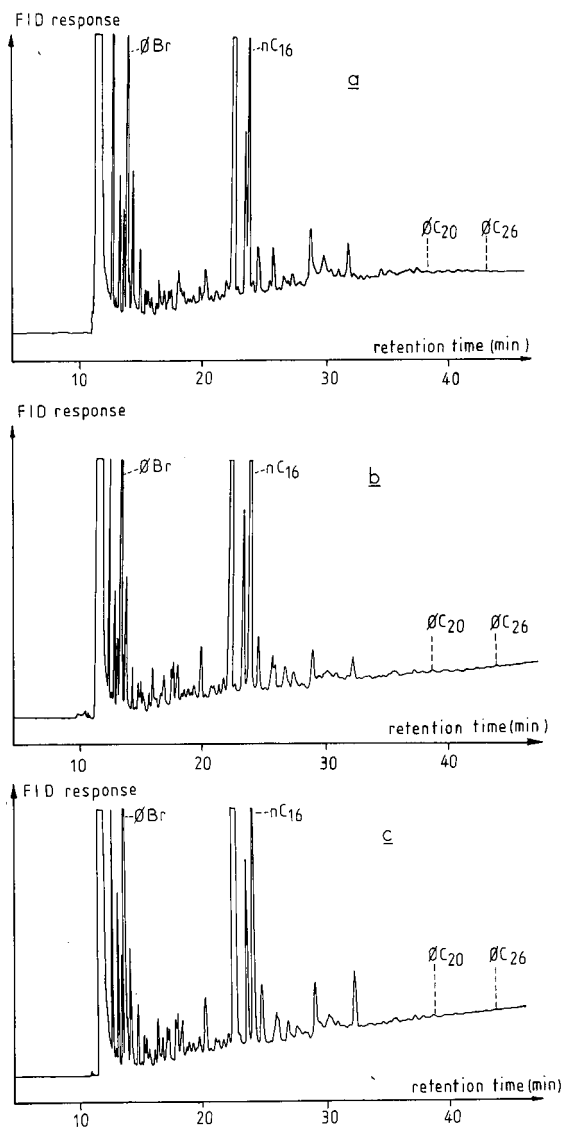


Fig. 4. SFC analysis of reaction media resulting from the transalkylation of various asphaltenes: (a) Arabian Light (Algeria); (b) Boscan (Venezuela); (c) Maya (Mexico). Conditions as in Fig. 1.

As transalkylation is a reaction which on the one hand is, in principle, an equilibrium (retro-Friedel-Crafts), and on the other is applied to very complex structures, reaction sites of which can be hindered, we concluded this study by examining the impact of one or more recyclings on the overall yields of transalkylation. Table IV reports the results ob-

TABLE III

OVERALL YIELDS OF TRANSALKYLATION PRODUCTS FROM VARIOUS ASPHALTENES DETERMINED BY CAPILLARY SFC AND CAPILLARY GC ANALYSES

The standard deviation is calculated from five independent transalkylations.

Asphaltenes	Overall yield (%)	
	SFC	GC
Arabian Light	7.5 ± 0.9	6.9 ± 0.3
Boscan	5.2 ± 0.2	4.6 ± 0.9
Kirkouk	7.5 ± 0.8	7.0 ± 0.8
Maya	5.9 ± 0.6	5.7 ± 0.8

tained by SFC analysis after one recycling of Kirkouk, Boscan, Maya and Arabian Light asphaltenes and after recycling Kirkouk asphaltenes twice.

These experiments show clearly that one transalkylation is not sufficient to transfer efficiently the totality of alkyl chains substituting the aromatic matrix of heavy crude oil fractions. The yields obtained in the second and third transalkylations are far from negligible. However, SFC and GC-MS analyses indicate clearly that almost no long chains are transferred in the course of these further transalkylations. Hence it appears that the transfer of

TABLE IV

EVOLUTION OF OVERALL TRANSALKYLATION YIELDS OF VARIOUS ASPHALTENES AS A FUNCTION OF RECYCLING

Asphaltene	Transalkylation number	Overall yield by SFC (%)
Boscan	1	5.2
	2	4.3
	3	0.9
Arabian Light	1	7.5
	2	3.5
Maya	1	5.9
	2	3.9
Kirkouk	1	7.5
	2	3.2

long alkyl chains substituting aromatic matrices was efficient in the first transalkylations.

The short chains transferred in the first and second recyclings give mainly di- and triphenylmethanes and were previously considered to be responsible for the distribution of aromatic entities in the composition of heavy crude oil fractions [7]. They can also be attributed to the fragmentation of longer or branched alkyl chains substituting heteroaromatic molecules (in place of simple aromatics), which are also present in heavy oil fractions [13,14].

Because of the lack of studies concerning the behaviour of alkyl heteroaromatics under transalkylation conditions, we cannot answer this fundamental question at present.

## CONCLUSIONS

SFC, which is well adapted to the study of the transalkylation of alkyl chains substituting the complex aromatic matrices of heavy crude oil fractions (regardless of chain length), allowed us to confirm that if relatively long linear alkyl chains are present, their length does not exceed  $C_{27}$ – $C_{29}$ .

The study of asphaltenes of various origins by combining transalkylation and SFC indicated that in spite of the differences observed in the distribution of alkyl chains substituting the aromatic matrices as a function of the origin of the asphaltenes, the length of the longer chains varies only slightly in the different asphaltenes. The maximum chain length is greater in Kirkouk asphaltenes than in Boscan, Maya and Arabian Light asphaltenes. As the alkyl chains substituting the oil aromatic matrix are only slightly longer than those previously identified by capillary GC, the non-quantitativeness of the alkyl chain transfer must have a cause other than the analytical procedure. Using successive transalkylations of the same asphaltenes we proved that an efficient transfer of alkyl chains cannot be obtained after only one transalkylation. This may

be due to an equilibrium (in spite of the excess of light aromatic acceptor) or to poor accessibility of reaction sites in oil aromatic matrices which are very complex.

The nature of the alkyl chains transferred after recycling, which are relatively short, raised the question of whether they are short chains distributed in heavy crude oil fractions or degradation products of longer linear or branched chain substituted heteroaromatic molecules (containing nitrogen, oxygen and mainly sulphur) which constitute part of heavy oil fractions. In order to answer this last question, we are currently studying the transalkylation of *n*-alkyl heteroaromatic molecules.

## REFERENCES

- 1 J. G. Speight, *The Chemistry and Technology of Petroleum*, Marcel Dekker, New York, 1980.
- 2 L. Petrakis and D. Allen, *N.M.R. for Liquid Fossil Fuels*, Elsevier, Amsterdam, 1984.
- 3 A. A. Herod, W. R. Ladner and C. E. Snape, *Philos. Trans. R. Soc. London, Ser. A*, 300 (1981) 3.
- 4 C. E. Snape, *Fuel*, 62 (1983) 621.
- 5 C. E. Snape, W. R. Ladner, L. Petrakis and B. C. Gates, *Fuel Process Technol.*, 2 (1984) 155.
- 6 C. E. Snape, W. R. Ladner, K. D. Bartle and N. Taylor, *Characterization of Heavy Crude Oils and Petroleum Residues (Collection Colloques et Séminaires, Vol. 40)*, Technip, Paris, 1984, p. 315.
- 7 P. L. Desbène, N. Jauseau-Pierre, B. Desmazières and J. J. Basselier, *Chromatographia*, 26 (1988) 70.
- 8 P. L. Desbène, N. Jauseau-Pierre, B. Desmazières and J. J. Basselier, *Anal. Chim. Acta*, submitted for publication.
- 9 P. L. Desbène, N. Jauseau-Pierre, A. Abderrezag and B. Desmazières, *Bull. Soc. Chim. Fr.*, submitted for publication.
- 10 P. L. Desbène, A. Abderrezag, B. Desmazières, J. J. Basselier, F. Béhar and M. Vandenbroucke, *Org. Geochem.*, 16 (1990) 969.
- 11 B. Tissot and D. Welte, *Petroleum Formation and Occurrence*, Springer, Berlin, 1978.
- 12 *French Standard*, NFT 6011S, AFNOR, Paris, 1970.
- 13 F. Béhar and M. Vandenbroucke, *Org. Geochem.*, 11 (1987) 15.
- 14 J. L. Faulon, M. Vandenbroucke, J. M. Drappier, F. Béhar and M. Romero, *Org. Geochem.*, 16 (1990) 981.





# Retention behaviour of closely related coumarins in thin-layer chromatographic preassays for high-performance liquid chromatography according to the “PRISMA” model

Pia Härmälä\*, Heikki Vuorela, Eeva-Liisa Rahko and Raimo Hiltunen

*Pharmacognosy Division, Department of Pharmacy, University of Helsinki, Fabianinkatu 35, SF-00170 Helsinki (Finland)*

---

## ABSTRACT

The retention behaviour of fourteen closely related coumarins in normal-phase thin-layer chromatography (TLC) and high-performance liquid chromatography (HPLC) was studied with the aim of testing the suitability of TLC as a preassay for HPLC when the optimization of the mobile phase has been carried out according to the “PRISMA” system. The retention (retardation) in TLC and HPLC was measured at 37 and 13 selective points, respectively. The retention behaviour at different solvent strengths was also examined. Capacity factors ( $k'$ ) and separation factors ( $\alpha$ ) were calculated to study the retention behaviour in the two systems. Two- and three-dimensional evaluations of  $k'$  against selectivity points showed similar retention behaviour for the coumarins in TLC and HPLC. According to quadratic regression,  $k'$  showed a dependency on the change in solvent strength. Similar behaviour of  $\alpha$  values for TLC and for HPLC was demonstrated in three-dimensional evaluations.

---

## INTRODUCTION

Coumarins are widely distributed in plants, especially in the Apiaceae and Rutaceae families. Coumarins usually contain many heteroatoms. The number and position of the various substituents in the coumarin molecule significantly influence their adsorption behaviour in thin-layer chromatography (TLC) and column chromatography [1].

Głowniak and Bieganowska [1,2] have studied the retention behaviours of coumarins using both normal- and reversed-phase TLC and high-performance liquid chromatography (HPLC). They studied the effects on retention of solvent composition and the individual substituents in the solute molecules. They found a linear relationship between the experimentally obtained retentions and the concentration of the organic modifier. The most selective mobile phase with respect to the effects of a substituent on retention was chosen by plotting the retention values of the coumarins against the mobile phase.

Some theoretical aspects concerning the use of TLC as a pilot technique for column liquid chromatography (CLC) have been presented by Różyło and Janicka [3]. Their work utilizes a thermodynamic description of adsorbent–binary solution–solute systems to characterize a given chromatographic process, and they investigated the effect of the chromatographic technique employed on the thermodynamic description of the chromatographic system. Różyło and Janicka [3] concluded that retention data obtained from sandwich chambers described adsorption from solutions in the same way as measurements from column liquid chromatography.

Nyiredy *et al.* [4] have presented strategies of mobile phase transfer from thin-layer to medium-pressure liquid column chromatography (MPLC) with silica as the stationary phase. The major advantage of the strategies was that mobile phase transfer started from a TLC separation in which the whole  $R_F$  range was used, in contrast to the general rule [5] that all zones should be below  $R_F=0.3$  in TLC.

However, the prediction of the final MPLC result was improved when overpressured layer chromatography (OPLC) was used as a pilot method.

The "PRISMA" optimization model assists in the selection of optimal eluent systems for both planar chromatographic techniques and column chromatographic techniques [6]. The PRISMA model can be visualized as a graphic representation of the solvent strengths ( $S_T$ ) and the proportions of the solvents ( $P_S$ ). The prism described by PRISMA consists of an unlimited number of triangular solvent diagrams (horizontal functions;  $P_S$ ) in which every triangular plane corresponds to a different solvent strength (vertical function;  $S_T$ ) [7]. The PRISMA optimization system consists of three parts. In the first part the basic parameters such as the stationary phase and the solvents are selected. In the second part of the system the optimal combination of the selected solvents is achieved using the actual PRISMA model. The third part includes selection of a suitable method and transfer of the optimized mobile phase to the various chromatographic techniques.

The aim of this study was to test TLC as a pre-assay for HPLC when optimization of the mobile phase has been carried out according to the PRISMA system [6], as demonstrated by fourteen closely related coumarins. A total of 37 selectivity points ( $P_S$ ) in the PRISMA model were examined using TLC, and 13 selectivity points were examined using HPLC. The retention was measured at five solvent strengths ( $S_T$ ) at  $P_S = 333$ . The capacity factors ( $k'$ ), and the separation factors ( $\alpha$ ) of the two methods were calculated and compared. Regression analysis and three-dimensional evaluations were performed in order to study the predictability of the HPLC behaviour and optimization on the basis of the TLC experiments.

## EXPERIMENTAL

### Apparatus

A Linomat IV TLC spotter (Camag, Muttentz, Switzerland) was used to apply the samples to TLC plates, and a CS-900 dual-wavelength flying-spot scanner (Shimadzu, Kyoto, Japan) was used for the densitometric evaluations. A 425 HPLC gradient former and 420 pump (Kontron Instruments, Rot-

kreuz, Switzerland) equipped with an ERC-7210 UV detector (ERMA Optical Works, Tokyo, Japan) and a Shimadzu C-R1B integrator were used. The HPLC system was connected to an Olivetti M24 personal computer (Olivetti, Ivrea, Italy).

### Chemicals

The coumarins (Fig. 1) bergapten, imperatorin, osthol, ostruthol, oxypeucedanin, psoralen, 2'-angeloyl-3'-isovaleryl vaginate and xanthotoxin were isolated from *Angelica archangelica* L. at the Pharmacognosy Division, Department of Pharmacy, University of Helsinki. Angelicin, herniarin and umbelliferone were obtained from Roth (Karlsruhe, Germany). Isobergapten, pimpinellin and sphondin were isolated from *Heracleum sphondylium* L. and identified at the Department of Pharmacy, ETH Zürich, Switzerland. The *n*-hexane was of technical grade (Oy Exxon Chemicals; Espoo, Finland) and was filtered before use. 1,4-Dioxane, methyl ethyl ketone, 2-propanol and toluene were of reagent grade and they were obtained from Merck (Darmstadt, Germany). Diethyl ether and acetic acid of analytical quality were from May & Baker (Dagenham, UK). The chloroform stabilized with ethanol of analytical quality was from RP Normapur (Paris, France), and absolute ethanol was from Alko (Helsinki, Finland). All other solvents, *i.e.* dichloromethane, tetrahydrofuran and ethyl acetate, were of HPLC quality (Rathburn, Walkerburn, UK).

### Chromatographic conditions

The TLC separations were performed on 10 × 4 cm plates in ascending one-dimensional mode in 22 × 6 cm unsaturated N-chambers (Camag) at ambient temperature. The solvent volume was 5 ml and the migration distance was 8.5 cm. The assays were carried out on alufoil, silica gel 60 F<sub>254</sub> (average particle size 10 µm) TLC plates (Merck, Germany). The migration distances and the solvent fronts were measured with the densitometer at 320 nm.

The column for the HPLC separations was a Li-chrosorb Si 60 (average particle size 10 µm), 250 × 4 mm I.D. (Merck) at ambient temperature. The flow-rate was 1.0 ml/min and detection was effected at 320 nm. The solvent peak was treated as the dead volume.

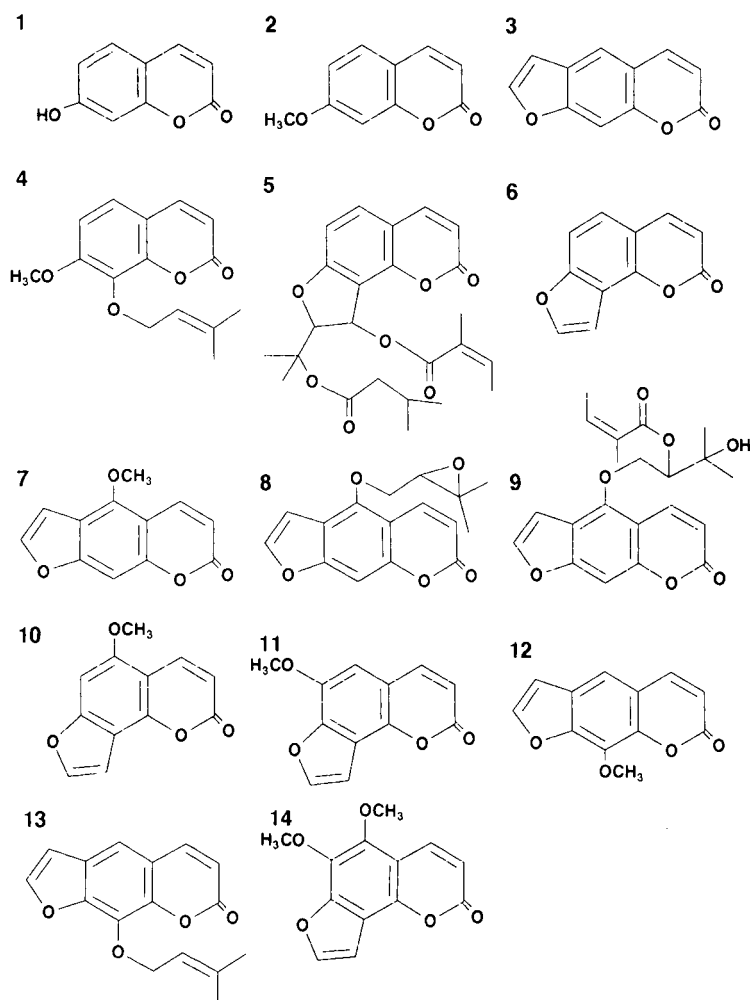


Fig. 1. Structures of the coumarins used in the study in the order according to the classification of Murray *et al.* [8]. 1 = Umbelliferone; 2 = herniarin; 3 = psoralen; 4 = osthol; 5 = 2'-angeloyl-3'-isovaleryl vaginate; 6 = angelicin; 7 = bergapten; 8 = oxypeucedanin; 9 = ostruthol; 10 = isobergapten; 11 = sphondin; 12 = xanthotoxin; 13 = imperatorin; 14 = pimpinellin.

#### Correlation between retention data obtained from TLC and HPLC

Calculation of the correlations and the regression analysis were performed with Stat View SE + Graphics software on a Macintosh SE computer. The Systat procedure was used for three-dimensional evaluation of the retention data and the separation factors.

#### RESULTS AND DISCUSSION

Ethyl acetate ( $S_T=4.4$ ), chloroform ( $S_T=4.1$ ) and tetrahydrofuran ( $S_T=4.0$ ) in *n*-hexane ( $S_T=0$ )

were selected according to the PRISMA model [6] to give the best separation of the fourteen coumarins in unsaturated chambers with normal-phase TLC plates. Retention measurements were performed in TLC at 37 selectivity points ( $P_S$ ) using the three selected solvents, *n*-hexane serving as the solvent strength ( $S_T$ ) regulator (Fig. 2).  $P_S$  describes the proportions of the selected solvents for the mobile phase. For example, a mobile phase characterized by  $P_S=181$  and  $S_T=2.0$  is a combination consisting of 4.5% ethyl acetate, 39.0% chloroform and 5.0% tetrahydrofuran adjusted with 51.5% *n*-hexane. The influence of  $S_T$  at the middle selectivity

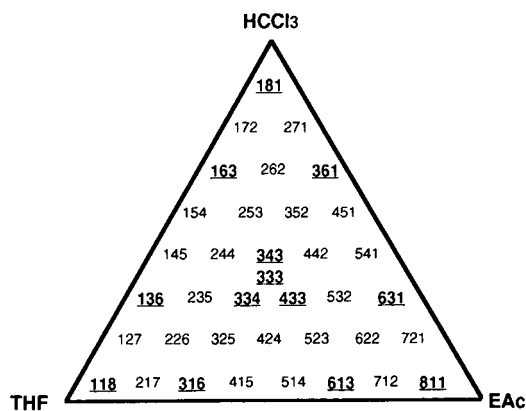


Fig. 2. The solvents selected for the analysis and selectivity points ( $P_s$ ) studied (TLC, all; HPLC, underlined). EAc = Ethyl acetate; THF = tetrahydrofuran.

point,  $P_s = 333$ , was tested by varying  $S_T$  from 1.4 to 2.2. Solvent strength was adjusted to  $S_T = 2.0$ , on the basis of these experiments, to give retardation factor ( $R_F$ ) values between 0.2 and 0.8 for the solutes in the TLC assays.

HPLC retention measurements were performed at thirteen selectivity points (Fig. 2) using the same solvents and *n*-hexane as the  $S_T$  regulator, as in the TLC runs. The influence of  $S_T$  at the middle selectivity point,  $P_s = 333$ , was tested by varying  $S_T$  from 0.8 to 1.6. For HPLC analysis  $S_T$  was adjusted to  $S_T = 1.2$  to give the last-eluting compound a capacity factor ( $k'$ ) of less than 20.

The capacity factors for HPLC ( $k'_c$ ) were calculated from the equation  $k'_c = (t_R - t_0)/t_0$ , where  $t_R$  is the retention time of the compound and  $t_0$  is the dead volume. The  $R_F$  values from TLC were transformed so as to obtain capacity factor values ( $k'_p$ ) similar to  $k'_c$  values in HPLC,  $k'_p = [1/(R_F)_{\text{obs}}] - 1$ , using the observed values ( $R_F$ )<sub>obs</sub> from the plate without correction [9,10].

The obtained experimental capacity factors were plotted against the selectivity points along the edges of the prism. Three representative compounds are shown in Fig. 3. The compounds were chosen according to elution, *i.e.* one from the beginning (pimpinellin; 14), one from the middle (herniarin; 2) and one from the end (umbelliferone; 1). The mobile phase composition has a similar effect on the elution of all the coumarins in both TLC and HPLC. The  $k'$  value is highest at  $P_s = 181$ .

The possible existence of a mathematical dependency between the capacity factor and  $P_s$  was also investigated. Regression functions of different order for the measured two-dimensional retention data were compared at constant  $S_T$ , *i.e.* 2.0 for TLC and 1.2 for HPLC. The capacity factors of the coumarins at selectivity points along one edge, *i.e.*, 118–181, 181–811 or 811–118, of the PRISMA showed high dependences, with quadratic regressions of the type  $k' = A(P_s)^2 + B(P_s) + C$  ( $r = 0.99$ – $0.91$  for TLC and  $r = 1.00$ – $0.95$  for HPLC). In reversed-phase HPLC similar findings for retention have been obtained by Nyiredy *et al.* [11].

Three-dimensional  $k'$  surfaces of each compound were constructed at all the investigated tertiary selectivity points. The three numerical values of  $P_s$  were plotted on an  $x$ – $y$  coordinate against a fourth parameter ( $z$ -coordinate;  $k'$ ) in order to obtain three-dimensional figures of the  $P_s$  in the prism. Coumarins have similar three-dimensional surfaces in both TLC and HPLC, as demonstrated by pimpinellin (14), herniarin (2) and umbelliferone (1) in Fig. 4. Selectivity point 181 gives the highest capacity factor values, falling to the corner of 118 with the lowest  $k'$  values. The surface follows this decreasing trend rather smoothly, the corner 811  $k'$  values being about half of the maximum values for each compound.

The influence of solvent strength in TLC was compared with that in HPLC.  $S_T$  values of 1.4, 1.6, 1.8, 2.0 and 2.2 in TLC were examined and 0.8, 1.0, 1.2, 1.4 and 1.6 in HPLC at selectivity point 333. The capacity factors ( $k'_p$  and  $k'_c$ ) of the coumarins were calculated and plotted against the solvent strengths, as demonstrated by pimpinellin, herniarin and umbelliferone (Fig. 5). The capacity factors in both methods showed high dependences, with quadratic regression of the type  $k' = A(S_T)^2 + B(S_T) + C$  ( $r = 1.00$ – $0.99$ ). In this study the dependences for the coumarins were not linear over the investigated  $k'$  range and the solvent strengths used, which is in accordance with the findings of Vuorela *et al.* [12].

The behaviour of  $S_T$  in these two methods was studied further. In order to compare the changes in retention with different  $S_T$  values in the two methods,  $k'_p$  and  $k'_c$  values at the joint  $S_T$  value of 1.4 were plotted against  $k'_p$  and  $k'_c$  values at the other  $S_T$ , and regression analysis was carried out (Table

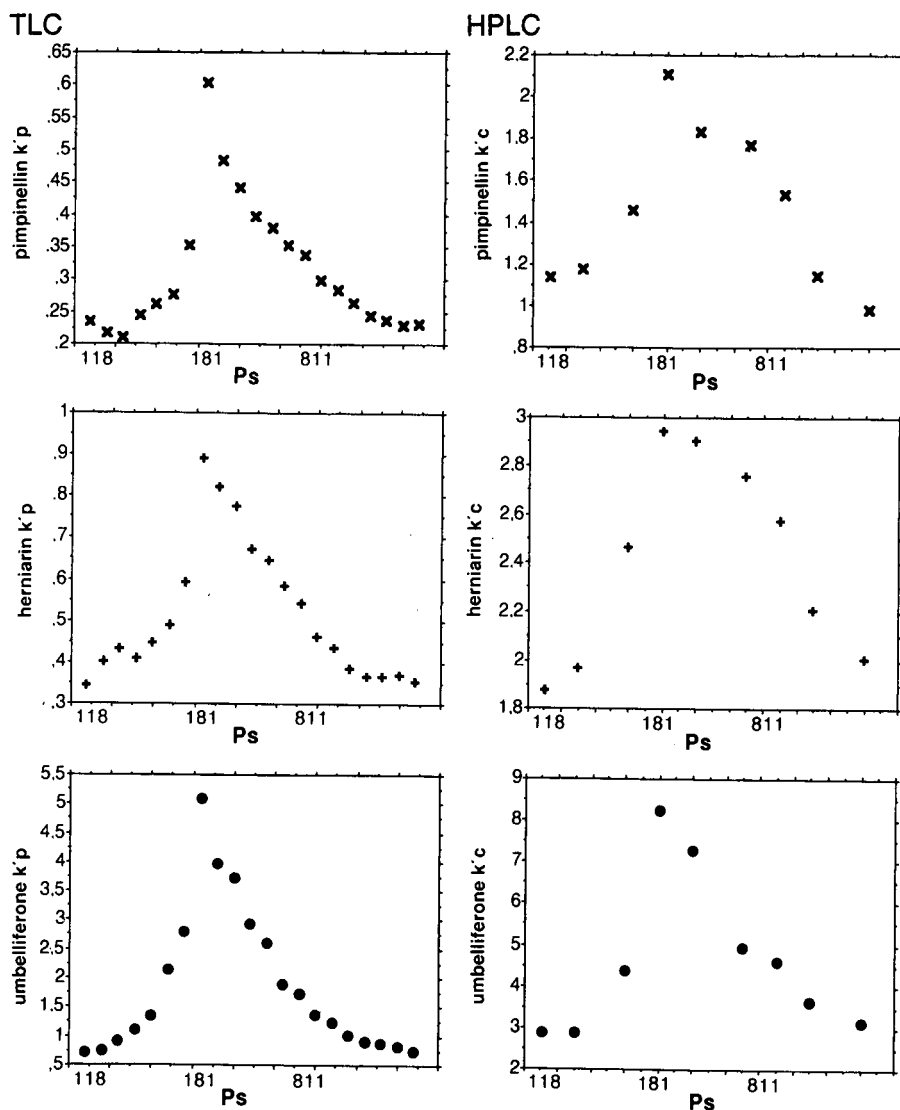


Fig. 3. The capacity factors ( $k'$ ) of three coumarins in  $P_s$  along the edges, i.e. 118, 181 and 811.

I). The slopes of the curves ( $A$  in Table I) were further plotted against  $S_T$  (Fig. 6). Two curves for TLC and HPLC were obtained with different slope values. The functions for TLC and HPLC showed clearly different  $S_T$  behaviour. This indicates that a change in  $S_T$  causes a different change in the retention behaviour of the compounds in TLC and HPLC. This has to be taken into consideration when transferring the mobile phase from TCL to HPLC.

The possibility of predicting the retention in HPLC from TLC experiments at the change in  $S_T$  was tested. TLC  $S_T=2.0$  capacity factors were plotted against HPLC  $S_T=1.2$ . Fitted  $k'_c$  values for HPLC at  $S_T=1.2$   $k'_c$  were calculated using the regression function (Stat View SE + Graphics software). The fitted and experimental  $k'_c$  values in HPLC at  $S_T=1.2$  were compared (Fig. 7). A high dependency ( $r=0.93$ ) was obtained between the fitted and experimental  $k'_c$ , thus making it possible to

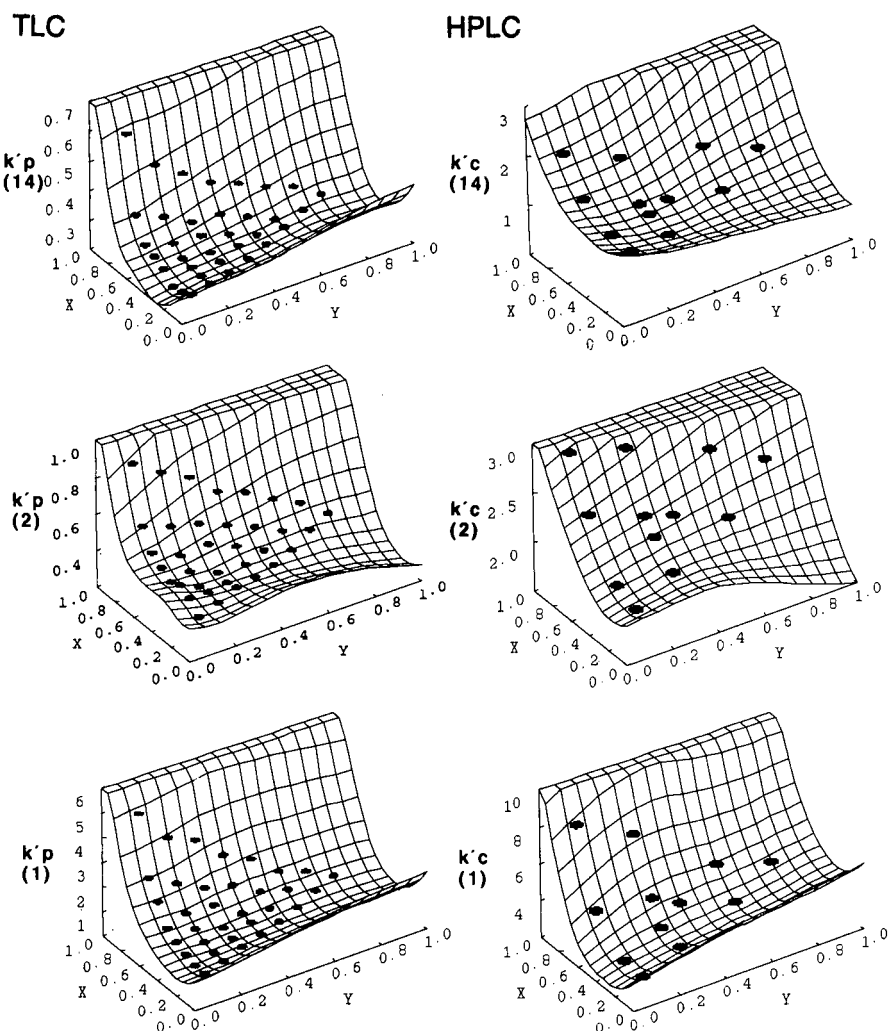


Fig. 4. The three-dimensional  $k'$  surfaces in TLC and HPLC for the three representative compounds ( $P_s=118$  at the front,  $P_s=181$  at the top,  $P_s=811$  on the right).

evaluate the effect of  $S_T$  on HPLC from TLC runs.

The separation factor ( $\alpha$ ) was defined as  $k'_2/k'_1$ , where  $k'_2$  is the capacity factor for the second-eluting peak and  $k'_1$  that for the first-eluting peak. The three-dimensional  $\alpha$  surfaces for each compound at all  $P_s$  values were constructed as described for the three-dimensional  $k'$  surfaces. Fig. 8 shows the behaviour of  $\alpha$  as demonstrated by the two first- ( $\alpha_1$ ) and two last- ( $\alpha_{13}$ ) eluting coumarins, and an average value ( $\alpha_x$ ) for seven coumarins eluting in the middle of the run. The average value was calculated

because the coumarins elute close to each other over a  $k'$  range of less than 1.25, and their relative elution order changed from one selectivity point to another.

The  $\alpha_1$  values give a starting inverted saddle for TLC and an inverted saddle for HPLC. In  $\alpha_x$  the saddles are no longer so pronounced. In  $\alpha_{13}$  the surfaces decrease quite smoothly from  $P_s$  118 down to the corner of 118 in TLC and HPLC. The  $\alpha$  surfaces behave alike in the two methods. This is in agreement with the fact that the distances between the

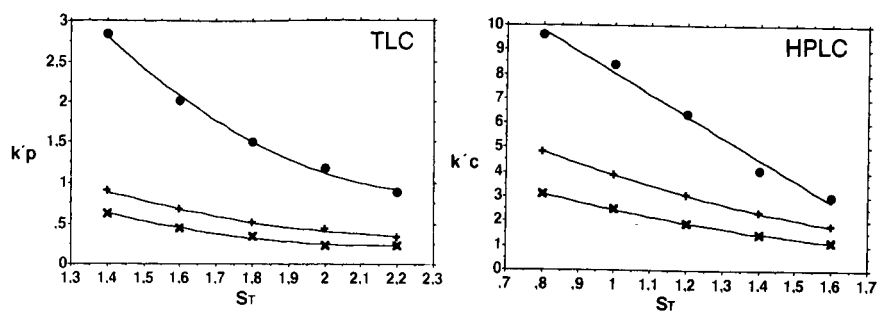


Fig. 5. The capacity factors plotted against the five solvent strengths ( $S_T$ ) tested in TLC and HPLC at  $P_s = 333$ .  $\times$  = Pimpinellin;  $+$  = herniarin;  $\bullet$  = umbelliferone.

TABLE I

SLOPES ( $A$ ), INTERCEPTS ( $B$ ) AND CORRELATION COEFFICIENTS ( $r$ ) FOR EQUATIONS OBTAINED FROM  $k'_{S_{Tx}} = Ak'_{S_{T1.4}} + B$  FOR TLC AND HPLC AT  $P_s = 333$

$S_T$	TLC			HPLC		
	$A$	$B$	$r$	$A$	$B$	$r$
0.8				3.47	-3.00	0.99
1.0				2.43	-1.58	0.99
1.2				1.53	-0.46	1.00
1.4	1.00	0	1.00	1.00	0	1.00
1.6	0.87	-0.19	0.99	0.47	0.66	0.97
1.8	0.43	0.11	0.99			
2.0	0.35	0.08	0.95			
2.2	0.20	0.14	0.95			

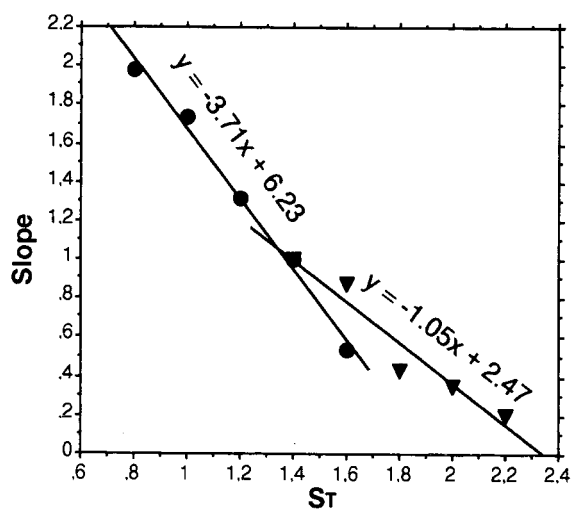


Fig. 6. The slope values plotted against various  $S_T$ .  $\nabla$  = TLC;  $\bullet$  = HPLC.

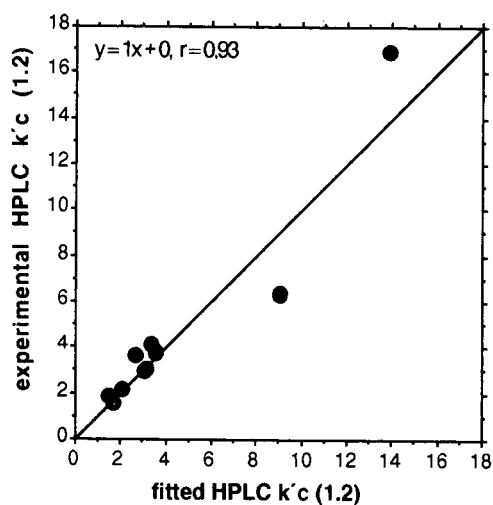


Fig. 7. Comparison of fitted  $k'_c$  values and experimentally obtained  $k'_c$  values.

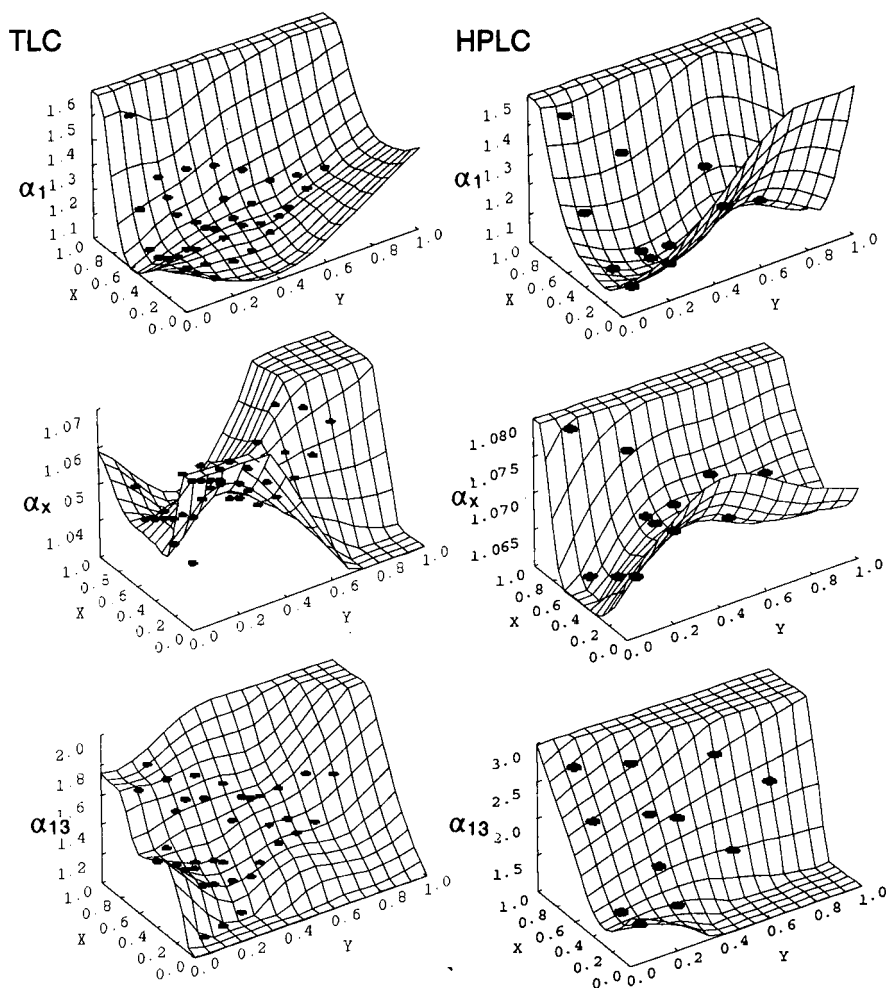


Fig. 8. The separation factors constructed as  $\alpha$  surfaces of the PRISMA ( $P_s = 118$  at front,  $P_s = 181$  at the top,  $P_s = 811$  to the right).

peaks follow an opposite order of detection in TLC and HPLC. It should also be borne in mind that the first-eluting compound in HPLC, which is usually the sharpest, is the compound with the longest elution in TLC (broadest). This is the case for the space between two compounds as well, *e.g.* the distance between compounds eluting furthest on the TLC plate is large, whereas in HPLC it is smaller and *vice versa*. The range of the  $\alpha$  values is kept rather constant in the methods.

To conclude, using a multicomponent eluent results in the same kind of behaviour with regard to the capacity factors of these fourteen coumarins. In the two- and three-dimensional evaluations of the

capacity factors in TLC and HPLC, rather similar behaviour of the coumarins can be observed when the mobile phase selectivity is changed. In TLC and HPLC, retention of the compounds is similarly dependent on mobile phase composition. It should be noted that a change in  $S_T$  in TLC has a different effect on the retention behaviour of the compounds than a change in  $S_T$  in HPLC. The range of the  $\alpha$  values is kept rather constant in TLC and HPLC. A similar, three-dimensional figure for the  $\alpha$  values is obtained with the methods.

The results showed that in normal-phase chromatography TLC can be used as an HPLC preassay method in the PRISMA system. The use of TLC



has the advantage that a great number of solvents can be screened for optimization of the mobile phase. It also gives preliminary information about the retention behaviour in HPLC ( $k'$  and  $\alpha$ ). The selectivity in HPLC can be described by experiments in TLC. However, the following must be taken into account when transferring the mobile phase: the elution process with regard to solvent strength is different in TLC and HPLC.

#### ACKNOWLEDGEMENTS

This work was supported by a grant from the Finnish Cultural Foundation, which is gratefully acknowledged.

#### REFERENCES

- 1 M. L. Bieganska and K. Glowinski, *Chromatographia*, 25 (1988) 111.
- 2 K. Glowinski and M. L. Bieganska, *J. Liq. Chromatogr.*, 8 (1985) 2927.
- 3 J. K. Rózylo and M. Janicka, *J. Planar Chromatogr.*, 3 (1990) 413.
- 4 S. Nyiredy, K. Dallenbach-Tölke, G.C. Zogg and O. Stichler, *J. Chromatogr.*, 499 (1990) 453.
- 5 K. Hostettmann, M. Hostettmann and A. Marston, *Preparative Chromatography Techniques*, Springer, Berlin, 1986, pp. 29–32.
- 6 S. Nyiredy, *Application of the "PRISMA" Model for the Selection of Eluent Systems in Over-Pressure Layer Chromatography (OPLC)*, Labor MIM, Budapest, 1987.
- 7 S. Nyiredy, K. Dallenbach-Tölke and O. Stichler, *J. Planar Chromatogr.*, 4 (1988) 336.
- 8 R. D. H. Murray, J. Méndez and S. A. Brown, *The Natural Coumarins*, Wiley, Chichester, 1982.
- 9 F. Geiss, *Fundamentals of Thin Layer Chromatography (Planar Chromatography)*, Hüthig, Heidelberg, 1987.
- 10 B. A. Bidlingmeyer, *Preparative Liquid Chromatography*, Elsevier, Amsterdam, 1987, pp. 50–55.
- 11 S. Nyiredy, K. Dallenbach-Tölke and O. Stichler, *J. Liq. Chromatogr.*, 12 (1989) 95.
- 12 H. Vuorela, K. Dallenbach-Tölke, R. Hiltunen and O. Stichler, *J. Planar Chromatogr.*, 1 (1988) 123.



# Asymmetric-channel flow field-flow fractionation with exponential force-field programming

J. J. Kirkland\*, C. H. Dilks, Jr., S. W. Rementer and W. W. Yau

*E. I. DuPont de Nemours Co., Experimental Station, P.O. Box 80228, Wilmington, DE 19880-0228 (USA)*

---

## ABSTRACT

Equipment and techniques have been developed to program the crossed-flow force fields with parallel-plate, asymmetric channels in flow field-flow fractionation (FIFFF). Force-field programming permits the rapid separation of samples with a wide range of molecular sizes; resolution is easily varied. Detectability of late-eluting components is enhanced as a result of band sharpening. Force-field programming probably can be performed with many functions. Exponential force-field decay method produces retention times vs. diffusion coefficient or particle size plots that are more linear than those from a constant force field. Resolution and measurement precision is more constant over the separation range. The exponential function also simplifies computer software measuring diffusion-coefficient and particle-size distributions. Optimum operating parameters for a desired FIFFF separation are predicted with a quantitative exponential force-field decay theory. Force-field programming significantly enhances the utility of the mild FIFFF method. Appropriate samples for this method include synthetic and natural polymers, organic and inorganic colloids and a variety of particulates.

---

## INTRODUCTION

Flow field-flow fractionation (FIFFF) is one of a family of field-flow fractionation (FFF) methods that exhibit unique properties for separating and characterizing a wide variety of macromolecular samples [1–5]. However, FIFFF is proving to be one of the most versatile and generally applicable of all of the FFF methods. FIFFF is capable of separating smaller macromolecules such as  $\geq 10^4$  molecular weight proteins [6,7], but also is well suited for describing the size of a wide range of colloidal particulates [4,7–9]. Retention in FIFFF is based on physical first principles [8]. Fundamental information such as diffusion coefficients is available from FIFFF retention data, and purified components are easily isolated during separations. FIFFF competes with sedimentation FFF (SdFFF) for many potential applications [4,5], but SdFFF equipment is more complicated and expensive, and compounds with molecular weights less than about  $2 \cdot 10^5$  are not retained with the highest force fields yet reported for this method [10].

In FIFFF, the force field needed for the separation is generated by flowing a carrier liquid across the channel thickness by means of semi-porous membranes forming the walls of the thin separating channel. FIFFF separations have been successfully carried out in channels made with parallel plates using two semi-permeable membranes [4,11] or in a porous hollow fiber [12]. However, the most successful FIFFF separations to date have been performed with the so-called asymmetric channel [6,7,13,14]. This approach uses only a single semi-permeable membrane at the channel bottom as the accumulation wall. A solid plate at the top forms the upper wall of the channel. To date most FIFFF separations with asymmetric channels have been conducted with constant force fields, that is, a constant volumetric flow of liquid carrier across the channel through the single semi-porous membrane. Equipment for this form of FIFFF is relatively inexpensive, and a simple theory describes sample properties as a function of observed retention [6]. FIFFF can be conveniently performed using constant force fields if sample components do not span too large a range in

molecular sizes (typically <50-fold). The highest resolution of closely eluting components is generally obtained with this approach.

However, as with the other FFF methods, the use of constant force fields limits the range of useful elution of components in a single separation [11]. In constant force-field separations, the resolution varies during the separation; the resolution of components increases with increasing retention. Detection is also difficult for highly retained materials owing to inherent broadening of bands with increasing retention. In theory, programming the flow eluting from the channel minimizes some of these limitations. Unfortunately, however, this approach has serious practical problems. Changes in the channel effluent flow cause significant difficulties in maintaining constant baselines and detector response for quantification.

To reduce the limitations of constant force-field operation in FIFFF, Wahlund *et al.* [11] programmed the force field during separations of water-soluble polymers using a rectangular channel with two semi-permeable membranes. The most successful programming used by these workers involved exponential decay of the force field. This is the programming form previously used extensively by Kirkland and co-workers for both sedimentation [15–17] and thermal [18,19] FFF separations. Other forms of continuous force-field programming undoubtedly also can be used advantageously in FIFFF. It is often convenient to field program the initial separation of an unknown sample to include a possible broad range of molecular sizes. This preliminary run is then followed by runs under constant field to focus on a desired narrower size range.

This paper describes the theory, equipment and technique for programming the force field exponentially within the channel during separation using asymmetric FIFFF channels. Although more complicated equipment is required for automation, this approach eliminates many of the limitations of the constant force-field method. Quantitative theory and software have been developed to describe elution when the force field is exponentially decayed during the separation. This combination permits the convenient measurement of diffusion-constant and particle-size distributions of macromolecules and particulates. Exponential decay of the force field during the separation results in more uniform

resolution of components across the elution profile. With a programmed force field, bands for highly retained components are compressed, making detection and quantitative measurement easier. Finally, the described method permits a constant flow through the detector during the separation, facilitating good detector baselines and subsequent quantitative measurements.

## EXPERIMENTAL

### *FIFFF apparatus*

Fig. 1 shows the general arrangements of components in our FIFFF equipment. Solvent metering devices 1–3 were Model 870 reciprocating pumps (DuPont Instruments, Wilmington, DE, USA). Pump 4 was a Model LC-5000 syringe pump (Isco, Lincoln, NE, USA). This pump was modified electrically to permit it to be used as an “unpump” to meter out precisely the channel effluent during the separation. This arrangement allows a constant flow out of the channel and through the detector. Flows from these systems were monitored by collecting pumped mobile phase in a volumetric flask for an observed time period. Model EC3W electronically actuated valves (Valco Instruments, Houston, TX, USA) were used as “on–off” and “focus–detector” valves. A Model EC6W electronically actuated valve (Valco Instruments) was the sample injector. All of these units were controlled with in-house-developed Turbo-Pascal software used on a PS-2 Model 30-286 personal computer (IBM, Boca Raton, FL, USA).

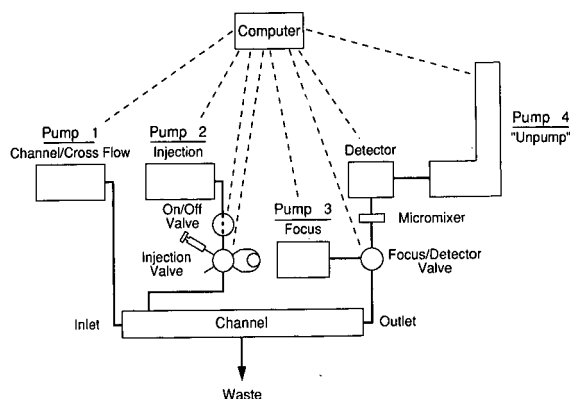


Fig. 1. Schematic diagram of FIFFF apparatus for cross-flow programming.

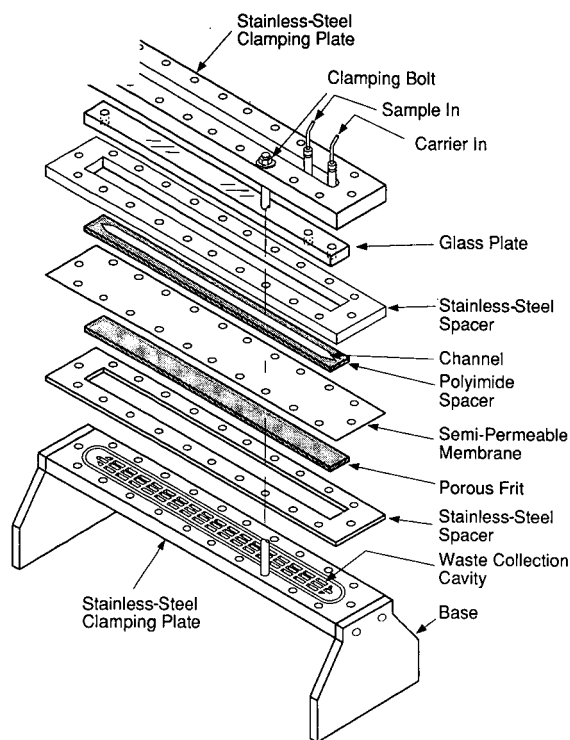


Fig. 2. Asymmetric FIFFF channel assembly: exploded view.

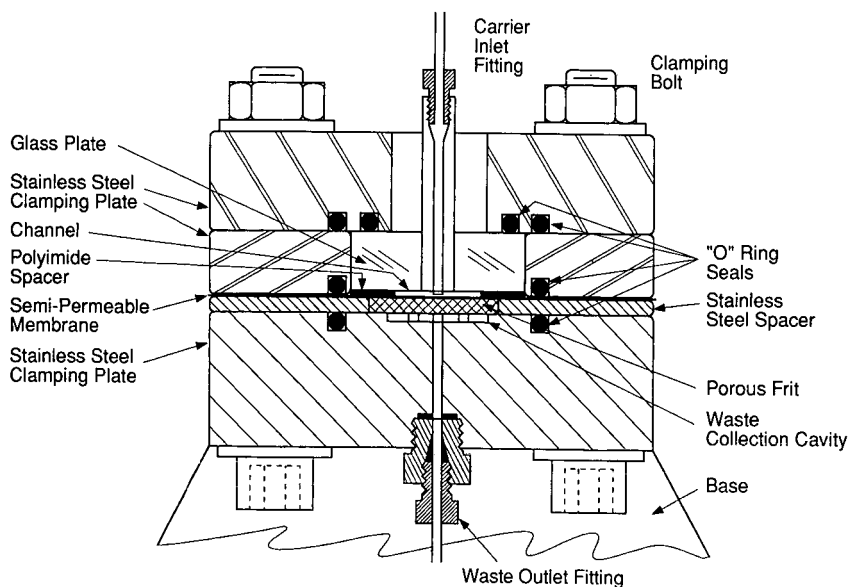


Fig. 3. Asymmetric FIFFF channel assembly: end-view.

The micromixer was a 0.25-ml magnetically stirred stainless-steel chamber. Detection was with a Model 783 UV-visible spectrophotometric high-performance liquid chromatographic detector (Kratos Analytical, Ramsey, NJ, USA). Detector output was displayed on a Model 822B10-3 recorder (Esterline-Angus Instrument, Indianapolis, IN, USA).

The FIFFF channel assembly is depicted by the exploded view in Fig. 2. Fig. 3 shows a scaled end-view of the channel assembly. The channel was of the rectangular asymmetric configuration [6], as depicted in Fig. 4. The separating channel was  $41.0 \times 2.0$  cm, formed with a nominal 0.025-cm thick Mylar polyester or Kapton polyimide film spacer (DuPont, Wilmington, DE, USA). The actual channel thickness was measured as 0.0241 cm by injecting a small sample of cytochrome *c* with no force field several times, and noting the average first moment of the eluted peak at a flow-rate of 0.20 ml/min (corrections were made for the extra-channel volume leading to the detector). As the volume, length and width of the channel were known, the thickness could be calculated. This channel was formed with  $90^\circ$  triangular inlet and outlet configurations.

The semi-permeable channel accumulation wall was a YM10 Diaflo ultrafiltration membrane (Amicon, Danvers, MA, USA). This membrane was

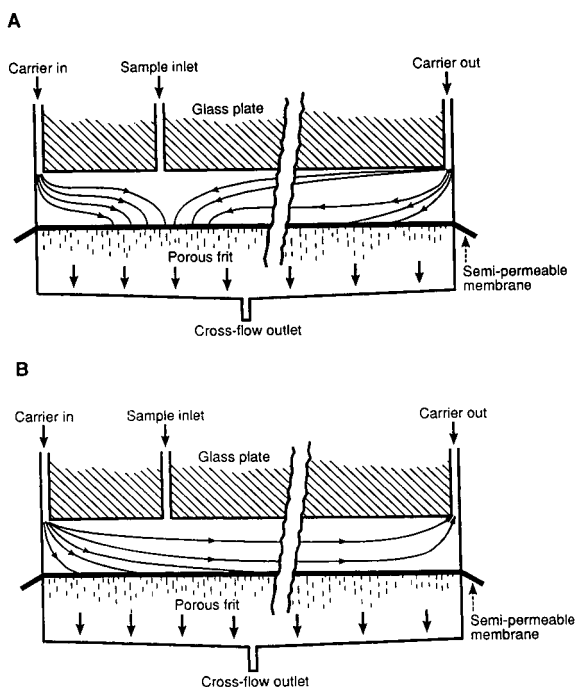


Fig. 4. Asymmetric channel for FIFFF. (A) Sample injection, relaxation and focusing step; (B) elution step.

supported by a precision-grade, 1/8-in. thick, 5- $\mu$ m porous polyethylene frit (General Polymer, West Reading, PA, USA). Buna-N O-rings (Mercer Rubber, Philadelphia, PA, USA) were used to seal the channel to the supporting plates. A drilled float-glass plate (Kaufman Glass, Wilmington, DE, USA) was the upper wall of the asymmetric channel. Sample injection was carried out through an injection port that was 3.5 cm downstream from the liquid carrier inlet port, in a manner similar to that described by Wahlund and Litzen [7]. The various units of the channel assembly were fabricated at the DuPont Experimental Station.

Operation of the FIFFF apparatus in the force-field programmed mode typically proceeds as follows (see Fig. 1). Simultaneously using pump 1 and "unpump" 4, the channel is first conditioned with the mobile phase carrier until a constant detector baseline is obtained. Pump 4 is then isolated with the "focus-detector" valve. The sample is slowly injected into the channel with mobile phase carrier by actuating pump 2 and displacing the sample from the loop of the injector valve (usually at 0.06–0.1

ml/min for a volume about twice the total volume of the sample loop and the connecting line). Simultaneously during this injection period, pumps 1 and 3 are actuated at flow-rates appropriate to focus the sample in a narrow band just below the sample inlet. This focusing approach is similar to that developed by Wahlund *et al.* [6,7,14]. Following the injection–focusing period, the "on–off" valve is closed. Sample focusing–relaxation can be continued with flow from pumps 1 and 3, if desired, or, if sufficient focusing–relaxation has been accomplished during injection, the "focus–detector" valve is actuated to close off pump 3 and access the "unpump" 4. Appropriate flow metering is then set on pumps 1 and 4 to conduct the desired separation. All steps in this procedure are conducted by the computer. The operator specifies the operating procedure by completing a software parameter block prior to the desired separation. The sample loop is filled manually, and the operator actuates the computer program to conduct the experiment automatically.

Separation data were collected on a PE/Nelson ACCESS-CHROM data-handling system (Nelson Analytical, Cupertino, CA, USA). In-house-developed software for the diffusion-coefficient or particle-size calculations and outputs was in FORTRAN 77 on a Vax 3100 computer (Digital Equipment, Maynard, MA, USA).

#### Reagents and chemicals

The proteins, Col E1 amp plasmid DNA, and Tris buffer were obtained from Sigma (St. Louis, MO, USA). Plasmid pSP 65 DNA was from Boehringer Mannheim Biochemicals (Indianapolis, IN, USA). Silica sol samples were prepared within DuPont. Samples of *Streptococcus faecalis* bacteria were kindly supplied by R. C. Ebersole of DuPont. Other materials for buffers and mobile phase additives were from J. T. Baker (Phillipsburg, NJ, USA).

#### THEORY

##### Retention with constant force field

Retention in FIFFF separations with a rectangular asymmetric channel and a constant force field (cross-flow) has previously been described by Wahlund and Giddings [6]. Retention times for well-retained components in such a system are described by

$$t_R = \left( \frac{W^2}{6D} \right) \ln \left[ \frac{\frac{z}{L} - \left( \frac{V_c + V_{out}}{V_c} \right)}{\left( 1 - \frac{V_c + V_{out}}{V_c} \right)} \right] \quad (1)$$

where  $t_R$  is the retention time of the component (s),  $W$  is the channel thickness (cm),  $D$  is the diffusion coefficient ( $\text{cm}^2/\text{s}$ ),  $z$  is the sample focusing distance from the channel inlet (cm),  $L$  is the channel length (cm),  $V_c$  is the cross-flow flow-rate (ml/min) and  $V_{out}$  is the flow-rate out of the channel (ml/min). Hence, component diffusion coefficients can be directly calculated from the retention time if all operating parameters are known.

Using the well known Einstein diffusion equation [20], retention can be directly related to the size of comparable spherical particles. Therefore, particle sizes can be determined by measuring the retention time, according to

$$d_p = \frac{2RTt_R}{(W^2 N \pi \eta) \ln \left[ \frac{\frac{z}{L} - \left( \frac{V_c + V_{out}}{V_c} \right)}{1 - \left( \frac{V_c + V_{out}}{V_c} \right)} \right]} \quad (2)$$

where  $d_p$  is the particle diameter (cm),  $R$  is the gas constant ( $8.31 \cdot 10^7 \text{ g cm}^2/\text{s}^2 \cdot \text{K} \cdot \text{mol}$ ),  $T$  is temperature (K),  $N$  is Avogadro's constant ( $6.02217 \cdot 10^{23}/\text{mol}$ ) and  $\eta$  is the mobile phase viscosity (Poise;  $\text{g/cm} \cdot \text{s}$ ). With this expression, the size of particulates can be calculated directly from retention using known operating parameters.

The relationship between retention time and diffusion coefficient for a rectangular asymmetric channel and a constant force field can be depicted graphically as shown in Fig. 5. This log-linear plot was calculated from eqn. 1 using the arbitrary but typical operating parameters given. As noted above, important characteristics of constant force-field operation in FIFFF are illustrated in this plot. First, less than two decades of diffusion coefficients (or particle sizes) can be accessed in a single experiment with good precision and in a convenient time span. Second, the difference in retention for two components with the same relative difference in diffusion coefficient (or particle size) is non-linear. The difference in retention between two large particles with small diffusion coefficients is much greater than that

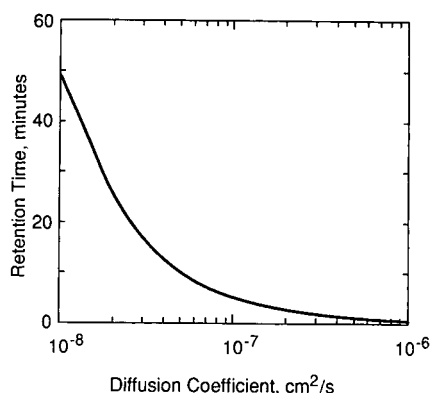


Fig. 5. Retention in FIFFF with asymmetric channel and constant force field.  $V_c = 1.0 \text{ ml/min}$ ;  $V_{out} = 0.5 \text{ ml/min}$ ;  $W = 0.0132 \text{ cm}$ ;  $L = 41.0 \text{ cm}$ ;  $z = 2.0 \text{ cm}$ ; breadth =  $2.0 \text{ cm}$ .

for small particles with larger diffusion coefficients. This comparison is made for particle pairs having the same relative diffusion coefficient difference, related to the same percentage change, or the same spacing of the two diffusion coefficients on a logarithmic scale.

#### *Retention using programmed force field with exponential decay*

To remove some of the limitations of constant force-field FIFFF operation, we developed the apparatus described above to permit programmed force-field operation. This equipment can be used to create virtually any form of force-field program. What type of force-field programming would be optimum for convenient and accurate measurements in FIFFF? We found no clear theoretical basis that a particular function for programming the force field would create the best compromise for the desired conditions, mainly uniform resolution across a wide range of component sizes in a reasonable separation time. However, constant force-field data such in Fig. 5 produced retention vs. diffusion coefficient relationships that were suggestive of a logarithmic form. Previously, we had found that in both sedimentation [15–17] and thermal [18,19] FFF, exponential-decay of the force field results in a simple calibration: a plot of particle size or molecular weight vs. retention time produces a straight line. This format provides several practical advantages, including essentially uniform resolution (and uniform measurement precision) across the separa-

tion range and convenient quantification of data. Our previous success with exponential programming in sedimentation and thermal FFF and the preliminary results of Wahlund *et al.* [11] encouraged us to develop the theory and software for performing FIFFF with this force-field programming function for asymmetric rectangular channels.

Retention in FFF can be represented by the retention ratio,  $R = V_o/V_R$ , where  $V_o$  is the channel volume and  $V_R$  is the retention volume of the sample component. Components that are well retained can be represented by  $R = 6\lambda$ , where  $\lambda$  is the ratio of the mean height of the sample cloud from the accumulation wall to channel thickness [4]. Retention for well retained components in asymmetric rectangular channels using programmed force fields with exponential decay during the separation can be described by

$$t_R = \left[ \frac{\tau}{\left(1 + \frac{6D\tau}{W^2}\right)} \right] \ln \left[ 1 + \left( \frac{L-z}{L} \right) \left( \frac{V_{co}}{V_{out}} \right) \left( 1 + \frac{W^2}{6D\tau} \right) \right] \quad (3)$$

where  $\tau$  is the time constant of the exponential decay (s) and  $V_{co}$  is the initial cross-flow flow rate (ml/min). Results can be expressed in terms of spherical particle size by using the Einstein relationship previously described for eqn. 2. Eqn. 3 is analogous to that described by Wahlund *et al.* [11] for rectangular channels with two semi-permeable membranes.

Previous studies in sedimentation [15–17] and thermal [18,19] FFF further demonstrated that a delay period equal to the time constant  $\tau$  of the exponential decay added to the range of linearity for the molecular weight or particle size *vs.* retention time plot. This method also is useful in providing additional separation between early eluting peaks and the potentially interfering channel dead-volume peak. The usefulness of this approach suggested that this also should be investigated for FIFFF separations. We found that retention in rectangular asymmetric channels using programmed force field with exponential delay and decay can be described by

$$t_R = \tau + \left( \frac{\tau}{1 + \frac{6D\tau}{W^2}} \right) \ln \left\{ 1 + \left[ \left( \frac{L-z}{L} \right) \cdot \frac{V_{co}}{V_{out}} \right] \cdot \left( 1 + \frac{W^2}{6D\tau} \right) + \left[ \frac{W^2}{6D\tau} \left( e^{-\frac{6D\tau}{W^2}} - 1 \right) \right] \right\} \quad (4)$$

Derivations of eqns. 3 and 4 are given in the Appendix.

#### SOFTWARE FOR QUANTIFICATION

To quantify desired diffusion-coefficient and particle-size distribution measurements, it was necessary to solve eqn. 3 for the diffusion coefficient,  $D$ , (or the corresponding particle diameter,  $d_p$ ) as a function of retention time,  $t_R$ . For this, an iterative numerical process was developed. This approach was simplified by combining certain parameters, so that

$$\alpha \equiv [(L-z)/L] [V_{co}/V_{out}] \quad (5)$$

and

$$S \equiv (6D\tau)/W^2 \quad (6)$$

Then, by iteration on  $S_i$  for the  $i$ th iteration,

$$S_i = \{ \tau \ln[1 + \alpha(1 + 1/S_{i-1})]/t_R \} - 1 \quad (7)$$

This approach relates the diffusion coefficient,  $D$ , to the retention time,  $t_R$ , that is,  $S = f(D)$ . Initially,

$$1/S_o \equiv 0; \quad S_1 = (\tau/t_R) \ln(1 + \alpha) - 1 \quad (8)$$

$S_i$  is solved by iteration when  $S$  is large. For late-eluting particles,  $\Delta S_j$  is calculated by

$$\Delta S_j = S(t_R + \Delta t_R) - S(t_R) \quad (9)$$

and

$$t_{R,j+1} = \tau / (1 + S_j + \Delta S_j) \ln \{ 1 + \alpha [1 + 1/(S_j + \Delta S_j)] \} \quad (10)$$

Here,  $\Delta S_j$  is manipulated to achieve equal steps in  $t_R$ , which is defined by the sampling rate.

For retention near zero,  $S$  (being inversely related to  $t_R$ ) is large and  $1/S$  is small. For this case, the mathematical relationship  $S = f(t_R, 1/S)$  is well behaved and eqn. 7 converges nicely, because the logarithmic term in eqn. 7 is dominated by  $\ln(1 + \alpha)$ . For later retentions,  $S$  is small and  $1/S$  is large. The



logarithmic term in eqn. 7 is then dominated by  $\ln(\alpha/S)$ , and the iteration behaves poorly. Therefore, for later retentions, the  $S$  value for the previous retention slice  $j$  is used to estimate  $S_{j+1}$ , and the corresponding retention time is determined. The iteration searches for  $\Delta S$  with eqn. 10 to achieve the known value of  $t_R$ : Fig. 6 is a graphical representation of  $\ln S$  vs. retention time,  $t_R$ , for several values of the exponential-decay time constant  $\tau$ .

## RESULTS AND DISCUSSION

### Effect of exponential-decay $\tau$ value on retention

The plots in Fig. 7 (based on eqns. 3 and 4) show the effect of changing the  $\tau$  value on retention with asymmetric rectangular channels using exponentially programmed force fields. Plots are given for exponential programs devised with arbitrary but realistic operating parameters with and without delay prior to the force field programming. As expected, the delay increases the time of elution between the first peak and the channel dead volume peak. Smaller  $\tau$  values result in plots that are increasingly more linear across the diffusion coefficient range selected for study. Larger  $\tau$  values increase the non-linearity of the calibration. As noted previously, a linear calibration generally is advantageous. More uniform resolution and mea-

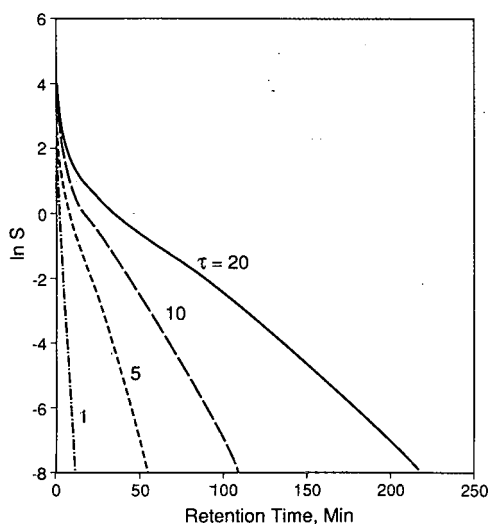


Fig. 6. Effect of combined retention parameters on retention time. See eqn. 10 for details.

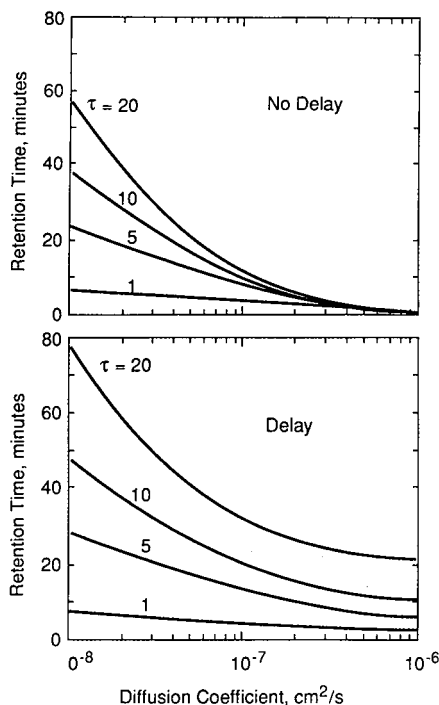


Fig. 7. Effect of  $\tau$  value on retention in FIFFF with asymmetric channel using exponentially programmed force field.  $V_{\infty} = 9.5$  ml/min;  $V_{out} = 0.5$  ml/min;  $W = 0.0132$  cm;  $L = 41.0$  cm;  $z = 4.3$  cm; breadth = 2.0 cm.

surement precision occurs across the separation range of interest in a practical analysis time. Contrary to experiences in sedimentation and thermal FFF, imposing a delay before starting the exponential decay does not appear to improve the calibration linearity.

The results presented in Fig. 7 and the following simulated plots represent a rough first attempt to determine the effects of the various operating parameters for exponentially programming the force field in FIFFF for asymmetric channels. In these simulation plots, results at very low retention are less valid because of the assumption of  $R = 6\lambda$  in eqns. 3 and 4. Still, these plots have been found useful in selecting useful experimental conditions for exponential programming in FIFFF.

As expected, similar effects were seen for retention time vs. particle diameter relationships, as shown in Fig. 8. In this instance, different operating parameters from those in Fig. 7 were selected to verify the general trends. Again, log-linear calibration and

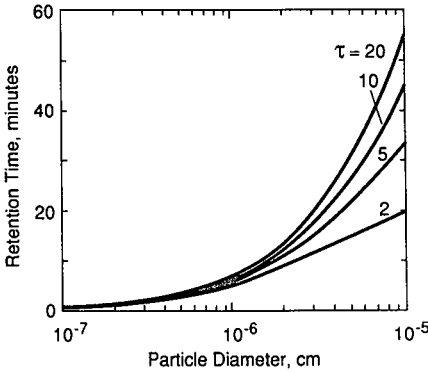


Fig. 8. Effect of  $\tau$  value on particle retention in FIFFF with asymmetric channel using exponentially programmed force field. Conditions as in Fig. 7, except  $V_{out} = 1.0$  ml/min.

approximately uniform separation are more nearly approached at smaller  $\tau$  values. In this instance, calibration plots with delay in the force field before exponential decay were not prepared.

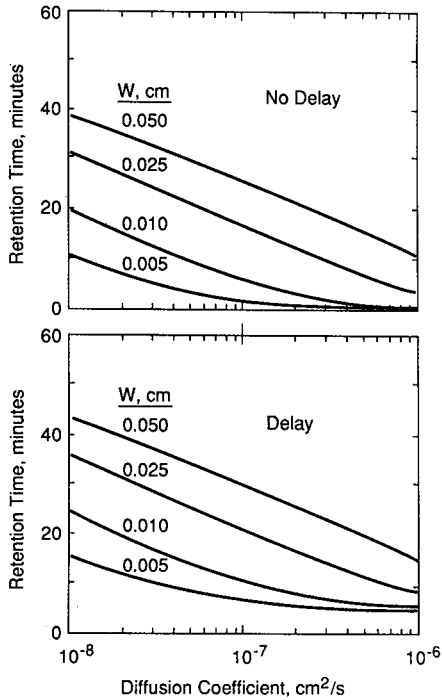


Fig. 9. Effect of channel thickness on retention in FIFFF with asymmetric channel using exponentially programmed force field. Conditions as in Fig. 7, except for  $W$  and  $\tau = 5.0$  min.

*Effect of channel thickness on retention*

The effect of channel thickness on retention with exponential force-field decay is shown in Fig. 9. These results suggest that log-linear calibration linearity is favored with wider channels, with channel thicknesses of 0.025 cm being about optimum for these particular operating conditions. No difference in calibration linearity is shown between separations carried out with and without delay before exponential decay. However, use of the delay does permit better separations of early-eluting peaks from the peak at the channel dead-time,  $t_0$ , at the expense of increased separation time. Note that increasing the channel thickness involves other compromises, as the separation time and band width also change [8]. Increasing the channel thickness does not appear to change significantly the relative separation between the same two components, as indicated by the approximately constant slope of the log-linear calibration graphs. The exception is very narrow channels and components with larger diffusion coefficients.

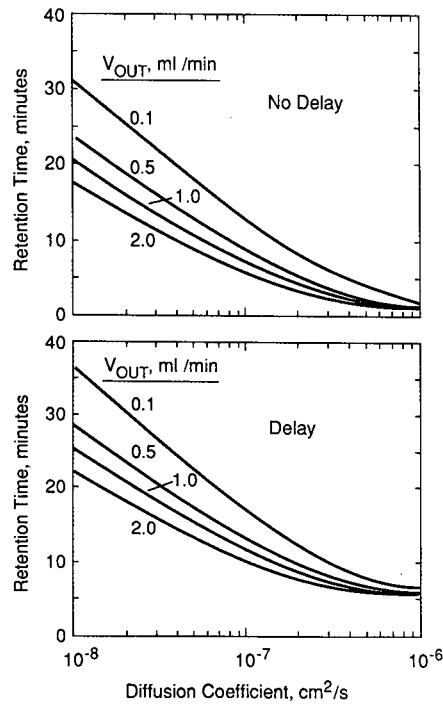


Fig. 10. Effect of channel effluent out-flow on retention in FIFFF with asymmetric channel using exponentially programmed force field. Conditions as in Fig. 7, except for  $V_{out}$  and  $\tau = 5.0$  min.

### Effect of channel effluent out-flow on retention

Fig. 10 shows the effect of channel effluent out-flow  $V_{out}$  with an asymmetric rectangular channel on retention using exponential force-field programming. Calibration linearity is not seriously influenced by the level of  $V_{out}$ . However, larger retention time differences occur at lower flow-rates. Bands also should be narrower at lower flow-rates because of more favorable mass-transfer effects [8]. Again, imposing a delay before exponential decay does not affect calibration linearity.

### Effect of initial cross-flow on retention

The effect of initial cross-flow,  $V_{co}$ , on retention in exponential force-field programming is shown in Fig. 11. As expected, increasing the initial force field increases retention. Calibration linearity also is better approached at higher initial force fields. Relative separations are not affected by the initial force field, except for small components with larger diffuson coefficients. The possible deleterious effect

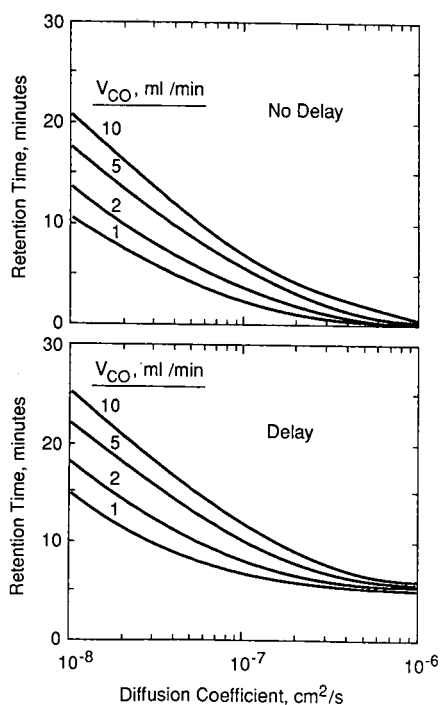


Fig. 11. Effect of initial cross-flow force field on retention in FIFFF with asymmetric channel using exponentially programmed force field. Conditions as in Fig. 7, except for  $V_{co}$  and  $\tau = 5.0$  min.

of higher initial force fields causing problems with unwanted interaction of components with rough semi-permeable membranes forming the accumulation is not predicted by this analysis. The effect of possible steric interactions also is not featured.

### Effect of channel length on retention

With a constant initial cross-flow, changes in channel length have little effect on retention in exponential programming, as shown in Fig. 12. These results suggest that shorter asymmetric channels (10–20 cm?) might be better suited for programmed separations in FIFFF under these conditions. This plot pictures components that are well retained on the channel until a certain lower force field is reached during programming. At that point components move rapidly down and out of the channel. The use of shorter channels may be practical because of the ability to focus the injected sample into a narrow band before starting the separation [7]. Focusing the injected sample mini-

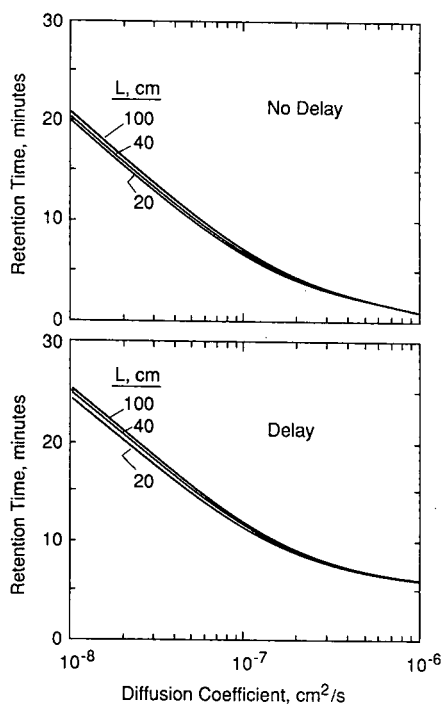


Fig. 12. Effect of channel length on retention in FIFFF with asymmetric channel using exponentially programmed force field: constant cross-flow. Conditions as in Fig. 7, except for  $L$  and  $\tau = 5.0$  min.

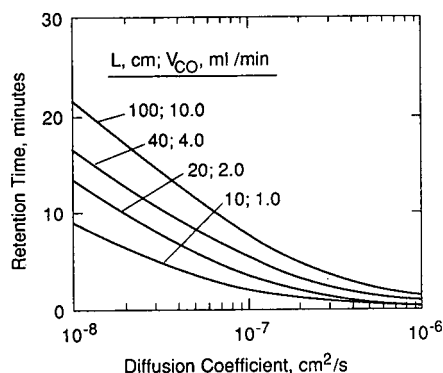


Fig. 13. Effect of channel length on retention in FIFFF with asymmetric channel using exponentially programmed force field: constant force field. Conditions as in Fig. 7, except for  $L$ ,  $V_{CO}$  and  $\tau = 5.0$  min.

mizes band-broadening difficulties that arise from utilizing some of the channel length at the inlet to contain the injected sample, as is often the case in sedimentation [15,21] and thermal [22,23] FFF separations.

However, the results are different if the initial

force field is maintained constant by proportionately decreasing the cross-flow as the channel is shortened, as shown in Fig. 13. Here, decreasing the channel length with exponential programming also decreases retention. This situation may be more typical of actual experiments where the channel length is not usually changed as an operating parameter. The results in Fig. 13 suggest that channel lengths in the range 20–40 cm may be a good compromise for many FIFFF separations, whether constant-field or programmed-field operation is considered.

## APPLICATIONS

### *Biological macromolecules*

The ability to program the force field during the FIFFF separation allows the elution of a wide range of component sizes (molecular weight) to be eluted in a convenient time. This capability is illustrated in Fig. 14 by the 35-min separation of a synthetic mixture of proteins and plasmid DNAs (no time delay was used in the exponential decay program

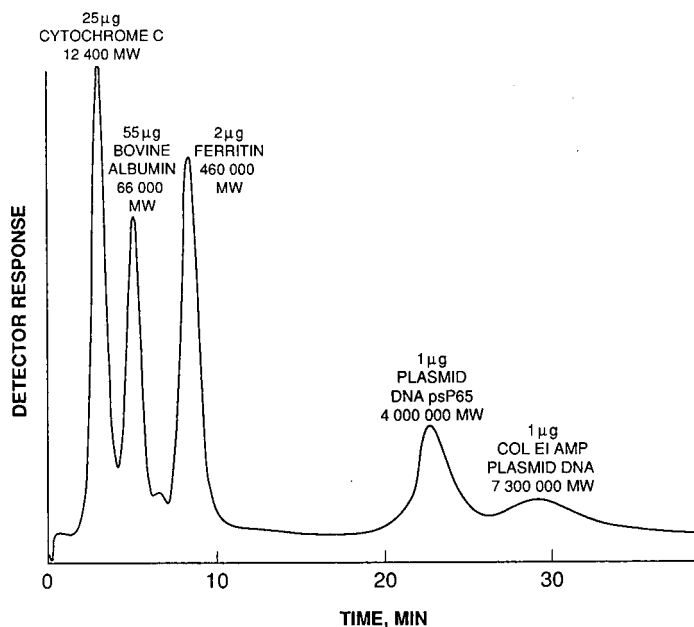


Fig. 14. Fractionation of proteins and nucleic acids with asymmetric channel using exponentially programmed force field. Channel,  $41 \times 2.0 \times 0.0241$  cm; focus distance, 4.3 cm; initial cross-flow, 9.0 ml/min; channel out-flow, 1.0 ml/min; sample injection at 0.06 ml/min for 4.0 min; sample injection/focus: pump (1) 1.0 ml/min, pump (2) 10.0 ml/min for a total of 8.0 min; exponential decay constant, 6.0 min; mobile phase, 0.05 *M* Tris buffer (pH 7.67)–0.05 *M*  $K_2SO_4$ –0.02% sodium azide; detector, UV, 260 nm, 0.02 a.u.f.s.; sample volume, 0.050 ml; components as shown.

used for this and the other applications reported in this paper). The first- and last-eluting compounds in the mixture in Fig. 14 have molecular weights of 12 400 and 7 300 000, respectively. This represents a molecular weight range ratio of about 600 separated in a single experiment. A stepwise gradient was previously used to separate human serum albumin from the dimer and trimer, but this approach involved a much narrower molecular weight range of components [13].

Calculation of the diffusion coefficients for the proteins in Fig. 14 produced values that closely correlated with those in the literature (e.g., for cytochrome *c* and bovine serum albumin,  $11.0 \cdot 10^{-7}$  and  $5.8 \cdot 10^{-7}$  cm<sup>2</sup>/s, respectively, compared with  $11.1 \cdot 10^{-7}$  and  $5.9 \cdot 10^{-7}$  cm<sup>2</sup>/s reported [24]). However, values for the high-molecular-weight plasmids appeared to be considerably larger than those predicted, suggesting that these materials were retained additionally by some other mechanism. It appears unlikely that this additional retention was caused by chemical interaction with the membrane. This cellulosic membrane material normally does not display such effects, particularly in the pH-ionic strength environment used in this study. We speculate, therefore, that the added retention is due to physical interaction with micro-imperfections of the membrane surface. The strong initial force used for the separation probably pushes the large plasmids into observable micro-crevices or pockets in the membrane surface. Because of poor diffusion for these large components, significant time is required for diffusion out of the micro-crevices back into the normal channel flow streams. The net effect is that the components then elute at retention times that are larger than predicted. Apparently, more lightly retained components (such as the proteins in Fig. 14) do not interact deleteriously with the rough membrane surface, probably because they are not pushed sufficiently close to the surface by the particular crossed-flow force field used. These postulates are substantiated by constant force-field FIFFF separations with the same membrane (and membranes with similar surface-roughness properties) that elute components with predicted diffusion coefficients [6,7,13,14]. In these instances, modest force fields apparently did not push the components into a region in which the deleterious interaction with the membrane could occur.

The results with the large components in the separation in Fig. 14 and other similar experiments strongly suggest that much smoother membranes are needed for FIFFF. This is especially the case when programming with high initial force fields is used with samples containing large components. Studies to identify better membranes for FIFFF are in progress.

No attempt was made in Fig. 14 to optimize the range of component resolution or separation time. Therefore, all of these separation goals probably could be improved, if desired. Optimizing such a separation could be carried out by manipulating channel thickness, initial and outlet channel flow-rates and the value of the exponential time constant,  $\tau$ . We believe that more than three decades of molecular weight difference can be comfortably spanned in a single FIFFF separation using optimized programming techniques.

#### *Biological particulates*

The use of exponential programming in FIFFF to separate a "real" sample of biological material is illustrated in Fig. 15. A 4-day-old isolate of *Streptococcus faecalis* bacteria was observed to have two minor and two major constituents. The minor components may be contaminating proteins that were expressed by the bacteria during storage at 4°C. The larger component eluting at *ca.* 21 min appears to be the "singles" or individual bacteria. The last large peak at *ca.* 30 min represents "chains" of these bacteria that are known to occur and are microscopically observed. Fig. 16 shows the particle-size ( $P_s$ ) distributions associated with the two major peaks. These plots were obtained with software based on eqn. 3, using a special deconvolution method [25] to isolate each population effectively. The material in the first large peak eluting at 21 min demonstrated a weight-average diameter of 0.45  $\mu$ m (Fig. 16A), with a sample polydispersity (weight-average/number-average) of 1.32 (uncorrected for band dispersion). This size is in keeping with microscopically observed values [26]. The differential plots in Fig. 16 relate the relative component concentration to the log (particle size) ( $P_s$ ). The cumulative plot relates the relative weight fraction of the component to the log (particle size). The material in the second large peak at 30 min in Fig. 15 showed a weight-average diameter of 2.1  $\mu$ m (Fig. 16B), with

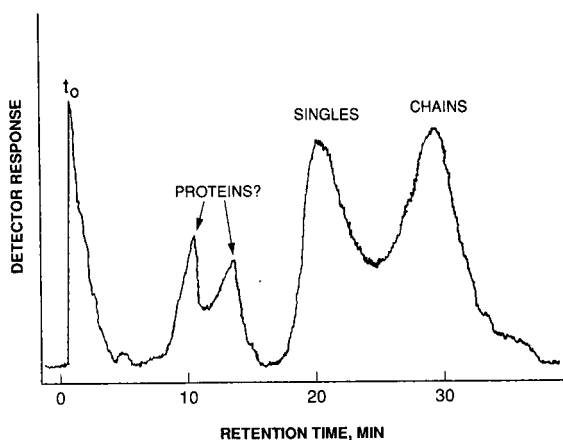


Fig. 15. Fractionation of *Streptococcus faecalis* bacteria sample with exponentially programmed FIFFF. Conditions as in Fig. 14, except initial cross-flow, 5.0 ml/min; channel out-flow, 2.0 ml/min; injection-focus, pump (1) 0.5 ml/min, pump (2) 4.5 ml/min for a total of 8.0 min; exponential decay time constant, 5.0 min; detector, 220 nm, 0.05 a.u.f.s.

a polydispersity of 1.52. These data suggest that this population is largely a mixture of 4–6-mer chains, with much smaller amounts of dimers largely in the “valley” between the two peaks. The data also

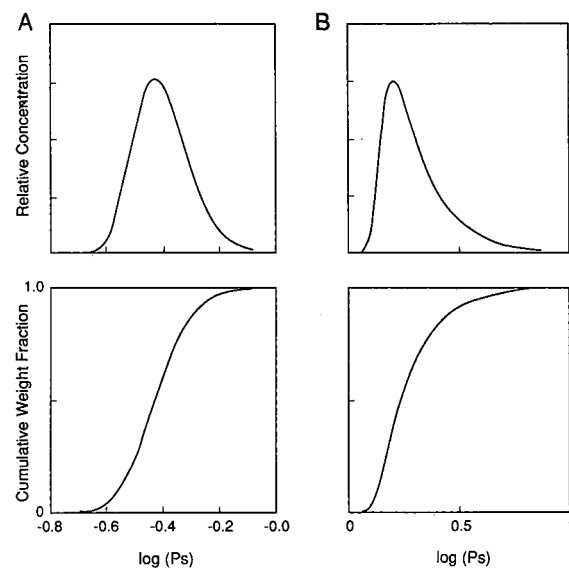


Fig. 16. Particle size distribution plots for *Streptococcus faecalis* bacteria. (A) 21-min peak (Fig. 15); (B) 30-min peak (Fig. 15). (A) Particle diameter: weight-average (A) 0.45  $\mu\text{m}$ ; (B) 2.1  $\mu\text{m}$ ; number-average: (A) 0.34  $\mu\text{m}$ ; (B) 1.4  $\mu\text{m}$ ; polydispersity: (A) 1.32, (B) 1.52.

suggest decreasing amounts of longer chains in the “tail” of the latter peak. Again, these results are in keeping with known properties associated with this bacterium and with microscopic observations [26].

The size of the “chains” in Fig. 15 might be expected to lead to earlier retention because of steric effects for these large components [27,28]. However, this effect apparently is not a strong feature under the conditions of force-field programming used. These and other of our studies in both FIFFF and SdFFF have suggested that force-field programming can be adapted to minimize steric effects associated with large components in mixtures of a wide size range. It is not intuitive that exponential programming actually minimizes the potential for steric interaction, if properly invoked. Smaller  $\tau$  and  $V_{\text{out}}$  values reduce the tendency for steric interaction during an exponentially programmed separation. At the beginning of the separation, the initial high force field holds the components tightly so they essentially do not move down the channel; steric forces are inoperable. As the force field is decreased exponentially, the components rapidly move away from the accumulation wall, so that steric forces quickly become less effective.

Another phenomenon may have compensated for any steric effects that might have occurred in the separation in Fig. 15. Other studies in sedimentation FFF have shown that particle conformation can seriously affect retention. Components with high aspect ratios are apparently intercepted by faster flow streams than theoretical, causing earlier retention and smaller calculated particle sizes than expected [29].

### Inorganic colloids

The utility of programmed FIFFF for measuring the particle-size distribution of inorganic colloids is shown in Fig. 17. This fractogram of a synthetic mixture containing three different silica sols of widely different sizes demonstrates the capability of the exponential programming method to analyze rapidly a sample of wide particle size distribution in a single experiment. A micro-mixing device was used between the channel and the detector to eliminate severe noise within the detector as the colloidal sample passed through the cell. This “noise” is caused by inhomogeneity in the channel effluent emerging from the channel. This effect can be

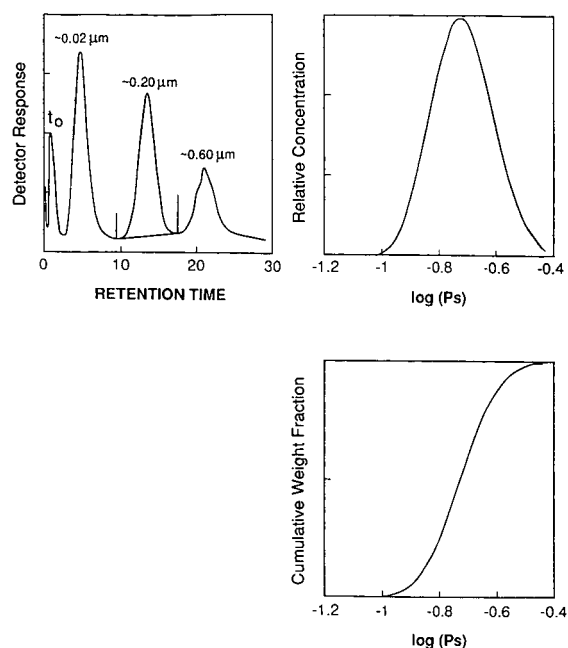


Fig. 17. Fractionation of silica sol mixture by exponentially programmed FIFFF. Conditions as in Fig. 14, except initial cross-flow, 3.0 ml/min; channel out-flow, 2.0 ml/min; injection-focus, pump (1) 0.3 ml/min, pump (2) 2.7 ml/min for a total of 5.0 min; exponential decay time constant, 4.0 min; sample, 0.050 ml of 2.5, 0.05 and 0.005% each of the increasingly larger silica sols; UV detector, 220 nm, 0.05 a.u.f.s. Particle diameter: weight-average  $0.21\ \mu\text{m}$ ; number-average  $0.18\ \mu\text{m}$ ; particle dispersity = 1.22. Retention time in min.

removed by using the stirring micro-mixer depicted in Fig. 1, or by using a low-volume packed-bed column of *ca.*  $150\text{-}\mu\text{m}$  glass beads. Fig. 17 shows the differential and cumulative particle-size distribution plots of the middle-size component of this mixture, with a weight-average of  $0.21\ \mu\text{m}$  and a polydispersity of 1.22. Results for the  $0.020\text{-}$  and  $0.20\text{-}\mu\text{m}$  silica sols correlate closely with values obtained by sedimentation FFF for these samples. However, the calculated value for the  $0.60\text{-}\mu\text{m}$  sample was significantly higher than that measured by transmission electron microscopy. This suggests an interaction of this material with the rough surface of the membrane in the same manner discussed for the plasmids in Fig. 14.

#### Synthetic polymers

FIFFF is well suited for characterizing a wide range of synthetic polymers, as illustrated by the

separation of a commercial sample of polyacrylamide in Fig. 18. Fig. 18A is the detector signal obtained during the exponentially programmed separation. The values listed in the figure caption are various diffusion-coefficient averages and the sample polydispersity calculated for this sample. The smoothed differential and cumulative plots in Fig. 18B and C are the result of a computer deconvolution method used for the presentation.

The FIFFF method is not limited to water-soluble polymers. Organic-soluble polymers should be handled following minor alterations of our equipment. Future studies will investigate the proposed method for determining not only diffusion-coefficient distributions, but also molecular-weight distributions based on fundamental hydrodynamic volume relationships.

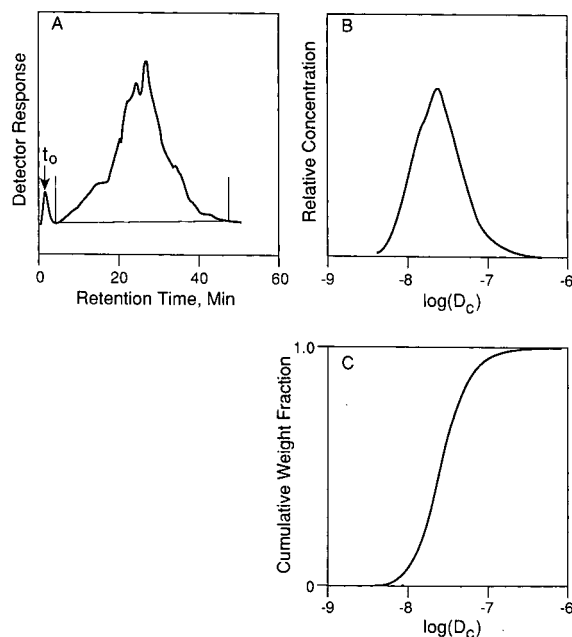


Fig. 18. FIFFF characterization of Septran MLG polyacrylamide sample. Conditions as in Fig. 14, except mobile phase,  $0.01\ M\ \text{KH}_2\text{PO}_4$  adjusted to pH 6.2 with NaOH; initial cross-flow, 5.0 ml/min; channel out-flow, 1.0 ml/min; exponential decay time constant, 7.0 min; sample  $50\ \mu\text{l}$ , 0.5% in mobile phase; detection, UV, 215 nm.  $[D_c]_0 = 1.74 \cdot 10^{-8}$ ;  $[D_c]_{+1} = 4.06 \cdot 10^{-8}$ ;  $[D_c]_{+2} = 1.05 \cdot 10^{-7}$ ;  $d_{[D_c]} = 2.33$ .

## CONCLUSIONS

This study has shown that exponentially programming the (cross-flow) force field in FIFFF is a convenient and effective way to provide data that permit the measurement of diffusion-coefficient- and particle-size-distributions of macromolecular components and particulates. Although an asymmetric rectangular channel was used as a model in this study, the described approach can be used for channels of any configuration. The method has certain distinct advantages over constant force-field operation, including (a) the ability to separate a wide range of components with a single experiment in a convenient time span; (b) maintaining more uniform resolution over a wide retention range; (c) easier

detection of highly retained components; and (d) constant flow out the channel for constant detector response and good baseline stability. Although force-field programming involves more complicated apparatus, operation is simplified and made more reproducible with the use of automated computer-directed interfaces.

## ACKNOWLEDGEMENTS

We thank V. Ivansons and E. R. Tinder, Jr., of the DuPont Experimental Station Engineering Crafts and Utilities Service Division for developing the computer-controlling system for the FIFFF instrument. We also thank R. C. Ebersole for the sample of *Streptococcus faecalis* bacteria.

## APPENDIX

## Derivation of eqns. 3 and 4

$$\chi = W$$

$$\begin{array}{c} \langle v \rangle_{\text{in}} \rightarrow \hspace{15em} \rightarrow \langle v \rangle_{\text{out}} \\ \hline \begin{array}{ccc} \chi = 0 & \downarrow & \downarrow & \downarrow \\ z = 0 & & u = v\chi \cdot \frac{W}{L} & z = L \end{array} \end{array}$$

The migration of retained solutes moving downstream a distance  $z$  can be described as

$$\frac{dz}{dt} + \left( \frac{6D}{W^2} \right) z = \frac{6DL}{W^2} \left[ \frac{\langle v \rangle_{\text{in}}}{\langle v \rangle_{\text{in}} - \langle v \rangle_{\text{out}}} \right] \quad (\text{A1})$$

Let  $v_\chi = \langle v \rangle_{\text{in}} - \langle v \rangle_{\text{out}}$ , then eqn. A1 becomes

$$\frac{dz}{dt} + \left( \frac{6D}{W^2} \right) z = \frac{6DL}{W^2} \left[ \frac{v_\chi + \langle v \rangle_{\text{out}}}{v_\chi} \right] = \frac{6DL}{W^2} + \frac{6DL}{W^2} \cdot \frac{\langle v \rangle_{\text{out}}}{v_\chi}$$

or

$$\frac{dy}{dt} + \left( \frac{6D}{W^2} \right) y = - \left( \frac{6DL}{W^2} \right) \frac{\langle v \rangle_{\text{out}}}{v_\chi} \quad (\text{A2})$$

with  $y = (L - z)$ . The solution to the first-order ordinary differential equation of the type of eqn. A2 is readily available in the following form (with  $c$  = integration constant):

$$y = e^{\frac{-6Dt}{W^2}} \left\{ c + \int e^{\frac{6Dt}{W^2}} \left[ - \frac{6DL}{W^2} \frac{\langle v \rangle_{\text{out}}}{v_\chi} \right] \frac{1}{v_\chi} \cdot dt \right\} \quad (\text{A3})$$



*Derivation of eqn. 3*

For the case of exponential-decay force-field programming,

$$v_x = v_{x^0} e^{-t/\tau} \quad (\text{A4})$$

and eqn. A3 becomes (with constant  $\langle v \rangle_{\text{out}}$ )

$$\begin{aligned} y &= e^{-\frac{6Dt}{W^2}} \left\{ c + \int e^{\frac{6Dt}{W^2}} \left[ -\frac{6DL \langle v \rangle_{\text{out}}}{v_{x^0} W^2} \right] e^{t/\tau} dt \right\} \\ &= c e^{-\frac{6Dt}{W^2}} - \frac{L \langle v \rangle_{\text{out}}}{v_{x^0}} \left( \frac{1}{1 + \frac{W^2}{6D\tau}} \right) e^{t/\tau} \end{aligned} \quad (\text{A5})$$

With the initial condition of  $y = L - z$  at  $t = 0$  (recalling that  $z$  is the sample focus distance in the channel), eqn. A5 gives the following expression for the integration constant  $c$ :

$$c = L - z + \frac{L \langle v \rangle_{\text{out}}}{v_{x^0}} \left( \frac{1}{1 + \frac{W^2}{6D\tau}} \right) \quad (\text{A6})$$

At  $t = t_R$ , the solute emerges from the channel, when  $z = L$  or  $y = 0$ . By combining eqns. A5 and A6 and setting  $y = 0$ :

$$\left[ L - z + \frac{L \langle v \rangle_{\text{out}}}{v_{x^0}} \left( \frac{1}{1 + \frac{W^2}{6D\tau}} \right) \right] e^{-\frac{6Dt_R}{W^2}} = \left[ \frac{L \langle v \rangle_{\text{out}}}{v_{x^0}} \left( \frac{1}{1 + \frac{W^2}{6D\tau}} \right) \right] e^{t_R/\tau} \quad (\text{A7})$$

By rearranging and taking logarithms, eqn. A7 becomes

$$t_R = \frac{\tau}{1 + \frac{6D\tau}{W^2}} \cdot \ln \left[ 1 + \frac{L - z}{L} \cdot \frac{V_{\text{co}}}{V_{\text{out}}} \left( 1 + \frac{W^2}{6D\tau} \right) \right] \quad (\text{A8})$$

As  $\langle v \rangle_{\text{out}} WB = v_{\text{out}}$  (volumetric flow-rate of channel effluent) and  $u_0 LG = V_{\text{co}}$  (initial volumetric cross-flow-rate),

$$\frac{V_{\text{co}}}{V_{\text{out}}} = \frac{U_0 L}{\langle v \rangle_{\text{out}} W} = \frac{v_{x^0}}{\langle v \rangle_{\text{out}}} \quad (\text{A9})$$

By substituting eqn. A9 in eqn. A8, we complete the derivation of eqn. 3:

$$t_R = \frac{\tau}{1 + \frac{6D\tau}{W^2}} \cdot \ln \left[ 1 + \frac{L - z}{L} \cdot \frac{V_{\text{co}}}{V_{\text{out}}} \left( 1 + \frac{W^2}{6D\tau} \right) \right] \quad (\text{A10})$$

*Derivation of eqn. 4*

For  $t < \tau$ ,  $v_x = v_{x^0}$ , and for  $t \geq \tau$ ,  $v_x = v_{x^0} e^{-\frac{t-\tau}{\tau}}$ . For  $t < \tau$ , from eqn. A3:

$$\begin{aligned} y &= e^{-\frac{6Dt}{W^2}} \left\{ c + \int e^{\frac{6Dt}{W^2}} \left[ -\frac{6DL \langle v \rangle_{\text{out}}}{v_{x^0} W^2} \right] dt \right\} \\ &= c e^{-\frac{6Dt}{W^2}} - \frac{L \langle v \rangle_{\text{out}}}{v_{x^0}} \end{aligned}$$

With the initial condition  $y = L - z'$  at  $t = 0$ :

$$y_{\tau} = y_{t=\tau} = (L - z') e^{-\frac{6D\tau}{W^2}} + \frac{L \langle v \rangle_{\text{out}}}{v_{\chi^0}} \left( e^{-\frac{6D\tau}{W^2}} - 1 \right) \quad (\text{A11})$$

For  $t \geq \tau$ , let  $t' = t - \tau$  and from eqn. A3:

$$y = c' e^{-\frac{6Dt'}{W^2}} - \frac{6DL \langle v \rangle_{\text{out}}}{v_{\chi^0} W^2} \cdot \frac{1}{\left( \frac{6D}{W^2} \right) + \frac{1}{\tau}} \cdot e^{t'/\tau} \quad (\text{A12})$$

With the initial condition  $y = y_{\tau}$  at  $t' = 0$ :

$$c' = y_{\tau} + \frac{L \langle v \rangle_{\text{out}}}{v_{\chi^0}} \cdot \frac{1}{1 + \frac{W^2}{6D\tau}}$$

and

$$y = \left[ (L - z') e^{-\frac{6D\tau}{W^2}} + \frac{L \langle v \rangle_{\text{out}}}{v_{\chi^0}} \left( e^{-\frac{6D\tau}{W^2}} - 1 + \frac{1}{1 + \frac{W^2}{6D\tau}} \right) \right] e^{-\frac{6Dt'}{W^2}} - \frac{L \langle v \rangle_{\text{out}}}{v_{\chi^0}} \left( \frac{1}{1 + \frac{W^2}{6D\tau}} \right) e^{t'/\tau} \quad (\text{A13})$$

Since, at the time of solute elution,  $t' = t_R - \tau$  at  $y = 0$ :

$$e^{\frac{t_R}{\tau} \left( 1 + \frac{6D\tau}{W^2} \right)} = e \cdot \left\{ \left( 1 + \frac{W^2}{6D\tau} \right) \cdot \left[ \frac{(L - z') v_{\chi^0}}{L \langle v \rangle_{\text{out}}} + 1 \right] - \frac{W^2}{6D\tau} e^{\frac{6D\tau}{W^2}} \right\} \quad (\text{A14})$$

or

$$\begin{aligned} t_R &= \left( \frac{\tau}{1 + \frac{6D\tau}{W^2}} \right) \left( 1 + \ln \left\{ 1 + \left( \frac{L - z'}{L} \right) \frac{V_{\text{co}}}{V_{\text{out}}} + \frac{W^2}{6D\tau} \left[ 1 + \left( \frac{L - z'}{L} \cdot \frac{V_{\text{co}}}{V_{\text{out}}} \right) - e^{\frac{6D\tau}{W^2}} \right] \right\} \right) \\ &= \left( \frac{\tau}{1 + \frac{6D\tau}{W^2}} \right) \left\{ \left( 1 + \frac{6D\tau}{W^2} \right) + \ln \left[ \left( 1 + \frac{L - z'}{L} \cdot \frac{V_{\text{co}}}{V_{\text{out}}} \right) \left( 1 + \frac{W^2}{6D\tau} \right) e^{-\frac{6D\tau}{W^2}} - \frac{W^2}{6D\tau} \right] \right\} \end{aligned}$$

And, finally we obtain eqn. 4:

$$t_R = \tau + \left( \frac{\tau}{1 + \frac{6D\tau}{W^2}} \right) \ln \left\{ 1 + \left[ \left( \frac{L - z'}{L} \cdot \frac{V_{\text{co}}}{V_{\text{out}}} \right) \left( 1 + \frac{W^2}{6D\tau} \right) \right] + \left[ \frac{W^2}{6D\tau} \left( e^{-\frac{6D\tau}{W^2}} - 1 \right) \right] \right\} \quad (\text{A15})$$

## REFERENCES

- 1 J. C. Giddings, *Sep. Sci.*, 1 (1966) 123.
- 2 E. Grushka, K. D. Caldwell, M. N. Myers and J. C. Giddings, in E. S. Perry, C. J. Van Oss and E. Grushka (Editors), *Separation and Purification Methods*, Vol. 2, Marcel Dekker, New York, 1973, p. 127.
- 3 J. C. Giddings, *J. Chem. Educ.*, 50 (1973) 667.
- 4 J. C. Giddings, M. N. Myers, K. D. Caldwell and S. R. Fisher, *Methods Biochem. Anal.*, 26 (1980) 79.
- 5 K. D. Caldwell, *Anal. Chem.*, 60 (1988) 959A.
- 6 K.-G. Wahlund and J. C. Giddings, *Anal. Chem.*, 59 (1987) 1332.
- 7 K.-G. Wahlund and A. Litzen, *J. Chromatogr.*, 461 (1989) 73.
- 8 J. C. Giddings, F. J. Yang and M. N. Myers, *Anal. Chem.*, 48 (1976).

- 9 J. C. Giddings, G. C. Lin and M. N. Myers, *J. Colloid Interface Sci.*, 65 (1978) 67.
- 10 J. J. Kirkland, C. H. Dilks, Jr. and W. W. Yau, *J. Chromatogr.*, 255 (1983) 255.
- 11 K.-G. Wahlund, H. S. Winegarner, K. D. Caldwell and J. C. Giddings, *Anal. Chem.*, 58 (1986) 573.
- 12 J. A. Jönsson and A. Carlshaf, *Anal. Chem.*, 61 (1989) 11.
- 13 A. Litzen and K.-G. Wahlund, *J. Chromatogr.*, 476 (1989) 413.
- 14 A. Litzen and K.-G. Wahlund, poster presented at the *International Symposium on Polymer Analysis and Characterization*, Brno, July 23–25, 1990.
- 15 J. J. Kirkland, W. W. Yau, W. A. Doerner and J. W. Grant, *Anal. Chem.*, 52 (1980) 1944.
- 16 W. W. Yau and J. J. Kirkland, *Sep. Sci. Technol.*, 16 (1981) 577.
- 17 J. J. Kirkland and W. W. Yau, *US Pat.*, 4 285 810 (1981).
- 18 J. J. Kirkland and W. W. Yau, *Macromolecules*, 18 (1985) 2305.
- 19 J. J. Kirkland, S. W. Rementer and W. W. Yau, *Anal. Chem.*, 60 (1988) 610.
- 20 S. Glasstone, *Textbook of Physical Chemistry*, Van Nostrand, New York, 2nd ed., 1946, p. 260.
- 21 C. H. Dilks, Jr., W. W. Yau and J. J. Kirkland, *J. Chromatogr.*, 315 (1984) 45.
- 22 J. C. Giddings, S. Li, P. S. Williams and M. E. Schimpf, *Makromol. Chem., Rapid Commun.*, 9 (1988) 817.
- 23 J. C. Giddings, L. K. Smith and M. N. Myers, *Anal. Chem.*, 48 (1976) 1587.
- 24 H. A. Sober (Editor), *Handbook of Biochemistry*, Chemical Rubber Co., Cleveland, OH, 2nd ed., 1970, Section C.
- 25 S. W. Rementer, Experimental Station, DuPont, Wilmington, DE, unpublished studies, 1991.
- 26 R. C. Ebersole, Experimental Station, DuPont, Wilmington, DE, unpublished studies, 1990.
- 27 M. N. Myers and J. C. Giddings, *Anal. Chem.*, 54 (1982) 2284.
- 28 S. Lee and J. C. Giddings, *Anal. Chem.*, 60 (1988) 2328.
- 29 J. J. Kirkland, L. E. Schallinger and W. W. Yau, *Anal. Chem.*, 57 (1985) 2271.



# Simple solution of velocity profiles of laminar flows in channels of various cross-sections used in field-flow fractionation

Jiří Pazourek\* and Josef Chmelík

*Institute of Analytical Chemistry, Czechoslovak Academy of Sciences, Veveří 97, 611 42 Brno (Czechoslovakia)*

---

## ABSTRACT

A simple method for the two-dimensional description of the flow velocity profile of Newtonian liquids in narrow channels is presented. This procedure is applied to a few types of cross-sections used in field-flow fractionation because the solutions of the flow velocity profiles are necessary for the theoretical description of the separation process in which the flow plays an active role. Limitations of the approach are discussed, and published results on this subject are compared.

---

## INTRODUCTION

Field-flow fractionation (FFF) is an analytical method based on simultaneous actions of physical field forces and the flow of the carrier liquid passing through the separation channel [1]. The carrier liquid takes an active part exhibiting the non-uniform flow velocity profile caused by viscosity effects and by the channel cross-section. Vectors of effective forces of the field and of the carrier liquid are mutually perpendicular: the field acts across the channel and the liquid flows longitudinally. Having different properties and consequently different spatial distributions due to the action of the field, components of a sample migrate along the channel with different elution velocities and thus separation occurs. It follows from the principle of FFF that the most important exploitations are separations of very high-molecular-weight samples; FFF thus holds a promising position in separations of polymers and particles, especially those of biological origin. These compounds, with respect to the properties of biological substances, could be irreversibly changed under conditions currently used in other separation methods, *e.g.*, high pressures, organic solvents and multiple transfers from the mobile to the stationary phases [2].

Channels of various cross-sections can be employed in FFF. Channels of rectangular cross-sections are commonly used for the classical mode of exponential concentration distribution [3] and in some instances for the focusing mode [4–7]. A disadvantage of this cross-section for focusing techniques is the symmetry of the flow velocity profile. This fact implies the application of asymmetric flow profiles in channels of trapezoidal cross-sections for focusing techniques [8–10]. Channels of circular cross-section are used, for example, in FFF techniques operating with an internally induced field (pressure FFF) [11] or with an external electrical field [12].

In all these instances a theoretical description of the separation is impossible without a knowledge of a mathematical expression of the velocity profile of the carrier liquid. While the velocity profiles for the channels of rectangular, circular and elliptical cross-sections have been solved [13–15], the sofar published results for the channels of trapezoidal and parabolic cross-sections [16,17] have not brought generally applicable solutions. This work is concentrated on a simple procedure for finding a two-dimensional description of the flow velocity profiles in channels which are or can be used in FFF.

# THEORY

For a unidirectional, horizontal and steady-state laminar flow of an incompressible viscous liquid in a channel of given length  $L$ , the general Navier-Stokes equations hold in the following form (the coordinate system is shown in Fig. 1):

$$\nabla^2 \vec{v} = -\frac{G}{\eta} \quad (1)$$

where  $\nabla^2$  is the Laplacean,  $\vec{v}$  is the  $z$ -component of the velocity vector of the streamline,  $G$  is equal to  $-\partial p/\partial z$  or approximately to  $\Delta p/L$  ( $\Delta p$  is the difference in pressures between the inlet and outlet of the channel) and  $\eta$  is the fluid viscosity.

The solution of eqn. 1 is simple for two infinitely wide parallel planes with a distance  $w$  ( $\nabla^2 = \partial^2/\partial y^2$ ):

$$v(y) = \frac{\Delta p}{2\eta L} (\frac{1}{4}w^2 - y^2) \quad (2)$$

When we rewrite eqn. 2 in the form

$$v(x,y) = \frac{\Delta p}{k\eta L} [\frac{1}{4}w^2(x) - y^2] \quad (3)$$

where for the above mentioned case  $k = 2$  and  $x$  is a real constant, the channel is divided into abstract elements coplanar to the plane  $yz$  and eqn. 3 describes the velocity profile in such an arbitrary element  $x$ .

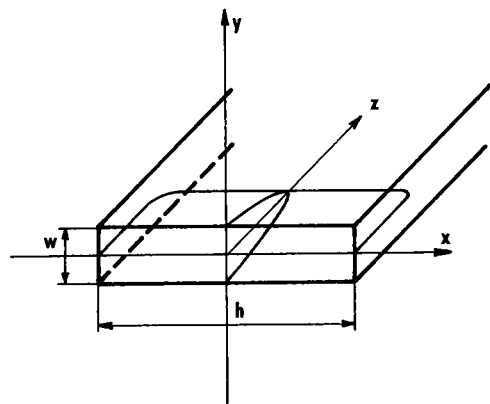


Fig. 1. Channel of rectangular cross-section. The velocity profile is schematically represented by the parabola in the plane  $yz$  and by the curve in the plane  $xz$  (see eqns. 2 and 5 for  $x = 0$  or  $y = 0$ ),  $h$  is the channel width and  $w$  is the channel height.

For the real flow velocity profile of the liquid in a rectangular cross-section channel with cross-sectional dimensions  $h$  and  $w$  (see Fig. 1) and for  $h \gg w$ , Takahashi and Gill [14] derived the relationship

$$v(x,y) = v(y)f(x) \quad (4)$$

where  $v(y)$  is the velocity profile defined by eqn. 2 and

$$f(x) = 1 - \frac{\cosh(\sqrt{3}a2x/h)}{\cosh(\sqrt{3}a)} \quad (5)$$

where  $a = h/w$ . The notation of the cross-section, with  $h$  as the larger and  $w$  as the smaller dimension, could seem to be unusual for the rectangular cross-section, but in the following cases of triangular and trapezoidal cross-sections, this approach is common. That is why this notation is also used for the rectangular cross-section channel. The course of eqn. 4 is schematically drawn in Fig. 1 as the curve in the plane  $xz$  for  $y = 0$  and as the parabola in the plane  $yz$  for  $x = 0$ .

Eqn. 4 does not fulfil eqn. 1 because of the term  $f(x)$ . We used the term  $f(x)$  to display approximate flow velocity profiles in real channels. However, for most analytical purposes, the central parts of channels are utilized. With respect to this fact (expressed by the condition  $|x| < h/2$ ), eqn. 5 is approximately equal to 1 and eqn. 4 converts into eqn. 2, which does fulfil eqn. 1.

To solve the problem of the velocity profile in channels with non-rectangular cross-sections, let us start with eqn. 3. If we are able to express  $w(x)$  as a function of the variable  $x$  that describes the width of the cross-section of the channel in a point  $x$ , then we can substitute  $w(x)$  for this function and provide a function of two variables:  $v(x,y)$ . To become the solution of eqn. 1, the new function must satisfy eqn. 1. This appropriate modification can be achieved by substituting  $v(x,y)$  into eqn. 1 and the following calculation of  $k$ , however, only for polynomial functions  $v(x,y)$  of second or first order with respect to both  $x$  and  $y$ , so that their second derivatives are constant. This limitation is fulfilled by the functions  $w(x)$  of the types  $w(x) = \sqrt{ex + f}$ ,  $w(x) = \sqrt{ex^2 + f}$  and  $w(x) = ex + f$ , where  $e$  and  $f$  are constants. Therefore, the above-described procedure will be further applied to these possible cross-sections of the channels.

The triangular cross-section is described by the expression  $w(x) = 2q(x + h/2)$ , where  $q = \tan(\beta/2)$  (the coordinate system is shown in Fig. 2). After substituting this equation for  $w(x)$  in eqn. 3 and calculating of  $k$ , we obtain

$$v(x, y) = \frac{\Delta p}{2\eta L} \cdot \frac{1}{1 - q^2} [q^2(x + \frac{1}{2}h)^2 - y^2] \quad (6)$$

If we use the equation for the mean velocity:

$$\langle v(y) \rangle_x = \frac{1}{h} \int_{-h/2}^{h/2} v(x, y) dx, \quad y = \text{constant} \quad (7)$$

we obtain the mean velocity in the plane  $xz$  ( $y = 0$ ):

$$\langle v \rangle_x = \frac{\Delta p}{6\eta L} \cdot \frac{q^2}{1 - q^2} \cdot h^2 \quad (8)$$

and then we can write eqn. 6 as

$$v(x, 0) = 3 \langle v \rangle_x \left( \frac{1}{2} + x/h \right)^2 \quad (9)$$

which is valid for each  $y = cw(x)$ , where  $c \in \langle 0, 1/2 \rangle$ . The analogous process yields the following results.

For the trapezoidal cross-section  $w(x) = 2q(x + K)$  (see Fig. 2) the following holds:

$$v(x, y) = \frac{\Delta p}{2\eta L} \cdot \frac{q^2 K^2}{1 - q^2} [(1 + x/K)^2 - y^2/q^2 K^2] \quad (10)$$

$$\langle v \rangle_x = \frac{\Delta p}{2\eta L} \cdot \frac{q^2 K^2}{1 - q^2} (1 + h^2/12w^2) \quad (11)$$

$$v(x, 0) = \frac{\langle v \rangle_x}{(1 + h^2/12K^2)} (1 + x/K)^2 \quad (12)$$

For the parabolic cross-section with the upper restricting wall we can write  $w(x) = 2\sqrt{2P}(x + h/2)$  (the coordinate system is shown in Fig. 3) and

$$v(x, y) = \frac{\Delta p}{2\eta L} \cdot hP(1 + 2x/h - y^2/hP) \quad (13)$$

$$\langle v \rangle_x = \frac{\Delta p}{2\eta L} \cdot hP \quad (14)$$

$$v(x, 0) = \langle v \rangle_x (1 + 2x/h) \quad (15)$$

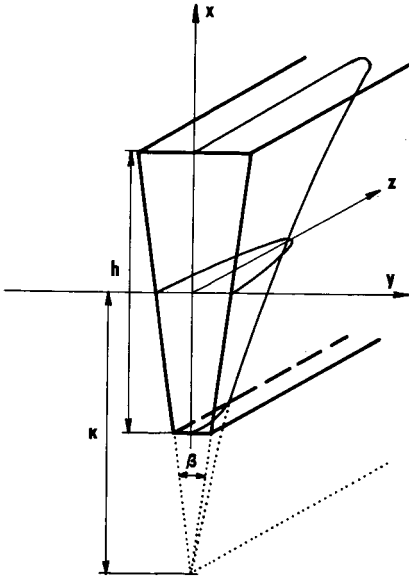


Fig. 2. Channel of trapezoidal cross-section. The velocity profile is schematically represented by the curves in the planes  $yz$  or  $xz$  (see eqn. 20 for  $x = 0$  or  $y = 0$ ),  $h$  is the channel height,  $w$  is the channel width,  $\beta$  is the angle between the side walls of the channel and  $K$  is the distance of the apex line from the axis  $z$ . The dotted line represents the channel of triangular cross-section and the corresponding velocity profile.

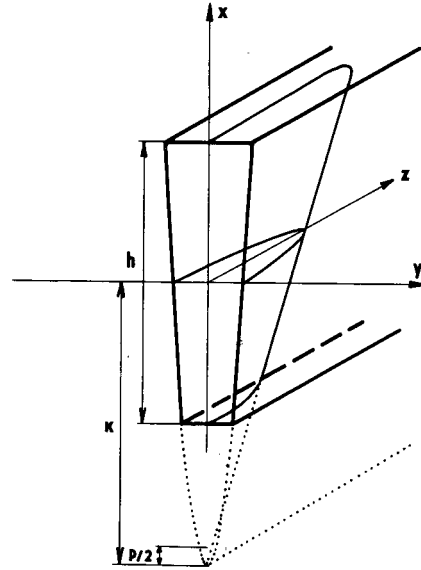


Fig. 3. Channel of parabolic cross-section with two restricting walls. The velocity profile is represented schematically by the curves in the planes  $yz$  or  $xz$  (see eqn. 21 for  $x = 0$  or  $y = 0$ ),  $h$  is the height of the channel,  $P$  is the parameter of the parabola of the edge of the channel cross-section and  $K$  is the distance of the apex line from the axis  $z$ . The dotted line represents the channel with only one limiting (upper) wall and the corresponding velocity profile.

For a parabolic cross-section with two restricting walls, the following relationship holds:

$$w(x) = 2\sqrt{2P(x+K)}$$

(see Fig. 3) and, consequently,

$$v(x,y) = \frac{\Delta p}{\eta L} \cdot KP (1 + x/K - y^2/2KP) \quad (16)$$

$$\langle v \rangle_x = \frac{\Delta p}{\eta L} \cdot KP \quad (17)$$

$$v(x,0) = \langle v \rangle_x (1 + x/K) \quad (18)$$

It is obvious from the procedure of derivations of the above-mentioned expressions that eqns. 6, 9, 10, 12, 13, 15, 16 and 18 do not generally vanish for  $x = \pm h/2$  (the upper and lower walls of the channel). Similarly to the case with the rectangular cross-section channel, we can eliminate this fact by rearranging these equations according to Takahashi and Gill [14]. However, one has to keep in mind that the validity of the equations generated by this procedure is limited only for  $|x| < h/2$ .

For both the trapezoidal and parabolic cross-sections we can write [provided that  $h \gg w(x)$  for  $x \in \langle -h/2, h/2 \rangle$ ]

$$a' = h/w(x) \quad (19)$$

By multiplying eqns. 10 and 16, respectively, by  $f(x)$  from eqn. 5 in which  $a'$  is used, the final velocity profile is obtained. Hence, for the trapezoidal cross-section

$$v(x,y) = \frac{\Delta p}{2\eta L} \cdot \frac{1}{1-q^2} [q^2(x+K)^2 - y^2] \cdot \left[ 1 - \frac{\cosh(\sqrt{3a'} \cdot 2x/h)}{\cosh(\sqrt{3a'})} \right] \quad (20)$$

and analogously for the parabolic cross-section

$$v(x,y) = \frac{\Delta p}{2\eta L} [2P(x+K) - y^2] \cdot \left[ 1 - \frac{\cosh(\sqrt{3a'} \cdot 2x/h)}{\cosh(\sqrt{3a'})} \right] \quad (21)$$

The courses of eqns. 20 and 21 are shown in Fig. 4. In Figs. 2 and 3, the final velocity profiles are schematically drawn for  $y = 0$  in the plane  $xz$  and for  $x = 0$  in the plane  $yz$ , respectively.

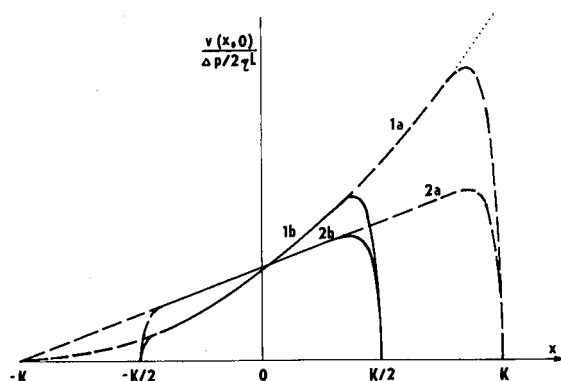


Fig. 4. Velocity profiles in channels of triangular, trapezoidal and parabolic cross-sections. Curves 1a and 1b represent the courses of eqn. 20 and curves 2a and 2b those of eqn. 21 for the case  $h = K$  (two limiting walls) (full lines 1b and 2b) and for the case  $h = 2K$  (one restricting wall) (dashed line). The dotted line displays the course of eqn. 6. Selected values:  $\beta = 5^\circ$ ;  $P = 0.001$ ;  $y = 0$ .

In the following two cases, we can obtain well known relationships [15] using the same basic procedure. For a circular cross-section with radius  $R$  [ $w(x) = 2\sqrt{R^2 - x^2}$ , Fig. 5], we provide

$$v(x,y) = \frac{\Delta p}{4\eta L} (R^2 - x^2 - y^2) \quad (22)$$

and for the elliptic cross-section with semi-axes  $a, b$  [ $w(x) = 2a\sqrt{1 - x^2/b^2}$ , Fig. 6] analogously

$$v(x,y) = \frac{\Delta p}{2\eta L} \cdot \frac{a^2 b^2}{a^2 + b^2} (1 - x^2/b^2 - y^2/a^2) \quad (23)$$

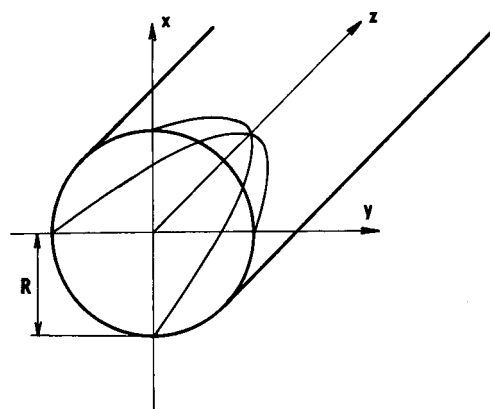


Fig. 5. Channel of circular cross-section. The velocity profile is represented schematically by two parabolas in the planes  $xz$  or  $yz$  (see eqn. 22 for  $y = 0$  or  $x = 0$ );  $R$  is the radius of the tube.



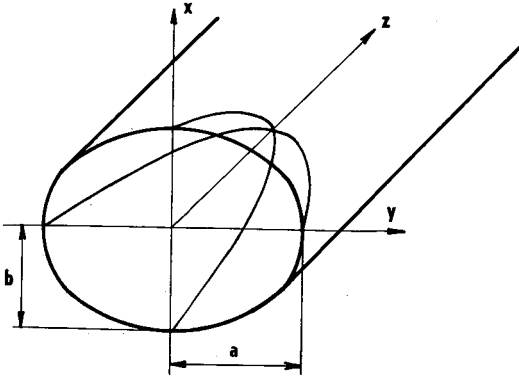


Fig. 6. Channel of elliptical cross-section. The velocity profile is schematically represented by two parabolas in the planes  $xz$  or  $yz$  (see eqn. 23 for  $y = 0$  or  $x = 0$ );  $a$  and  $b$  are the semi-axes of the channel cross-section.

## DISCUSSION

Several workers have tried to find the mathematical description of the velocity profiles in channels with non-rectangular cross-sections.

Janča and Jahnová [16] solved the cases of channels with trapezoidal and parabolic cross-sections. Their solutions are mathematical modifications of the velocity profile (eqn. 4) according to Takahashi and Gill [14]. The flow velocity profile for the trapezoidal cross-section obtained by Janča and Jahnová [16] can be written as [without the term  $f(x)$ , see eqn. 5]

$$v(x, y) = \frac{\Delta p}{2\eta L} \cdot q^2 K^2 (1 - y^2/q^2 K^2)(1 + x/K)^2 \quad (24)$$

Fig. 7 shows the courses of eqns. 10 and 24 for  $y = cw(x)$  ( $c = 0, 0.25, 0.50$ ). It is obvious that eqn. 24 has a different course for  $y < 0$  and even negative values. These authors' solution for the parabolic cross-section exhibits analogous differences (see Fig. 8):

$$v(x, y) = \frac{\Delta p}{\eta L} \cdot KP (1 - y^2/2KP)(1 + x/K) \quad (25)$$

The two solutions have another disadvantage as they do not satisfy the general eqn. 1 [regardless of the term  $f(x)$ ]. This discrepancy was introduced by Wičar [18].

Janča and Chmelík [17] published the following relationship for the description of the flow velocity

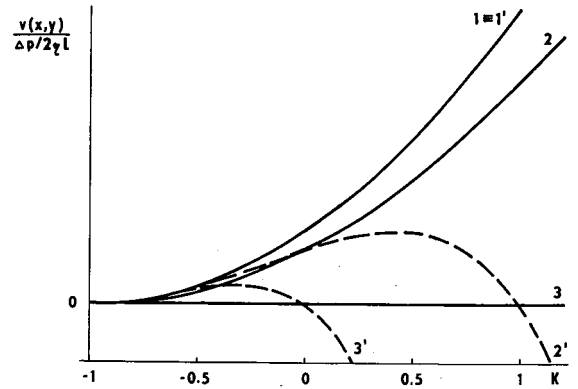


Fig. 7. Comparison of solutions of the velocity profile in a channel of triangular cross-section. Presented are the solution of eqn. 10 (full line) and the solution of ref. 16 (eqn. 24) (dashed line). Values used:  $y = 0$  (curves 1 and 1') (plane of channel symmetry),  $y = w(x)/4$  (curves 2 and 2') and  $y = w(x)/2$  (curves 3 and 3') (the side walls of the channel). Selected values:  $K = h/2$ ;  $\beta = 5^\circ$ .

profile in a channel with a trapezoidal cross-section:

$$v(x) = \frac{\langle v \rangle_x}{1 + \frac{1}{3} \tan^2 \beta} [1 + (2x/h) \tan \beta]^2 \quad (26)$$

which was derived from eqn. 24 for  $y = 0$  and  $\beta \rightarrow 0$ . This equation may be obtained from eqn. 24 or 10 but only for  $h/w(0) = 2$ , which contradicts the premise conditioning the validity of the solutions of

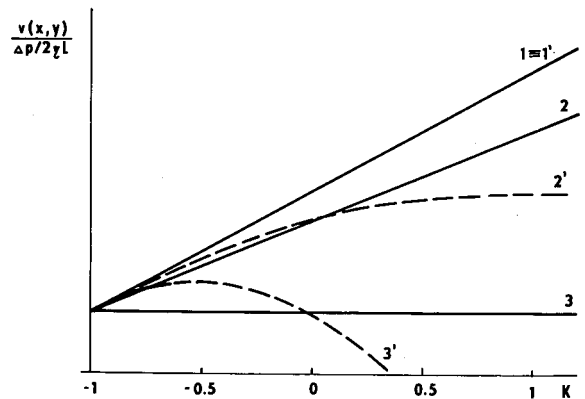


Fig. 8. Comparison of solutions of the velocity profile in a channel of parabolic cross-section with one restricting wall. Presented are the solution of eqn. 16 (full line) and the solution of ref. 16 (eqn. 25) (dashed line). Values used:  $y = 0$  (curves 1 and 1') (plane of channel symmetry),  $y = w(x)/4$  (curves 2 and 2') and  $y = w(x)/2$  (curves 3 and 3') (the side walls of the channel). Selected values:  $K = h/2$ ;  $P = 0.001$ .

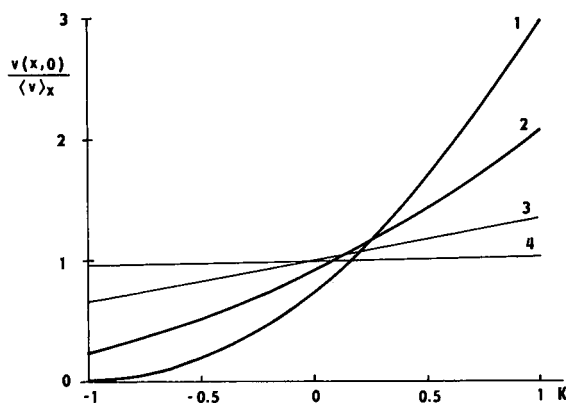


Fig. 9. Comparison of solutions of the velocity profiles in channels of triangular and trapezoidal cross-sections. Presented are solutions of eqn. 9 (curve 1) and eqn. 12 (curve 2). Curves 3 and 4 show the course of the solution of ref. 17 (eqn. 26) for  $\beta = 10^\circ$  and  $\beta = 1^\circ$ , respectively.

eqns. 4 and 24, respectively:  $h \gg w$ . In Fig. 9 the different course of eqn. 26 to that of eqns. 9 and 12 can be seen.

Wičar [18] solved the case of the flow velocity profile in a channel of a triangular cross-section without the restricting upper wall. His solution is identical with eqn. 6 (see Fig. 4, dotted line).

Eqn. 20 displays the course of the flow velocity profile in the plane  $xz$  ( $y = 0$ ) for the trapezoidal cross-section channel. In the central part ( $|x| < h/2$ ) one can see the parabolic shape of the flow velocity profile (see Fig. 2). In the case of a parabolic cross-section channel (eqn. 21) and under the same conditions, the shape of the flow velocity profile is linear (see Fig. 3). The solution of the flow velocity profile for a channel with a circular cross-section is a circular paraboloid (see eqn. 22 and Fig. 5). For the elliptical cross-section channel the solution is an elliptical paraboloid (see eqn. 23 and Fig. 6).

As a comparison criterion for channels of different cross-sections, the limiting ratio defined as

$$R = \lim_{\substack{a' \rightarrow \infty \\ x \rightarrow h/2}} v_{\max}(x,0)/\langle v \rangle_x$$

can be used [ $v_{\max}(x,0)$  is the maximum velocity in the plane  $xz$  ( $y = 0$ ) and the other symbols have the above-mentioned meanings]. As follows from eqns. 9 and 15, for channels with triangular cross-sections this limiting ratio is equal to 3 and for parabolic cross-sections to 2. Consequently, channels with triangular or trapezoidal cross-sections are of greater advantage than those of parabolic cross-sections because of their easier design and because of the values of the comparison criterion.

The results of this work permit the design of a theoretical model of the FFF separation process in channels of trapezoidal cross-sections and, consequently, a comparison of the efficiencies of channels with different cross-sections for the individual techniques of FFF.

## REFERENCES

- 1 J. C. Giddings, *Sep. Sci.*, 1 (1966) 123.
- 2 K. D. Caldwell, in C. J. King and J. D. Navratil (Editors), *Chemical Separations, Vol. 1, Principles*, Litarvan Literature, Denver, CO, 1986.
- 3 K. D. Caldwell, *Anal. Chem.*, 60 (1988) 959A.
- 4 J. C. Giddings, S. Li, P. S. Williams and M. E. Schimpf, *Macromol. Chem. Rapid Commun.*, 9 (1988) 817.
- 5 W. Thormann, M. A. Firestone, M. J. Dietz, T. Cecconie and R. A. Mosher, *J. Chromatogr.*, 461 (1989) 95.
- 6 K. G. Wahlund and A. J. Litzén, *J. Chromatogr.*, 461 (1989) 73.
- 7 S. K. Ratanathanawongs and J. C. Giddings, *J. Chromatogr.*, 467 (1989) 341.
- 8 J. Chmelík and J. Janča, *J. Liq. Chromatogr.*, 9 (1986) 55.
- 9 J. Chmelík, M. Deml and J. Janča, *Anal. Chem.*, 61 (1989) 912.
- 10 E. Urbánková and J. Janča, *J. Liq. Chromatogr.*, 13 (1990) 1877.
- 11 A. Carlshaf and A. J. Jönsson, *J. Chromatogr.*, 461 (1988) 89.
- 12 E. N. Lightfoot, *Sep. Sci. Technol.*, 14 (1979) 453.
- 13 R. J. Cornish, *Proc. R. Soc. London, Ser. A*, 120 (1928) 691.
- 14 T. Takahashi and W. N. Gill, *Chem. Eng. Commun.*, 5 (1980) 367.
- 15 Hicks, *British Association Report*, 1882, p. 63; cited in H. Lamb, *Hydrodynamics*, Dover, New York, 1945, p. 587.
- 16 J. Janča and V. Jahnová, *J. Liq. Chromatogr.*, 6 (1983) 1559.
- 17 J. Janča and J. Chmelík, *Anal. Chem.*, 56 (1984) 2481.
- 18 S. Wičar, *J. Chromatogr.*, 454 (1988) 335.

# Separation of pristinamycins by high-speed counter-current chromatography

## I. Selection of solvent system and preliminary preparative studies

S. Drogue, M.-C. Rolet, D. Thiébaut\* and R. Rosset

Laboratoire de Chimie Analytique, Ecole Supérieure de Physique et de Chimie Industrielles de la Ville de Paris, 10 Rue Vauquelin, 75005 Paris (France)

---

### ABSTRACT

Partition coefficient determination and direct application of high-speed counter-current chromatography allowed the selection of suitable chloroform–ethyl acetate–methanol–water solvent systems for the separation of macrolide antibiotics. Sample loading limits were found to be 10 ml and 200 mg for a total volume capacity of 108 ml. This allows scale-up to higher volume counter-current chromatographic apparatus and direct competition with semi-preparative high-performance liquid chromatography for crude extract samples.

---

### INTRODUCTION

Pristinamycins are macrolide antibiotics mainly acting on Gram-positive *Staphylococcus* and *Streptococcus*. They consist of two families: pristinamycins I with acid–base properties and pristinamycins II without such properties. Fig. 1 shows the molecular structure of the four components that we investigated, *i.e.*, pristinamycins IA and B and pristinamycins IIA and B. As pristinamycins are obtained from a fermentation broth, the direct preparative separation of the crude extract by high-performance liquid chromatography (HPLC) is not possible without damage to the stationary phase and a tedious crystallization pretreatment is necessary to obtain the purified samples that can be injected on to the columns.

Counter-current chromatography (CCC) uses a liquid stationary phase retained in the apparatus by a centrifuged force field. The planetary motion of the column promotes solute mass transfer between

the stationary and mobile phases. Consequently, efficient separations can be obtained and there is no risk of stationary phase degradation. The principles and examples of applications of the technique can be found in special issues of *Journal of Chromatography* and *Journal of Liquid Chromatography* devoted to CCC [1–5].

This paper described how suitable solvent systems for the separation of pristinamycins were selected and modified until satisfactory resolution was obtained on our analytical unit. Then, sample loading limits were studied for comparison with semi-preparative HPLC. Preliminary promising results are presented.

### EXPERIMENTAL

#### *Apparatus*

*High-speed counter-current chromatography (HSCCC)*. The HSCCC system was a Model CPHV 2000 (SFCC, Neuilly-Plaisance, France)

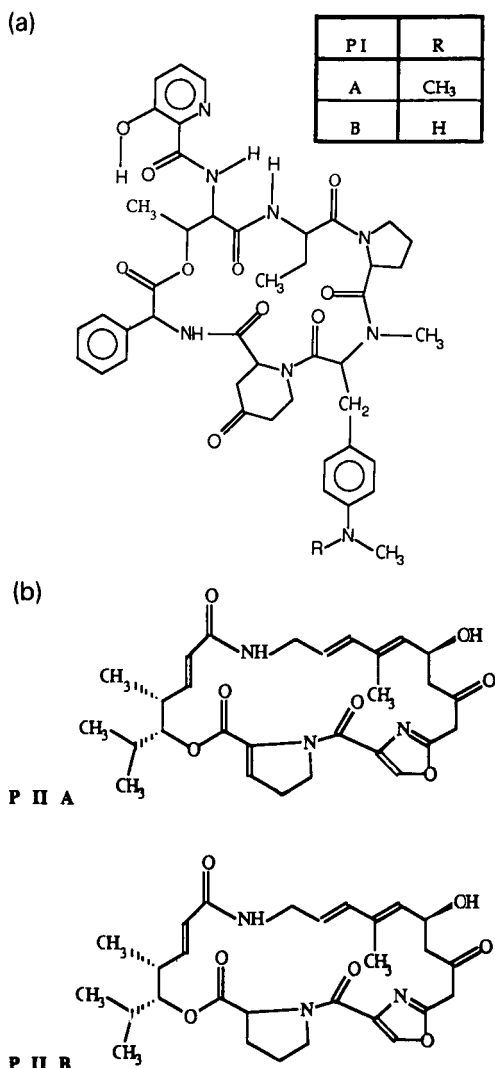


Fig. 1. Structures of (a) pristina-mycins IA and B and (b) pristina-mycins IIA and B.

equipped with three identical columns connected in series and arranged symmetrically around the central axis of the centrifuge. The columns were prepared from 1.6 mm I.D. polytetrafluoroethylene (PTFE) tubing wound on to a holder to give a total capacity of 108 ml and the connections between the columns were made of 0.8 mm I.D. PTFE tubing. The columns underwent synchronous planetary motion and revolved around their own axis, avoiding twisting of the column flow tubes. The maxi-

mum revolution speed attainable was 2000 rpm. The  $\beta$  value (ratio of the rotational radius to the revolution radius) ranged from 0.5 at the internal terminal to 0.85 at the external terminal.

Apart from the HSCCC system, the complete HSCCC apparatus consisted of a Shimadzu Model LC 5 A reciprocating HPLC pump (Touzart et Matignon, Vitry sur Seine, France) for the mobile organic phase and a preparative pump (LC-XPS pump, Pye Unicam, Philips Industries, Bobigny, France) for the stationary aqueous phase. The columns were connected to the pumps by 0.8 mm I.D. PTFE tubing via a three-way valve. Samples were injected into the column via a Rheodyne Model 7125 injection valve equipped with different loops of variable volume. Each solvent system was thoroughly equilibrated in a separating funnel at room temperature and the two phases were separated shortly before use. After filling the columns with the stationary phase, injections of the samples dissolved either in the mobile or the stationary phase were carried out into the mobile phase according to a special injection procedure.

A Sedex 45 evaporative light-scattering detector (ELSD) (Sédéré, Vitry sur Seine, France) manufactured for HPLC was used without modification. The basic principles of the ELSD were described previously [6]. This detector allows the detection of samples whose UV absorption is poor and also the use of high-UV cut-off solvents, and the baseline obtained is very stable even with slight bleeding of the stationary phase during the separation.

**HPLC.** Using the procedure developed by Rhône-Poulenc Rorer (Centre de Recherche de Vitry-Alfortville, France), HPLC analyses of sample solutions for the determination of partition coefficients were performed on a Pecosphere 5 CR C<sub>8</sub> (5  $\mu$ m) column (150  $\times$  4.6 mm I.D.) (Perkin Elmer, Saint Quentin en Yvelines, France), thermostated at 35°C in a Crocosil oven, with 0.1 M phosphate buffer (pH 2.9)–acetonitrile (67.5:32.5, v/v) as mobile phase pumped by a Shimadzu Model LC 5 A reciprocating HPLC pump (Touzart et Matignon) at a flow-rate of 1 ml/min. The injection solvent was water–acetonitrile (60:40, v/v). Injections of the sample vials by a Rheodyne Model 7125 injection valve equipped with a 20- $\mu$ l sample loop were automatically carried out by an Kontron 360 automatic injector (Kontron Instruments, Montigny-Le-Bre-

tonneux, France), the column effluent was monitored at 220 nm by a Model 2550 UV detector (Varian, Orsay, France) and all chromatographic data were stored in a CR4A Shimadzu data system (Touzart et Matignon).

### Reagents

All organic solvents were of HPLC grade except methanol, which was of analytical-reagent grade. Alcohols were purchased from Prolabo (Paris, France) and other organic solvents from Rathburn (Chromoptic, Montpellier, France). Each phase was filtered before use through on-line filters (2  $\mu$ m) after the pumps. Water was doubly distilled. Nitrogen (L'Air liquide, Paris, France) supplied the nebulizer of the ELSD system.

Pure pristinamycins IA and IB were provided by Rhône-Poulenc Rorer.

## RESULTS AND DISCUSSION

### Selection of solvent systems

In CCC, there are three main criteria in choosing a solvent system. First, the solvent systems must be composed of two immiscible phases, second, their selectivity towards samples of interest has to be sufficient to lead to separations with good resolution and third, the stationary phase retention must be at least of 50% of the total column volume when applied on a CCC unit.

The main criterion is the second one. The selectivity of different solvent systems can be evaluated by determination of the partition coefficients for each component. All partition coefficients are expressed as the ratio of the concentration in the organic phase to that in the aqueous phase, whichever phase is the mobile phase, whereas the ratios of concentration in the stationary phase to that in the mobile phase were used to predict possible separations. The selectivity ( $\alpha$ ) of the solvent system is the ratio of the partition coefficients of the solutes. Different methods are commonly used for the determination of partition coefficients [7–9]. As crude pristinamycins consisted of four main components, HPLC, which allowed the simultaneous determination of the four partition coefficients and did not require the use of pure samples, was chosen to measure their concentrations.

Taking into account the relative hydrophobicity

of pristinamycins, several hydrophobic solvent systems based on heptane–water mixtures were investigated. The basic system heptane–water (1:1, v/v) was not selective enough so modifiers such as methanol and ethyl acetate were added in various proportions to modify the polarity of this system. Unfortunately, with heptane–methanol–water or heptane–ethyl acetate–water solvent systems, all the partition coefficient values were of the same magnitude and, considering the accuracy of their determination, no solvent system with sufficient selectivity could be found.

Based on the data for the Craig separation of these macromolecules [10], dichlorethane–water–methanol solvent systems were studied. The solvent system used with Craig's Machine, dichlorethane–water–methanol (40:7:30, v/v/v) gave partition coefficients and selectivity that were too low. Partition coefficients and selectivity were increased, by first modifying the proportion of water in the system, then changing the pH of the aqueous phase (pristinamycins I have acid–base properties) and then increasing the proportion of another components of the solvent system. In this investigation, two kinds of difficulties were encountered. Some proportions resulted in miscible solvent systems which were therefore not consistent with CCC and, second, neither the aqueous nor the organic phase was retained as the stationary phase in the CCC unit irrespective of the mobile phase flow-rate and the rotation speed.

As reported in numerous papers, most separations of antibiotics by counter-current chromatography use a two-phase solvent system based on chloroform–water systems [11–18]. Commonly, methanol, carbon tetrachloride, ethyl acetate or an aqueous buffer is added to modify the polarity of the solvent system and increase its selectivity. The first attempts were to add methanol, which is miscible in the two phases. All solvent system compositions are presented in Table I and on a ternary diagram (Fig. 2) that is very useful in CCC [19–23] to study the influence of each component of solvent systems on partition coefficient and in HPLC to study the polarity and selectivity of various solvents (Snyder selectivity diagram [24]). Ternary diagrams were used to determine ranges where solvent systems provided separations not too slowly and with good resolution. Either the partition coefficients

TABLE I

PARTITION COEFFICIENTS FOR CHLOROFORM–METHANOL–WATER SOLVENT SYSTEMS

No.	Solvent system composition (volumes)			P IA	P IB	P IIA	P IIB
	Chloroform	Methanol	Water				
1	3	1	3	$\infty$	$\infty$	$\infty$	$\infty$
2	1	1	1	$\infty$	$\infty$	$\infty$	$\infty$
3	2	5	4	99	86	31	22
4	1	2	1	23	4.9	3.9	— <sup>a</sup>
5	1	3	1	single phase			
6	1	5	1				

<sup>a</sup> Partition coefficient not available.

values were too high (solvent systems 1–4) or the solvent system was composed of a single phase (solvent systems 5 and 6). As methanol was mostly miscible with water, ethyl acetate which was mostly miscible with chloroform was added; hence both the aqueous and organic phase polarities were modified. The solvent system chloroform–ethyl acetate–methanol–water (3:1:3:2, v/v) was applied on the

CPHV 2000 unit with the organic phase as mobile phase pumped from head to tail and promising results for the separation of pristnamycins II were obtained. Hence this solvent system had to be improved and adapted to the separation of pristnamycins I.

#### *Separation of pristnamycins I and II using chloroform–ethyl acetate–methanol–water solvent systems*

Using the analytical HSCCC CPHV 2000 unit, modified solvent systems were tried directly without wasting any time in calculating low-accuracy partition coefficients.

The separation of pristnamycins IIA and B was first improved. Ethyl acetate was the component of the solvent system with the greatest influence on selectivity. Its proportion was modified until a separation with sufficient analytical resolution to allow scale-up to preparative separation was obtained. All the results in terms of solvent systems, resolution, selectivity and stationary phase retention for CPHV 2000 are presented in Table II. Fig. 3 shows chromatograms of the separation of pristnamycins IIA and B with increasing proportion of ethyl acetate, the total volume of chloroform and ethyl acetate being constant. If too much ethyl acetate was added (Table II, solvent system 5), there was no longer any retention of the aqueous stationary phase. The best resolution between pristnamycins IIA and B was obtained when chloroform and ethyl acetate were in equal proportions (Table II, solvent system 4, *i.e.*,  $R_s = 2.21$  against  $R_s = 1.2$  with the first solvent system).

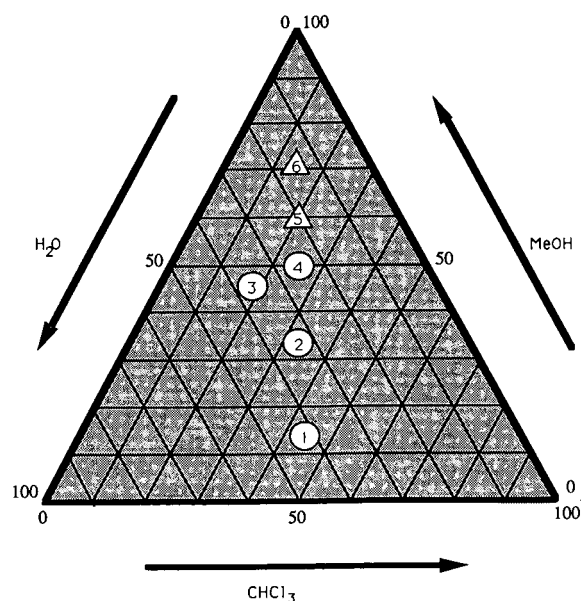


Fig. 2. Ternary diagram for chloroform–methanol–water solvent systems. Compositions of each components are expressed in volume percentage and numbers refer to Table I.  $\Delta$ , Single-phase solvent system.

TABLE II

## IMPROVEMENT OF THE PRISTINAMYCINS IIA AND IIB SEPARATION

Chloroform–ethyl acetate–methanol–water solvent system compositions in volumes, resolution between pristnamycins IIA and B, solvent system selectivity and stationary phase retention obtained on CPHV 2000. Aqueous stationary phase. Mobile phase flow-rate, 2 ml/min.

No.	Solvent system composition (volumes)				$R_s$ (P IIA/ P IIB)	$\alpha$ (P IIB/ P IIA)	Capacity factor, $k'$		Stationary phase retention (%)
	Chloroform	Ethyl acetate	Methanol	Water			P IIA	P IIB	
1	3	1	3	2	1.2	1.5	0.52	0.8	81
2	2.5	1.5	3	2	1.87	1.67	0.30	0.61	80
3	2.4	1.6	3	2	2.0	1.7	0.83	1.4	78
4	2	2	3	2	2.21	1.76	0.61	1.06	77
5	1.5	2.5	3	2					0

Solvent system 4 in Table II, which offered the best resolution between pristnamycins IIA and B, was not at all selective towards pristnamycins IA and B. Through the protonable nitrogen and hydroxyl groups, pristnamycins I present acid–base properties so formic acid was added to solvent system 4 to control the aqueous phase pH and thus increase selectivity. Table III summarizes the results. Formic acid was added until there was less stationary phase retention (which induced a decrease in resolution), then the proportions of chloroform and ethyl acetate were changed (their total volume remaining constant) and the proportion of formic acid increased again, etc. As the proportions of methanol and water were maintained constant, the more interesting solvent systems, that is solvent systems 1 and 6–16 in Table III, were plotted on a ternary diagram (Fig. 4). For limited component proportions, general trends of resolution, solutes retention and stationary phase retention could be highlighted.

When the proportion of formic acid was increased (solvent systems 1–7 and 8 against 9), solute solubility in the stationary phase and retention increased, stationary phase retention tended to decrease until it became zero and resolution increased as long as there was no bleeding of the stationary phase. With a significant proportion of formic acid (solvent systems 7–16), the same trend as before was observed with increasing amount of ethyl acetate. Solvent system 12 was not selective; it showed the need for ethyl acetate to obtain sufficient selectivity,

which was already observed for ethyl acetate to obtain sufficient selectivity, which was already observed for the optimization of the separation of pristnamycins IIA and B. The effect of an increasing proportion of chloroform on separation was mainly to lower the solute retention and to give excellent stationary phase retention (solvent systems 7, 8 and 10). As far as resolution was concerned, no obvious influence could be seen. The best solvent system for the separation of pristnamycins IA and B seemed to be solvent system 8, which combined rapidity (the separation lasted less than 30 min) and a resolution close to 2, which would allow easy semi-preparative scale-up studies that are now in progress.

#### Preliminary semi-preparative studies

The maximum volume and amount that can be injected on to the CPHV 2000 system without appreciable losses in efficiency and resolution were determined. A 1-mg amount of pristnamycin IA was injected while the sample volume was increased from 50  $\mu$ l to 20 ml. For each injected volume, samples were diluted alternately with the mobile phase and the stationary phase. Figs. 5a and b and 6a and b show respectively the variation of efficiency *versus* injected volume and the ratio of injected volume to peak volume *versus* injected volume. Figs. 5a and 6a refer to mobile phase as sample diluent and Figs. 5b and 6b to stationary phase as sample diluent. As injection in mobile phase did not disturb the phase equilibrium and distribution, no stationary phase bleeding was observed but a dramatic decrease in

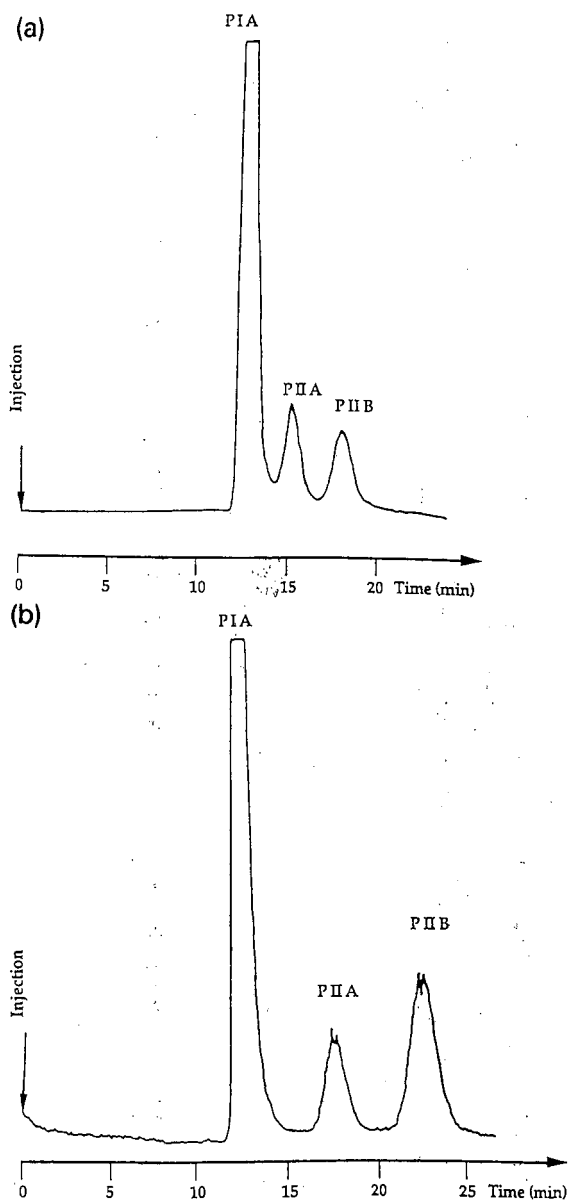


Fig. 3. Chromatograms for separation of pristinamycins IIA and B on CPHV 2000. Solvent systems: chloroform-ethyl acetate-methanol-water, (a) 3:1:3:2 and (b) 2.4:1.6:3:2 (v/v). Organic mobile phase flow-rate, 2 ml/min; injection, 50  $\mu$ l; rotation speed, 1400 rpm; ELSD, 40°C; nitrogen pressure, 2 bar.

peak efficiency occurred (1500 theoretical plates for a 50- $\mu$ l sample loop against 20 theoretical plates for a 20-ml sample loop). In contrast, although injection in stationary phase disturbed the phase equilib-

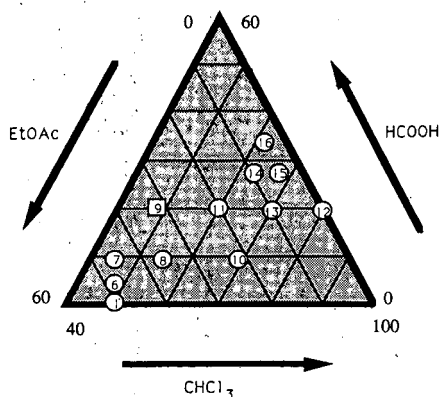


Fig. 4. Ternary diagram for chloroform-ethyl acetate-methanol-water-formic acid solvent systems, all with 3 volumes of methanol and 2 volumes of water; compositions of the other three components are expressed in volume percentage and numbers refer to Table III. □, Interesting but no stationary phase retention.

rium and induced significant bleeding of the stationary phase for injected volumes over 5 ml, the peak efficiency increased slightly up to 2000 theoretical plates for 10 ml injected. A higher peak efficiency would have been obtained without taking into account that loss of stationary phase during separation induced artificially longer retention times. In additions with injections over 5 ml, peak compression occurred. This has already been observed [25-27] and could be of advantage for one-step pre-concentration and separation of diluted samples.

Hence the maximum injection volume was 10 ml (10% of the column total capacity) in stationary phase sample diluent. The injected amount was then increased from 0.5 mg to 200 mg of a mixture of pristinamycins IA and B to study the variation of resolution. Each injection, consecutive or not, was performed in stationary phase and had to follow a specific procedure in order not to induce bleeding of the stationary phase and to obtain good reproducibility of solute retention times. It consisted in filling the apparatus while the injection valve was in the "inject" position. Then the injection valve was commuted to the "load" position and the stationary phase sample solution was loaded in the 10-ml sample loop. Before starting rotation and pumping the mobile phase, the injection valve was commuted to "inject" and 1 or 2 ml of pure stationary phase were pumped to prevent direct mixing between mobile



TABLE III

## IMPROVEMENT OF THE SEPARATION OF PRISTINAMYCINS IA AND IB

Partial system compositions in chloroform (x), ethyl acetate (y) and formic acid (z) in volumes for typical solvent systems: chloroform-ethyl acetate-methanol-water-formic acid (x:y:z:z:v/v), resolution between pristinemycins IA and B, solvent system selectivity and stationary phase retention obtained on CPHV 2000. Aqueous stationary phase. Mobile phase flow-rate, 2 ml/min.

No.	Solvent system composition (volumes)			$N_s$	$\alpha$	Retention time (min)		Capacity factor $k'$		Stationary phase retention (%)	Comments
	Chloroform	Ethyl acetate	Formic acid			P IA	P IB	P IA	P IB		
1	2	2	0.0019	0.55	1.54	16.98	18.05	0.13	0.20	72	
2	2	2	0.002	0.5	1.48	17.30	18.40	0.15	0.23	72	
3	2	2	0.005	0.6	1.44	15.20	16.35	0.21	0.31	77	
4	2	2	0.02	0.8	1.3	20.35	22.03	0.36	0.47	72	
5	2	2	0.04	1.1	1.43	20.28	22.53	0.35	0.50	73	
6	2	2	0.2	2.16	1.35	29.70	34.85	0.98	1.32	73	
7	2	2	0.2	1.7	1.36	25.85	29.35	0.70	0.95	73-63	Slight bleeding of stationary phase
8	2.4	1.6	0.4	1.7	1.33	35.20	42.08	1.35	1.80	73-35	Bleeding of stationary phase
9	2.4	1.6	0.4	2.49	1.51	21.98	28.33	0.90	1.36	81	
10	3	1	0.4	2.04	1.96	20.17	26.10	0.44	0.86	77-72	
11	3	1	1	1	1.4	12.63	15.58	0.26	0.56	0	No stationary phase retention
12	4	0	1	2.7	1.58	26.48	36.63	1.94	3.07	81	Weak resolution
13	3.5	0.5	1	0	1	17.22	17.22	0.38	0.38	77	No selectivity
14	3.5	0.5	1.5	1.3	1.44	18.00	21.50	0.80	1.15	81	
15	3.75	0.25	1.5	2.5	1.32	31.80	39.60	2.18	2.96	80	
16	3.75	0.25	2	0	1	- <sup>a</sup>	- <sup>a</sup>	- <sup>a</sup>	- <sup>a</sup>	- <sup>a</sup>	No selectivity
				0.65	1.24	15.40	16.40	0.43	0.52	80	Weak selectivity

<sup>a</sup> Data not available.

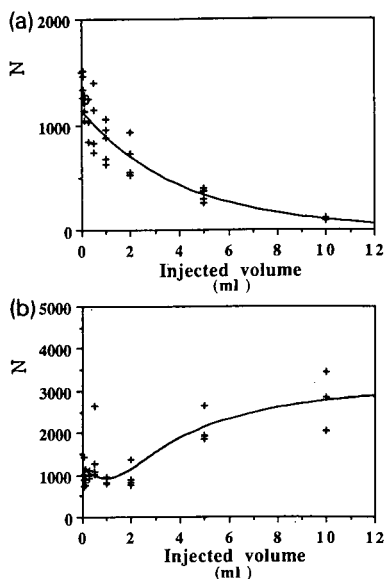


Fig. 5. Variation of the separation efficiency *versus* injected volume on CPHV 2000 for (a) mobile phase sample diluent and (b) stationary phase sample diluent. Solvent system: chloroform-ethyl acetate-methanol-water-formic acid (2.4:1.6:3:2:0.4, v/v). Organic mobile phase flow-rate, 2 ml/min; injection, pristinamycin IA 1 mg, 0.05–10 ml; rotation speed, 1400 rpm; ELSD, 40°C; nitrogen pressure, 2 bar.

phase and sample solution. Hence the first injection was made before the phases were equilibrated. For consecutive injections, mobile phase pumping was stopped but not the rotation and before being filled

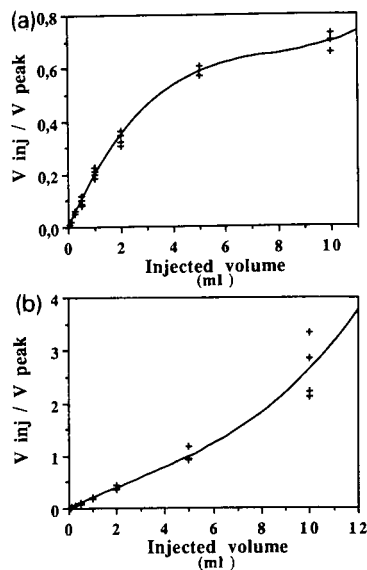


Fig. 6. Variation of the ratio of injected volume to peak volume ( $V_{inj}/V_{peak}$ ) *versus* injected volume on CPHV 2000 for (a) mobile phase sample diluent and (b) stationary phase sample diluent. Operating conditions as in Fig. 5.

the sample loop was rinsed with 20 ml of pure stationary phase, the injection valve having been commuted to the “load” position. It ends as for the first injection: the injection valve in the “inject” position, a small volume of stationary phase was pumped and mobile phase pumping was resumed. Fig. 7 shows three consecutive chromatograms with

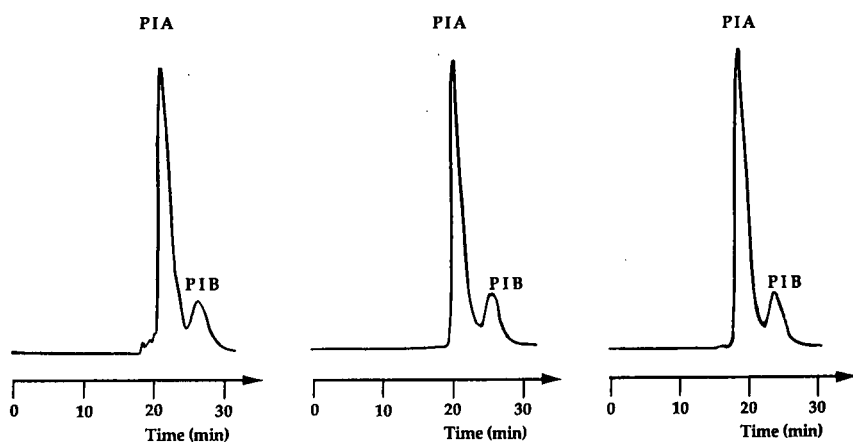


Fig. 7. Three consecutive chromatograms of the separation of pristinamycin IA following the special injection procedure. Operating conditions as in Fig. 5 except for sample size: 100 mg of pristinamycin IA dissolved in 10 ml of stationary phase.

100 mg injected in 10 ml of stationary phase. As a result of this injection procedure, mean retention times  $\pm$  standard deviations were  $21.9 \pm 1.3$  min for pristinamycin IA and  $26.6 \pm 1.2$  min for pristinamycin IB and the stationary phase displaced corresponded to the 10 ml injected. Up to 200 mg of pristinamycins IA and B dissolved in stationary phase were injected (the sample solution corresponded to the solubility limit of the compounds) and the separation still had a mean efficiency blank (1000 theoretical plates) but no resolution.

## CONCLUSION

No direct transposition of solvent systems from Craig Machine separation of pristinamycins to CCC was possible because of the high stationary phase retention requirement of HSCCC. Therefore, an original solvent system was developed allowing the rapid separation of pristinamycins when the stationary phase was the aqueous phase. Injections in stationary phase permitted large amounts of purified sample to be separated without too much loss of resolution. Further investigations are being carried out directly on the crude extract to scale-up the separation (300 to 1000 mL column volume) and to evaluate the yield of the process in terms of amount and purity. These preliminary results demonstrate that HSCCC can be a powerful tool for the fractionation of compounds.

## ACKNOWLEDGEMENT

The authors thank Rhône-Poulenc Rorer for providing financial support for this work.

## REFERENCES

- 1 *J. Liq. Chromatogr.*, 7, No. 2 (1984).
- 2 *J. Liq. Chromatogr.*, 8, No. 12 (1985).
- 3 *J. Liq. Chromatogr.*, 11, No. 1 (1988).
- 4 *J. Liq. Chromatogr.*, 13, No. 12 (1990).
- 5 *J. Chromatogr.*, 538, No. 1 (1991).
- 6 S. Drogue, M.-C. Rolet, D. Thiébaud and R. Rosset, *J. Chromatogr.*, 538 (1991) 91–97.
- 7 K. Hostettmann, M. Hostettmann-Kaldes and K. Nakanishi, *J. Chromatogr.*, 170 (1979) 355–361.
- 8 W. D. Conway and Y. Ito, *J. Liq. Chromatogr.*, 7 (1984) 275–289.
- 9 W. D. Conway and Y. Ito, *J. Liq. Chromatogr.*, 7 (1984) 291–302.
- 10 J. Preud'homme, P. Tarridec and A. Belloc, *Bull. Soc. Chim. Fr.*, (1968) 585–591.
- 11 G. M. Brill, J. B. McAlpine and J. E. Hochlowski, *J. Liq. Chromatogr.*, 8 (1985) 2259–2280.
- 12 D. G. Martin, C. Biles and R. E. Peltonen, *Am. Lab.*, 18 (1986) 21.
- 13 J. B. McAlpine, D. N. Whittern, J. E. Jochlowski and L. M. Ranfranz, poster presented at the 26th Interscience Conference on Antimicrobial Agents and Chemotherapy, September 29, 1986.
- 14 J. E. Hochlowski, G. M. Brill, W. W. Andres and J. B. McAlpine, poster presented at the 26th Interscience Conference on Antimicrobial Agents and Chemotherapy, September 29, 1986.
- 15 J. E. Hochlowski, S. J. Swanson, D. N. Whittern, A. M. Buko and J. B. McAlpine, poster presented at the 26th Interscience Conference on Antimicrobial Agents and Chemotherapy, September 29, 1986.
- 16 H. Nakazawa, P. A. Andrews, N. R. Bachur and Y. Ito, *J. Chromatogr.*, 205 (1981) 482–485.
- 17 J. W. Lightbown, P. Newland, I. A. Sutherland and J. W. A. Dymond, *Proc. Anal. Div. Chem. Soc.*, 14 (1977) 34.
- 18 T. Y. Zhang, *J. Chromatogr.*, 315 (1984) 287–297.
- 19 A. Berthod, J. D. Duncan and D. W. Armstrong, *J. Liq. Chromatogr.*, 11 (1988) 1171–1185.
- 20 D. W. Armstrong, *J. Liq. Chromatogr.*, 11 (1988) 2433–2446.
- 21 W. D. Conway, presented at the Pittsburgh Conference, New Orleans, 1988.
- 22 A. Foucault and K. Nakanishi, *J. Liq. Chromatogr.*, 13 (1990) 3583–3602.
- 23 W. D. Conway, *Counter-Current Chromatography — Apparatus, Theory and Applications*, VCH, New York, 1990.
- 24 L. R. Snyder, *J. Chromatogr. Sci.*, 16 (1978) 223–234.
- 25 H. Oka, K.-I. Harada and M. Suzuki, H. Nakazawa and Y. Ito, *J. Chromatogr.*, 482 (1989) 197–205.
- 26 J. A. Glinski, G. O. Caviness and J. R. Mikell, *J. Liq. Chromatogr.*, 13 (1990) 3625–3635.
- 27 H. Oka, K.-I. Harada, M. Suzuki, H. Nakazawa and Y. Ito, *J. Chromatogr.*, 538 (1991) 213–218.



# Author Index Vols. 592 and 593

- Abderrezag, A., see Desbène, P.-L. 593(1992)321
- Abete, C., see Colombini, M. P. 592(1992)255
- Aguilar, M. I., see Purcell, A. W. 593(1992)103
- Anderson, K., see Boppana, V. K. 593(1992)29
- Arcelloni, C., see Fermo, I. 593(1992)171
- Arm, H., see Brügger, R. 592(1992)309
- Arrigoni Martelli, E., see Zezza, F. 593(1992)99
- Balmér, K., Lagerström, P.-O., Persson, B.-A. and Schill, G.  
Reversed retention order and other stereoselective effects  
in the separation of amino alcohols on Chiralcel OD  
592(1992)331
- Bán, T., Papp, E. and Inczédy, J.  
Reversed-phase high-performance liquid chromatography  
of anionic and ethoxylated non-ionic surfactants and  
pesticides in liquid pesticide formulations 593(1992)227
- Bargossi, A. M., see Grossi, G. 593(1992)217
- Baruffini, A., De Lorenzi, E., Gandini, C., Kitsos, M. and  
Massolini, G.  
High-performance liquid chromatographic determination  
of  $\alpha$ -tocopheryl nicotinate in cosmetic preparations  
593(1992)95
- Battino, M., see Grossi, G. 593(1992)217
- Baumann, J., see Yamamoto, H. 593(1992)313
- Berek, D., see Macko, T. 592(1992)109
- Berg-Candolfi, M., Borlakoglu, J. T., Dulery, B., Jehl, F. and  
Haegele, K. D.  
Assessment of the biotransformation of the cardiotonic  
agent piroximone by high-performance liquid  
chromatography and gas chromatography-mass  
spectrometry 593(1992)1
- Berger, M., Cadet, J., Berube, R., Langlois, R. and Van Lier,  
J. E.  
Reversed-phase high-performance liquid  
chromatography-thermospray mass spectrometry of  
radiation-induced decomposition products of thymine and  
thymidine 593(1992)133
- Bertolasi, V., see Pietrogrande, M. C. 592(1992)65
- Berube, R., see Berger, M. 593(1992)133
- Bianchi, G. P., see Grossi, G. 593(1992)217
- Blake, T. J. A., see Boppana, V. K. 593(1992)29
- Boppana, V. K., Geschwindt, L., Cyronak, M. J. and Rhodes,  
G.  
Determination of the enantiomers of fenoldopam in  
human plasma by reversed-phase high-performance liquid  
chromatography after chiral derivatization 592(1992)317
- Boppana, V. K., Simpson, R. C., Anderson, K., Miller-Stein,  
C., Blake, T. J. A., Hwang, B. Y.-H. and Rhodes, G. R.  
High-performance liquid chromatographic determination  
of monohydroxy compounds by a combination of pre-  
column derivatization and post-column reaction  
detection 593(1992)29
- Borlakoglu, J. T., see Berg-Candolfi, M. 593(1992)1
- Bourguignon, B., Vankeerberghen, P. and Massart, D. L.  
CRISEBOOK, a Hypermedia version of an expert system  
for the selection of optimization criteria in high-  
performance liquid chromatography 592(1992)51
- Brenneisen, R., see Helmlin, H.-J. 593(1992)87
- Brenneisen, R., see Mathys, K. 593(1992)79
- Brown, P. R., see Roman, M. 592(1992)3
- Brown, P. R., see Weston, A. 593(1992)289
- Brügger, R. and Arm, H.  
Investigations of the influence of silanol groups on the  
separation of enantiomers by liquid and supercritical fluid  
chromatography 592(1992)309
- Bruno, A., see Pietta, P. 593(1992)165
- Bruns, A., Waldhoff, H., Wilsch-Irrgang, A. and Winkle, W.  
Automated high-performance liquid chromatographic and  
size-exclusion chromatographic sample preparation by  
means of a robotic workstation 592(1992)249
- Břizová, K., Králová, B., Demnerová, K. and Vinš, I.  
Isolation and characterization of  $\alpha$ -glucosidase from  
*Aspergillus niger* 593(1992)125
- Bucheli, F., see Wyss, R. 593(1992)55
- Burton, F. W., see Gadde, R. R. 593(1992)41
- Cadet, J., see Berger, M. 593(1992)133
- Cantafora, A. and Masella, R.  
Improved determination of individual molecular species  
of phosphatidylcholine in biological samples by high-  
performance liquid chromatography with internal  
standards 593(1992)139
- Carrai, P., see Colombini, M. P. 592(1992)255
- Caslavská, J., see Thormann, W. 593(1992)275
- Castledine, J. B., Fell, A. F., Modin, R. and Sellberg, B.  
Assessment of chromatographic peak purity by means of  
multi-wavelength detection and correlation-based  
algorithms 592(1992)27
- Caturla, M. C., Cusido, E. and Westerlund, D.  
High-performance liquid chromatography method for the  
determination of aminoglycosides based on automated  
pre-column derivatization with *o*-phthalaldehyde  
593(1992)69
- Chalykh, A. E., Kolomiets, L. N., Larionov, O. G. and  
Vinogradova, N. I.  
Investigation of solid surfaces by high-performance liquid  
chromatography 592(1992)121
- Chmelík, J., see Pazourek, J. 593(1992)357
- Chollet, D. and Salanon, M.  
Determination of Zy 17617B in plasma by solid-phase  
extraction and liquid chromatography with automated  
pre-column exchange 593(1992)73
- Coenen, A. J. J. M., Kerkhoff, M. J. G., Heringa, R. M. and  
Van der Wal, S.  
Comparison of several methods for the determination of  
trace amounts of polar aliphatic monocarboxylic acids by  
high-performance liquid chromatography 593(1992)243

- Colombini, M. P., Carrai, P., Fuoco, R. and Abete, C.  
Rapid and sensitive determination of urinary 2,5-hexanedione by reversed-phase high-performance liquid chromatography 592(1992)255
- Cooke, N., see Guttman, A. 593(1991)297
- Courthaudon, L. O., see Fujinari, E. M. 592(1992)209
- Cserhádi, T., see Forgács, E. 592(1992)75
- Cunico, B., see Dollinger, G. 592(1992)215
- Cusido, E., see Caturla, M. C. 593(1992)69
- Cyronak, M. J., see Boppana, V. K. 592(1992)317
- Däppen, R. and Molnar, I.  
Application of the gradient elution technique. Demonstration with a special test mixture and the DryLab G/plus method development software 592(1992)133
- Del Nero, S., Di Somma, M. and Vigevari, A.  
High-performance liquid chromatographic analysis of FCE 24304 (6-methylenandrosta-1,4-diene-3,17-dione) and FCE 24928 (4-aminoandrosta-1,4,6-triene-3,17-dione), two new aromatase inhibitors 593(1991)25
- De Lorenzi, E., see Baruffini, A. 593(1992)95
- Demnerová, K., see Břizová, K. 593(1992)125
- Desbène, P.-L., Abderrezag, A. and Desmazières, B.  
Analytical study of heavy crude oil fractions by coupling of the transalkylation reaction with supercritical fluid chromatography 593(1992)321
- Desmazières, B., see Desbène, P.-L. 593(1992)321
- De Vecchi, E., see Fermo, I. 593(1992)171
- Dilks, Jr., C. H., see Kirkland, J. J. 593(1992)339
- Di Somma, M., see Del Nero, S. 593(1991)25
- Djordjevic, N. M., see Liu, G. 592(1992)239
- Dolan, J. W., see Lewis, J. A. 592(1992)183
- Dolan, J. W., see Lewis, J. A. 592(1992)197
- Dollinger, G., Cunico, B., Kunitani, M., Johnson, D. and Jones, R.  
Practical on-line determination of biopolymer molecular weights by high-performance liquid chromatography with classical light-scattering detection 592(1992)215
- Dondi, F., see Pietrogrande, M. C. 592(1992)65
- Dreyer, U., Melzer, H. and Möckel, H. J.  
Increasing data precision in reversed-phase liquid chromatography leads to new information level 592(1992)13
- Drogue, S., Rolet, M.-C., Thiébaud, D. and Rosset, R.  
Separation of pristinamycins by high-speed counter-current chromatography. I. Selection of solvent system and preliminary preparative studies 593(1992)363
- Dulery, B., see Berg-Candolfi, M. 593(1992)1
- Emmrich, F., see Guse, A. H. 593(1992)157
- Erdin, R., see Timm, U. 593(1992)63
- Eriksson, B.-M. and Wikström, M.  
Determination of catecholamines in urine by liquid chromatography and electrochemical detection after on-line sample purification on immobilized boronic acid 593(1992)185
- Erni, F.  
Foreword 592(1992)1
- Erni, F., see Liu, G. 592(1992)239
- Erni, F., see Yamamoto, H. 593(1992)313
- Fanali, S., see Quaglia, M. G. 593(1992)259
- Farina, M., see Rossini, M. L. 593(1992)47
- Fell, A. F., see Castledine, J. B. 592(1992)27
- Fell, A. F., see Zimina, T. M. 593(1992)233
- Fermo, I., Arcelloni, C., De Vecchi, E., Viganò, S. and Paroni, R.  
High-performance liquid chromatographic method with fluorescence detection for the determination of total homocyst(e)ine in plasma 593(1992)171
- Fettingner, J. C., see Manz, A. 593(1992)253
- Fiorella, P. L., see Grossi, G. 593(1992)217
- Fischer, C.-H.  
Trace analysis of phthalocyanine pigments by high-performance liquid chromatography 592(1992)261
- Forgács, E., Cserhádi, T. and Valkó, K.  
Retention behaviour of some ring-substituted phenol derivatives on a porous graphitized carbon column 592(1992)75
- Forni, E., Polesello, A., Montefiori, D. and Maestrelli, A.  
High-performance liquid chromatographic analysis of the pigments of blood-red prickly pear (*Opuntia ficus indica*) 593(1992)177
- Fujima, H., see Haginaka, J. 592(1992)301
- Fujinari, E. M. and Courthaudon, L. O.  
Nitrogen-specific liquid chromatography detector based on chemiluminescence. Application to the analysis of ammonium nitrogen in waste water 592(1992)209
- Fuoco, R., see Colombini, M. P. 592(1992)255
- Gadde, R. R. and Burton, F. W.  
Simple reversed-phase high-performance liquid chromatographic method for 13-*cis*-retinoic acid in serum 593(1992)41
- Galushko, S. V., Shishkina, I. P. and Soloshonok, V. A.  
High-performance ligand-exchange chromatography of some amino acids containing two chiral centres 592(1992)345
- Gandini, C., see Baruffini, A. 593(1992)95
- Gebauer, P., see Thormann, W. 593(1992)275
- Geschwindt, L., see Boppana, V. K. 592(1992)317
- Giannini, R., see Zezza, F. 593(1992)99
- Gill, R., see Smith, R. M. 592(1992)85
- Görög, S., see Herényi, B. 592(1992)297
- Greenhagen, R. D., see O'Shea, T. J. 593(1992)305
- Gross, G. A. and Grüter, A.  
Quantitation of mutagenic/carcinogenic heterocyclic aromatic amines in food products 592(1992)271
- Grossi, G., Bargossi, A. M., Fiorella, P. L., Piazzzi, S., Battino, M. and Bianchi, G. P.  
Improved high-performance liquid chromatographic method for the determination of coenzyme Q<sub>10</sub> in plasma 593(1992)217
- Grüter, A., see Gross, G. A. 592(1992)271
- Guse, A. H. and Emmrich, F.  
Determination of inositol polyphosphates from human T-lymphocyte cell lines by anion-exchange high-performance liquid chromatography and post-column derivatization 593(1992)157
- Guttman, A., Nelson, R. J. and Cooke, N.  
Prediction of migration behavior of oligonucleotides in capillary gel electrophoresis 593(1991)297
- Haegele, K. D., see Berg-Candolfi, M. 593(1992)1

- Haerdi, W., see Maeder, G. 593(1992)9
- Haginaka, J., Seyama, C., Yasuda, H., Fujima, H. and Wada, H.  
Retention and enantioselectivity of racemic solutes on a modified ovomucoid-bonded column. I. Cross-linking with glutaraldehyde 592(1992)301
- Halmekoski, J., see Salo, M. 592(1992)127
- Hang Huynh, N., see Heldin, E. 592(1992)339
- Hann, J. T., see Perez-Souto, N. 593(1992)209
- Härmälä, P., Vuorela, H. and Rahko, E.-L.  
Retention behaviour of closely related coumarins in thin-layer chromatographic preassays for high-performance liquid chromatography according to the "PRISMA" model 593(1992)329
- Harrison, D. J., see Manz, A. 593(1992)253
- Hearn, M. T. W., see Purcell, A. W. 593(1992)103
- Heckenberg, A. L., see Weston, A. 593(1992)289
- Heldin, E., Hang Huynh, N. and Pettersson, C.  
(2S,3S)-Dicyclohexyl tartrate as mobile phase additive for the determination of the enantiomeric purity of (S)-atropine in tablets 592(1992)339
- Helmlin, H.-J. and Brenneisen, R.  
Determination of psychotropic phenylalkylamine derivatives in biological matrices by high-performance liquid chromatography with photodiode-array detection 593(1992)87
- Herényi, B. and Görög, S.  
Chiral high-performance liquid chromatographic separations on an  $\alpha_1$ -acid glycoprotein column. II. Separation of the diastereomeric and enantiomeric analogues of vinpocetine (Cavinton) 592(1992)297
- Heringa, R. M., see Coenen, A. J. J. M. 593(1992)243
- Hirata, N., Tamura, Y., Kasai, M., Yanagihara, Y. and Noguchi, K.  
New, stable polyamine-bonded polymer gel column 592(1992)93
- Huang, C.-Y., see Wen, K.-C. 593(1992)191
- Hwang, B. Y.-H., see Boppana, V. K. 593(1992)29
- Inczédy, J., see Bán, T. 593(1992)227
- Ito, S., see Ota, A. 593(1992)37
- Jandik, P., see Weston, A. 593(1992)289
- Jehl, F., see Berg-Candolfi, M. 593(1992)1
- Johnson, D., see Dollinger, G. 592(1992)215
- Jones, R., see Dollinger, G. 592(1992)215
- Jones, W. R., see Weston, A. 593(1992)289
- Kahie, Y. D., see Pietrogrande, M. C. 592(1992)65
- Kasai, M., see Hirata, N. 592(1992)93
- Kawashima, Y., see Ota, A. 593(1992)37
- Kerkhoff, M. J. G., see Coenen, A. J. J. M. 593(1992)243
- Kerner, J., see Zezza, F. 593(1992)99
- Kever, J. J., see Zimina, T. M. 593(1992)233
- Kim, H.-J. and Richardson, M.  
Determination of 5-hydroxymethylfurfural by ion-exclusion chromatography with UV detection 593(1992)153
- Kira, R., see Ôi, N. 592(1992)291
- Kirkland, J. J., Dilks, Jr., C. H., Rementer, S. W. and Yau, W. W.  
Asymmetric-channel flow field-flow fractionation with exponential force-field programming 593(1992)339
- Kitahara, H., see Ôi, N. 592(1992)291
- Kitamura, F., see Ueda, T. 592(1992)229
- Kitamura, F., see Ueda, T. 593(1992)265
- Kitsos, M., see Baruffini, A. 593(1992)95
- Kolomiets, L. N., see Chalykh, A. E. 592(1992)121
- Koza, T., see Wurst, M. 593(1992)201
- Králová, B., see Břizová, K. 593(1992)125
- Kunitani, M., see Dollinger, G. 592(1992)215
- Kuwana, T., see Ueda, T. 593(1992)265
- Kysilka, R., see Wurst, M. 593(1992)201
- Lagerström, P.-O., see Balmér, K. 592(1992)331
- Langlois, R., see Berger, M. 593(1992)133
- Larionov, O. G., see Chalykh, A. E. 592(1992)121
- Lewis, J. A., Dolan, J. W., Snyder, L. R. and Molnar, I.  
Computer simulation for the prediction of separation as a function of pH for reversed-phase high-performance liquid chromatography. II. Resolution as a function of simultaneous change in pH and solvent strength 592(1992)197
- Lewis, J. A., Lommen, D. C., Raddatz, W. D., Dolan, J. W., Snyder, L. R. and Molnar, I.  
Computer simulation for the prediction of separation as a function of pH for reversed-phase high-performance liquid chromatography. I. Accuracy of a theory-based model 592(1992)183
- Liu, F.-S., see Wen, K.-C. 593(1992)191
- Liu, G., Djordjevic, N. M. and Erni, F.  
High-temperature open-tubular capillary column liquid chromatography 592(1992)239
- Lommen, D. C., see Lewis, J. A. 592(1992)183
- Lo Moro, A., see Raspi, G. 593(1992)119
- Lopes Marques, R. M. and Schoenmakers, P. J.  
Modelling retention in reversed-phase liquid chromatography as a function of pH and solvent composition 592(1992)157
- Lüdi, H., see Manz, A. 593(1992)253
- Ludwig, R. C.  
Application of a pellicular anion-exchange resin to the separation of inorganic and organic anions by single-column anion exchange 592(1992)101
- Lunte, C. E., see O'Shea, T. J. 593(1992)305
- Lunte, S. M., see O'Shea, T. J. 593(1992)305
- Lynch, R. J., see Perez-Souto, N. 593(1992)209
- Macko, T. and Berek, D.  
Experimental evaluation of sorbent bed homogeneity in high-performance liquid chromatographic columns 592(1992)109
- Maeder, G., Pelletier, M. and Haerdi, W.  
Determination of amphetamines by high-performance liquid chromatography with ultraviolet detection. On-line pre-column derivatization with 9-fluorenylmethyl chloroformate and preconcentration 593(1992)9
- Maestrelli, A., see Forni, E. 593(1992)177
- Manz, A., Harrison, D. J., Verpoorte, E. M. J., Fettingner, J. C., Paulus, A., Lüdi, H. and Widmer, H. M.  
Planar chips technology for miniaturization and integration of separation techniques into monitoring systems. Capillary electrophoresis on a chip 593(1992)253
- Masella, R., see Cantafora, A. 593(1992)139

- Massart, D. L., see Bourguignon, B. 592(1992)51
- Massart, D. L., see Vandenbosch, C. 592(1992)37
- Massolini, G., see Baruffini, A. 593(1992)95
- Mathys, K. and Brenneisen, R.  
Determination of (S)-(-)-cathinone and its metabolites (R,S)-(-)-norephedrine and (R,R)-(-)-norpseudoephedrine in urine by high-performance liquid chromatography with photodiode-array detection 593(1992)79
- Mauri, P., see Pietta, P. 593(1992)165
- Measures, G., see Perez-Souto, N. 593(1992)209
- Melenevskaya, E. Y., see Zimina, T. M. 593(1992)233
- Melzer, H., see Dreyer, U. 592(1992)13
- Metcalfe, T., see Ueda, T. 593(1992)265
- Meyer, V. R.  
Peak purity, yield and throughput in preparative liquid chromatography with self-displacement 592(1992)17
- Miles, C. J.  
Determination of National Survey of Pesticides analytes in groundwater by liquid chromatography with postcolumn reaction detection 592(1992)283
- Miller-Stein, C., see Boppana, V. K. 593(1992)29
- Minger, A., see Thormann, W. 593(1992)275
- Mitchell, R., see Ueda, T. 592(1992)229
- Mitchell, R., see Ueda, T. 593(1992)265
- Moats, W. A.  
High-performance liquid chromatographic determination of penicillin G, penicillin V and cloxacillin in beef and pork tissues 593(1991)15
- Möckel, H. J., see Dreyer, U. 592(1992)13
- Modin, R., see Castledine, J. B. 592(1992)27
- Molnar, I., see Däppen, R. 592(1992)133
- Molnar, I., see Lewis, J. A. 592(1992)183
- Molnar, I., see Lewis, J. A. 592(1992)197
- Molteni, S., see Thormann, W. 593(1992)275
- Montefiori, D., see Forni, E. 593(1992)177
- Nakamoto, A., see Ueda, T. 592(1992)229
- Nakamoto, A., see Ueda, T. 593(1992)265
- Nardi, A., see Quaglia, M. G. 593(1992)259
- Nelson, R. J., see Guttman, A. 593(1991)297
- Nicolotti, A., see Pellegrino, S. 592(1992)279
- Noguchi, K., see Hirata, N. 592(1992)93
- Öi, N., Kitahara, H. and Kira, R.  
Direct separation of enantiomers by high-performance liquid chromatography on a new chiral ligand-exchange phase 592(1992)291
- O'Shea, T. J., Greenhagen, R. D., Lunte, S. M., Lunte, C. E., Smyth, M. R., Radzik, D. M. and Watanabe, N.  
Capillary electrophoresis with electrochemical detection employing an on-column Nafion joint 593(1992)305
- Osselton, M. D., see Smith, R. M. 592(1992)85
- Ota, A., Ito, S. and Kawashima, Y.  
Direct high-performance liquid chromatographic resolution of a novel benzothiazine  $\text{Ca}^{2+}$  antagonist and related compounds 593(1992)37
- Papgis, M., see Swart, K. J. 593(1992)21
- Papp, E., see Bán, T. 593(1992)227
- Paroni, R., see Fermo, I. 593(1992)171
- Pascale, M. R., see Zezza, F. 593(1992)99
- Patterson, S. D.  
Use of solvent selectivity optimization procedures for high-performance liquid chromatographic method development. 592(1992)43
- Patthy, M.  
Gradient elution with shorter equilibration times in reversed-phase ion-pair chromatography 592(1992)143
- Paulus, A., see Manz, A. 593(1992)253
- Pazourek, J. and Chmelik, J.  
Simple solution of velocity profiles of laminar flows in channels of various cross-sections used in field-flow fractionation 593(1992)357
- Pellegrino, S., Petrarulo, M., Testa, E. and Nicolotti, A.  
Rapid high-performance liquid chromatographic determination of urinary N-(1-methylethyl)-N'-phenyl-1,4-benzenediamine in workers exposed to aromatic amines 592(1992)279
- Pelletier, M., see Maeder, G. 593(1992)9
- Perez-Souto, N., Lynch, R. J., Measures, G. and Hann, J. T.  
Use of high-performance liquid chromatographic peak deconvolution and peak labelling to identify antiparasitic components in plant extracts 593(1992)209
- Persson, B.-A., see Balmér, K. 592(1992)331
- Petrarulo, M., see Pellegrino, S. 592(1992)279
- Pettersson, C., see Heldin, E. 592(1992)339
- Piazzì, S., see Grossi, G. 593(1992)217
- Pietrogrande, M. C., Reschiglian, P., Dondi, F., Kahie, Y. D. and Bertolasi, V.  
Correlations between high-performance liquid chromatographic retention, X-ray structural and  $^{13}\text{C}$  NMR spectroscopic data of flavonoid compounds 592(1992)65
- Pietta, P., Bruno, A., Mauri, P. and Rava, A.  
Separation of flavonol-2-O-glycosides from *Calendula officinalis* and *Sambucus nigra* by high-performance liquid and micellar electrokinetic capillary chromatography 593(1992)165
- Polesello, A., see Forni, E. 593(1992)177
- Purcell, A. W., Aguilar, M. J. and Hearn, M. T. W.  
High-performance liquid chromatography of amino acids, peptides and proteins. CXV. Thermodynamic behaviour of peptides in reversed-phase chromatography 593(1992)103
- Quaglia, M. G., Fanali, S., Nardi, A., Rossi, C. and Ricci, M.  
Separation of leucinostatins by capillary zone electrophoresis 593(1992)259
- Raddatz, W. D., see Lewis, J. A. 592(1992)183
- Radzik, D. M., see O'Shea, T. J. 593(1992)305
- Rahko, E.-L., see Härmälä, P. 593(1992)329
- Raspi, G., Lo Moro, A. and Spinetti, M.  
Direct determination of kallikrein by high-performance liquid chromatography 593(1992)119
- Rava, A., see Pietta, P. 593(1992)165
- Rementer, S. W., see Kirkland, J. J. 593(1992)339
- Reschiglian, P., see Pietrogrande, M. C. 592(1992)65
- Rhodes, G., see Boppana, V. K. 592(1992)317
- Rhodes, G. R., see Boppana, V. K. 593(1992)29
- Ricci, M., see Quaglia, M. G. 593(1992)259
- Richardson, M., see Kim, H.-J. 593(1992)153
- Rolet, M.-C., see Drogue, S. 593(1992)363



- Roman, M. and Brown, P. R.  
Separation techniques for biotechnology in the 1990s 592(1992)3
- Rosset, R., see Drogue, S. 593(1992)363
- Rossi, C., see Quaglia, M. G. 593(1992)259
- Rossini, M. L. and Farina, M.  
Stability studies with a high-performance liquid chromatographic method for the determination of a new anthracycline analogue, 3'-deamino-3'-[2-(*S*)-methoxy-4-morpholino]doxorubicin (FCE 23762), in the final drug formulation 593(1992)47
- Salanon, M., see Chollet, D. 593(1992)73
- Salo, M., Vuorela, H. and Halmekoski, J.  
Effect of temperature and mobile phase on the retention of retinoates in reversed-phase liquid chromatography 592(1992)127
- Schad, H., Schäfer, F., Weber, L. and Seidel, H. J.  
Determination of benzene metabolites in urine of mice by solid-phase extraction and high-performance liquid chromatography 593(1992)147
- Schäfer, F., see Schad, H. 593(1992)147
- Schill, G., see Balmér, K. 592(1992)331
- Schoenmakers, P. J., see Lopes Marques, R. M. 592(1992)157
- Seidel, H. J., see Schad, H. 593(1992)147
- Sellberg, B., see Castledine, J. B. 592(1992)27
- Seyama, C., see Haginaka, J. 592(1992)301
- Shishkina, I. P., see Galushko, S. V. 592(1992)345
- Simpson, R. C., see Boppana, V. K. 593(1992)29
- Slégel, P., see Valkó, K. 592(1992)59
- Smith, R. M., Westlake, J. P., Gill, R. and Osselton, M. D.  
Retention reproducibility of basic drugs in high-performance liquid chromatography on a silica column with a methanol-high-pH buffer eluent. Changes in selectivity with the age of the stationary phase 592(1992)85
- Smyth, M. R., see O'Shea, T. J. 593(1992)305
- Snyder, L. R., see Lewis, J. A. 592(1992)183
- Snyder, L. R., see Lewis, J. A. 592(1992)197
- Soloshonok, V. A., see Galushko, S. V. 592(1992)345
- Spinetti, M., see Raspi, G. 593(1992)119
- Swart, K. J. and Paggis, M.  
Automated high-performance liquid chromatographic method for the determination of rifampicin in plasma 593(1992)21
- Tamura, Y., see Hirata, N. 592(1992)93
- Testa, E., see Pellegrino, S. 592(1992)279
- Thiébaud, D., see Drogue, S. 593(1992)363
- Thormann, W., Minger, A., Molteni, S., Caslavská, J. and Gebauer, P.  
Determination of substituted purines in body fluids by micellar electrokinetic capillary chromatography with direct sample injection 593(1992)275
- Timm, U. and Erdin, R.  
Determination of the catechol-O-methyltransferase inhibitor Ro 40-7592 in human plasma by high-performance liquid chromatography with coulometric detection 593(1992)63
- Tuinstra, L. G. M. T., see Van Rhijn, J. A. 592(1992)265
- Ueda, T., Mitchell, R., Kitamura, F., Metcalf, T., Kuwana, T. and Nakamoto, A.  
Separation of naphthalene-2,3-dicarboxaldehyde-labeled amino acids by high-performance capillary electrophoresis with laser-induced fluorescence detection 593(1992)265
- Ueda, T., Mitchell, R., Kitamura, F. and Nakamoto, A.  
Constant-potential amperometric detection of carbohydrates at metal electrodes in high-performance anion-exchange chromatography 592(1992)229
- Valkó, K., see Forgács, E. 592(1992)75
- Valkó, K. and Slégel, P.  
Chromatographic separation and molecular modelling of triazines with respect to their inhibition of the growth of L1210/R71 cells 592(1992)59
- Vandenbosch, C., Vannecke, C. and Massart, D. L.  
Optimization of the separation of (6*R*)- and (6*S*)-leucovorin and evaluation of the robustness of the optimum 592(1992)37
- Van der Wal, S., see Coenen, A. J. J. M. 593(1992)243
- Vankeerberghen, P., see Bourguignon, B. 592(1992)51
- Van Lier, J. E., see Berger, M. 593(1992)133
- Vannecke, C., see Vandenbosch, C. 592(1992)37
- Van Rhijn, J. A., Viveen, J. and Tuinstra, L. G. M. T.  
Automated determination of aflatoxin B<sub>1</sub> in cattle feed by two-column solid-phase extraction with on-line high-performance liquid chromatography 592(1992)265
- Verpoorte, E. M. J., see Man, A. 593(1992)253
- Vigano', S., see Fermo, I. 593(1992)171
- Vigevani, A., see Del Nero, S. 593(1991)25
- Vinogradova, N. I., see Chalykh, A. E. 592(1992)121
- Vinš, I., see Břizová, K. 593(1992)125
- Viveen, J., see Van Rhijn, J. A. 592(1992)265
- Vuorela, H., see Härmälä, P. 593(1992)329
- Vuorela, H., see Salo, M. 592(1992)127
- Wada, H., see Haginaka, J. 592(1992)301
- Waldhoff, H., see Bruns, A. 592(1992)249
- Watanabe, N., see O'Shea, T. J. 593(1992)305
- Weber, L., see Schad, H. 593(1992)147
- Wen, K.-C., Huang, C.-Y. and Liu, F.-S.  
Determination of cinnamic acid and paeoniflorin in traditional chinese medicinal preparations by high-performance liquid chromatography 593(1992)191
- Westerlund, D., see Caturla, M. C. 593(1992)69
- Westlake, J. P., see Smith, R. M. 592(1992)85
- Weston, A., Brown, P. R., Jandik, P., Jones, W. R. and Heckenberg, A. L.  
Factors affecting the separation of inorganic metal cations by capillary electrophoresis 593(1992)289
- Widmer, H. M., see Manz, A. 593(1992)253
- Wikström, M., see Eriksson, B.-M. 593(1992)185
- Wilsch-Irrgang, A., see Bruns, A. 592(1992)249
- Winkle, W., see Bruns, A. 592(1992)249
- Wurst, M., Kysilka, R. and Koza, T.  
Analysis and isolation of indole alkaloids of fungi by high-performance liquid chromatography 593(1992)201
- Wyss, R. and Bucheli, F.  
Use of direct injection precolumn techniques for the high-performance liquid chromatographic determination of the retinoids acitretin and 13-*cis*-acitretin in plasma 593(1992)55

- Yamamoto, H., Baumann, J. and Erni, F.  
Electrokinetic reversed-phase chromatography with  
packed capillaries 593(1992)313
- Yanagihara, Y., see Hirata, N. 592(1992)93
- Yasuda, H., see Haginaka, J. 592(1992)301
- Yau, W. W., see Kirkland, J. J. 593(1992)339
- Zezza, F., Kerner, J., Pascale, M. R., Giannini, R. and  
Arrigoni Martelli, E.  
Rapid determination of amino acids by high-performance  
liquid chromatography: release of amino acids by  
perfused rat liver 593(1992)99
- Zimina, T. M., Kever, J. J., Melenevskaya, E. Y. and Fell, A.  
F.  
Analysis of block copolymers by high-performance liquid  
chromatography under critical conditions 593(1992)233

# Journal of Chromatography

## NEWS SECTION

### SHORT CONFERENCE REPORT

15TH INTERNATIONAL SYMPOSIUM ON COLUMN LIQUID CHROMATOGRAPHY (HPLC'92), BASEL, SWITZERLAND, JUNE 3-7, 1991

The fifteenth Column Liquid Chromatography (HPLC '92) meeting, excellently organized by Dr. Fritz Erni and his many co-workers, was attended by more than 1200 participants from all over the world. In addition to the scientific programme (consisting of about 60 lectures, close to 500 posters and a number of discussion sessions), there was a large exhibition of scientific instruments and other accessories, where almost a hundred



Fig. 1. Professor W. Simon (Chairman of the First Symposium on Column Liquid Chromatography, held in Interlaken in 1973) presents a typical Swiss cowbell to the Chairman of HPLC'91, Fritz Erni, to allow the latter to subtly remind the speakers not to exceed their time.

manufacturers presented their latest products in the field of separation science. An extensive social programme offered the participants plenty of opportunity to meet less formally during receptions, dinners and a concert. These photographs attempt to recapture some of the atmosphere during the event.

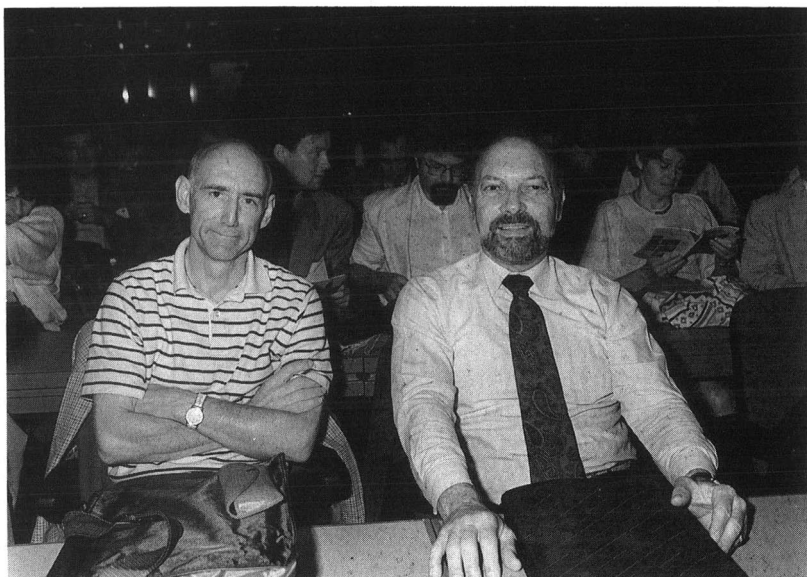


Fig. 2. Roger Giese (Northeastern University, Boston) and Michael Widmer (Ciba-Geigy, Basel) in anticipation of things to come at one of the plenary sessions.

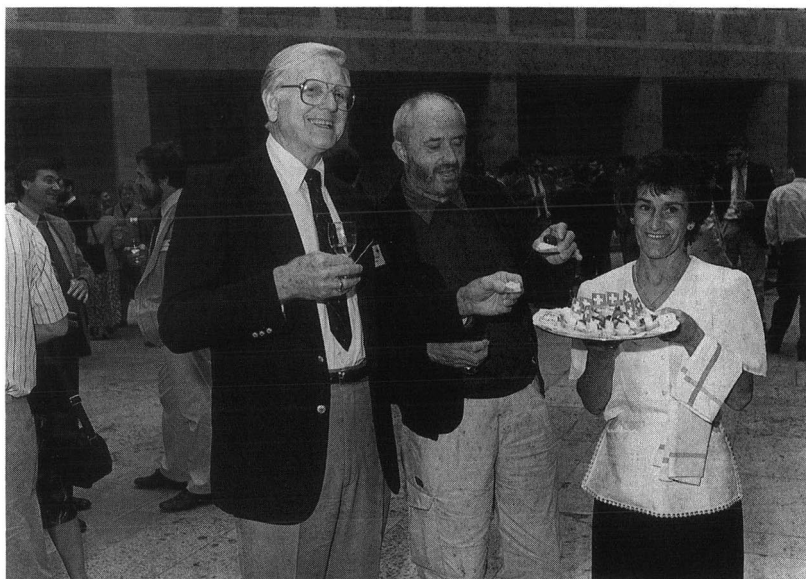


Fig. 3. Jack Kirkland (DuPont, Wilmington) and Klaus Unger (Johannes Gutenberg University, Mainz) sampling Swiss cheese at the reception offered by the Government of the canton of Basel.

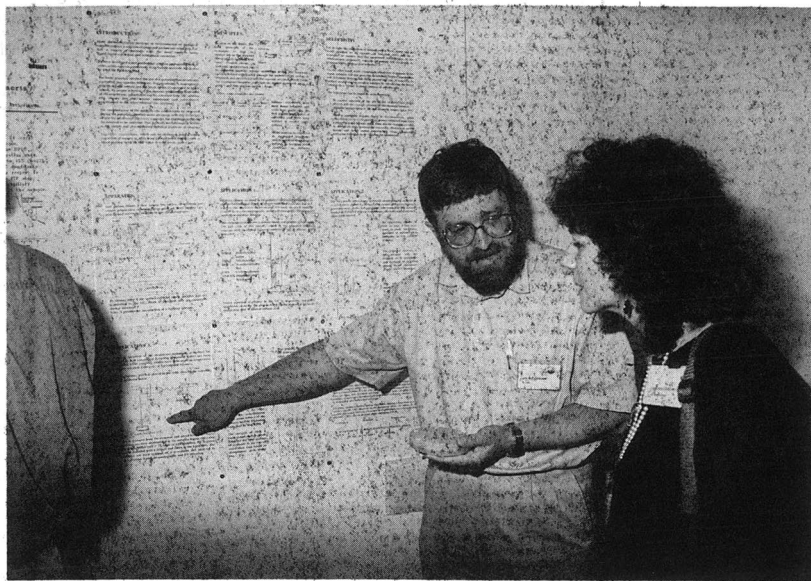


Fig. 4. Jan-Ake Jönsson (University of Lund) explains to Claudia Lipschitz (Elsevier, Amsterdam) the advantages of applying supported liquid membranes to sample preparation.



Fig. 5. Klaas Bij (Elsevier), Csaba Horváth (Yale University, New Haven), John Haken (University of New South Wales, Kensington) and Guy van Dam (Elsevier's promotion manager, who attended his last chromatography symposium before retiring) at the informal get-together on Sunday.



## PUBLICATION SCHEDULE FOR 1992

*Journal of Chromatography and Journal of Chromatography, Biomedical Applications*

MONTH	O 1991	N 1991	D 1991	J	F	M	
Journal of Chromatography	585/1	585/2 586/1 586/2 587/1	587/2 588/1 + 2	589/1 + 2 590/1 590/2	591/1 + 2 592/1 + 2 593/1 + 2	594/1 + 2 595/1	The publication schedule for further issues will be published later
Cumulative Indexes, Vols. 551–600							
Bibliography Section						610/1	
Biomedical Applications				573/1 573/2 574/1	574/2	575/1 575/2	

## INFORMATION FOR AUTHORS

(Detailed *Instructions to Authors* were published in Vol. 558, pp. 469–472. A free reprint can be obtained by application to the publisher, Elsevier Science Publishers B.V., P.O. Box 330, 1000 AH Amsterdam, The Netherlands.)

**Types of Contributions.** The following types of papers are published in the *Journal of Chromatography* and the section on *Biomedical Applications*: Regular research papers (Full-length papers), Review articles and Short Communications. Short Communications are usually descriptions of short investigations, or they can report minor technical improvements of previously published procedures; they reflect the same quality of research as Full-length papers, but should preferably not exceed five printed pages. For Review articles, see inside front cover under Submission of Papers.

**Submission.** Every paper must be accompanied by a letter from the senior author, stating that he/she is submitting the paper for publication in the *Journal of Chromatography*.

**Manuscripts.** Manuscripts should be typed in double spacing on consecutively numbered pages of uniform size. The manuscript should be preceded by a sheet of manuscript paper carrying the title of the paper and the name and full postal address of the person to whom the proofs are to be sent. As a rule, papers should be divided into sections, headed by a caption (*e.g.*, Abstract, Introduction, Experimental, Results, Discussion, etc.). All illustrations, photographs, tables, etc., should be on separate sheets.

**Introduction.** Every paper must have a concise introduction mentioning what has been done before on the topic described, and stating clearly what is new in the paper now submitted.

**Abstract.** All articles should have an abstract of 50–100 words which clearly and briefly indicates what is new, different and significant.

**Illustrations.** The figures should be submitted in a form suitable for reproduction, drawn in Indian ink on drawing or tracing paper. Each illustration should have a legend, all the *legends* being typed (with double spacing) together on a *separate sheet*. If structures are given in the text, the original drawings should be supplied. Coloured illustrations are reproduced at the author's expense, the cost being determined by the number of pages and by the number of colours needed. The written permission of the author and publisher must be obtained for the use of any figure already published. Its source must be indicated in the legend.

**References.** References should be numbered in the order in which they are cited in the text, and listed in numerical sequence on a separate sheet at the end of the article. Please check a recent issue for the layout of the reference list. Abbreviations for the titles of journals should follow the system used by *Chemical Abstracts*. Articles not yet published should be given as "in press" (journal should be specified), "submitted for publication" (journal should be specified), "in preparation" or "personal communication".

**Dispatch.** Before sending the manuscript to the Editor please check that the envelope contains four copies of the paper complete with references, legends and figures. One of the sets of figures must be the originals suitable for direct reproduction. Please also ensure that permission to publish has been obtained from your institute.

**Proofs.** One set of proofs will be sent to the author to be carefully checked for printer's errors. Corrections must be restricted to instances in which the proof is at variance with the manuscript. "Extra corrections" will be inserted at the author's expense.

**Reprints.** Fifty reprints of Full-length papers and Short Communications will be supplied free of charge. Additional reprints can be ordered by the authors. An order form containing price quotations will be sent to the authors together with the proofs of their article.

**Advertisements.** The Editors of the journal accept no responsibility for the contents of the advertisements. Advertisement rates are available on request. Advertising orders and enquiries can be sent to the Advertising Manager, Elsevier Science Publishers B.V., Advertising Department, P.O. Box 211, 1000 AE Amsterdam, Netherlands; courier shipments to: Van de Sande Bak-huyzenstraat 4, 1061 AG Amsterdam, Netherlands; Tel. (+31-20) 515 3220/515 3222, Telefax (+31-20) 6833 041, Telex 16479 els vi nl. UK: T. G. Scott & Son Ltd., Tim Blake, Portland House, 21 Narborough Road, Cosby, Leics. LE9 5TA, UK; Tel. (+44-533) 753 333, Telefax (+44-533) 750 522. USA and Canada: Weston Media Associates, Daniel S. Lipner, P.O. Box 1110, Greens Farms, CT 06436-1110, USA; Tel. (+1-203) 261 2500, Telefax (+1-203) 261 0101.

# new! Laboratory information management

An International Journal  
Section of Chemometrics and Intelligent Laboratory Systems

Editor:

**R.D. McDowall**, Beckenham, Kent, UK

Editor for North America:

**R.R. Mahaffey**, Eastman Chemicals  
Division, Kingsport, TN, USA

The journal covers all aspects of information management in a laboratory environment, such as information technology, storage, processing and flow of data. The following topics are covered:

- \* **Laboratory Information Management Systems (LIMS)**
- \* **Means of integrating and merging laboratory information**
- \* **Networks**
- \* **Regulatory Aspects**
- \* **Electronic Laboratory Notebooks**
- \* **Human aspects of laboratory automation**

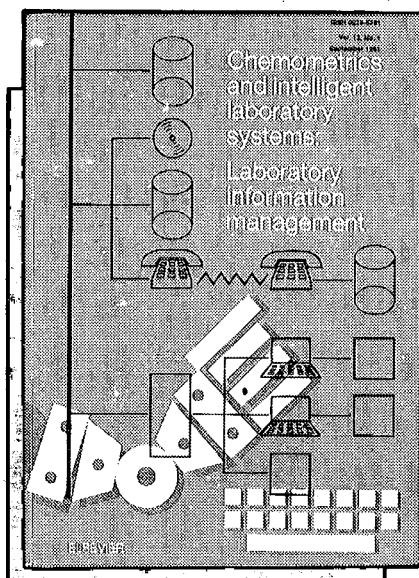
Subscription Information:

1992: Vol. 17 (3 issues)

Dfl. 406.00 / US\$ 201.00

(including postage)

ISSN 0925-5281



***A Free Sample Copy is Available on Request***

Elsevier Science Publishers  
P.O. Box 330  
1000 AH Amsterdam  
The Netherlands  
Tel: (31-20) 5862 873  
Fax: (31-20) 5862 845



in the USA and Canada  
P.O. Box 882  
Madison Square Station  
New York, NY 10159, USA  
Tel: (212) 633 3750  
Fax: (212) 633 3764

**ELSEVIER SCIENCE PUBLISHERS**